CATALOG OF APOLLO 15 ROCKS

Part 1. 15015—15299

Curatorial Branch Publication 72
JSC 20787
October 1985

GRAHAM RYDER
(Lunar and Planetary Institute;
Northrop Services, Inc.)

National Aeronautics and
Space Administration

Lyndon B. Johnson Space Center
Houston, Texas

CATALOG OF APOLLO 15 ROCKS

Part 1. 15015—15299

GRAHAM RYDER
(Lunar and Planetary Institute;
Northrop Services, Inc.)

October 1985

TABLE OF CONTENTS

PART 1.

PART 2.

PART 3.

INTRODUCTION

This catalog characterizes each of 267 individually numbered rock samples in the Apollo 15 collection, showing what each sample is and what is known about it. Unconsolidated regolith (soil) samples are not included. The catalog is intended to be used by both researchers requiring sample allocations and a broad audience interested in Apollo 15 rocks. The sample descriptions are arranged in numerical order, closely corresponding to the sample collection stations. Some samples which were numbered as rocks are actually collections of small fragments.

Information on sample collection, petrography, chemistry, stable and radiogenic isotopes, surface characteristics, physical properties, and curatorial processing is summarized and referenced as far as it is known. The intention has been to be comprehensive--to include all published studies of any kind which provide information on a sample, as well as some unpublished information. Some exceptions are made where the same research group published the same data and conclusions in two journals, in which case one reference (usually the earlier) is chosen; if one is the Proceedings of the Lunar Science Conference, this reference is selected. References which are primarily bulk interpretations of existing data (such as mixing models) or mere lists of samples are rarely included. The references are complete to early 1985. Foreign language journals were not scrutinized, but as far as we can tell little data has been published only in such journals.

This catalog differs from the Catalog of Apollo 16 Rocks, JSC 16904 (1980) in that all chemical data is tabulated, instead of "best-guess" averages. Rare-earth diagrams are computer-plotted to a consistent scale for easy comparison; analyses with fewer than three rare-earth points are in most cases not plotted.

Much valuable information exists in the original Apollo 15 Sample Information Catalog (1971). However, that catalog was compiled and published only three months after the mission itself, from rapid descriptions of usually dust-covered rocks, usually without anything other than macroscopic observations, and less often thin sections. Since then, the rocks have been studied, analyzed, and split, with many published papers. These make the original catalog inadequate, outmoded, and in some cases erroneous, providing the motivation for this revision. However, the Apollo 15 Sample Information Catalog (1971) contains more information on macroscopic observations for most samples than does the present volume.

ACKNOWLEDGEMENTS

Many Northrop Services, Inc., personnel in the Planetary Materials Laboratory worked on the compilation of this catalog, over a period of a few years. Alene Simmons diligently translated unintelligible handwriting into accurate inputs for all text and tables. Jenny Seltzer, Lee Smith, and Jo Ann Wolfshohl supported data pack research and thin section library work. Andrea Mosie assisted in inspection of several rock samples in the laboratory. Claire Dardano produced the computer-generated rare earth element diagrams. Final production was supervised by Judy Allton. Claudine Robb served as graphics teacher and coordinator for the data input and layout team of Joe Hodapp, Robbie Marlow, Rene Martinez, Cecilia Satterwhite, and Linda Watts.

Outside of the Curatorial Laboratory, several persons directly or indirectly provided assistance. Sources of unpublished data are quoted directly in the text. G.J. Taylor (University of New Mexico) provided several photomicrographs of rake samples.

The catalog was produced with the encouragement, support, and pressure of D. Blanchard (NASA: Planetary Materials Curator); S. Waltz (NSI: Planetary Materials Laboratory Manager); the Lunar and Planetary Sample team during its chairmanships by O.B. James and L.A. Taylor; and K. Burke (Director, Lunar and Planetary Institute).

THE APOLLO 15 MISSION

On July 30, 1971, the Apollo 15 lunar module Falcon, descending over the 4,000 meter Apennine Mountain front, landed at one of the most geologically diverse sites selected in the Apollo program, the Hadley-Apennine region. Astronauts Dave Scott and Jim Irwin brought the spacecraft onto a mare plain just inside the most prominent mountain ring structure of the Imbrium basin, the Montes Apennines chain which marks its southeastern topographic rim, and close to the sinuous Hadley Rille (Fig. 1). The main objectives of the mission were to investigate and sample materials of the Apennine Front itself (expected to be Imbrium ejecta and pre-Imbrium materials), of Hadley Rille, and of the mare lavas of Palus Putredinis (Fig. 2). A package of seven surface experiments, including heat flow and passive seismic, was also set up and 1152 surface photographs were taken. A television camera, data acquisition (sequence) camera, and orbital photography and chemical data provided more information. The Apollo 15 mission was the first devoted almost entirely to science, and the first to use a Rover vehicle which considerably extended the length of the traverses, from a total of 3.5 km on Apollo 14 to 25.3 km during three separate traverses on Apollo 15 (Fig. 3). The collected sample mass was almost doubled, from 43 kg on Apollo 14 to 78 kg on Apollo 15. A reduction in the planned traverse length was made necessary, in part by unexpected and time-consuming difficulties in the collection of the deep core sample (at the experiments package area). Thus the North Complex, a hilly, cratered region of disputable origin, was not visited. Nonetheless the mission was very successful.

The Apollo 15 mission produced both expected and unexpected results. As expected, mare basalt samples were collected on the mare plains. No evidence was found to change the pre-mission interpretation of Hadley Rille as a collapsed lava tube or channel. Mare basalts were also sampled almost in situ at the rille edge and the only observations of in situ bedrock ever made on the Moon were those on the Hadley Rille wall. The mare basalts form two distinct chemical groups, both of which have the same age (3.3 b.y.), Sr-isotopic characteristics, and rare-earth element patterns. The one group, olivine-normative, contains many vesicular specimens, and shows an olivine fractionation trend. Samples are mainly medium- to coarse-grained. The other group, quartz-normative, is pigeonite-phyric and includes both vitrophyric and coarse-grained examples. However, it shows little fractionation at all. A few other mare basalts may represent distinct flows.

An unexpected find was emerald green glass, which is a mare volcanic product. It is primitive in chemistry and isotopic characteristics but has an age similar to the mare basalts. It is ubiquitous, but most common on the Apennine Front where it is locally present as fairly pure clods. Several slightly but distinctly different chemical subgroups of this very low-Ti glass

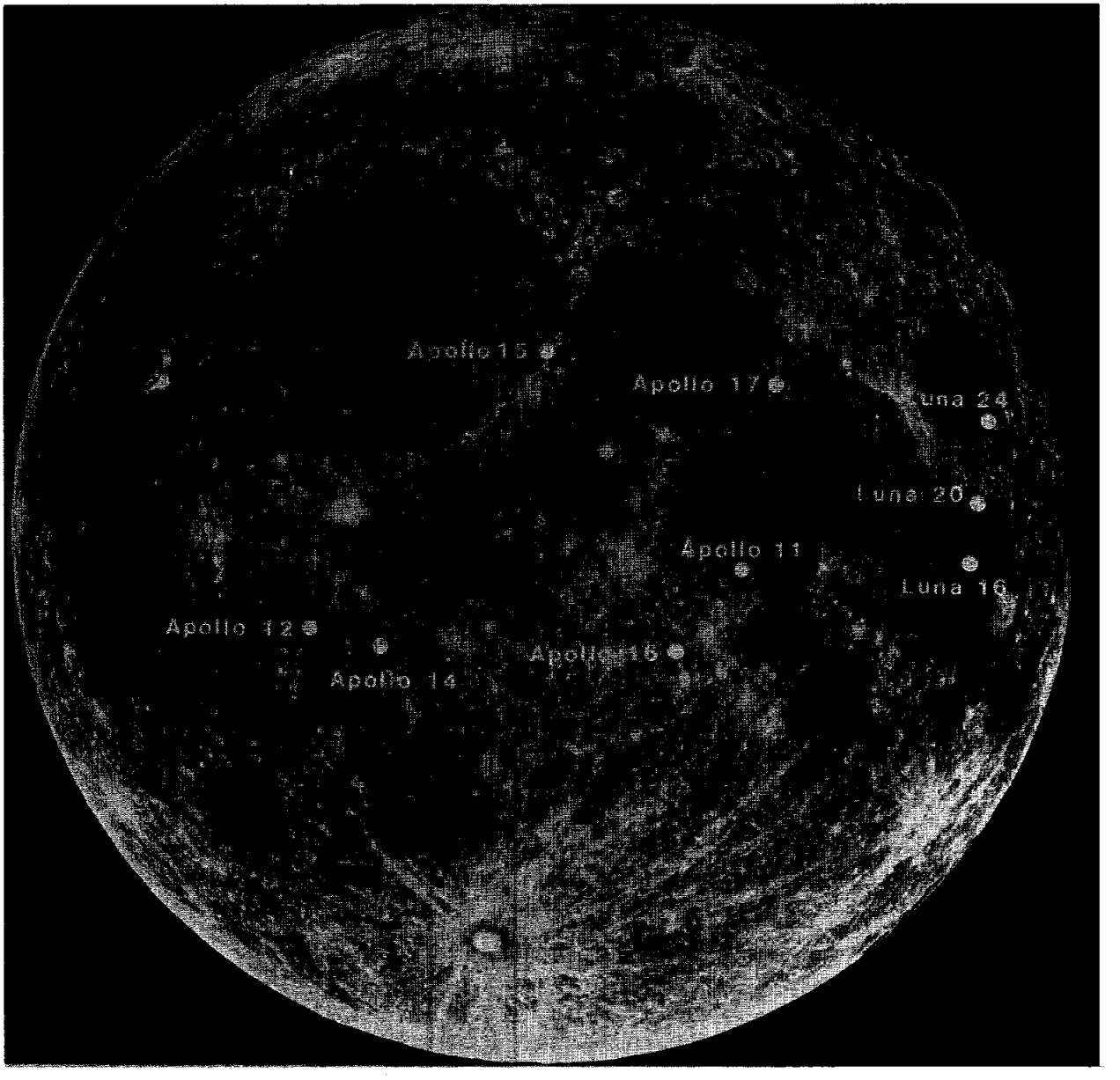

Figure (i). Apollo and Luna sampling locations (S84-31673)

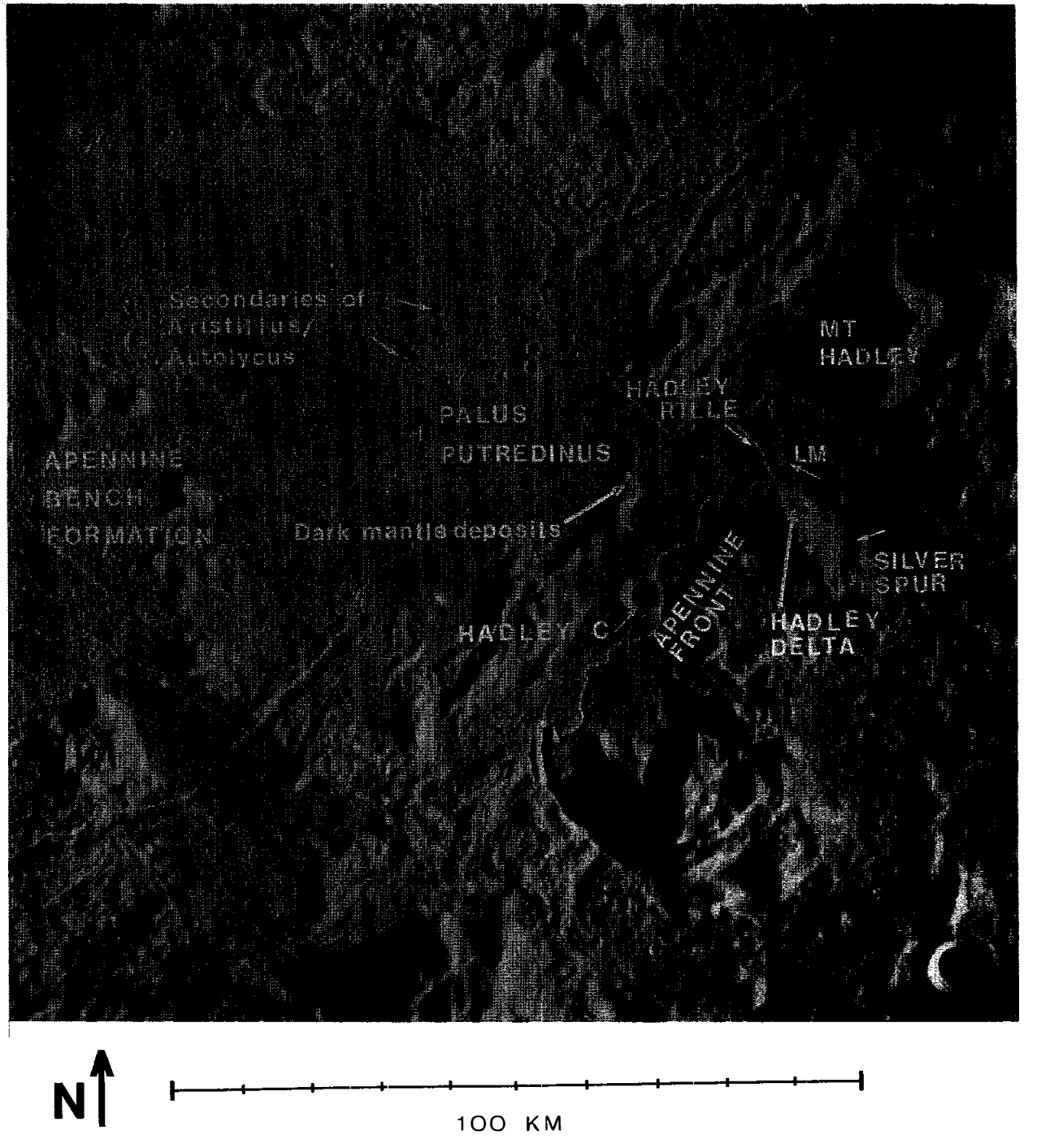

Figure (ii). Apollo 15 landing site area (metric camera frame AS-15-M-0415)

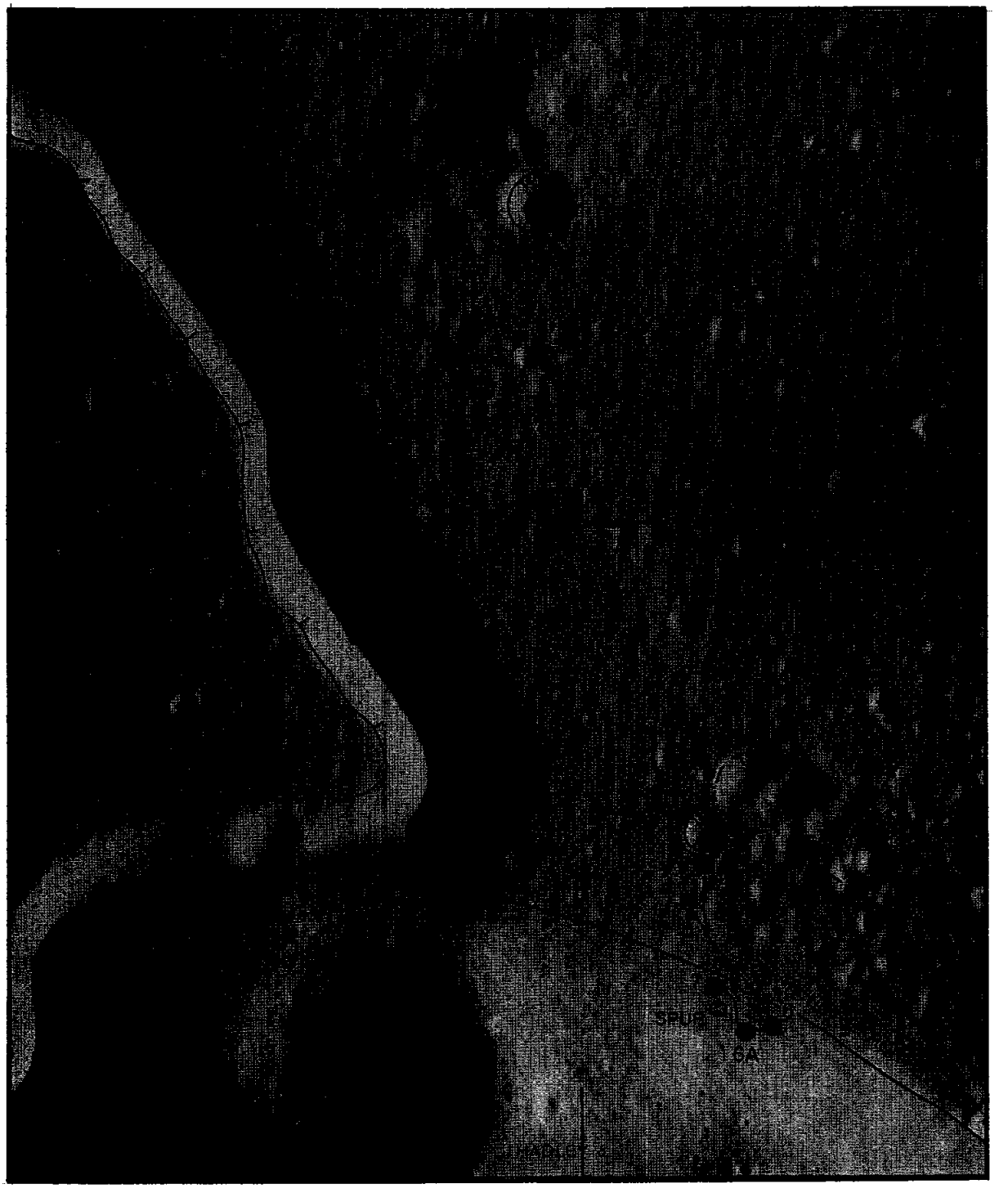

Figure (iii). Apollo 15 traverses and sampling locations (AS-15-M-0415)

occur. Two other volcanic glass types of grossly different chemistry, yellow intermediate-Ti and red high-Ti, are present at the site but are dispersed deposits.

The Apennine Front samples include many brown glassy regolith breccias ranging from friable clods to coherent rocks. These breccias contain mare basalt and green glass and only minor conspicuous highland-derived materials, hence have an origin much later than Imbrium. Such regolith breccias, with varied chemistry generally similar to local regoliths, are common throughout the landing site. Highlands materials include cataclasized or brecciated igneous rocks including ferroan anorthosites (e.g., "Genesis rock" 15415), norites, and spinel-bearing troctolites, as well as impact melts and metamorphosed breccias. Unexpectedly though, distinctly highlands samples are rare and generally small. The Apennine Front is in fact rather smooth, and only three meter-sized boulders were observed close enough to the planned traverses to sample. Two of these are post-Imbrium exotics. The average composition of the Apennine Front, as suggested by regolith chemistry mixing models and the compositions of impact glasses in the regolith, is a low-K KREEP basaltic composition ("Low-K Fra Mauro"). Several impact melt rocks have this general composition which has never been found as a pristine igneous rock type.

Another unexpected discovery was the common presence of volcanic KREEP (K, REE, P, and other incompatible-element-enriched) basalts, though only as small fragments. Only two are included among numbered rocks. They are ~3.85 b.y. old, an age indistinguishable from that of the Imbrium basin. The KREEP fragments are ubiquitous, but although pre-mare, are most common in regoliths from around the lunar module, on top of the mare flows.

The variety of Apollo 15 samples reflects the variety of terrains in the vicinity of the landing site, and the impressive stratigraphic section ranging from pre-Imbrian to Copernican.

References to detailed studies on the Apollo 15 samples are cited in the individual rock descriptions. The following list is a more general selected bibliography pertaining to the geological interpretation and rock samples of the Apollo 15 landing site.

ALGIT (Apollo Lunar Field Geology Investigation Team) (1972) Geologic setting of the Apollo 15 samples. Science 175, 376-384.

Allen J.P. (1972) Apollo 15: Scientific journey to Hadley-Apennine. American Scientist 60, 162-174.

Apollo 15 Preliminary Science Report (1972), NASA SP-289.

Apollo 15 Preliminary Examination Team (1972) The Apollo 15 Lunar Samples: A Preliminary Description. Science 175, 363-375.

Bailey N.E. and Ulrich G.E. (1975) Apollo 15 Voice Transcript Pertaining to the Geology of the Landing Site. USGS Rept. USGS-GD-74-029.

Carr M.H., Howard K.A., and El-Baz F. (1971) Geologic map of the Apennine-Hadley region of the Moon. U.S. Geol. Surv., Map 1-723, Sheet 1.

Chamberlain J.W. and Watkins C. (Eds.) (1972) The Apollo 15 Lunar Sample. Lunar Science Inst., Houston, 525 pp.

Hackman R.J. (1966) Geologic map of the Montes Apenninus region of the Moon. U.S. Geol. Surv., Map 1-463.

Howard K.A., Head J.W., and Swann E.A. (1972) Geology of Hadley Rille. Proc. Lunar Sci. Conf. 3rd, 1-14.

Sutton R.L., Hait M.H., Larson K.B., Swann G.A., Reed V.S., and Schaber G.G. (1972) Documentation of Apollo 15 samples. U.S. Geol. Surv. Interagency Report: Astrogeology 47, 257 pp.

Swann G.A., Hait M.H., Schaber G.G., Freeman V.L., Ulrich G.G., Wolfe E.W., Reed V.S., and Sutton R.L. (1971) Preliminary description of Apollo 15 sample environments. U.S. Geol. Surv. Interagency Report: 36, 219 pp.

NUMBERING OF APOLLO 15 SAMPLES

A five digit sample number was assigned each rock (generally coherent material greater than about 1 cm), the unsieved reserve and each sieve fraction of scooped <1 cm material, each drill stem and drive tube section and each sample of special characteristics. The explanation of the numbering system, below, is for all samples, but only rocks, or samples numbered as rocks, are included in this catalog.

The first two digits, 15, designate the mission number for all of the samples of this catalog. The last three digits were assigned with a dual purpose: to indicate sample type and to group samples by locality.

Without regard to sampling locations, the first 14 numbers (15001-15014) were assigned to drill stems, drive tubes, and special environment sample containers (SESC). 15900-15999 were housekeeping numbers used for sweepings, for material caught on filters from dusting operations, for small amounts of fines from sample containers with rocks only, and for any material not easily categorized. All of the other sample numbers were grouped by sampling locality (station) and the groups arranged in order of the traverses.

Materials from the three paired rake and soil samples were assigned the centuries: 15001-15199, 15300-15399, and 15600-15699. Within each the fines were numbered in the first one or two decades according to the fines convention explained below. The remaining numbers were given to rocks which are grouped by lithology.

A decade or more of sample numbers was used for the contents of each documented bag (DB). Fines (soil samples) were ascribed numbers according to the following system:

15XY0	Unsieved "reserve"
15XY1	<1 mm sieve fraction
15XY2	1-2 mm sieve fraction
15XY3	2-4 mm sieve fraction
15XY4	4-10 mm sieve fraction

The rocks were given numbers ranging from 15XY5-15XY9 for each number decade. Large rocks returned loose in the sample collection bags (SCB) were assigned unused rock numbers in the decades, as were some rocks returned in documented bags without fines.

Any material removed from a sample (splits, chips, aliquots, thin

sections, etc.) is given a "specific" number, which is placed to the right of the sample number and separated from it by a comma (e.g., 15426,17).

APOLLO 15 ROCK SAMPLES: BASIC INVENTORY

The following pages are an inventory of all numbered Apollo 15 rock samples, updated from the Apollo 15 Sample Information Catalog (1971); regolith and core samples are not included. Rock sample columns comprise the type of sample, its mass, a brief descriptive name, and the container(s) in which it was brought to earth.

Under SAMPLE TYPE, a blank indicates that the sample was an individually collected hand sample, in some cases chipped from boulders. An "R" indicates that the sample was collected with many others by raking the regolith. A "P" indicates that the sample was picked from a regolith sample during laboratory processing in Houston. Details on sample collection can be found in the Interagency Report: Astrogeology 47 (1972), the Apollo 15 Preliminary Science Report NASA SP-289 (1972), and Bailey and Ulrich "Apollo 15 Voice Transcript" (1975).

The DESCRIPTION is not meant to be a formal classification nor to replace any existing classifications. For samples for which thin sections have not been made the nature and genesis of a rock is far less well-known than for those for which thin sections do exist. Thus some of the rocks are less specifically characterized than others, and this is partly reflected in the descriptive name by the use of a question mark.

The descriptive names used in this inventory are:

Olivine-normative mare basalt (modifiers: fine-grained, medium-grained, coarse-grained): Mare volcanic rock containing about 10% olivine with textures generally ranging from porphyritic-subophitic or ophitic to gabbroic. Fine-grained refers to maximum grain sizes of less than about 0.5 mm; medium-grained refers to groundmass grain sizes less than about 1 mm and phenocrysts less than about 2 mm; coarse-grained refers to any coarser varieties. A few are brecciated or melted or both.

Quartz-normative mare basalt (modifiers: porphyritic, vitrophyric, spherulitic, variolitic, radiate, subophitic): Mare volcanic rock in which pigeonite phenocrysts are embedded in a finer-grained groundmass. In general, the coarser the phenocrysts, the coarser the groundmass. Mg-olivine is rare. Vitrophyric have small phenocrysts in a glassy groundmass; spherulitic and variolitic have coarser phenocrysts in a groundmass with fine radiating pyroxene/plagioclase/glass intergrowths; radiate have coarser phenocrysts in a coarsely radially-grown groundmass; subophitic have the coarsest phenocrysts and a subophitic to intergranular groundmass.

Feldspathic peridotite (mare basalt): Olivine-rich mare basalts

which are probably cumulates.

Feldspathic microgabbro (mare basalt): Feldspathic mare basalt which is probably a cumulate.

KREEP basalt: Non-porphyritic feldspar/pyroxene volcanic basalt with textures ranging from vitric to variolitic to intersertal to subophitic. They are considerably enriched in imcompatible elements (K, REE, P, etc.) compared with mare basalts.

Anorthosite (modifiers: ferroan, cataclastic): Very feldspathic rock of highland's origin, mainly brecciated but originally coarse-grained. Ferroan indicates shown to be a member of the ferroan anorthosite suite. Cataclastic implies in situ crushing rather than pervasive brecciation and mixing.

Regolith breccia, Regolith Clods: A brecciated, mixed assemblage containing glass, agglutinates, and other regolith components, and with at least some coherency. Clods are extremely friable and have largely disintegrated.

Green Glass Clods: Extremely friable regolith-like clods with a very high proportion of emerald green glass debris, in some cases close to 100%, at least in part. Only one is indurated.

Shocked/melted breccia: Breccia with obvious and pervasive melting produced by shock and with intensely shocked clasts.

Impact melt (modifiers: glassy, fine-grained): Breccia with a melt matrix, and clasts without intense shock features. Most are highlands samples with low-K KREEP composition.

Glass, glass bombs, agglutinates: Varied glassy objects are present. Glassy refers to more homogeneous glassy objects, agglutinates to more heterogeneous objects in which a relationship between glass and clasts is more obvious. Several rocks have conspicuous complete or partial glass coats, and are so designated.

APOLLO 15 ROCK INVENTORY

KEY: F.G.=fine-grained M.G.=medium-grained C.G.=coarse-grained

SAMPLE NUMBER	SAMPLE TYPE	MASS g	DESCRIPTION	SCB/DB
15015		4770.0	Regolith breccia	SCB4/
15016		923.7	M.G. ol-norm mare basalt	SCB4/
15017		9.8	Glass shell	SCB5/162
15018		5.7	Vesicular glass	SCB5/162
15019		1.2	Agglutinitic breccia	SCB5/162
15025		77.3	Regolith breccia	CSB
15026		1.1	Regolith breccia, glass-coated	CSB
15027		51.0	Regolith breccia/vesicular glass	SCB5/162
15028		59.4	Regolith breccia, glass-coated	SCB5/162
15058		2672.0	Porphyritic subophitic qz-norm mare basalt	SCB6/
15059		1149.0	Regolith breccia, glass-coated	SCB6/
15065		1475.0	Porphyritic subophitic qz-norm mare basalt	SCB1/156
15075		809.3	Porphyritic subophitic qz-norm mare basalt	SCB1/157
15076		400.5	Porphyritic subophitic qz-norm mare basalt	SCB1/157
15085		471.3	Porphyritic subophitic qz-norm mare basalt	SCB1/158
15086		216.5	Regolith breccia	SCB1/158
15087		5.7	Porphyritic subophitic qz-norm(?) mare basalt	SCB1/158
15088		1.8	Regolith breccia	SCB1/158
15095		25.5	Polymict breccia, glass-coated	SCB1/159
15105	P	5.6	F.G. ol-norm mare basalt	SCB1/187
15115	R	4.0	Porphyritic subophitic qz-norm mare basalt	SCB1/186
15116	R	7.2	Porphyritic subophitic qz-norm mare basalt	SCB1/186
15117	R	23.3	Porphyritic subophitic qz-norm mare basalt	SCB1/186
15118	R	27.6	Porphyritic radiate qz-norm mare basalt	SCB1/186
15119	R	14.1	F.G. ol-norm mare basalt and regolith breccia	SCB1/186
15125	R	6.5	Porphyritic spherulitic qz-norm mare basalt	SCB1/186
15135	R	1.6	Agglutinate	SCB1/186
15145	R	15.1	Ol-norm(?) mare basalt breccia	SCB1/186
15146	R	1.0	Mare basalt (monomict?) breccia	SCB1/186
15147	R	3.7	Regolith breccia	SCB1/186
15148	R	3.0	Regolith breccia	SCB1/186
15205		337.3	Regolith breccia, glass-coated	SCB1/161
15206		92.0	Melted regolith breccia	SCB1/160
15245		115.5	Fragments of regolith breccia and glass	SCB3/163
15255		240.4	Regolith breccia, glass-coated	SCB5/190

APOLLO 15 ROCK INVENTORY

KEY: F.G.=fine-grained M.G.=medium-grained C.G.=coarse-grained

SAMPLE NUMBER	SAMPLE TYPE	MASS g	DESCRIPTION	SCB/DB
15256		201.0	Shock-melted ol-norm mare basalt (breccia?)	SCB5/190
15257		22.5	Regolith breccia, glass-coated	SCB5/190
15259		0.7	Regolith breccia	SCB5/192
15265		314.1	Regolith breccia	SCB5/193
15266		271.4	Regolith breccia	SCB5/193
15267		1.8	Regolith breccia	SCB5/193
15268		11.0	Regolith breccia	SCB5/192
15269		6.0	Regolith breccia, glass-coated	SCB5/192
15285		264.2	Regolith breccia, glass-coated	SCB5/192
15286		34.6	Glass and regolith breccia	SCB5/192
15287		44.9	Regolith breccia	SCB5/192
15288		70.5	Regolith breccia, glass-coated	SCB5/192
15289		24.1	Regolith breccia	SCB5/192
15295		947.3	Regolith breccia	SCB3/188
15297		34.9	Regolith breccia fragments	SCB3/
15298		1731.0	Regolith breccia, glass-coated	SCB3/
15299		1692.0	Regolith breccia	SCB3/
15306	P	134.2	Regolith breccia	SCB3/173
15307	P	1.3	Hollow glass sphere	SCB3/173
15308	P	1.7	Glassy impact melt(?)	SCB3/173
15315	R	35.6	Regolith breccia	SCB3/172
15316	R	6.1	Regolith breccia	SCB3/172
15317	R	0.6	Regolith breccia	SCB3/172
15318	R	5.4	Regolith breccia	SCB3/172
15319	R	8.0	Regolith breccia	SCB3/172
15320	R	4.7	Regolith breccia	SCB3/172
15321	R	0.3	Regolith breccia	SCB3/172
15322	R	8.4	Regolith breccia	SCB3/172
15323	R	4.4	Regolith breccia	SCB3/172
15324	R	32.3	Regolith breccia	SCB3/172
15325	R	57.8	Regolith breccia, glass-coated	SCB3/172
15326	R	2.5	Regolith breccia	SCB3/172
15327	R	12.4	Clast-rich glassy melt breccia	SCB3/172
15328	R	0.3	Regolith breccia	SCB3/172
15329	R	2.2	Regolith breccia, glass-coated	SCB3/172
15330	R	57.8	Regolith breccia	SCB3/172
15331	R	2.6	Regolith breccia	SCB3/172
15332	R	2.3	Agglutinate	SCB3/172
15333	R	0.3	Regolith breccia(?)	SCB3/172
15334	R	7.5	Regolith breccia	SCB3/172
15335	R	6.0	Regolith breccia	SCB3/172
15336	R	0.2	Regolith breccia(?), glass-coated	SCB3/172
15337	R	4.3	Regolith breccia	SCB3/172
15338	R	11.1	Regolith breccia	SCB3/172
15339	R	0.4	Regolith breccia(?)	SCB3/172
15340	R	0.9	Glass/regolith breccia(?)	SCB3/172
15341	R	1.6	Regolith breccia	SCB3/172
15342	R	7.5	Regolith breccia	SCB3/172

APOLLO 15 ROCK INVENTORY

KEY: F.G.=fine-grained M.G.=medium-grained C.G.=coarse-grained

SAMPLE NUMBER	SAMPLE TYPE	MASS g	DESCRIPTION	SCB/DB
15343	R	6.9	Regolith breccia	SCB3/172
15344	R	7.9	Regolith breccia, glass-coated	SCB3/172
15345	R	12.3	Vesicular glass/breccia clast	SCB3/172
15346	R	3.1	Regolith breccia	SCB3/172
15347	R	3.2	Regolith breccia	SCB3/172
15348	R	0.3	Regolith breccia(?)	SCB3/172
15349	R	2.3	Regolith breccia	SCB3/172
15350		2.9	Regolith breccia	SCB3/172
15351	R	4.2	Regolith breccia	SCB3/172
15352	R	2.9	Regolith breccia, glass-coated	SCB3/172
15353	R	10.6	Regolith breccia	SCB3/172
15354	R	0.3	Regolith breccia(?)	SCB3/172
15355	R	5.2	Regolith breccia	SCB3/172
15356	R	2.0	F.G. impact melt	SCB3/172
15357	R	11.8	F.G. impact melt	SCB3/172
15358	R	14.6	Glassy breccia with KREEP basalt clasts	SCB3/172
15359	R	4.2	F.G. impact melt	SCB3/172
15360	R	9.3	Regolith breccia	SCB3/172
15361	R	0.9	Anorthosite	SCB3/172
15362	R	4.2	Cataclastic anorthosite	SCB3/172
15363	R	0.5	Anorthosite	SCB3/172
15364	R	1.5	Anorthositic (monomict?) breccia	SCB3/172
15365	R	2.9	Indurated green glass clod	SCB3/172
15366	R	3.3	Green glass clod	SCB3/172
15367	R	1.1	Green glass clod	SCB3/172
15368	R	0.4	Green glass clod	SCB3/172
15369	R	2.5	Green glass clod	SCB3/172
15370	R	2.9	Green glass clod	SCB3/172
15371	R	0.5	Green glass clod	SCB3/172
15372	R	0.8	Green glass clod	SCB3/172
15373	R	0.6	Green glass clod	SCB3/172
15374	R	1.0	Green glass clod	SCB3/172
15375	R	0.4	Green glass clod	SCB3/172
15376	R	1.0	Green glass clod	SCB3/172
15377	R	0.5	Green glass clod	SCB3/172
15378	R	3.3	Regolith breccia	SCB3/172
15379	R	64.3	F.G. ol-norm mare basalt	SCB3/172
15380	R	5.2	F.G. ol-norm mare basalt	SCB3/172
15381	R	0.3	F.G. (ol-norm mare?) basalt	SCB3/172
15382	R	3.2	KREEP basalt	SCB3/172
15383	R	1.4	Glass with monomict (basalt) clast assemblage	SCB3/172
15384	R	1.4	M.G. ol-norm mare basalt	SCB3/172
15385	R	8.7	Feldspathic peridotite (mare basalt)	SCB3/172
15386	R	7.5	KREEP basalt	SCB3/172
15387	R	2.0	Feldspathic peridotite (mare basalt)	SCB3/172

APOLLO 15 ROCK INVENTORY

KEY: F.G.=fine-grained M.G.=medium-grained C.G.=coarse-grained

SAMPLE NUMBER	SAMPLE TYPE	MASS g	DESCRIPTION	SCB/DB
15388	R	9.0	Feldspathic microgabbro (mare basalt)	SCB3/172
15389	R	2.8	Agglutinate	SCB3/172
15390	R	3.5	Vesicular glass and breccia	SCB3/172
15391	R	0.3	Glass (with breccia clasts?)	SCB3/172
15392	R	0.4	Glass	SCB3/172
15405		513.1	F.G. impact melt (KREEP)	SCB6/168
15415		269.4	Ferroan anorthosite	SCB3/196
15417		1.3	Regolith breccia	SCB3/194
15418		1141.0	Shocked/melted breccia ("anorthositic gabbro")	SCB3/194
15419		17.7	Regolith breccia, glass-coated	SCB3/194
15425		136.3	Green glass clods	SCB3/195
15426		223.6	Green glass clods	SCB3/195
15427		115.9	Green glass clods	SCB3/195
15435		206.8	Regolith clod	SCB5/170
15436		3.5	F.G. impact melt	SCB5/170
15437		1.0	Ferroan anorthosite	SCB5/170
15445		287.2	F.G. impact melt with pristine clasts	SCB6/171
15455		937.2	F.G. impact melt with pristine clasts	SCB5/198
15459		5854.0	Regolith breccia	SCB6/
15465		376.0	Glass with regolith breccia clasts	SCB5/199
15466		119.2	Glass with regolith breccia clasts	SCB5/199
15467		1.1	Regolith breccia/glass	SCB5/199
15468		1.3	Glassy breccia	SCB5/199
15475		406.8	Porphyritic subophitic qz-norm mare basalt	SCB5/203
15476		266.3	Porphyritic radiate qz-norm mare basalt	SCB5/203
15485		104.9	Vitrophyric qz-norm mare basalt	SCB5/204
15486		46.8	Vitrophyric qz-norm mare basalt	SCB5/204
15495		908.9	Porphyritic radiate qz-norm mare basalt	SCB5/174
15498		2340.0	Regolith breccia, glass-coated	SCB6/
15499		2024.0	Vitrophyric qz-norm mare basalt	SCB5/
15505		1147.0	Regolith breccia, glass-coated	SCB7/255
15506		22.9	Regolith breccia, glass-coated	SCB7/255
15507		3.9	Glass, vesicular ellipsoid	SCB7/255
15508		1.4	Regolith breccia, glass-coated	SCB7/255
15515		144.7	Regolith clods	SCB7/273
15528		4.7	Regolith breccia	SCB2/274
15529		1531.0	M.G. ol-norm(?) mare basalt	SCB2/274
15535		404.4	F.G. ol-norm mare basalt	SCB7/275
15536		317.2	M.G. ol-norm mare basalt	SCB7/275
15537		1.9	M.G. ol-norm mare basalt	SCB7/275

APOLLO 15 ROCK INVENTORY

KEY: F.G.=fine-grained M.G.=medium-grained C.G.=coarse-grained

SAMPLE NUMBER	SAMPLE TYPE	MASS g	DESCRIPTION	SCB/DB
15538		2.6	M.G. ol-norm mare basalt	SCB7/275
15545		746.6	F.G. ol-norm mare basalt	SCB7/278
15546		27.8	C.G. ol-norm mare basalt	SCB7/278
15547		20.1	C.G. ol-norm mare basalt	SCB7/278
15548		3.3	F.G. ol-norm mare basalt	SCB7/278
15555		9614.0	M.G. ol-norm mare basalt	BSLSS
15556		1542.0	F.G. ol-norm mare basalt	SCB2/
15557		2518.0	F.G. ol-norm mare basalt	SCB2/
15558		1333.0	Regolith breccia, glass-coated	SCB2/
15565		822.6	Regolith breccia fragments	SCB2/
15595		237.6	Porphyritic spherulitic qz-norm mare basalt	SCB7/281
15596		224.8	Porphyritic spherulitic qz-norm mare basalt	SCB7/281
15597		145.7	Vitrophyric qz-norm mare basalt	SCB7/281
15598		135.7	F.G. ol-norm mare basalt	SCB7/281
15605	R	6.1	C.G. ol-norm mare basalt	SCB7/283
15606	R	10.1	M.G. ol-norm mare basalt	SCB7/283
15607	R	14.8	F.G. ol-norm mare basalt	SCB7/283
15608	R	1.2	Porphyritic spherulitic qz-norm mare basalt	SCB7/283
15609	R	1.1	F.G. ol-norm mare basalt	SCB7/283
15610	R	1.5	C.G. ol-norm mare basalt	SCB7/283
15612	R	5.9	M.G. ol-norm mare basalt	SCB7/282
15613	R	1.0	M.G. ol-norm mare basalt	SCB7/282
15614	R	9.7	C.G. ol-norm mare basalt	SCB7/282
15615	R	1.7	M.G. ol-norm mare basalt	SCB7/282
15616	R	8.0	M.G. ol-norm mare basalt	SCB7/282
15617	R	3.1	M.G. ol-norm mare basalt(?)	SCB7/282
15618	R	0.8	M.G. ol-norm mare basalt(?)	SCB7/282
15619	R	0.6	M.G. ol-norm mare basalt(?)	SCB7/282
15620	R	6.6	M.G. ol-norm mare basalt	SCB7/282
15621	R	1.6	M.G. ol-norm mare basalt	SCB7/282
15622	R	29.5	M.G. ol-norm mare basalt	SCB7/282
15623	R	3.0	M.G. ol-norm mare basalt	SCB7/282
15624	R	0.2	M.G. ol-norm mare basalt	SCB7/282
15625	R	0.5	M.G. ol-norm mare basalt(?)	SCB7/282
15626	R	0.6	M.G. ol-norm mare basalt	SCB7/282
15627	R	0.4	M.G. ol-norm mare basalt(?)	SCB7/282
15628	R	0.4	M.G. ol-norm mare basalt(?)	SCB7/282
15629	R	0.4	M.G. ol-norm mare basalt(?)	SCB7/282
15630	R	23.2	M.G. ol-norm mare basalt	SCB7/282
15632	R	2.3	M.G. ol-norm mare basalt	SCB7/282
15633	R	7.4	C.G. ol-norm mare basalt	SCB7/282
15634	R	5.2	C.G. ol-norm mare basalt	SCB7/282
15635	R	0.5	M.G. ol-norm mare basalt(?)	SCB7/282
15636	R	336.7	C.G. ol-norm mare basalt	SCB7/282
15637	R	0.9	M.G. ol-norm mare basalt(?)	SCB7/282
15638	R	3.6	M.G. ol-norm mare basalt	SCB7/282

APOLLO 15 ROCK INVENTORY

KEY: F.G.=fine-grained M.G.=medium-grained C.G.=coarse-grained

SAMPLE NUMBER	SAMPLE TYPE	MASS g	DESCRIPTION	SCB/DB
15639	R	7.0	C.G. ol-norm mare basalt	SCB7/282
15640	R	0.5	M.G. ol-norm mare basalt(?)	SCB7/282
15641	R	6.9	M.G. ol-norm mare basalt	SCB7/282
15642	R	1.9	M.G. ol-norm mare basalt(?)	SCB7/282
15643	R	17.9	M.G. ol-norm mare basalt	SCB7/282
15644	R	0.4	M.G. ol-norm mare basalt(?)	SCB7/282
15645	R	0.5	M.G. ol-norm mare basalt(?)	SCB7/282
15647	R	58.2	M.G. ol-norm mare basalt	SCB7/282
15648	R	9.1	Brecciated/melted M.G. ol-norm mare basalt	SCB7/282
15649	R	6.2	F.G. ol-norm mare basalt	SCB7/282
15650	R	3.4	F.G. ol-norm mare basalt(?)	SCB7/282
15651	R	1.6	F.G. ol-norm mare basalt	SCB7/282
15652	R	0.7	F.G. ol-norm mare basalt(?)	SCB7/282
15653	R	0.4	F.G. ol-norm mare basalt(?)	SCB7/282
15654	R	0.2	F.G. ol-norm mare basalt(?)	SCB7/282
15655	R	0.4	F.G. ol-norm mare basalt(?)	SCB7/282
15656	R	0.2	F.G. ol-norm mare basalt(?)	SCB7/282
15658	R	11.6	M.G. ol-norm mare basalt	SCB7/282
15659	R	12.6	M.G. ol-norm mare basalt	SCB7/282
15660	R	8.9	M.G. ol-norm mare basalt(?)	SCB7/282
15661	R	5.9	F.G. ol-norm mare basalt	SCB7/282
15662	R	4.9	M.G. ol-norm mare basalt	SCB7/282
15663	R	10.3	M.G. ol-norm mare basalt	SCB7/282
15664	R	7.4	M.G. ol-norm mare basalt	SCB7/282
15665	R	10.2	F.G. ol-norm mare basalt	SCB7/282
15666	R	3.9	Porphyritic variolitic qz-norm mare basalt	SCB7/282
15667	R	1.1	Porphyritic variolitic qz-norm mare basalt	SCB7/282
15668	R	15.1	F.G. ol-norm mare basalt	SCB7/282
15669	R	4.4	F.G. ol-norm mare basalt	SCB7/282
15670	R	2.0	M.G. ol-norm mare basalt	SCB7/282
15671	R	6.1	M.G. ol-norm mare basalt	SCB7/282
15672	R	21.4	M.G. ol-norm mare basalt	SCB7/282
15673	R	5.9	M.G. ol-norm mare basalt	SCB7/282
15674	R	35.7	F.G. ol-norm mare basalt	SCB7/282
15675	R	34.5	F.G. ol-norm mare basalt	SCB7/282
15676	R	25.3	F.G. ol-norm mare basalt	SCB7/282
15677	R	6.4	F.G. ol-norm basalt	SCB7/282
15678	R	7.5	F.G. ol-norm mare basalt	SCB7/282
15679	R	0.7	F.G. ol-norm mare basalt(?)	SCB7/282
15680	R	0.3	F.G. ol-norm mare basalt(?)	SCB7/282
15681	R	0.3	F.G. ol-norm mare basalt(?)	SCB7/282
15682	R	50.6	Porphyritic spherulitic qz-norm mare basalt	SCB7/282
15683	R	22.0	F.G. ol-norm mare basalt	SCB7/282
15684	R	1.4	Glass containing mare basalt clasts	SCB7/282

APOLLO 15 ROCK INVENTORY

KEY: F.G.=fine-grained M.G.=medium-grained C.G.=coarse-grained

SAMPLE NUMBER	SAMPLE TYPE	MASS g	DESCRIPTION	SCB/DB
15685	R	0.8	Regolith breccia/glass	SCB7/282
15686	R	0.9	Regolith breccia/glass	SCB7/282
15687	R	1.4	Agglutinitic glass	SCB7/282
15688	R	5.3	Agglutinitic glass	SCB7/282
15689	R	2.8	Regolith breccia	SCB7/282
15695	P	10.7	M.G. ol-norm(?) mare basalt	SCB7/283
15696	P	12.8	M.G. ol-norm(?) mare basalt	SCB7/283
15697	P	4.1	F.G. ol-norm(?) mare basalt	SCB7/283
15698	P	3.9	Glass bomb	SCB7/283

PLANIMETRIC SKETCH MAPS OF THE APOLLO 15 SAMPLES SITES
SHOWING LOCATIONS OF ROCK SAMPLES

Individual station maps are modified from U.S.G.S. Interagency Report: Astrogeology 47, "Documentation of Apollo 15 Samples", April 1972.

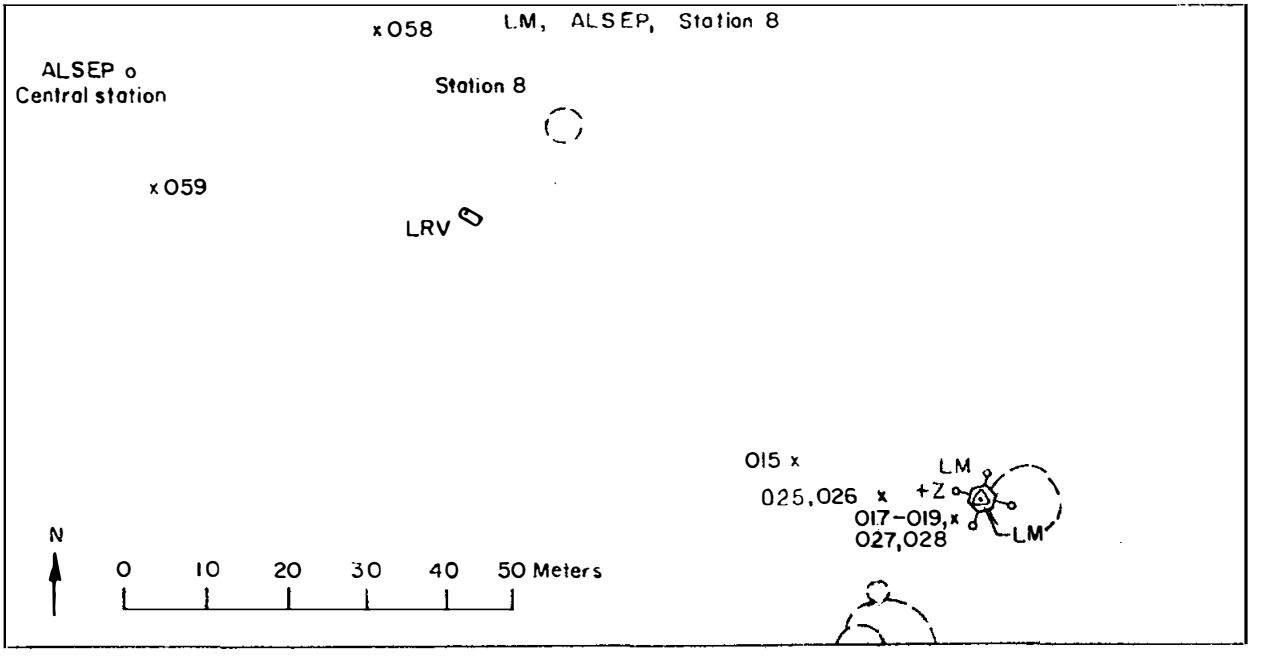

LM, STATION 8, ALSEP ROCK SAMPLES:

15015	15026
15017	15027
15018	15028
15019	15058
15025	15059

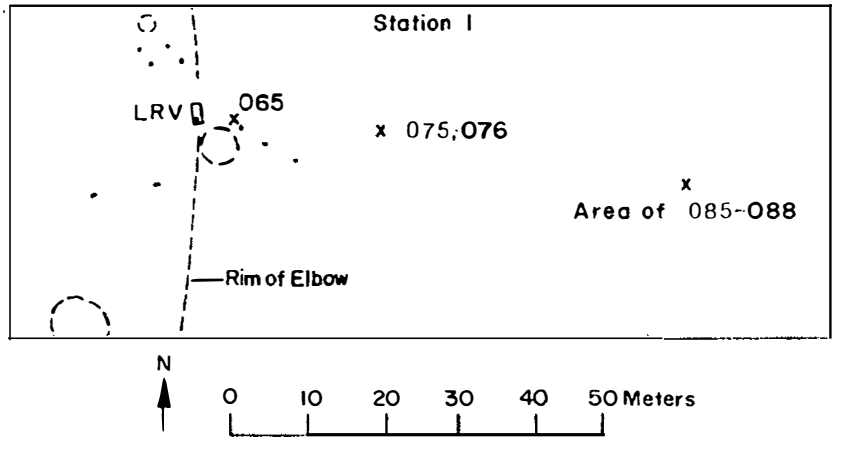

STATION 1

ROCK SAMPLES:

15065
15075
15076
15085
15086
15087
15088

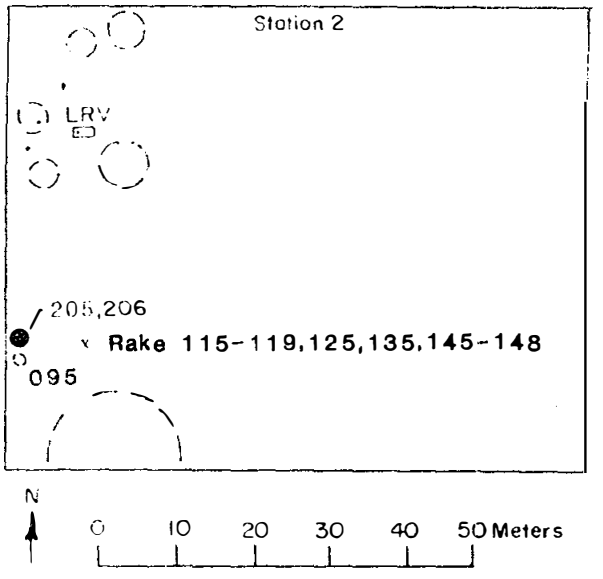

STATION 2 ROCK SAMPLES:

15095
15105
15115
15116
15117
15118
15119
15125
15135
15145
15146
15147
15148
15205
15206

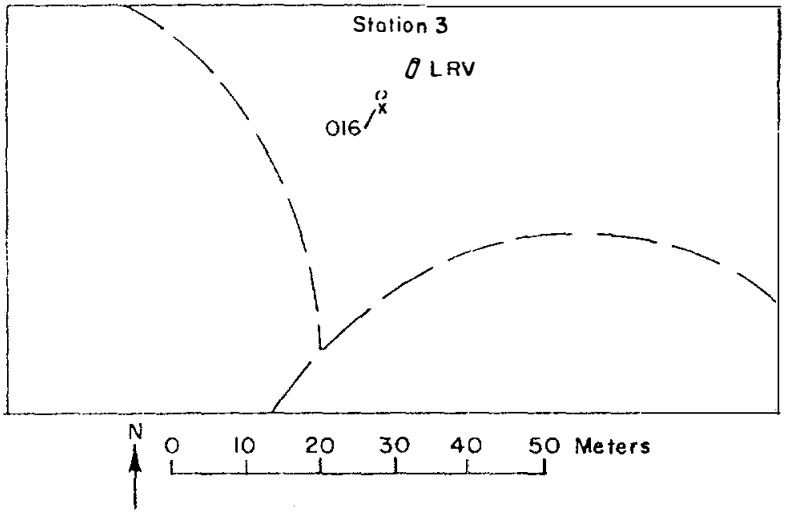

STATION 3 ROCK SAMPLE:

15016

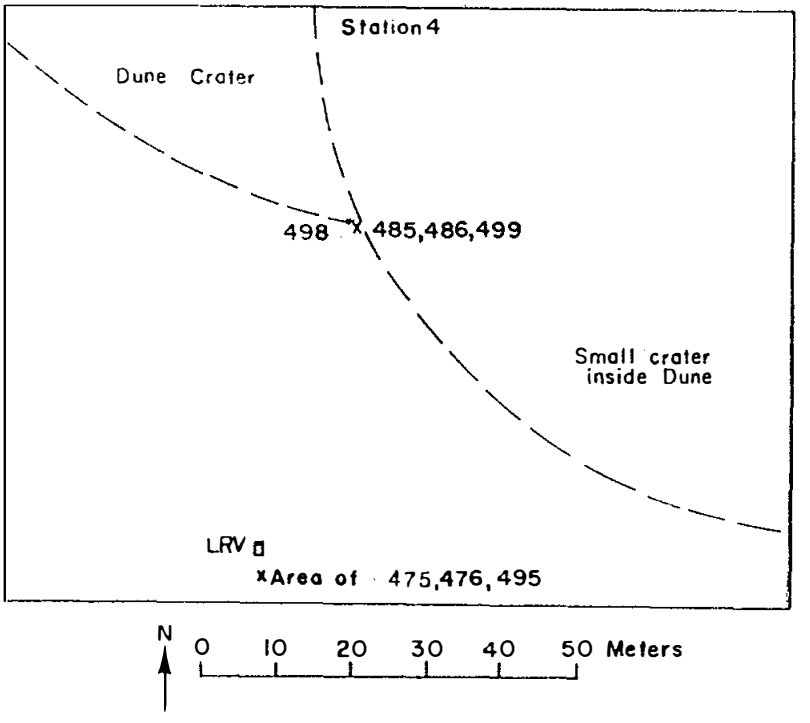

STATION 4 ROCK SAMPLES:

15475
15476
15485
15486
15495
15498
15499

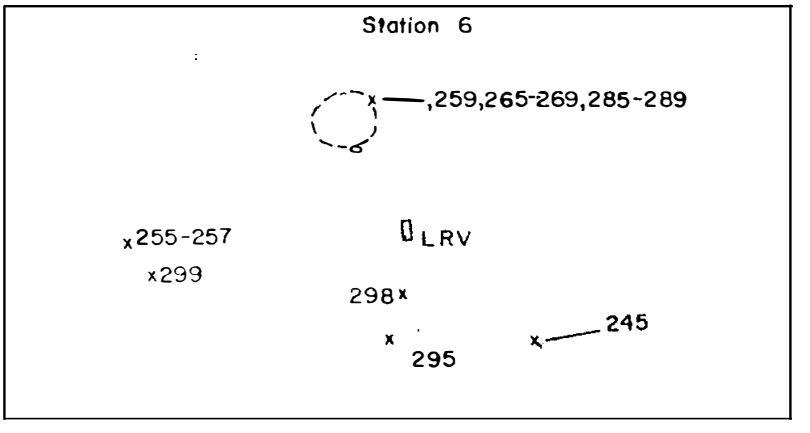

STATION 6 ROCK SAMPLES:

15245	15285
15255	15286
15256	15287
15257	15288
15259	15289
15265	15295
15266	15297*
15267	15298
15268	15299
15269	

*unlocated, fragment residue from collection bag

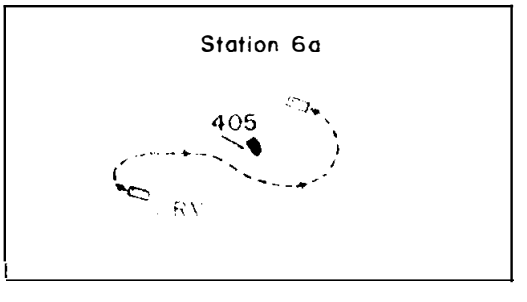

STATION 6A ROCK SAMPLE:

15405

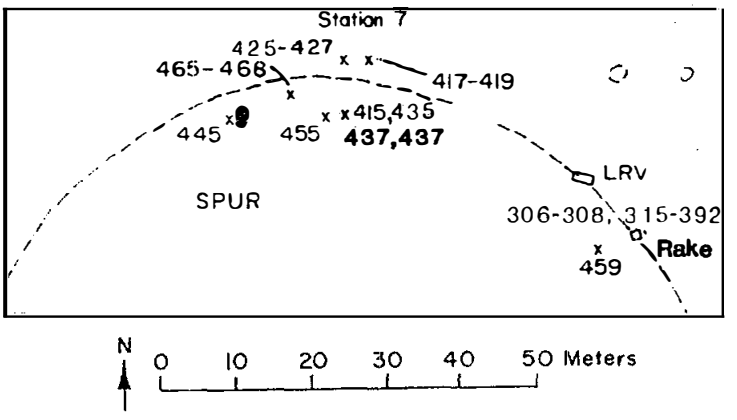

STATION 7 ROCK SAMPLES:

15306	15329	15346	15362	15378	15417
15307	15330	15347	15363	15379	15418
15308	15331	15348	15364	15380	15419
15315	15332	15349	15365	15381	15425
15316	15333	15350	15366	15382	15426
15317	15334	15351	15367	15383	15427
15318	15335	15352	15368	15384	15435
15319	15336	15353	15369	15385	15436
15320	15337	15354	15370	15386	15437
15321	15338	15355	15371	15387	15445
15322	15339	15356	15372	15388	15455
15323	15340	15357	15373	15389	15459
15324	15341	15358	15374	15390	15465
15325	15342	15359	15375	15391	15466
15326	15343	15360	15376	15392	15467
15327	15344	15361	15377	15415	15468
15328	15345				

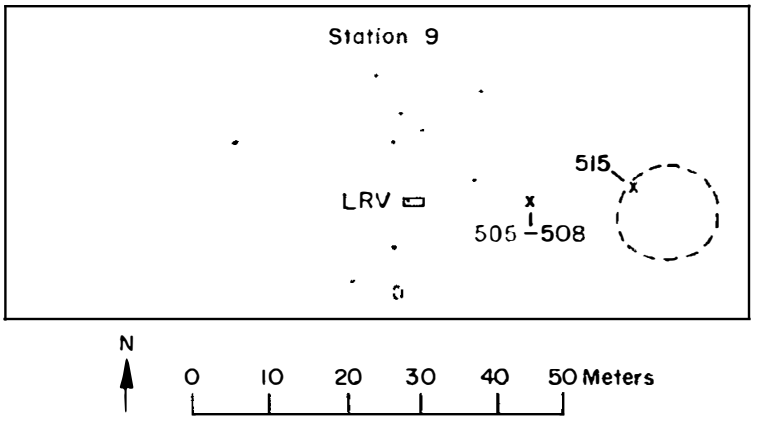

STATION 9 ROCK SAMPLES:

15505
15506
15507
15508
15515
15558*

*Collection site is uncertain. According to Bailey and Ulrich (1975), 15558 was probably collected at station 9.

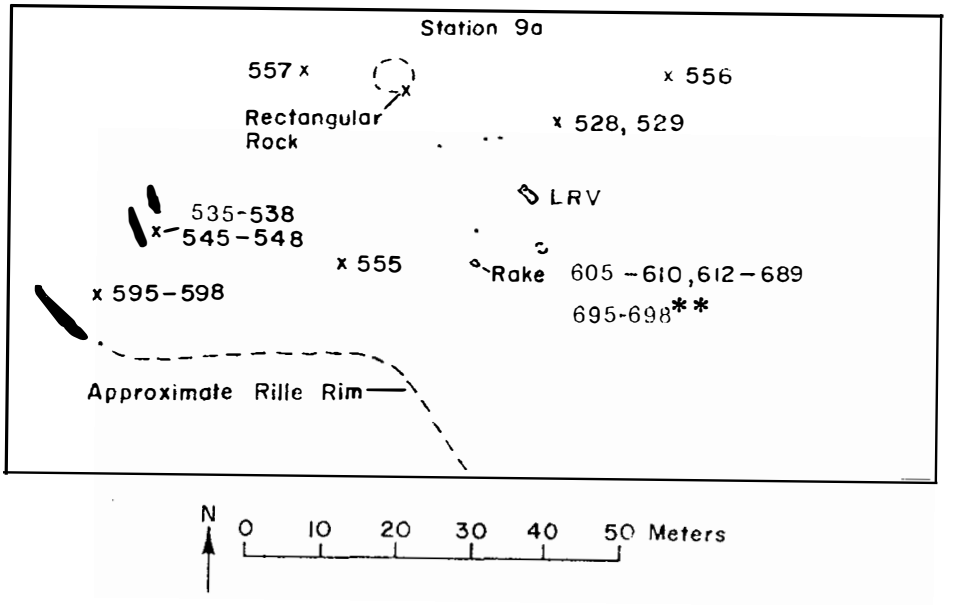

STATION 9A ROCK SAMPLES:

15528	15607	15629	15652	15674
15529	15608	15630	15653	15675
15535	15609	15632	15654	15676
15536	15610	15633	15655	15677
15537	15612	15634	15656	15678
15538	15613	15635	15658	15679
15545	15614	15636	15659	15680
15546	15615	15637	15660	15681
15547	15616	15638	15661	15682
15548	15617	15639	15662	15683
15555	15618	15640	15663	15684
15556	15619	15641	15664	15685
15557	15620	15642	15665	15686
15565*	15621	15643	15666	15687
15595	15622	15644	15667	15688
15596	15623	15645	15668	15689
15597	15624	15647	15669	15695
15598	15625	15648	15670	15696
15605	15626	15649	15671	15697
15606	15627	15650	15672	15698
	15628	15651	15673	

**plucked from rake fines during laboratory processing

*unlocated, fragment residue from collection bag

15015 REGOLITH BRECCIA LM 4770 g

INTRODUCTION: 15015 is a coherent, glassy matrix breccia containing abundant glass balls, shards, and schlieren, most of mare and KREEP basalt derivation. It is largely coated with a glass which is either splashed on or melted from the rock. The breccia has a composition very similar to LM soils.

15015 was collected ~20 m west of the LM +Z footpad, in a flat, smooth area, but its sampling was not documented. Its appearance on the surface was unique. Its lunar orientation has been approximately reconstructed from long-range photography. It is a brownish gray, blocky and angular breccia sample, with a glass surface (Fig. 1). The glass is vesicular, brownish black, and of varied thickness. Zap pits occur on only one side and are small. 15015 was extensively studied by the European Consortium (1974, 1977).

PETROLOGY: The petrology of 15015 has been extensively described by the European Consortium (1974, 1977), with many microprobe analyses, with less extensive studies by Sewell et al. (1974), Gleadow et al. (1974), McKay and Wentworth (1983), Wentworth and McKay (1984), and McKay et al. (1984). The rock is a shock-fused, polymict soil breccia (Fig. 3). The matrix is composed of glass and devitrified glass crowded with tiny mineral fragments. Larger rock, mineral, and glass fragments are set in the matrix. The whole is a low-grade breccia (Warner Grade 2). The rock fragments include basalts of several types (84%) including mare basalts, plagioclase basalts, Fra Mauro basalts; and subsidiary (16%) metaclastic fragments. No distinct banding or segregation is visible. McKay et al. (1983) found it to be compact but with a high fracture porosity, agglutinates to be very rare, spheres to be rare, and shock features to be common. Wentworth and McKay found it to have a bulk density of 2.53 g/cm^3 (intrinsic density 3.15 g/cm^3) and a calculated porosity of 19.7%. McKay et al. (1984) and Korotev (1984 unpublished) reported a very immature I_s/FeO of 3.

Most mineral clasts have shock features, and include coarser-grained varieties than the lithic clasts, indicating another source. Analyses are presented by the European Consortium (1977). Pyroxene varieties are shown in Figure 4a and embrace those of pyroxene in lithic clasts. Some magnesian varieties may represent noritic plutonic rocks. Plagioclases (Fig. 4b) range from An_{97} to An_{80}, and are not in general zoned. Part of the population is more An-rich than any in lithic clasts.

Vitric fragments constitute about 10% of 15015, and include indeterminate plastic forms, twisted and ropey forms, spheres, and broken fragments. Five main chemical categories have been recognized. Fra Mauro basaltic glass is most abundant, with agglutinates, mare-type basaltic glasses, highland basalt glasses, and green glass spheres subordinate. Representative analyses are quoted by the European Consortium and shown in Fig. 4c.

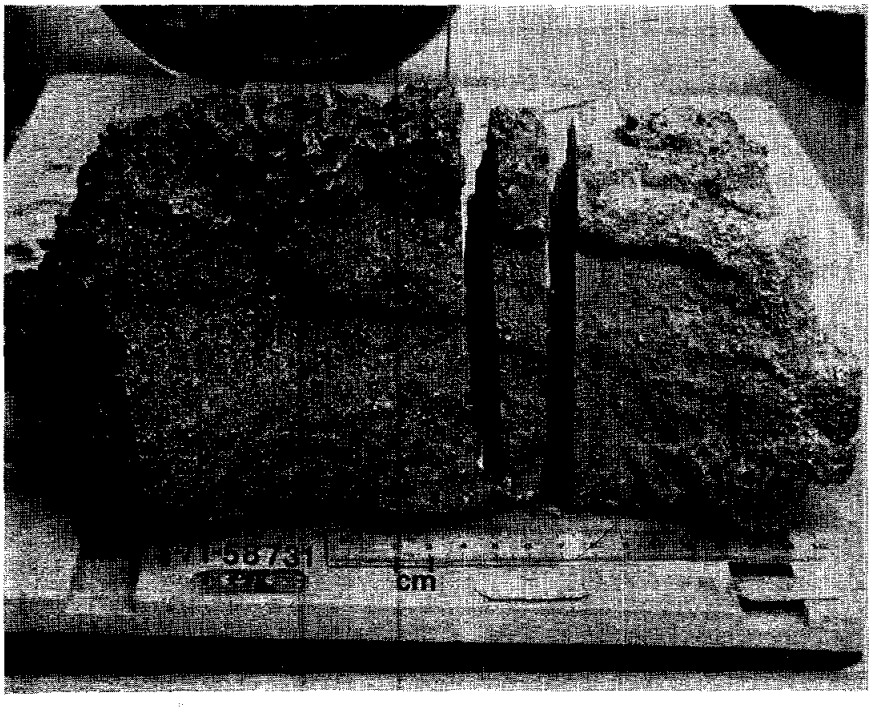

Figure 1. Sawing of 15015, showing vesicular glassy coat.

Figure 2. Pieces from subdivision of slab ,8.

Fig. 3a

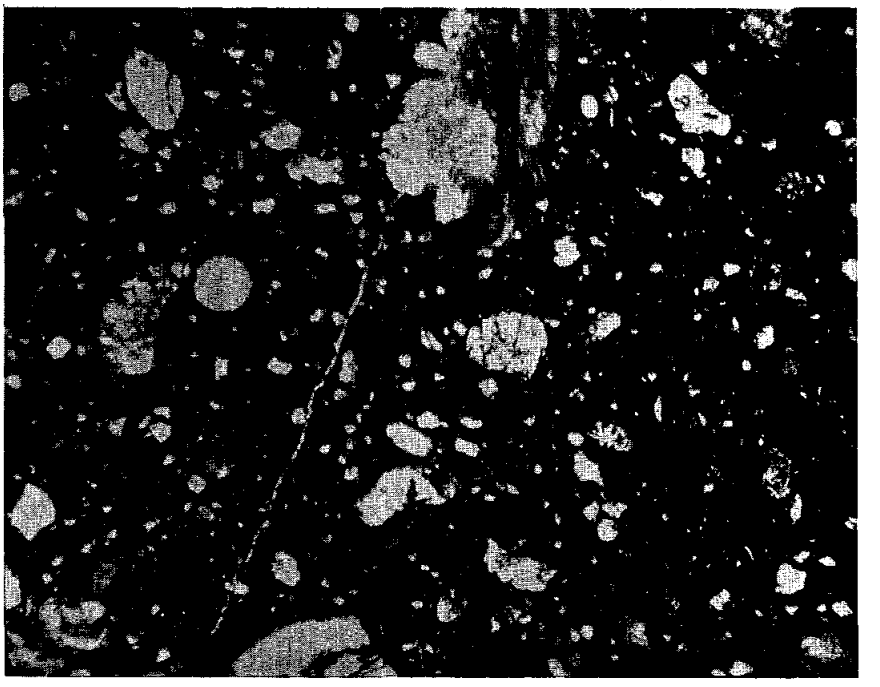

Fig. 3b

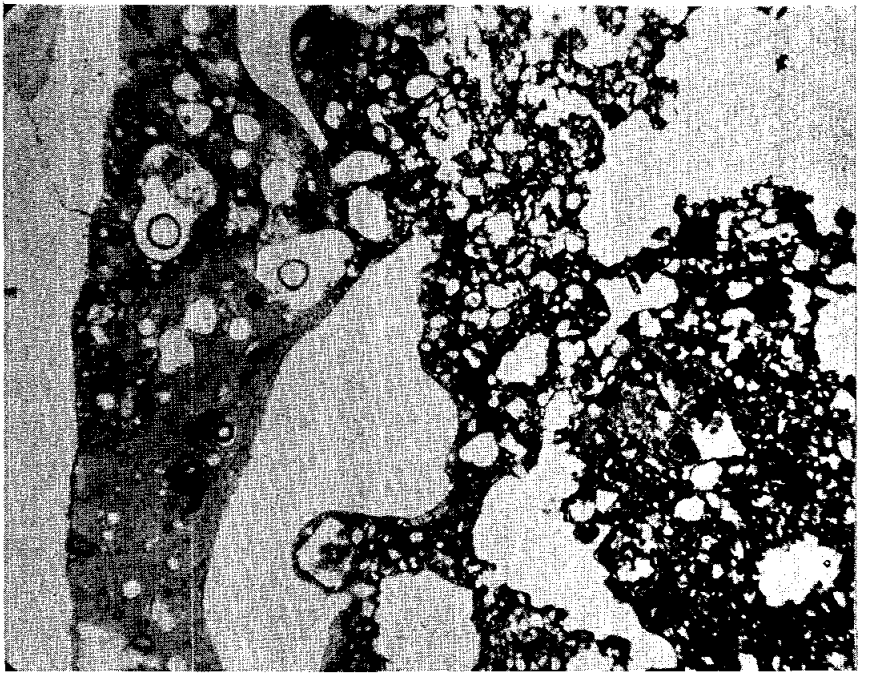

Figure 3. Photomicrographs of 15015. Transmitted light. Widths about 3 mm. a) general matrix; b) matrix (top) and vesicular glass coat.

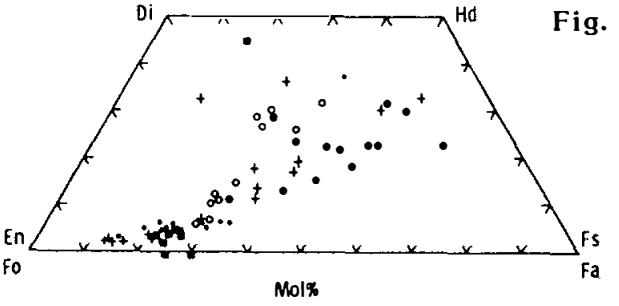

Fig. 4a

- ○ Mare-type basalts
- • Feldspathic basalts
- · Fra Mauro-type basalts
- ● Metamorphic (recrystallized) rocks, probably metaclastic, some Fra Mauro, others ANT suite
- \+ Single-crystal clasts

Fig. 4b

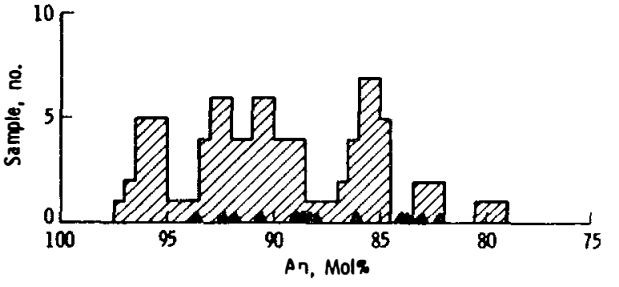

▲ Composition of plagioclase in lithic fragments

15015 histogram of plagioclase compositions in mineral clasts, size 100 to 400 μm.

Fig. 4c

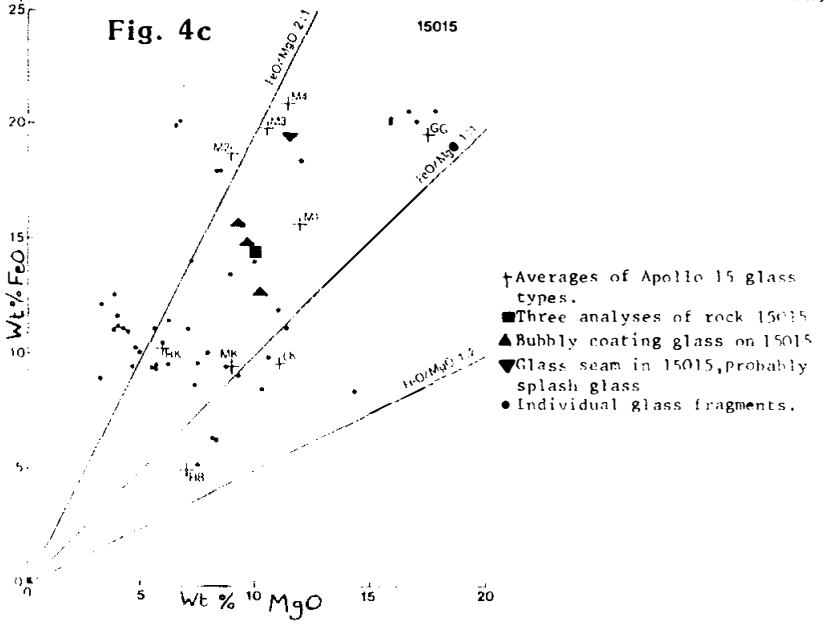

†Averages of Apollo 15 glass types.
■Three analyses of rock 15015
▲Bubbly coating glass on 15015
▼Glass seam in 15015, probably splash glass
● Individual glass fragments.

Figure 4. a) Pyroxene compositions; b) plagioclase compositions; c) FeO vs. MgO for glasses in 15015. (all European Consortium, 1977).

Lithic clasts also constitute about 10%, of which 30% are mare basalts, 33% Fra Mauro basalts, 22% feldspathic basalts, and 15% metaclastic. The mare basalts can be matched texturally with larger samples of mare basalts, but olivine-bearing types are rare. Gleadow et al. (1974) also found mare basalts to be well-represented in 15015. Fra Mauro basalts are the typical, olivine-free, clast-free KREEP basalts which are widely believed to be volcanic (represented by 15386, etc). These were also recognized by Gleadow et al. (1974). Feldspathic basalts have higher An in their plagioclase and typically higher Fe/(Fe + Mg) than the Fra Mauro basalts. The metaclastic samples include feldspathic granulites and porphyroclastic rocks with a fine-grained (5 to 30 micron) matrix.

The glass coat is thick and frothy on the upper surface, thinner and smoother lower down (European Consortium, 1974, 1977). Its polarization properties show it to be smooth and complex. The composition is similar to the composition of the bulk rock (European Consortium, 1977, Table 1-11), and is interpreted by those authors and by Cadenhead and Stetter (1975) as a melt of 15015, not a splash coat. (However, local soils are the same composition, so a splash coat is not precluded.) Wilshire and Moore (1974) noted that the glass does not mask the very angular character of the rock, whose planar surfaces appear to be conjugate fractures formed in previously consolidated breccia. Thin sections of the glass and breccia show a gradual increase in glass and vesiculation outwards over the last few millimeters into the glass coat, without a sharp contact.

Electron microscope examination of micron-sized grains from a bottom chip (European Consortium, 1977) showed that less than 10% of grains were amorphous, but many showed evidence of shock. Almost 30% of the grains contain microcrystallites similar to those in artificially heated lunar dust grains and in mildly metamorphosed Apollo 11 and 14 breccias of Warner Grade 1 and 2.

Carter (1972, 1973) described various surface features on the glass coat from the lower part, as observed with the SEM and analyzed with an energy dispersive system. He found the glass surface to be very frothy and hummocky, with depressions and blisters connected by valleys. He described four types of features: (1) low-velocity impact features, rare (and no high-velocity), (2) out-gassing structures e.g., blisters, (3) metallic mounds, which grew in place and were not splashed on, and (4) whisker structures--metallic iron (?) stalks 0.015 μm diameter with bulbous tips of iron and sulfur mixtures. Morrison et al. (1973) also describe the mounds, but as accretionary objects.

Fabel et al. (1972) tabulated x-ray emission shifts and diagrammed Raman spectra for glass particles with an apparent wide range of composition from mare to anorthositic.

Mehta and Goldstein (1979) conducted TEM and STEM x-ray studies

to determine the composition and structure of submicroscopic metal inclusions in the glass. There are several sub-micron sized metal inclusions distributed throughout, most larger than 0.1 μm. The smallest have cubic symmetry with well-developed crystallographic facets; the larger ones are more spherical. (They note that Morris pers. comm. found that a few pieces of glass contain a substantial amount of metal in the 40-330 Å range.) The metal grains contain modest (1 to 3.8%) Ni, and microdiffraction studies (STEM) show them to be α-Fe. The metal probably precipitated from the melt because of solar-wind induced reduction of Fe^{2+} during impact. The size distribution suggests growth of some metal during slow cooling of the melt or during the time the rock may have been in a hot ejecta blanket. Twins are probably the result of low temperature deformation during shock in a hot debris cloud.

CHEMISTRY: All analyses in Table 1 and Figure 5 are for breccia matrix samples and are consistent with each other. The analysis of the European Consortium is a bulk analysis from dust produced during their sawing operations. These authors and Laul et al. (1972) stated that 15015 is identical in composition with the contingency soil sample 15021 from a nearby location, hence 15015 is probably lithified local soil; this similarity is also evident in elements not analyzed by Laul and Schmitt (1972), e.g., indium (Chou et al. 1974), and lead (Silver 1973). Glass analyses, including the surface glass, from microprobe determinations were given by the European Consortium (1977). They also made x-ray photoelectron spectroscopic studies from two chips showing three kinds of surface: bottom exterior glass face and interior chipped and sawn surfaces.

STABLE ISOTOPES/LIGHT ELEMENTS: Three samples from the top, middle, and bottom of the rock were analyzed for C, N, S and their isotopes (Table 2). C and S abundances are similar to local soils, but N is lower by almost half. All three elements show heavy isotopic depletion relative to the local fines 15012 and 15013: fines average δC^{13} = +11 °/oo, breccia -4.3 °/oo. δS^{34} fines = +8.1 °/oo, breccia +7.1 °/oo. δN^{15} fines = +35.6 °/oo , breccia = +0.9 °/oo. The European Consortium (1977) also studied methane and carbide in the sample.

Leich et al. (1973a,b) studied the depth distribution of hydrogen in two glass samples from the bottom part of 15015, finding a sharp near-surface peak, with very little hydrogen at depths greater than 1000 A. Running the interior side showed little contamination, with a peak 1/5 that of the exposed side. The data are tabulated in Leich et al. (1973a) who noted that they are unlike soil fragment data, and discussed the origin of the hydrogen.

GEOCHRONOLOGY AND RADIOGENIC ISOTOPES: Six samples from ,15 were subjected to ^{40}Ar-^{39}Ar analysis by the European Consortium (1974, 1977): (i) matrix (ii) gray clast (variolitic basalt) (iii) white clast (KREEP basalt), and (iv) (v) (vi) samples of bubbly glass from the upper surface. The release patterns for the two

TABLE 15015-1. Chemical analyses of matrix of 15015

		15	,30	,11	,15,11	,15 2B	,15,2B	,40	
Wt %	SiO2	47.11			47.30		47.50		
	TiO2	1.90	1.5	1.70	1.74	1.04	1.76		
	Al2O3	14.46	14.2		14.16		13.99		
	FeO	14.38	15.2		14.56		14.63		
	MgO	9.93	10		10.09		10.12		
	CaO	10.49	10.2		10.62		10.52		
	Na2O	0.31	0.462	0.49	0.50	0.51	0.50		
	K2O	0.28a	0.25	0.234	0.22	0.248	0.24		
	P2O5	0.22			0.22		0.24		
(ppm)	Sc		27						
	V		130						
	Cr	2700	2800	2685		2755			
	Mn	1500	1400		1700		1650		
	Co		43						
	Ni							236	
	Rb			6.34		6.86			
	Sr			135.4		133.6			
	Y								
	Zr		560[b]	387		445			
	Nb								
	Hf		10.0	11.2		12.9			
	Ba		300	294		319			
	Th		4.5	4.4		4.9			5.04
	U		1.4	1.33		1.42			1.357
	Pb								2.837
	La		30	28.0		29.8			
	Ce		80	72.7		79.1			
	Pr								
	Nd			44.7		48.1			
	Sm		14.2	13.0		13.8			
	Eu		1.6	1.44		2.01			
	Gd			15.2		16.5			
	Tb		2.5						
	Dy		17	17.3		18.6			
	Ho								
	Er			10.2		11.2			
	Tm								
	Yb		9.9	9.30		9.86			
	Lu		1.4	1.34		1.46			
	Li			14.7		15.4			
	Be								
	B								
	C	121							
	N	54							
	S	630							
	F								
	Cl								
	Br								
	Cu								
	Zn							13.1	
(ppb)	I								
	At								
	Ga							4200	
	Ge							378	
	As								
	Se								
	Mo								
	Tc								
	Ru								
	Rh								
	Pd								
	Ag								
	Cd							40	
	In							3.0	
	Sn								
	Sb								
	Te								
	Cs								
	Ta		1400						
	W								
	Re								
	Os								
	Ir							7.3	
	Pt								
	Au							3.1	
	Hg								
	Tl								
	Bi								
		(1)	(2)	(3)	(1)	(3)	(1)	(4)	(5)

References for TABLE 15015-1.

References and method
(1) European Consortium (1974, 1977); ,15,wet chemical (Scoon); ,15 2B and ,15,11, XRF (Rhodes).
(2) Laul and Schmitt (1973) INNA.
(3) Wiesmann and Hubbard (1975) IDMS. Partially reported in Church et al. (1972) and Nyquist et al. (1973).
(4) Chou et al. (1974) RNAA (averages of 3 replicates).
(5) Silver (1973) IDMS.

Notes:
(a) reported as I.28 (not 1.28) in the 1974 publication.
(b) large uncertainty of +120 ppm.
(c) see also Table 15015-2.

15015

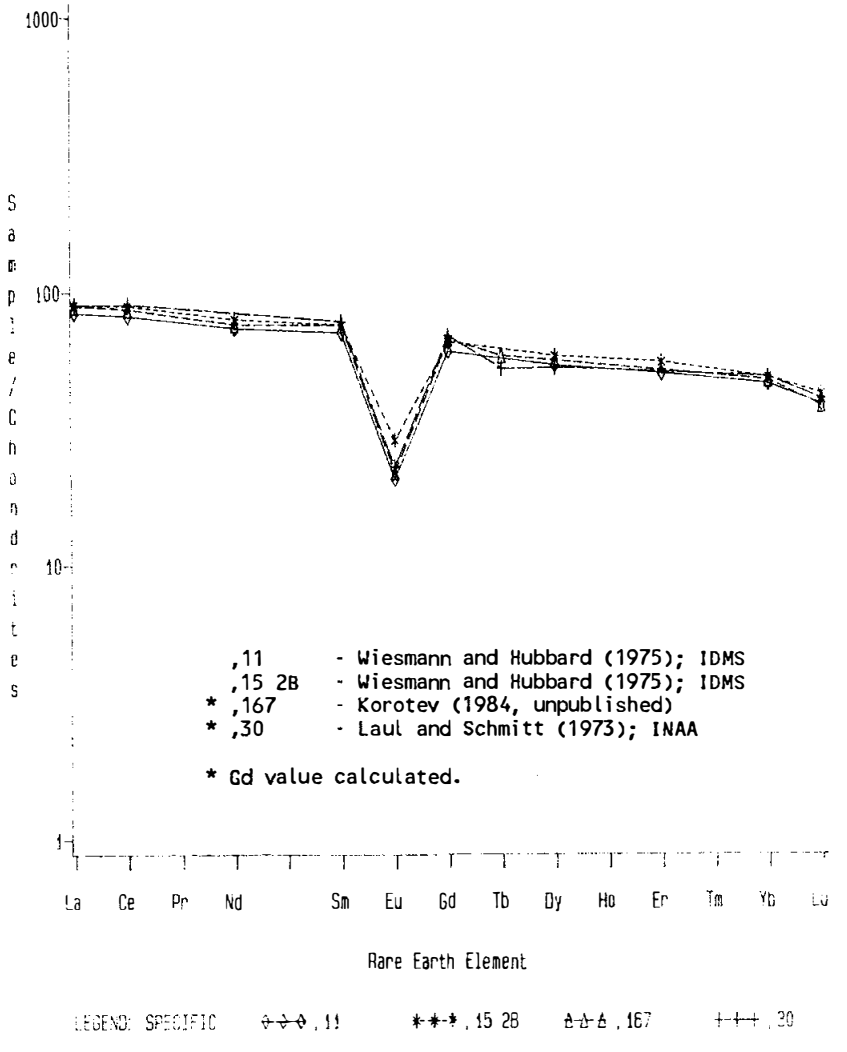

Figure 5. Rare earth elements for matrix analyses of 15015.

TABLE 15015-2. Carbon, sulfur, and nitrogen in 15015, obtained by combustion in partial oxygen atmosphere (European Consortium, 1977)

Sample no.	Location in consortium slab	Weight, g	C, ppm	δC^{13} PDB (a)	S, ppm	δS^{34} C.D. (b)	N, ppm	δN^{15} air	He, ppm
15015,15,17	Top	0.5568	131	[c] -2.8	673	7.4	42	-1.5	[d] <1
15015,15,7	Middle	.6393	121	-4.5	586	7.6	61	3.2	<1
15015,15,3	Bottom	.4607	110	-5.5	628	6.3	59	(e)	<1
Average		--	121	-4.3	630	7.1	54	.9	

[a] PDB = Pee Dee belemnite.

[b] C.D. = Canyon Diablo.

[c] CO_2 repurified.

[d] Below detection limit.

[e] Impure.

clasts are shown in Figure 6, and show the effects of extreme (75% or more) radiogenic argon loss. The high temperature release for the Fra Mauro (KREEP) basalt indicate that the parent crystallized 3.7 ± 0.1 b.y. or earlier. The variolitic basalt crystallized at 3.4 ± 0.2 b.y. or earlier; it is apparently not considered to be a mare basalt. The presence of mare basalt clasts however requires formation of the breccia less than 3.3 b.y. ago. The isochron ages of two of the glass samples, about 1.0 b.y., may represent the formation time of the glass, and possibly the time of lithification.

Nyquist et al. (1973) determined Rb and Sr isotopic ratios for two breccia matrix samples, which show old model ages (Table 3).

Silver (1973) presented Pb isotopic data showing characteristics similar to other breccias and soils.

EXPOSURE AGES, TRACKS, AND MICROCRATERS: The European Consortium (1974, 1977) found different exposure ages for different clasts using the Ar method. The Fra Mauro basalt gave 490 m.y., the variolitic basalt 1290 m.y.; both samples had experienced 25% cosmogenic argon loss. ^{21}Ne on both matrix and the Fra Mauro clasts gave 250-310 m.y. exposure, and presumably there has been ^{21}Ne loss. ^{3}He gave an exposure age of less than 100 m.y. The overall conclusion is that 15015 formed from well-mixed local soil with components of varied exposure age and maturity, not before 2.7 ± 0.2 b.y., and probably 1.2 b.y. It was then buried at more than 2 meters depth until ejection ~30 m.y. ago. An extensive discussion of the noble gas data is given in the European Consortium (1977).

The European Consortium (1977) used high voltage and scanning electron microscopy to study radiation damage and textural features. Because bubbles are superimposed on the track distribution, no track density gradient from the exterior can be identified. The very heavy exposure of the glass coating is less than 10^7 years. Feldspar grains have track densities of 10^7 to 4 x 10^9 tracks 1 cm^2, pyroxenes from 10^6 to about 4 x 108 tracks/cm^2. These "intermediate" characteristics suggest that the breccia formed from a mixture of mature and immature soil or that a nonthermal process has been responsible for track metamorphism.

Schneider et al. (1972, 1973) and Storzer et al. (1973) deduced an exposure age of 13 yrs (actually 4<age<40 yrs) from track density/depth relationships (Fig. 7); a recalibration revised this age to 40 yrs (Fechtig et al. 1974). The sample used was a glass chip from the bottom side, free of microcraters. Morrison et al. (1973) studied crater densities (Fig. 8) and have a best guess exposure age of 0.01-0.02 m.y., a large extrapolation from their calibrated range but 15015 clearly shows a shorter exposure history than most other rocks. Essentially the surface is young and uneroded. The sample used was from the top surface, and counts are erratic from area to area. Mandeville (1975) also studied microcraters (SEM), finding 35 definite craters with

Fig. 6a

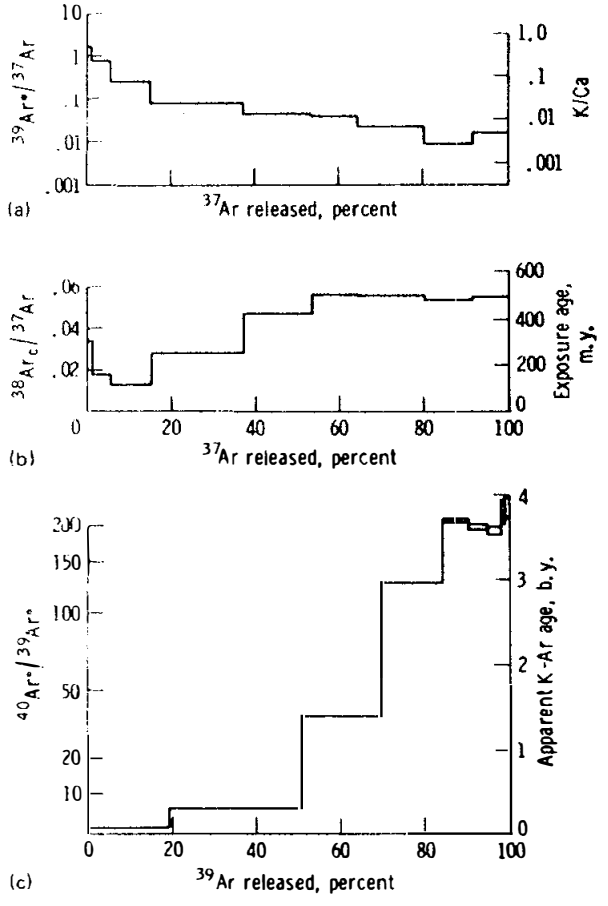

Argon isotope release pattern for Fra Mauro basalt-type fragment 23b, indicating a 75-percent loss of radiogenic ^{40}Ar and a 20-percent loss of cosmogenic $^{38}Ar_c$. The high-temperature $^{40}Ar/^{39}Ar$ age attains a value of 3.7 ± 0.1 b.y. despite the extreme loss and is comparable to, but slightly lower than, more precise ages of other Fra Mauro basalts. A well-defined cosmic ray exposure age of 490 m.y. is determined.

Fig. 6b

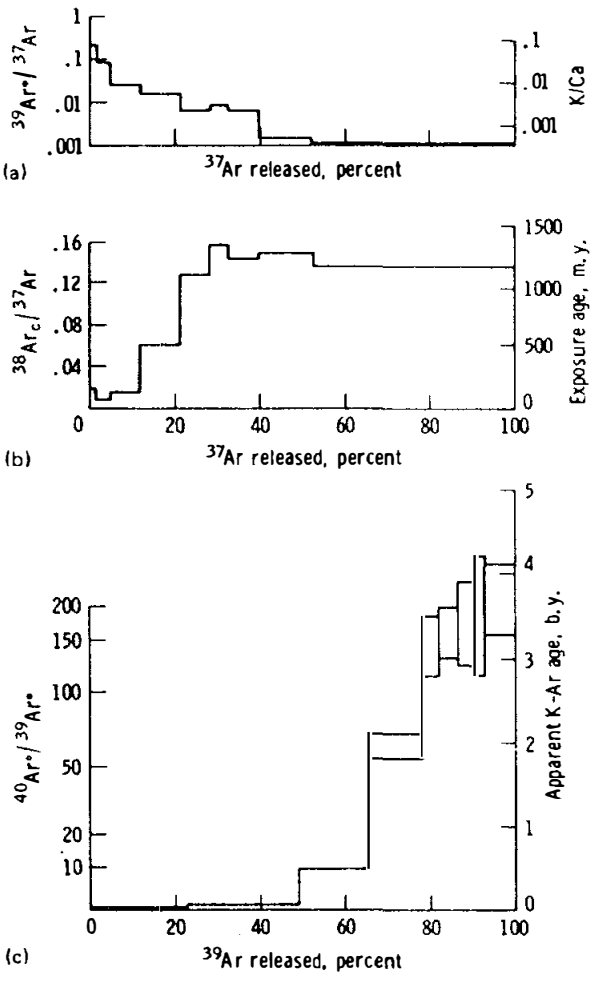

Argon isotope release pattern for variolitic basalt fragment 5b, indicating ^{40}Ar and $^{38}Ar_c$ loss similar to that of fragment 23b. The high-temperature $^{40}Ar/^{39}Ar$ age is imprecise, 3.4 ± 0.2 b.y. The cosmic ray exposure age is well defined and extremely high, 1290 m.y., indicating that 5b received extensive cosmic ray irradiation for at least 800 m.y. after crystallization and before incorporation in the part of the regolith that was later to be lithified to form 15015.

Figure 6. Argon release patterns from (a) Fra Mauro basalt-type fragment 23b and (b) variolitic basalt fragment 5b.

TABLE 15015-3. Rb-Sr Whole Rock Isotopic Data (Nyquist et al., 1973)

	$^{87}Rb/^{86}Sr$	$^{87}Sr/^{86}Rb$	T_{BABI}	T_{LUNI}
,11	0.1355±11	0.70785±7	4.50±0.07	4.55±0.07
,15 2B	0.1486±16	0.70885±8	4.57±0.09	4.62±0.09

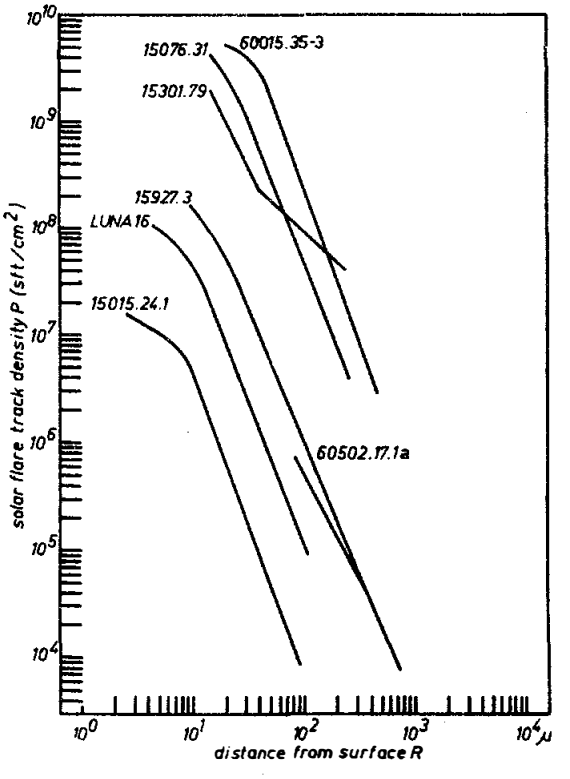

Figure 7. Track density vs. depth for a bottom glass sample (Storzer et al., 1973).

Figure 8. Microcrater density data for a top glass sample (Morrison et al., 1973).

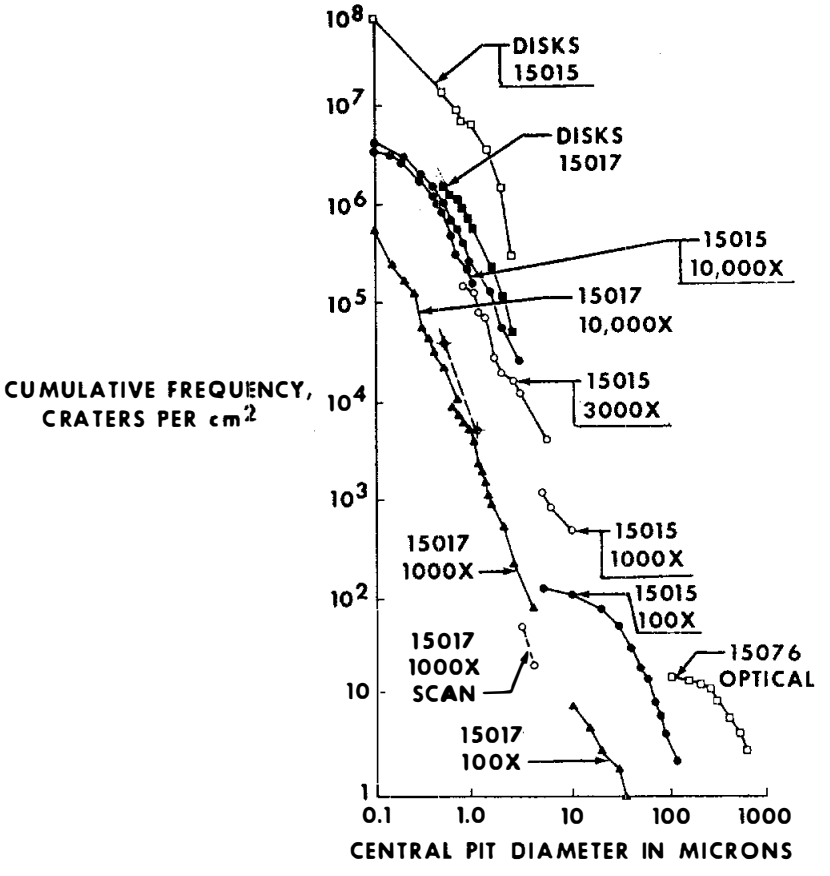

Cumulative frequency distributions for category 4 rocks and accretionary objects on 15017 and 15015. Numbers refer to magnifications of SEM mosaics. 15076 SEM points from Schneider *et al.* (1972) shown as crossed circles. Open circles for diameters between 1 and 10 microns represent visual scans at 1000×.

TABLE 15015-4. P-Wave Velocities (Todd et al. 1972)

bars	1	100	250	500	750	1000	1500	2000	3000	4000	5000
Pwave km/sec	3.50	3.68	3.90	4.13	4.27	4.38	4.49	4.54	4.64	4.74	4.85

diameters from 5 to 120 microns, and found the low solar flare track density and the microcrater density consistent with an exposure age of ~3,000 yrs.

PHYSICAL PROPERTIES: Todd et al. (1972) measured P-wave velocities for a breccia matrix (2x1x1 cm) sample at room temperature, up to 5 kb confining pressure (Table 4). The determination of S-wave velocity was not possible because of the poor coherence of the sample.

Baldridge et al. (1972) measured the thermal expansion of 15015 over the temperature range -1000°C to +25 C (Fig. 9). Cadenhead and Stetter (1975) measured a density of 3.0 ± 0.1 gm cm^{-3} for a glass sample.

Greenman and Gross (1972) diagrammed luminescence data for visible wavelength luminescence from soft x-rays, and possible ultraviolet luminescence from the same source, for bottom glass, adjacent matrix, and a top glass sample. Dollfus and Geake (1975) measured polarimetric and photometric characteristics of reflected light (5800 to 3520 A).

Cadenhead and Stetter (1974) studied water sorption on a cindery glass sample at 15-20°C following outgassing at 25° to 320°C, as part of an attempt to study the general characteristics of water sorption on lunar sample surfaces.

The European Consortium (1977) measured the geometric albedo and polarization properties of a dark, glassy piece from the top surface.

PROCESSING AND SUBDIVISIONS: A slab was cut through the center of the breccia (Figs. 2, 10) and most allocations made from it. A piece of this slab, 15, was allocated to the European Consortium. All the thin sections (,132-,143) were made serially from ,14, except two made of the glass exterior from a small piece from ,7. ,0 is 2870 g. ,7 had four large pieces (100-200 gm) removed for PAO exhibits and the remainder of it, 808 g, was placed in remote storage.

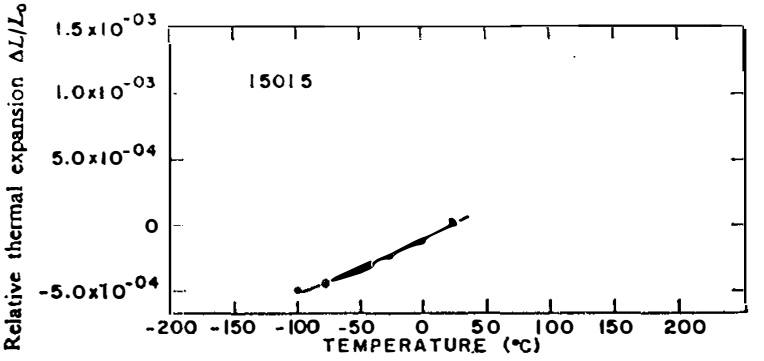

Figure 9. Thermal expansion of 15015 (Baldridge et al., 1972).

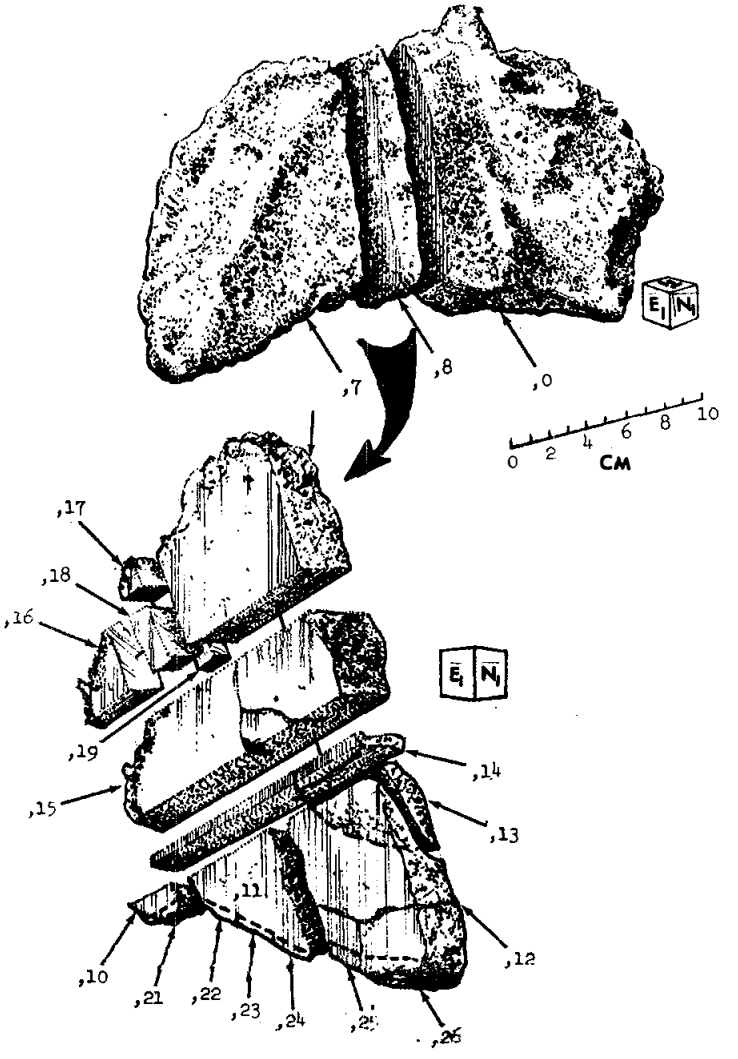

Figure 10. Main subdivisions of 15015 from sawing of a slab.

15016 MEDIUM-GRAINED OLIVINE-NORMATIVE MARE BASALT ST. 3 923.7 g

INTRODUCTION: 15016 is a medium-grained, very vesicular (Fig. 1) olivine-normative basalt. It crystallized about 3.4 or 3.3 b.y. ago.

15016 is the only sample collected at Station 3, an unscheduled stop on a mature mare surface. The area has abundant, subdued 10 cm-to 1 m-diameter craters. The sample appeared to be representative in shape, burial, and filleting of the other nearby large fragments; an adjacent rock of similar size was also vesicular. 15016 is light brownish gray, blocky and sub-rounded, and tough. Its lunar orientation is known and it was embedded in soil only at one end. It apparently has no zap pits, despite its long exposure age (~300 m.y., below).

PETROLOGY: 15016 is a porphyritic olivine-normative basalt (Fig. 2) with yellow-green olivine and light brown pyroxene phenocrysts. Its most conspicuous character is its vesicularity, like 15556 and 15529, and is the reason the sample was noticed and collected. The sample has been described by Brown et al. (1972a), Papike et al. (1972), Bence and Papike (1972), and Kushiro (1972, 1973). Brown et al. (1972) quote 45% vesicles. Like other olivine-nomative basalts, the sample contains ~70% mafic minerals. Some x-ray diffraction data is reported by Papike et al. (1972), and microprobe data for pyroxenes by Bence and Papike (1972) and Kushiro (1972, 1973).

The sample differs from the isochemical basalt 15555 in its texture: it has lathy, not poikilitic feldspars, and cooled faster. The groundmass is subophitic to intersertal. The olivine phenocrysts are zoned, with a total range of Fo_{72-7} (Kushiro 1972). Compared with 15555, the pyroxene compositions are truncated at both ends (Bence and Papike, 1972) (Fig. 3), leading Brown et al. (1972) to state that there are no detectable pigeonites. However, all other authors refer to the low-Ca pyroxene phase as pigeonite. The pyroxenes, the second crystallizing phase, are complexly zoned, with pigeonitic cores and with the transition to augitic rims barely discernable. A sharp reversal to low-Ca augites, correlated with increasing Ti/Al, corresponds with the onset of plagioclase crystallization (Bence and Papike, 1972; Kushiro, 1972, 1973). Plagioclases are zoned from $An_{94-80.7}$ (Kushiro, 1972). Other phases include chromite, Cr-ulvospinel, cristobalite, ilmenite, and traces of FeNi metal. The vesicles have ilmenite plates lined around them. Engelhardt (1979) tabulates ilmenite paragenesis.

EXPERIMENTAL PETROLOGY: Low pressure crystallization experiments were conducted by Humphries et al. (1972) with fO_2 buffered at Fe^o/FeO equilibrium. The sample has a high temperature olivine + spinel liquidus (Fig. 4a), with pigeonite crystallizing at 1170°C, and plagioclase at ~1150°C. Humphries et al. (1972) prefer a (minority) interpretation that 15016 is a mafic accumulation from a liquid multiply saturated with olivine,

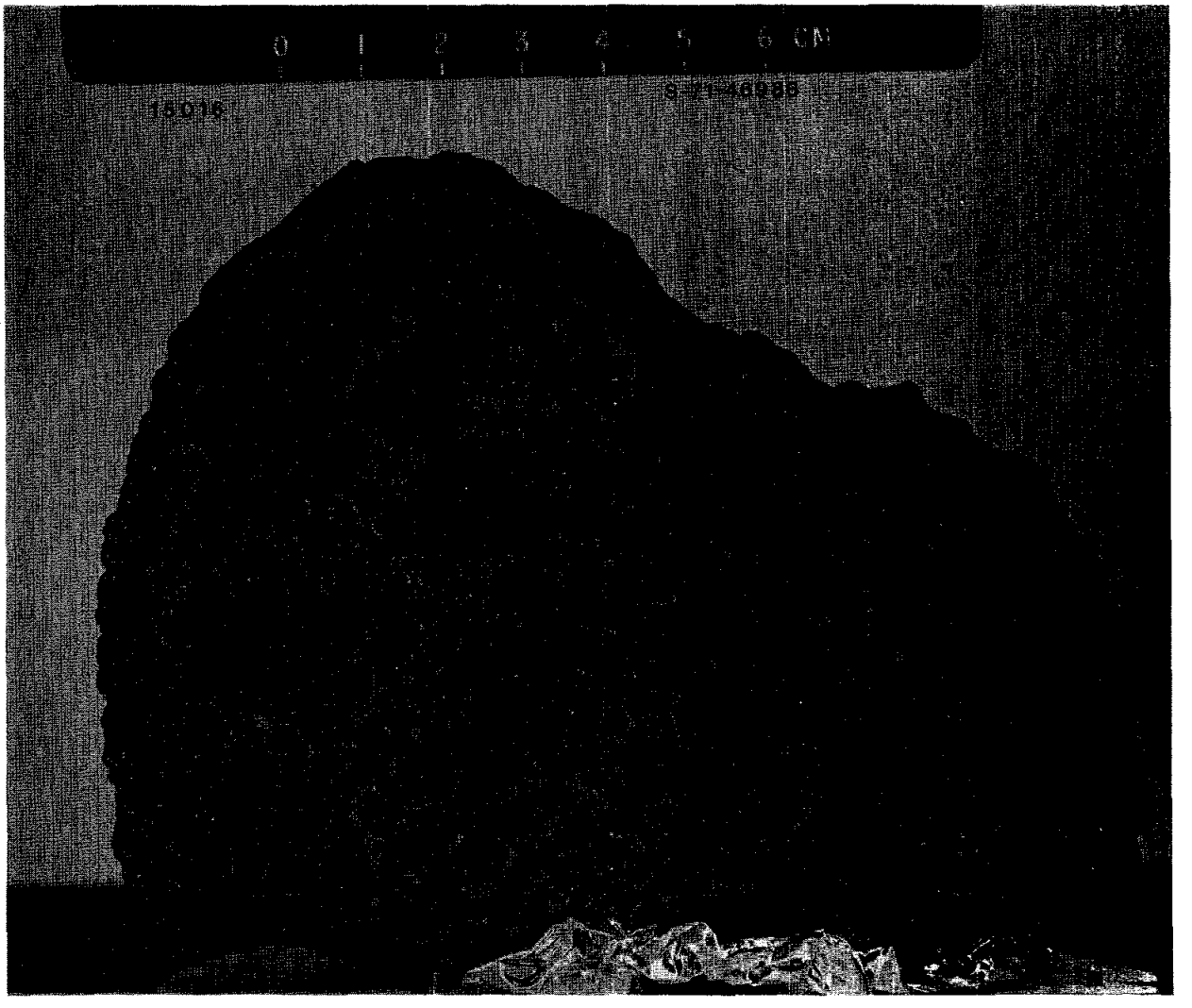

Figure 1: Macroscopic view, pre-splitting, showing vesicularity.

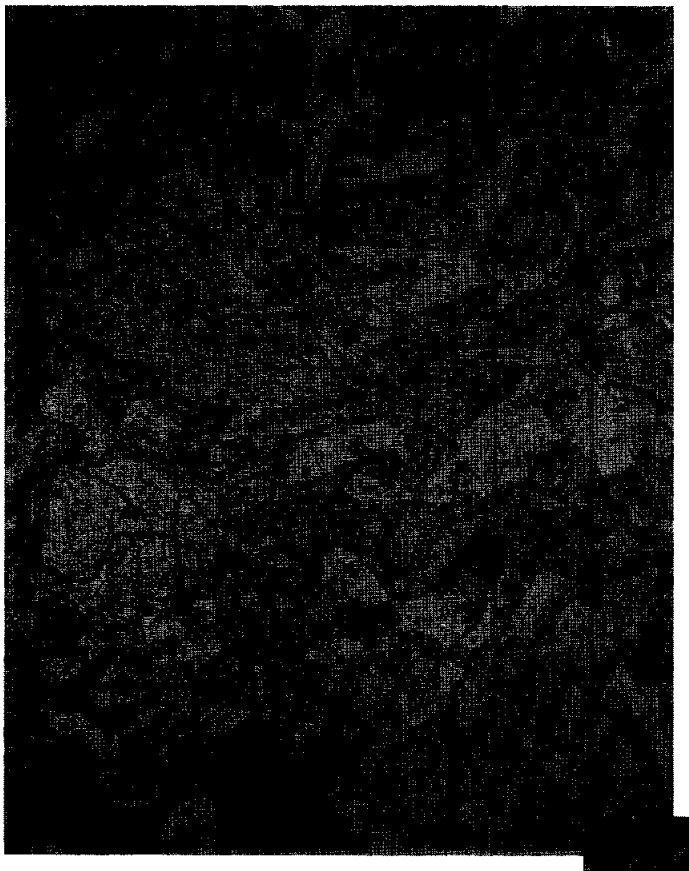

Fig. 2a

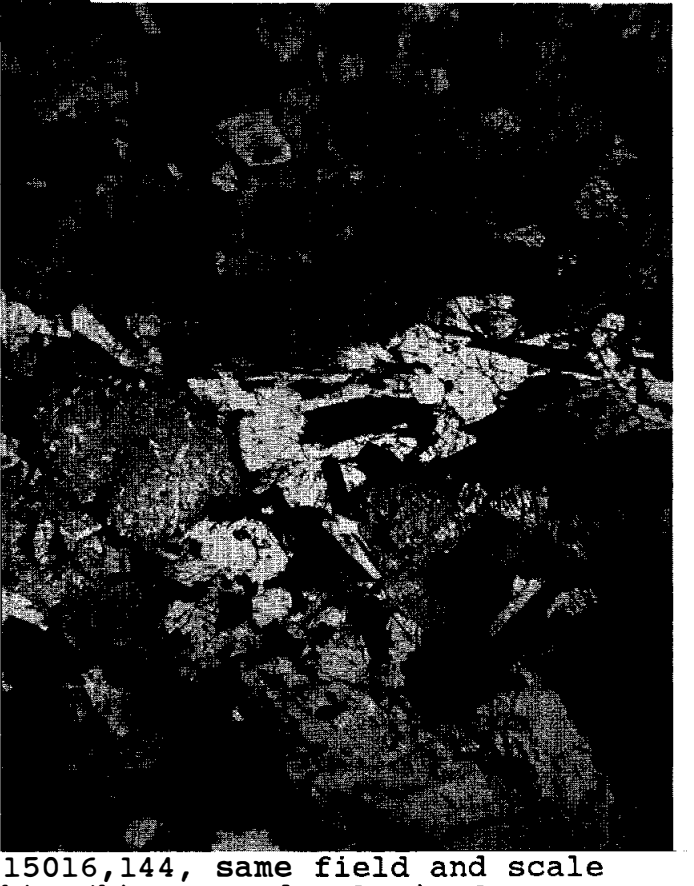

Fig. 2b

Figure 2: Photomicrograph of 15016,144, same field and scale (a) transmitted light; (b) crossed polorized.

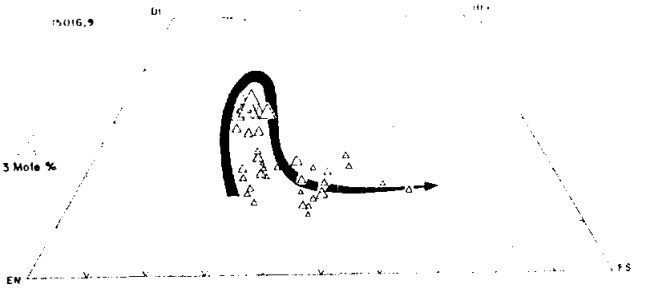

Fig. 3a

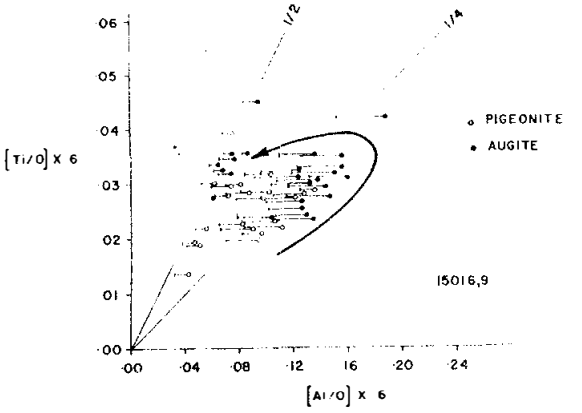

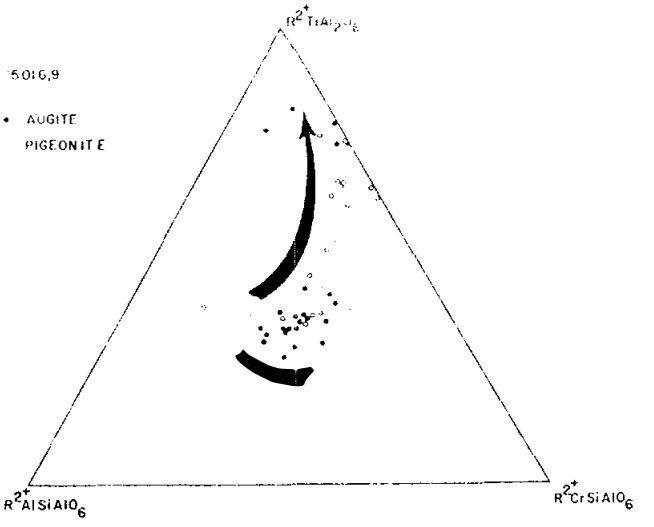

Figure 3: Pyroxene compositional data (a) Bence and Papike (1972); (b) Kushiro (1973).

Fig. 3b

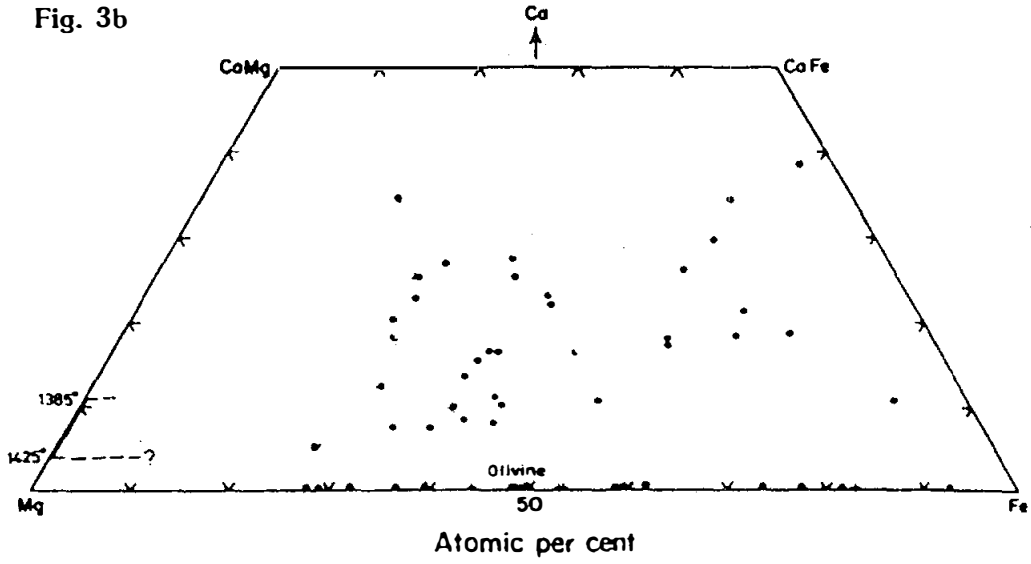

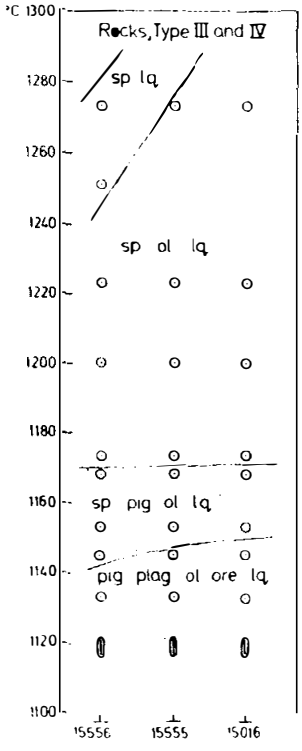

Fig. 4a

Fig. 4b

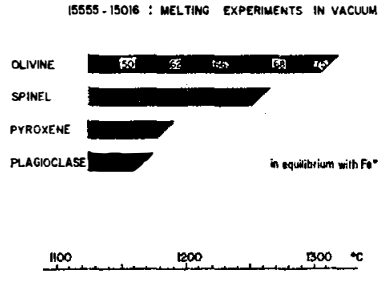

Equilibrium crystallization sequence for 15555–15016 in vacuum. Numbers in olivine field refer to mol % Fo.

Figure 4: Low pressure experimental data (a) Humphries et al. (1972); (b) Kesson (1977).

pigeonite, and plagioclase. Kesson (1975, 1977) also conducted low-pressure crystallization experiments (Fig. 4b), on a synthetic 15016-15555 composition, providing mineral compositional data and residual liquid compositions. Later crystallization of spinel in her experiments than in those of Humphries et al. (1972) is attributed by Kesson (1975, 1977) to the "unreasonably high fO_2" of the Humphries et al. (1972) experiments. O'Hara and Humphries (1972) in discussing the effects of Fe-loss on experimental results, claim that Kesson's (1975) experiments were not immune from chemical changes.

High pressure experiments were conducted by Kushiro (1972) and Hodges and Kushiro (1973) in the range 4 to 16 kb (Fig. 5a), and by Kesson (1975, 1977) (Fig. 5b). Kushiro's (1972) experiments were at wustite stability, and have olivine as a liquidus or near-liquidus phase above 15 kb. Plagioclase exists only below 10 kb, and never on the liquidus. Mineral compositional data for some runs is given by Kushiro (1972). Kesson (1975, 1976) obtained rather similar results--olivine the liquidus phase to 12 kb--but spinel always 50°C below the liquidus, again resulting from the lower fO_2 used. A multiple saturation point exists at ~12 kb, 1350°C; assuming some olivine fractionation during ascent, a minimum depth of 240 km to an olivine-pyroxene source is required.

CHEMISTRY: Chemical analyses are listed in Table 1 and rare-earths are shown in Figure 6. In general the data has not been discussed specifically, only in terms of relationships with other olivine-normative basalts by olivine control. The sample is one of the more magnesian members of the group. The sample analyzed by S.R. Taylor et al. (1973) is considerably less mafic in major element composition than other analyses, but the trace elements are similar to those of other analyses. Chappel et al. (1973) suggest that the high Cr abundance is a result of spinel accumulation in 15016.

Data by Ehmann et al. (1972) and Rhodes (1972) is included only in averages of basalts and not presented until later publications. Christian et al. (1972) and Cuttitta et al. (1973) analyzed for Fe^{3+}, finding none, and tabulated "excess reducing capacity". Janghorbani et al. (1973) analyzed for oxygen. Gibson et al. (1975) analyzed for CO, CO_2, H_2, H_2S, AND Fe°.

Barker (1974) made a study aimed at determining the composition of the gas which formed the vesicles, from analysis of gases trapped in glass inclusions released by heating. He concluded that the original gas contained 46% O, 42% C, and 12% H, and became more H_2O-rich as crystallization proceeded (similar to results from 15065). The gases released at 1200°C to 1300°C provide the best estimates of the gas composition. A peak in CO2 at 490°C is interpreted to result from the breakdown of ~5 ppm siderite which is not a product of sample handling.

Goldberg et al. (1976) analyzed F on vesicle walls and in

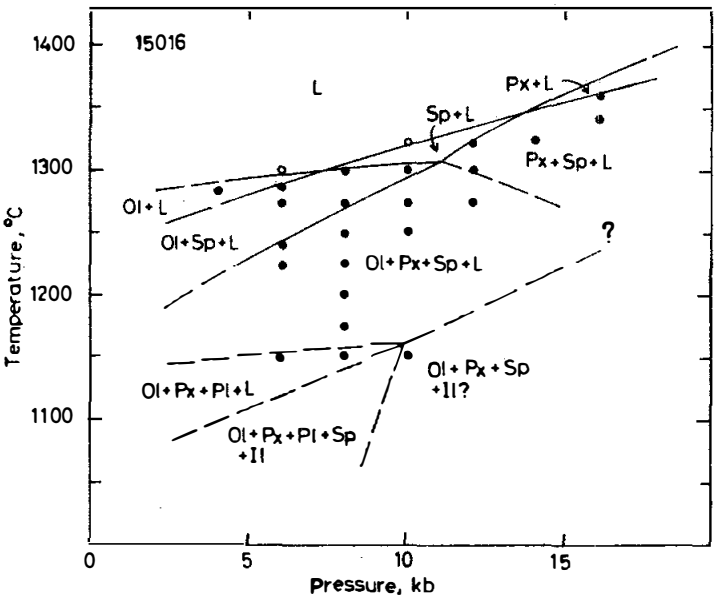

Fig. 5a

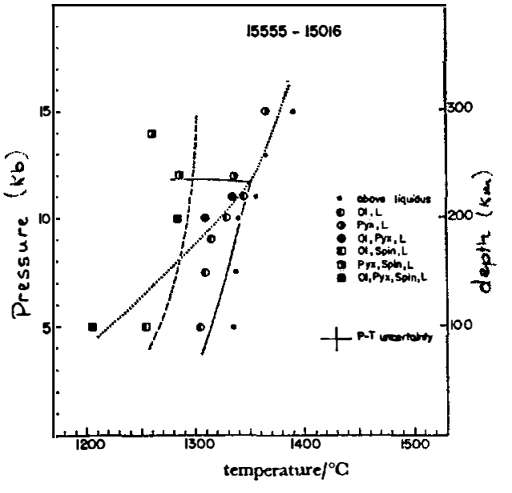

Fig. 5b

Figure 5: High pressure experimental data (a) Kushiro (1972); (b) Kesson (1977).

15016

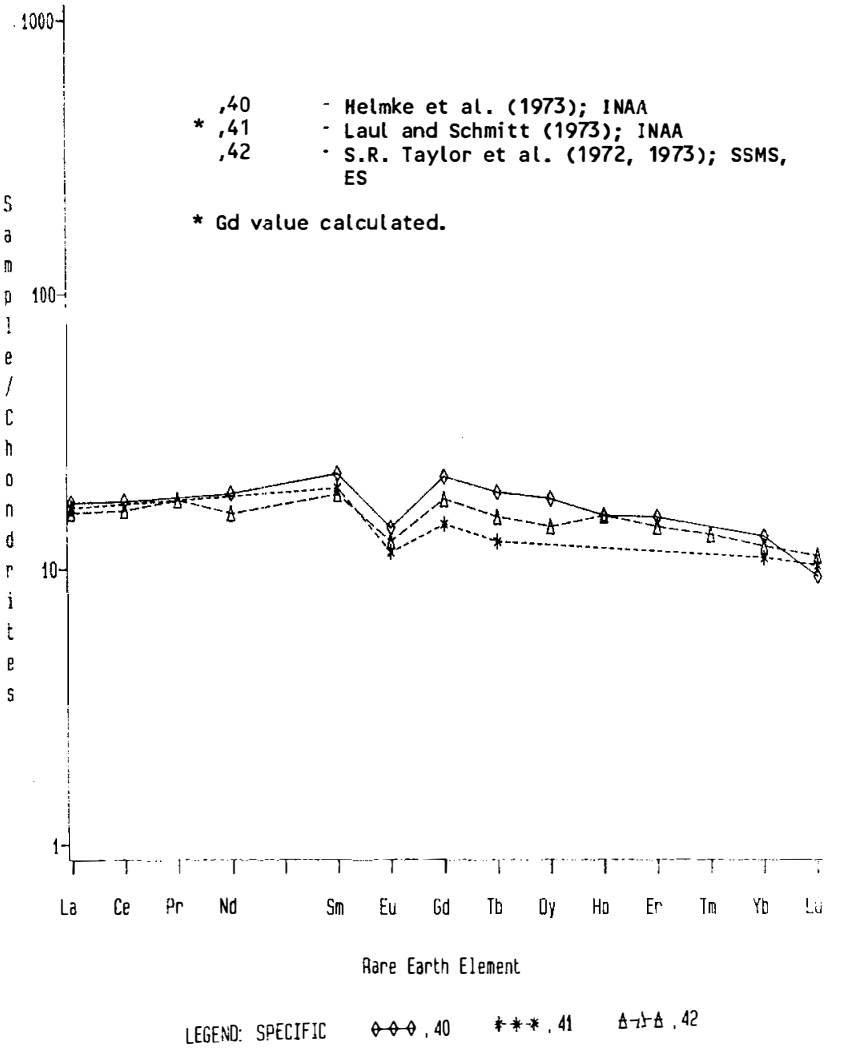

Figure 6: Rare earths in bulk rock 15016.

TABLE 15016-1

		,37	,41	,33		,42	,38	,31	,39[d]	,46		
Wt %	SiO2	43.78	43.97	44.30				43.9		43.9		
	TiO2	2.28	2.31	2.27	2.1			1.77		3.0		
	Al2O3	8.17	8.43	8.39	8.8			15.8		8.3		
	FeO	22.50	22.58	22.95	21.8			16.53		21.7		
	MgO	11.58	11.14	11.65	11	11.12		9.16		11.4		
	CaO	9.06	9.40	9.20	9.0	9.05		10.9				
	Na2O	0.24	0.21	0.32	0.251	0.2510b		0.32				
	K2O	0.04	0.03	0.05	0.041	0.0410	0.0451					0.0405
	P2O5	0.25	0.07	0.06		0.0410						
(ppm)	Sc			32	36			25.0				
	V			200	250			140				
	Cr	7530		4500	5860			4100				
	Mn	2600	2600	2200	2000			2550,1200	1680			
	Co			65	53			56.0				
	Ni			86				74.0			85	
	Rb			<1		1.0		0.83	0.73,0.81,0.65			0.670
	Sr		83	80		99			89.7,91.4,93.3			90.7
	Y			21				26.0				
	Zr		95	69	150			94.0				
	Nb			<10				6.2				
	Hf				2.5			2.04				
	Ba			30	70	132		61.0				
	Th						0.52	0.5				
	U					0.51	0.15	0.12				
	Pb							0.56				
	La			<10	5.5	13		5.3				
	Ce							14.4				
	Pr							2.0				
	Nd							9.6				
	Sm				3.6			3.42				
	Eu				0.80			0.87				
	Gd							4.5				
	Tb				0.59			0.73				
	Dy							4.55				
	Ho							1.1				
	Er							2.86				
	Tm							0.40				
	Yb			4.2	2.2			2.42				
	Lu				0.35			0.38				
	Li			4.6		7.5						
	Be			1.0								
	B											
	C											
	N											
	S	1900	700[c]									
	F											
	Cl											
	Br											
	Cu			11a				10.0				
	Zn										1.8	
(ppb)	I											
	At											
	Ga			4600				4400			3600	
	Ge										28	
	As											
	Se											
	Mo											
	Tc											
	Ru											
	Rh											
	Pd											
	Ag											
	Cd										2.0	
	In										0.36	
	Sn							190				
	Sb											
	Te											
	Cs					40						
	Ta				400							
	W											
	Re											
	Os											
	Ir										0.12	
	Pt											
	Au										0.27	
	He											
	Tl											
	Bi											
		(1)	(2)	(3)	(4)	(5)	(6)	(7)	(8)	(9)	(10)	(11)

TABLE 15016-1 Continued

		,31	,41	,44	,78		,40	,32	,33
Wt %	SiO2					44.26			
	TiO2					2.29			
	Al2O3					8.52			
	FeO					22.93			
	MgO					10.84			
	CaO					9.43		7.1	8.3
	Na2O					0.32			
	K2O					0.05		0.0340	0.036
	P2O5					0.08			
(ppm)	Sc						39.1		
	V								
	Cr					5500	6400		
	Mn					2400			
	Co						54		
	Ni				68				
	Rb				0.879	0.65			
	Sr					93.3			
	Y					23			
	Zr	94.7d,a				86			
	Nb					7			
	Hf	2.53d					2.6		
	Ba								
	Th								
	U				0.160				
	Pb								
	La						5.77		
	Ce						15.6		
	Pr								
	Nd						11.4		
	Sm						4.05		
	Eu						0.970		
	Gd						5.4		
	Tb						0.90		
	Dy						5.74		
	Ho						1.1		
	Er						3.1		
	Tm								
	Yb						2.62		
	Lu						0.321		
	Li								
	Be								
	B								
	C			11					
	N			<2					
	S		860e	790e		400			
	F								
	Cl								
	Br								
	Cu								
	Zn				1.05		<4		
(ppb)	I								
	At								
	Ga					2700	3200		
	Ge				4.38				
	As								
	Se				114				
	Mo								
	Tc								
	Ru								
	Rh								
	Pd				<0.33				
	Ag				0.84				
	Cd				2.05				
	In				0.34				
	Sn				<60				
	Sb				3.8				
	Te				2.4				
	Cs				33.5		29		
	Ta								
	W								
	Re				0.033				
	Os				<0.01				
	Ir				0.018				
	Pt								
	Au				0.025				
	Hg								
	Tl				0.32				
	Bi				0.36				
		(12)	(13)	(14)	(15)	(16)	(17)	(18)	(19)

References to Table 15016-1

References and methods:

(1) Kushiro et al. (1972) convention
(2) PET (1972), Rhodes and Hubbard (973) XRF, AAS
(3) Christian et al. (1972); Cuttitta et al. (1973) XRF, etc.
(4) Laul and Schmitt (1973) INAA
(5) Muller (1972,1975) INAA, AAS
(6) O'Kelley et al. (1972a,b,c) GRS
(7) S.R. Taylor et al. (1972,1973) SSMS, ES
(8) Compston et al. (1972) ID, XRF
(9) Janghorbani et al. (1973) NAA
(10) Baedecker et al. (1973) RNAA
(11) Evensen et al. (1973) IDMS
(12) Ehmann and Chyi (1974); Garg and Ehmann (1976) RNAA
(13) Gibson et al. (1975) combustion
(14) Kaplan et al. (1976) combustion
(15) Wolf et al. (1979) RNAA
(16) Chappell et al. (1973) XRF
(17) Helmke et al. (1973) INAA
(18) Husain et al. (1974) from argon isotopes
(19) Kirsten et al. (1973) from argon isotopes

Notes:

(a) erron
Cutti
(b) revis
(1972
(c) Rhode
(d) all d
(e) lower
hydro
(f) corre
(1974

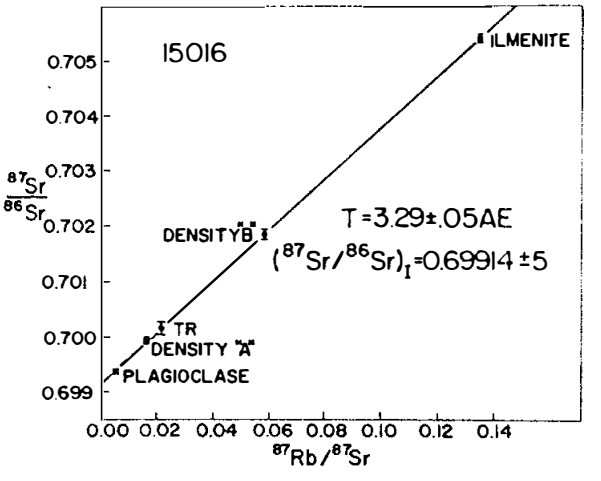

Rb-Sr internal isochron for 15016. TR = total rock; density "A" = $2.89 < \rho < 2.96$; density "B" = $3.24 < \rho < 4.1$; Errors for $^{87}Rb/^{86}Sr$ are ±2%; Errors for $^{87}Sr/^{86}Sr$ are noted in Table 1. Best fit line obtained by York (1966) type of weighted regression analysis, with 2 σ errors.

Figure 7: Rb-Sr isochron (Evensen et al., 1973).

intervesicle areas. The thin F deposits are of lunar origin, but are thinner than occur on Apollo 15 Green Glass. The amount of F present is not enough to have caused the vesicles, but if a lot of gas escaped, HF or HF/HCl gas could have been the cause. However, Goldberg et al. (1976) consider CO a more likely phase.

RADIOGENIC ISOTOPES AND GEOCHRONOLOGY: Evensen et al. (1973) measured Rb and Sr isotopes on total rock and mineral separates from 15016, finding an internal isochron age of 3.29 ± 0.05 b.y. and initial $^{87}Sr/^{86}Sr$ of 0.69914 ± 0.0005 (Fig. 7). The whole rock data corresponds with T_{BABI} of 4.27 b.y. after adjusting for inter-laboratory bias (Nyquist et al. (1977). Compston et al. (1972) also measured Rb and Sr isotopes in whole rock samples, finding substantially higher $^{87}Sr/^{86}Sr$ ratios (Table 2) (even when adjusted for inter-laboratory bias). These higher values give substantially older T_{BABI} ages (Nyquist 1977). The duplicate whole rock analyses spread along a 3.3 b.y. isochron.

Kirsten et al. (1973) found a ^{40}Ar-^{39}Ar plateau age of 3.38 ± 0.08 b.y., but no details are given. Husain (1974) on the other hand did not find any consistent plateau from his tabulated data, and 19% of the radiogenic ^{40}Ar was lost (Husain 1972). A K-Ar age of 2.90 ± 0.04 b.y. (Husain 1974) reflects this Ar loss.

Anderson and Hinthorne used an ion probe to measure Pb isotopes on a phosphate, determining an age of 3.75 ± 0.27 b.y.

EXPOSURE: Kirsten et al. (1972) and Husain (1974) determined ^{38}Ar exposure ages of 285 m.y. and 315 m.y. respectively. Eldridge et al. (1972) studied cosmogenic radionuclides; according to Yokoyama et al. (1974) the ^{26}Al is at saturated values, indicating an exposure of at least 2 m.y.

PHYSICAL PROPERTIES: Gose et al. (1972) and Pearce et al. (1973) studied and tabulated the basic magnetic properties (from room temperature hysteresis loops) and NRM of chips of 15016. 15016,28 demagnetized systematically and a stable magnetization is indicated (Fig. 8) but ,29, although it contained no soft component, showed a random scatter of direction. The magnetization gives a low field estimate (e.g., Cisowski et al., 1975).

Charette and Adams (1975) depict a reflectance spectra in the 0.5 to 2.5 micron region which is similar to that for 15555.

PROCESSING AND SUBDIVISIONS: A few small chips were taken, (including ,3 for a potted butt to make thin sections ,5 to ,14) prior to substantial sawing of the rock (Fig. 9). ,0 remains as 601.8 g; ,16 (80.3 g) is in remote storage; and ,20 (64.7 g) was encapsulated for display. Most subsequent splits and allocations were from the two central sawn pieces ,17 and ,19 (Fig. 9). More thin sections were made from ,22 (thin sections ,140 to ,150), and three P.I. made thin sections were from ,47 (thin sections ,157 to ,159).

Table 15016-2. Whole Rock Rb-Sr Isotopic Data

Reference	$^{87}Rb/^{86}Sr$	$^{87}Sr/^{86}Sr$	I $^{87}Sr/^{86}Sr$
Evensen et al. (1973)	0.0214	0.70016 ± 13	0.69914a
Compston et al. (1972)	0.0233	0.70064 ± 10	0.69954b
Compston et al. (1972)	0.0255	0.70083 ± 10	0.69963b

(a) from isochron
(b) assuming 3.3 b.y. age

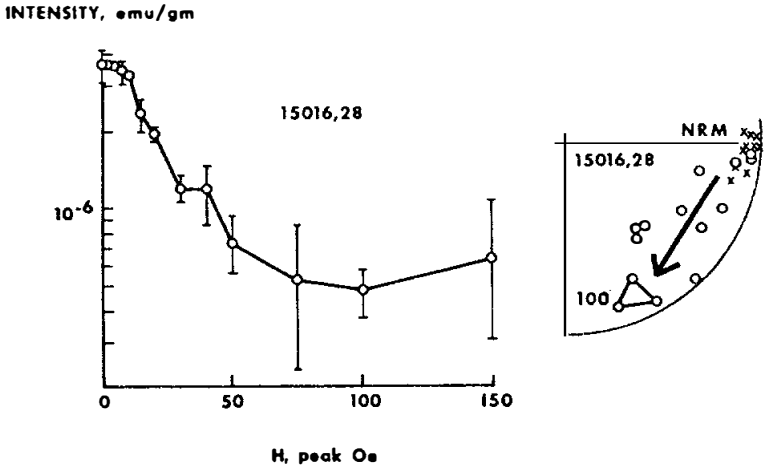

AF demagnetization of 15016. Arrows show change in direction upon demagnetization.

Figure 8: AF demagnetization (Pearce et al., 1973).

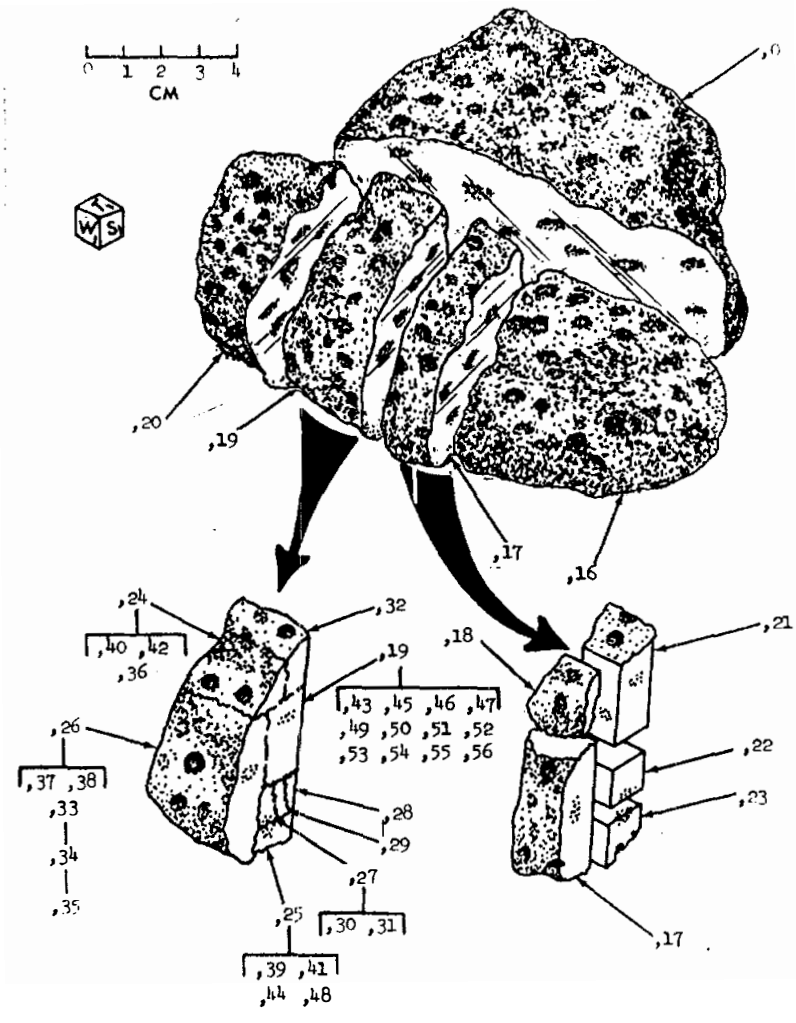

B1 WORK ORIENTATION (LRL "MUG" PHOTOGRAPHY)

Figure 9: Main sawing and subsplits of 15016.

15017 GLASS SHELL ST. LM 9.8 g

INTRODUCTION: 15017 is a hollow glass sphere which was 3 to 4 cm in diameter (Fig. 1). It had broken by the time of receipt at LRL. Its composition is very similar to local regolith, except perhaps very slightly more felsic. The glass sphere is dark gray, and its walls vary from 1 to 3 mm thick. The inside surface is vesicular (Fig. 1); the outside surface is smooth where glassy but hackly to irregular where breccia fragments are embedded or vesicles are open. There are very few zap pits, indicating a very young age.

15017 was noticed from the LM window, and is atypical. It was collected and bagged with 15018, 15019, 15027, and 15028; all were lying in a subdued 1-m crater 4 m south of the LM + Z footpad. It had no fillet; sampling was documented but its orientation was not decipherable because of its spherical shape.

Figure 1. Six chips of 15017, as received. S-71-43662

PETROLOGY: 15017 is a vesicular, thin glass with a smooth surface on both the interior and exterior sides (Fig. 2). Larger vesicles open to the interior. The glass is pale green, banded, with some portions slightly devitrified. Some portions contain or grade into a glassy breccia or clast-rich glass, which contains mineral and glass fragments. Fabel et al. (1972) made electron probe analyses and found the sample to be inhomogeneous; however, they probably analyzed inclusions which gave the ranges. Their analyses are suspect because the silica ranges as low as 25%, and their highest alumina content is not as high as the bulk chemical analysis. Fabel et al. (1972) also reported X-ray emission shift data for SiK_β, AlK_β, and OK_α, as well as Rama spectra which showed pyroxene bands. Morrison et al. (1973), in a detailed examination of the glass surface, found it to be smooth, full of vesicles, and to have a few superposed glass splashes. Most of the accretionary objects are less than 10 microns across, very thin, and mainly elliptical.

Figure 2. Photomicrograph of 15017,22. Width about 2 mm. Transmitted light. Section cut across shell; interior is to left.

CHEMISTRY: Chemical analyses are listed in Table 1 and rare earths are shown in Figure 3. The composition is very similar to local regolith compositions except slightly richer in Al_2O_3 and poorer in FeO. The SiO_2 content (Wanke et al., 1977) appears to be too high; the major elements listed, even without TiO_2 or P_2O_5 (which can be expected to sum to nearly 2%) is 100.2%, suggesting some analytical error.

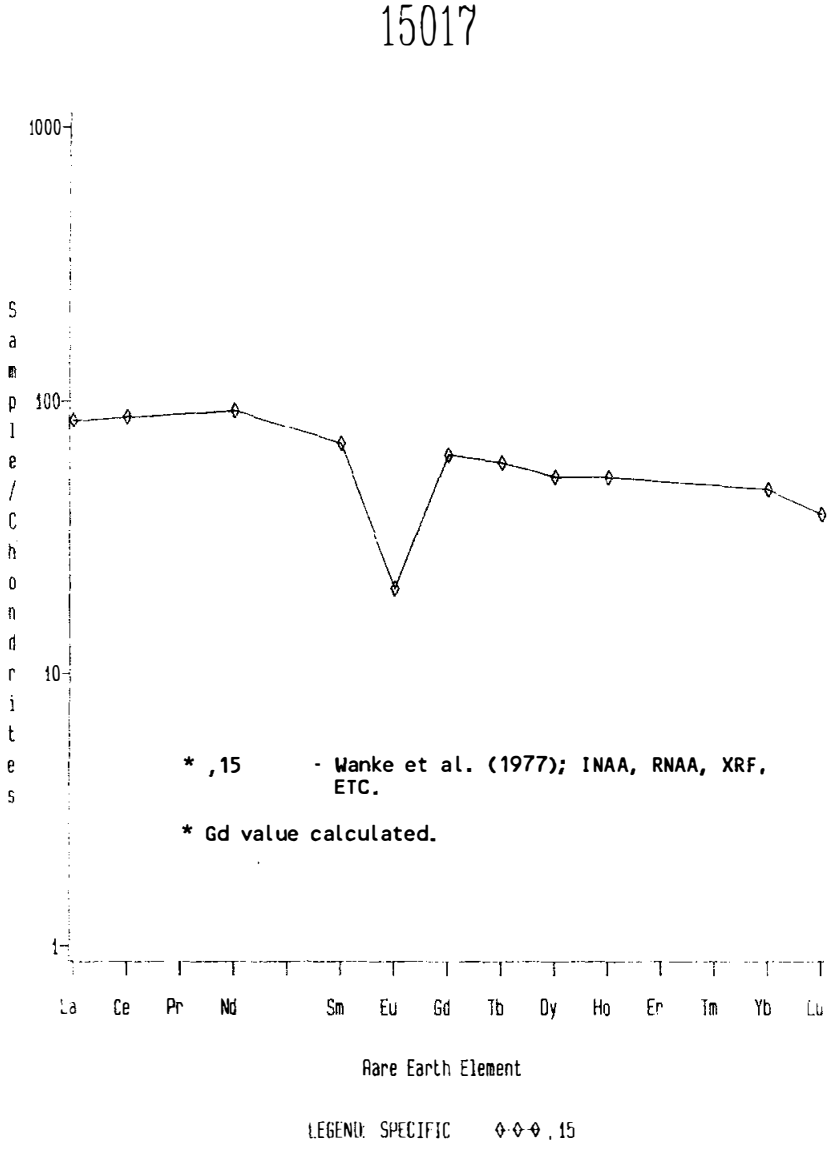

Figure 3. Rare earths in 15017.

TABLE 15017-1. Chemical analyses

		,15	,16
Wt %	SiO2	49.88	
	TiO2		
	Al2O3	14.91	
	FeO	14.34	
	MgO	10.72	
	CaO	9.74	
	Na2O	0.442	
	K2O	0.211	
	P2O5		
(ppm)	Sc	29.9	
	V		
	Cr	3000	
	Mn	1530	
	Co	40.6	49
	Ni	260	
	Rb		2.2
	Sr	135	
	Y		
	Zr	437	
	Nb		
	Hf	10.3	
	Ba	300	
	Th	3.93	
	U		1.410
	Pb		
	La	28.2	
	Ce	77.7	
	Pr		
	Nd	56	
	Sm	12.7	
	Eu	1.42	
	Gd		
	Tb	2.79	
	Dy	16.8	
	Ho	3.7	
	Er		
	Tm		
	Yb	9.49	
	Lu	1.32	
	Li		
	Be		
	B		
	C		
	N		
	S		
	F		
	Cl		
	Br		0.076
	Cu		
	Zn		5.8
(ppb)	I		
	At		
	Ga		
	Ge		241
	As		
	Se		363
	Mo		
	Tc		
	Ru		
	Rh		
	Pd		
	Ag		2.3
	Cd		4.2
	In		1.95
	Sn		
	Sb		47
	Te		20
	Cs		273
	Ta	1260	
	W		
	Re		0.87
	Os		
	Ir	8	9.1
	Pt		
	Au		2.9
	Hg		
	Tl		1.55
	Bi		0.59
		(1)	(2)

References and methods:

(1) Wanke et al. (1977); INAA, RNAA, XRF, etc.
(2) Ganapathy et al. (1973); RNAA

TRACKS, MICROCRATERS, AND EXPOSURE: Fleischer et al. (1973) found that the exterior of ,6 had a low density of impact pits; one area of about 1 cm^2 has one pit larger than 200 microns, three larger than 100 microns, and six larger than 50 microns. From the flux of Hartung et al. (1973), such a density would suggest 14,000 years exposure. Tracks (Fig. 4) suggest an age of 2-1/2 months, a discrepancy of a factor of 10^5, and suggests thermal fading of tracks. Experiments showed that 50 minutes at 230°C removed nearly all tracks. Fleischer et al. (1973) suggested that the flux in the 2-1/2 months prior to the Apollo

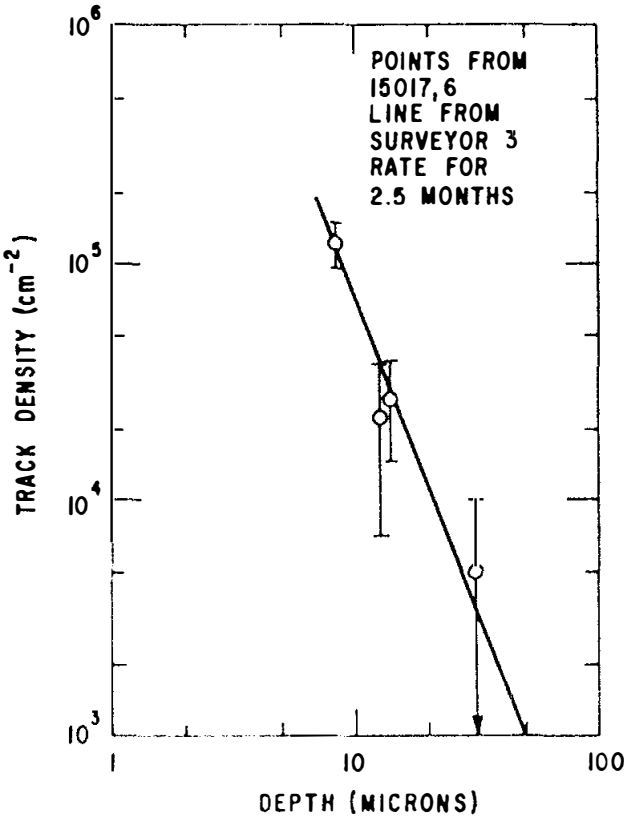

Figure 4. Track density gradient in 15017,6 (Fleischer et al., 1973).

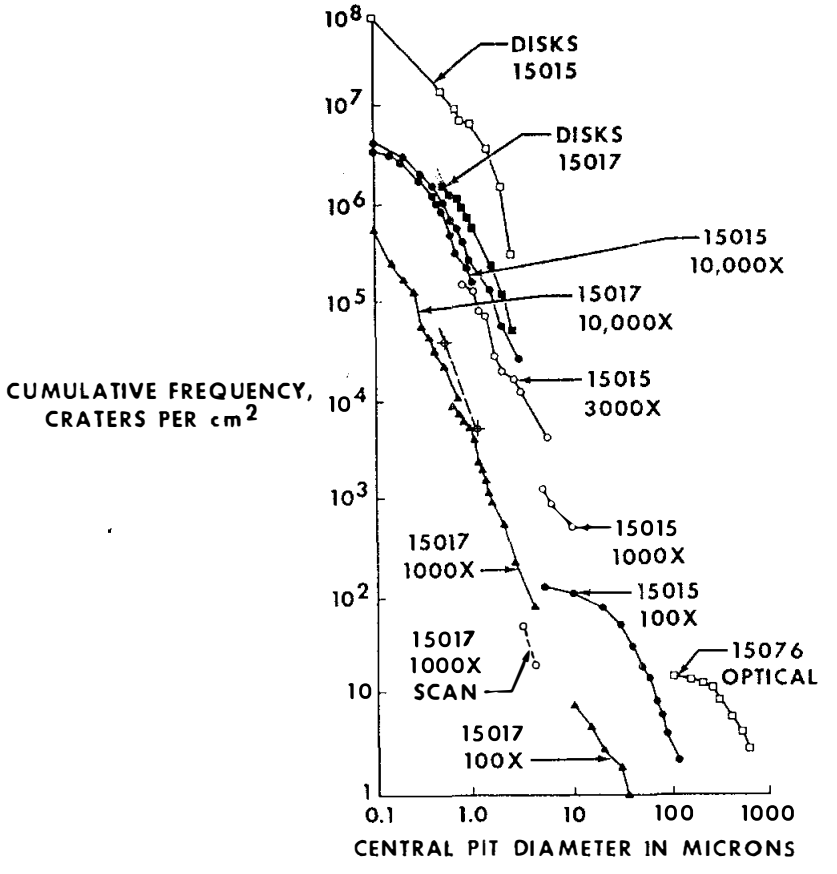

Figure 5. Cumulative microcrater and accretioning object frequency distributions for 15017 exterior, and for 15015 (Morrison et al., 1973).

15 mission was too low to produce the tracks, and that the glass retained tracks for about one year (using the Surveyor 3 solar flare energy spectrum determination).

Morrison et al. (1973) studied microcraters, and placed 15017 in their Category 4 (exceptionally low frequency of microcraters), suggesting it is very young. Cumulative frequencies were obtained from photomosaics, visual scanning at greater magnification, and SEM. The cumulative frequency distribution (Fig.5) has a flat slope in the 10 to 30 micron region. The frequencies are more than three orders of magnitude below a steady state. The bimodal distribution is typical, like 15205 and 15076 (Horz et al., 1975). Morrison et al. (1973) noted that the exposure age was difficult to determine because of the few craters larger than 100 microns, and the probable flexure on the frequency distribution below but near that size. They suggested that 15017 was probably about 1/30 the age of 15015, i.e., 300 to 700 years old. They interpreted the distribution in terms of a mass-flux distribution (Fig. 6). Accretionary objects (glass splashes) have a distribution similar to the craters.

PROCESSING AND SUBDIVISIONS: The sphere was received as 6 separate pieces (Fig. 1), and numbered ,1 to ,6. ,2 was chipped to produce ,7, from which thin sections ,22 to ,25 were made, and other allocations were also made from ,2; ,5; and ,6. The other three chips remain untouched.

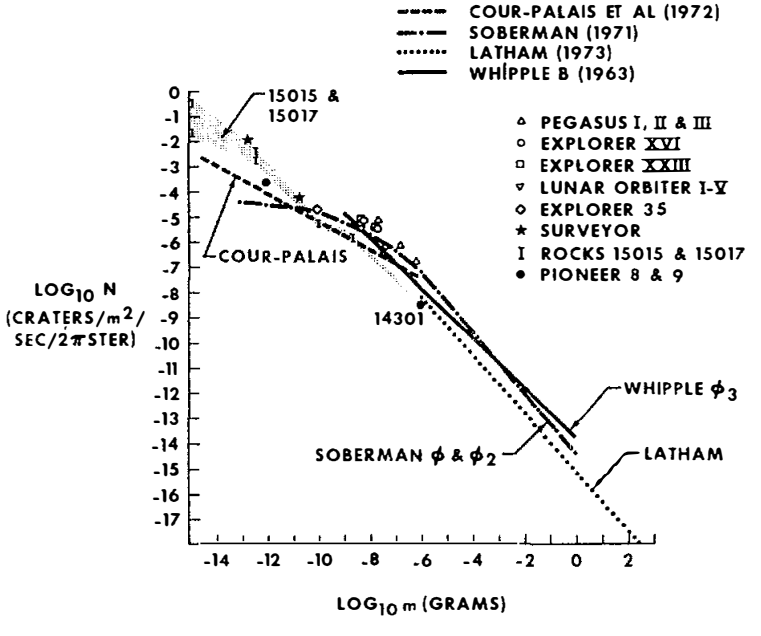

Figure 6. Mass-flux distribution estimates based on 15017 and other samples (Morrison et al., 1973).

15018 VESICULAR GLASS ST. LM 5.7 g

INTRODUCTION: 15018 is an olive gray, round glassy object (Fig. 1). It is tough, smooth to vesicular, with patchy irridescence. Basalt and microbreccia fragments stuck to the glass are small and rare. 15018 was collected and bagged with 15017, 15019, 15027, and 15028; all were lying in a subdued 1-m crater 4 m south of the LM+Z footpad. It has not been recognized in site photographs. It has never been allocated or subdivided.

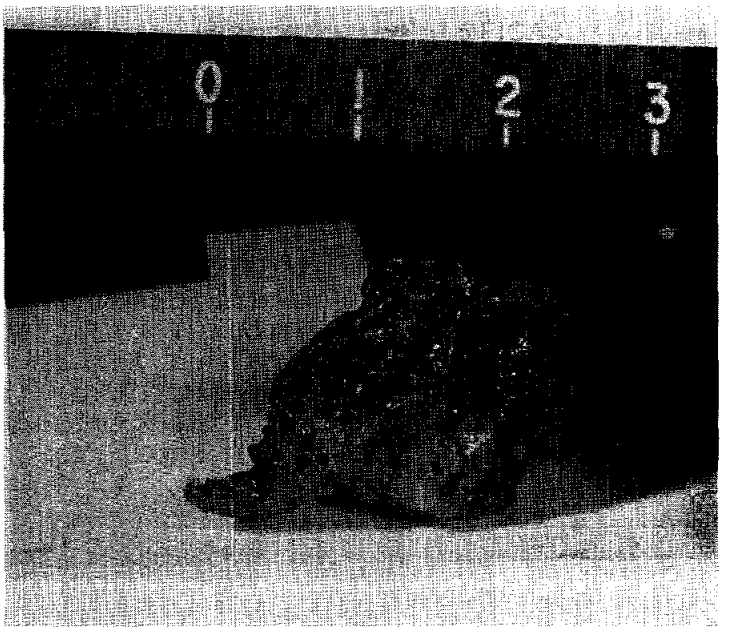

Figure 1. Sample 15018. S-71-43631

15019 AGGLUTINITIC BRECCIA ST. LM 1.2 g

INTRODUCTION: 15019 is a vesiculated, glassy breccia which could be described as either a glassy regolith breccia or an agglutinatic breccia (Fig. 1). It is medium dark gray, blocky and angular, tough, and has only a few zap pits, which are confined to one side. 15019 was collected and bagged with 15017, 15018, 15027, and 15028; all were lying in a subdued 1-m crater 4 m south of the LM + Z footpad. It has not be recognized in site photographs.

PETROLOGY: 15019 is a vesiculated, non-porous, very glassy regolith breccia or agglutinate (Fig. 2). Most of the vesicles are in a restricted band. The clasts include mineral fragments which are dominantly mare debris, and several very pale, homogeneous glass shards which have tended to devitrify, especially along their edges. Wilshire and Moore (1974) noted 15019 as an example of a rock with a glass selvage, presumably because it grades from a compact interior to a frothy edge.

PROCESSING AND SUBDIVISIONS: 15019 was chipped in 1975 to produce ,1 (0.48 g, allocated to Wasserburg); ,2 (for thin sections ,4 to ,6); and ,3 (0.04 g chips and fines). ,0 is now 0.63 g. The chips were intended to represent two distinct lithologies with a sharp contact, one a fine-grained vesicular breccia, the other a coarse basalt. Thin sections indicate that the "coarse basalt" is nonetheless breccia.

Figure 1. Pre-split view of 15019. S-71-43664

Figure 2. Photomicrograph of 15019,6. Width about 2 mm. Transmitted light. Vesicular band is to left. Pale piece at lower right with "stirrup" shape is a partly-devitrified glass shard.

15025 REGOLITH BRECCIA ST. LM 77.3 g

INTRODUCTION: 15025 is a coherent regolith breccia (Fig. 1) whose composition is a little more FeO and rare-earth enriched, and correspondingly Al_2O_3-poorer, than the local regolith. Clasts of mare basalt and KREEP basalt are conspicuous, along with typical regolith components such as glass. The sample is dark gray and subrounded. There are many zap pits on one side. 15025 was collected in the contingency sample approximately 12 m west of the LM + Z footpad, and is of about average size for the larger fragments in the local area. Photographs are inadequate to assess orientation.

PETROLOGY: 15025 is a regolith breccia (Fig. 2). It is subporous (porosity 2.73 g/cm^3; Wentworth and McKay, 1984), and submature, with an I_s/FeO of 42 (McKay et al., 1984), reported also as 30 (Korotev, 1984 unpublished). The thin sections consist of a matrix of brown glass and fine debris (mainly plagioclase, pyroxene, and glass) enclosing coarser mineral, glass, and lithic fragments. Most glasses are colorless spheres and shards, with some red spheres. Yellow glass appears to be rare to absent. Best and Minkin (1972) noted that "peridotite" glass (=Apollo 15 green glass) appears to be absent from this sample. They listed an analysis of a pale brown/gold glass wtih 57.4% SiO_2 and 1.04% K_2O from 15025,6 as a representative of their "KREEP" glass group from the entire landing site.

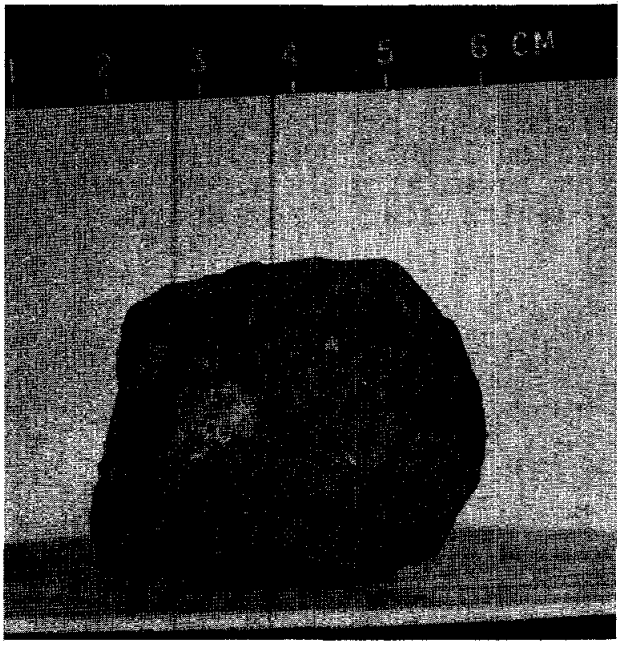

Figure 1. Pre-split view of 15025. S-71-45104

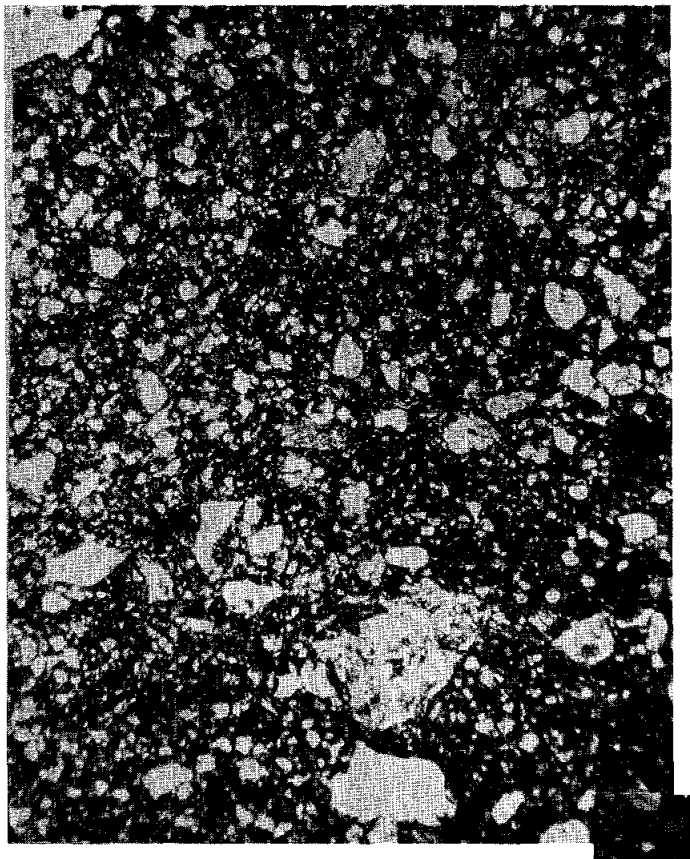

Fig. 2a

Fig. 2b

Figure 2. Photomicrographs of 15025,4. Widths about 2 mm. Transmitted light. a) general matrix; b) mare basalt clast; c) KREEP basalt clast.

Fig. 2c

Lithic clasts include mare basalts, KREEP basalts, and some highlands materials. The thin sections display a 3 mm fragment of medium-grained basalt (70% zoned pyroxenes, 30% plagioclase, 1% opaques) (Fig. 2b). They also show a 2-mm subophitic-intersertal KREEP basalt (Fig. 2c) with a prominent clear yellow glass mesostasis. One 1-1/2-mm lithic clast is a single grain of low-Ca pyroxene enclosing plagioclase (feldspathic granulite).

CHEMISTRY: The two chemical analyses (Table 1, Fig. 3) are consistent in suggesting that 15025 is slightly higher in FeO, TiO_2, Sc, Cr, and incompatible elements, and slightly lower in alumina, than the local regoliths. Hence 15025 appears to be enriched in both mare and KREEP basalt materials and correspondingly lower in some aluminous, presumably highlands, material than the local regolith.

PROCESSING AND SUBDIVISIONS: 15025 was chipped in 1971 to obtain chip ,1 (for thin sections ,3 to ,6); ,2 (0.20 g) also came off at that time. Chipping of the "T" face in 1976 produced ,7 for chemical analysis; further chipping in 1980 produced ,9 (0.94 g); and more chipping in 1983 and 1984 produced further splits for petrological and chemical analysis. ,0 is now 69.82 g.

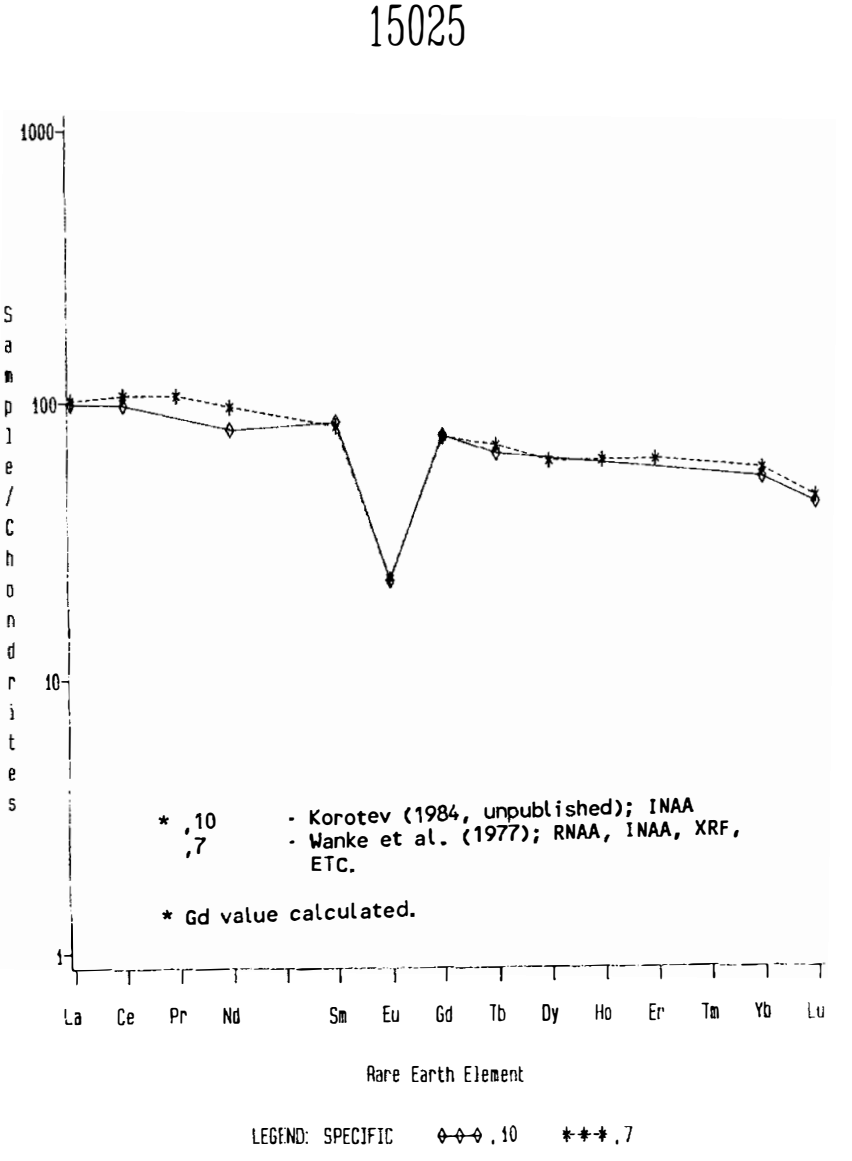

Figure 3. Rare earths in 15025 matrix.

TABLE 15025-1. Chemical analyses

		,7	,10
Wt %	SiO2	48.15	
	TiO2	1.84	1.88
	Al2O3	13.11	12.4
	FeO	15.22	15.9
	MgO	9.86	9.8
	CaO	10.42	10.3
	Na2O	0.497	0.50
	K2O	0.274	
	P2O5	0.275	
(ppm)	Sc	31.6	31.2
	V	108	104
	Cr	2950	2940
	Mn	1550	1555
	Co	41.5	50.4
	Ni	210	200
	Rb	6.27	
	Sr	139/135	138
	Y	115	
	Zr	472	460
	Nb	35	
	Hf	11.8	12.3
	Ba	375	357
	Th	4.9	5.1
	U	1.43	1.41
	Pb		
	La	33.6	32.6
	Ce	93.6	86
	Pr	11.9	
	Nd	58	48
	Sm	14.9	15.5
	Eu	1.58	1.56
	Gd	18.7	
	Tb	3.28	3.06
	Dy	19.3	
	Ho	4.3	
	Er	12.4	
	Tm		
	Yb	11.5	10.7
	Lu	1.54	1.47
	Li	16.6	
	Be	5.26	
	B		
	C		
	N		
	S	580	
	F	94	
	Cl	28.3	
	Br	0.073	
	Cu	19.8	
	Zn	10.0	
(ppb)	I		
	At		
	Ga	3920	
	Ge	360	
	As	39	
	Se	230	
	Mo		
	Tc		
	Ru		
	Rh		
	Pd		
	Ag		
	Cd		
	In		
	Sn		
	Sb		
	Te		
	Cs	300	320
	Ta	150	1480
	W	680	
	Re	0.7	
	Os		
	Ir	5	6.1
	Pt		
	Au	2.1	2.7
	Hg		
	Tl		
	Bi		
		(1)	(2)

References and methods:

(1) Wanke et al. (1977); RNAA, INAA, XRF, etc.

(2) Korotev (1984 unpublished); INAA

15026 REGOLITH BRECCIA, GLASS-COATED ST. LM 1.1 g

INTRODUCTION: 15026 is a small regolith breccia fragment with a vesicular glass coating. The breccia is medium-dark gray and contains typical regolith components. The glass coat is greenish-black and contains a few fragments. The whole sample is slabby, subangular, and friable. It was collected as part of the contingency sample approximately 12 m west of the LM + Z footpad. It has not been identified in site photographs.

PETROLOGY: 15026 consists of regolith breccia coated with vesicular glass (Fig. 2). The breccia is not very porous. It has an I_s/FeO of 61 to 94 (McKay et al., 1984), listed as 68 by Korotev (1984 unpublished) hence is mature, unlike most Apollo 15 regolith breccias which are submature or immature. The breccia consists mainly of mineral and glass fragments; the minerals are angular and generally unshocked. The glass fragments are mainly colorless or pale tan, and spheres are rare. The lithic fragments include some fine-grained feldspathic crystalline breccias and some small (mare?) basalts. The vesicular glass coat is greenish-gray, banded,and clast-poor. Its contact with the breccia is sharp and marked by a darker, glassy zone a few microns wide in the breccia.

CHEMISTRY: The 15026 regolith breccia has a composition very similar to the local regolith (Table 1, Fig. 3) from which it was presumably derived. No composition for the glass coat is available.

PROCESSING AND SUBDIVISIONS: 15026 was chipped in 1975 and thin sections ,3 to ,5 (all breccia plus glass coat) were cut from ,1. Subsequently more chipping of ,0 produced chips ,6 (for petrological and chemical analysis), and ,7. ,0 is now 0.817 g.

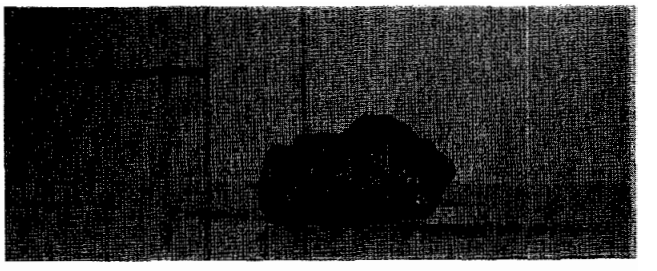

Figure 1. Pre-split view of 15026. S-71-43042

Figure 2. Photomicrograph of 15026,4. Width about 2 mm. Transmitted light.

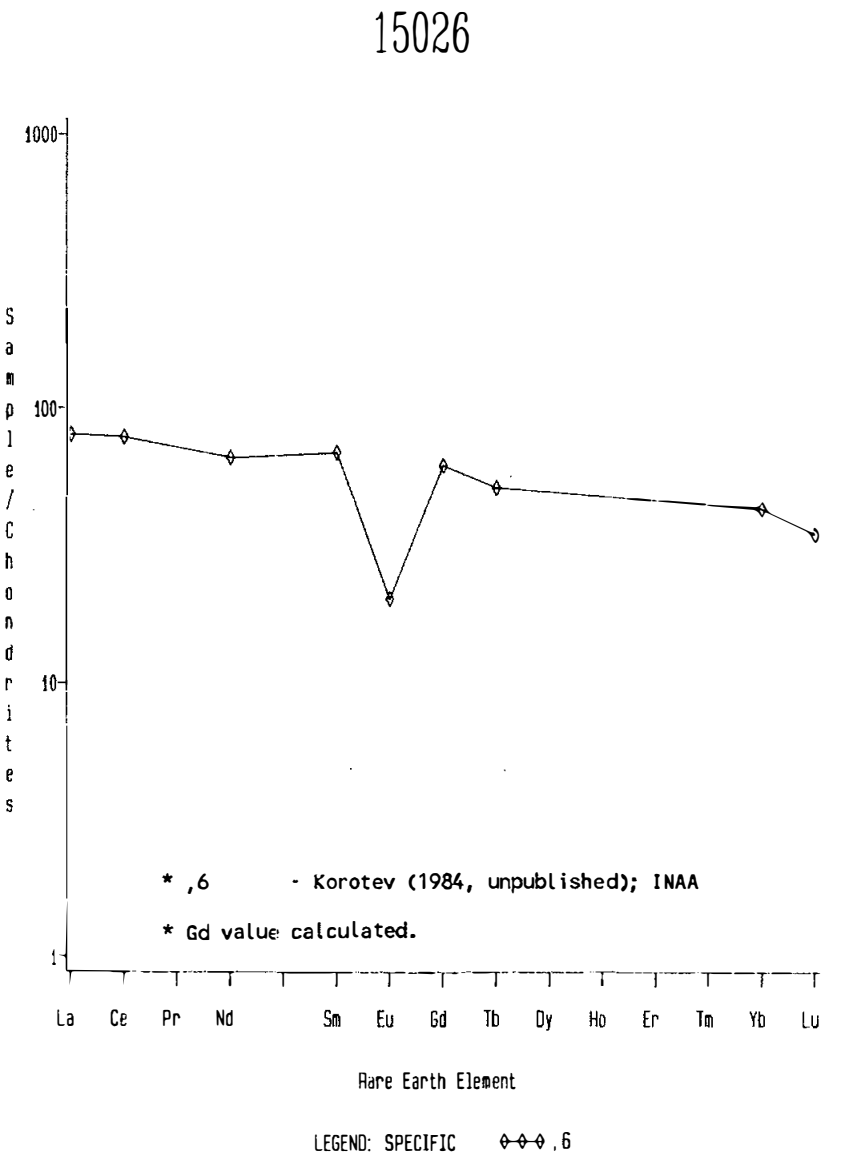

Figure 3. Rare earths in 15026 regolith breccia.

TABLE 15026-1. Chemical analysis

		,6
wt %	SiO2	
	TiO2	1.93
	Al2O3	13.2
	FeO	15.2
	MgO	10.4
	CaO	10.0
	Na2O	0.40
	K2O	
	P2O5	
(ppm)	Sc	29.5
	V	100
	Cr	2820
	Mn	1515
	Co	49.2
	Ni	289
	Rb	
	Sr	130
	Y	
	Zr	360
	Nb	
	Hf	9.9
	Ba	259
	Th	4.8
	U	0.97
	Pb	
	La	26.6
	Ce	69
	Pr	
	Nd	40
	Sm	12.6
	Eu	1.40
	Gd	
	Tb	2.43
	Dy	
	Ho	
	Er	
	Tm	
	Yb	8.7
	Lu	1.19
	Li	
	Be	
	B	
	C	
	N	
	S	
	F	
	Cl	
	Br	
	Cu	
	Zn	
(ppb)	I	
	At	
	Ga	
	Ge	
	As	
	Se	
	Mo	
	Tc	
	Ru	
	Rh	
	Pd	
	Ag	
	Cd	
	In	
	Sn	
	Sb	
	Te	
	Cs	290
	Ta	1250
	W	
	Re	
	Os	
	Ir	10.3
	Pt	
	Au	2.2
	Hg	
	Tl	
	Bi	
		(1)

References and methods:

(1) Korotev (1984 unpublished); INAA

15027 REGOLITH BRECCIA/VESICULAR GLASS ST. LM 51.0 g

INTRODUCTION: 15027 is varied, from a vesicular glass phase to a glassy regolith breccia (Fig. 1). At least the glass phase is considerably enriched in rare-earths over local regolith compositions. Macroscopically, the boundary between glass and breccia is not distinct. The vesicles are up to 4 mm across. The sample is medium gray, blocky to angular, and tough. One prominent clast is a basalt of unknown type visible on the "S" face (Fig. 1). 15027 has many zap pits on one side, few on others.

15027 was collected and bagged with 15017 to 15019, and 15028; all were lying in a subdued 1-m crater 4 m south of the LM + Z footpad. Its sampling was documented and its orientation known.

PETROLOGY: Thin sections represent two pieces chipped from different places, and show a brown, glassy, fairly dense regolith breccia (Fig. 2) which is faintly foliated in places. It contains many glass fragments and spheres, many of which are devitrified, especially around their margins. Clasts are mainly mineral, glass, and small basaltic fragments. The vesicular glass portion is brown and clast-poor, and the transition from glass to breccia is fairly rapid and distinct, suggesting a separate identity.

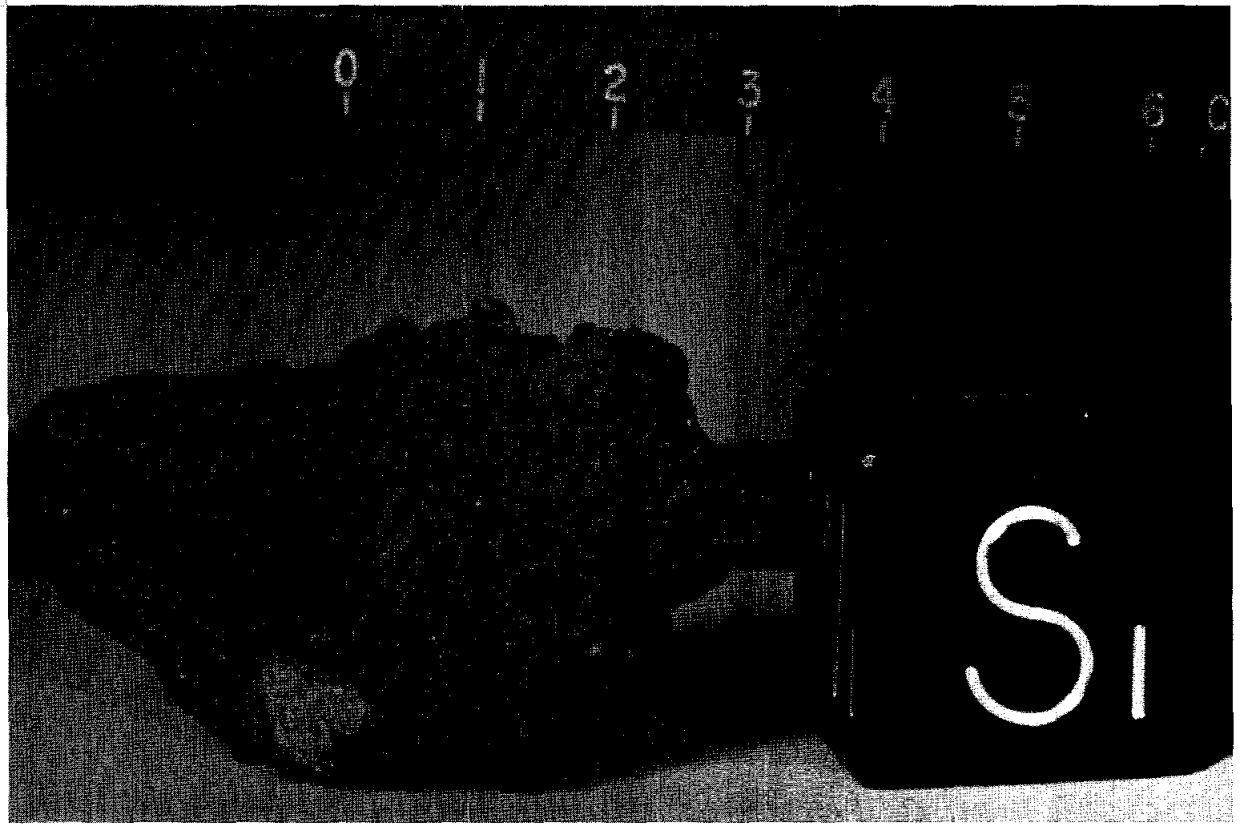

Figure 1. Pre-chip view of 15027. S-71-43635

CHEMISTRY: The chemical analysis (Table 1, Fig. 3) is of the vesicular glass, according to data pack photographs of the allocated material, which was vesicular. Although its major elements are fairly similar to local regolith, the incompatible elements are enriched almost two-fold, and the chemistry is very similar to 15028, collected close by. TiO_2 and especially SiO2 are also enriched compared with local regolith. The sum of major elements (Wanke et al., 1977) is slightly more than 100% but the high SiO_2 appears to be real.

PROCESSING AND SUBDIVISIONS: Two small chips from separate places were combined to make ,1 (Fig. 4), from which thin sections ,6 and ,7 were made. One of the chips was included to sample the prominent basaltic clast (labelled A), but the clast does not appear in either thin section. A large piece broken off during processing (Fig. 4) was not given a daughter number but combined with ,0. Subsequently a further chipping produced ,2, which appears to be dominantly vesicular glass, for the chemical analysis. ,0 is now 48.64 g.

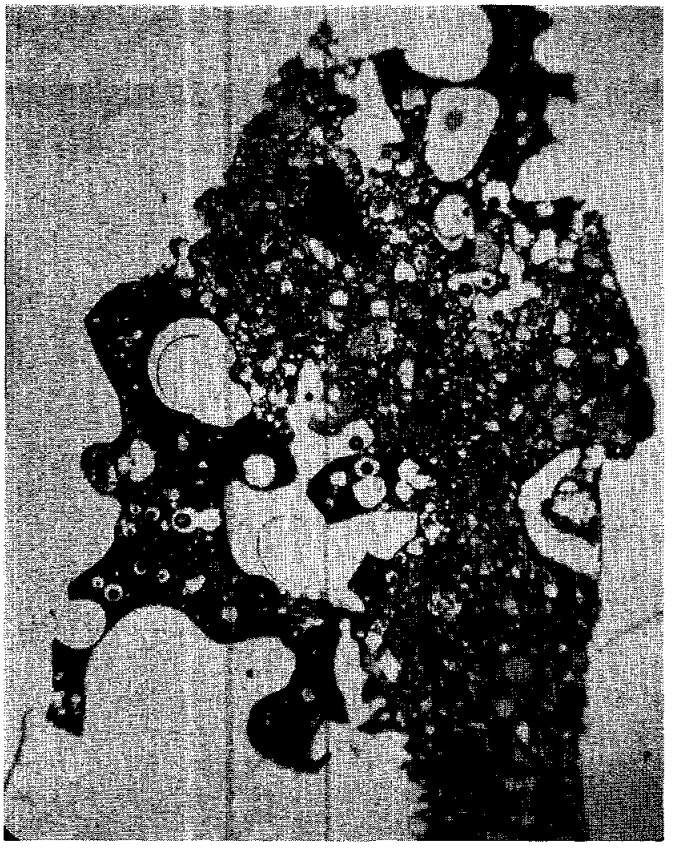

Figure 2. Photomicrograph of 15027,6. Width about 2 mm. Transmitted light. View shows both vesicular glass and glassy breccia.

15027

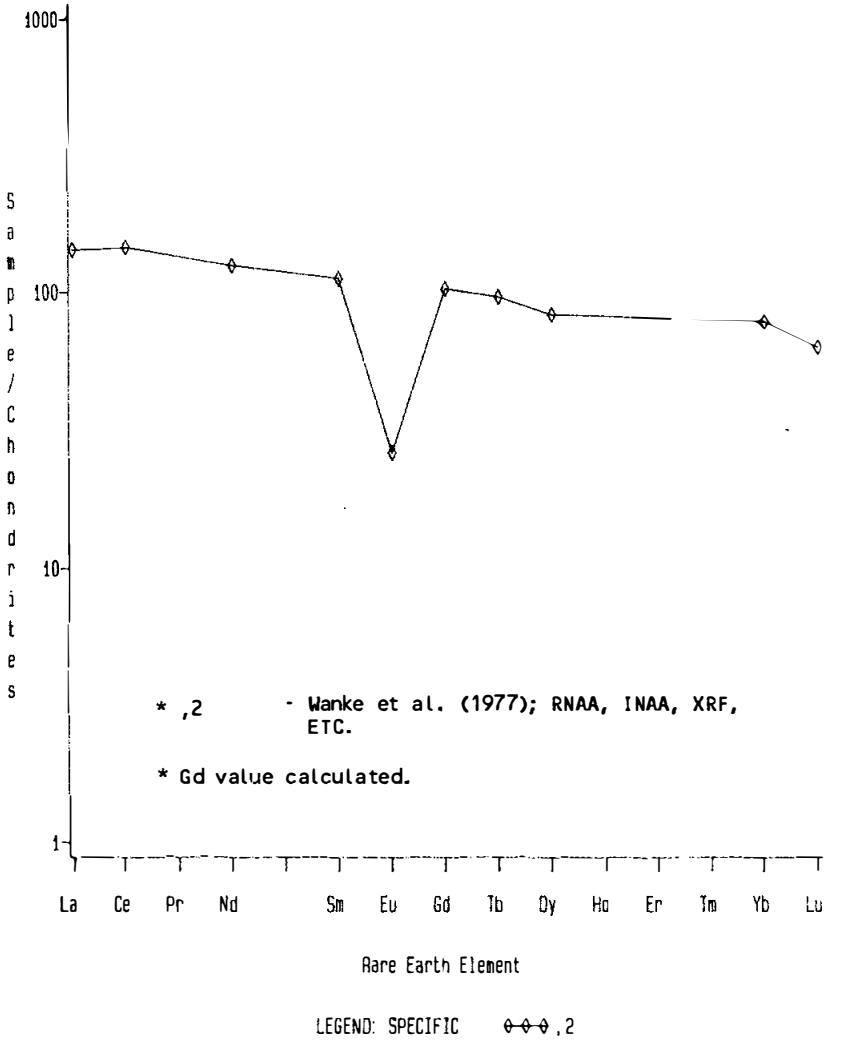

Figure 3. Rare earths in vesicular glass (Wanke et al., 1977).

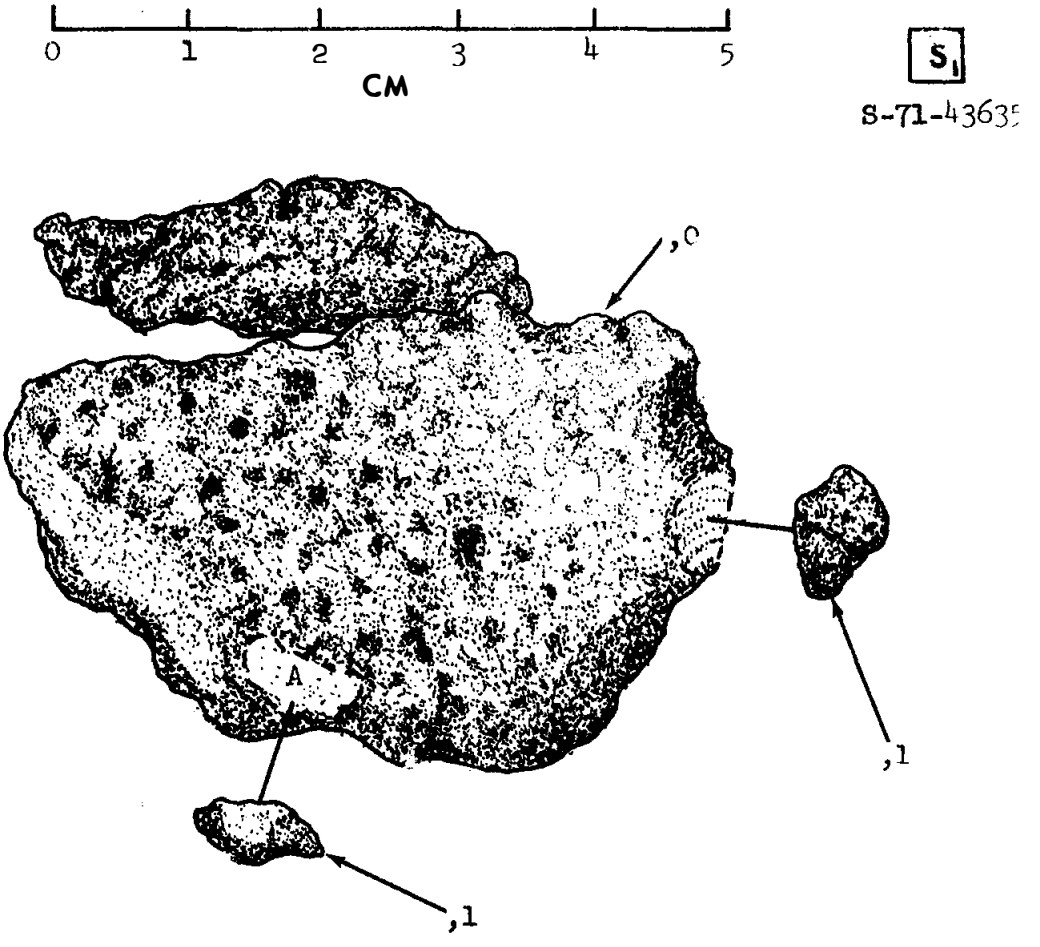

Figure 4. Original chipping of 15027.

TABLE 15027-1. Chemical analysis of vesicular glass in 15027

		,2
Wt %	SiO2	49.35
	TiO2	1.89
	Al2O3	13.78
	FeO	14.23
	MgO	9.19
	CaO	10.44
	Na2O	0.601
	K2O	0.422
	P2O5	0.394
(ppm)	Sc	30.8
	V	97.9
	Cr	2620
	Mn	1500
	Co	38.9
	Ni	180
	Rb	
	Sr	145
	Y	158
	Zr	662
	Nb	47
	Hf	17.0
	Ba	515
	Th	7.45
	U	2.3
	Pb	
	La	47.3
	Ce	129
	Pr	
	Nd	75
	Sm	20.4
	Eu	1.81
	Gd	
	Tb	4.54
	Dy	26.4
	Ho	
	Er	
	Tm	
	Yb	15.7
	Lu	2.17
	Li	
	Be	
	B	
	C	
	N	
	S	1040
	F	
	Cl	
	Br	
	Cu	
	Zn	
(ppb)	I	
	At	
	Ga	
	Ge	
	As	
	Se	
	Mo	
	Tc	
	Ru	
	Rh	
	Pd	
	Ag	
	Cd	
	In	
	Sn	
	Sb	
	Te	
	Cs	
	Ta	2050
	W	
	Re	
	Os	
	Ir	3
	Pt	
	Au	
	Hg	
	Tl	
	Bi	
		(1)

References and methods:

(1) Wanke et al. (1977); RNAA, INAA, XRF, etc.

15028 REGOLITH BRECCIA, GLASS-COATED ST. LM 59.4 g

INTRODUCTION: 15028 is a regolith breccia consisting of lithic, mineral, and glass fragments in a glassy matrix. It has an extensive, vesicular glass coat and thin veins of glass (Fig. 1). It is more enriched in incompatible elements than local regolith compositions, and is chemically similar to 15027.

15028 was collected and bagged with 15017, 15018, 15019, and 15027. They were lying in a subdued 1-m crater 4 m south of the LM +Z footpad; 15028 was apparently typical of rocks in its size range in the area. It is subangular, tough, and light gray (Fig. 1). Its lunar orientation is known; there are a few zap pits on the (laboratory) "S" and "T" surfaces.

PETROLOGY: 15028 is petrographically similar to 15027, which was collected near it. Kridelbaugh et al. (1972) described 15028 as a glass-coated breccia (Fig. 2) which shows a preferred orientation defined by elongate glass shards (Fra Mauro or KREEP composition) and vesicular glass veinlets. Normal to the preferred orientation is a set of microfaults, which truncate all components except the veinlets. There are two dominant types of lithic clasts: basalts and microbreccias. The basalts are porphyritic olivine basalt (mare). The olivine is zoned normally, Fo_{68} to Fo_{34}; pyroxenes have pigeonitic cores and augitic rims. Other minerals are plagioclase, ilmenite, chromite, Fe-metal, troilite, and residual phases. The microbreccias are well-rounded and noritic (orthopyroxene and plagioclase). Crystal fragments in the matrix include low-Ca pyroxenes (opx + pig), augitic pyroxenes, plagioclase, olivine, ilmenite, Fe-metal, troilite, and chromite.

Glass fragments constitute about 30% of 15028 by volume, and each is generally homogeneous, without devitrification. Fra Mauro (KREEP) glasses are the most abundant type in 15028, as colorless or light brown spherules, droplets, and elongate shards. Mare glasses, including AP15 Green Glass, are common. The volume distribution of the major glass compositional group is similar to that in local soils. The glass veinlets are compositionally homogeneous and similar in composition to the matrix (Tables 1 and 2).

McKay et al. (1984) found 15028 to have an I_s/FeO of 22 to 34 (listed as 26 by Korotev, 1984 unpublished), an immature to submature signature.

The glass analysis of Uhlmann et al. (1981) is probably of the glass coat. They studied glass crystallization kinetics, including this glass composition, and estimated viscosity-temperature relations. A simplified model (1.2°C/sec) and measured (0.9°C/sec) cooling rate required to produce glass without any nucleation agree well. These rapid cooling rates could readily be attained in a body of the observed size (although whether this means the size of 15028 or of the glass

Figure 1. Photographs of 15028 showing vesicular glassy coat and fine breccia.

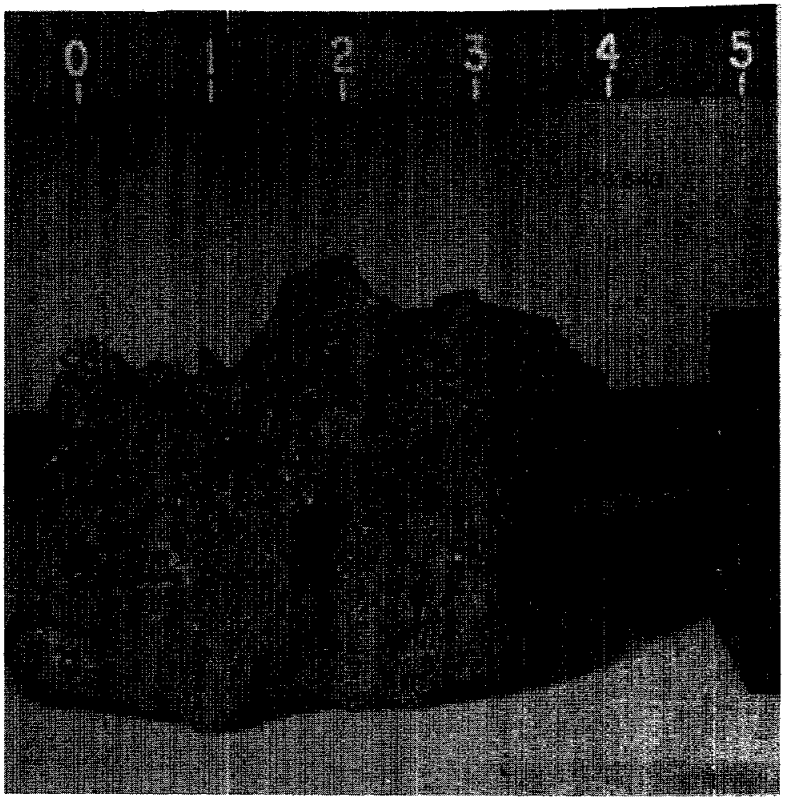

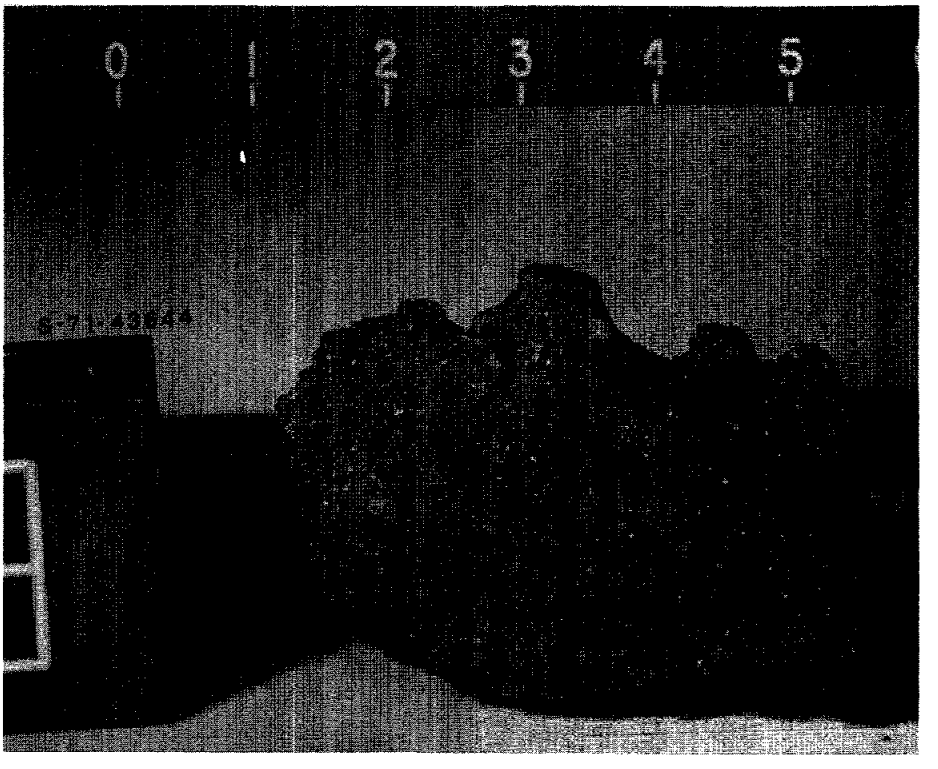

Figure 2. Photomicrographs of 15028 matrix showing foliation. Widths about 2 mm. Transmitted light. (a) 15028,5; (b) 15028,6.

Fig. 2a

Fig. 2b

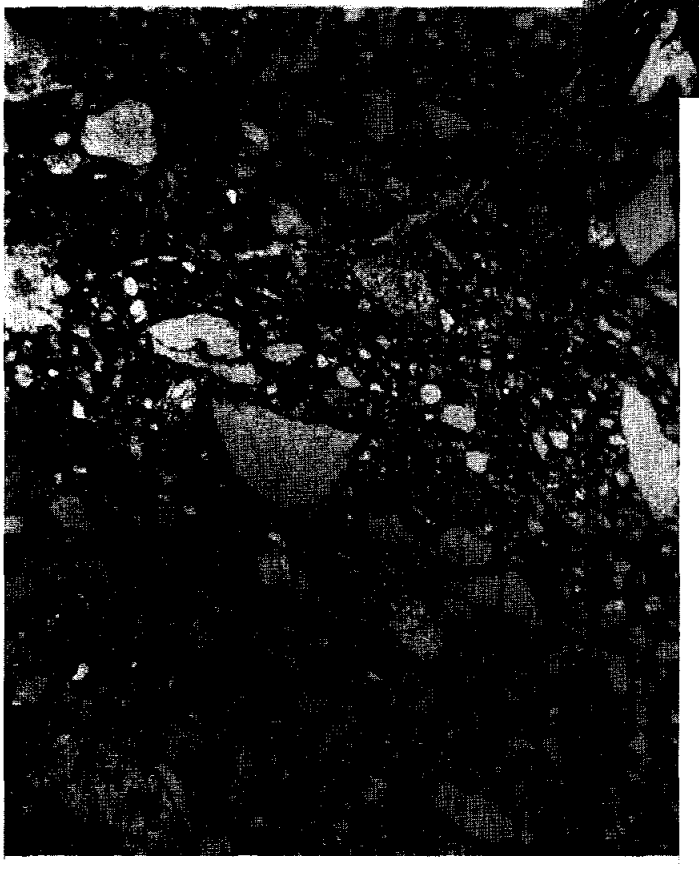

1 mm

coat is not actually specified in Uhlmann et al., 1981) cooling by radiation.

CHEMISTRY: Chemical analyses of the breccia matrix are shown in Table 2 and Figure 3. Wanke et al. (1977) also analyzed for oxygen (42.82%); they did not specifically discuss the data. The breccia is enriched in incompatible elements compared with local regolith, by a factor of almost 2, but the major elements are fairly similar to those of local regolith. The chemistry is similar to that of 15027.

PROCESSING AND SUBDIVISIONS: Only a few pieces have been chipped from the sample, with ,0 now having a mass of 56.70 g. Chip ,1 was made into thin sections ,2 to ,6.

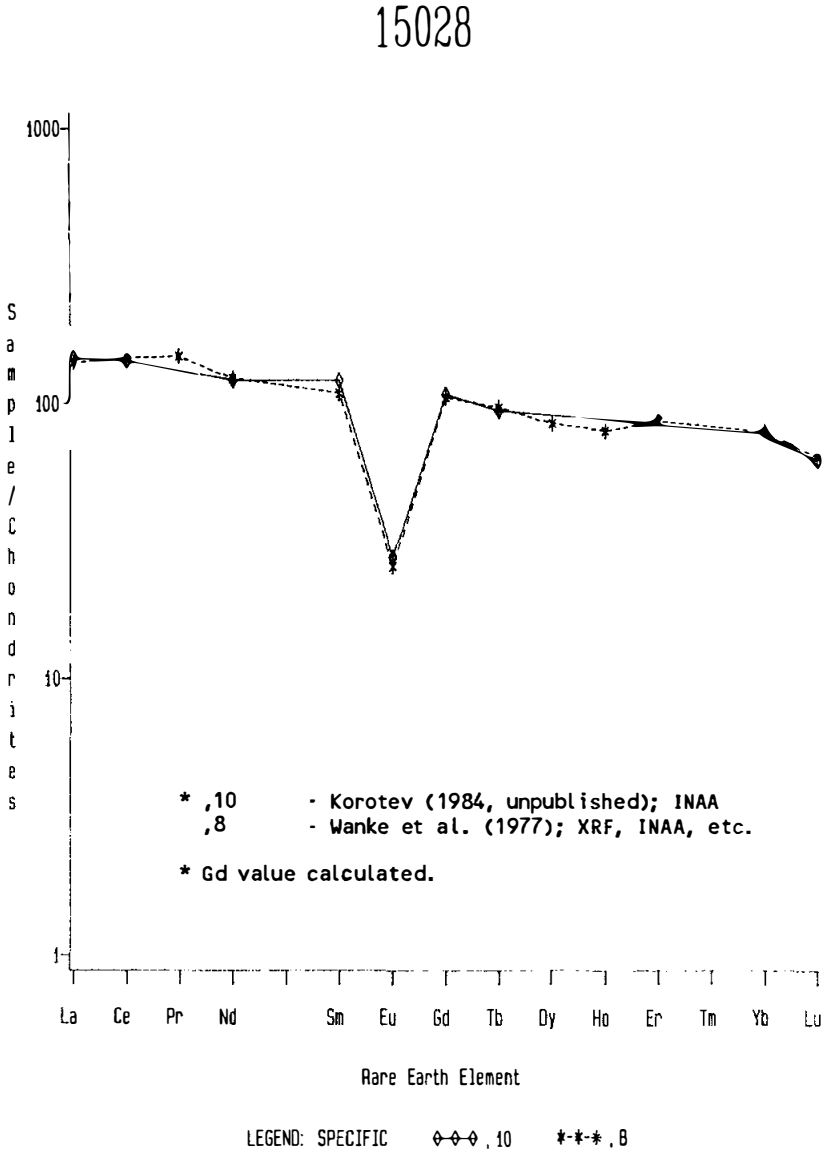

Figure 3. Rare earths in 15028 matrix.

TABLE 15028-1. Microprobe analyses of glass

		a	a	b
Wt %	SiO2	47.98	46.47	48.8
	TiO2	1.75	1.60	1.4
	Al2O3	14.66	16.49	12.9
	FeO	14.10	13.72	14.1
	MgO	8.73	8.56	7.4
	CaO	10.30	10.69	9.5
	Na2O	0.59	0.64	0.6
	K2O	0.41	0.36	0.4
	P2O5	0.30	0.37	
ppm	Cr	1600	950	1300
		(1)	(1)	(2)

References:

(1) Kridelbaugh et al. (1972)
(2) Uhlmann et al. (1981)

Notes:

(a) glass veins
(b) glass coat(?)

TABLE 15028-2. Chemical analyses of matrix of 15028

		,8	,10
Wt %	SiO2	48.90	
	TiO2	1.79	2.00
	Al2O3	12.87	13.6
	FeO	14.16	14.5
	MgO	9.25	9.2
	CaO	10.37	9.8
	Na2O	0.5852	0.55
	K2O	0.4061	
	P2O5	0.3595	
(ppm)	Sc	29.9	28.7
	V	95.6	78
	Cr	2570	2410
	Mn	1470	1460
	Co	39.1	35.2
	Ni	200	135
	Rb	10.7	
	Sr	139,148	170
	Y	154	
	Zr	666	660
	Nb	48	
	Hf	17.0	18.0
	Ba	501	523
	Th	7.49	8.3
	U	2.37	2.37
	Pb		
	La	46.9	48.6
	Ce	130	127
	Pr	16.7	
	Nd	74	73
	Sm	19.7	21.9
	Eu	1.77	1.896
	Gd	26.2	
	Tb	4.53	4.42
	Dy	26.9	
	Ho	5.6	
	Er	17.4	
	Tm		
	Yb	15.8	15.5
	Lu	2.18	2.12
	Li	26.2	
	Be	7.59	
	B		
	C		
	N		
	S		
	F	84	
	Cl	29.7	
	Br	0.24	
	Cu	5.29	
	Zn	8.0	
(ppb)	I		
	At		
	Ga	3360	
	Ge	300	
	As	63	
	Se	350	
	Mo		
	Tc		
	Ru		
	Rh		
	Pd		
	Ag		
	Cd		
	In		
	Sn		
	Sb		
	Te		
	Cs	530	440
	Ta	2010	2080
	W	980	
	Re	0.51	
	Os		
	Ir		3.8
	Pt		
	Au	4.0	9.6
	Hg		
	Tl		
	Bi		
		(1)	(2)

References and methods:

(1) Wanke et al. (1977); XRF, INAA, etc.
(2) Korotev (1984 unpublished); INAA

15058 PORPHYRITIC-SUBOPHITIC QUARTZ-NORMATIVE MARE BASALT ST.8 2672.0 g

INTRODUCTION: 15058 is a coarse-grained and vuggy quartz-normative basalt containing pigeonite phenocrysts up to 2 cm long. It crystallized approximately 3.3 or 3.4 b.y. ago.

The rock was collected about 30 m east-northeast of the ALSEP central station. No other rocks as big as 15058 occur in the area (Fig. 1). It was less than one-fourth buried, and lacked fillets or dust. It is olive-gray, tough, blocky, and angular (Fig. 2), with a few zap pits.

PETROLOGY: 15058 is readily classified as a member of the Apollo 15 quartz-normative group of basalts: macroscopically it has abundant greenish pyroxene phenocrysts 1 to 2 cm long, and lacks olivine phenocrysts. Diktytaxitic vugs, acicular plagioclases (some with radiate patterns) (Fig. 3), and interstitial brown mafic grains and opaque phases are conspicuous. Thin sections (Figs. 4, 5) show the prominent complexly-zoned and twinned pigeonite phenocrysts, plagioclase laths and plates which evidently grew with hollow cores, and interstitial pyroxene, mesostasis, opaque phases, and cristobalite. Radiate structures are common, and rare relict olivines are surrounded by pigeonite.

The sample has always been classified as a quartz-normative basalt, under the different names used for that group; e.g. Brown et al. (1972a) call it a "pyroxene-rich, tridymite gabbro" of their Mare Basalt Type 1. Most petrographic reports have been restricted in scope but short general descriptions were given by Gay et al. (1972) and Juan et al. (1972). Pyroxenes have received most attention. They contain inclusions, including spinels and Ni-iron, and exsolved platelets. Microprobe analyses of the pyroxenes (Gay et al., 1972; Morawski et al., 1972; Papike et al., 1972; and Bence and Papike, 1972) are summarized in Figure 6 and Table 2. Cores of Mg-pigeonite ($En_{68}Wo_5$) are zoned to ~$En_{43}Wo_{17}$, then mantled by sub-calcic augite which is also zoned ($En_{43}Wo_{33}$ to $En_{34}Wo_{36}$). The pyroxenes in the cores of plagioclase are distinct ($En_{38}Wo_{14}$) according to Gay et al. (1972), who also did not find pyroxferroite (although Grove and Bence, 1978 refer to the existence of pyroxferroite in 15058, and Papike et al., 1972, and Bence and Papike, 1972, show an analysis close to pyroxferroite in composition). Bence and Papike (1972) discuss minor element trends, noting a sharp increase in Ti/Al to ~1/2 (corresponding to a drop in Al) when augite enters the crystallization sequence. Exsolution is visible under the microscope, and was studied by single-crystal x-ray diffraction (Gay et al., 1972; Papike et al., 1972) and TEM (Grove, 1982) methods. Papike et al. (1972) stress that the pigeonite cores do not show exsolution (Fig. 7). The exsolution features are consistent with slow cooling (Papike et at., 1972; Grove, 1982). Bence and Papike (1972) also note that the phenocrysts have no regular forms and may be resorbed. Mossbauer studies by Burns et al. (1973), made possible because of the large phenocrysts, show

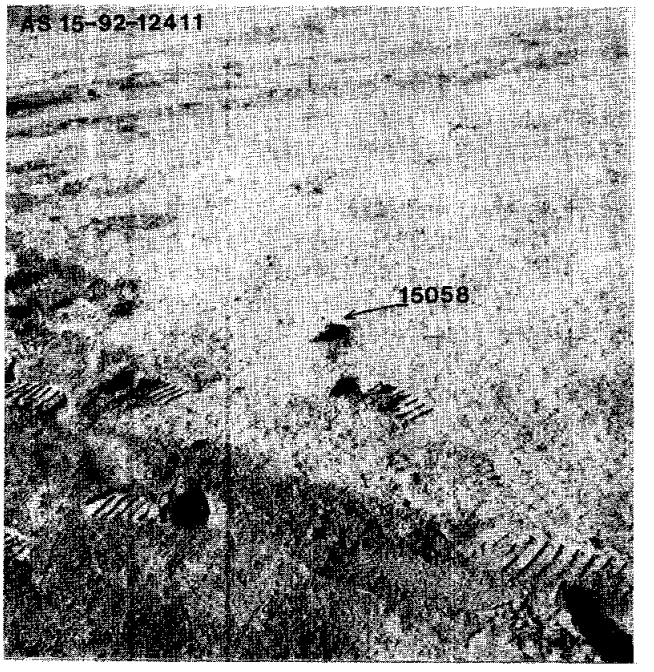

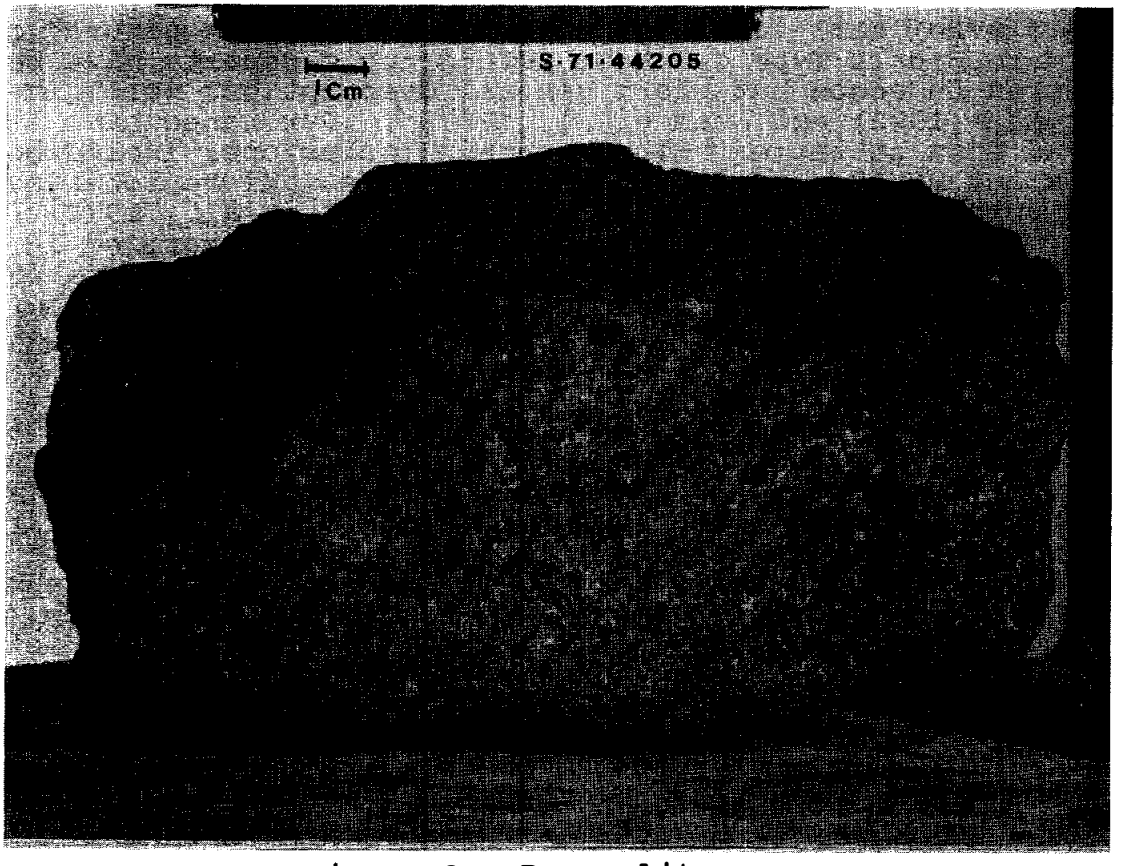

Figure 2. Pre-split.

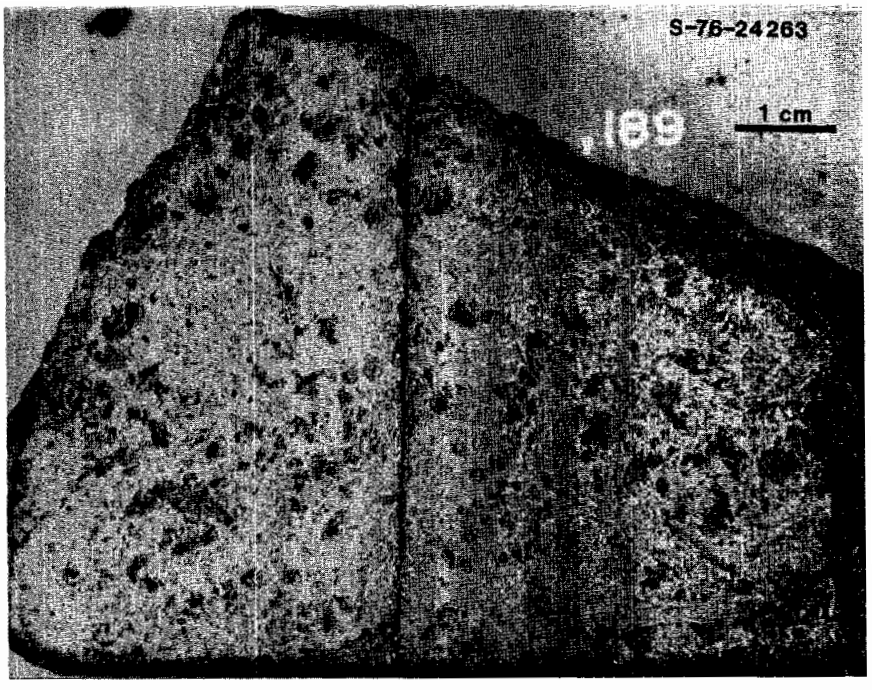

Figure 3. Diktytaxitic texture in sawn faces.

Figure 4. Whole thin section 15058,130.

Fig. 5a

Fig. 5b

Figure 5. Photomicrographs of 15058,130, all crossed polarizers.
(a) olivine phenocryst and lathy hollow plagioclases;
(b) radiate growth of plagioclase, pigeonite twins;
(c) twinned, zoned pigeonite phenocrysts.

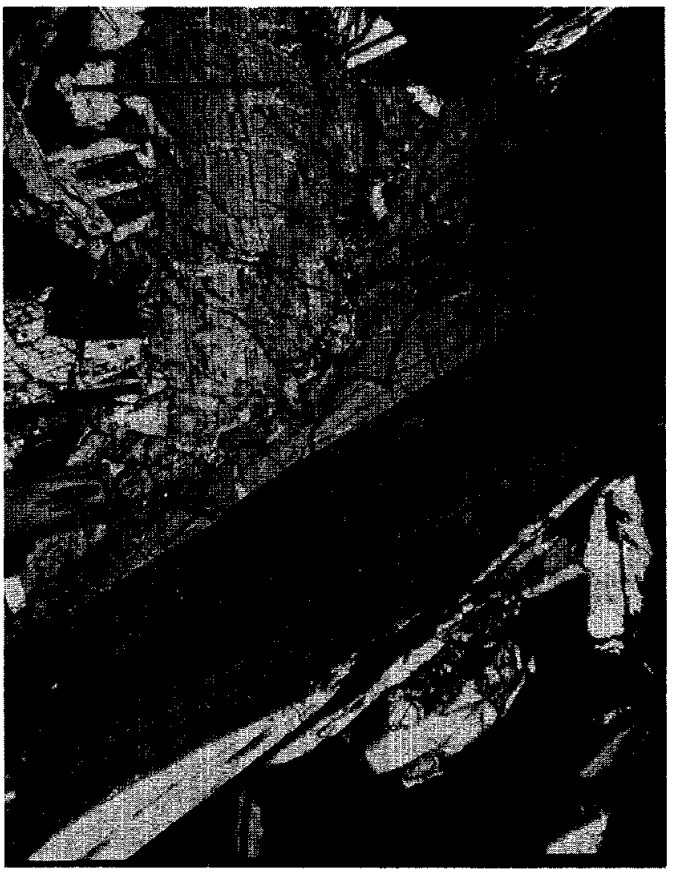

Fig. 5c

TABLE 15058-1. Modes of 15058

Reference	Cpx	Pl	Opq	Crist	Meso	Ol	Tr/Fe
A15 Info. Cat. (1971)	71[a]	24	2-3	1	1	tr	<0.6
Rhodes and Hubbard (1973)	68.3	27.1	3.5	1.5	0.6	1.8	0.3
Juan et al. (1972)	72	22	2	3			<1

(a) 56% phenocrysts, 15% groundmass

Figure 6. Compositions of pyroxenes (Papike et al., 1972).

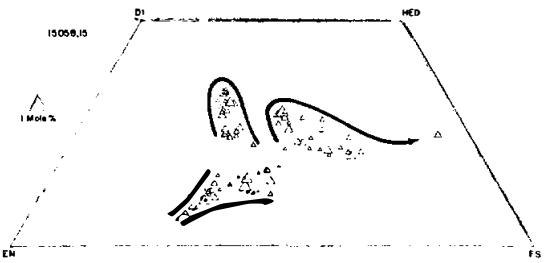

TABLE 15058-2. Representative microprobe analyses of pyroxenes in 15058 (Bence and Papike, 1972)

	1	2	3	4	5	6	7	8	9	10	11
SiO_2	52.0	50.9	51.4	52.5	51.7	51.3	50.7	50.4	48.2	51.6	51.5
Al_2O_3	2.01	3.95	1.81	3.07	2.41	2.81	2.07	1.31	1.43	2.47	2.77
TiO_2	0.53	0.58	0.40	0.61	0.65	0.71	0.66	0.84	1.11	0.73	0.63
FeO	23.4	22.1	24.2	18.8	18.1	23.7	23.8	27.0	30.2	15.4	14.5
MgO	15.3	15.6	15.4	17.9	14.6	14.0	13.9	10.4	7.41	14.4	14.2
CaO	5.24	6.50	5.37	6.14	11.1	7.40	7.46	9.80	10.8	14.1	14.7
Na_2O	0.0	0.0	0.0	0.05	0.06	0.02	0.01	0.01	0.03	0.04	0.03
Cr_2O_3	0.86	0.58	0.66	1.18	1.14	0.93	0.74	0.54	0.45	1.05	1.06
	99.3	100.2	99.2	100.3	99.8	100.9	99.3	100.3	99.6	99.8	99.4
Si	1.982	1.921	1.973	1.946	1.953	1.943	1.956	1.969	1.942	1.943	1.941
Al^{IV}	0.018	0.079	0.027	0.054	0.047	0.057	0.054	0.031	0.058	0.057	0.059
Al^{VI}	0.072	0.097	0.055	0.080	0.060	0.068	0.040	0.029	0.010	0.053	0.064
Ti	0.015	0.017	0.012	0.017	0.018	0.020	0.019	0.025	0.034	0.021	0.018
Fe	0.745	0.698	0.778	0.584	0.571	0.752	0.769	0.882	1.017	0.486	0.458
Mg	0.872	0.875	0.879	0.990	0.824	0.790	0.798	0.606	0.444	0.805	0.798
Ca	0.214	0.263	0.221	0.244	0.447	0.300	0.309	0.410	0.464	0.568	0.593
Na	0.000	0.000	0.000	0.004	0.004	0.002	0.001	0.000	0.002	0.003	0.002
Cr	0.026	0.017	0.020	0.035	0.034	0.028	0.022	0.017	0.014	0.031	0.031

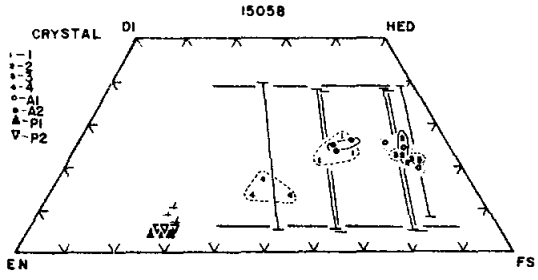

Figure 7. Pyroxene exsolutions (Papike et al., 1972).

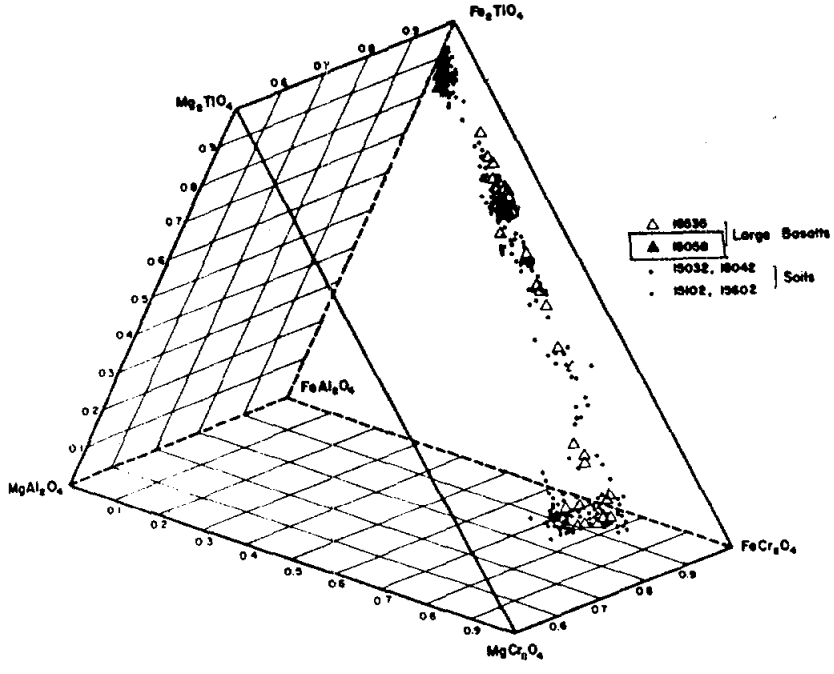

Figure 8. Spinel compositions (Haggerty, 1972d).

negligible Fe^{3+} and Cr^{2+}, but significant Cr^{3+} and Ti^{3+}, as well as Fe^{2+}. Absorption spectral measurements also failed to show Fe^{3+}. Morawski et al. (1972) did Mossbauer studies, on hand-separated pyroxenes, finding that Fe^{2+} site preference differed in pigeonite and augite. They also did not detect Fe^{3+}, but also did not find Ti^{3+} in their polarized absorption spectra. Abu-Eid et al. (1973) did not find Fe^{3+}, did find Ti^{3+} in rims, Cr^{3+} in core pigeonites, and probably no Cr^{2+} in pyroxene. They depict their absorption spectra for a 15058 zoned pyroxene. The characteristics of pyroxene nucleation density, size and trace element zoning trends, and exsolution, have been extensively used in deciphering the cooling history of 15058 (below).

According to Gay et al. (1972) plagioclases are ~An_{90} and are unzoned, with x-ray diffraction showing transitional anorthite structures. Some have rectangular cores of Fe-pigeonite, which are probably trapped because there is no orientation relationship. In contrast, Juan et al. (1972) report that the composition of the plagioclase is An_{78}. Wenk et al. (1973) report An_{89}, and describe antiphase b-domains found in their TEM studies, as well as submicroscopic structures which characterize the beginning of exsolution. They did not observe c-domains.

Haggerty (1972b,c) reported studies of the spinel series; 15058 contains only Cr-Al-ulvospinel (Fig. 8). Taylor and McCallister (1972a,b) and Taylor et al. (1972) analyzed Zr in ilmenite and ulvospinel to elucidate the thermal history (below). Roedder and Weiblen (1972) observed late immiscible high-Si and high-Fe melt inclusions in 15058 but report no data. Engelhardt (1979) inferred a paragenesis of plag-->ilm-->px from ilmenite textural relations, which contrast with other workers' conclusions that pyroxene is the obvious first-crystallizing phase. Drever et al. (1973) and Donaldson et al. (1977) published the same diagram (Fig. 9) illustrating subophitic/ophitic textural relationships between pyroxenes and plagioclase as well as chemical trends (microprobe data) in a discussion of radiate structures, but did not specifically discuss the diagram or 15058. Simmons et al. (1975) studied microcracks, using techniques which essentially determine the pressures at which cracks close. A large proportion of the cracks in 15058 close at ~300 bars. Simmons et al. (1975) illustrate sigmoidal cracks in matrix pyroxenes, and state that they are probably from the same process that produced curved cracks in phenocrysts. Huffman et al. (1972, 1974) tabulate magnetic and Mossbauer data obtained to elucidate the state and distribution of iron: no metal was detected in the Mossbauer study but a very small amount, 0.058%, was revealed in the magnetic studies. 98.6% of the Fe^{2+} resides in pyroxene, 1.4% in ilmenite, and no olivine was detected.

Cooling rate: Thermal histories have been deduced from mineralogical and textural characteristics, in many cases using the results of experimental studies for comparison. Bence and Papike (1972) preferred a two-stage cooling history, the first fast while phenocrysts crystallize, the second slower during

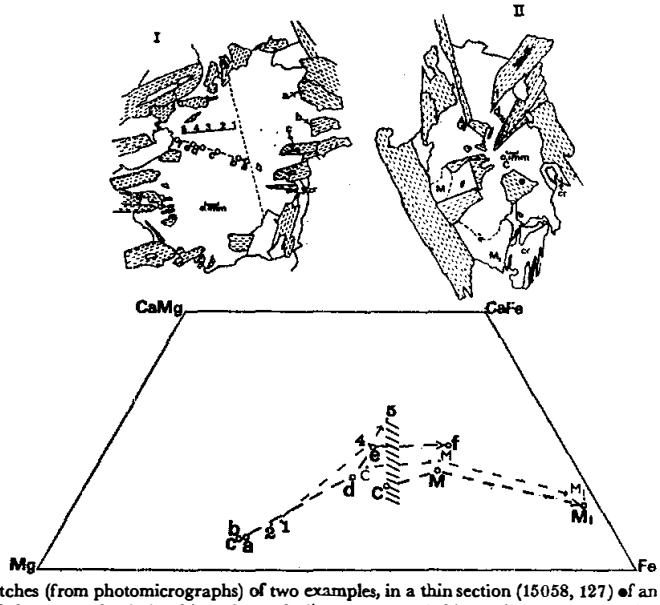

Sketches (from photomicrographs) of two examples, in a thin section (15058, 127) of an Apollo 15 mare basalt, of the textural relationships of zoned clinopyroxenes (white, subophitic and twinned in I; white, ophitic in II) and zoned plagioclase (dashed). The numbers or letters (C, M, M_1 refer to pyroxene II) correspond approximately with microprobe analyses in the positions shown in these sketches; arrows indicate in the quadrilateral the inferred directions of crystal growth; cr-cristobalite, opaques omitted. In pyroxene II the position of the second three determinations only approximately coincided with the first three but are given the same lettering (C, M, M_1). The area hachured is the approximation to the pyroxene composition at the time when plagioclase began to crystallize, inferred from the textural relations. Two independent series of microprobe analyses on these pyroxenes were made as a check on accuracy.

Figure 9. Radial growth in 15058,127 (Donaldson et al., 1977).

plagioclase crystallization. Taylor and McCallister (1972a,b) used the distribution of Zr between ilmenite and ulvospinel to deduce thermal aspects, concluding that Zr was "quenched in" at a high temperature compared with other rocks. Lofgren et al. (1975), with a direct comparison of phenocryst morphologies and rock textures with the products of experiments run at known linear cooling rates, concluded that both phenocrysts and matrix cooled at <1°C/hr. Grove and Walker (1977) used an experimental study on (the near isochemical) 15597 as a basis for comparison of pyroxene nucleation density (Fig. 10) to deduce an early rate of 0.04°C-0.2°C/hr., and from plagioclase size (Fig. 11) deduced a later rate of ~0.1°C/hr, i.e., roughly linear. They caution that no real significance could in any case be attached to differences between deduced early and late-stage cooling rates for such coarse basalts, and their slowest experiments (0.5°C/hr) did not quite reproduce the crystal sizes of the rock. They calculate that 15058 crystallized at least 300 cm from a conductive boundary. Grove and Bence (1977) used the minor element chemistry of pyroxenes produced in the same experiments as a basis for comparision with natural 15058 data. 15058 pigeonite cores are similar to those produced in 3.75°C/hr, but the absolute rates are not well-constrained. 15058 cooled rapidly enough for plagioclase nucleation to be supressed, but probably less than 0.5°C/hr. Grove (1982) used a "lamellae coarsening speedometer" for exsolution, using TEM techniques, comparable with grainsize-based cooling rate estimates. Pyroxene microlites have structures similar to those in slow cooling-rate experiments. An integrated cooling rate of ~0.02°C/hr is similar to that derived from plagioclase data (Walker et al., 1977) which gave 0.1°C/hr from ~1050°C to 950°C, from which a 300°C average of ~0.03°C/hr can be deduced.

EXPERIMENTAL PETROLOGY: While experiments on the near-isochemical sample 15597 (e.g., Bence and Grove 1977) are relevant, little experimental data for 15058 rock powders themselves are available. Humphries et al. (1972) briefly report the results of equilibrium, low-pressure experiments on 15058 (Fig. 13), and these results are shown in various projections by O'Hara and Humphries (1977). The sample crystallizes a little olivine prior to pigeonite entry, and the olivine is resorbed before plagioclase crystallizes. They claim there is little iron loss in their experiments. As for other Apollo 15 quartz-normative basalt samples, Humphries et al. (1972) prefer the hypothesis that 15058 is a pyroxene cumulate from a cotectic (px + pl) liquid, and was erupted at ~1150°C, not the ~1220°C liquidus of the experiments (see Walker et al., 1977 for the case against this hypothesis).

CHEMISTRY: Published chemical analyses are listed in Table 3. While comprehensive, there is not much duplication for minor elements; only one set of rare-earth data exists (Fig. 14). Little specific comment on the analyses exist other than to note the similarity with other Apollo 15 quartz-normative basalts. Gibson et al. (1975) note that sulfur abundances measured

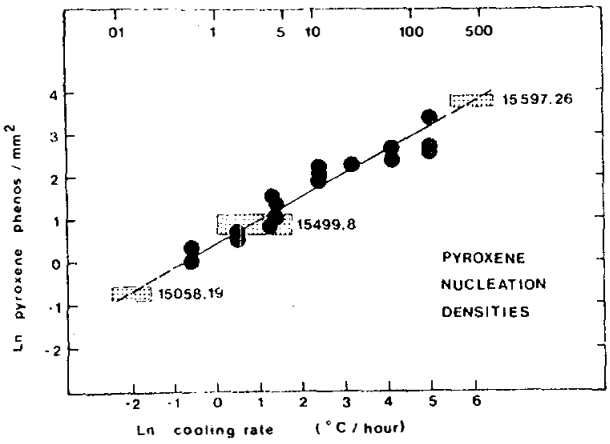

Figure 10. Pyroxene nucleation density/cooling rate (Grove and Walker 1977).

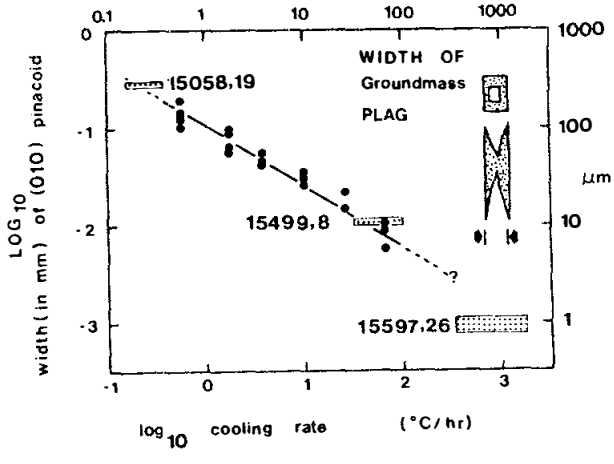

Figure 11. Plagioclase "size"/cooling rate (Grove and Walker 1977).

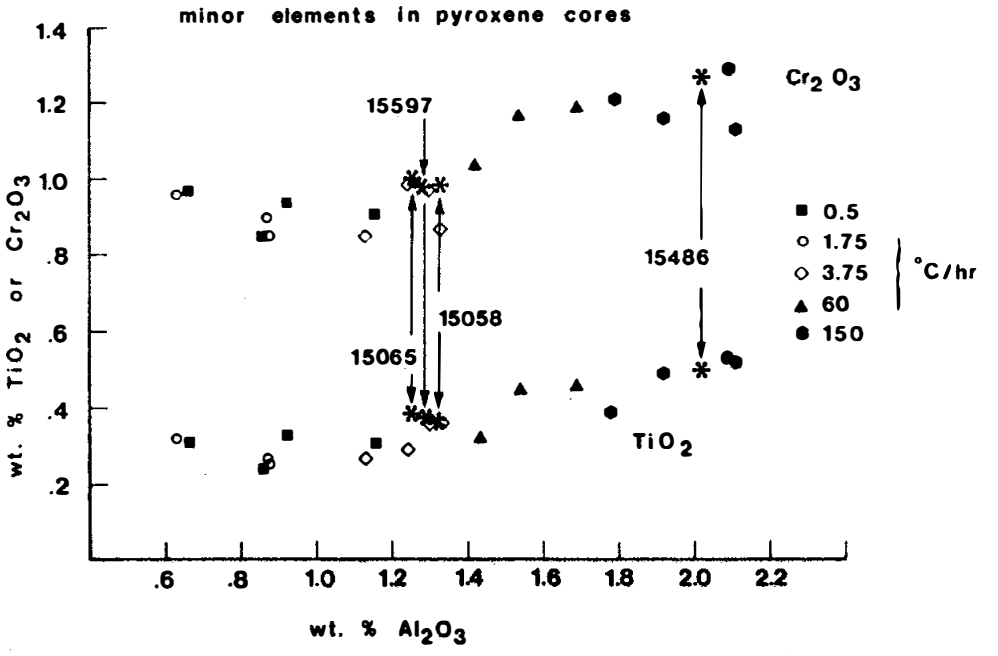

Comparison of minor element contents of pyroxene cores in Apollo 15 quartz-normative basalts with the pyroxene cores of the controlled cooling rate experiments. Weight percent Al_2O_3 is plotted against wt.% TiO_2 and Cr_2O_3. Asterisks indicate lunar samples and other symbols indicate the cooling rate experiments.

Figure 12. Minor elements in pigeonite cores/cooling rate (Grove and Bence 1977).

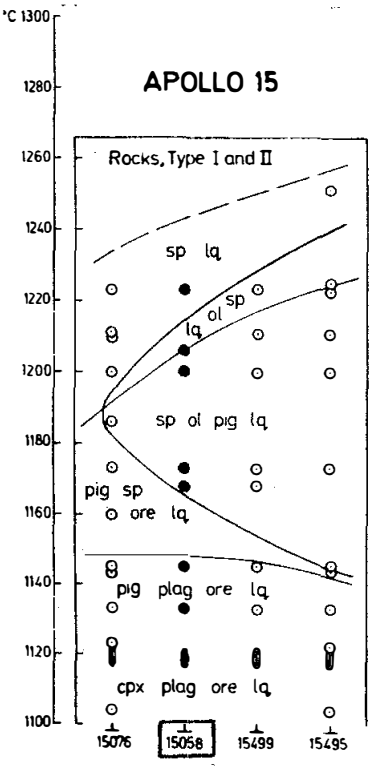

Figure 13. Low-pressure relationships (black dots) (Humphries et al., 1972).

TABLE 15058-3.

		,39	,76	,5	,9	,76	WR	,4	,86	,74	,72	,95	,32
Wt %	SiO2	48.47	46.7	47.81									
	TiO2	1.60	2.3	1.77	1.80								
	Al2O3	8.90	9.1	8.87	9.3								
	FeO	19.75	19.1	19.97	20.1	19.5							
	MgO	9.56	10.8a	9.01									
	CaO	10.23		10.32									12.3
	Na2O	0.28		0.28	0.2957								
	K2O	0.038		0.03			0.0486						0.0642
	P2O5	0.049		0.08									
(ppm)	Sc				46	42							
	V												
	Cr	4600			2865	2840		5870, 3800, 4790					
	Mn	2120	2600	2200									
	Co				42								
	Ni												
	Rb	<2											
	Sr	99.2											
	Y	21.1											
	Zr	70.9				74,97b							
	Nb	4.9											
	Hf				2.6	1.80, 2.52							
	Ba	49											
	Th						0.52						
	U						0.13						
	Pb												
	La				6.0								
	Ce												
	Pr												
	Nd												
	Sm				4.1								
	Eu				1.08	0.96							
	Gd												
	Tb				0.9								
	Dy												
	Ho												
	Er												
	Tm												
	Yb				2.5								
	Lu				0.43								
	Li												
	Be								0.45				
	B												
	C							27 27		10			
	N												
	S	570		700							970	950	
	F												
	Cl												
	Br												
	Cu												
	Zn												
(ppb)	I												
	At												
	Ga												
	Ge												
	As												
	Se												
	Mo												
	Tc												
	Ru												
	Rh												
	Pd												
	Ag												
	Cd												
	In												
	Sn												
	Sb												
	Te												
	Cs												
	Ta				460								
	W												
	Re												
	Os												
	Ir												
	Pt												
	Au												
	Hg												
	Tl												
	Bi												
		(1)	(2)	(3)	(4)	(5)	(6)	(7) (8)	(9)	(10)	(11)	(11)	(12)

TABLE 15058-3 Continued

		,85	,209	,207
Wt %	SiO2			
	TiO2			
	Al2O3			
	FeO			
	MgO			
	CaO			
	Na2O			
	K2O	0.0398		
	P2O5			
(ppm)	Sc			
	V			
	Cr			
	Mn			
	Co			
	Ni		0.50	
	Rb	0.811c	0.646	
	Sr	99.5d		
	Y			
	Zr			
	Nb			
	Hf			
	Ba			
	Th			
	U		0.089	
	Pb			
	La			
	Ce			
	Pr			
	Nd			
	Sm			
	Eu			
	Gd			
	Tb			
	Dy			
	Ho			
	Er			
	Tm			
	Yb			
	Lu			
	Li			
	Be			
	B			
	C			5.3e
	N			<0.1
	S			671
	F			
	Cl			
	Br			
	Cu			
	Zn		0.94	
(ppb)	I			
	At			
	Ga			
	Ge		6.47	
	As			
	Se		56	
	Mo			
	Tc			
	Ru			
	Rh			
	Pd		<0.51	
	Ag		0.27	
	Cd		3.35	
	In		0.40	
	Sn		83	
	Sb		0.43	
	Te		2.0	
	Cs		26.7	
	Ta			
	W			
	Re		0.0006	
	Os		<0.02	
	Ir		0.0063	
	Pt			
	Au		0.081	
	Hg			
	Tl		0.22	
	Bi		<0.17	
		(13)	(14)	(15)

References to Table 15058-3

References and methods:

(1) Willis et al. (1972); XRF
(2) Janghorbani et al. (1973); NAA
(3) Rhodes and Hubbard (1973),PET (1972); XFR/AA
(4) Fruchter et al. (1973); INAA
(5) Ehmann et al. (1975); INAA, RNAA
(6) O'Kelley et al. (1972); -ray
(7) Desmarais et al. (1972); Combustion
(8) Moore et al. (1972); Combustion
(9) Eisentraut et al. (1972)
(10) Moore et al. (1973); Combustion
(11) Gibson et al. (1975); Combustion, hydrolysis
(12) Husain (1974); MS
(13) Birck et al. (1975); ID/MS
(14) Wolf et al. (1979); RNAA
(15) Desmarais (1978); Temp. releases

Notes:

(a) Authors reservation on accuracy.
(b) Averaged and corrected to 84.1 ppm by Garg and Ehamnn (1976)
(c) Calc. from ^{87}Rb.
(d) Calc. from ^{86}Sr.
(e) Only 2.5 ppm indigenous.

15058

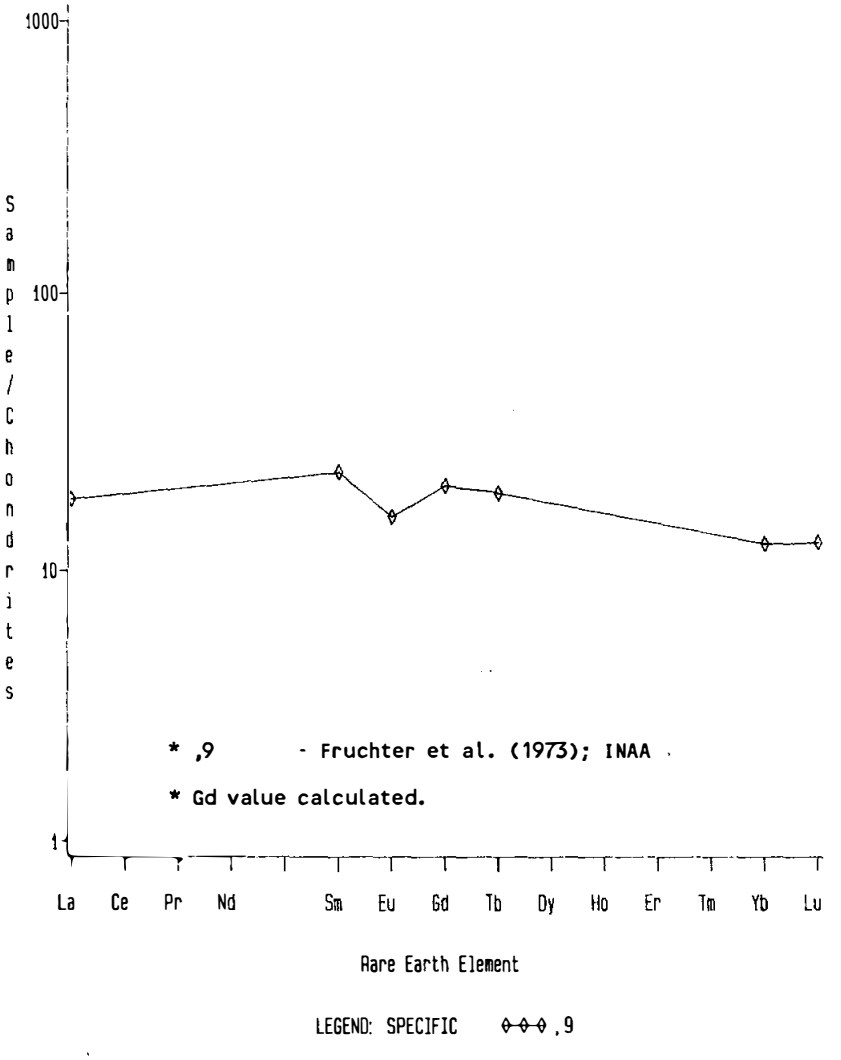

Figure 14. Rare earths in bulk rock.

following hydrolysis are lower than those following combustion, presumably because some sulfur is in an acid-resistant phase. Desmarais (1978) using a more refined method, found much lower carbon than in previous analyses and concluded (partly from isotopic analyses) that the carbon released at low temperature is a terrestrial contaminant. Apart from the data in Table 3, 12 micron moles H/gm were found by Desmarais et al. (1974); 17.4 and 21.2 ppm H by Gibson et al. (1975); and Janghorbani et al. (1973) analyzed for O (38.6%). Desmarais (1978) also quotes S=400 ppm in an unpublished check list of Moore. Oxides of carbon and CH4 data were presented by Gibson and Moore (1972), Gibson et al. (1975) and Desmarais et al. (1972).

Wolf and Anders (1980) quoted 15058 as a mare basalt with an atypically low Se content, a characteristic correlated with low U and Rb, and suggestive that the source reservoir has too little S and Se to be saturated with a sulfide at large degrees of partial melting.

Sato (1973) measured the oxygen fugacity in two splits over a range of temperatures, finding values (Fig. 15, Table 4) similar to other mare basalts and midway between the iron-wustite and iron-rutile-ferrospeudobrookite buffers.

STABLE ISOTOPES: Epstein and Taylor (1972) reported oxygen and silicon isotopic analyses (Table 5) for mineral separates. The data show no unusual characteristics; the plagioclase-clino-pyroxene difference is similar to other lunar basalts and appropriate for magmatic temperatures. Gibson et al. (1975) reported $^{34}S_{CDT}$0/00 = -0.5 and -0.6 for two splits. Desmarais (1978) reported ^{13}C data, finding a variation from -33.1% for a 420°C release to -3.3% for a 1270°C release. The lower temperature carbon is similar to terrestrial cloth fibers and plastics, etc. Assessing the possibility of spallation produced ^{13}C (because the high temperature value is high), Desmarais calculates a spallation age of 470 m.y., assuming original ^{13}C = -20.

RADIOGENIC ISOTOPES AND GEOCHRONOLOGY: Birck et al. (1975) determined a Rb-Sr internal isochron with an age of 3.46 ± 0.07 b.y. and initial $^{87}Sr/^{86}Sr$ of 0.69928 (Fig. 16, Table 6). They discuss and conclude they cannot deny the possibility that the "isochron" is a mixing line.

Husain (1974) found a good high temperature Ar-Ar plateau corresponding to an age of 3.358 ± 0.025 b.y. (Fig. 17), although significant radiogenic ^{40}Ar has been lost from the samples (variously stated as 7.5%, 8.6%, and 8.9% in the paper; 9% in Husain, 1972). This loss leads to a lower K-Ar age of 3.213 ± 0.015 b.y.

RARE GASES, EXPOSURE AND TRACKS: Husain (1974) tabulates an exposure age of 135 ± 7 m.y. derived from high temperature (>1000°C) Ar releases. Eldridge et al. (1972) list ^{22}Na, ^{26}Al,

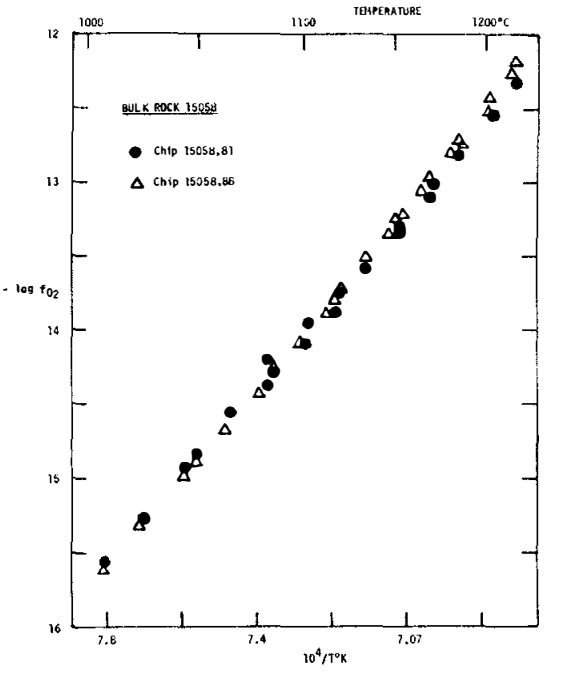

Figure 15. fO_2 of two chips measured separately (Sato et al., 1973).

TABLE 15058-4. Oxygen fugacity (-log fO_2) as a function of temperature (Sato et al., 1973)

	1000°C	1050°C	1100°C	1150°C	1200°C
15058,81	15.7	14.9	14.0	13.3	12.6
15058,88	15.7	14.9	14.0	13.3	12.5

TABLE 15058-5. O and Si isotopic data (Epstein and Taylor, 1972)

	δO^{18}	δSi^{30}
cpx	5.73 ± 0.04	-0.31 ± 0.05
pl	6.13 ± 0.05	-0.14 ± 0.10

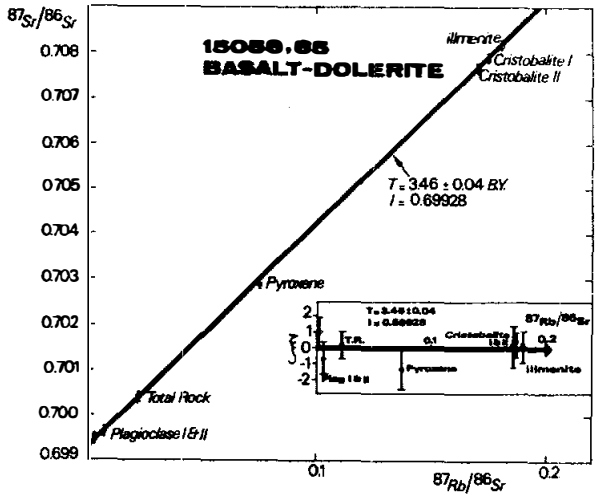

Figure 16. Rb-Sr internal isochron (Birck et al., 1975).

TABLE 15058-6. K, Rb, Sr concentrations and isotopic composition for 15058,85 (Birck et al., 1975)

Samples	Weight (mg)	K (ppm)	^{87}Rb (ppm)	^{86}Sr (ppm)	$^{87}Rb/^{86}Sr$[1]	$^{87}Sr/^{86}Sr$[2,3]
15058,85						
Total rock	26.7	332	0.2254	9.85	0.02262	0.70040 (6)
Plagioclase	38.3	545	0.1197	35.9	0.00320	0.699507 (60)
Plagioclase	31.2	605	0.297	40.44	0.0073	0.69659 (7)
Pyroxene	12.9	143	0.1364	1.800	0.0749	0.70288 (9)
Cristobalite	2.7	2275	1.361	7.715	0.1743	0.70789 (5)
Ilmenite	3.2	367	0.366	2.005	0.1804	0.70818 (7)
Cristobalite	1.5	3360	1.416	1.416	8.223	0.70767 (8)

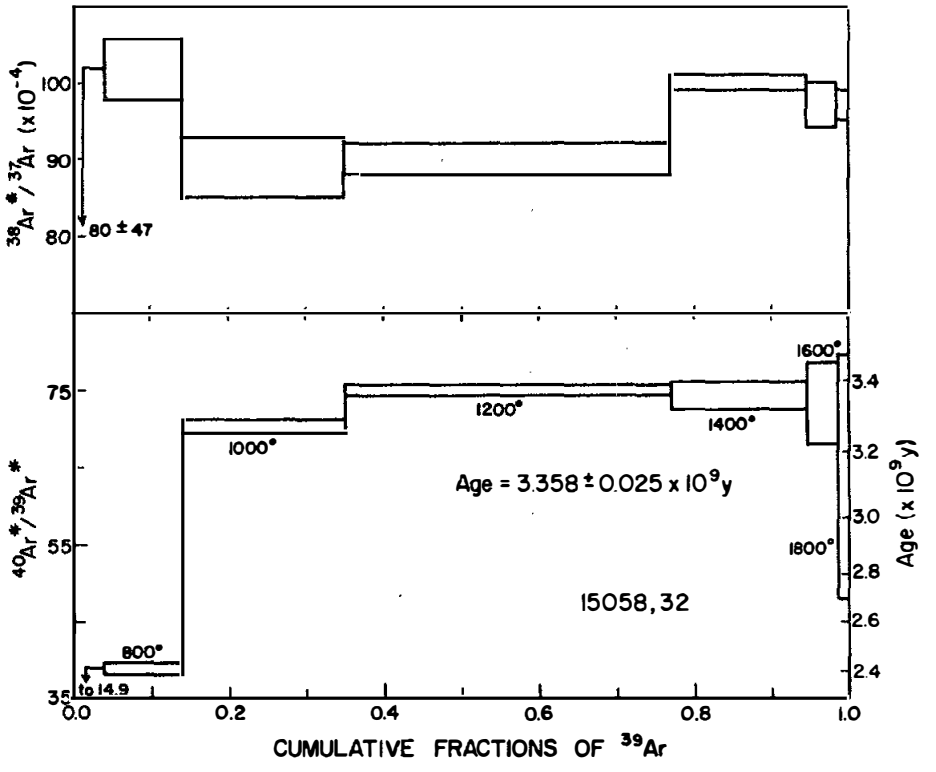

Comparison of the $^{40}Ar^*/^{39}Ar^*$ and $^{38}Ar^*/^{37}Ar$ release diagrams for crystalline rock 15058.32. The 1000° and 1200°C fractions show an $^{38}Ar^*/^{37}Ar$ plateau. The 1200°C and higher-temperature fractions exhibit an $^{40}Ar^*/^{39}Ar^*$ plateau typical of many lunar basalts.

Figure 17. Ar release diagram (Husain, 1974).

and ^{54}Mn data without specific discussion. The data are similar to that for (near-isochemical) 15065 in which ^{22}Na and ^{26}Al appear to be saturated, and 15058 is listed as saturated with ^{26}Al by Yokoyama et al. (1974). Thus 15058 has been exposed for at least ~2 m.y.

Track determinations result in lower ages. Bhandari et al. (1972, 1973) illustrate the track density/depth profile, which is steep at depths less than 0.1 cm (Fig. 18). A suntan age (2 m.y.) is lower than the subdecimeter age (10 m.y.) and illustrates a multiple history; the low suntan age probably results from the friability of the rock, as with other Apollo 15 samples. Poupeau et al. (1972) studied tracks and produced a density vs. depth profile for feldspar. The lunar top-face showed no solar flare irradiation, in contrast with the bottom, which gives an exposure age of 1/2-2 m.y. Generally the track density is low, and in the outer millimeter variable because of erosion differences. Galactic tracks have a flat profile with little variation, indicating that most were registered under heavy shielding. Crozaz et al. (1974) in tabulating exposure ages for 15058 (and other rocks), list a "single-point determination" of 25 m.y., referencing Poupeau et al. (1972) as the source. Fleischer et al. (1973) studied track densities in located samples. Olivine has a low density, probably because some heating event has erased tracks--the relevant shock event was less than 7 m.y. ago. Short tracks, if produced by spallation, suggest a near-surface age of a few hundred million years; cosmic ray track densities require 2,000 m.y. under 10 cm of cover or a few hundred million years at shallower depth, suggesting a long near-surface exposure history prior to the 7 m.y. track-erasing event. Crozaz et al. (1974) tabulate a 10 m.y. "single point determination" unpublished data by Yuhas.

PHYSICAL PROPERTIES: Nagata et al. (1972a,b, 1973, 1975) tabulate basic magnetic data and the results of NRM determinations from demagnetization (Fig. 19). 15058 has a hard component of NRM ~1×10^{-6} emu/gm, with a direction which is reasonably invariant for fields greater than 100 Oe.rms. TRM demagnetizing experiments suggest that the NRM is attributable to a TRM acquired by cooling from at most 300°C. If the stable component of NRM can be attributed to PTRM, the ambient lunar magnetic field is estimated to be 2,000 . Banerjee and Mellema (1974) used an ARM method and determined a field of 4,900 , a result which Collinson et al. (1975) suggested must be treated with caution: the method is valid for single domain grains whereas lunar mare basalts are dominantly multidomain.

Schwerer et al. (1974) determined the variation of electrical conductivity with temperature (Fig. 20). They found large decreases in conductivity following heating in reducing atmospheres, a process which produces Fe-metal. (They also show Mossbauer spectra.) Schwerer et al. (1974) note that Housley, in a review of the paper, suggested that the low conductivity of 15058 might result from its high porosity and its high density of

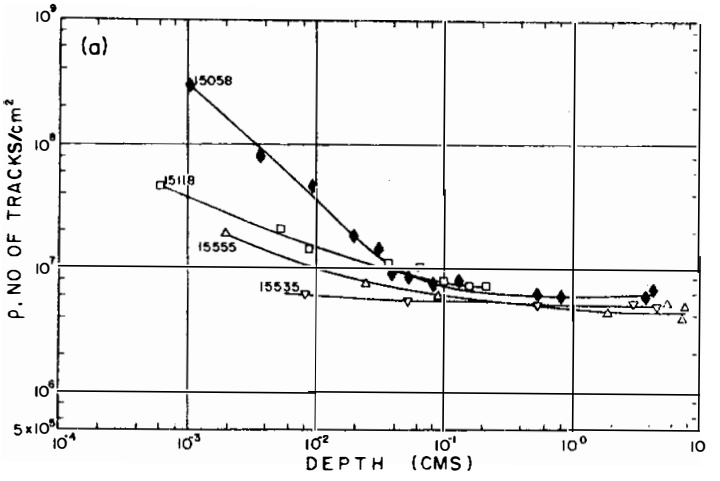

Fig. 18a

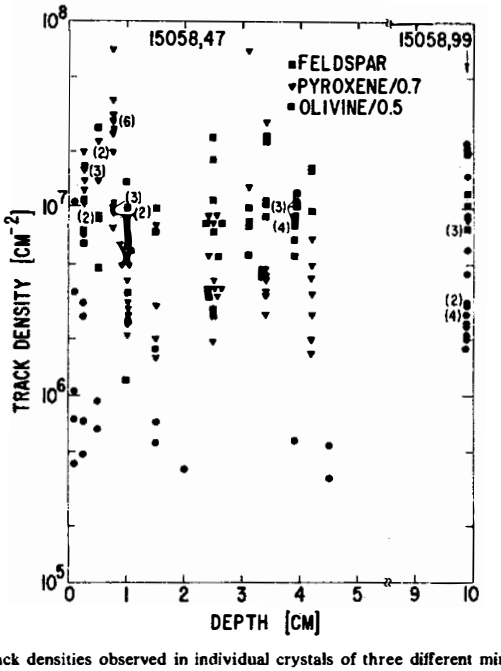

Track densities observed in individual crystals of three different minerals of 15058,47 and 15058,99. The pyroxenes show evidence of shock.

Fig. 18b

Figure 18. Track density studies (a) Bhandari et al. (1973), black diamonds; (b)-(d) Fleischer et al. (1973).

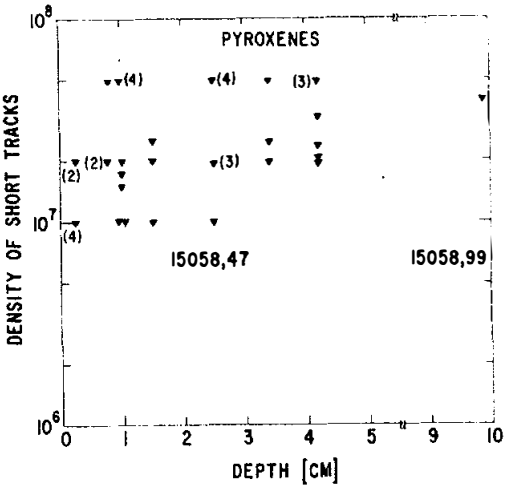

Density of short tracks (≤ 1.5 μ in length) in pyroxenes from 15058.

Fig. 18c

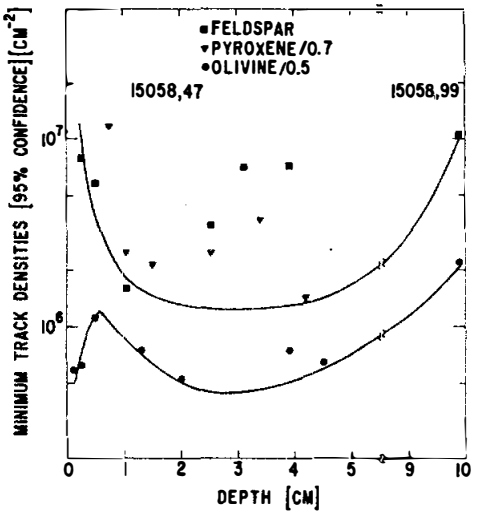

Minimum track densities (95% confidence) at each position sampled in 15058. Curves show the smoothed lower limits for feldspars plus pyroxenes and for olivines.

Fig. 18d

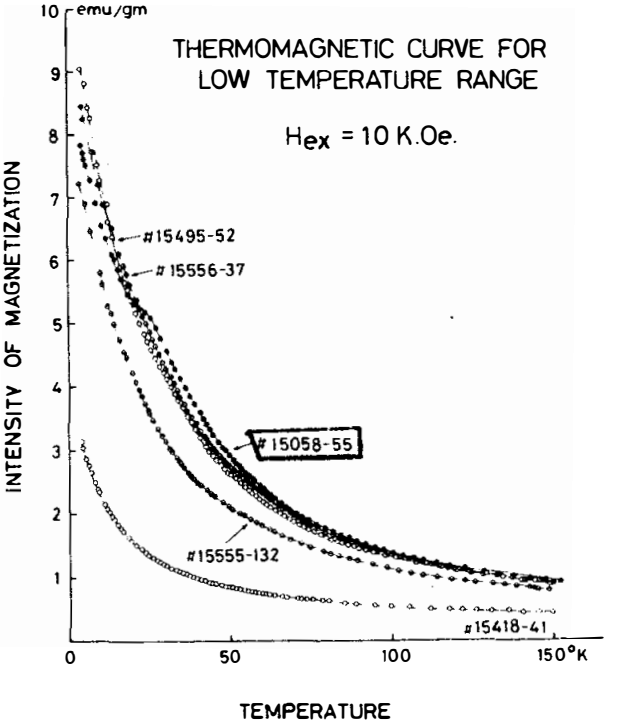

Thermomagnetic curves of Apollo 15 samples in a temperature range between 4.2°K and 150°K.

Figure 19. Thermomagnetic curve for 15058 and other Apollo 15 samples (Nagata et al., 1973).

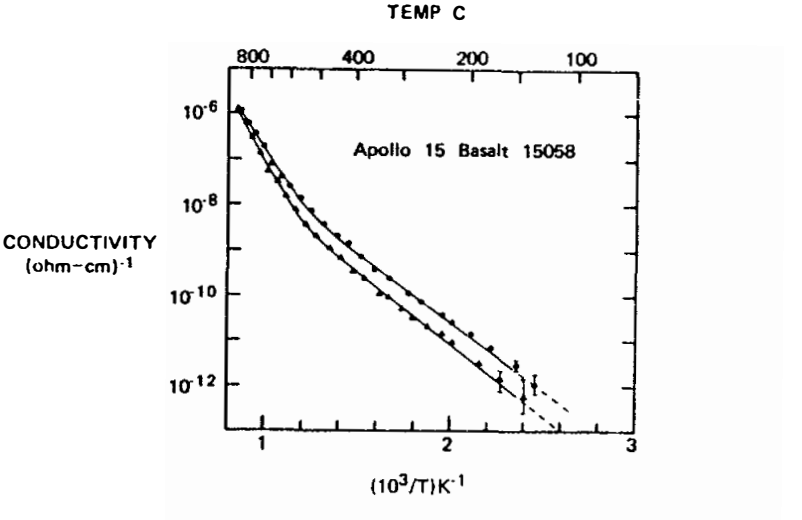

Figure 20. Conductivity vs. temperature (Schwerer et al., 1974).

microcracks.

Mitzutani and Newbigging (1973) list a density of 2.99 gm/cc and measurements of velocity as a function of pressure are tabulated as depicted (Fig. 21, Table 7). At high pressures 15058 is seismically similar to other rocks.

Charette and Adams (1975) depict the spectra from 0.5-2.5 microns for a powdered sample of 15058. It has a typical quartz-normative basalt pattern, with a narrow pyroxene band not widened by the presence of olivine.

PROCESSING AND SUBDIVISIONS: Following chipping of a few exterior fragments, 15058 was substantially sawn (Fig. 22). The interior slab ,24 and the orthogonal slab pieces ,27 (now 53 g) and ,30 (now 102 g) were substantially subdivided. ,29 (originally 558 g) has been totally subdivided, mainly into four large pieces >100 g, for PAO exhibits. The remaining large pieces ,26 (337 g) ,28 (321 g), and ,31 (620 g, in BSV) remain intact.

Thin sections were made from exterior chips (,11 and ,12) from the E face, and from ,60, a portion of the interior slab ,24 (Fig. 22).

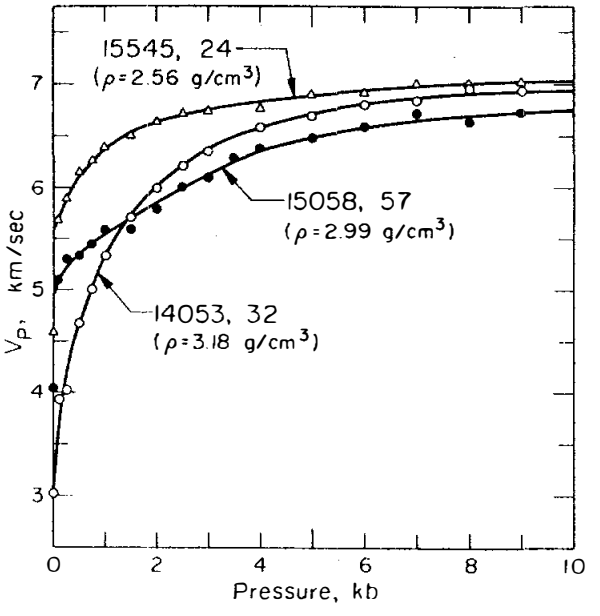

Figure 21. Seismic velocity vs. pressure (Mizutani and Newbigging, 1973).

TABLE 15058-7. Vp v. Pressure (Mitzutani and Newbigging, 1973)

Kb	0.0	0.5	1.0	2.0	3.0	5.0	7.0	9.0
Vp (km/spc)	4.03	5.33	5.54	5.85	6.12	6.49	6.65	6.73

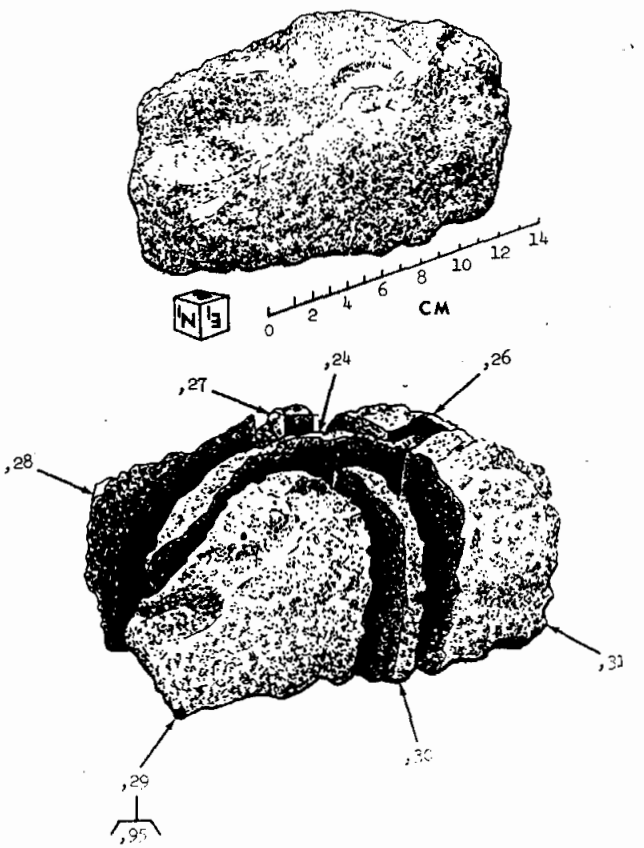

Figure 22. Main subdivision of 15058.

Figure 2. Sawing of 15059 to show glass coat.

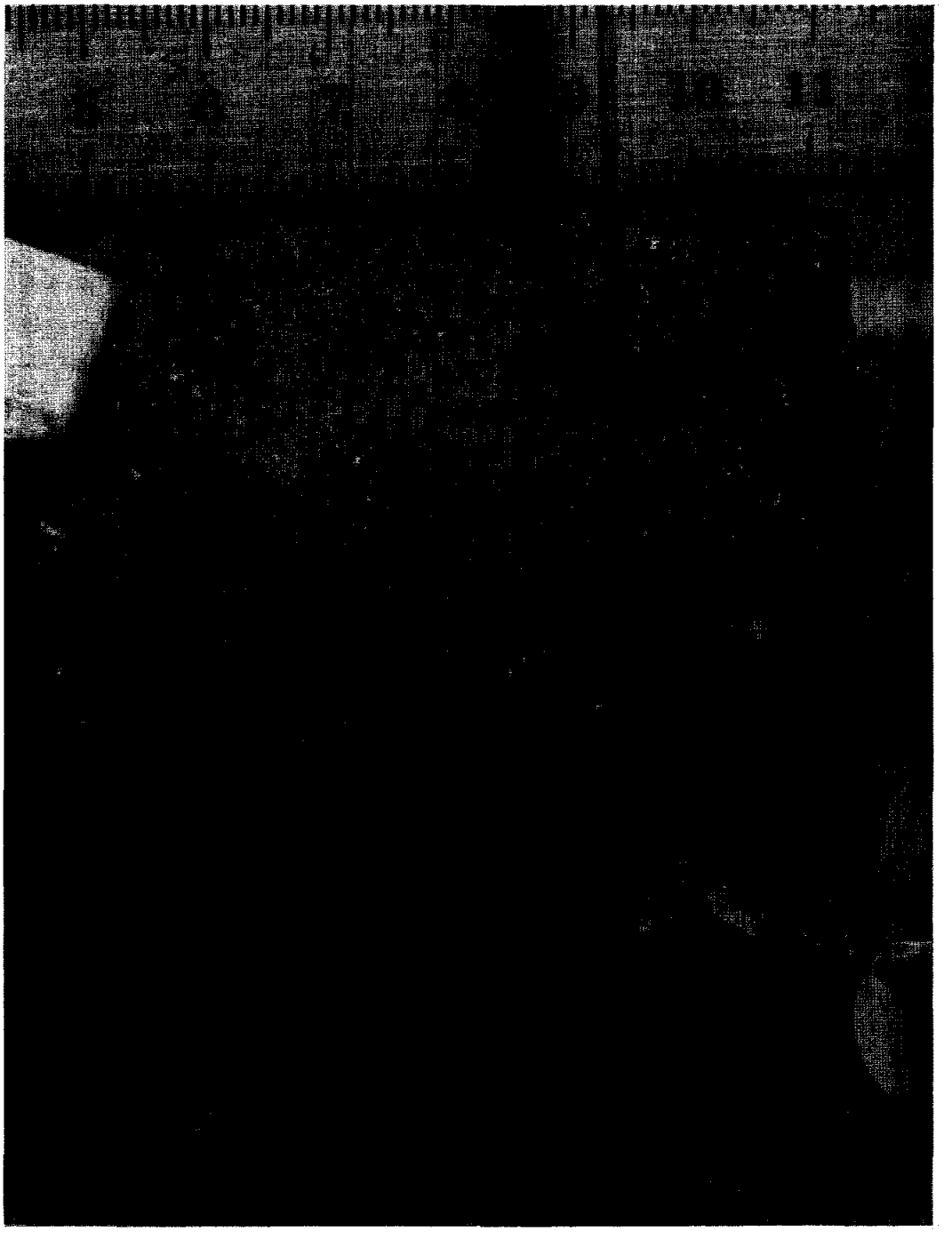

PETROLOGY: Macroscopically 15059 consists of about 55% unresolvable gray matrix enclosing identifiable fragments which are dominantly white or pale-colored but including green and orange materials. McKay and Wentworth (1983) found 15059 to have a compact intergranular porosity, an intermediate fracture porosity, spheres and agglutinates to be rare, and shock features to be common. Wentworth and McKay (1984) found the sample to have a bulk density of 2.19 g/cm^3. An I_s/FeO of 32-49 was reported by McKay et al. (1984) (reported as 36 by Korotev, 1984 unpublished), i.e., a submature index.

Kridelbaugh et al. (1972) provided a petrographic description. The sample consists of lithic fragments of basalt, microbreccias, glass of various shapes and colors, and monomineralic fragments set in a cryptocrystalline, unrecrystallized matrix (Figs. 3, 4). There are crosscutting veinlets of a highly vesicular glass. The basalts are ophitic pyroxene basalts without olivine, containing plagioclase (An_{87-92}), ilmenite, Ti-chromite, Fe-metal, troilite, and residual phases. Microbreccia clasts are subordinate to the basalts and are noritic (orthopyroxene and plagioclase) with minor high-Ca pyroxene, ilmenite, olivine, and whitlockite. The monomineralic fragments are low-Ca pyroxenes, augitic pyroxenes, plagioclases (An_{95-76}), olivines (Fo_{89-44}), ilmenite (0 to 5% MgO), Fe-metal (1.5-14.0% Ni), troilite, and Ti-chromites.

Figure 3. Interior breccia matrix of 15059 as exposed in sawn slab.

Fig. 4a

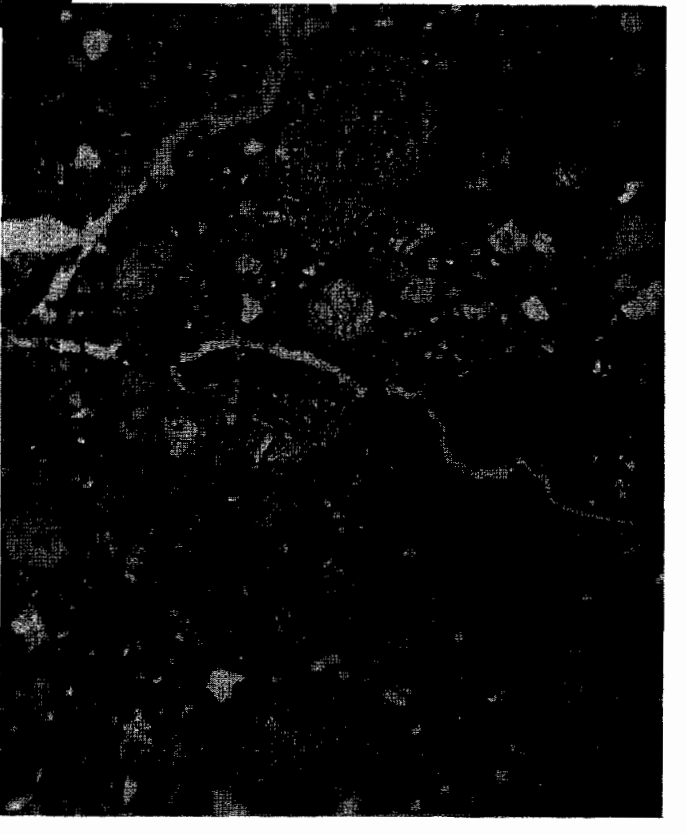

Fig. 4b

Figure 4. Photomicrographs of the 15059,48 breccia matrix, transmitted light (a) also shows vesicular glass coat.

Glasses form 20% by volume, and individual pieces are generally homogeneous. Mare basalts are most abundant, with Fra Mauro (KREEP) slightly less. Apollo 15 green glasses are present. Analyses presented by Kridelbaugh et al. (1972) did not distinguish glasses from 15028 and 15059. The glass in the veinlets is the same as the coat, and both were probably emplaced during excavation of the sample.

CHEMISTRY: Fruchter et al. (1973) reported the acquisition of data for 22 subsamples, including physically separated clasts. The published data are presented in Tables 1 and 2 and Figure 5. The matrix samples show 15059 to be homogeneous on a mm-scale, and to be very similar to neighboring soil, e.g. 15021; the

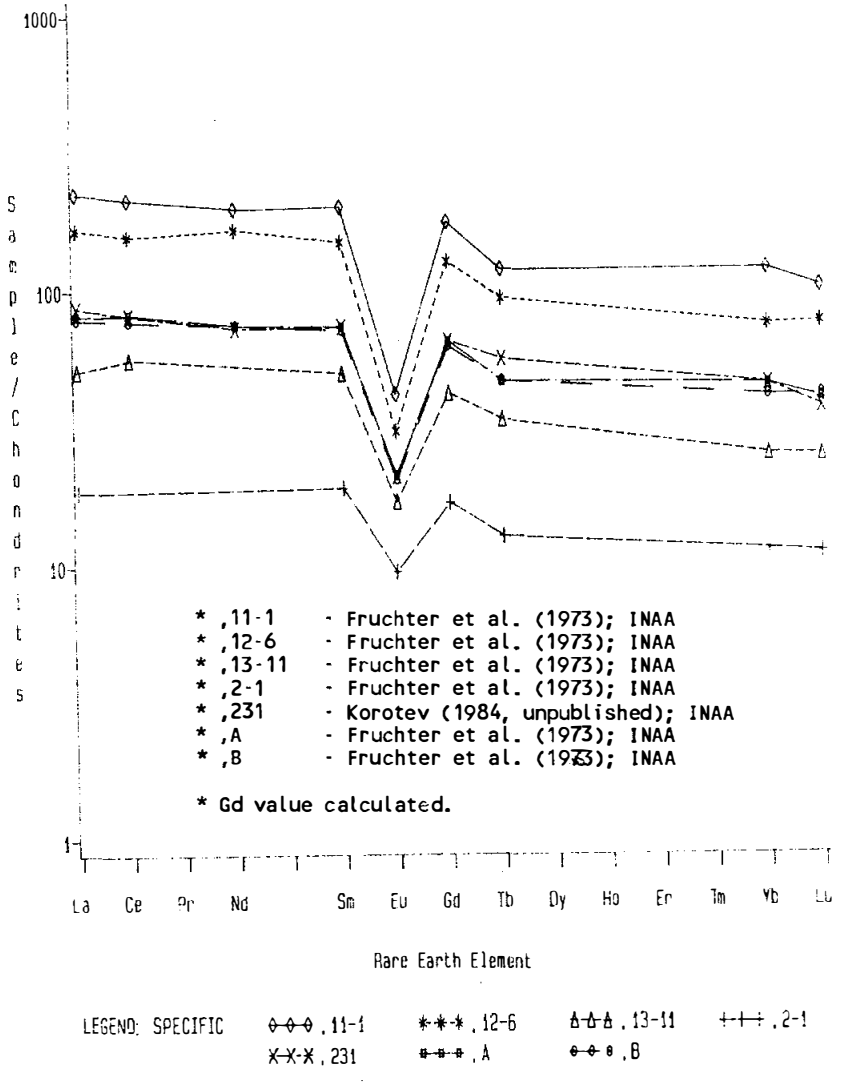

Figure 5. Rare earths in matrix (upper two curves) and clasts in 15059.

TABLE 15059-1. Chemical analyses of breccia matrix

		,13-1	,Aa	,231
Wt %	SiO2			
	TiO2		1.99	1.73
	Al2O3		13.31	13.6
	FeO		14.8	15.0
	MgO			10.4
	CaO			10.2
	Na2O		0.4631	0.45
	K2O		0.196	
	P2O5			
(ppm)	Sc		30	28.9
	V			100
	Cr		2890	2840
	Mn			1520
	Co		42	61.6
	Ni			615
	Rb	5.8		
	Sr			165
	Y			
	Zr		330	420
	Nb			
	Hf		10.0	10.7
	Ba		300	287
	Th		4.8	4.9
	U	1.31		1.35
	Pb			
	La		27.0	28.8
	Ce		73	72
	Pr			
	Nd		45	44
	Sm		13.4	13.4
	Eu		1.48	1.46
	Gd			
	Tb		2.2	2.65
	Dy			
	Ho			
	Er			
	Tm			
	Yb		9.1	9.1
	Lu		1.38	1.28
	Li			
	Be			
	B			
	C			
	N			
	S			
	F			
	Cl			
	Br	0.115		
	Cu			
	Zn	13.5		
(ppb)	I			
	At			
	Ga			
	Ge	306		
	As			
	Se	225		
	Mo			
	Tc			
	Ru			
	Rh			
	Pd			
	Ag	5.4		
	Cd	35.5		
	In	2.7		
	Sn			
	Sb	0.99		
	Te	15.5		
	Cs	2455		280
	Ta		1200	1310
	W			
	Re	0.55		
	Os			
	Ir	7.0		6.2
	Pt			
	Au	2.45		<4
	Hg			
	Tl	2.4		
	Bi	0.88		
		(1)	(2)	(3)

References and Methods:

(1) Ganapathy et al. (1973); INAA
(2) Fruchter et al. (1973); INAA
(3) Korotev (1984 unpublished); INAA

Notes:

(a) average of 7 analyses

TABLE 15059-2. Chemical analyses of glass coat and clasts

		,Bb	,2-1c	,13-11d	,11-1	,12-6e
Wt %	SiO2					
	TiO2	2.00	1.60	1.87	2.8	2.09
	Al2O3	13.8	6.03	9.96	15.5	16.0
	FeO	14.8	21.8	17.5	13.5	11.9
	Mg					
	CaO					
	Na2O	0.4700	0.189	0.339	0.850	0.767
	K2O	0.215	0.041	0.128	0.593	0.419
	P2O5					
(ppm)	Sc	30	27	30	29	24
	V					
	Cr	2880	4600	4300	2400	2550
	Mn					
	Co	44	73	57	30	28
	Ni					
	Rb					
	Sr					
	Y					
	Zr	300			730	680
	Nb					
	Hf	9.4	2.5	6.3	25.5	19.3
	Ba	270			820	670
	Th	4.2	1.1	2.9	13.4	9.7
	U					
	Pb					
	La	26.0	6.2	17.0	75.0	55.0
	Ce	68		50	189	140
	Pr					
	Nd	45			120	100
	Sm	13.0	3.5	9.1	36.7	27.3
	Eu	1.42	0.66	1.18	2.91	2.14
	Gd					
	Tb	2.2	0.6	1.6	5.6	4.4
	Dy					
	Ho					
	Er					
	Tm					
	Yb	8.3	2.3	5.1	24.0	15.0
	Lu	1.42	0.38	0.86	3.48	2.59
	Li					
	Be					
	B					
	C					
	N					
	S					
	F					
	Cl					
	Br					
	Cu					
	Zn					
(ppb)	I					
	At					
	Ga					
	Ge					
	As					
	Se					
	Mo					
	Tc					
	Ru					
	Rh					
	Pd					
	Ag					
	Cd					
	In					
	Sn					
	Sb					
	Te					
	Cs					
	Ta	1200			3000	210
	W					
	Re					
	Os					
	Ir					
	Pt					
	Au					
	Hg					
	Tl					
	Bi					
		(1)	(1)	(1)	(1)	(1)

References and Methods:

(1) Fruchter et al. (1973); INAA

Notes:

(b) glass coat/veins, average of 3 analyses
(c) mare clast
(d) mare-appearing clast macroscopically
(e) norite (probably A15 KREEP basalts)

15065 PORPHYRITIC SUBOPHITIC QUARTZ-NORMATIVE MARE BASALT ST. 1 1475.5 g

INTRODUCTION: 15065 is a coarse-grained quartz-normative basalt with pigeonite phenocrysts. It contains a pyroxene-rich segregation on one end. It is 3.3 b.y. old. It is blocky, subrounded (Fig. 1), and tough except on rounded surfaces. One end (laboratory W) is much more mafic than the rest of the rock and is a pyroxene accumulation--this portion is also more vuggy than the rest of the sample (Fig. 1). A few zap pits appear on most surfaces.

15065 was collected on the east flank of Elbow Crater, as one of several samples collected on a line extending out from the crater (Fig. 2). 15065 was closest to the crater, only 4 m east of the rim crest. The lunar orientation is known.

PETROLOGY: 15065 is a coarse-grained inequigranular basalt (often termed gabbro) with prismatic/euhedral pigeonite crystals which have greenish cores and red-brown rims. Most are 3 to 5 millimeters long. Plagioclases are white, anhedral to subhedral, and up to approximately 2.5 mm long.

15065 is a coarse member of the quartz-normative basalt group (e.g., Brown et al., 1972; Gay et al., 1972 and others), and is one of the most slowly-cooled members of that group. It is a little unusual for this group in containing a few percent magnesian olivine (Brown et al., 1972 and others) (Fig. 3d) and conspicuous tridymite laths (Fig. 3d,f). Published modes are listed in Table 1. (According to Juan et al., 1972 the sample contains nepheline but they have apparently misidentified tridymite.) Fayalite is conspicuous with residual phases (tridymite, ulvospinel, etc.) in some sections, growing larger than 1 mm (Fig. 3d). In general the sample has been described as consisting of phenocrysts in a finer-grained groundmass of Ca-poor ferroaugite, calcic plagioclase, Fe-Ti oxides, minor sulfide and metal, prominent accessory apatite, and a residuum containing cristobalite and tridymite.

The few ragged anhedral Mg-olivines (Fo_{50-52}; Longhi et al. (1972) are enclosed by pyroxenes (Fig. 3d). Walker et al. (1977) record that grains of such olivine (which is unstable below 1100°C) are unzoned and homogeneous but each has a slightly different composition (Fo_{50-55}). The grains are large (~60 um) and differ from liquidus olivines for this composition (Fo_{74}). The cooling rate was apparently slow enough to homogenize olivines by diffusion. The olivines produce some peculiar effects in crystallization experiments (see Walker et al. 1977).

The pyroxenes are composite, complexly zoned, and twinned (Fig. 3); some are hollow crystals (Fig. 3c). Some are complexly intergrown with plagioclase (Fig. 3b), with patches of pyroxene appearing to be poikilitically enclosed in plagioclase but optically continuous with larger pyroxenes. According to Longhi

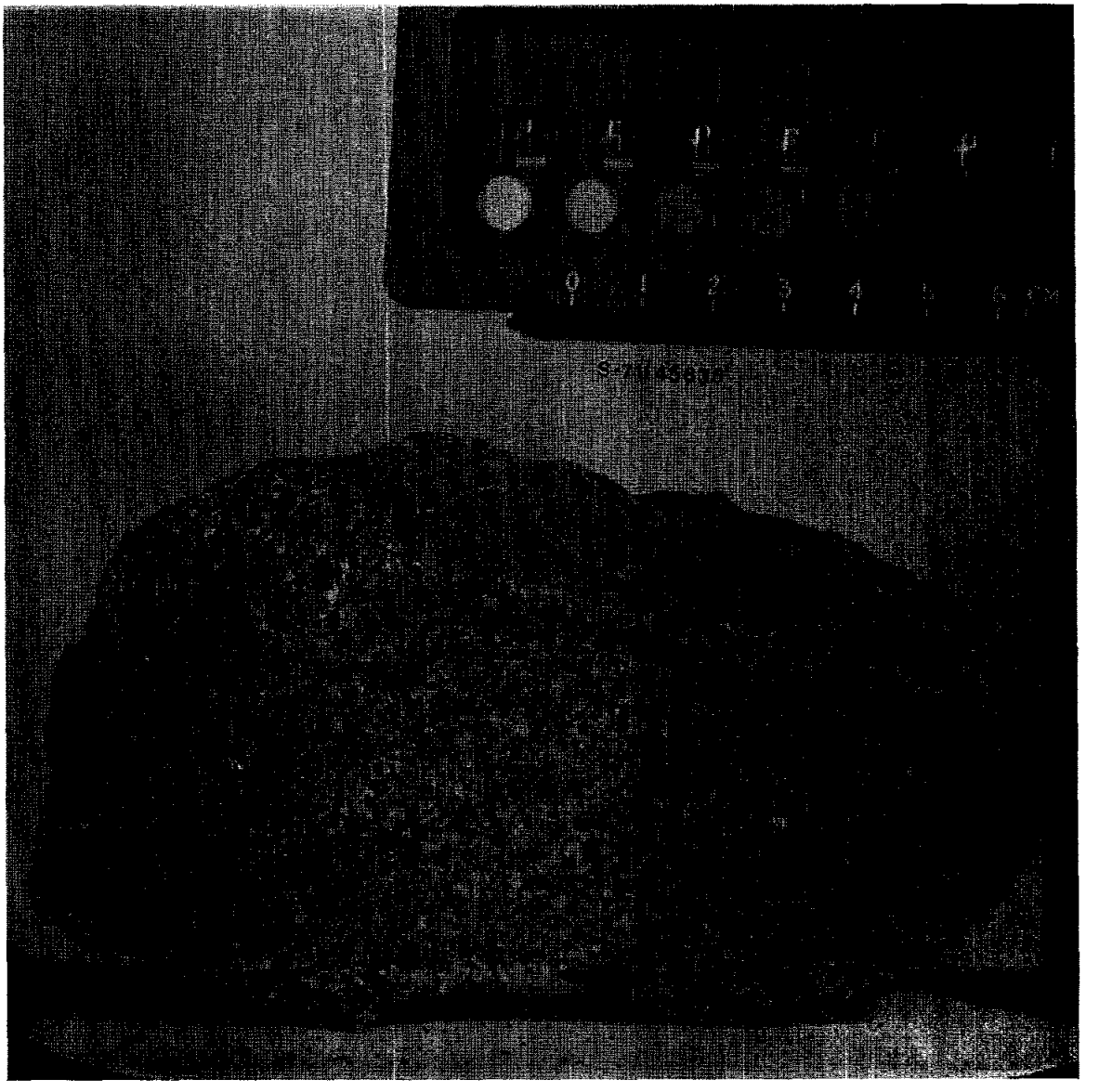

Figure 1. Pre-split picture of 15065, showing vuggy mafic segregation on B/W end (left), and normal coarse texture.

Figure 2. Sampling location of 15065 near the Elbow Crater rim.

Fig. 3a

Figure 3. Photomicrographs of 15065 all to same scale. (a) Gabbroic aspect in ,90, crossed polarizers; (b) pyroxene plagioclase complex intergrowth in ,74, crossed polarizers; (c) pyroxene phenocrysts showing hollow core in ,91, crossed polarizers; (d) Mg-olivine cores (fo) surrounded by pyroxene and residual fayalite (fa) olivine grain tridymite (tr) and ulvospinel (opaque) in ,81, crossed polarizers; (e) euhedral chromites in pyroxene core, with anhedral interstitial ulvospinel and ilmenite in ,90, plane transmitted light (f) tridymite (tr) laths with ulvospinel (opaque) in ,81, transmitted light.

Fig. 3b

Fig. 3c

Fig. 3d

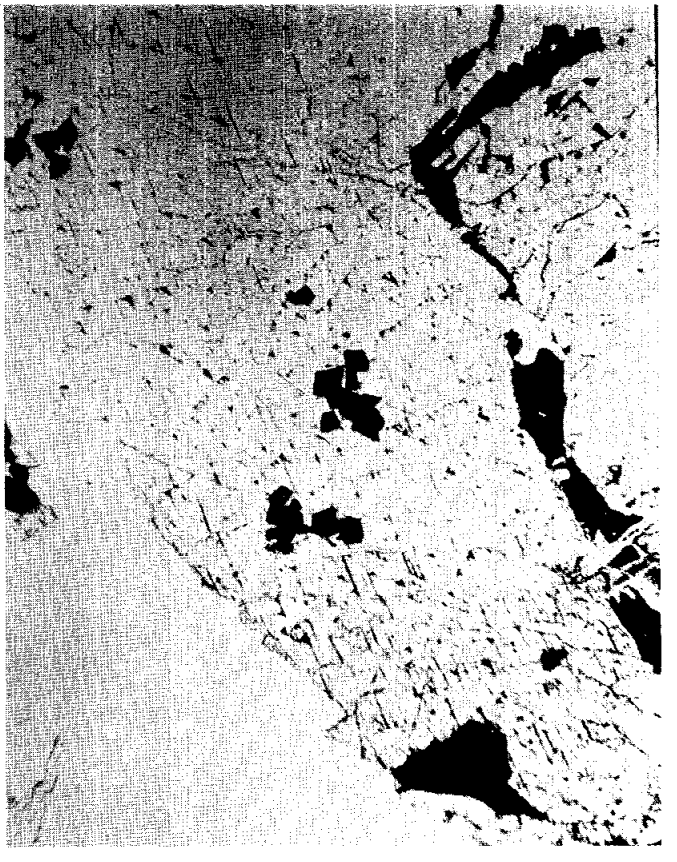

Fig. 3e

TABLE 15065-1. Published modes of 15065

Sample	Ol	Plag	Cpx	Gl+Sil	Opaques	Reference
,90	--	27	70	--	2	Juan et al.(1972)
,86	1.3	31.6	63.0	1.9	2.2	Longhi et al. (1972
--	2					Brown et al. (1972)

Fig. 3f

et al. (1972) this texture results from slow late-stage crystallization of these two phases. Details of pyroxene compositions are given by Grove and Bence (1977) (Fig. 4), in a study aimed at assessing cooling rates (below). Yajima and Hafner (1974) used x-ray diffraction and Mossbauer techniques to find the distribution of Fe^{2+} and Mg^{2+} over the M, and M_2 sites, finding a distribution corresponding to equilibration close to 600°C; they also provided microprobe analyses of pyroxenes. They found no trace of exsolved augite or of cation distribution resulting from shock. Nakazawa and Hafner (1976) noted that the precession plots of Yajima and Hafner (1974), while not showing high-temperature exsolution, do show a small amount of low-temperature augite exsolution. Jedwab (1972) described microvugs in pyroxenes as characterized with SEM, EMP, and photon microscope techniques. The vugs are complex and zonally arranged and contain small opaques and/or K-feldspar. Juan et al. (1972) reported 2v data for pyroxenes: 90° in the core pigeonites and 30° in subcalcic augite rims.

Most plagioclases are anhedral and they are often complexly twinned. They are zoned and often enclose pyroxenes poikilitically. According to Longhi et al. (1972) they are zoned from An_{91} to An_{80}, while Juan et al. (1972) merely reported a single value of An_{77}. Longhi et al. (1976) plotted An vs. Fe (Fe+Mg) of plagioclase crystals (Fig. 5), demonstrating a positive correlation of iron and sodium. Juan et al. (1972) stated that plagioclase probably crystallized earlier than clinopyroxene but with some coprecipitation; however this is in contrast with textural observations and experimental data which indicate that plagioclase crystallized later than pyroxene.

El Goresy et al. (1976) noted that 15065 and other coarse basalts contain corroded and rounded chromite cores as inclusions in Cr-ulvospinel, while idiomorphic Ti-chromites without any sign of optical zoning are included in olivine. The earliest chromite crystallized before plagioclase, probably before pyroxenes, and before or during olivine crystallization. El Goresy et al. (1976) diagrammed the zoning trends (Fig. 6a) and discussed the substitutions involved. Taylor et al. (1975) also analyzed spinels (Fig. 6b). Taylor and McCallister (1972a,b), Taylor et al. (1973, 1975), and Onorato et al. (1979) discussed the partitioning of Zr between ilmenite and ulvospinel, and the subsolidus reduction of ulvospinel to ilmenite and Fe-metal, as informants on cooling rates (below). Taylor et al. (1975) also analyzed Fe-metal compositions (Fig. 7). Jedwab (1972) described the iron as facetted and isometric, and probably of late crystallization. He also reported Ca-Fe phosphate deposited as hexagonal plates on a face-growing ilmenite crystal. Wark et al. (1973) presented an analysis of zirconolite, and Blank et al. (1982) used a proton probe to analyze for Zr and Nb in ilmenite/spinel pairs; they found ~200 ppm Zr in chromite, ~1000 ppm in ulvospinel, and ~10,000 ppm in ilmenite (Fig. 8).

Cooling rates: Lofgren et al. (1975), in a comparison of the

Figure 4. Pyroxene compositions (a) Grove and Bence (1977); (b) Yajima and Hafner (1974).

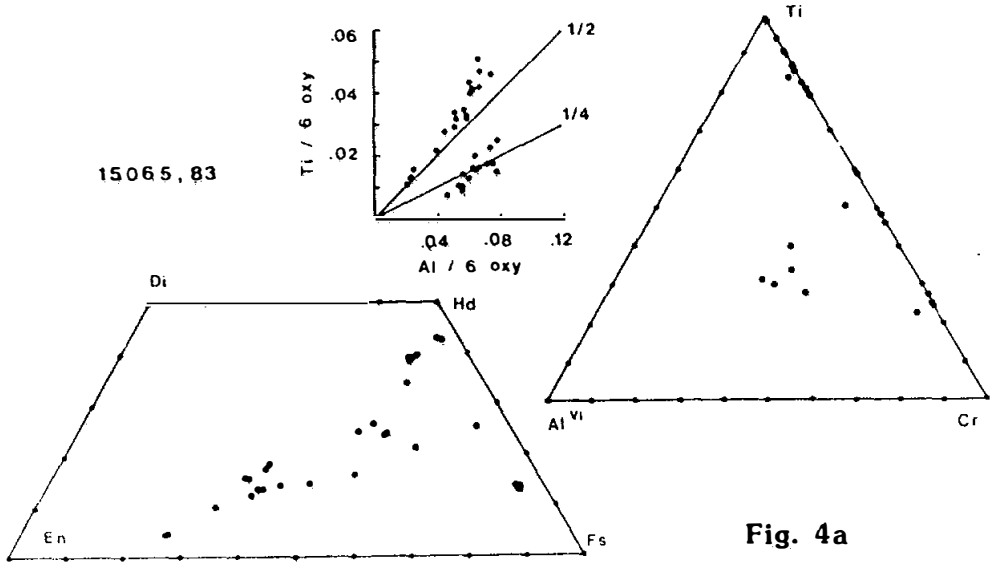

Fig. 4a

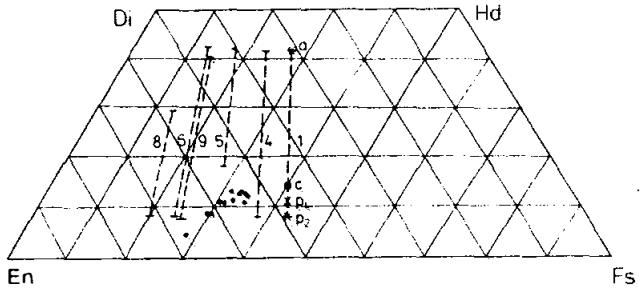

Fig. 4b

Figure 5. Plagioclase compositions (Longhi et al., 1976).

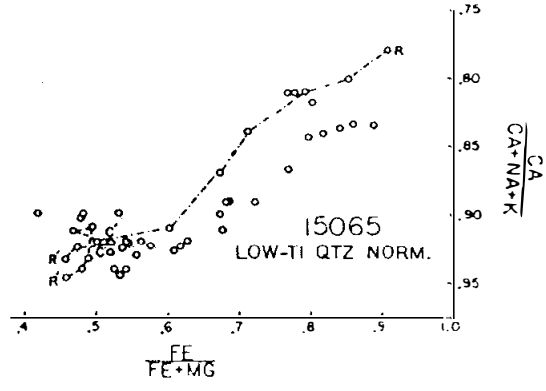

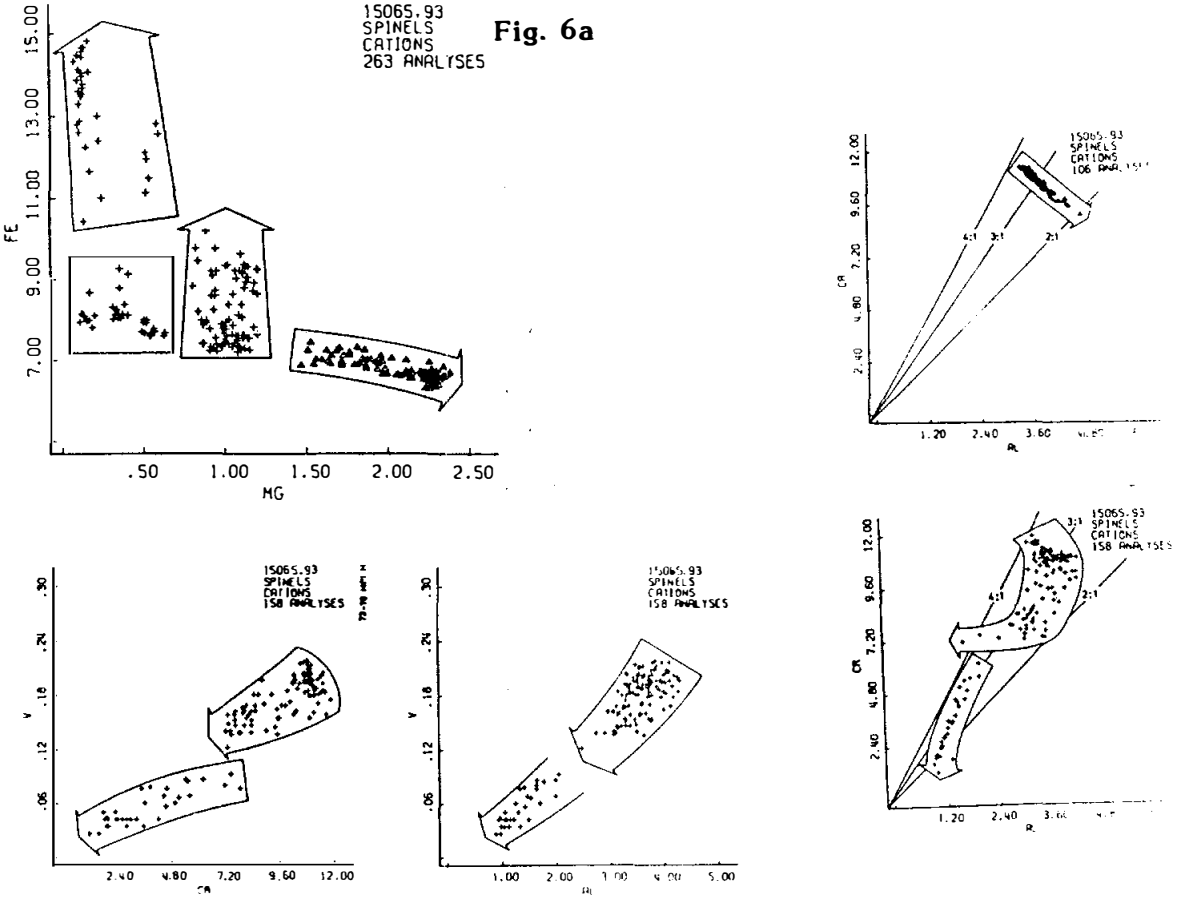

Fig. 6a

Fig. 6b

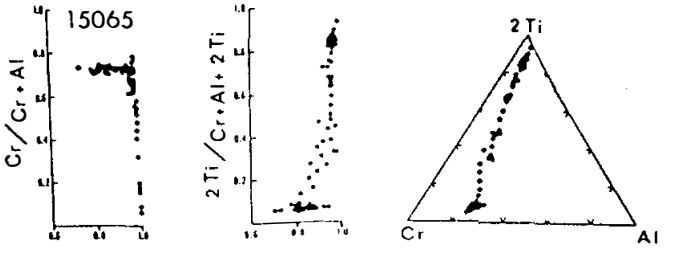

Figure 6. Spinel compositions. (a) El Goresy et al. (1976); (b) Taylor et al. (1975).

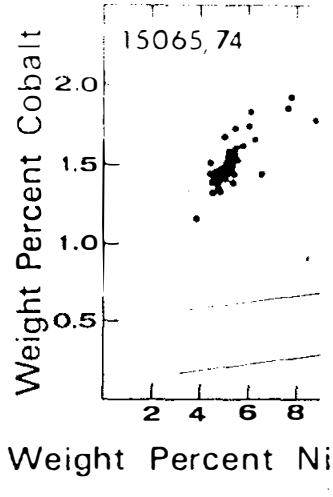

Figure 7. Fe-metal compositions (Taylor et al., 1975).

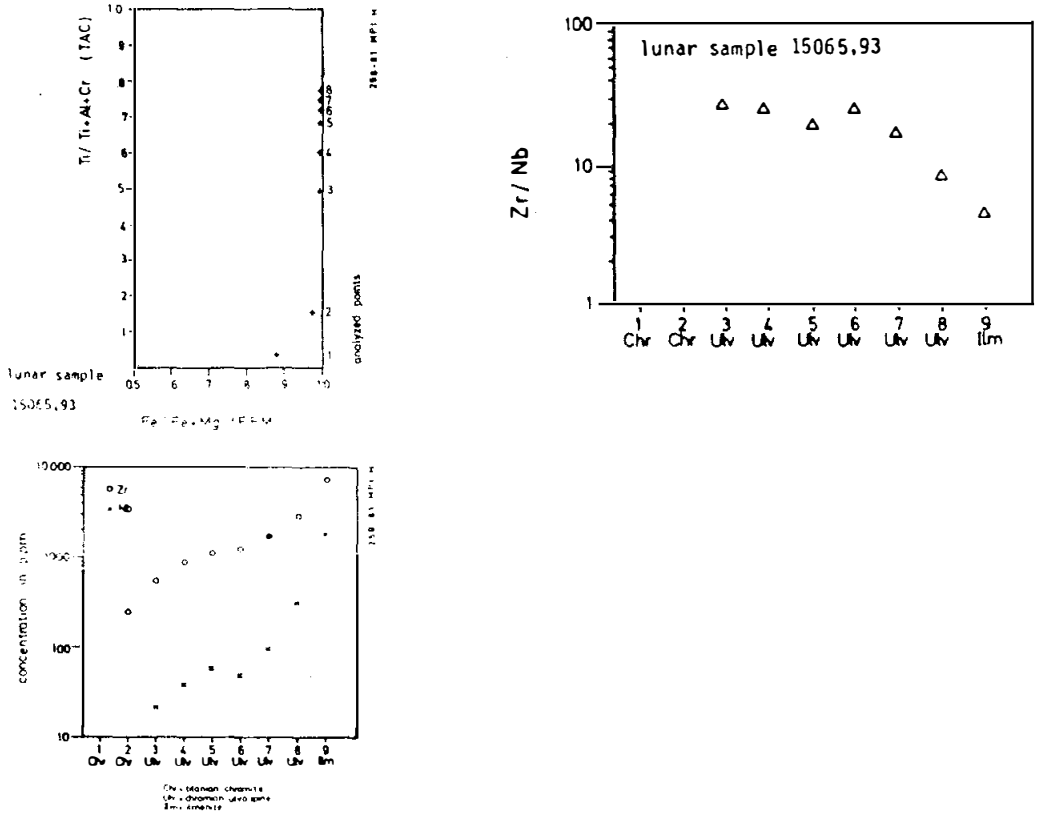

Figure 8. Zr abundances in opaque phases (Blank et al., 1982).

products of linear cooling rate dynamic experiments with the natural rock, deduced a cooling rate of less than 1°C/hr from both the pyroxene phenocryst shapes and the "groundmass" textures for 15065, making it one of the slowest-cooled of the quartz-normative basalts. In a more detailed but similar type of analysis, Grove and Walker (1977) deduced cooling rates of 0.03°C to 0.1°C/hr at first (from pyroxene nucleation density), and a late stage cooling rate of 0.01°C/hr (from plagioclase "size"). The pyroxenes were larger than any produced in experiments cooled at 0.5°C/hr. The results are consistent with a slow, nearly linear cooling rate and suggest a distance of 1032 cm from a conductive boundary. The chemistry of the pyroxene cores is similar to those of equilibrium experiments (Grove and Bence, 1977). Walker et al. (1977) concluded that the similarity of natural cores with experimental products precluded the presence of any significant cumulus pyroxene, and that the sample was not supercooled at pyroxene entry. Neither is the olivine (very little, and more Fe-rich than liquidus olivines) a possible cumulus phase. The cooling rates were slow enough to homogenize olivine (but not pyroxene); modelling olivine diffusion produces a cooling rate of 0.3°C/day. The 15065 magma body must have taken a year or two to traverse the solidification interval.

Taylor and McCallister (1972a,b), Taylor et al. (1973, 1976), and Onorato et al. (1979) used the distribution of Zr between ulvolspinel and ilmenite to deduce equilibration temperatures (~850°C) and cooling rates (~0.15°C to 1.0°C/day), consistent with other data showing lower cooling rates and equilibration temperatures than most other quartz-normative basalts. Brett (1975) used available kinetic data to deduce crystallization ~2 m from a boundary.

EXPERIMENTAL PETROLOGY: Longhi et al. (1972) conducted equilibrium crystallization experiments on a 15065 rock powder, from low pressure to 20 kb (Fig. 9). The low pressure crystallization sequence is similar to that inferred from the natural rock, but the late-stage phases were not crystallized.

Fe-loss is a problem (see discussion of 15065 experiments in O'Hara and Humphries, 1977) making liquidus mafics too magnesian; even so Longhi et al. (1972) concluded that cumulus pyroxene was probably present.

Walker et al. (1977) conducted detailed experiments on 15065 natural powders in attempts to determine the optimum experimental conditions and containers. They reported results for low pressure (various containers) and for pressures up to 30 kb (molybdenum containers). Neglecting spinel, whose crystallization is enhanced in molybdenum containers, clinopyroxene is the liquidus phase at elevated pressures; there is a problem with reproducibility in these high pressure, near-solidus experiments.

Longhi et al. (1978) used the 15065 composition in studying olivine-liquid distribution coefficients for iron and magnesium,

providing analyses of one olivine-liquid pair for a low pressure experiment at 1249°C. All other experiments (Lofgren et al., 1976; Grove and Bence, 1977) were dynamic experiments on an analog composition, not precisely 15065.

CHEMISTRY: The published chemical data are separated into "normal" rock (Table 2) and mafic segregation (Table 3) according to the split location. Rare earths are shown on Figure 10. If the limited data of Christian et al. (1972)/Cuttitta et al. (1973) are credible, then the mafic segregation is richer in rare earths than "normal" rock. The mafic segregation is certainly richer in K_2O and P_2O_5, it is also vuggier (macroscopic observations), and contains more conspicuous tridymite and fayalite (microscopic observation). One "normal" rock analysis seems wholly inconsistent: that of Juan et al., which is low in silica, high in CaO and Na_2O, and produces normative nepheline as well as 30% normative olivine. Otherwise the "normal" rock is fairly similar to other Apollo 15 quartz-normative basalts, but is more magnesian. Rhodes and Hubbard (1973) found that its composition could not be derived from other members of the group by additions or removal of potential low-pressure liquidus phases. Hence it actually represents a separate magma type or unusual crystallization processes. One other inconsistency is that Ganapathy et al. (1973) refer to ,41, not ,5, as their mafic split (also in Wolf and Anders, 1980), in contradiction to the allocation records. Their analysis of ,5, allocated as mafic, has higher Rb, Cs, and U than ,41, consistent with the higher rare earths, K_2O, and P_2O_5 of the other mafic splits.

Cuttitta et al. (1973) analyzed for Fe_2O_3, finding none, and found an excess reducing capacity for ,31 ("normal") not present in ,8 (mafic). They ascribe the 64 ppm Cu in ,31 and the 32 ppb B in ,8 to probable contamination in the lunar laboratory. Gibson and Moore (1972) studied inorganic gas releases of the sample on heating, noting an absence of solar-wind derived species such as H_2 and CO_2. The sample has lower abundances of volatiles than do soils, by a factor of 5 to 10. Bibring et al. (1974) studied carbon extracted by vacuum sublimation from a crushed internal piece in efforts to understand lunar carbon chemistry. Gibson et al. (1975) analysed for CO, CO_2, H_2, H_2S, Fe^o with combustion, hydrolysis, and magnetic techniques. Wanke et al. (1975) also specifically analyzed for oxygen. Gibson and Andrawes (1978) found very low upper limits for H_2, CN_4, Ar, CO, acid CO_2, finding the absence of C-containing gases to be surprising.

In their discussion of the chemistry of Apollo 15 basalts, Pratt et al. (1977) did not seem to be aware of the mafic segregation specifically sampled in 15065, noting only gross compositional heterogeneities.

Barker (1974) attempted to find the composition of gases in the 15065 magma, by attempting to analyze the gases in glass inclusions in 15065,44. The sample was heated and gases measured with mass spectrometry. Barker (1974) diagrammed the evolution

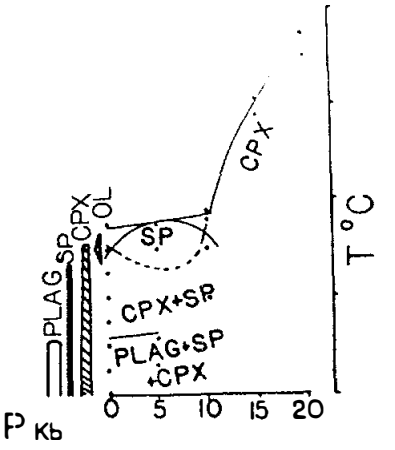

Figure 9. Phase relationships (Longhi et al., 1972).

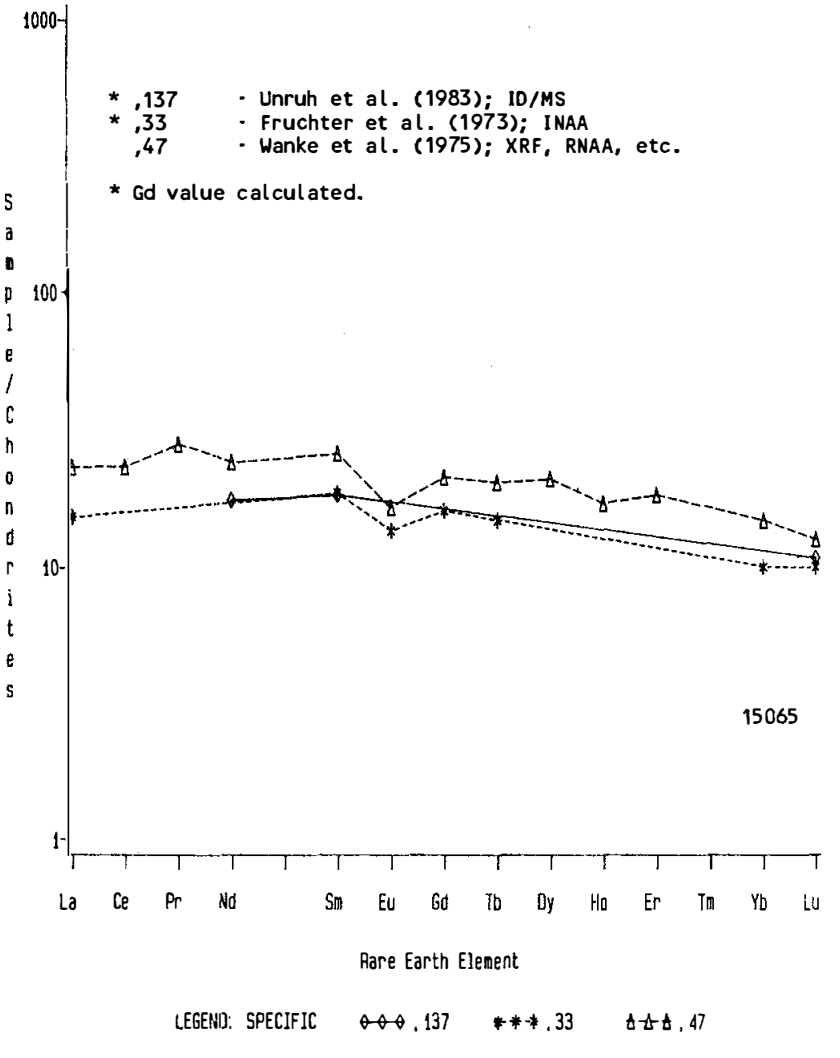

Figure 10. Rare earths.

TABLE 15065-2

		,48	,29	,31	—	.32	—	,40	,33	,41	,37	,42	,39	,47	,126
Wt %	SiO2	43.30	48.66	48.47		47.24						48.2		49.0	
	TiO2	1.88	1.55	1.48		1.54			1.21			1.44		1.33	
	Al2O3	10.10	9.17	9.26		9.33			11.3			10.32		12.76	
	FeO	19.20	19.07	19.18		19.17			19.2			18.46		17.8	
	MgO	11.50	10.57	10.58		10.69						10.35		8.81	
	CaO	12.12	9.70	9.94		9.53						9.55		11.24	
	Na2O	0.715	0.36	0.34		0.23			0.282			0.33		0.3672	
	K2O	0.068	0.11	0.05	0.0464	0.05						0.041		0.0365,0.058	
	P2O5			0.05		0.08						0.104		0.062	0.076
(ppm)	Sc			38					41					39.1	
	V			158		185									
	Cr	5507	5600	3600		4400			4600			3200		3160	
	Mn	2300		2000		2000						1800		1890	
	Co	70		52		47			46	40				37.7	
	Ni	147		151		78		63							
	Rb			<1		5				0.39				0.70	
	Sr	214		110		98								134	
	Y			23		29								24	
	Zr			63		79								94	
	Nb			12		13								6	
	Hf								2.1					3.36	
	Ba			50		85								96	
	Th				0.51		0.5244							0.70	
	U				0.15		0.1368			0.085				0.190	0.14
	Pb						0.236								
	La			<10					5.1					7.73	
	Ce													20.6	
	Pr													3.15	
	Nd													14.6	
	Sm								3.4					4.72	
	Eu								0.94					1.14	
	Gd													5.3	
	Tb								0.7					0.96	
	Dy													6.66	
	Ho													1.2	
	Er													3.7	
	Tm														
	Yb			3.8					2.0					2.98	
	Lu								0.34					0.43	
	Li	7		5.9											6.7
	Be														
	B														
	C										12		11.2		
	N														
	S												600		
	F														40
	Cl														4.23a
	Br									8					12.2
	Cu	56		64		48								5.42	
	Zn	38						0.92		1.0				<1	
(ppb)	I														0.37
	At														
	Ga	24000		4100				3100						3760	
	Ge							21		6.7				<100	
	As													0.90	
	Se									53				80	
	Mo														
	Tc														
	Ru														
	Rh														
	Pd														
	Ag	5450								0.88					
	Cd							1.2		1.1					
	In							0.32		0.18					
	Sn														
	Sb									0.24					
	Te									0.96					
	Cs									23				50	
	Ta								400					450	
	W													102	
	Re									0.0094				<0.1	
	Os														
	Ir							0.048		0.144					
	Pt														
	Au	4						0.19		0.014				0.031	
	Hg														
	Tl									0.21					
	Bi									0.11					
		(1)	(2)	(3)	(4)	(5)	(6)	(7)	(8)	(9)	(10)	(11)	(12)	(13)	(14)

Reference to Table 15065-2

References and methods:

(1) Juan et al. (1972); AAS, colorimetric
(2) Longhi et al. (1972); microprobe fused bead
(3) Christian et al. (1972), Cuttitta et al. (1973); XRF, etc.
(4) O'Kelley et al. (1972); Gamma ray spectroscopy
(5) Strasheim et al. (1972); XRF, and others
(6) Tatsumoto et al. (1972); MS/ID
(7) Baedecker et al. (1973); RNAA
(8) Fruchter et al. (1973); INAA
(9) Ganapathy et al. (1973); GNAA
(10) Moore et al. (1973)
(11) Nava (1974); AAS, colorimetry, etc.
(12) Gibson et al. (1975); combustion, hydrolysis
(13) Wanke et al. (1975); XRF, RNAA, etc.
(14) Jovanovic and Reed (1976)

Note:

a = ril

References and methods:

(3) Christian et al. (1972); Cuttitta et al. (1973) XRF, etc.

(9) Ganapathy et al. (1973) GNAA

(11) Nava (1974) AAS, colorimetry, etc.

TABLE 15065-3

		,8	,5	,6
Wt %	SiO2	47.95		47.7
	TiO2	2.30		2.86
	Al2O3	5.33		6.05
	FeO	23.60		23.77
	MgO	10.15		9.52
	CaO	9.30		9.33
	Na2O	0.25		0.27
	K2O	0.07		0.081
	P2O5	0.09		0.119
(ppm)	Sc	53		
	V	178		
	Cr	3400		3700
	Mn	2400		2400
	Co	66	45	
	Ni	54		
	Rb	1.0	0.76	
	Sr	100		
	Y	39		
	Zr	103		
	Nb	<10		
	Hf			
	Ba	75		
	Th			
	U		0.235	
	Pb			
	La	22		
	Ce			
	Pr			
	Nd			
	Sm			
	Eu			
	Gd			
	Tb			
	Dy			
	Ho			
	Er			
	Tm			
	Yb	6.6		
	Lu			
	Li	6.3		
	Be	<1		
	B	32		
	C			
	N			
	S			
	F			
	Cl			
	Br			
	Cu	14		
	Zn		1.6	
(ppb)	I			
	At			
	Ga	5300		
	Ge		5.3	
	As			
	Se		167	
	Mo			
	Tc			
	Ru			
	Rh			
	Pd			
	Ag		0.91	
	Cd		1.5	
	In		0.51	
	Sn			
	Sb		0.016	
	Te		3.4	
	Cs		60	
	Ta			
	W			
	Re		0.0015	
	Os			
	Ir		0.0054	
	Pt			
	Au		0.021	
	Hg			
	Tl		0.47	
	Bi		0.11	
		(3)	(9)	(11)

of H_2O, CO_2, and CO as a function of temperature. He concluded that the gas in the parent magma started with a composition close to 46% O, 42% C, and 12% H, and became more H_2O-rich as crystallization progressed. This result is in contradiction with the general conclusion that lunar basalts are and were devoid of water.

STABLE ISOTOPES: Clayton et al. (1973) reported oxygen isotope analyses for mineral separates from "normal" 15065 (Table 4), finding the fractionations consistent with typical magmatic temperatures of equilibration, i.e., ~1100°C. Strasheim et al. (1972) reported a $^7Li/^6Li$ ratio of 13.5, also for a "normal" sample.

RADIOGENIC ISOTOPES AND GEOCHRONOLOGY: Papanastassiou and Wasserburg (1973) determined a Rb-Sr internal isochron age of 3.28 ± 0.04 b.y. ($\lambda^{87}Rb = 1.39 \times 10^{-11}$ yr^{-1}) with an initial $^{87}Sr/^{86}Sr$ of 0.69937 ± 4 (Fig. 11), within error the same as other Apollo 15 mare basalts. The isochron is based on plagioclase, "ilmenite", and "cristobalite" separates, and both mechanical and density separation techniques were used.

Nakamura et al. (1977) studied the Sm-Nd isotopic system. Although Sm/Nd fractionations among separated phases were small, the data defined an isochron corresponding to 3.34 ± 0.09 b.y. ($\lambda^{147}Sm = 0.00654 \times 10^{-9}$ yr^{-1}) with an initial $^{143}Nd/^{144}Nd$ of 0.50844 ± 0.00011. This age is consistent with the Rb-Sr age. Using the Moore County initial ratio, the source of 15065 was calculated to have $^{147}Sm/^{144}Nd$ of 0.1998 for a two-stage model, within the "chondritic" range of 0.195 ± 0.015.

Unruh et al. (1984) reported Sm/Nd and Lu/Hf isotopic data for a whole-rock sample of 15065. The whole-rock values (Table 5) are similar to those for other Apollo 15 mare basalts, except that present day ϵNd (ϵNd_o in Table 5) is lower than olivine-normative basalt 15555. With the other analyzed quartz-normative mare basalt, 15076, it has the lowest ϵNd_o among mare basalt groups except for the aluminous basalt 12038. Like all mare basalts, the Lu/Hf ratio is less than chondritic, thus ϵHf has been falling since crystallization.

Strasheim et al. (1972) stated that the $^7Li/^6Li$ relationship gives an age of 3.30 b.y., but no information as to the derivation of this age is given. Rosholt (1972) discussed Th isotopes which contribute to radioactivity in the sample.

EXPOSURE AND TRACKS: Eldridge et al. (1972) reported cosmogenic radionuclide data: ^{22}Na and ^{26}Al have equilibrium values indicating a surface exposure of at least 2 m.y.

Bhattacharya et al. (1975) studied track densities for an interior chip. They did not provide specific data but bracketted the results with other rocks as a track density between 6 and 20 x 10^6/cm^2, with an upper limit to the exposure (because no

TABLE 15065-4. Oxygen isotopes (°/oo, rel. SMOW) for mineral separates from 15065 (Clayton et al.)

Mineral	Plag	Pig	Cpx	Ilm	Trid
$\delta^{18}O$	5.84	5.60	5.47	4.08	6.72

TABLE 15065-5. Sm/Nd and Lu/Hf whole-rock data for 15065,137 (Unruh et al. (1984)

$^{147}Sm/^{144}Nd$	$(^{143}Nd/^{144}Nd)_o$	ϵNd_o	$(^{143}Nd/^{144}Nd)_I$	ϵNd_I	$^{176}Lu/^{177}Hf$	$(^{176}Hf/^{177}Hf)_o$	ϵHf_o	$(^{176}Hf/^{177}Hf)_I$	ϵHf_I
.1961±2	0.512723±22	+1.7±.4	0.50851±2	+2.0±.4	.02179±3	0.282481±74	-13.5±2.6	0.28106±7	+13.4±2.6

o = at present day; I = at time of crystallization

TABLE 15065-6. Elastic wave velocities (Km sec^{-1}) as a function of hydrostatic pressure (Chung, 1973)

Confining pressure in kilobars

	0.5	1.0	1.5	2	3	4	5	6	7
P	3.9	4.7	5.25	5.62	6.20	6.52	6.76	6.84	6.98
S	2.5	2.8	3.06	3.29	3.50	3.68	3.75	3.86	3.90

Figure 11. Deviations of mineral separates data from best fit isochron (Papanastassiou and Wasserburg, 1973).

surface chip was studied) of 10-30 m.y.

PHYSICAL PROPERTIES: Hargraves and Dorety (1972) reported NRM and its variation with alternating field demagnetization (Fig. 13) finding a weak remanence after demagnetization, similar to 15555.

Chung (1973) reported seismic wave velocities under confining pressures (Table 6) for sample ,27. Chung and Westphal (1973) reported dielectric spectra (Fig. 14) which are similar to 15555 and typical of gabbroic basalts.

Adams and McCord (1972) and Charrette and Adams (1975) reported diffuse reflection spectra (0.35 to 2.5 μm) for a powdered sample. The data show the preponderance of pigeonite as a slope in the 0.5 μm to 0.75 μm region steeper than the glassy vitrophyres.

PROCESSING AND SUBDIVISIONS: Prior to slabbing, the mafic segregation was chipped, providing ,2 from which thin sections ,87 and ,91 were made. From the same region ,3 and ,4 were chipped, and another several grams ground into a homogeneous powder and aliquotted into splits ,5 to ,11, some of which has not been allocated.

The "normal" rock was slabbed and the slab substantially dissected (Fig. 15). Several thin sections were made from ,24; ,25; and ,55. The large end piece (,0 in Fig. 15) was subsequently broken into smaller pieces along natural fractures; the two largest pieces are ,117 (575.6 g) in remote storage, and ,118 (544 g).

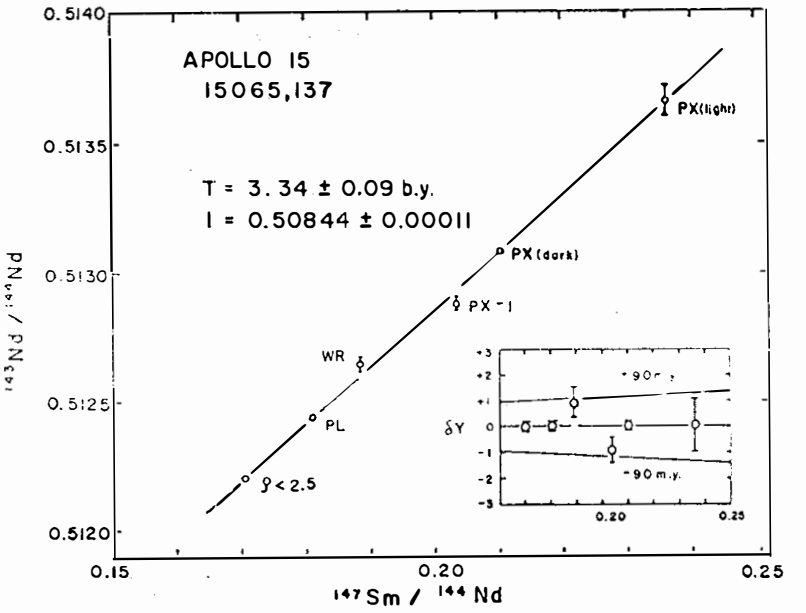

Sm-Nd evolution diagram for basalt 15065. The data are for "cristobalite" ($\rho < 2.5$), plagioclase ($\rho = 2.6$-2.8), whole rock, pyroxene + ilmenite ($\rho > 3.3$), hand-picked dark pyroxene (rim), and hand-picked light pyroxene (core) fractions. The data define a line which corresponds to a 3.34 ± 0.09 x 10^9yr age (2.77σ at 95% confidence). The whole rock and $\rho > 3.3$ fractions appear to deviate slightly from the line as can be seen in the δY (in 10^4) vs. X plot in the insert.

Figure 12. Sm-Nd internal isochron (Nakamura et al., 1977).

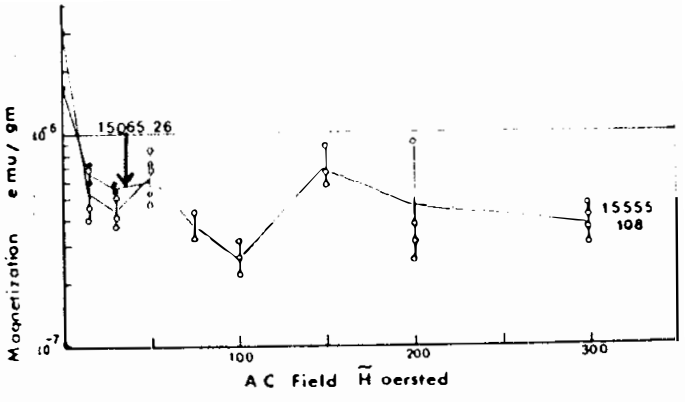

Figure 13. AF demagnetization (Hargraves and Dorety, 1972).

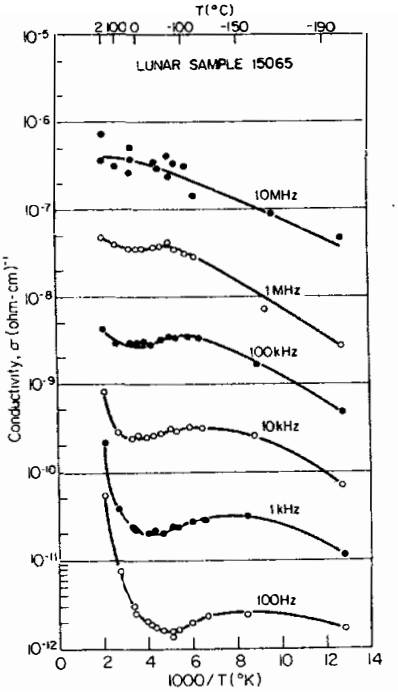

Electrical conductivity of sample 15065,27 as a function of frequency and temperature.

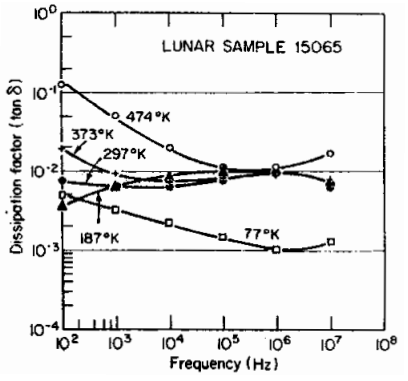

Dielectric losses in sample 15065,27 as a function of frequency and temperature

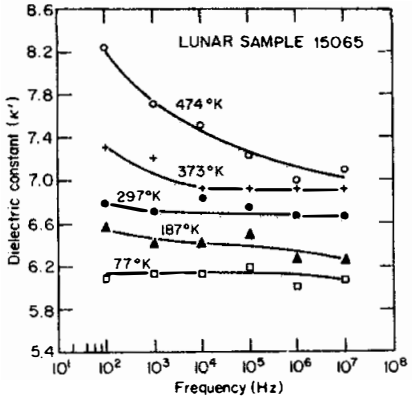

Dielectric constant of sample 15065,27 as a function of frequency and temperature.

Figure 14. Dielectric data (Chung and Westphal, 1973).

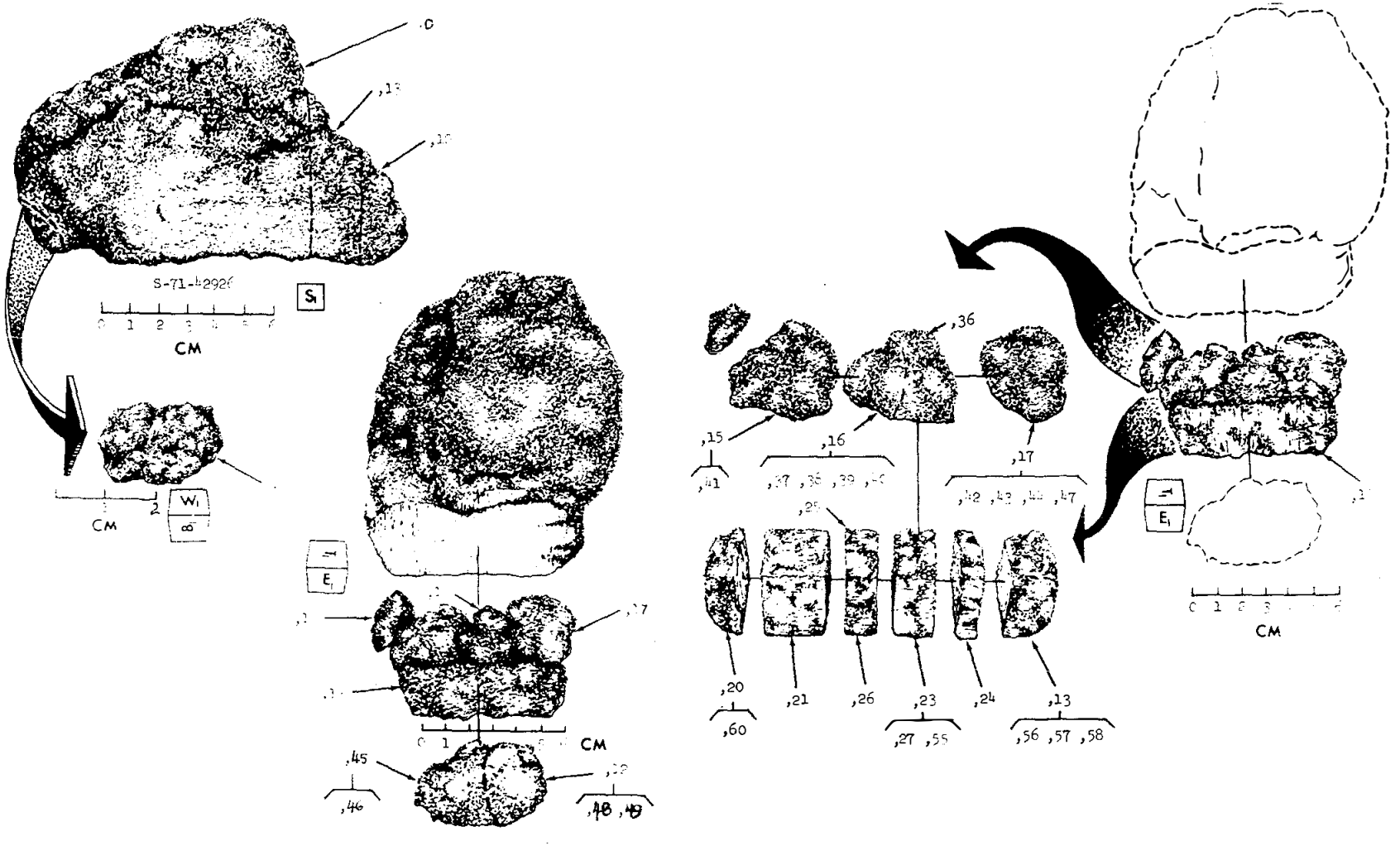

Figure 15. Main processing subdivisions. Mafic segregation splits ,3 to ,11 not shown, but are from same region as ,2.

15075 PORPHYRITIC SUBOPHITIC QUARTZ-NORMATIVE MARE BASALT ST. 1 809.3 g

INTRODUCTION: 15075 is among the coarsest-grained quartz-normative basalts, and contains pigeonite phenocrysts. It has been dated as ~3.4 b.y. old. The sample (Fig. 1) is blocky, rounded, tough, and a light olive gray. It had a small fillet when collected, and it has a few zap pits on some surfaces.

15075 was collected on the east flank of Elbow Crater, as one of 5 basalt samples collected on a line extending out from the crater (see Fig. 15065-1). 15075 was collected, with 15076 and soil samples, about 25 m east of the Elbow Crater rim crest, as one of a cluster of rocks, all of which had the same surface texture and albedo. The orientation of 15075 is known.

PETROLOGY: 15075 is a coarse, quartz-normative basalt lacking magnesian olivine (Fig. 2). A detailed description was given by Taylor and Misra (1975) who described the texture, reported mineral analyses, and interpreted the paragenesis and cooling rate. The most striking feature is the presence of pyroxene phenocrysts up to 6 mm long and invariably zoned. The interstitial regions are dominated by lathy to tabular plagioclases (up to 2 mm long) and anhedral to subhedral pyroxenes. Pyroxenes and plagioclase compose 90% of the rock; accessories include pyroxferroite, cristobalite, tridymite, ilmenite, spinels, baddelyite, troilite, Fe-Ni metal, and fayalite.

Pyroxenes show spectacular zoning (Figs. 3, 4) from "hypersthene" and pigeonite cores outwards, with a sharp discontinuity with the appearance of subcalcic augite, marking the beginning of plagioclase crystallization. Pyroxferroite constitutes 2 to 5% of the sample, as late-stage material, usually with cristobalite. Many have broken down to a fayalite + Ca-rich pyroxene + silica intergrowth, but others persist metastably. Plagioclases are zoned normally, from An_{90-95} cores to An_{70-80} rims (Fig. 5). Iron increases as plagioclase becomes more calcic. Cristobalites and tridymite constitute 3-5% of the sample, cristobalite as fairly large subhedral grains in the groundmass, tridymite typically as bladed crystals. Spinels of the chromite-ulvospinel are common. Ilmenites typically occur near the center portions of ulvospinel grains and have low MgO (<0.3%). The few Fe-Ni metal grains occur mainly as inclusions in pyroxene cores, less commonly in subcalcic augite, and rarely in ferropyroxenes. They are rounded in form and contain more than 1% cobalt (Fig. 7). Troilite is rare.

According to Taylor and Misra (1975) the liquidus phases were chromite, Fe-metal, and low-Ca pyroxene. Plagioclase started crystallizing very late; olivine was also very late, crystallizing only as fayalite. Metal and spinel apparently crystallized throughout the cooling of the rock. Subsolidus reduction of late-stage phases (pyroxferroite, ulvospinel) and

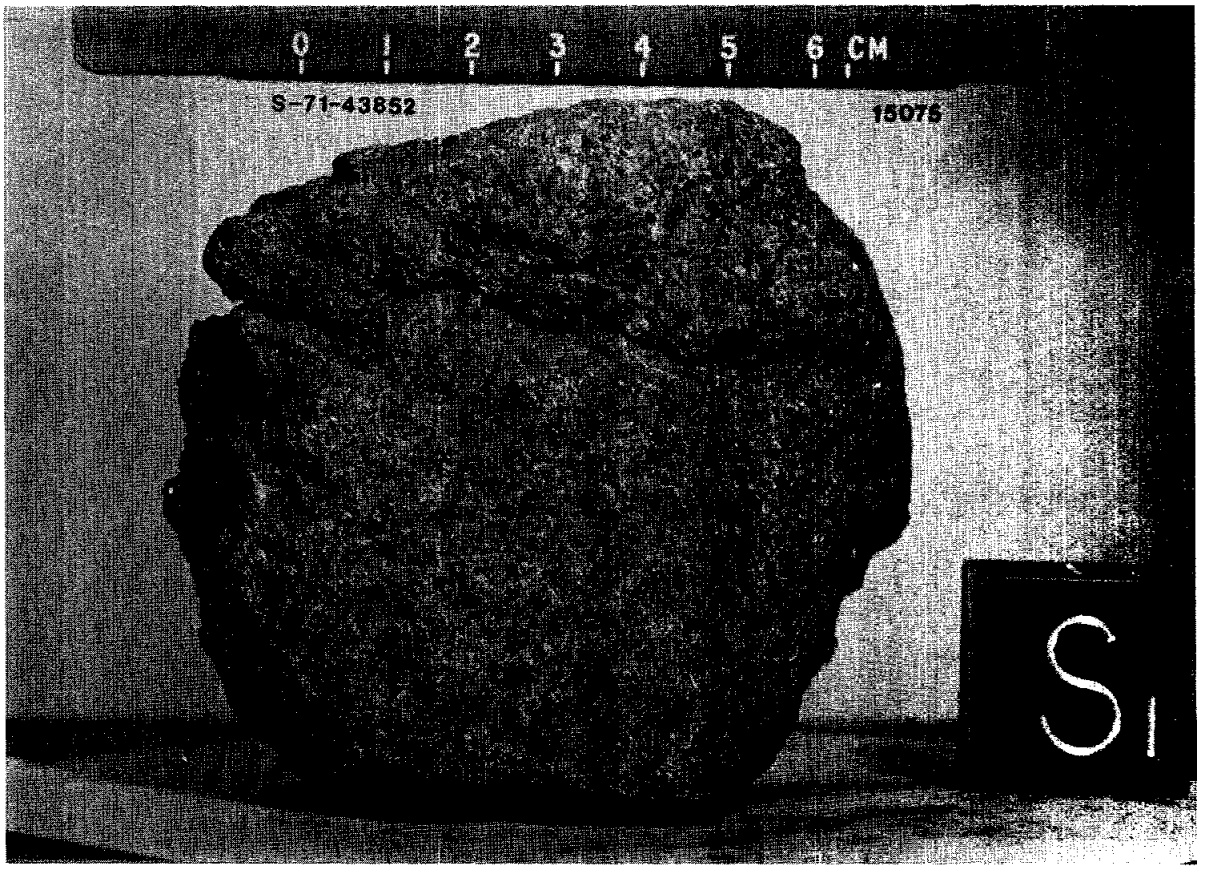

Figure 1. Macroscopic view of 15075.

Fig. 2a

Fig. 2b

Figure 2. Photomicrographs of 15075,45. Same field, same scale; (a) transmitted light; (b) crossed polarizers.

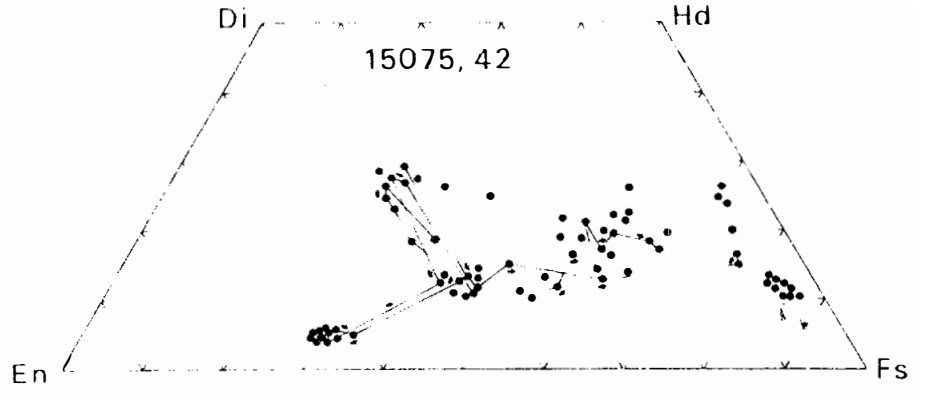

Figure 3. Pyroxene compositions (Taylor and Misra, 1975).

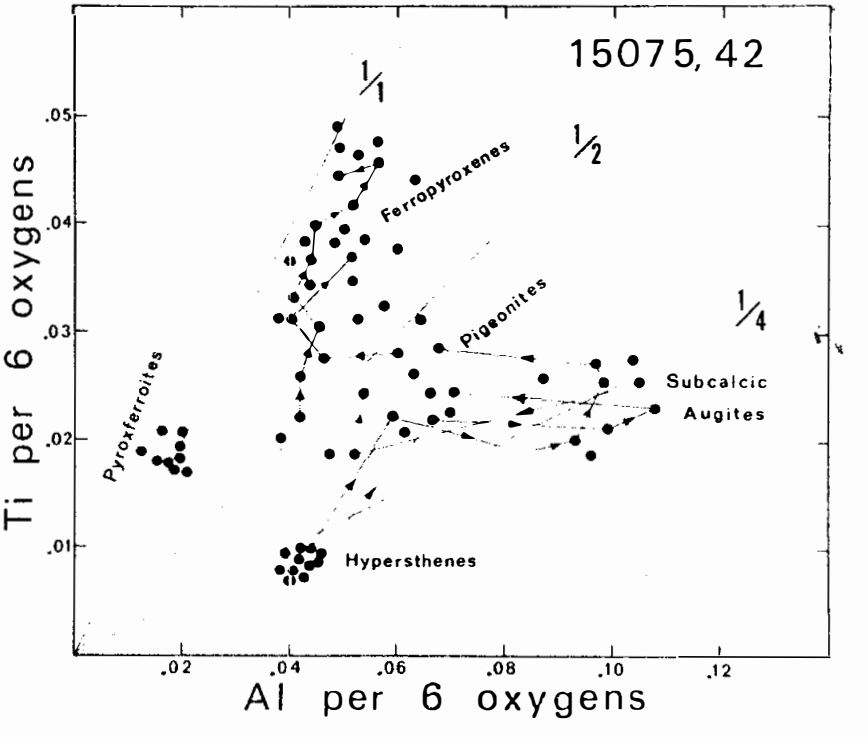

Figure 4. Ti/Al of pyroxenes (Taylor and Misra, 1975).

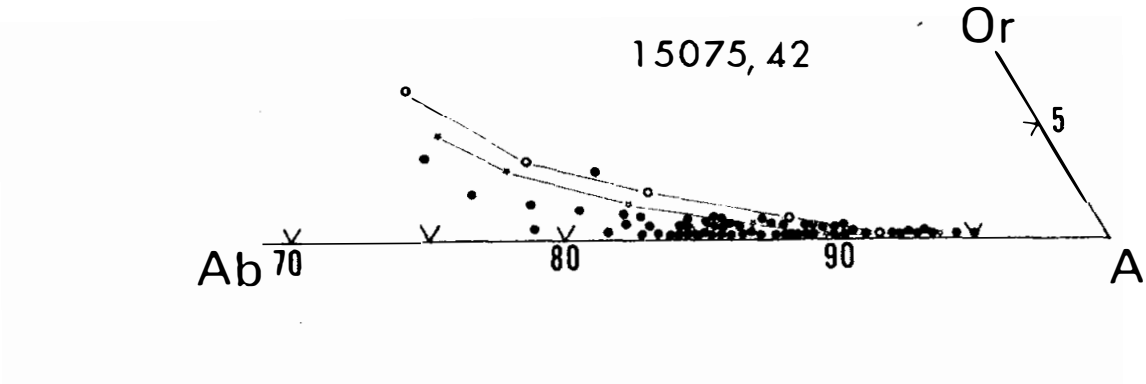

Figure 5. Plagioclase compositions (Taylor and Misra, 1975).

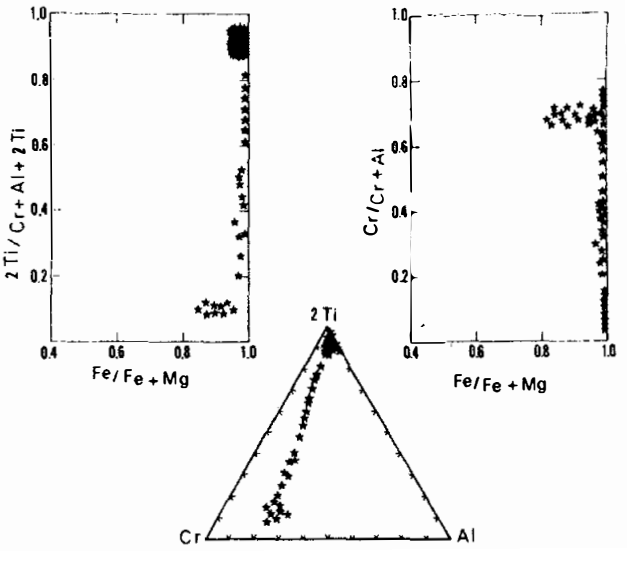

Figure 6. Spinel compositions (Taylor and Misra, 1975).

reactions to form fayalite rims probably took place in the subsolidus.

Simmons et al. (1975) studied microcracks with optical and SEM methods, identifying shock-induced cracks and showing the curved cracks across the cleavage which are characteristic of the cores of pigeonites. The sample is highly cracked. The rock was subjected to "differential strain analysis", and Simmons et al. (1975) plotted differential strain v. pressure, and crack closure pressure distributions. The crack spectra, like other lunar samples, are quite different from terrestrial samples, probably because of shock effects on lunar samples.

Cooling Rates: Taylor and Misra (1975) attributed the porphyritic texture to a one-stage cooling history, as concluded by Lofgren et al. (1975) on the basis of linear cooling rate studies (but see also Grove and Walker, 1977, even though they did not specifically discuss 15075). They deduced an equilibration temperature of 918°C for the partitioning of Zr between ilmenite and ulvospinel, calculating from that a cooling rate of 3°C/day (also Taylor et al. 1975). Lofgren et al. (1975) concluded that the cooling rates were less than 1°C/day, on the basis of phenocryst shapes and matrix textures, thus 15075 is one of the slowest-cooled of the quartz-normative basalts. Onorato et al. (1979) refined the Zr partitioning model and calculated cooling rates of 0.2°C to 1°2°C/day.

CHEMISTRY: Little chemical data has been published. Cripe and Moore (1975) measured 390 ppm S. Schaeffer and Schaeffer (1977) in their Ar-Ar geochronology for two splits found 16.8 and 16.0% CaO (which seem very high) and 0.0370 and 0.0513% K_2O. These data alone are insufficient to classify the basalt.

GEOCHRONOLOGY AND EXPOSURE: Schaeffer and Schaeffer (1977) analyzed two splits with the Ar-Ar method, finding plateaus in the 800° to 1300°C release (Fig. 8) which correspond to ages of 3.45 ± 0.20. This age is among the oldest of Apollo 15 mare basalts. There is some gas loss in the less than 800°C fraction, and K/Ca decreases continuously over the entire analysis. Both splits give total K-Ar ages of 3.39 b.y. Exposure ages (^{38}Ar method) of 274 and 258 m.y. were determined from the plateau range gas releases.

PROCESSING AND SUBDIVISIONS: Initially, a small piece (,1) was chipped from the sample to make thin section ,4. Subsequently the sample was substantially sawn (Fig. 9) for allocations. End piece ,5 (171.5 g) is in remote storage; end piece ,25 has a mass of 382.6 grams. Slab piece ,15 was made into a potted butt for thin sections ,40 to ,46.

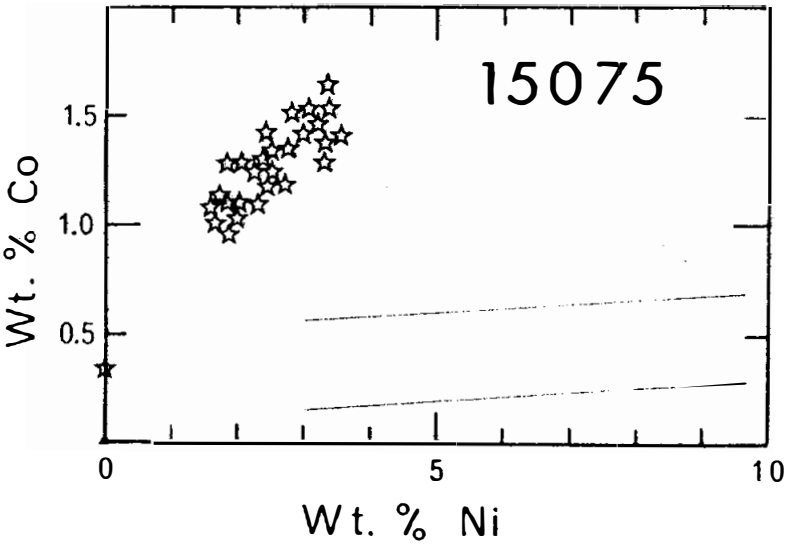

Figure 7. Fe-metal compositions (Taylor and Misra, 1975).

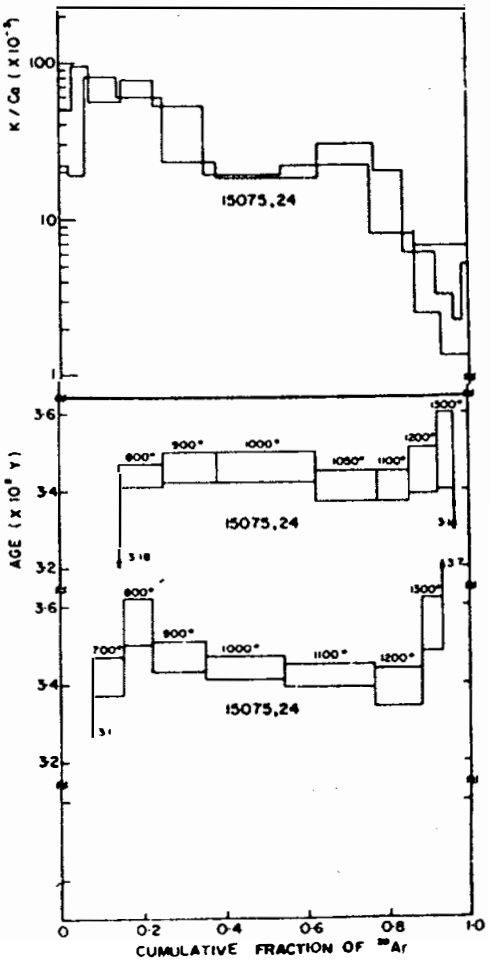

Figure 8. Ar release diagram (Schaeffer and Schaeffer, 1977).

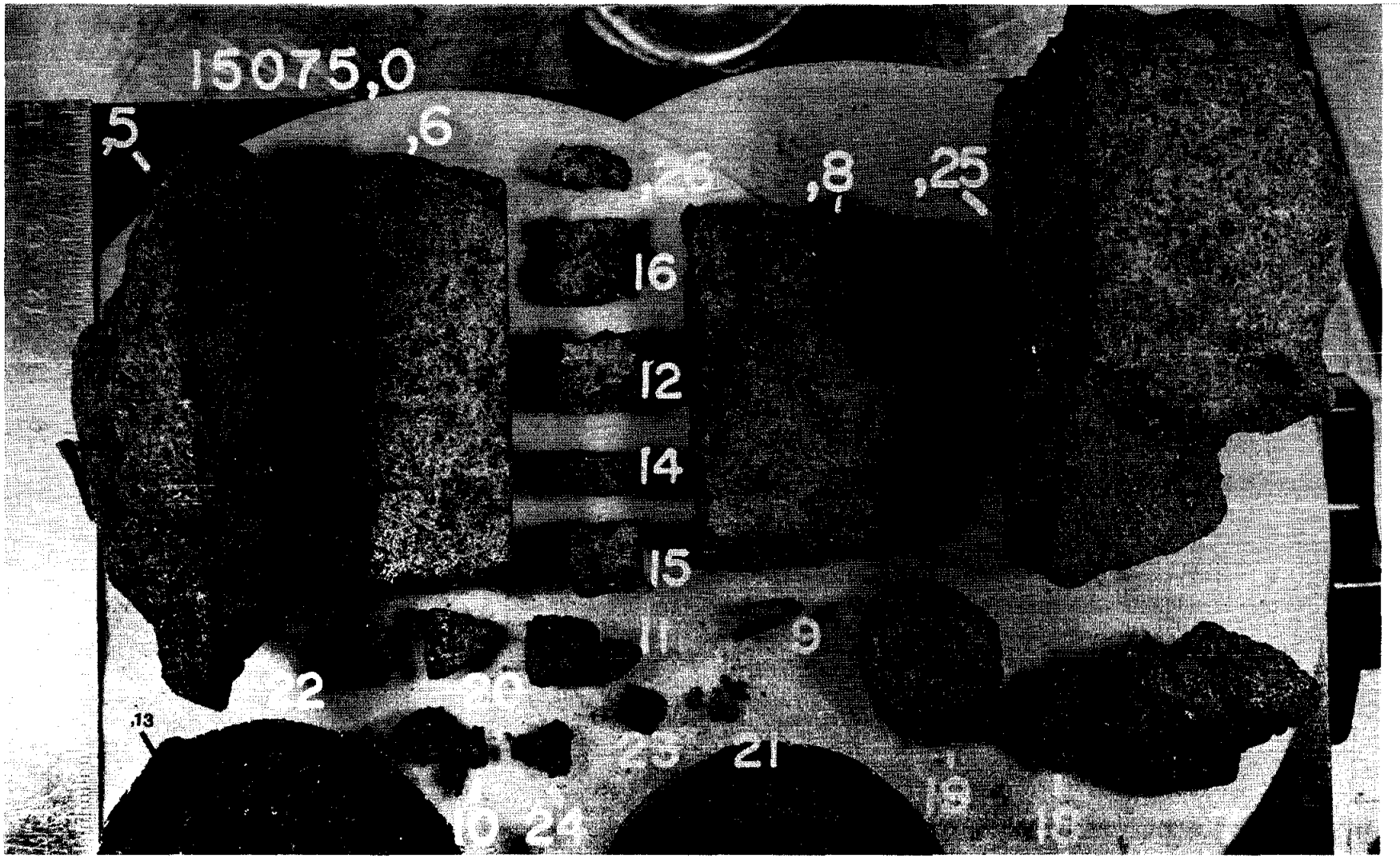

Figure 9. Slabbing of 15075. S-74-31232

15076 PORPHYRITIC SUBOPHITIC QUARTZ-NORMATIVE MARE BASALT ST. 1 400.5 g

INTRODUCTION: 15076 is tough, coarse-grained basalt (Fig. 1) with some pigeonite phenocrysts. It has been dated as close to 3.35 b.y. old. The sample is blocky and angular, with a few planar fractures. It is light olive gray with a few irregularly distributed vugs containing plagioclase crystals. Its surface has some slickensides on one face, and a few zap pits occur on two sides. It had a small fillet when collected.

15076 was collected on the east flank of Elbow Crater, as one of five basalt samples collected on a line extending out from the crater (see Fig. 15065-1). 15076 was collected with 15075 and soil samples, about 25 m east of the Elbow Crater rim crest, as one of a cluster of rocks, all of which had the same surface texture and albedo.

PETROLOGY: 15076 is a coarse, quartz-normative mare basalt, lacking magnesian olivine but containing pigeonite phenocrysts (Fig. 2). The texture is essentially porphyritic and subophitic with very little interstitial glass, and the pigeonite phenocrysts are twinned and zoned. Tridymite is conspicuous in thin sections. Rhodes and Hubbard (1973) reported a mode of 66.3% pyroxene, 28.5% plagioclase, 0.5% ilmenite, 1.4% ulvospinel, 2.1% cristobalite, 0.5% troilite, 0.6% mesostasis, and traces of Cr-spinel and Fe-metal. They apparently identified tridymite as cristobalite. The PET report for thin section ,12 (Lunar Sample Information Catalog Apollo 15, 1972) listed 55% clinopyroxene, 45% plagioclase, 2% tridymite, 2% ilmenite, 1% ulvospinel, and less than 0.1% each of Cr-spinel, troilite, and Fe-Ni metal. Brown et al. (1972a) reported 53% clinopyroxene and 36% plagioclase and noted the discrepancy with the PET report. The differences result from the coarse grain size and the small thin section size (less than 1 cm^2). Peckett et al. (1972) noted the presence of tranquillityite as an accessory phase. Macroscopically the mafic silicates are yellowish green and zoned to brown, or are honey brown to red brown, and include about 10% subhedral prisms. The plagioclases are white to translucent and are dominantly laths. The low density (2.4 g/cm^3) reported by O'Kelley et al. (1972) might reflect the vuggy nature of the sample analyzed.

The pyroxenes are mostly zoned, pigeonite to augite, and many are twinned. Most grains are not particularly elongated, but some are long, narrow, zoned phenocrysts (Fig. 2c,d). Microprobe analyses of pyroxenes were reported by Brown et al. (1972a,b), and by Virgo (1972,1973). These data are very similar (Fig. 3) and show heterogeneous zoning from pigeonite to subcalcic ferroaugite, or to subcalcic augite and then rapid zoning over narrow rims to subcalcic ferroaugite. One crystal showed oscillatory zoning of subcalcic augite (Virgo, 1972). The Ti/Al ratio starts at 1/6, and stays constant until subcalcic augite is reached, and then rapidly increases to 1/2 (Virgo, 1972) (Fig.

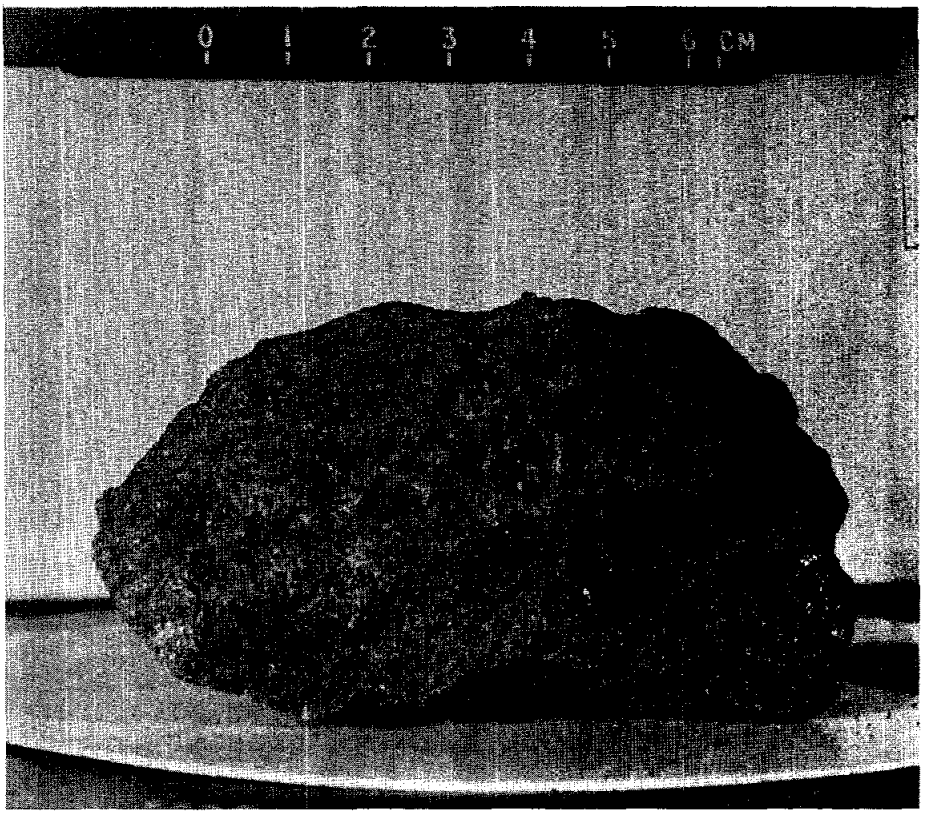

Figure 1. Pre-split view of 15076. S-71-47769

Fig. 2a Fig. 2b

Figure 2. Photomicrographs of 15076. Widths about 3 mm. a)c) transmitted light; b)d)e) crossed polarizers. a)-d) 15076,71; e) 15076,17. a)b) general groundmass view showing cored, stubby, lathy plagioclases. c)d) portion of a 1 cm long pigeonite phenocryst, and twinned pigeonite cross section. e) small tridymite laths at common extinction.

Fig. 2c

Fig. 2d

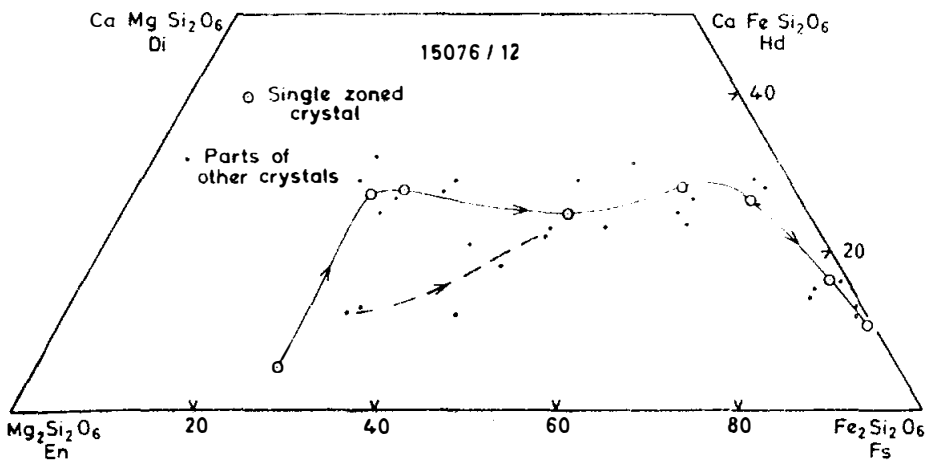

3a

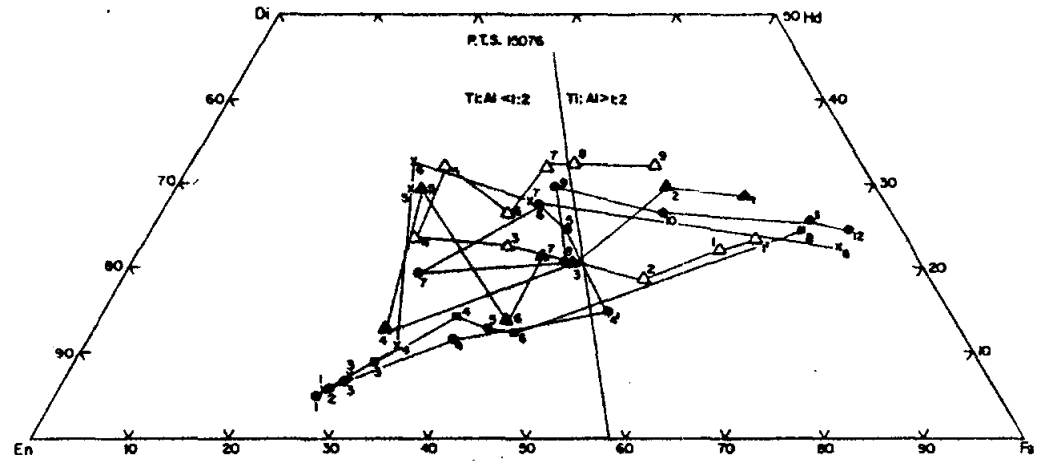

3b

Figure 3. Compositions of pyroxenes on pyroxene quadrilateral a) Brown et al. (1972b). b) Virgo (1972).

4), an abrupt change attributed to the start of plagioclase crystallization. Possibly Ti^{3+} is present. Brown et al. (1972b) diagrammed similar Ti/Al variations, but did not distinguish data for 15076 from data for 15085 and 15555. Papanastassiou and Wasserburg (1972) listed a pyroxferroite analysis (45% FeO, 47% SiO_2, 6% CaO, 1.8% MgO). Virgo (1972, 1973) used Mossbauer spectroscopy to provide information on the Fe^{2+}, Mg distribution, tabulating site occupancies, and calculated distribution coefficients. The site occupancies suggest a temperature of 560°C (Virgo, 1972) or 580°C (Virgo, 1973), significantly below the critical temperature for ordering (500°C-810°C), indicating slow cooling below the critical temperature. There is no evidence for Fe^{3+}. Virgo (1972) also reported x-ray diffraction data, showing diffuse streaking for pigeonite reflection along both a* and c*, which point toward the expected position of the augite reflections and hence indicate very fine-scale exsolution. Jagodzinski and Korekawa (1973) also found diffuse x-ray scattering resulting from the exsolution process, even though no reflections of the exsolved augite or pigeonite itself could be seen. In the same study, Berking et al. (1972) reported x-ray diffraction results for pigeonites, and found four to have the space group $P2_1/c$, and tabulated the lattice parameters, which indicate a low-Ca pyroxene. The other sample is different. Fernandez-Moran et al. (1973) studied homogeneous pigeonites using electron optical techniques, and showed electron micrographs and electron diffraction patterns. They observed exsolution in 32% of their samples, with a lamella structure with band widths of 100 to 1800 Å (average 1000 Å) and interband widths of 300 to 6200 Å (average 3100 Å).

Feldspars are dominantly lathy or prismatic, and some are hollow. Many contain a well-defined core-zone consisting of pyroxene and plagioclase. This core is commonly rectangular (Fig. 2b,c), and sharply bounded. Brown et al. (1972b) reported oscillatory zoning (An89-82-89-72), but little chemical data for the plagioclases has been reported. Berking et al. (1972), Jagodzinski and Korekawa (1973), and Korekawa and Jagodzinski (1974) reported compositions of An85 ± 3 (optical determinations) for three plagioclases protruding into vugs. X-ray data show that two of these crystals are untwinned, the other twinned (albite and carlsbad). The patterns show reflections and diffusions whose possible causes are discussed in Berking et al. (1972) and Jagodzinski and Korekawa (1973). Two of the plagioclase crystals have peculiar mound-shaped surface features with pillars or whiskers on the surface.

L. Taylor et al. (1975) plotted analyses of spinels (Fig. 5) and metals (Fig. 6). The sample is considered anomalous in that they observed no chromite, only ulvospinel, although this might be a sampling problem. The metal compositions show a substantial range compared with other coarse quartz-normative mare basalts. Jagodzinski and Korekawa (1973) showed Weissenberg photographs of tridymite, which has subcell dimensions like terrestrial high tridymite. The photographs also show additional reflections,

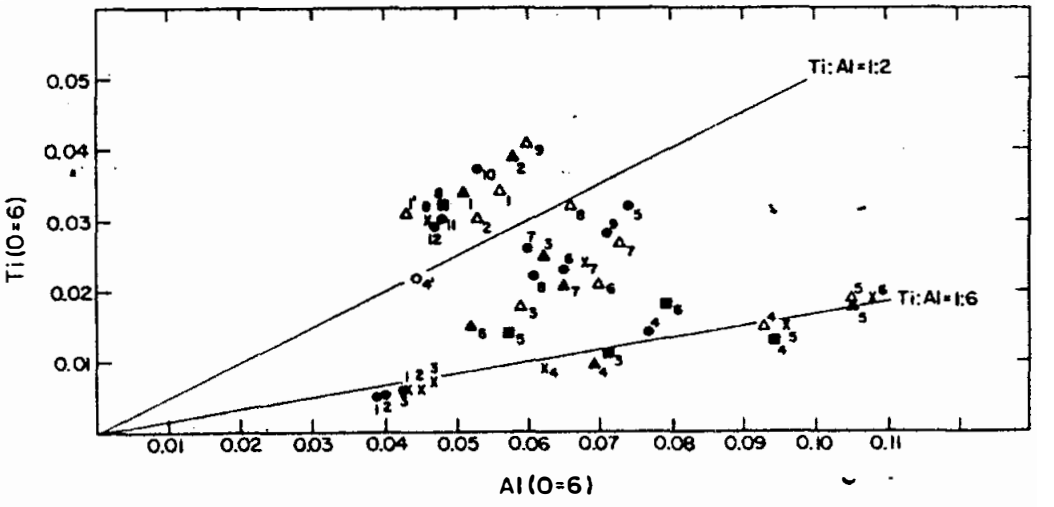

Figure 4. Ti vs. Al for pyroxenes (Virgo, 1972).

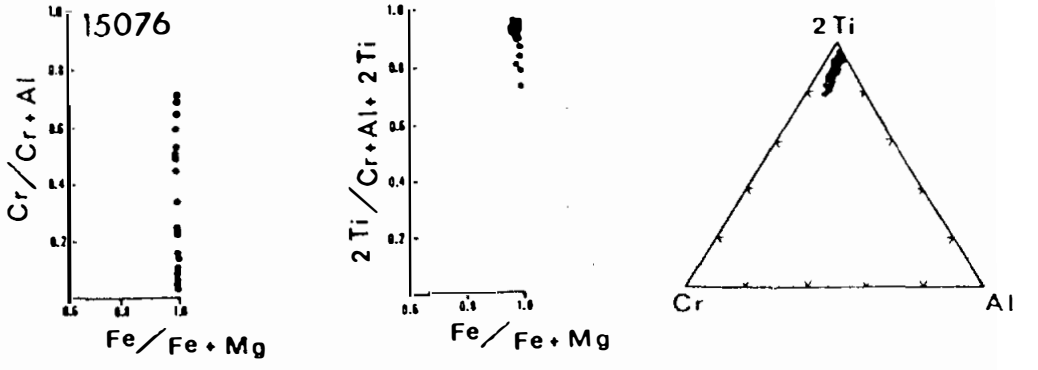

Figure 5. Compositions of spinels (L. Taylor et al., 1975).

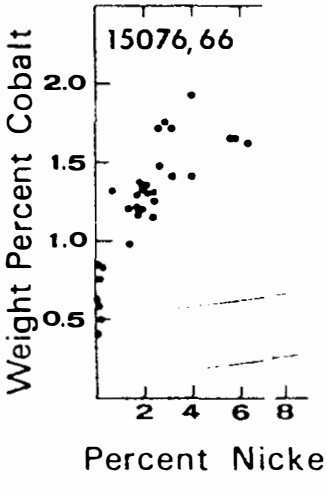

Figure 6. Compositions of metals(L. Taylor et al., 1975).

some of which are strong, others diffuse. Brown et al. (1972b) listed an analysis of a rhyolitic residuum.

Cooling Rates: In a series of papers, L. Taylor used the Zr partitioning between ilmenite and ulvospinel to determine cooling rates for 15076 (Taylor and McCallister 1972a,b; L. Taylor et al., 1973, 1975b; Onorato et al.,1979). Early data was reported erroneously, and L. Taylor et al. (1975) reported the correct data, with Zr ilmenite/Zr ulvospinel ratios of 1-1/2 to 2 (1.88 average), which, by comparison with their experimental data, is consistent with an equilibration temperature of 949°C and a cooling rate of 6°C/day (corrected from L. Taylor et al., 1975a, value of 95°C/day). The underlying solute partitioning model was further improved by Onorato et al. (1979) and, following experiments to find the Zr diffusion coefficient, a cooling rate of 0.6°C to 2.1°C/day was derived. A grain size function calculated in provided a variation from 2.1°C to 3.2°C/day.

Lofgren et al. (1975), using a comparison of phenocryst morphologies and rock textures with those produced in dynamic crystallization experiments (known linear cooling rates), determined that both the phenocrysts and the matrix crystallized during cooling at less than 1°C/hr. Grove and Walker (1977), in a similar but more refined study, also determined cooling rates. From the pyroxene nucleation density they determined a rate of about 0.1°C/hr for early stage cooling, and from plagioclase dimensions determined a rate of about 0.2°C/hr for the late stage cooling. They suggested that the final position from a conductive boundary was 263 cm; Brett (1975), on the basis of then-available and limited kinetic data, had suggested that 15076 cooled in a flow about 1 m thick.

EXPERIMENTAL PEROLOGY: Humphries et al. (1972) diagrammed the results of equilibrium crystallization experiments on 15076, at an $_{f}O_2$ of Fe/FeO equilibrium. The sequence is spinel at about 1230°C, ol + pig + spinel at about 1190°C (ol out by 1180°C), then sp + pig + oxide to 1150°C where plagioclase enters and spinel goes out. Clinopyroxene enters at about 1120°C and by then the charge is almost solid. As they do for other mare basalts, they believe the mafic nature of the rock is from mafic mineral accumulation, hence that the liquid was erupted at 1150°C at an ol-pig-plag cotectic. Most authors disagree with such an interpretation. Grove and Lindsley (1979) used the composition of 15076 in their study to determine pigeonite-liquid partition coefficients for Fe, Mg, Ca, Cr, Al, Ti, and Mn.

All other experimental work has been dynamic, referred to under "Cooling Rates", above.

CHEMISTRY: Chemical analyses for bulk rock are listed in Table 1, and rare earths are plotted in Figure 7. The data are not entirely consistent (e.g., variation in TiO_2, MgO), presumably a consequence of small sample size and coarse grain size. The data clealy show 15076 to be one of the quartz-normative mare basalts.

TABLE 15076-1. Chemical analyses of 15076

		,24	,2	,21	,21	,21	,52	?	,0	,23	,3	,10	?	,20
Wt %	SiO2	48.82	48.80	48.06										
	TiO2	1.83	1.46	2.01	1.90		1.47							
	Al2O3	8.31	9.30	9.63			9.26							
	FeO	20.45	18.62	20.22	18.5		19.74							
	MgO	9.43	9.46	7.80	7.75									
	CaO	10.30	10.82	10.74								10.6		
	Na2O	0.40	0.26	0.29	0.30		0.30							
	K2O	0.08	0.03	0.05	0.049				0.049			0.044		
	P2O5	0.05	0.03	0.08										
(ppm)	Sc	40					47							
	V	135												
	Cr	2123					3380							
	Mn	2250	2090	2250										
	Co	42					41							
	Ni	32		11										
	Rb	1.2		1.1	0.917	0.924								
	Sr	98		120	112	111.8								
	Y	26		29										
	Zr	64		97										
	Nb	<10		6.2										
	Hf						2.1							2.866
	Ba	58			62.7									
	Th							0.5901	0.45					
	U				0.149			0.1532	0.12					
	Pb							0.266						
	La	10			7.38		4.7							
	Ce				15.1									
	Pr													
	Nd				10.6									11.850
	Sm				3.52		3.4							3.796
	Eu				0.970		0.98							
	Gd				4.95									
	Tb						0.7							
	Dy				5.60									
	Ho													
	Er				3.40									
	Tm													
	Yb	3.7			2.77		2.4							
	Lu				0.326		0.40							0.394
	Li	5.6												
	Be	1.2												
	B													
	C										21			
	N													
	S		300	800						452/499			970	
	F													
	Cl													
	Br													
	Cu	9.1												
	Zn													
(ppb)	I													
	At													
	Ga	4100												
	Ge													
	As													
	Se													
	Mo													
	Tc													
	Ru													
	Rh													
	Pd													
	Ag													
	Cd													
	In													
	Sn													
	Sb													
	Te													
	Cs													
	Ta					440								
	W													
	Re													
	Os													
	Ir													
	Pt													
	Au													
	Hg													
	Tl													
	Bi													
		(1)	(2)	(2)	(2)	(3)	(4)	(5)	(6)	(7)	(8)	(9)	(10)	(11)

References to Table 15076-1

References and methods:

(1) Christian et al. (1972), Cuttitta et al. (1973); XRF, semi-micro chemical, optical emission spec.
(2) Rhodes and Hubbard (1973), Wiesmann and Hubbard (1975), Hubbard et al. (1973), Church et al. (1972); XRF, ID/MS
(3) Nyquist et al. (1972, 1973); ID/MS
(4) Fruchter et al. (1973); INAA
(5) Tatsumoto et al. (1972); ID/MS
(6) O'Kelley et al. (1972); gamma ray spec.
(7) Thode and Rees (1972);
(8) Moore et al. (1972, 1973); combustion, GC
(9) Stetter et al. (1973); Ar-isotopes, irradiation
(10) Gibson et al. (1975); combustion
(11) Unruh et al. (1983); ID/MS

Figure 7. Rare earths in 15076.

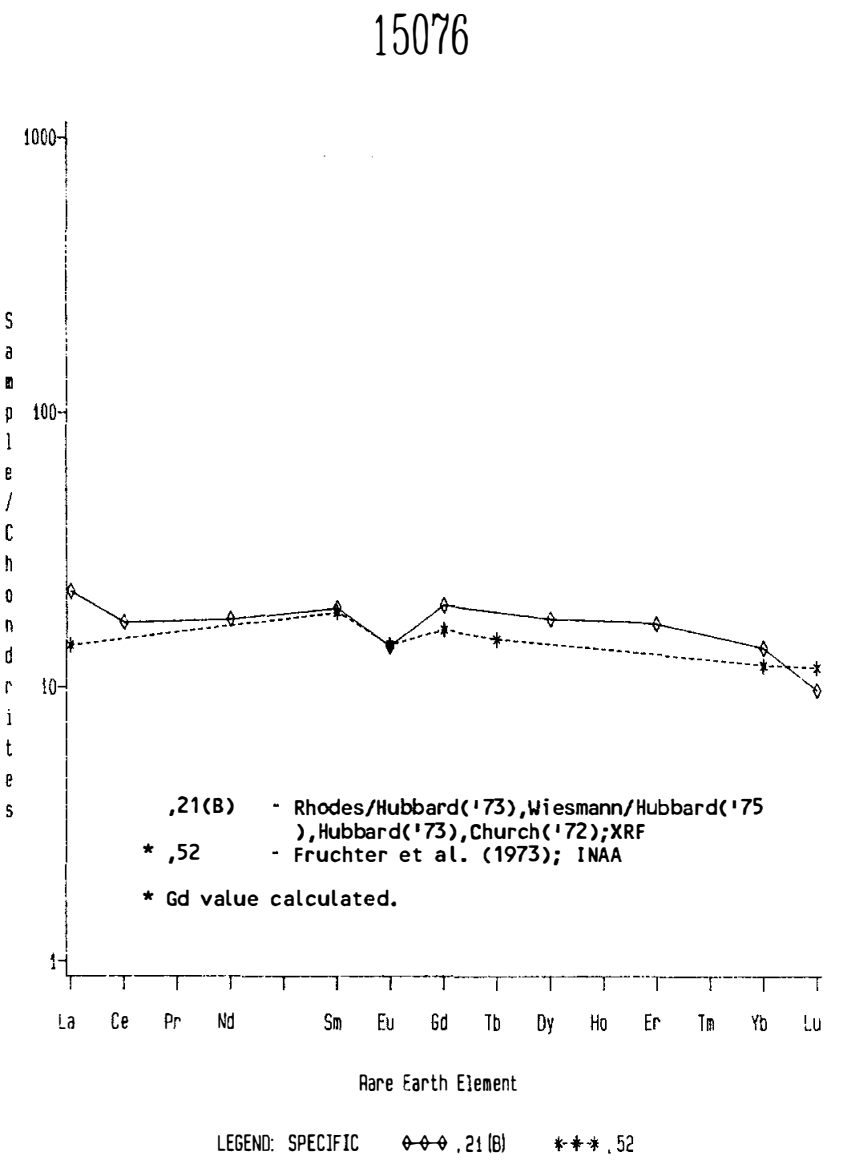

The averages would indicate that 15076 is a rather average Apollo 15 quartz-normative basalt. Hubbard and Rhodes (1973) noted that agreement between their two splits was poor. Rhodes (1972) used the composition in producing an average for the quartz-normative basalts. Christian et al. (1972) and Cuttitta et al. (1973) also reported an "excess reducing capacity" of +0.18, and analyzed for but found no Fe_2O_3. Light element abundances are similar to those for other mare basalts; the S analyses show a wide variation, and those data from combustion (e.g., Gibson et al., 1975, 970 ppm) are probably more reliable and reasonable than those from acid hydrolysis, etc. Gibson et al. (1975) also analyzed for C in CO (3.0 ppm C), in CO_2 (10.6 ppm C), for H in H_2 (18.6 ppm H), for S in H_2S (651 ppm S), and for Fe^o (1040 ppm by hydrolysis, 940 by magnetics).

STABLE ISOTOPES: Sulfur isotopic analyses were reported by Thode and Rees (1972) ($\delta^{34}S$ °/oo = 0.57) and Gibson et al. (1975) ($\delta^{34}S$ °/oo = -1.2). These isotopic values are similar to those of other mare basalts.

RADIOGENIC ISOTOPES AND GEOCHRONOLOGY: Papanastassiou and Wasserburg (1973) reported a Rb-Sr internal isochron age of 3.33 ± 0.08 b.y. with initial $^{87}Sr/^{86}Sr$ of 0.69927 ± 8, within error the same as other Apollo 15 mare basalts. The isochron is based on tabulated data for plagioclase, "ilmenite", and "cristobalite" separates. Nyquist et al. (1972, 1973) and Wiesmann and Hubbard (1975) reported whole rock $^{87}Rb/^{86}Sr$ of 0.0237 ± 4 and $^{87}Sr/^{86}Sr$ of 0.70051 ± 7, consistent with the internal isochron when an appropriate interlaboratory correction is made.

Stettler et al. (1973) reported a ^{40}Ar-^{39}Ar high temperature plateau age of 3.35 ± 0.04 b.y. (Fig. 8). The Ca/K release is similar to other mare basalts and demonstrates that K is not located in a single phase. Kirsten et al. (1973) reported a ^{40}Ar-^{39}Ar plateau age which is the same, 3.35 ± 0.15 b.y.

Tatsumoto et al. (1972) reported U, Th, and Pb isotopic data for a whole-rock sample (Table 2). The data lies, with 15065, 15085, and 15476, on a 3.5 to 4.65 b.y. model discordia line. Rosholt and Tatsumoto (1973) and Rosholt (1974) discussed α-spectrometry measurements of $^{232}Th/^{230}Th$ as compared with the value for that ratio expected from the $^{232}Th/^{238}U$ concentration ratio. The expected/measured ratio of 1.48 was the highest among A15 mare basalts, and Rosholt (1974) discussed possible and probable reasons for the discrepancy.

Unruh et al. (1984) reported Sm-Nd and Lu-Hf whole rock isotopic data (Table 3). The Sm/Nd, Lu/Hf, ϵNd, and ϵHf values are similar to those for other Apollo 15 mare basalts, which are discussed as a group. 15076 underwent Sm/Nd and Lu/Hf fractionations at the time of melting, 3.3 b.y. ago.

RARE GASES, COSMOGENIC NUCLIDES, TRACKS, MICROCRATERS, AND EXPOSURE: Stettler et al. (1973) and Kirsten et al. (1973)

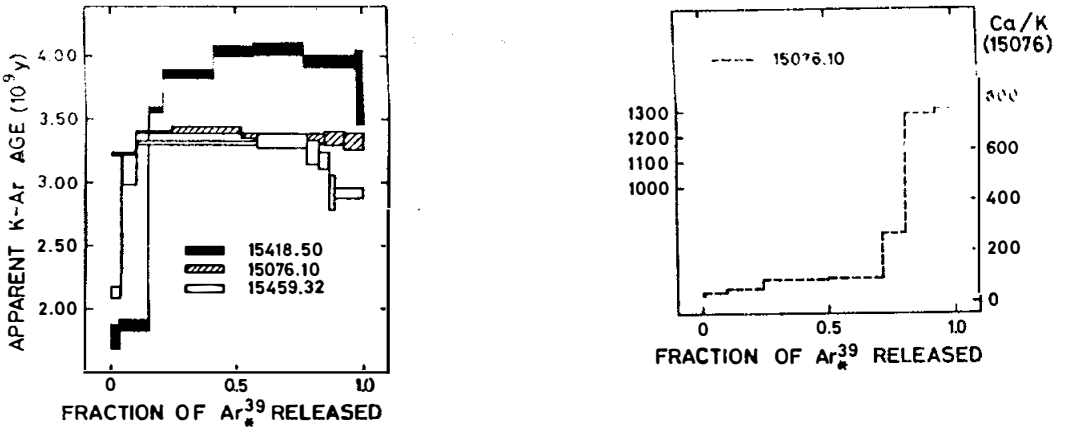

Figure 8. Ar release and Ca/K release for 15076,10 (Stettler et al., 1973).

TABLE 15076-2. U, Th, Pb isotopic data (Tatsumoto et al., 1972)

$^{206}Pb/^{204}Pb$	$^{207}Pb/^{204}Pb$	$^{208}Pb/^{204}Pb$	$^{232}Th/^{238}U$	$^{238}U/^{204}Pb$
374.4	155.8	393.1	3.98	460

Corrected for analytical blanks.

TABLE 15076-3. Sm/Nd and Lu/Hf whole-rock data for 15076,20 (Unruh et al., 1984)

$^{147}Sm/^{144}Nd$	$^{143}Nd/^{144}Nd_o$	ϵNd_o	$^{143}Nd/^{144}Nd_I$	ϵNd_I	$^{176}Lu/^{177}Hf$	$^{176}Hf/^{177}Hf_o$	ϵHf_o	$^{176}Hf/^{177}Hf_I$	ϵHf_I
0.1936 ± 2	0.512700 ± 16	+1.3 ±0.3	0.50854 ± 2	+2.6 ±0.4	0.01949 ± 3	0.282344 ±67	-18.3 ± 2.4	0.28108 ± 7	+13.8 ± 2.5

o = at present day; I = at time of crystallization

reported ^{38}Ar exposure ages of 330 m.y. and 280 m.y. respectively. This age is similar to that obtained by the same method for 15075, but much older than the track and microcrater ages (below).

Eldridge et al. (1972) reported cosmogenic nuclide disintegration count data for ^{22}Na, ^{26}Al, ^{46}Sc, and ^{54}Mn. They noted that the ^{22}Na appeared to have reached equilibrium, even though the chemistry was not known, but ^{26}Al was marginal; they suggested an exposure age of at least 2 m.y. Yokoyama et al. (1974) normalized the data for chemical composition, but were still unable to decide if the ^{26}Al activity was saturated or not.

Solar flare track density/depth relationships were studied by the Heidelberg group (Schneider et al., 1972, 1973a,b; Storzer et al., 1973; Fechtig et al., 1974). Their track density/depth measurements are summarized in Figure 9, with other samples for comparison. The original age determined, 8.5×10^4 years, was revised up to 2.6×10^5 years (Fechtig et al., 1974) or 2.8×10^5 years (Horz et al., 1975) using a new flux calibration. This track age is significantly lower than the ^{38}Ar age, suggesting a recent exposure from a shallow depth of burial. Kratschmer and Gentner (1975) used a method for identifying heavy ions from their etchable tracks in feldspars, applying the results to fossil cosmic-ray and Fe calibration tracks to obtain information about the nuclear composition of the ancient cosmic radiation. The distributions of the track etching rates and the residual ranges for both fossil and calibration tracks were compared, but a definitive interpretation was not possible because the influence of annealing and the crystallographic effects were insufficiently known.

Microcraters were studied by Schneider et al. (1973b) (0.1 to 10 microns) and by Morrison et al. (1973) (100 to 1,000 microns). Cumulative frequency/diameter diagrams are shown as Figure 10 and 11. Schneider et al. (1973b) used an SEM and noted that their statistics were good in the less than 1 micron range, but poor above this size. They estimated a cosmic dust flux in the submicron range from the size distribution and exposure age (solar flare) (Fig. 12); this flux was lower than that from satellite-borne detectors. (The later change in the solar flare calibration to make the exposure older would decrease the calculated flux.) Brownlee et al. (1972) noted that the crater density was very low, about 10 times less than 15286 or Luna 16 glass. Morrison et al. (1973) also found an exceptionally low frequency of craters, and estimated the age as 8 to 17 $\times 10^5$ years. Combined with the Schneider et al. (1973b) data, there appears to be a flexure in the distibution below 100 microns and probably at about 10 microns if both surfaces investigated are actually the same age.

PHYSICAL PROPERTIES: Gose et al. (1972) and Pearce et al. (1973) reported magnetic data (Table 4), including NRM in some detail. The NRM is similar to other basalts (between 10^{-5} and 10^{-6}

Figure 9. Depth dependence of solar flare tracks on 15076,31 and other samples (Storzer et al., 1973).

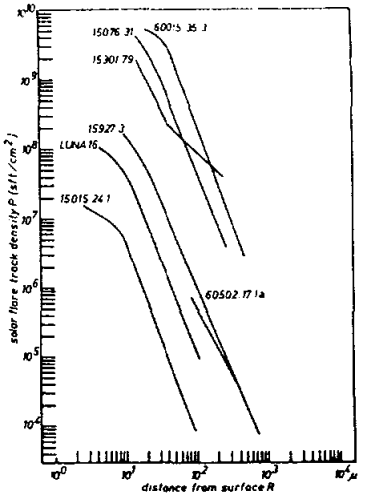

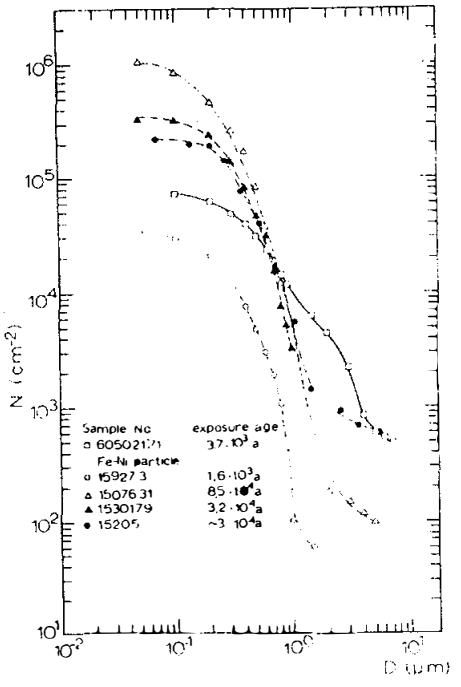

Figure 10. Cumulative crater densities N vs. pit diameter D for 15076 and other samples (Schneider et al., 1973b).

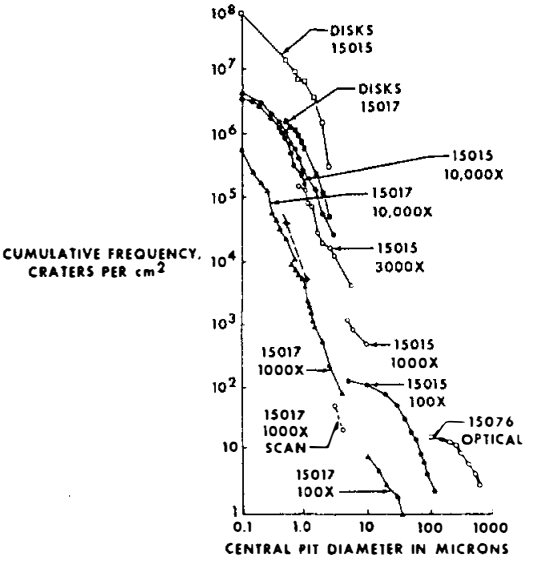

Figure 11. Cumulative crater density vs. pit diameter for 15076 and other samples (Morrison et al., 1973).

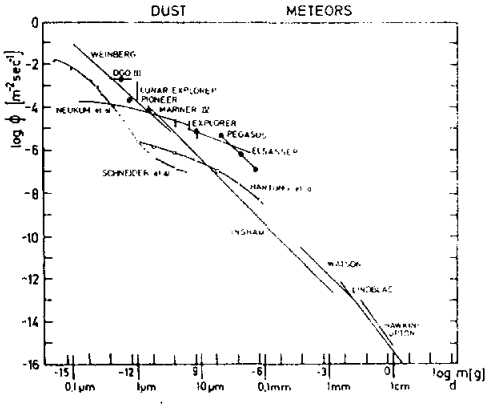

Figure 12. Cumulative cosmic dust fluxes plotted against particle masses and diameters. Line marked "Schneider et al." is from 15076 data (Schneider et al., 1973b).

TABLE 15076-4. Room temperature magnetic data (Pearce et al., 1973)

J emu/g	X_p emu/g Oe	X_o emu/g Oe	Jrs/Js	Hc Oe	J_s/X_o KOe	Equiv Fe°	Equiv. Fe²l
0.21	33.8	0.53	0.004	11.0	3.9	0.095	15.5

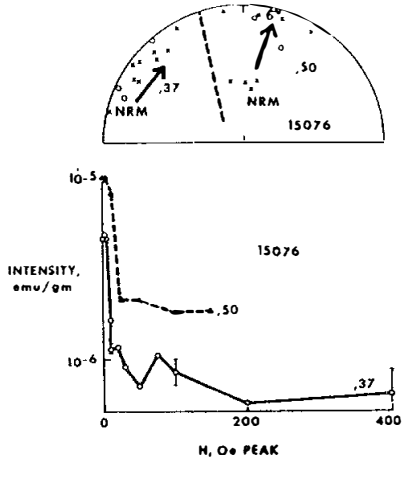

Figure 13. AF demagnetization of two splits of 15076. Arrows show change in direction upon demagnetization (Pearce et al., 1973).

emu/g). Under AF-demagnetization, two chips had stable magnetization (Fig. 13). A soft magnetization was eliminated after cleaning in 250 Oe, and there were no major changes in intensity or direction up to 150 Oe. However, Brecher (1975, 1976) listed 15076 under her category of rocks "inhomogeneous in NRM intensity or direction", presumably because of the higher stable intensity of ,50 (Fig. 13).

PROCESSING AND SUBDIVISIONS: A chip was taken from ,0, and subsplit to make samples ,1 to ,11, some of which were interior only and some of which had exterior. ,4 was potted and produced thin sections ,12 and ,14 to ,19, and ,11 was subsplit (,20 to ,24) for isotopic and chemical analyses. Subsequently, the sample was sawn (1972) and a slab subdivided as shown in Figure 14. Several of these pieces were further subdivided, including ,28, which was potted and produced thin sections ,68 to ,72. In 1975 the "W" end was sawn off (Fig. 14) and subdivided (,87, 6.6 g; ,88, 44.4 g; ,89, 3.96 g; and ,90, 5.2 g) for remote storage at Brooks. ,0 now has a mass of 239.5 g. Nearly all other pieces are less than 4 g each.

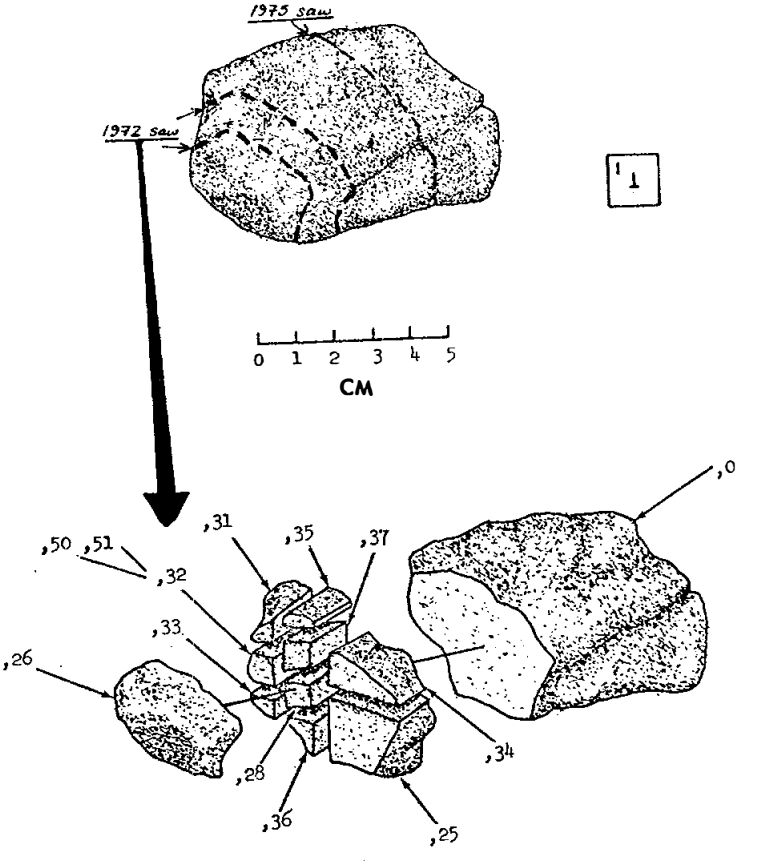

Figure 14. Sawing of 15076, in 1972 and 1975.

15085 PORPHYRITIC SUBOPHITIC QUARTZ-NORMATIVE ST. 1 471.3 g MARE BASALT

INTRODUCTION: 15085 is a coarse-grained basalt (Fig. 1), with large, zoned pigeonite crystals. It has been dated as close to 3.40 b.y. old. The sample is blocky and subrounded. It is generally tough or coherent, but there are penetrative fractures which make some portions quite friable. It is light brownish gray overall, but consists of yellow-brown mafic minerals and white plagioclases. It has no zap pits but about 2% vugs into which pyroxene and plagioclase grains project.

15085 was collected on the east flank of Elbow Crater, as one of five basalt samples collected on a line extending out from the crater (see Fig. 15065-1). It was collected with breccia 15086 about 60 m from the rim crest, in a flat area with distinctly spaced cobbles such as 15085. Its orientation is known.

PETROLOGY: 15085 is a coarse, quartz-normative mare basalt, lacking magnesian olivine but containing zoned pigeonite crystals (Fig. 2). These are less-easily described as phenocrysts in 15085 than in other quartz-normative basalts because the plagioclases are also very large (both pigeonite and plagioclase up to about 1 cm), although the plagioclase is less abundant and most is smaller. The pigeonites have simple twins, and zone to augite; in many cases the pigeonite to augite transition is very sharp. The rims contain inclusions; discrete augite grains also occur in the groundmass. The plagioclases are slightly zoned optically. Tridymite blades are a common accessory, frequently embedded in pyroxferroite, and there are small patches of mesostasis consisting of tridymite laths, glass, and opaque phases. Cristobalite occurs as irregular patches. Opaque phases range from chromite (in pigeonite cores) to ulvospinel and residual ilmenite. Some patches consist of brown material consisting of a fine-grained intergrowth of (probably) silica, fayalite, and a second mafic phase; these patches pseudomorph pyroxferroite(?) and some pyroferroite grains contain patches of this assemblage.

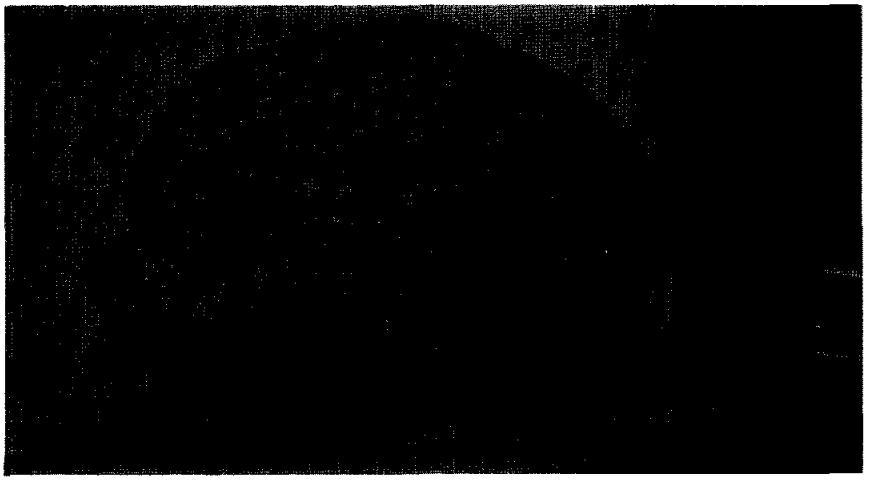

Figure 1. Pre-split view of 15085. S-71-45889

Fig. 2a

Fig. 2b

Figure 2. Photomicrographs of 15085,11. Widths about 3 mm. a)c) transmitted light. b)d) crossed polarizers. a)b) coarse groundmass with large plagioclases. Lath at right is tridymite. c)d) two zoned pigeonites (lower is twinned, and part of a 1 cm grain). Middle right are tridymite laths intergrown with opaque phases. Upper right are tridymite laths embedded in a 1 mm grain of pyroxferroite.

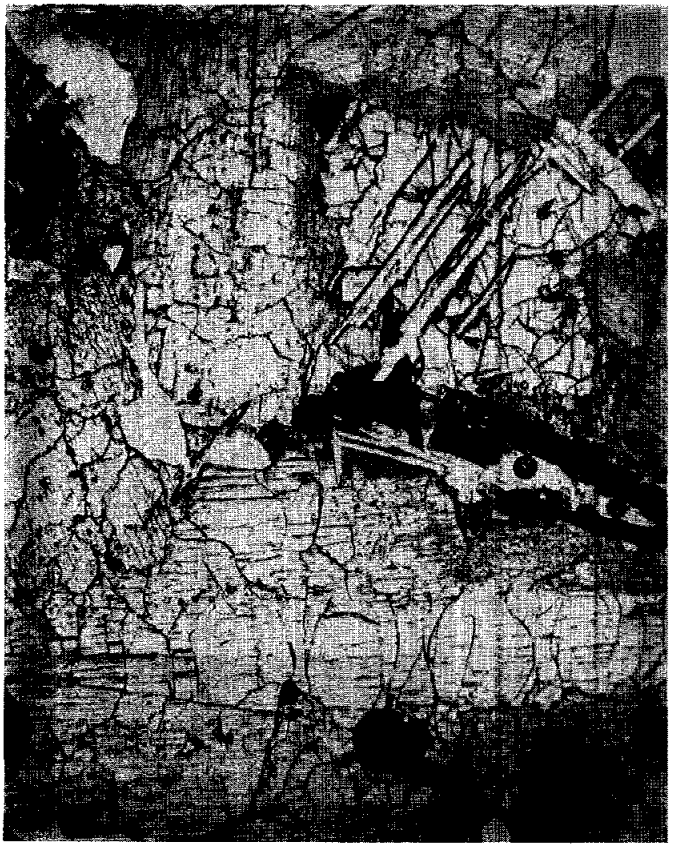

Fig. 2c

Fig. 2d

The Lunar Sample Information Catalog Apollo 15 (1972) reported a mode of 66% clinopyroxene, 22% plagioclase, 4% tridymite, 2% pyroxferroite, 1.5% ilmenite, 1.5% ulvospinel, and less than 0.1% each of Fe-Ni metal, troilite, Cr-spinel, and an unidentified phase. Mason (1972) reported that the sample contained 0.7% (wt) tridymite and 0.4% (wt) cristobalite. Papanastassiou and Wasserburg (1973) noted that plagioclase was fractured and there was clear indication of shock, but shock features are not apparent in most of the sample.

The pyroxenes are extensively zoned (Brown et al., 1972a,b), but the low-Ca pigeonite cores are extensive (60% or so of each crystal) (Fig. 3). The zoning is mainly to subcalcic ferro-augite; augite itself is rare. Some cores are subcalcic pigeonites (2.2% CaO) and might be hypersthene (Brown et al.

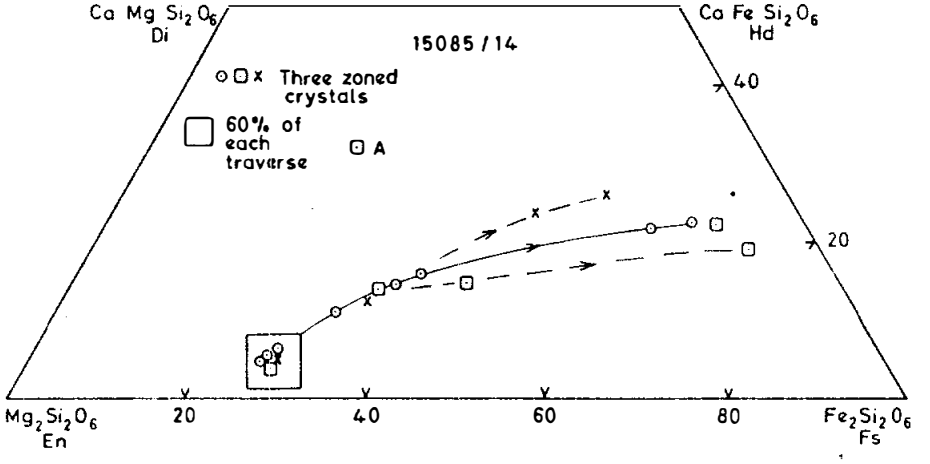

Figure 3. Pyroxene compositions (Brown et al., 1972b).

(1972b). Rims have Ti/Al less than 1/2, suggesting that Ti^{3+} is present. Takeda et al. (1975) made single crystal x-ray diffraction studies of pyroxenes, tabulating cell dimensions, relative orientations, and space groups ($P2_1/c$ for pigeonite, C2/c for augite). Microprobe analyses showed zoning from $En_{67.5}Wo_{5.1}$ to $En_{42.6}Wo_{36.7}$. The pigeonites have augite oriented on both (001) and (100) but a lack of distinct core/rim relations in the sample studied make it difficult to distinguish epitaxial growth from an exsoluton relationship. Exsolution is not visible optically. A subcalcic augite exsolved pigeonite on (001), with $\Delta\beta$ for the pair being 2.4°.

Mason (1972) described and analysed the tridymite and cristobalite crystals. The tridymite occurs as thin platy crystals (narrow laths in section) (see Fig. 2) and the cristobalite as anhedral grains showing a mosaic texture attributed to inversion. Tridymite also shows patchy extinction attributable to inversion. Both have low birefringence: tridymite about 0.003, cristobalite about 0.001. The analyses (Table 1) show them to be more than 99% SiO_2, but with appreciable TiO_2. The molecular ratio of Al_2O_3 to (Na_2O + K_2O + CaO) is close to unity, suggesting replacement is of the type K + Al ⇐⇒ Si. There appears to be little chemical difference between the two polymorphs, except perhaps lower K_2O and Al_2O_3 in the cristobalite. The tridymite indicates that crystallization was completed at 1000°C or less; the cristobalite clearly crystallized outside its thermodynamic stability field.

L. Taylor et al. (1975) reported analyses of spinel phases, ranging from Ti-chromites to Cr-ulvospinel (Fig. 4). They do not display the "core-rim" textures common in Apollo 12 spinels. Brown et al. (1972b) and Papanastassiou and Wasserburg (1973) each listed an analysis of a spinel. L. Taylor et al. (1975) also reported Fe-metal analysis (Fig. 5). The metals include some with unusually high Ni compared with other mare basalts, up to 58.2 wt%.

Cooling Rates: Lofgren et al. (1975), in a comparison of the natural rock textures with those produced in dynamic crystallization experiments, deduced cooling rates of <1°C/hr for both the pigeonites and for the groundmass, and 15085 appeared to have cooled the slowest among those studied. Grove and Walker (1977) determined a late-stage cooling rate of 0.01°C/hr from the plagioclase dimensions, also as compared with the products of dynamic crystallization experiments. The sample seems to have experienced a slow, nearly linear cooling rate throughout its entire cooling history. L. Taylor et al. (1975) used the partitioning of Zr between ilmenite and ulvospinel to determine a cooling rate of 7°C/day, in agreement with the Lofgren et al. (1975) estimate of less than 24°C/day. The underlying model was improved by Onorata et al. (1979) with experimental determination of the diffusion of Zr, revising the cooling rate to 1.00 to 2.8°C/day. A model taking grain size into account was also investigated. Takeda et al. (1975), on the basis of $\Delta\beta$ (2.4°)

TABLE 15085-1. Analyses of tridymite and cristobalite (Mason, 1972)

	tr	cr
SiO2	[99.05]	[99.13]
TiO2	.28	.38
Al2O3	.34	.18
FeO	<0.02	.09
MnO	<0.02	<0.02
MgO	<0.03	<0.03
CaO	0.02	<0.02
Na2O	0.05	0.05
K2O	0.26	0.17
P2O5	<0.03	<0.03

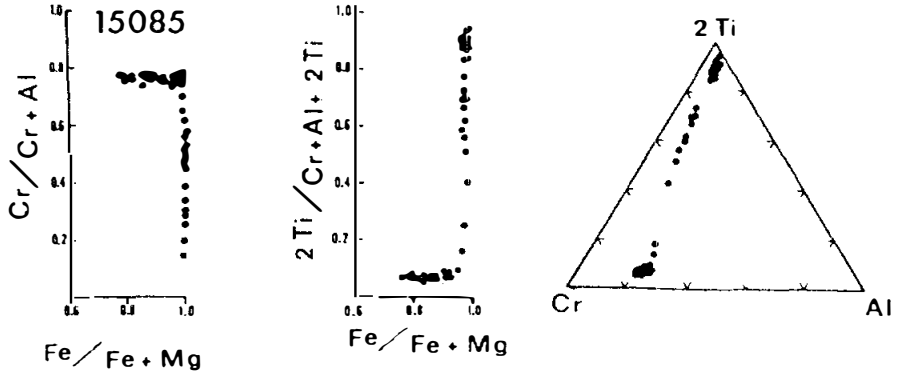

Figure 4. Spinel compositions (Taylor et al., 1975).

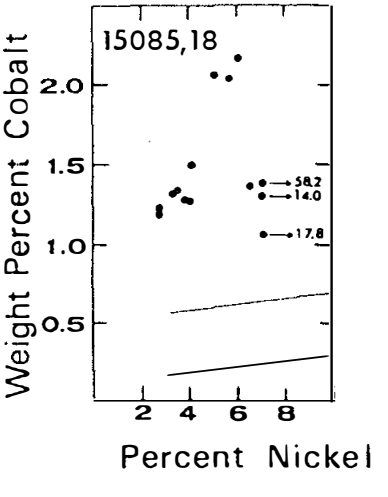

Figure 5. Metal compositions (Taylor et al., 1975).

for an augite-pigeonite exsolution pair, suggested that 15085 was slowly cooled, but not as slowly as 15058 or 15475 (a minor reversal of the sequence as determined from experimentally determined textures).

CHEMISTRY: Bulk rock analyses are listed in Table 2, with rare earths shown in Figure 6. There are some severe discrepancies among samples which are a result of the small sample sizes and the coarse grain size. The analysis of Rhodes and Blanchard (1983 and unpublished) is based on the most representative sampling: 10 g were reduced to medium sand size and then 2 g were used for the analysis. This analysis (data not available) removes any doubt that 15085 is a member of the quartz-normative basalt group. Sampling problems and discrepancies among splits had been referred to by previous workers (e.g., Mason et al., 1972). Ganapathy et al. (1973) found the siderophiles and volatiles to be similar to those in fine-grained sample 15597, indicating that there was little fractionation of these elements during shallow-level crystallization. Helmke and Haskin (1972) put 15085 in a group of high Sm/Eu quartz-normative basalts.

Gibson et al. (1975) reported data for C in CO (3.3 ppm C), in CO_2 (7.8 ppm C); for H in H_2 (9.7 ppm); and for S in H_2S (559 ppm S; acid hydrolysis). They also reported abundances of Fe^o of 542 and 340 ppm from hydrolysis and magnetic techniques respectively. Wanke et al. (1976) also reported a determination for oxygen.

Helmke et al. (1972) and Helmke and Haskin (1973) tabulated trace element data for separated minerals, in a study of the effects of closed-system crystallization (Fig. 7). The patterns are not distribution coefficients, although that for pigeonite could be close to one. The unusual pattern for augite can be understood in terms of closed-system crystallization. Jovanovic and Reed (1977) reported mineral separate data for Hg, Ru, and Os, and for the Hg released from these minerals at less than 130°C. The Ru and Os in the minerals (combined) were 6x as much as these in the whole rock, but the Ru/Os ratio was the same; apparently these elements are not uniformly distributed in the rock.

STABLE ISOTOPES: Gibson et al. (1975) reported $\delta^{34}S_{CDT}$ o/oo of -1.3, of the sulfur produced during their total combustion. This isotopic ratio is similar to that of other mare basalts.

RADIOGENIC ISOTOPES AND GEOCHRONOLOGY: Papanastassiou and Wasserburg (1973) reported a Rb-Sr two point isochron age of 3.40 ± 0.04 b.y. with an initial $^{87}Sr/^{86}Sr$ ratio of 0.69923 ± 6 b.y. The tabulated data are for the separates plagioclase and "ilmenite".

Tatsumoto et al. (1972) reported U, Th, and Pb isotopic data for a whole rock sample, which falls on a 3.5 to 4.65 b.y. discordia line ($^{206}Pb/^{238}U$ vs. $^{207}Pb/^{235}U$) when plotted with 15065, 15076, and 15476. Unruh and Tatsumoto made a detailed study of the U, Th, and Pb isotopic systems for whole rock and mineral separate

TABLE 15085-2. Bulk rock chemical analyses

	,21	,34	,6	,8	,71	,●	,5	,34	,39	,97	,47	,47	,50	,71(b)	,71(b)
SiO2		46.39						46.61	47.73				48.06		
TiO2		3.07	1.67	2.60				2.63	1.96				1.57		
Al2O3		5.79	10.0	6.61				7.13	9.92				11.17		
FeO		26.75	18.3	23.0				24.38	19.69				18.42		
MgO		8.20						7.90	8.84				7.85		
CaO		9.12						9.68	10.63				11.23		
Na2O		0.21	0.3●●	0.243				0.26	0.33				0.365		
K2O		●.07				0.048		0.059	0.035				0.54		
P2O5		0.09						0.107	0.064		0.068		0.055		
Sc			41	51									44.0		
V		110						172	165						
Cr		4●●0	3350	3980				4200	3570				2940		
Mn	2440	2870						2300	2160				2010		
Co		49	42	48				43	41				35.7		
Ni	37	45						20	23				31		
Rb		<5					0.86	1.8	<1.5				0.73		
Sr		92						120	112				107		
Y		54						44.0	28.6				21		
Zr		150						156	92				99		
Nb								10.0	6.6						
Hf			2.0	3.1									2.44		
Ba	68	87						110	60				62.1		
Th					0.4588	0.57							0.42	0.408	0.426
U					0.1183	0.138	0.135				0.16		0.13	0.106	0.111
Pt		2			0.208									0.186	0.174
La	4.92		4.5	6.5									5.88		
Ce	13.2												16.5		
Pr													2.5		
Nd	10.2												13.1		
Sm	3.86		3.15	4.5									3.79		
Eu	0.84		1.02	1.12									1.07		
Gd	4.9												5.4		
Tb	0.90		0.7	1.1									0.92		
Dy	5.79												5.65		
Ho	1.16												1.2		
Er													3.5		
Tm															
Yb	2.63		2.0	3.1									2.72		
Lu	0.393		0.36	0.53									0.43		
Li		8									6.5		7.8		
Be															
B		5													
C															
N															
S								1370	680	855			715		
F													22.4		
Cl										3.21		4.0			
Br							0.008				13.7		0.018		
Cu		18						9	29				10.6		
Zn							1.05	<1.5	17				3.33		
I											0.69				
At															
Ga		5000											3240		
Ge							2.8						50		
As													0.5		
Se							123						126		
Mo															
Tc															
Ru												0.5(a)			
Rh															
Pd															
Ag							1								
Cd							0.68								
In							0.6								
Sn															
Sb							0.035								
Te							6.2								
Cs							42						37		
Ta			460	770									410		
W													59		
Re							0.0015								
Os												0.19			
Ir							0.0069								
Pt															
Au							0.012						0.44		
Hg															
Tl							0.24								
Bi							0.12								
	(1)	(2)	(3)	(3)	(4)	(5)	(6)	(7)	(7)	(8)	(9)	(10)	(11)	(12)	(12)

References and methods:

(1) Helmke and Haskin (1972), Helmke et al. (1973); INAA
(2) Mason et al. (1972); general silicate analysis, gravimetric, flame photometry, colorimetry, emission spec.
(3) Fruchter et al. (1973); INAA
(4) Tatsumoto et al. (1972); ID/MS
(5) Keith et al. (1972); gamma ray spectrometry
(6) Ganapathy et al. (1973); RNAA
(7) Duncan et al. (1975); XRF
(8) Gibson et al. (1975); combustion
(9) Jovanovic and Reed (1976b); neutron and photron activation, colorimetry
(10) Jovanovic and Reed (1977); INAA
(11) Wanke et al. (1976); XRF, RNAA, INAA
(12) Unruh and Tatsumoto (1977); ID/MS

15085

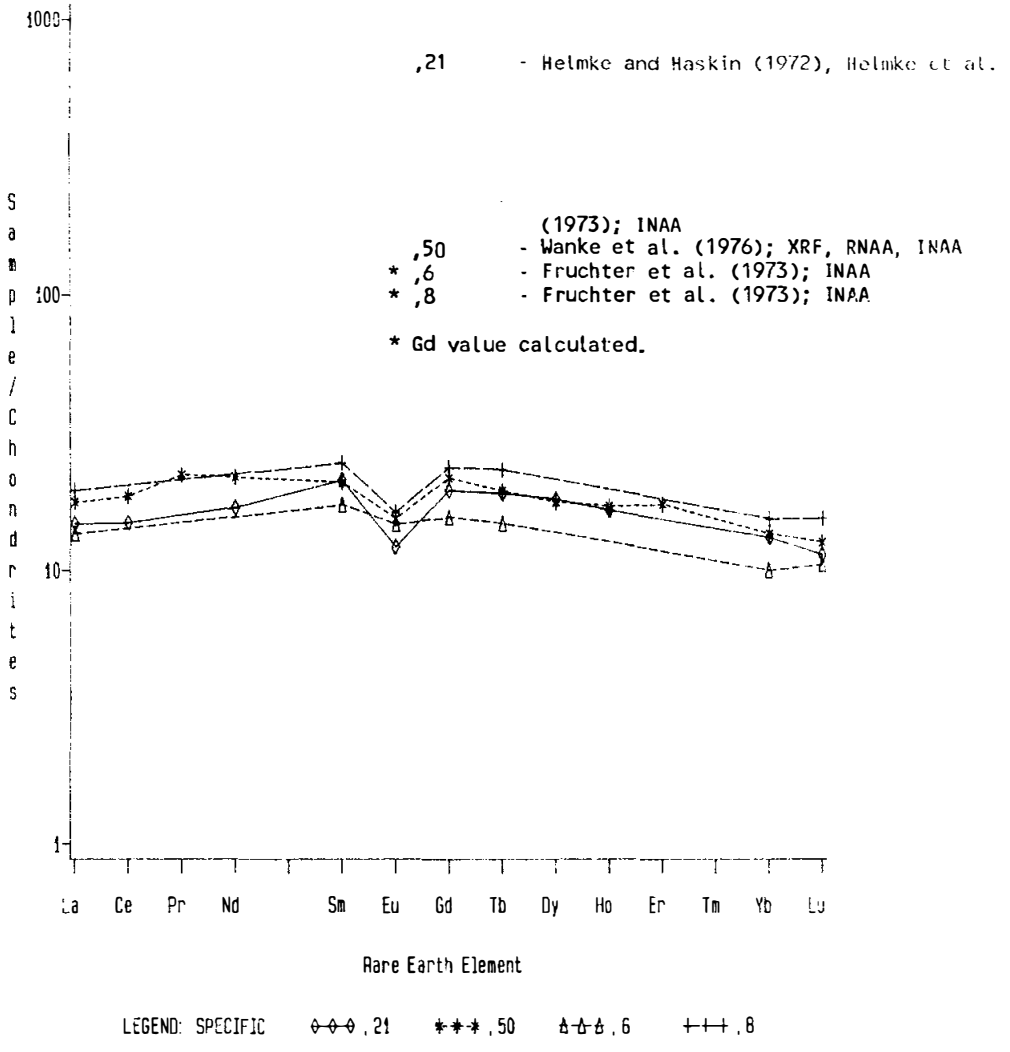

Figure 6. Rare earths in bulk rock samples.

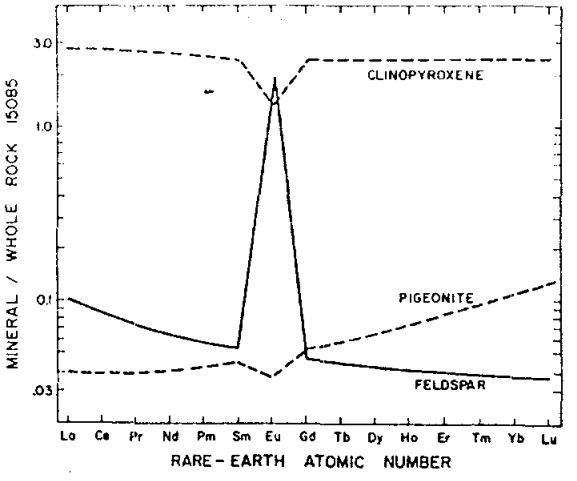

Figure 7. Rare earths in mineral separates (Helmke et al., 1973).

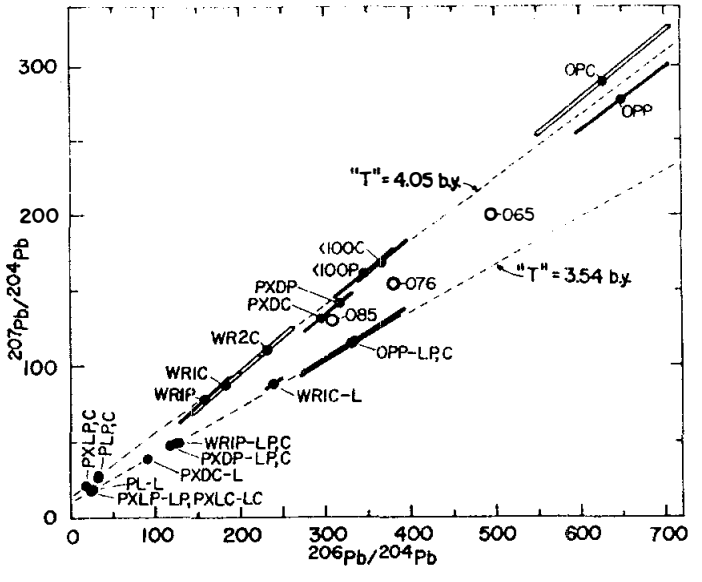

$^{206}Pb/^{204}Pb$ vs. $^{207}Pb/^{204}Pb$ plot of mineral separate residues and leaches from 15085. The leaches and residues define distinctly different trends yielding apparent ages of 3.54 ± 0.06 and 4.05 ± 0.08 b.y., respectively. The ages probably have no significance, and are much older than Rb-Sr and Sm-Nd ages of ~3.3-3.4 b.y. for this rock. The two trends suggest that post-crystallizational disturbances have affected the Pb-Pb system. The "old" ages suggest ^{207}Pb enrichment from an outside source or lack of isotopic homogenization prior to crystallization.

Figure 8. $^{206}Pb/^{204}Pb$ vs. $^{207}Pb/^{204}Pb$ in mineral separate residues and leaches from 15085 (Unruh and Tatsumoto, 1977).

samples of 15085. They tabulated data for separates, including leaches (HCl) and residues. Significant portions (20 to 50%) of the U, Th, and Pb were easily leachable, with the implication that such portions originally resided on grain boundaries, in microfractures, or in interstices. There is an apparent depletion of ^{207}Pb relative to ^{206}Pb on the leached fractions (Fig. 8), and an enrichment of ^{208}Pb. The trends cannot be explained by Pb contamination. The actual ages defined by the trends are both older than the actual crystallization age of about 3.4 b.y. and probably neither has any age significance. Similar trends on the U-Pb evolution diagram (Fig. 9) also have no real age significance other than that the lower concordia intercepts indicate some sort of post-crystallization disturbance. Individual parent-daughter diagrams for ^{206}Pb, ^{207}Pb, and ^{208}Pb are shown as Figure 10. The ^{206}Pb diagram shows an "age" for the residues of 3.44 ± 0.22 b.y. The ^{207}Pb shows an opposite effect: the leaches are younger, indicating ^{207}Pb depletion in grain boundaries. The anomalously old ages (3.6 b.y. leaches, 3.79 b.y. residues) suggest enrichment of ^{207}Pb relative to uranium. The ^{208}Pb shows relationships similar to the ^{206}Pb, with a combined "age" of 3.59 ± 0.25 b.y. Preferential leaching alone cannot account for the trends in Figure 10.

The distinct trends of the residues and leaches appear to represent either continuous or episodic post-crystallization disturbances, but a unique interpretation is not possible. Unruh and Tatsumoto (1977) proposed a two-stage, KREEP-mixing model to explain the U-Pb evolution in mare basalts, a model compatible with Rb-Sr and Sm-Nd data, but if the primary differentiation occurred at a time distinctly different from lunar accretion then a more complex model is required. They concluded that (according to reported and calculated U and Pb partition coefficients) the initial $^{238}U/^{207}Pb$ (μ) of the moon was quite high, i.e., 100 to 300.

Rosholt and Tatsumoto (1973) and Rosholt (1974) discussed α-spectrometry measurements of $^{232}Th/^{230}Th$ as compared with the value for that ratio expected from the $^{232}Th/^{238}U$ concentration ratio. The expected/measured ratio is 1.27, and its significance was discussed by Rosholt (1974).

EXPOSURE AND TRACKS: Keith et al. (1972) reported disintegration count data for ^{26}Al, ^{22}Na, ^{54}Mn, ^{56}Co, and ^{46}Sc. The ^{26}Al was saturated, implying a surface residence of a few million years. Yokoyama et al. (1974), correcting for composition, agreed that ^{26}Al was saturated.

Bhandari et al. (1972) and Bhattacharya et al. (1975) measured track densities in two surface chips of 15085. Densities of 6 and 12 x 10^6 cm^{-2}, and "suntan" ages of less than 1 m.y. were determined. Bhattacharya et al. (1975) reported the ages as less than 10 to 30 m.y.

PHYSICAL PROPERTIES: Collinson et al. (1972, 1973) determined

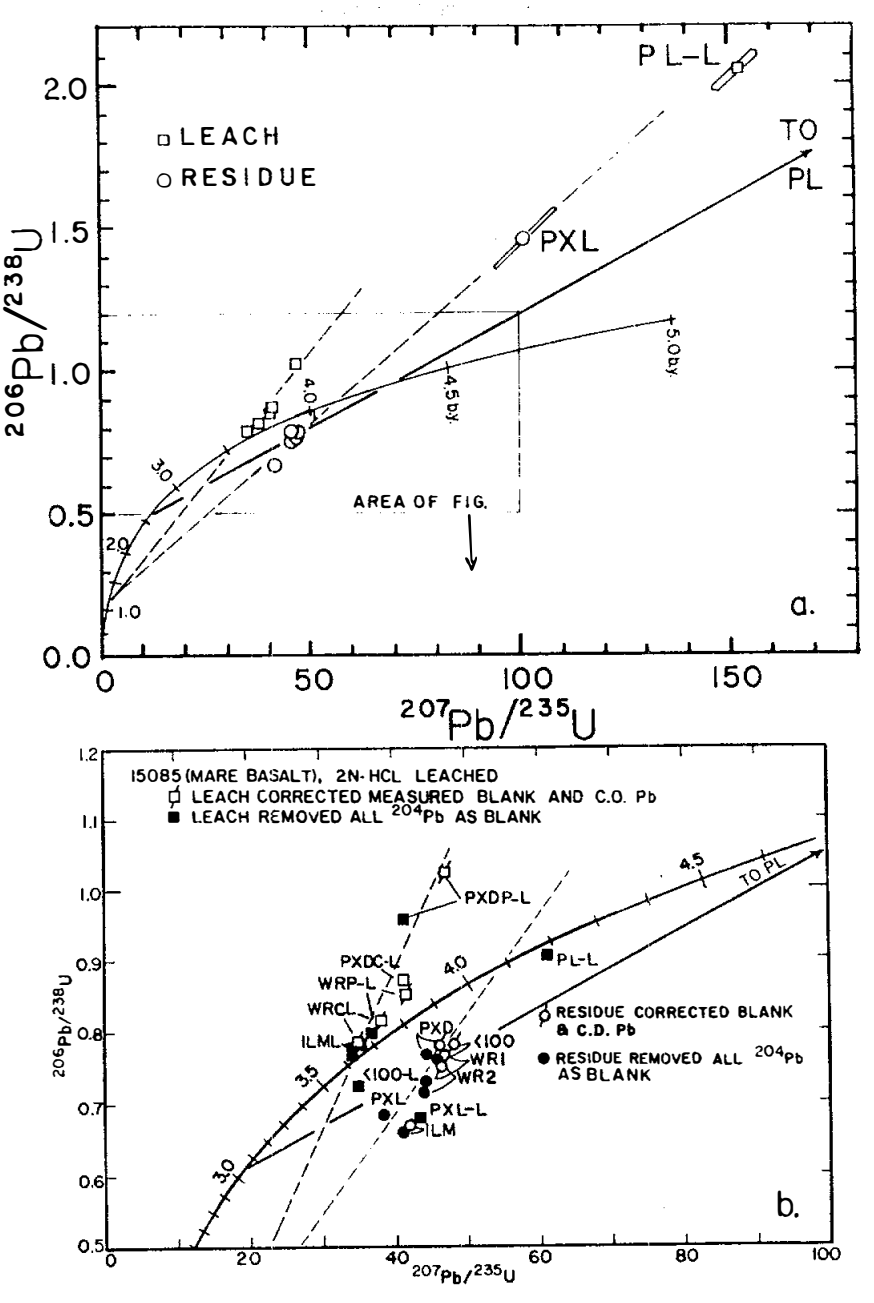

Figure 9. U-Pb evolution diagram. Corrected for Canyon Diablo troilite Pb (open symbols) and all ^{204}Pb as modern terrestrial (blank; closed symbols). Leach = squares. Residue = circles. (Unruh and Tatsumoto, 1977).

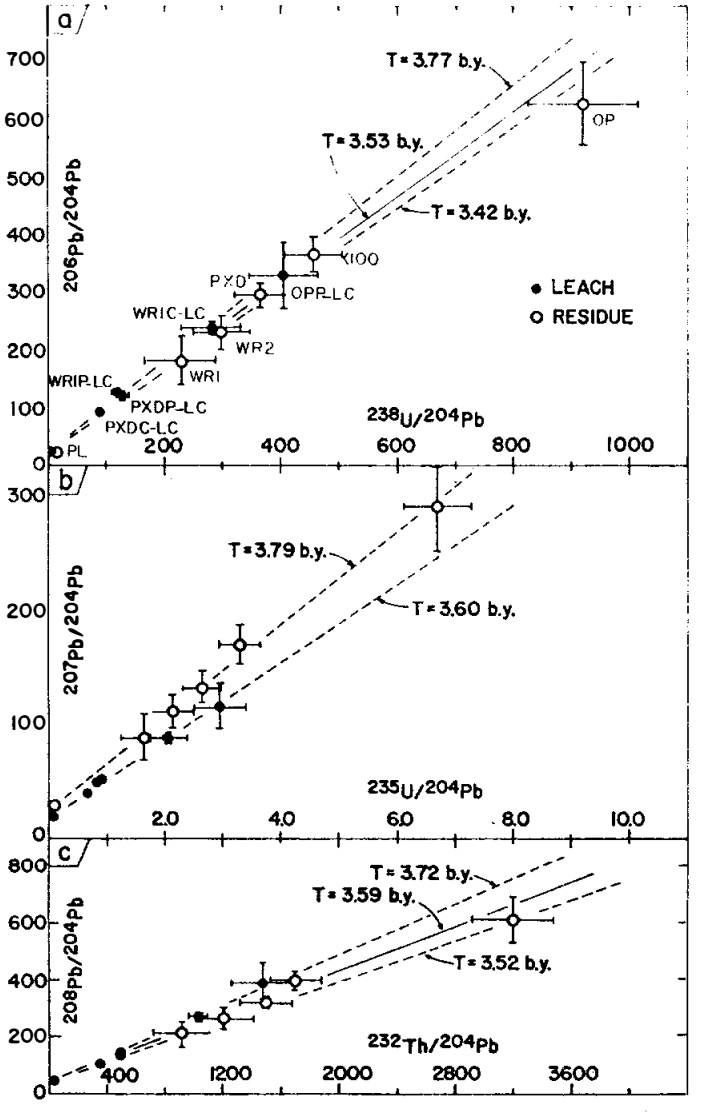

U–Pb and Th–Pb parent-daughter evolution diagrams for 15085. (a) $^{238}U/^{204}Pb$ vs. $^{206}Pb/^{204}Pb$ plot. The residues (open circles) define an "age" (lower broken line) of 3.42 ± 0.22 b.y. (95% confidence) which is in agreement with Rb–Sr and Sm–Nd ages. The leaches (closed circles) define a 3.77 ± 0.26 b.y. "age" (upper broken line). Combination of the data (solid line) yields a 3.53 ± 0.09 b.y. "age". (b) $^{235}U/^{204}Pb$ vs. $^{207}Pb/^{204}Pb$ plot. The residues (solid) line define a 3.79 ± 0.10 b.y. apparent age. The leach data (broken line) yield a 3.60 ± 0.12 b.y. "age". Both ages are older than the Rb–Sr and Sm–Nd ages which suggests ^{207}Pb enrichment relative to U (addition of "old" Pb). (c) $^{232}Th/^{204}Pb$ vs. $^{208}Pb/^{204}Pb$ plot. The residue trend (lower broken line) defines a 3.5 ± 0.5 b.y. apparent age, whereas the leaches (upper broken line) define a 3.72 ± 0.12 b.y. "age". However this very old age is mostly controlled by OP–L, which appears to have suffered Th–Pb fractionation during leaching. The combined data (solid line) yield an apparent age of 3.59 ± 0.25 b.y.

Figure 10. U-Pb and Th-Pb parent-daughter evolution diagrams. Residues = open circles. Leaches = closed circles. (Unruh and Tatsumoto, 1977).

the magnetic characteristics of two whole-rock samples. They had as-received natural remanent magnetisms (NRM) of 8.7, and 7.1, $x10^{-6}$ emu/g (Fig. 11). ,31 showed an approximately constant direction of NRM after removal of the soft components (AF demagnetization). Thermal demagnetization up to 500°C for ,32 produced the same general behaviour in NRM as AF treatment, but at high temperatures the directions scattered. Iron is the carrier of the magnetization. There is some evidence for anomalous variation in intensity during AF demagnetization. In rock magnetism studies, the two samples produced almost identical induced magnetization curves. They failed to saturate in a field of 8 KOe, and the slope of the graph at this field is 31 x 10^{-6} emu g^{-1} Oe^{-1}, which is still a significant fraction of the induced susceptibility. In thermoremanent magnetic studies, a sudden decrease in magnetization occurred at -150°C when being warmed from -196°C to 20°C. Measurements on a crystal near ulvospinel in composition gave almost identical results.

Greenmann and Gross (1972) reported luminescence studies of 15085, tabulating and diagramming peak wavelength, bandwidths, and band efficiencies for soft x-ray irradiation.

PROCESSING AND SUBDIVISIONS: A large chip (,2) was first removed from the "B"/"E" end corner, and split to produce daughters ,3 to ,9. ,4 was potted and produced thin sections ,11 to ,19 and ,23 to ,26. Several allocations were made from the other chips. Further chipping (Fig. 12) produced ,29 to ,33 from different parts of the sample, with ,33 producing thin section ,77; ,78; and ,16; some thin section mix-ups with sample 15285 were made and corrected. In 1974, large chips were made to produce samples for remote storage (,43, 20.00 g; ,44, 8.21 g; ,45, 27.99 g) at Brooks, producing several other daughters of small chips (,40 to ,56). In 1982, chipping was done to obtain about 10 g of representative sample, which was crushed to a medium sand size (,143). 2.3 g were allocated for chemical analysis (,152), the rest is stored. This action also produced a large piece (,142, 53.0 g) and other chips and fines.

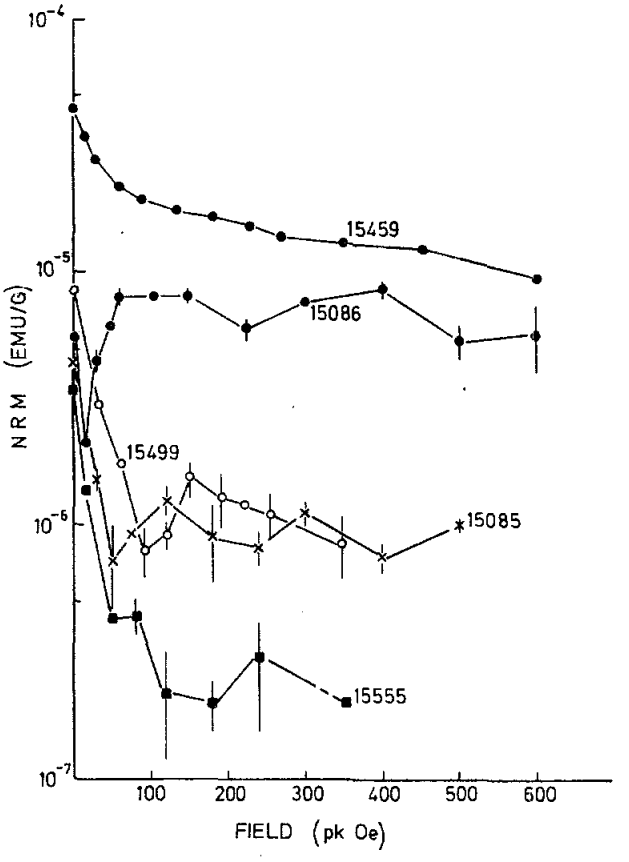

Figure 11. Alternating field demagnetization of 15085 and some other Apollo 15 samples. 15459 and 15086 (higher NRM) are breccias; the other samples are mare basalts (Collinson et al., 1973).

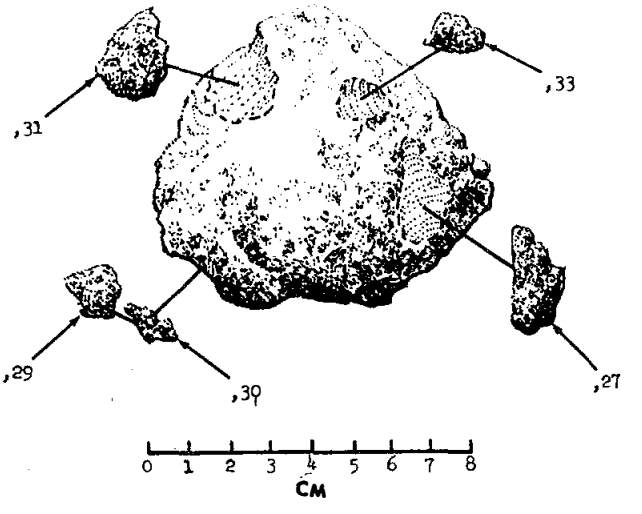

Figure 12. Part of the chipping of 15085.

15086 REGOLITH BRECCIA ST. 1 216.5 g

INTRODUCTION: 15086 is a very friable regolith breccia (Fig. 1) dominated by quartz-normative mare basalt fragments and green glass fragments and spheres. It has a composition similar to local regolith compositions. It is medium-gray and subrounded, and homogeneous. A few zap pits are present on several surfaces.

15086 was collected on the east flank of Elbow Crater, about 60 m from the rim crest. It lay about 30 or 40 cm from basalt 15085 in a flat area with distinctly spaced cobbles such as 15086. It did not have a resolvable fillet despite its friability. Its orientation is known.

PETROLOGY: 15086 is a friable, porous regolith breccia whose fragment population is dominated by quartz-normative mare basalt, ranging from vitrophyric to medium-grained, and by green glass spheres and shards (Fig. 2). Wentworth and McKay (1984) determined a bulk density of 2.03 g/cm^3 (intrinsic density 3.22 g/cm^3), and calculated a porosity of 37.0%, in agreement with an SEM point-count porosity determination of 35.4%. McKay and Wentworth (1983) found it to be the most agglutinate-rich of Apollo 15 breccias (21.5% in the 20 to 500 micron fraction), even though it is immature according to Is/FeO (18 to 27 in McKay et al., 1984; 19 in Korotev, 1984 unpublished). They also found shock features to be minor. Nagle (1982b) reported grain size distribution, rounding, packing, and clast orientation data. Hutcheon et al. (1972) found 15086 to be the least metamorphosed breccia studied by them; it contained no shock-produced glass, indicating very low peak shock pressures, and the tracks at boundaries between small grains were not erased, indicating consolidation either by the load of overburden or a very mild, cold, shock-compaction process.

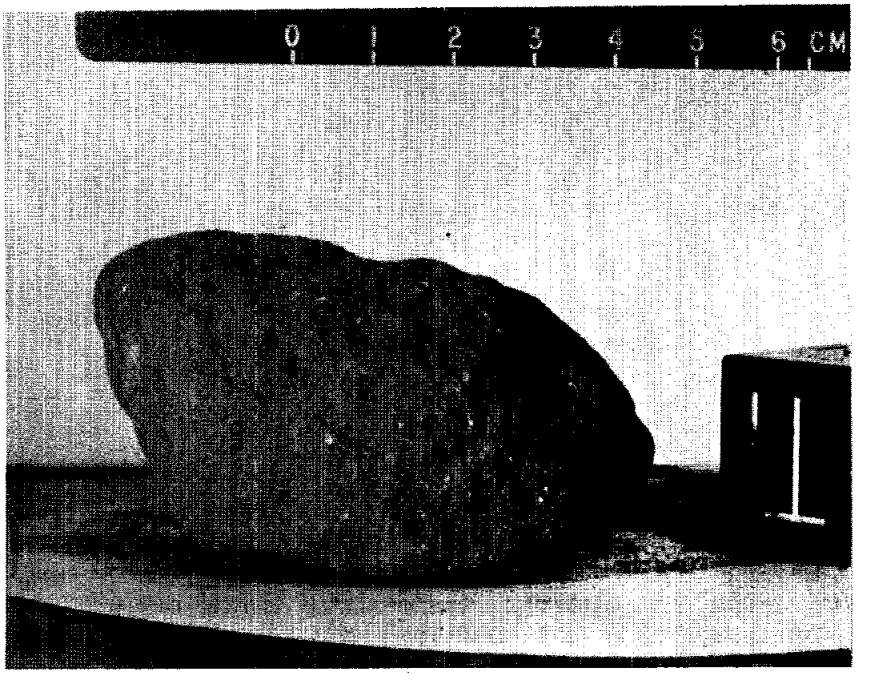

Figure 1. Pre-split view of 15086. S-71-47634

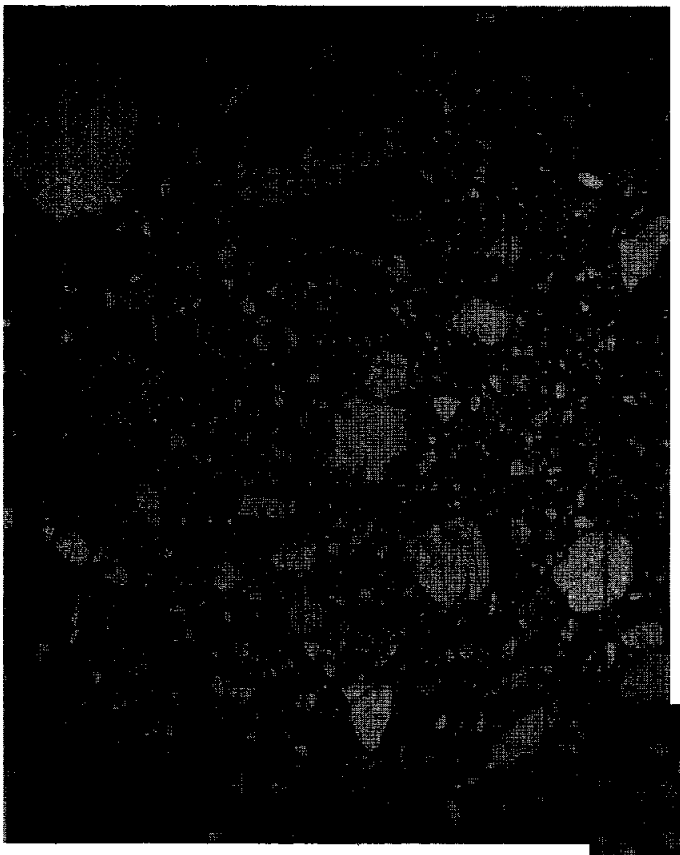

Fig. 2a

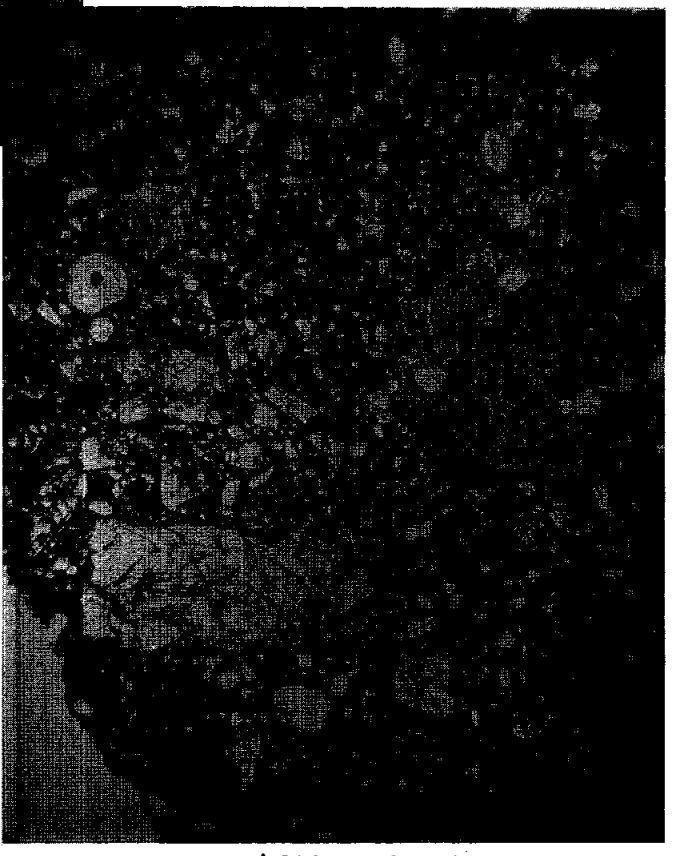

Fig. 2b

Figure 2. Photomicrographs of 15086,32. Widths about 3mm. Transmitted light. a) general matrix view, with two vitrophyric quartz-normative mare basalt clasts in upper right. b) general matrix view, with coarse mare basalt, lower left, and a highlands impact melt, middle right.

Figure 3. Compositions of pyroxenes and olivines in 15086,39 (Drake and Klein, 1973).

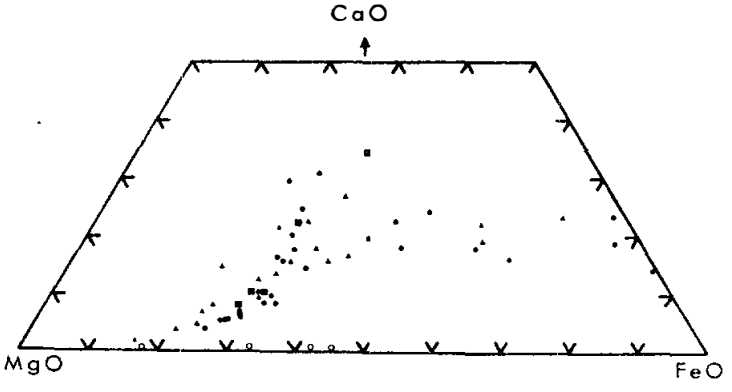

Relative molecular proportions of CaO, MgO, and FeO for pyroxene and olivine fragments in breccia 15096,39.

○ Olivine
▲ Pyroxenes in lithic fragments
● Pyroxene crystal fragments
■ Pyroxenes coexisting with group 4 angular glasses

Descriptions of fragmental materials were provided by Drake and Klein (1972, 1973), Brown et al. (1972a), Engelhardt et al. (1972, 1973), and Wenk et al. (1972). The most detailed description is that of Drake and Klein (1972, 1973). They found a diverse range of lithic and glass types and textures, and analyzed 291 glasses, 58 pyroxenes, 27 feldspars, 4 olivines, and 12 lithic clasts (the latter with defocussed beam), providing representative analyses. The lithic clasts include pyroxene porphyries (microporphyritic to vitrophyric), microgabbros, subophitic basalts, and anorthositic gabbros. The "recrystallized" fragments as depicted in Drake and Klein (1973, their Fig. 1d) are actually typical, rapidly crrystallized KREEP basalts. (Drake and Klein concluded that most lithic clasts were of igneous derivation. This is true, but a few, such as one depicted here in Figure 2b, are highland impact melt breccias, and some are anorthositic granulites.) Pyroxenes exhibit diverse chemical compositions (Fig. 3) but individual grains are little zoned; the mineral fragments represent the same population as the lithic population. Only one grain of pyroxferroite was found. Olivines range from $Fo_{91.2}$ to $Fo_{54.6}$, plagioclase from An_{92} to

An_{77}. Drake and Klein (1973) distinguished six clusters of glass compositions (Fig. 4). The spheres and some fragments form a cluster corresponding to the well-known Apollo 15 green glass group; other groups are aluminous (24.6 to 28.8% Al_2O_3), roughly highland basalt; KREEP (0.3 to 0.9% K_2O); medium-Ti mare (3.8% TiO_2); anorthositic (35% Al_2O_3); and a group of brown, opaque glasses with 19% FeO and less than 1% MgO which is similar to the glass of Apollo 15 pyroxene-vitrophyres and may well merely be such material. Brown et al. (1972) also concluded that the sample contained much quartz-normative mare basalt and green glass; they also observed yellow KREEP and high-Ti (10.4% TiO_2) glass. They found mineral fragments indicative of highlands derivation (An_{97}, $En_{83}Wo_2$, pleonaste, etc.), and found one olivine at Fo_{93} with less than 0.01% CaO; they suggested that this fragment was meteoritic, but it is similar to the olivines in the (lunar) spinel troctolite in 15445.

Wenk et al. (1972) studied plagioclases, loose crystals oriented in thin sections. Most showed only albite twins. They fit the optic curves for terrestrial feldspars, and the probe data suggests the low temperature curve is appropriate. The feldspars clearly are nonstoichiometric, being deficient in Al in comparison with Ca. L. Taylor et al. (1975) found that the compositions of Fe-Ni grains were scattered (Fig. 5) and some fell in the "meteoritic" field, indicating a non-equilibrium assemblage, as expected of a breccia. The opaque mineral population lacks chromite (Fig. 6) indicating that there is not an appreciable contribution from typical coarse-grained gabbros.

L. Taylor et al. (1975) included 15086 in their study of basalt cooling rates as determined from the partitioning of Zr between ilmenite and ulvospinel. The empirical data give a wide scatter, a result of mixing several rock types, and demonstrates that any post-breccia formation reheating and cooling was not of sufficient magnitude to completely equilibrate Zr among the oxides. The average partitioning indicates sources cooled at an average of 16°C/day. Onorato et al. (1979) continued the work of L. Taylor et al. (1975) with a more refined solute partitioning model, using the same data to deduce 5.6° to 9.5°C/day. They found grain-size effect to be negligible for this rock. They gave no indication that this rock is a breccia, and treated it as a basalt.

Uhlmann et al. (1981) used a bulk composition of 15086 (source unstated, but it appears to be microprobe-derived) in experiments to determine glass-forming characteristics and possible thermal histories. From experiments they constructed TTT and CT curves. For their composition (Table 15086-2) they determined a liquidus temperature of 1217°C and a glass transition temperature (Tg) of 677°C. They estimated viscosity-temperature relationships, and tabulated a nucleation barrier of 68KT* From their simplified model they calculated a cooling rate of 4.5°C/sec necessary to produce a glass, close to their measured rate of 3°C/sec. Uhlmann et al. (1981) erroneously described 15086 as a

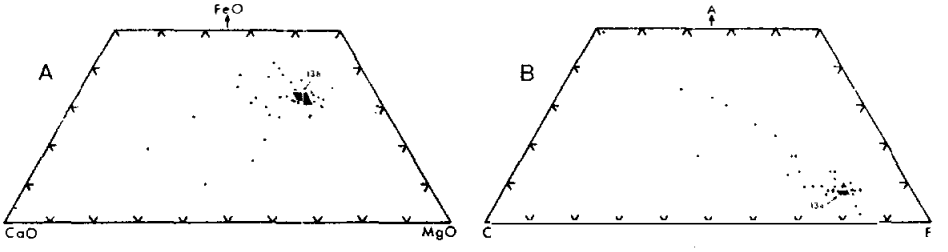

Compositional ranges of rounded glasses in microbreccia, 15086,39. The numbers refer to the total number of analyses plotting in the opaque areas. (a) Relative molecular proportions of CaO, MgO, and FeO. (b) ACF diagram (A = Al_2O_3 – Na_2O – K_2O, C = CaO, F = FeO + MgO + MnO).

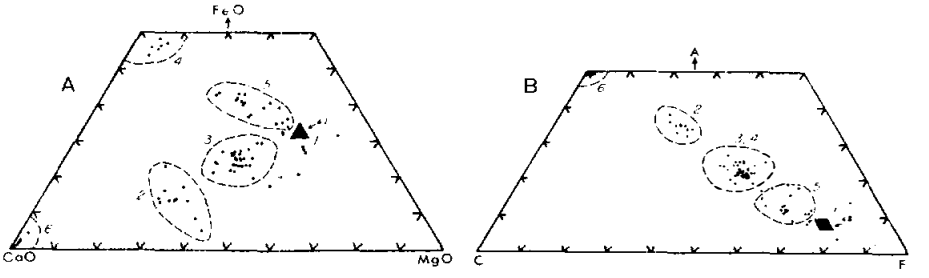

Compositional ranges of angular glasses and irregular patches of glass in microbreccia 15086,39. Numbers refer to sub-group designations described in text. (a) Relative molecular proportions of CaO, MgO, and FeO. (b) ACF diagram (A = Al_2O_3 – Na_2O – K_2O, C = CaO, F = FeO + MgO + MnO).

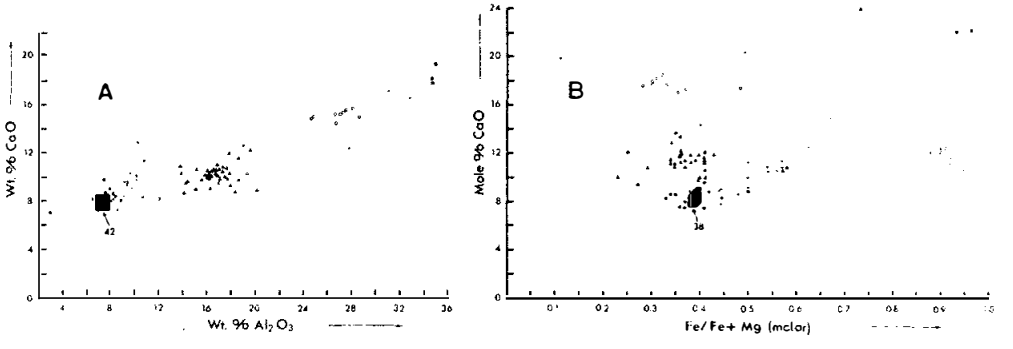

(a) Weight percent CaO vs. weight percent Al_2O_3 in angular glasses. (b) Molecular percentage of CaO vs. atomic fraction of Fe/Fe + Mg.

● Group 1 △ Group 4
○ Group 2 + Group 5
▲ Group 3 ■ Group 6
× Unclassified analyses.

Figure 4. Compositions of glasses in 15086,39 on various plots (Drake and Klein, 1973).

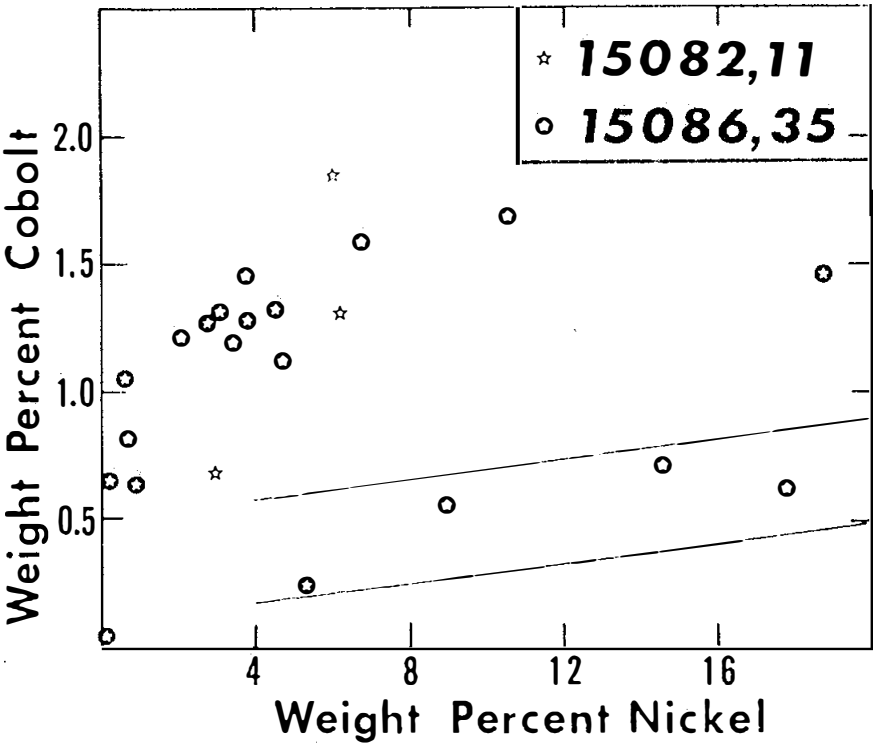

Figure 5. Compositions of metals in 15086, and 15082 (L. Taylor et al., 1976).

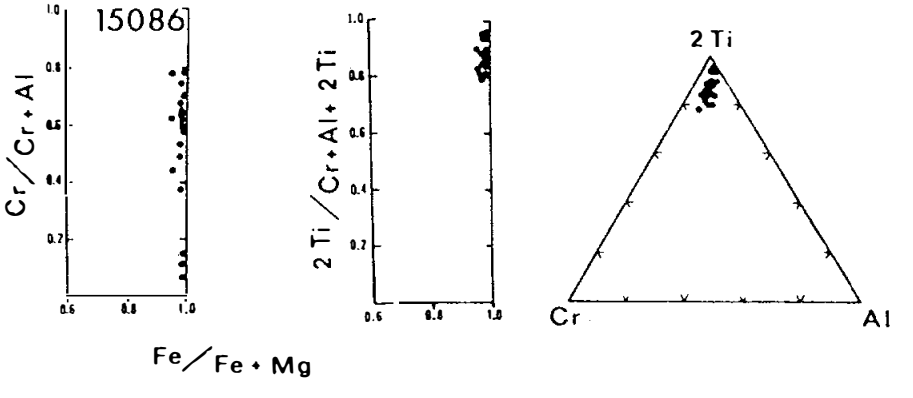

Figure 6. Compositions of spinels in 15086 (L. Taylor et al., 1976).

crystalline matrix breccia; the uncertainty in their bulk composition and the fact that sample is a friable breccia makes the direct application of their results to a thermal history of 15086 inappropriate.

Adams and McCord (1972) plotted the 1 micron and 2 micron pyroxene bands in diffuse reflection spectra against each other. 15086 is fairly intermediate in pyroxene type, at the transition from mare (calcic pyroxene) and non-mare (low-Ca pyroxene), and like 15555.

CHEMISTRY: Bulk rock chemical analyses are listed in Tables 1 and 2, and rare earths are plotted in Figure 7. The analyses in Table 1 show some small differences but generally show 15086 to be quite similar to the local regolith at Station 1. Rose et al. (1975) analyzed for, and found no, Fe_2O_3, and reported an "excess reducing capacity" of +0.63. Thiemens and Clayton (1979, 1980) reported stepwise heating release of nitrogen (Table 3, Fig. 8).

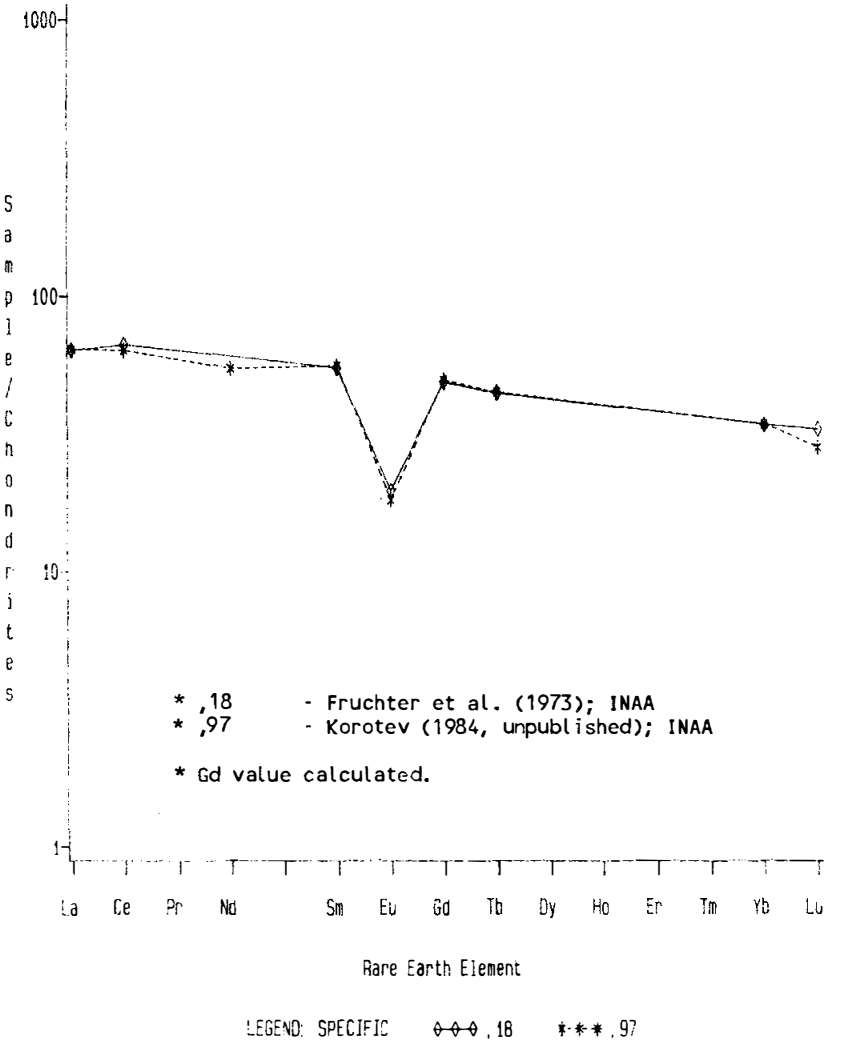

Figure 7. Rare earth elements in bulk samples of 15086.

TABLE 15086-1. Bulk rock chemical analyses

		,18	,29	,0	,97	,24	
Wt %	SiO2		47.50				
	Ti●2	1.72	1.67				
	Al2O3	12.3	11.01				
	FeO	15.9	17.49		16.0		
	MgO		10.55				
	CaO		10.26		10.0		
	Na2O	0.398	0.35		0.39		
	K2O		0.14	0.172			
	P2O5		0.17				
(ppm)	Sc	33	33		32.1		
	V		92				
	Cr	2700	2876		3010		
	Mn		2015				
	Co	41	42		44.8		
	Ni		79		146		
	Rb		4.1				
	Sr		83		145		
	Y		68				
	Zr	260	234		340		
	Nb		19				
	Hf	7.4			8.2		
	Ba	230	146		214		
	Th	3.7		3.2	3.1		
	U			0.76	1.00		
	Pb		14				
	La	21.0	19		21.1		
	Ce	59			56		
	Pr						
	Nd				33		
	Sm	10.0			10.2		
	Eu	1.35			1.25		
	Gd						
	Tb	2.1			2.11		
	Dy						
	Ho						
	Er						
	Tm						
	Yb	6.9	9.4		6.9		
	Lu	1.13			0.96		
	Li		13				
	Be		2.2				
	B						
	C					57	
	N						36.1
	S						
	F						
	Cl						
	Br						
	Cu		12				
	Zn		28				
(ppb)	I						
	At						
	Ga		5100				
	Ge						
	As						
	Se						
	Mo						
	Tc						
	Ru						
	Rh						
	Pd						
	Ag						
	Cd						
	In						
	Sn						
	Sb						
	Te						
	Cs				220		
	Ta	1400			1040		
	W						
	Re						
	●s						
	Ir				3.0		
	Pt						
	Au				<3		
	Hg						
	Tl						
	Bi						
		(1)	(2)	(3)	(4)	(5)	(6)

References and methods:

(1) Fruchter et al. (1973); INAA
(2) Rose et al. (1975); semi-microchemical, XRF, optical emiss. spec.
(3) Keith et al. (1972); gamma-ray spec.
(4) Korotev (1984 unpublished); INAA
(5) Moore et al. (1973); combustion, gas chromatography
(6) Thiemens and Clayton (1979, 1980); vacuum pyrolysis

TABLE 15086-2. Bulk chemical composition of 15086 (Uhlmann et al., 1981). Method unstated but appears to be microprobe.

Wt %	SiO2	48.3
	TiO2	1.7
	Al2O3	9.6
	FeO	16.9
	MgO	10.0
	CaO	10.0
	Na2O	0.4
	K2O	0.1
ppm	Cr	~2000
	Mn	~2300

STABLE ISOTOPES: The nitrogen isotopic data of Thiemens and Clayton (1979, 1980) (Table 3, Fig. 8) shows a pattern very much like that of the ALSEP core section 15003, from a depth of 157 to 146 cm, and is flanked by the 15005 (79 to 82 cm) and 15002 (202 to 205 cm) sections. This feature suggests that 15086 was derived from a similar depth. Cosmogenic ^{15}N is 2.8 ng/g, which also corresponds with a depth of 140 cm in the core, so both implanted and cosmogenic nitrogen suggest a similar depth of origin. The soils had a two-stage irradiation producing a correlation of implanted nitrogen abundance and isotopic composition. 15086 lies close to this line, suggesting a similar two-stage irradiation.

RADIOGENIC ISOTOPES AND GEOCHRONOLOGY: Huneke et al. (1974) measured Ar in stepwise heating of clear and devitrified glass spheres handpicked from 15086. Trajectory variations on diagrams to separate ^{40}Ar into trapped and radiogenic contributions are complex. A ^{40}Ar-^{39}Ar age of 3.29 ± 0.06 b.y. for undevitrified green glass from the 1075°C and 1195°C points was determined (Fig. 9); this fraction has 45% of the ^{39}Ar release and very little trapped Ar. Inclusion of the subsequent 1320°C release changes the calculated age only 0.02 b.y. This determination is consistent with and confirms the previous determination of 3.38 ± 0.06 b.y. of Huneke et al. (1973). For devitrified spheres, the last 65% of ^{39}Ar release yields an average apparent age of 3.1 b.y., only slightly younger than the undevitrified samples.

RARE GASES, COSMOGENIC NUCLIDES, TRACKS, MICROCRATERS AND EXPOSURE: Huneke et al. (1974) reported Ar data for stepwise heating release of clear and devitrified green glass spheres. The isotope variations are complex (Fig. 10), and no constant trapped argon composition is clearly established. The data serve to illustrate the complexity in trapped argon compositions. The systematics are better defined in the undevitrified glasses than in the devitrified material.

TABLE 15086-3. Stepwise heating release nitrogen and nitrogen-isotopic data (Thiemens and Clayton, 1980)

Temp °C	N_2 ppm	$\delta^{15}N$ (°/oo)
600	2.4	+46.0
800	14.3	-0.2
900	7.9	-50.0
1000	5.3	-54.6
1100	3.6	-11.0
1300	2.6	+167.5
TOTAL	36.1	-5.0

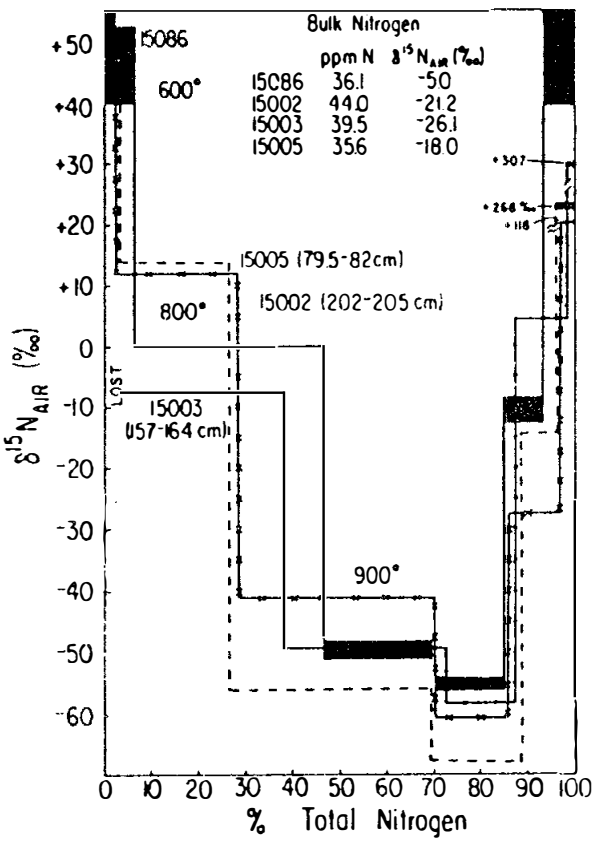

Figure 8. Stepwise heating analysis of 15086 and core samples 15002, 15003, and 15005 (Thiemens and Clayton, 1980).

Figure 9. K/Ca and apparent age for green glass spheres and devitrified glass spheres handpicked from 15086 (Huneke et al., 1974).

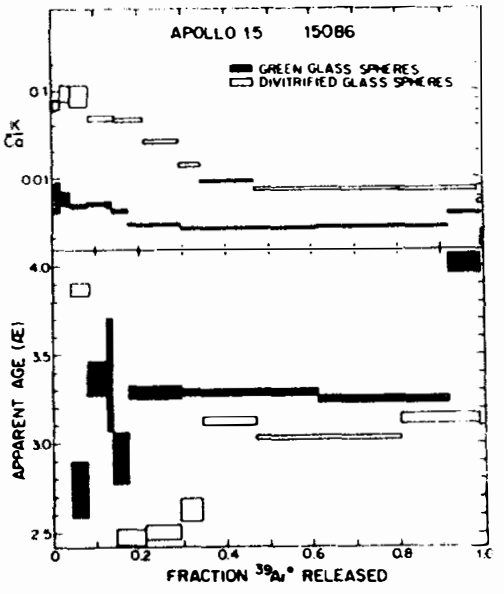

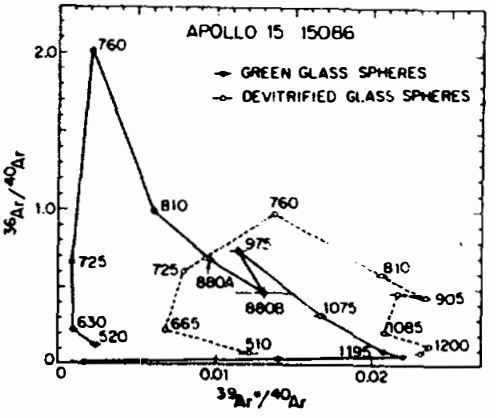

Figure 10. $^{36}Ar/^{40}Ar$ vs. $^{39}Ar^*/^{40}Ar$ for 15086 green glass spheres and devitrified glass spheres handpicked from 15086 (Huneke et al., 1974).

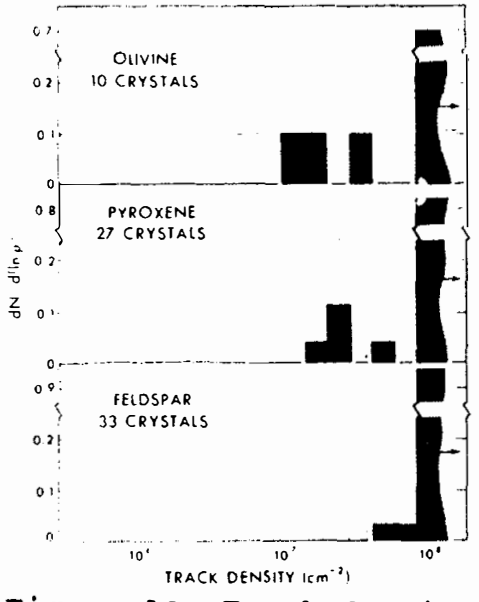

Figure 11. Track density distribution in hand-picked grains from 15086 (Macdougall et al., 1973).

Hintenberger et al. (1975) provided some He, Ne, Ar, Kr, and Xe isotopic data for a bulk 15086 sample. The $^{132}Xe/^{36}Ar$ is higher in 15086 and other Apollo 15 breccias than it is in soils, for unknown reasons (these authors erroneously refer in the text and Figure caption to Apollo 17 breccias rather than Apollo 15 breccias).

Cosmogenic radionuclide data (Keith et al., 1972) definitely show that ^{26}Al is unsaturated (Keith et al., 1972; Yokoyama et al., 1974) and that 15086 has been exposed to radiation for only 200,000 to 500,000 years. Thiemens and Clayton reported a nitrogen spallation age of 736 m.y.

Macdougall et al. (1973) found preserved etchable tracks in glasses, olivines, and feldspars. They showed SEM photomicrographs, including a feldspar with a density gradient. Track density distributions, for grains 50 micron to 300 microns, are shown in Figure 11. The fraction of grains with a density greater than $10^8/cm^2$ (N_H/N) is high, about 0.9. The densities in all three phases are about the same, and the values are typical of soils with a surface exposure of 80 to 100 m.y. (see also Price et al., 1975, for tabulations). The preservation of the tracks in glass indicates that reheating was to no more than 300°C. The green glasses show large and small etch pits, i.e., two distinct track sizes. The large-pit density does not correlate with U, but in a general way with solar flare track density; hence they are not fission tracks but solar tracks from nuclei with Z greater than 26. Even if all the large pits were fission tracks, the "age" would only be 0.7 b.y., raising the question of why the samples lack fission tracks. Macdougall et al. (1973) suggested that the glasses formed more recently than 0.7 b.y. ago, and that the 3.3 to 3.4 b.y. Ar-Ar ages are from some previous event; they cite the slow diffusion of Ar even at 1660°C, above the melting temperature. (However, there is a distinct possibility that the calculations of Macdougall et al., 1973, use a much higher U content for the interior of green glass spheres than is actually the case). Goswami et al. (1976) noted that the track densities greater than $10^8/cm^2$ are consistent with exposure within the upper 1 mm of regolith.

Rajan et al. (1974) studied craters on green glass spheres, and found the micrometeoroid complex to be similar to the contemporary one, with crater morophologies similar to currently-produced ones. There is an order-of-magnitude agreement with the present-day flux. Goswami et al. (1976) depicted two SEM photographs of microcraters. Three out of four feldspars and three out of five spherules studied had numerous microcraters with diameters 0.1 to 2 microns. Crater frequency/size for two feldspars are similar to the Murchison meteorite and a variety of uneroded lunar samples, and the craters are a production population. The relationship of craters and tracks gives a production rate for craters larger than 0.5 microns of 3 and 30 craters/cm^2/yr || sr for the two feldspars (assumes 0.5 m.y. age). The differences are posssibly a result of shielding. Neither shows a steep profile, so the fluxes are lower limits.

PHYSICAL PROPERTIES: Collinson et al. (1972, 1973) reported natural remanent magnetism (NRM) and rock magnetic data. 15086 has a higher NRM (about 9 x 10^{-6} emu/g) than mare basalts and is stable after removal of the soft components up to 100 Oe (Figs. 12, 13). There is some evidence for anomalous variations during AF demagnetization. 15086 also has a strong viscous remanent magnetism (VRM), acquiring a field of 130 x 10^{-6} emu/g in one week (1.0 to 2.0 Oe fields), with a corresponding viscosity coefficient of 33.5 x 10^{-6} emu/g/Oe. This VRM is anomalously stable to AF demagnetization fields in excess of 250 Oe. In comparison, basalts have a low VRM. The rock magnetism results showed that the saturation isothermal remanent magnetism level was 21 x 10^{-3} emu/g, much higher than basalts. The saturation anhysteric remanent magnetization in 0.6 Oe in a peak AF of 1200 Oe was 230 x 10^{-6} emu/g, about 50 times greater than the NRM. Brecher (1975, 1976) listed 15086 in her proposal of textural remanent magnetization as having "a common pattern of NRM directional change in AF and/or thermal demagnetization", based on the Collinson et al. (1972, 1973) data.

Geake et al. (1973) produced luminescence spectra for 15086; plagioclase is the component mainly responsible for the luminescence characteristics.

PROCESSING AND SUBDIVISIONS: Despite its friability, 15086 was originally sawn to produce a slab through its center, with oriented samples and interior and exterior pieces (Fig. 14). The slab (,3) was immediately split to produce ,4 to ,10 and subsequent daughters. ,10 was made into a potted butt and thin sections ,32 to ,38 made from it. Butt end ,2 was also partly subdivided, including the production of potted butt ,26 for thin sections ,39 to ,43. Later ,2 was entirely subdivided to produce an interior shielded portion and surrounding pieces (,53 to ,58). In 1975 ,0 was further sawn to produce butt end pieces of which ,63 (13.8 g) and ,64 (3.4 g) are in remote storage at Brooks. Subsequent chipping on ,0 produced a few more daughters (including potted butt ,200 which produced thin section ,205). ,0 now has a mass of 33.13 g and is the largest individual piece.

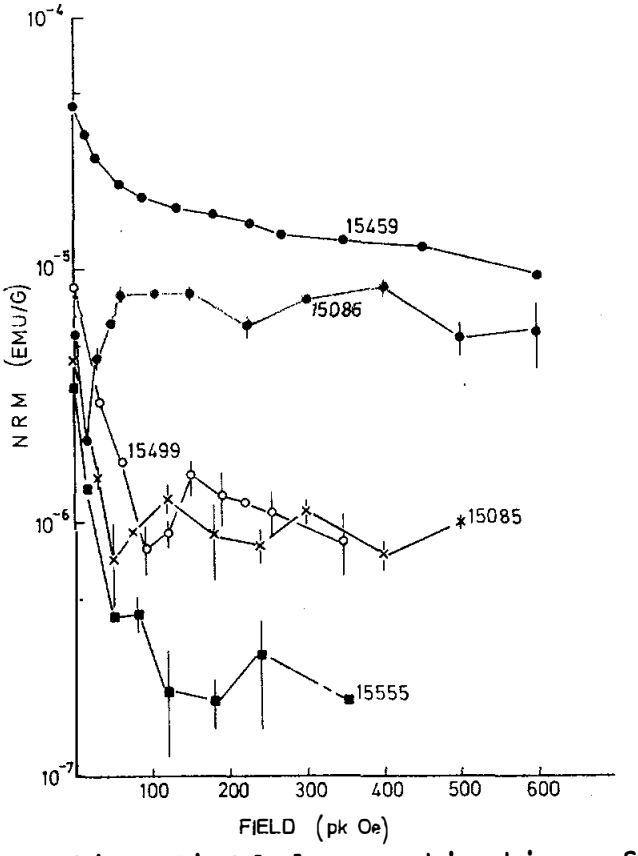

Figure 12. Alternating field demagnetization of Apollo 15 samples including 15086 (Collinson et al., 1973).

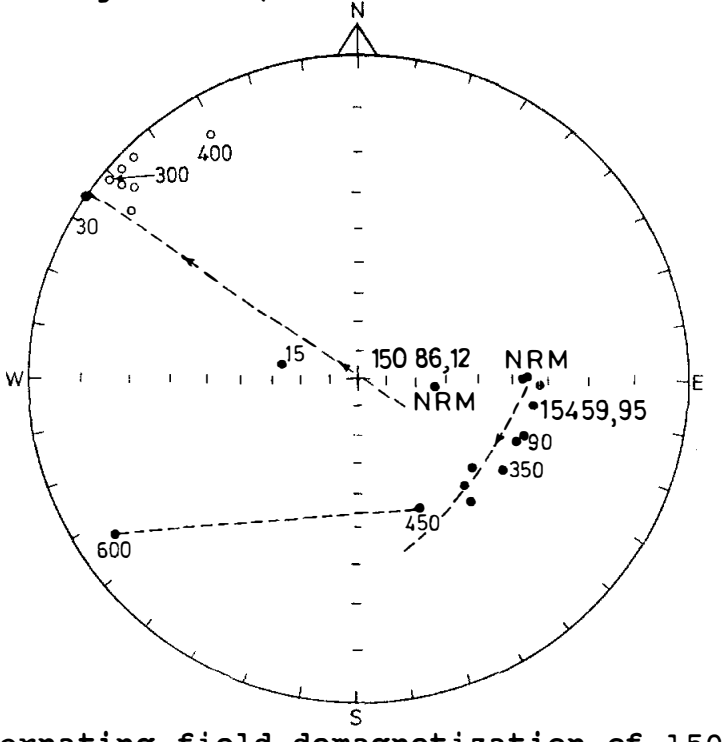

Figure 13. Alternating field demagnetization of 15086 and 15459, referred to arbitrary axes in the rocks (Collinson et al., 1973).

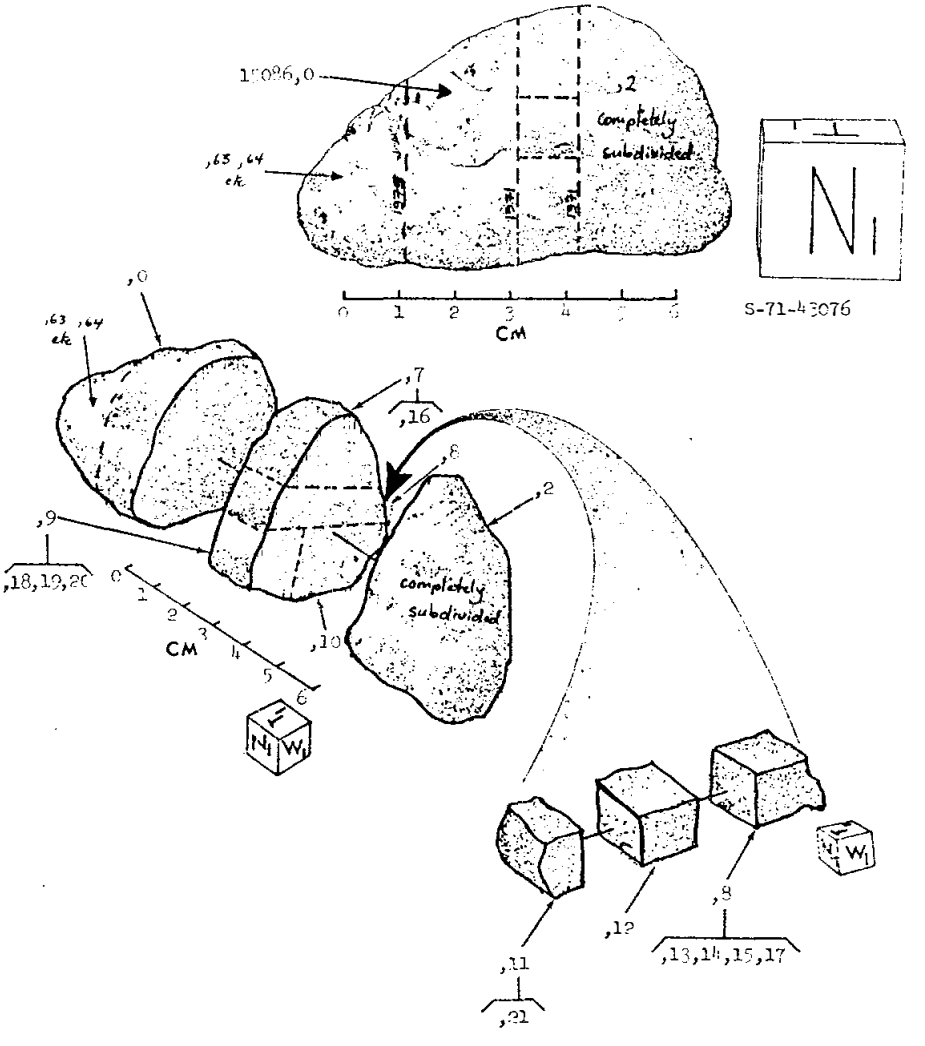

Figure 14. Essential splitting of 15086.

15087 PORPHYRITIC SUBOPHITIC QUARTZ-NORMATIVE(?) ST. 1 5.7 g
MARE BASALT

INTRODUCTION: 15087 is a medium-light gray fragment of a mare basalt (Fig. 1), containing yellow-green to cinnamon brown zoned pyroxenes up to 4 mm long, plagioclase laths up to 7 mm long, and a few opaque grains. It has about 4% irregularly distributed vugs, into which pyroxenes project. The sample is blocky and angular, and is varied in friability resulting from non-penetrative fractures. No zap pits are present. 15087 was collected with samples 15080 to 15088, about 60 m east of the rim of Elbow Crater (see Figs. 15065-1). It was probably buried in the regolith collected at that point. It has never been subdivided or allocated.

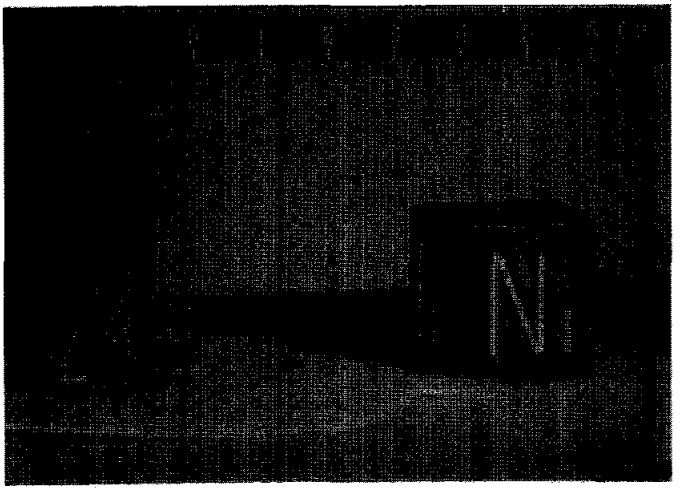

Figure 1. Macroscopic view of 15087. S-71-43070

15088 REGOLITH BRECCIA ST. 1 1.8 g

INTRODUCTION: 15088 is a medium gray regolith breccia (Fig. 1), containing small green spherules, felsic fragments, and mineral fragments. It is friable, subrounded, and its surface has no zap pits. 15088 was collected with samples 15080 to 15088, about 60 m east of the rim of Elbow Crater (see Fig. 15065-1). It was probably buried in the regolith collected at that point. It has never been subdivided or allocated.

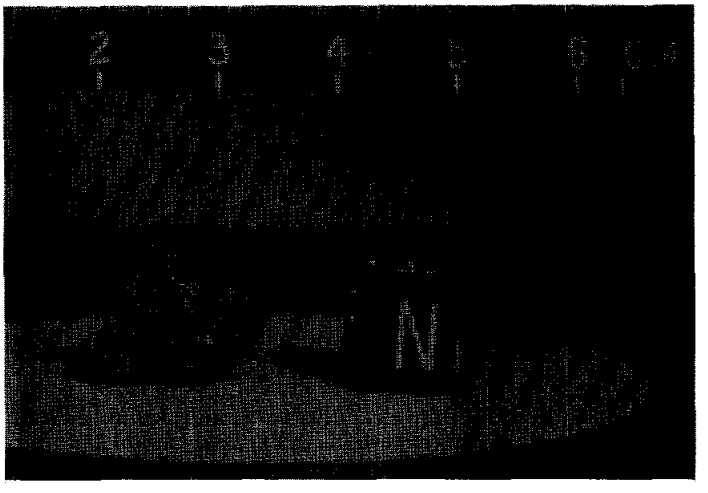

Figure 1. Macroscopic view of 15088. S-71-43082

15095 POLYMICT BRECCIA, GLASS-COATED ST. 2 25.5 g

INTRODUCTION: 15095 consists of a light gray breccia largely enclosed in a round, smooth-surfaced glass (Fig. 1). The glass is medium dark gray and vesicular. The breccia contains lithic and mineral clasts, appears to be polymict, and lacks regolithic materials. The sample is tough and the glass makes it rounded except where broken. There are many zap pits on the glass. 15095 was collected near the large boulder at Station 2.

PETROLOGY: The only thin section is extremely thin and consists of a polymict breccia surrounded by a clear, vesicular, very pale green or brown glass. The breccia contains basaltic clasts and shattered plagioclases, but regolith materials appear to be absent.

PROCESSING AND SUBDIVISIONS: Only an exterior chip ,1 was removed (Fig. 3) to make thin section ,4.

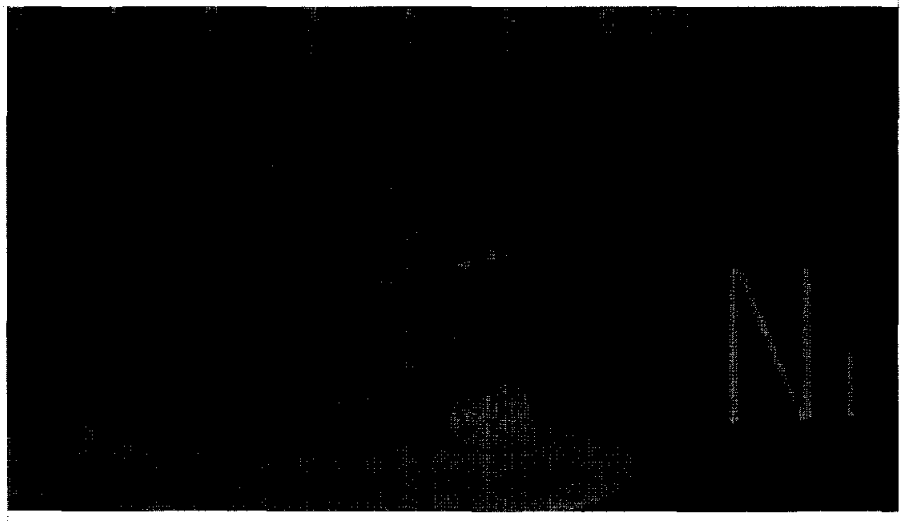

Figure 1. Pre-split view of 15095. S-71-42918.

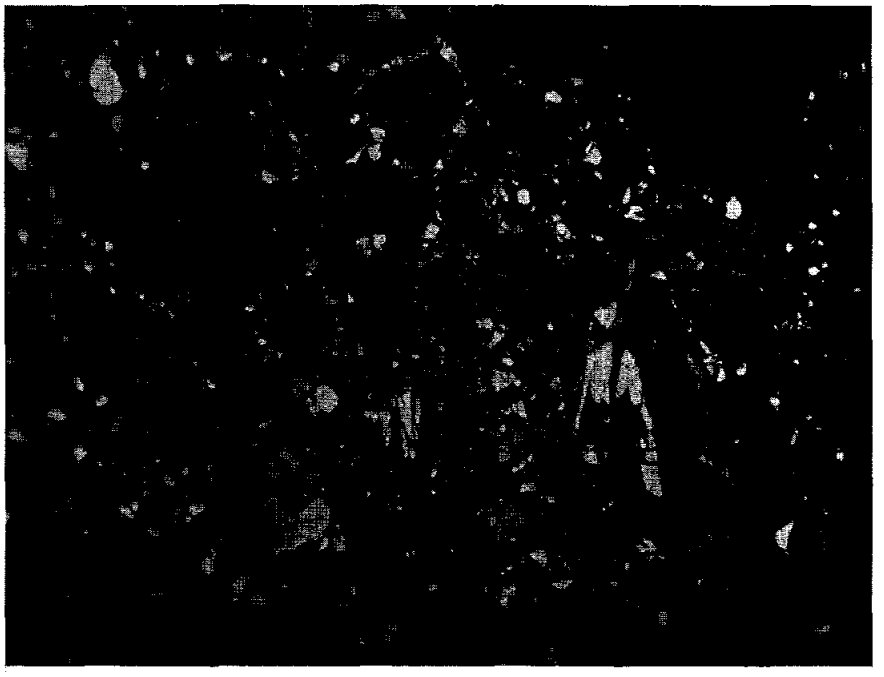

Figure 2. Photomicrograph of breccia portion of 15095,4. Crossed polarizers. Width about 1.25 mm. Photograph is dark because of extreme thinness of the section.

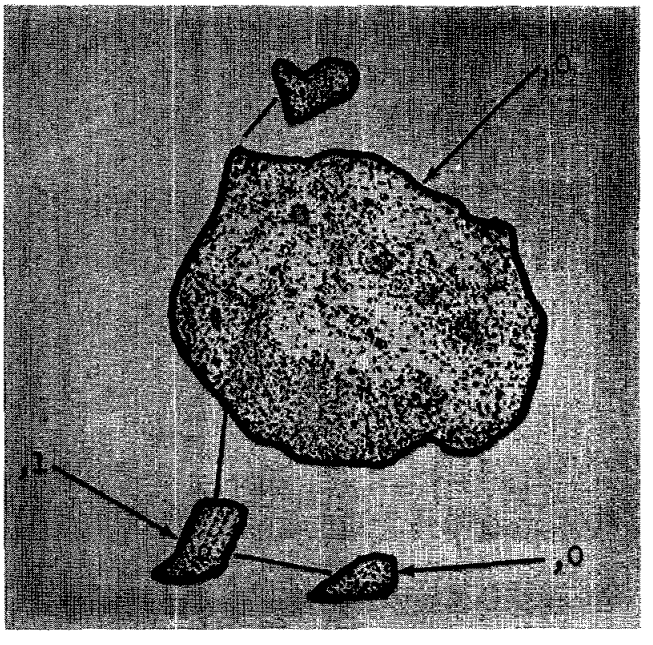

Figure 3. Chipping of 15095.

15105 FINE-GRAINED OLIVINE-NORMATIVE MARE BASALT ST. 2 5.6 g

INTRODUCTION: 15105 is an olivine-phyric mare basalt. It is vesicular (Fig. 1) with fine-grained microphenocrystic olivine and brown pyroxene visible macroscopically. 15105 was taken from the regolith sample collected with the rake sample 5 m east of the boulder at Station 2 (Fig. 2).

PETROLOGY: 15105 is a member of the olivine-normative mare basalt group. It is fine-to medium-grained (Fig. 3) with irregular small olivine phenocrysts. It was described by Dowty et al. (1973a,b), and microprobe analyses were tabulated of silicate minerals and metals by Dowty et al. (1973c) (Fig. 4). Nehru et al. (1973, 1974) provided spinel group and ilmenite microprobe analyses. The sample consists of 63% pyroxene, 24% plagioclase, 8% opaque minerals, 4% olivine, 0.4% silica, and 0.6% others. The olivine phenocrysts are up to about 2 mm across, but most are much smaller; they contain silicate melt inclusions and euhedral spinels. They are embayed and reacted and cusps enclose matrix pyroxene and plagioclase. Scarce euhedral pyroxene phenocrysts are present. The groundmass is a fairly uniform intergrowth of granular to lathy pyroxenes and irregular plagioclase laths which are partly poikilitic. According to Dowty et al. (1973a,b), ilmenites are large and irregular while chromite is fairly scarce and generally forms cores to ulvospinel. A rare metal phase contains 1.5 to 2.3% Co and 4.4 to 8.2% Ni. A K-rich phase is also present.

CHEMISTRY: A defocussed beam microprobe analysis by Dowty et al. (1973a,b) (Table 1) agrees fairly well with the INAA analysis of Ma et al. (1976) (Table 2). Rare earths are shown in Figure 5. The analyses conform with those for evolved members of the olivine-normative mare basalt group.

PROCESSING AND SUBDIVISIONS: A few small chips were taken from ,0 (now 3.48 g) and all subdivisions made from them (Fig. 1). These chips (,1) now are 1.34 g. Two thin sections ,5 and ,6 were made from separate chips.

Figure 1. Post-chipping view of 15105. The front chip ,2 was potted and thin section ,6 made from it. S-72-20376

Figure 2. Sample locations for most Station 2 rocks (AS15-85-11435). Looped area is rake area, samples 15100-15148. Boulder by astronaut was sampled as 15205 and 15206.

Figure 3. Photomicrograph of 15105,6. Crossed polarizers. Width about 1.25 mm.

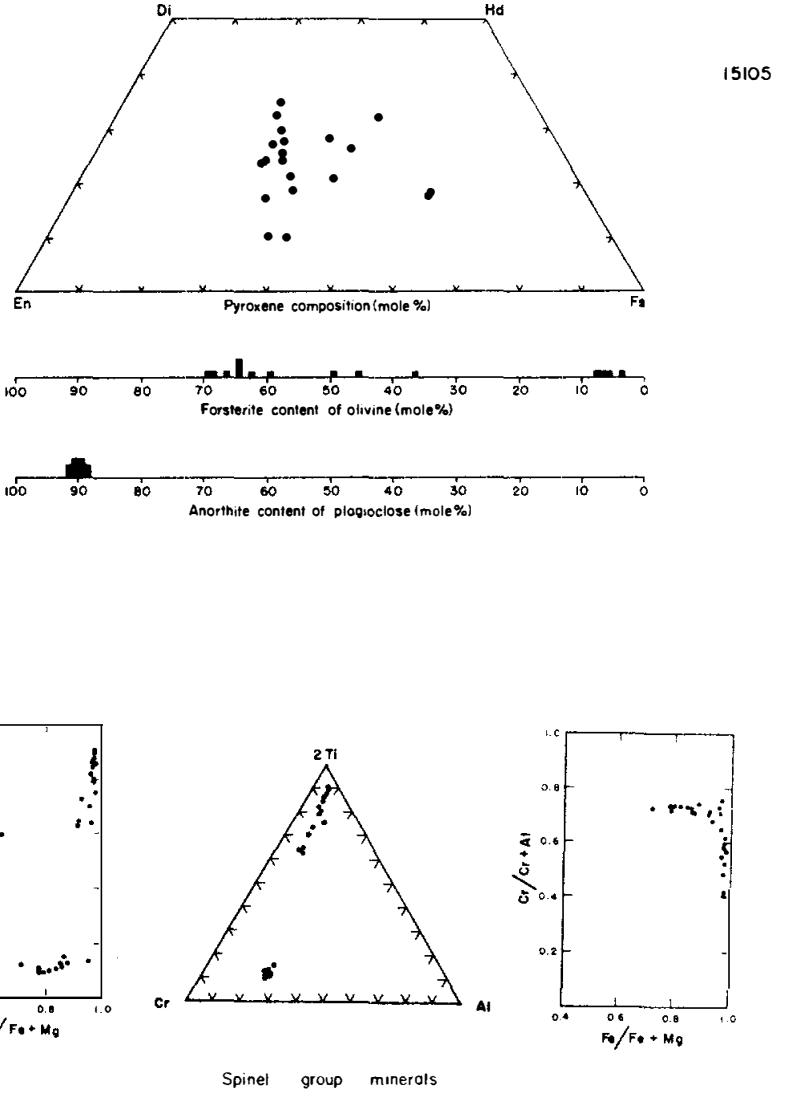

Figure 4. Silicate and opaque mineral analyses (Dowty et al., 1973b).

15105

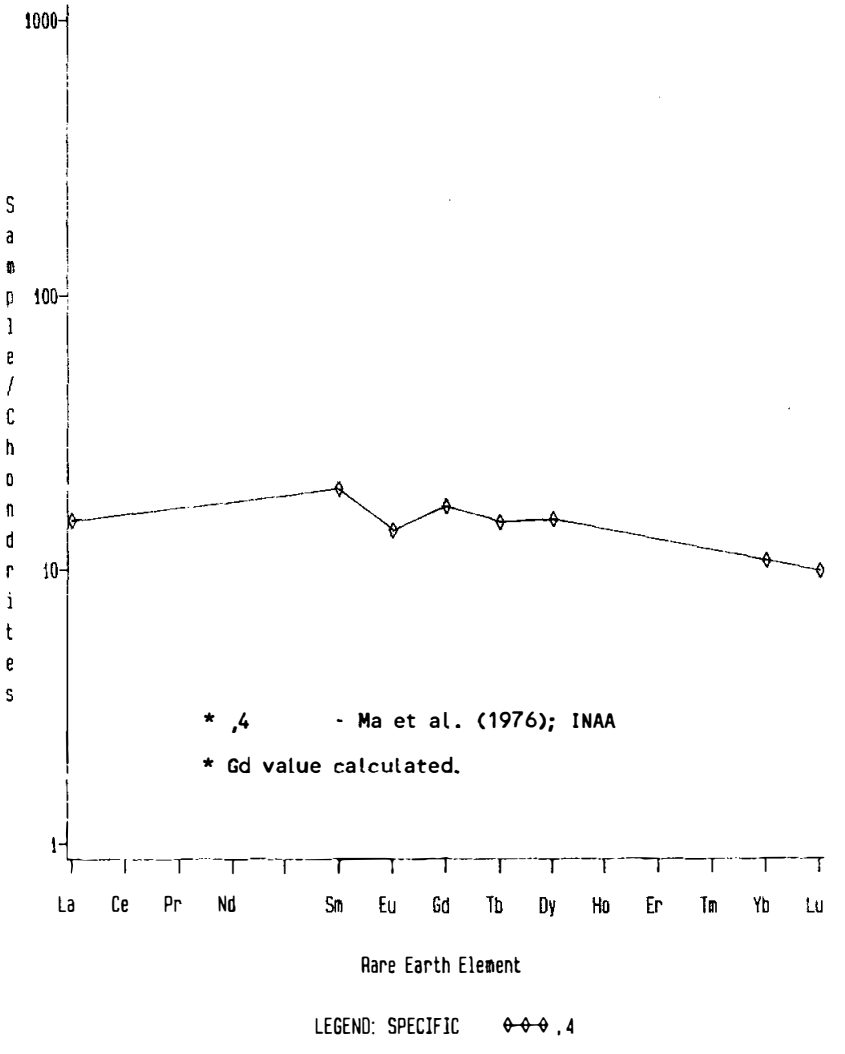

Figure 5. Rare earths.

TABLE 15105-1. Microprobe defocussed beam analysis (Dowty et al., 1973a, b)

Wt %	SiO2	46.0
	TiO2	2.97
	Al2O3	8.2
	FeO	22.7
	MgO	9.0
	CaO	10.2
	Na2O	0.33
	K2O	0.03
	P2O5	0.09
ppm	Cr	2600
	Mn	2015

TABLE 15105-2. Chemical analysis

		,4
Wt %	SiO2	
	TiO2	3.0
	Al2O3	8.5
	FeO	21.8
	MgO	9.3
	CaO	8.9
	Na2O	0.358
	K2O	0.047
	P2O5	
(ppm)	Sc	42
	V	204
	Cr	4040
	Mn	2210
	Co	44
	Ni	<66
	Rb	
	Sr	
	Y	
	Zr	
	Nb	
	Hf	3.1
	Ba	80(a)
	Th	
	U	
	Pb	
	La	5.0
	Ce	
	Pr	
	Nd	
	Sm	3.6
	Eu	0.97
	Gd	
	Tb	0.71
	Dy	4.9
	Ho	
	Er	
	Tm	
	Yb	2.2
	Lu	0.34
	Li	
	Be	
	B	
	C	
	N	
	S	
	F	
	Cl	
	Br	
	Cu	
	Zn	
(ppb)	I	
	At	
	Ga	
	Ge	
	As	
	Se	
	Mo	
	Tc	
	Ru	
	Rh	
	Pd	
	Ag	
	Cd	
	In	
	Sn	
	Sb	
	Te	
	Cs	
	Ta	4500
	W	
	Re	
	Os	
	Ir	
	Pt	
	Au	
	Hg	
	Tl	
	Bi	
		(1)

References and methods:

(1) Ma et al. (1976); INAA

Notes

(a) ±35 ppm

15115 PORPHYRITIC SUBOPHITIC QUARTZ-NORMATIVE MARE BASALT ST. 2 4.0 g

INTRODUCTION: 15115 is a coarse quartz-normative mare basalt (Fig. 1) with conspicuous yellow-green pyroxene phenocrysts. It is tough and angular, with a few vugs and no zap pits. It was collected as part of the rake sample 5 m east of the boulder at Station 2 (see Figure 15105-2).

PETROLOGY: 15115 is coarse-grained with a gabbroic texture similar to 15116 and 15117, although the thin sections lack the coarse phenocrysts typical of the quartz-normative mare basalts (Fig. 2). Macroscopically such phenocrysts appear to be present (Fig. 1). Plagioclases are more-or-less equant and commonly enclose single small pyroxene crystals (Ma et al., 1978). Trace amounts of olivine are present.

CHEMISTRY: The analysis of Ma et al. (1978) is listed in Table 1; rare earths are shown in Figure 3. The low MgO, FeO, and TiO2 and the high rare-earth abundances suggest that this basalt is a member of the quartz-normative group.

PHYSICAL PROPERTIES: Gose et al. (1972) and Pearce et al. (1973) using a Deveko cryogenic magnetometer, found a natural remanent magnetism intensity of 7.2 x 10^{-6} emu/g for the sample, typical of Apollo 15 mare basalts.

PROCESSING AND SUBDIVISIONS: 15115 was chipped to produce ,1 from which the thin section ,3 and the chemical analysis was made.

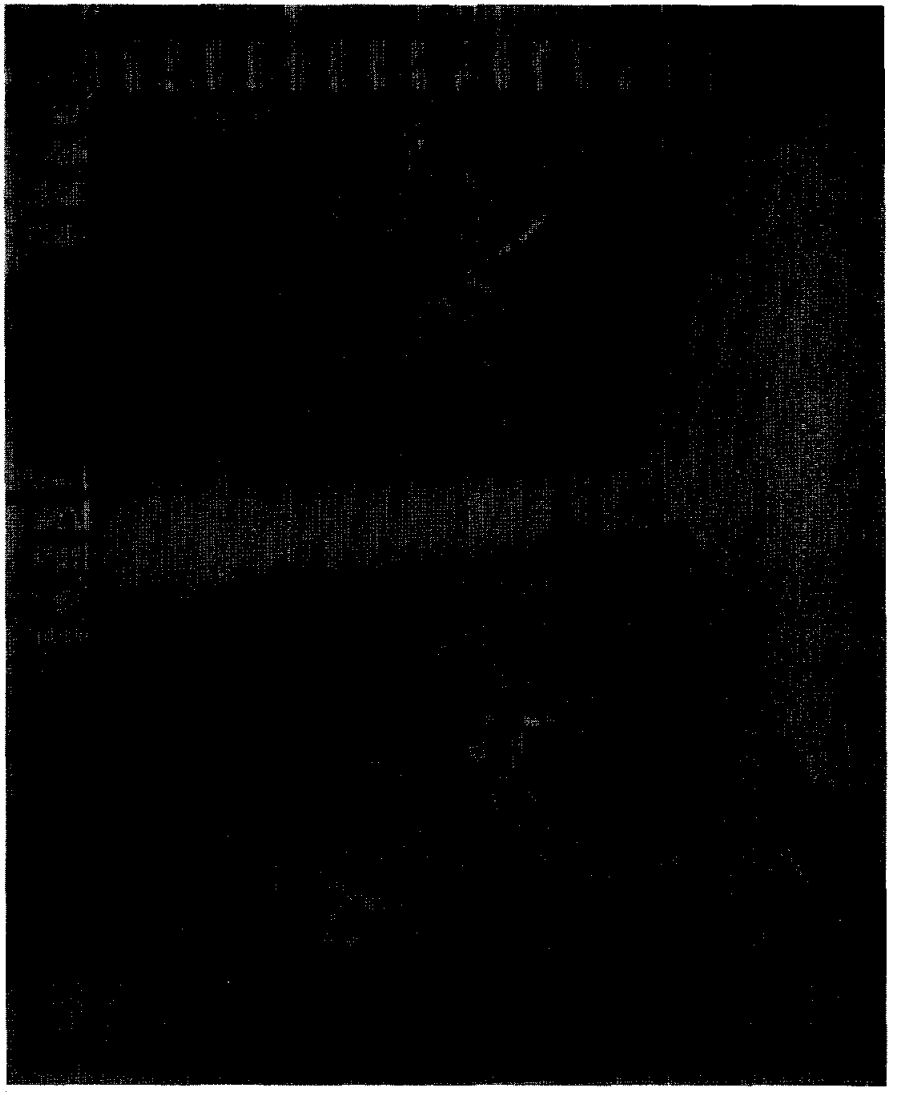

Figure 1. Post-split view of 15115,0. S-77-22585

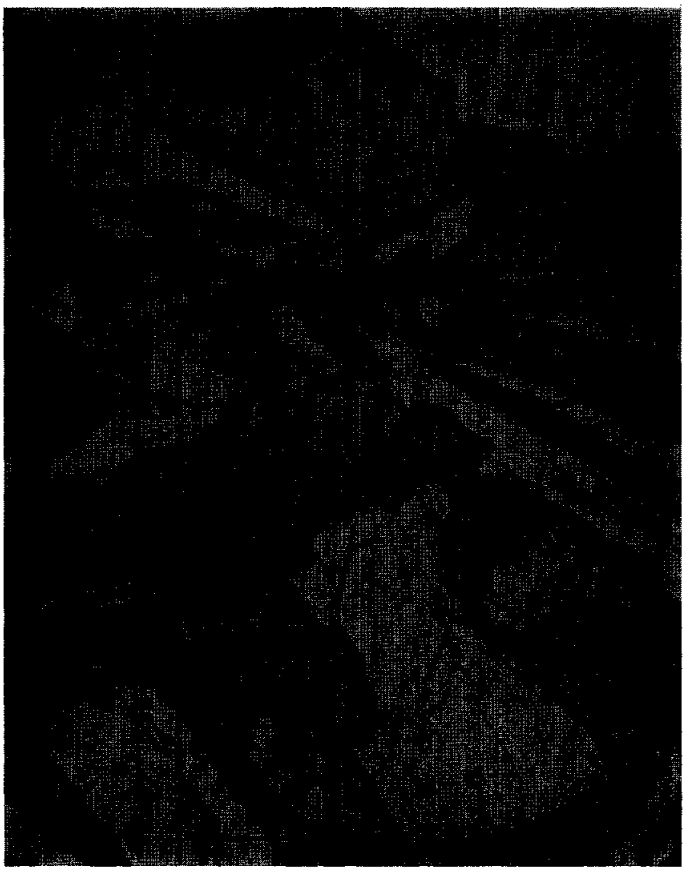

Figure 2. Photomicrograph of 15115,3. Cross polarizers. Width about 1.25 mm.

15115

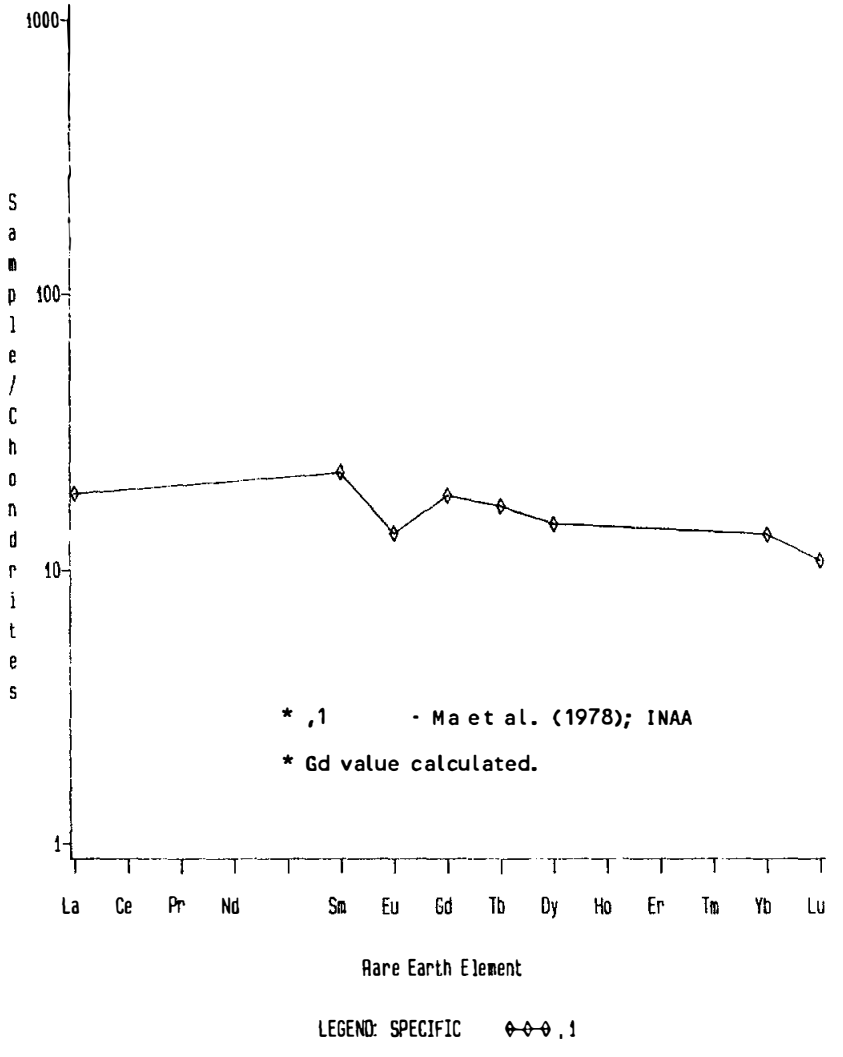

Figure 3. Rare earths in 15115,1.

TABLE 15115-1. Chemical analysis

		,1
Wt %	SiO2	
	TiO2	1.8
	Al2O3	9.6
	FeO	20.0
	MgO	8
	CaO	10.0
	Na2O	0.306
	K2O	0.055
	P2O5	
(ppm)	Sc	45
	V	187
	Cr	3055
	Mn	2130
	Co	41
	Ni	10(a)
	Rb	
	Sr	
	Y	
	Zr	
	Nb	
	Hf	2.6
	Ba	70(b)
	Th	
	U	
	Pb	
	La	6.3
	Ce	
	Pr	
	Nd	
	Sm	4.1
	Eu	0.94
	Gd	
	Tb	0.8
	Dy	4.7
	Ho	
	Er	
	Tm	
	Yb	2.7
	Lu	0.37
	Li	
	Be	
	B	
	C	
	N	
	S	
	F	
	Cl	
	Br	
	Cu	
	Zn	
(ppb)	I	
	At	
	Ga	
	Ge	
	As	
	Se	
	Mo	
	Tc	
	Ru	
	Rh	
	Pd	
	Ag	
	Cd	
	In	
	Sn	
	Sb	
	Te	
	Cs	
	Ta	4300
	W	
	Re	
	Os	
	Ir	
	Pt	
	Au	
	Hg	
	Tl	
	Bi	
		(1)

References and methods:

(1) Ma et al. (1978); INAA

Notes:

(a) ± 10
(b) ± 35

15116 PORPHYRITIC SUBOPHITIC QUARTZ-NORMATIVE MARE BASALT ST. 2 7.2 g

INTRODUCTION: 15116 is a coarse pyroxene-phyric mare basalt (Fig. 1), one of the coarsest of the quartz-normative group. It has conspicuous, yellow-green pyroxene phenocrysts. The sample is tough, with a few vugs, and no zap pits. It was collected as part of the rake sample 5 m east of the boulder at Station 2 (see Fig. 15105-2).

PETROLOGY: 15116 was described and analyzed by Dowty et al. (1973a,b,c; 1974) as one of the coarsest of the quartz-normative Apollo 15 mare basalts, with a gabbroic texture (Fig. 2). A lack of phenocrysts in the thin sections was suspected of being a sampling problem by Dowty et al. (1973a,b) and portions of large phenocrysts do occur. Macroscopically phenocrysts are visible and up to 5 mm long. The sample comprises 60% pyroxene, 30% plagioclase, 5% opaque minerals, 4% silica, and 1% residual phases; olivine is absent. Tridymite is conspicuous, occurring in parallel arrangements (1 mm laths); it crystallized earlier than cristobalite, and is embedded in the margins of silicates. Metal occurs in two compositional groups. The groundmass pyroxenes are coarser than the phenocrysts in many other quartz-normative basalts.

Microprobe analyses of minerals (Dowty et al., 1973a,b,c; 1974) and Nehru et al. (1973, 1974) are shown in Figure 3. The details of pyroxene zoning (Fig. 4) was described and discussed by Dowty et al. (1974). They also gave cell parameters for pyroxenes. The $\Delta\beta$ value for pigeonite-augite intergrowths (2.8) are very high, in accordance with slow cooling. Nehru et al. (1974) noted that the transition from chromite cores to ulvospinel rims was very sharp, but that the gap in compositions was narrower than in faster-cooled, finer-grained rocks. In a comparison of the textures (as described by Dowty et al., 1973a,b; 1974) with the products of dynamic experiments on a synthetic quartz-normative basalt compostion, Lofgren et al. (1974) suggested that both phenocrysts are groundmass cooled at rates less than 1°C/hour.

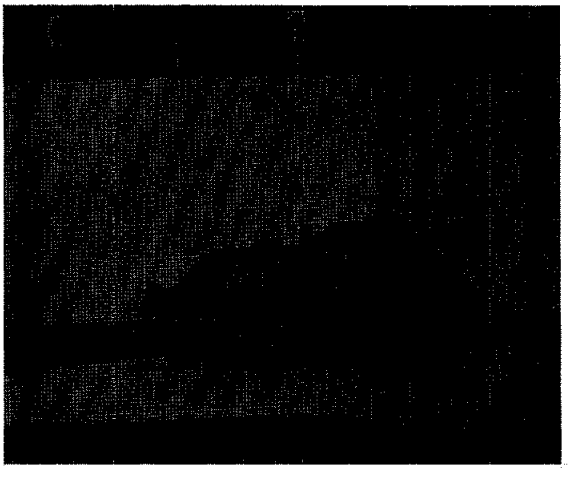

Figure 1. Macroscopic view of 15116, pre-split. S-71-48756

Figure 2. Photomicrograph of 15116,10. Crossed polarizers. Width about 2 mm.

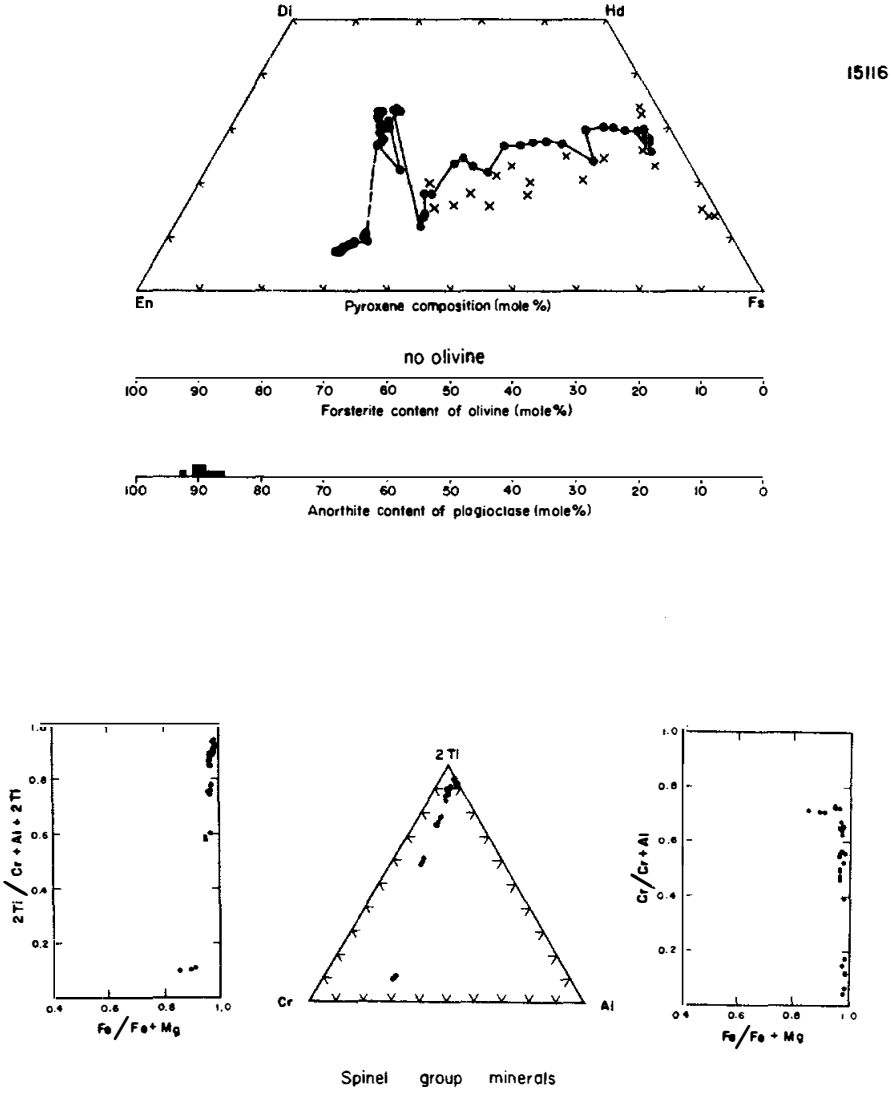

Figure 3. Silicate and opaque mineral analyses (Dowty et al., 1973b).

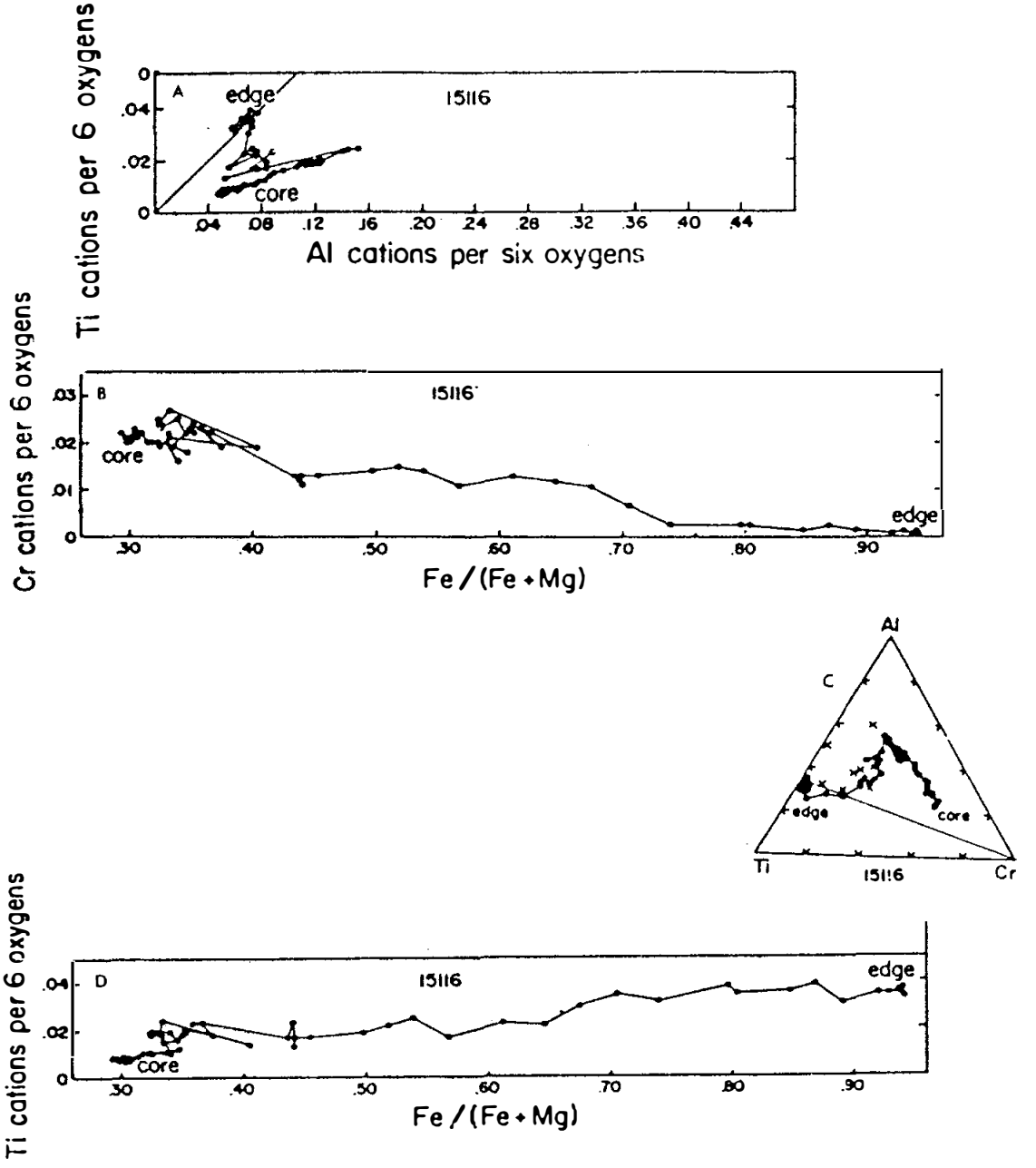

Figure 4. Zoning in pyroxenes. a) Ti vs. Al; b) Cr vs. Fe/(Fe + Mg); c) Ti-Al-Cr; d) Ti vs. Fe/(Fe + Mg) (Dowty et al., 1974).

CHEMISTRY: An analysis by Helmke et al. (1973) (Table 1, Fig. 5) clearly places 15116 in the quartz-normative mare basalt group. The defocussed beam microprobe analysis of Dowty et al. (1973a,b) (Table 2) is in reasonable agreement except for the low TiO_2.

PROCESSING AND SUBDIVISIONS: 15116 was split by chipping, with ,0 (4.79 g) and ,2 (1.52 g) the largest pieces remaining. Thin sections ,7 and ,10-,13 were cut from ,1 which was all but consumed in the process.

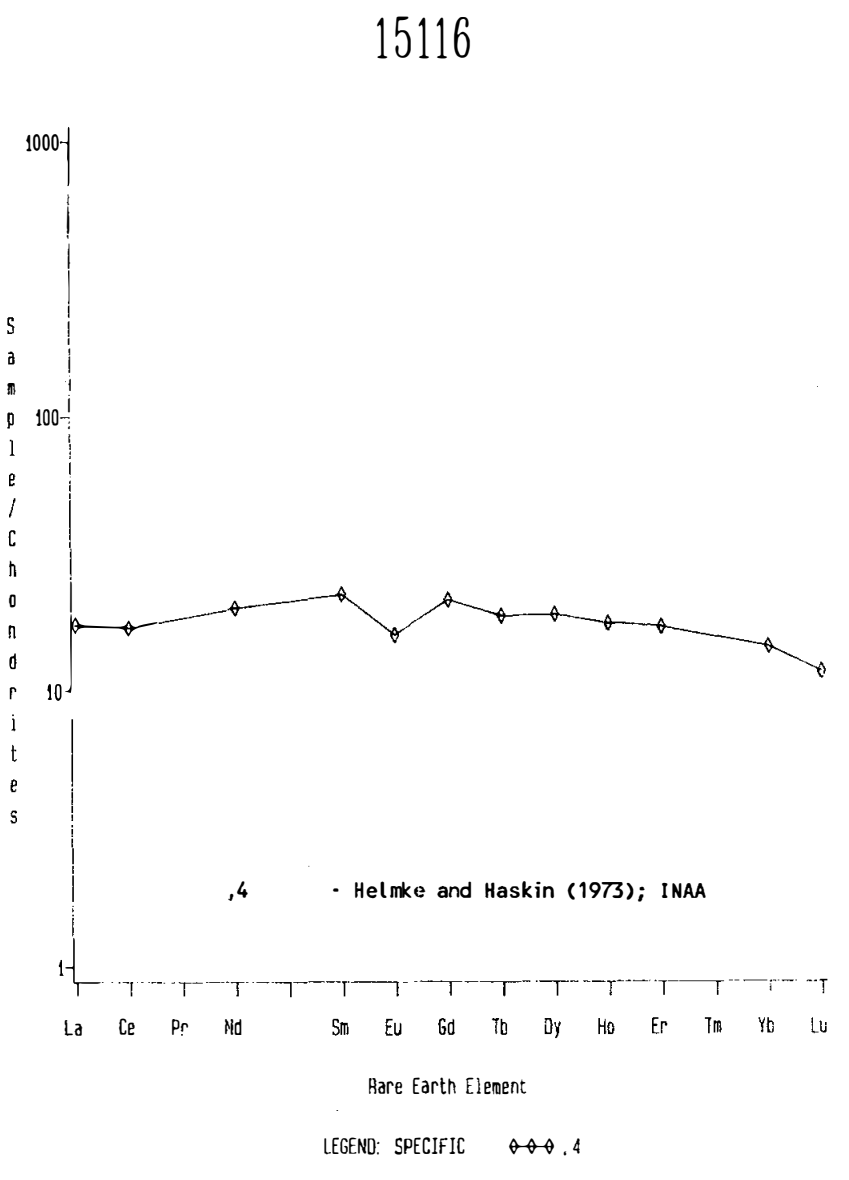

Figure 5. Rare earths in 15116.

TABLE 15116-1. Chemical analysis

		,4
Wt %	SiO2	51.0
	TiO2	1.78
	Al2O3	9.94
	FeO	20.0
	MgO	7.87
	CaO	9.57
	Na2O	0.335
	K2O	0.060
	P2O5	
(ppm)	Sc	50.8
	V	
	Cr	2650
	Mn	2040
	Co	35
	Ni	
	Rb	1.0
	Sr	
	Y	
	Zr	
	Nb	
	Hf	2.4
	Ba	
	Th	
	U	
	Pb	
	La	5.73
	Ce	14.8
	Pr	
	Nd	12.0
	Sm	4.05
	Eu	1.10
	Gd	5.3
	Tb	0.88
	Dy	6.02
	Ho	1.23
	Er	3.4
	Tm	
	Yb	2.90
	Lu	0.396
	Li	
	Be	
	B	
	C	
	N	
	S	
	F	
	Cl	
	Br	
	Cu	
	Zn	<2.7
(ppb)	I	
	At	
	Ga	4100
	Ge	
	As	
	Se	
	Mo	
	Tc	
	Ru	
	Rh	
	Pd	
	Ag	
	Cd	
	In	
	Sn	
	Sb	
	Te	
	Cs	51
	Ta	
	W	
	Re	
	Os	
	Ir	
	Pt	
	Au	
	Hg	
	Tl	
	Bi	
		(1)

References and methods:

(1) Helmke and Haskin (1973); INAA

TABLE 15116-2. Microprobe defocussed beam analysis (Dowty et al., 1973a, b)

Wt %	SiO2	49.2
	TiO2	1.16
	Al2O3	10.2
	FeO	19.0
	MgO	7.3
	CaO	10.4
	Na2O	0.38
	K2O	0.02
	P2O5	0.04
ppm	Cr	2190
	Mn	1705

15117 PORPHYRITIC SUBOPHITIC QUARTZ-NORMATIVE MARE BASALT ST. 2 23.3 g

INTRODUCTION: 15117 is a coarse, pyroxene-phyric mare basalt (Fig. 1) belonging to the quartz-normative group. The phenocrysts are yellow-green and conspicuous. The sample has been dated as 3.35 ± 0.04 b.y. old. The sample is tough, has a few vugs, and lacks zap pits. It was collected as part of the rake sample 5 m east of the boulder at Station 2 (see Figure 15105-2).

PETROLOGY: 15117 is a coarse basalt rather similar to 15115 and 15116. The pyroxene phenocrysts are zoned and in some cases twinned (Fig. 2). Plagioclases are irregular laths. Steele et al. (1972a) noted that the thin section lacked olivine; Papanastassiou and Wasserburg (1973) referred to it as a friable coarse basalt or gabbro containing ilmenite.

CHEMISTRY: Two analyses are listed in Table 1, with rare earths plotted in Figure 3. The major elements agree well, and are typical quartz-normative mare basalt abundances. The rare-earth abundances of Fruchter et al. (1973) conform closely with typical quartz-normative basalt abundances, but those of Cuttitta et al. (1973) are much higher and their Cr abundance is low. This is possibly a sampling problem due to the coarse grain size of the sample, but the rare earth data of Cuttitta et al. (1973) are generally higher than those of other groups on the same rocks, indicating a systematic error.

RADIOGENIC ISOTOPES AND GEOCHRONOLOGY: Papanastassiou and Wasserburg (1973) determined a Rb-Sr two-point isochron from plagioclase and "ilmenite" separates (Table 2). The age of 3.35 ± 0.04 and initial $^{87}Sr/^{86}Sr$ of 0.69928 ± 5 are identical with those of other Apollo 15 mare basalts.

PROCESSING AND SUBDIVISIONS: Several pieces were chipped from ,0 which is now 16.79 g. Two thin sections (,2 and ,9) were made from parts of ,2.

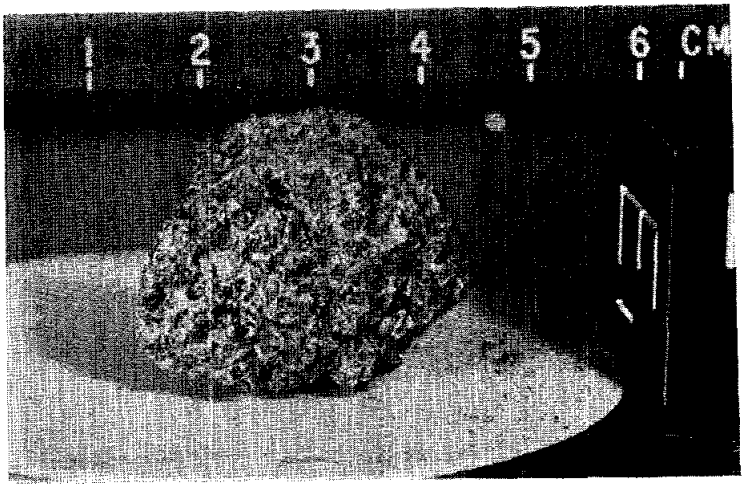

Figure 1. Pre-split view of 15115. S-71-48768

Figure 2. Photomicrograph of thin section 15117,2. Crossed polarizers. Width about 1.25 mm.

15117

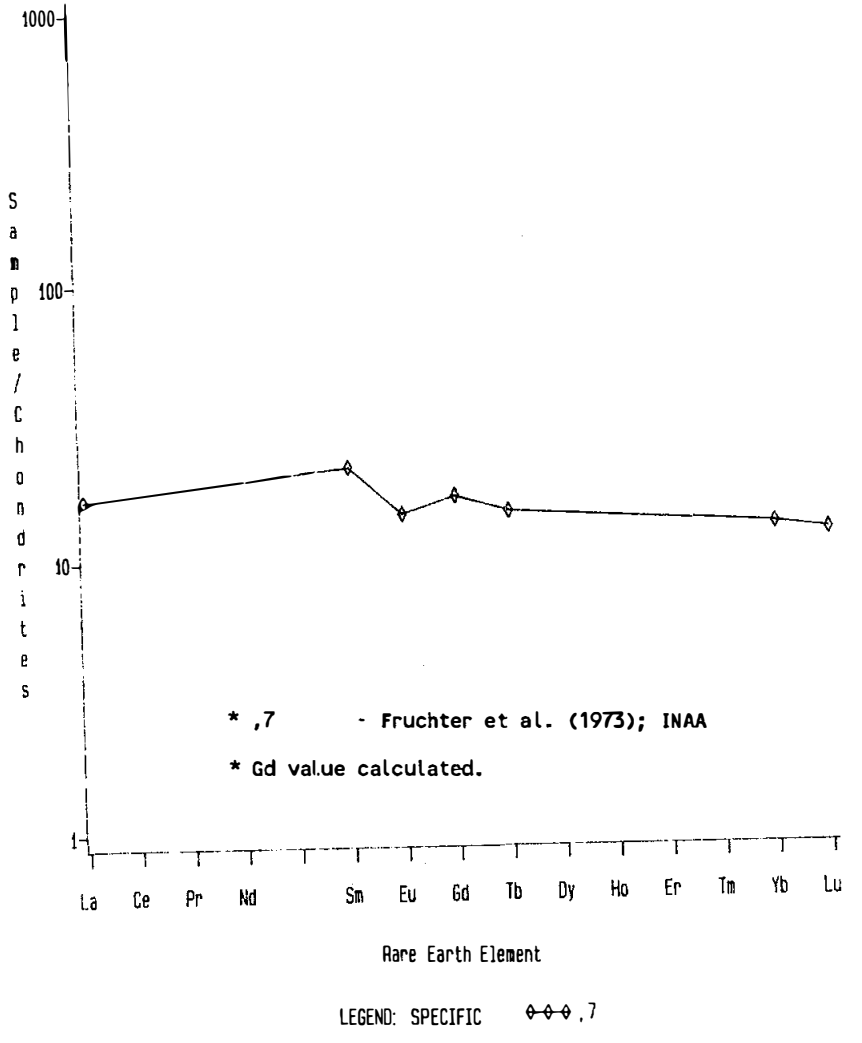

Figure 3. Rare earths in 15117.

TABLE 15117-2. Rb-Sr isotopic data (Papanastassiou and Wasserburg, 1973)

Separate	Separation	Weight mg	Rb 10^{-8} m/g	^{88}Sr 10^{-8} m/g	$^{87}Rb/^{86}Sr$ x10^2	$^{87}Sr/^{86}Sr$
Plagioclase	Mechanical	6.9	0.183	289.3	0.148±2	0.69935±5
"Ilmenite"	Density	6.2	2.029	31.70	14.93±6	0.70639±7

TABLE 15117-1. Chemical analyses

		,8	,7
Wt %	SiO2	47.80	
	TiO2	2.09	2.02
	Al2O3	9.89	8.78
	FeO	20.41	21.0
	MgO	8.02	
	CaO	10.98	
	Na2O	0.33	0.308
	K2O	0.07	
	P2O5	0.11	
(ppm)	Sc	43	46
	V	188	
	Cr	1920	4450
	Mn	2250	
	Co	38	53
	Ni	30	
	Rb	1.0	
	Sr	150	
	Y	26	
	Zr	90	
	Nb	<10	
	Hf		2.5
	Ba	100	
	Th		
	U		
	Pb		
	La	12	5.5
	Ce		
	Pr		
	Nd		
	Sm		3.9
	Eu		1.01
	Gd		
	Tb		0.7
	Dy		
	Ho		
	Er		
	Tm		
	Yb	4.3	2.6
	Lu		0.42
	Li	5.2	
	Be	1.4	
	B		
	C		
	N		
	S		
	F		
	Cl		
	Br		
	Cu	12	
	Zn		
(ppb)	I		
	At		
	Ga	3800	
	Ge		
	As		
	Se		
	Mo		
	Tc		
	Ru		
	Rh		
	Pd		
	Ag		
	Cd		
	In		
	Sn		
	Sb		
	Te		
	Cs		
	Ta		440
	W		
	Re		
	Os		
	Ir		
	Pt		
	Au		
	Hg		
	Tl		
	Bi		
		(1)	(2)

References and methods:

(1) Christian et al. (1972), Cuttitta et al. (1973); Chem, XRF, opt. emission spec.
(2) Fruchter et al. (1973); INAA

15118 PORPHYRITIC RADIATE QUARTZ-NORMATIVE MARE BASALT ST. 2 27.6 g

INTRODUCTION: 15118 is a pyroxene-phyric mare basalt belonging to the quartz-normative group. It has large yellow-green phenocrysts in a much finer-grained but wholly crystalline groundmass. The sample is tough, has a few vugs, and has zap pits on at least 3/4 of the surface. It was collected as part of the rake sample 5 m east of the boulder at Station 2 (see Figure 15105-2).

PETROLOGY: 15118 consists of pyroxene phenocrysts in a finer mass of plagioclase and pyroxene (Fig. 2). The phenocrysts are embayed or grew very irregularly, with spaces filled with the groundmass. The sample was described by Dowty et al. (1973a,b; 1974), and microprobe analyses of silicates and metals were tabulated by Dowty et al. (1973c). The opaque minerals were analyzed by Nehru et al. (1973, 1974). Dowty et al. (1973a,b) found a mode of 61% pyroxene, 29% plagioclase, 4% opaques, 3% silica, and 1% others. Mineral analyses are shown in Figure 3. The phenocrysts are skeletal and 1.0 to 3.0 mm wide, much larger than the groundmass pyroxenes: 0.6 x 0.2 to 0.4 mm wide. Dowty et al. (1974) provided pyroxene cell parameters and the $\Delta\beta$ for pigeonite-augite intergrowths; the value of 2.4 is consistent with slow cooling for the phenocrysts. The phenocrysts are zoned (Figs. 3, 4), with irregular shapes and zoning patterns. The groundmass is mainly subparallel stubby plagioclase laths which are enclosed in a mosaic of pyroxene grains; some plagioclase grains have pyroxene cores. Scarce metal contains 1.3 to 1.6% Co, 1.6 to 3.3% Ni. A K-rich phase is also present. Nehru et al. (1974) found that the chromite is exceptionally high in alumina (17.6 to 19.0%). Lofgren et al. (1975) used the Dowty et al. (1973a,b; 1974) description to estimate cooling rates of about <1°C/hour for the phenocrysts and 1 to 5°C/hour for the groundmass, by a comparison with textures produced in dynamic crystallization experiments on a synthetic composition.

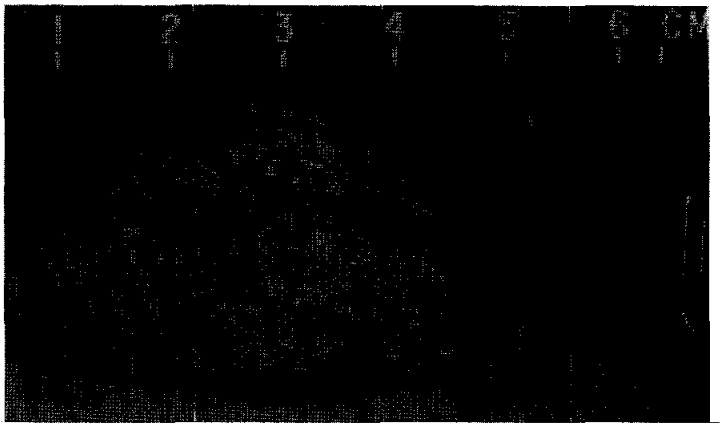

Figure 1. Pre-split view of 15118. S-71-48762

CHEMISTRY: Chemical analyses are listed in Table 1 and the rare earths are plotted in Figure 5. Except FeO, the major elements are consistent among analyses and are of a quartz-normative basalt, as the low-Mg end of the spectrum. The defocussed beam analysis (Table 2) is also quite consistent. The rare-earths are less consistent; those of Wiesmann and Hubbard (1975) seem rather high, although the Mg/Fe of the sample is rather fractionated. The FeO abundance of Ma et al. (1976) is anomalously high for an Apollo 15 mare basalt. Some of the inconsistencies might result from irregular distribution of the large phenocrysts.

TRACKS AND EXPOSURE: Bhandari et al. (1972, 1973) measured track densities of 8-50 ($x10^6 cm^{-2}$) in a surface chip. The variation of track density with depth is shown as Figure 6. Bhandari et al. (1972, 1973) determined a "suntan" age of 1.3 m.y.

PROCESSING AND SUBDIVISIONS: Chipping produced a few daughters, and ,0 is now 21.75 g. Thin sections ,6; ,9; and ,18 were made from ,1.

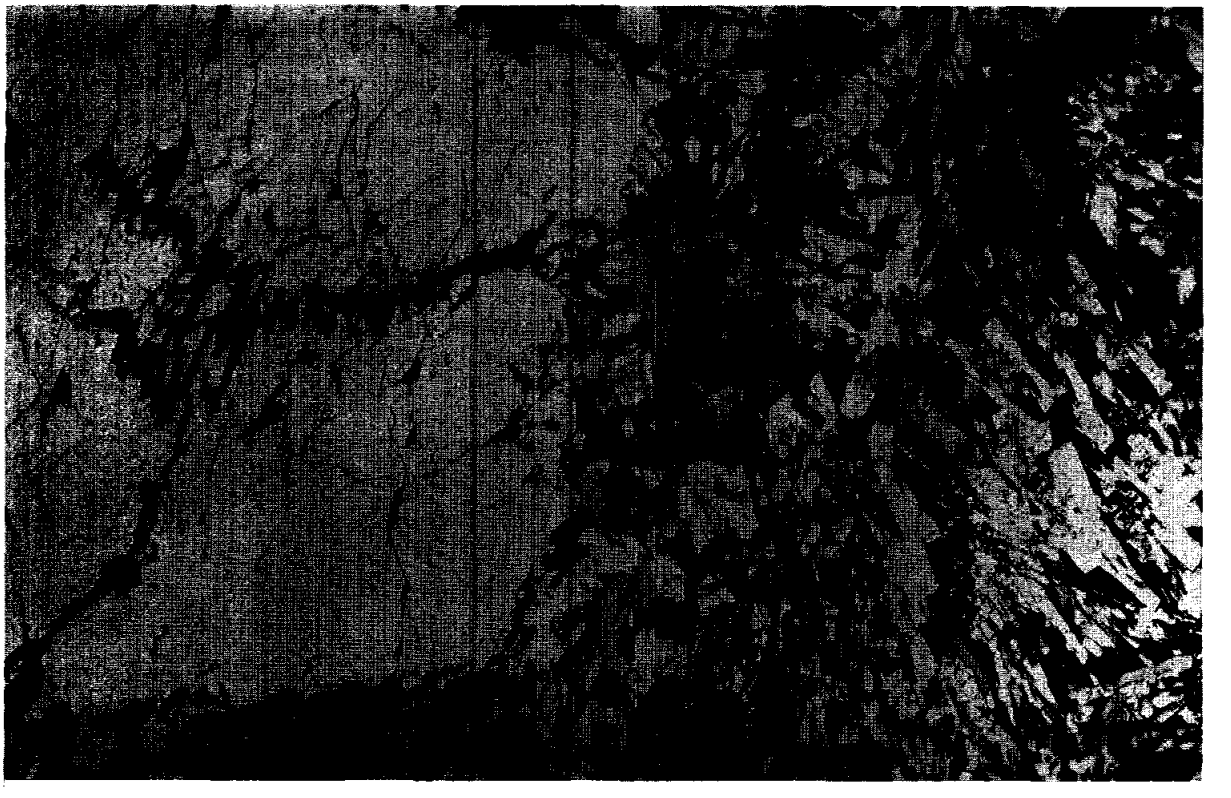

Figure 2. Photomicrograph of 15118,6, showing large irregular phenocryst (left) and contrasting groundmass (right). Crossed polarizers. Width about 2.5 mm.

Figure 3. Mineral analyses. In pyroxene quadrilateral, dots are phenocryst analyses, crosses are groundmass pyroxene analyses (Dowty et al., 1973b).

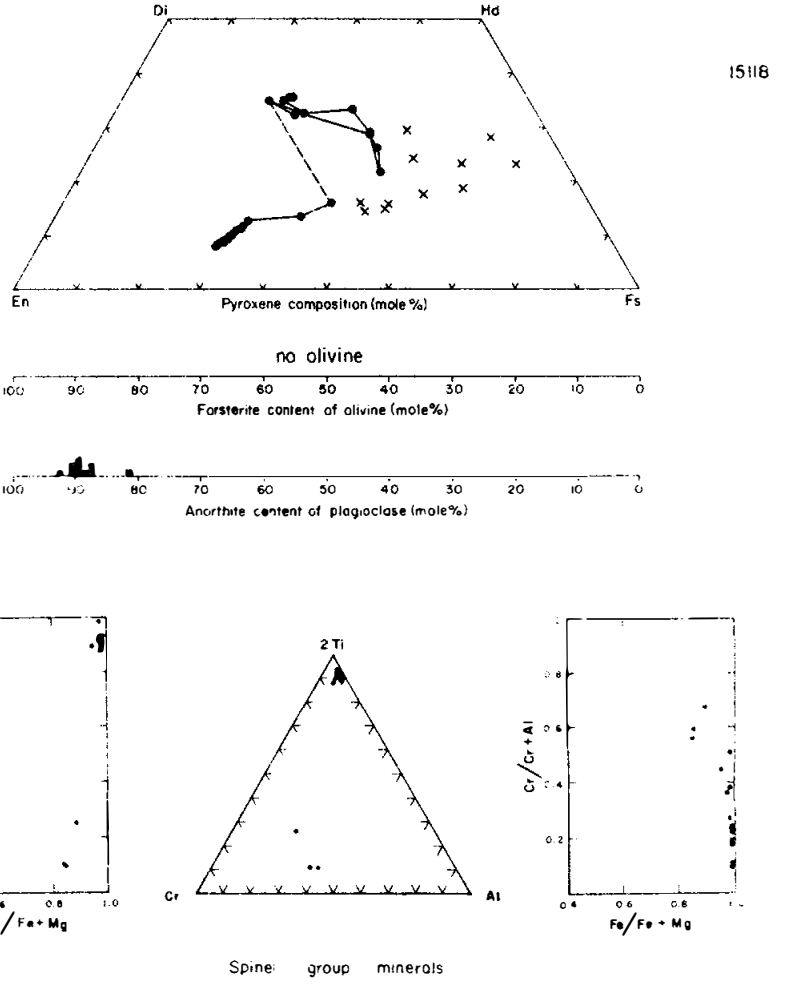

Figure 4. Zoning in pyroxenes. a) Ti-Al; b) Ti-Al-Cr (Dowty et al., 1974).

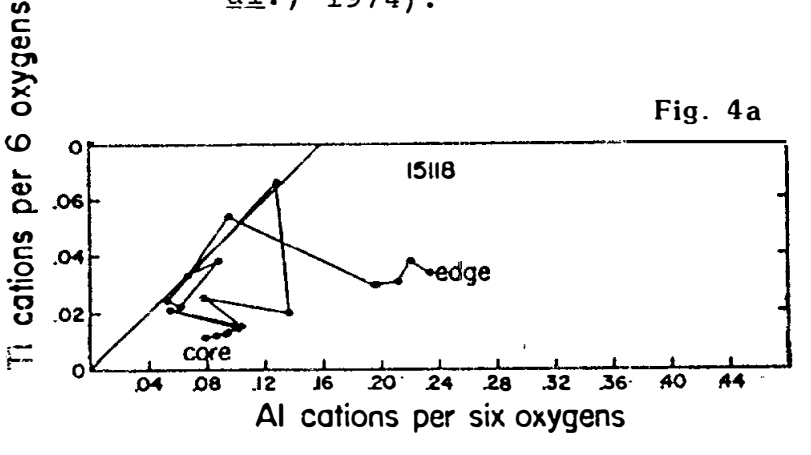

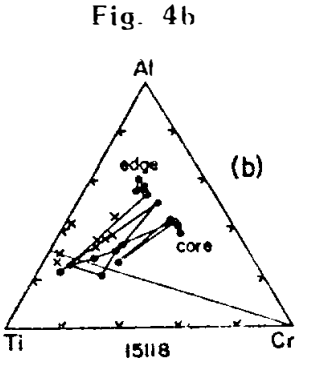

Figure 5. Rare earths in 15118.

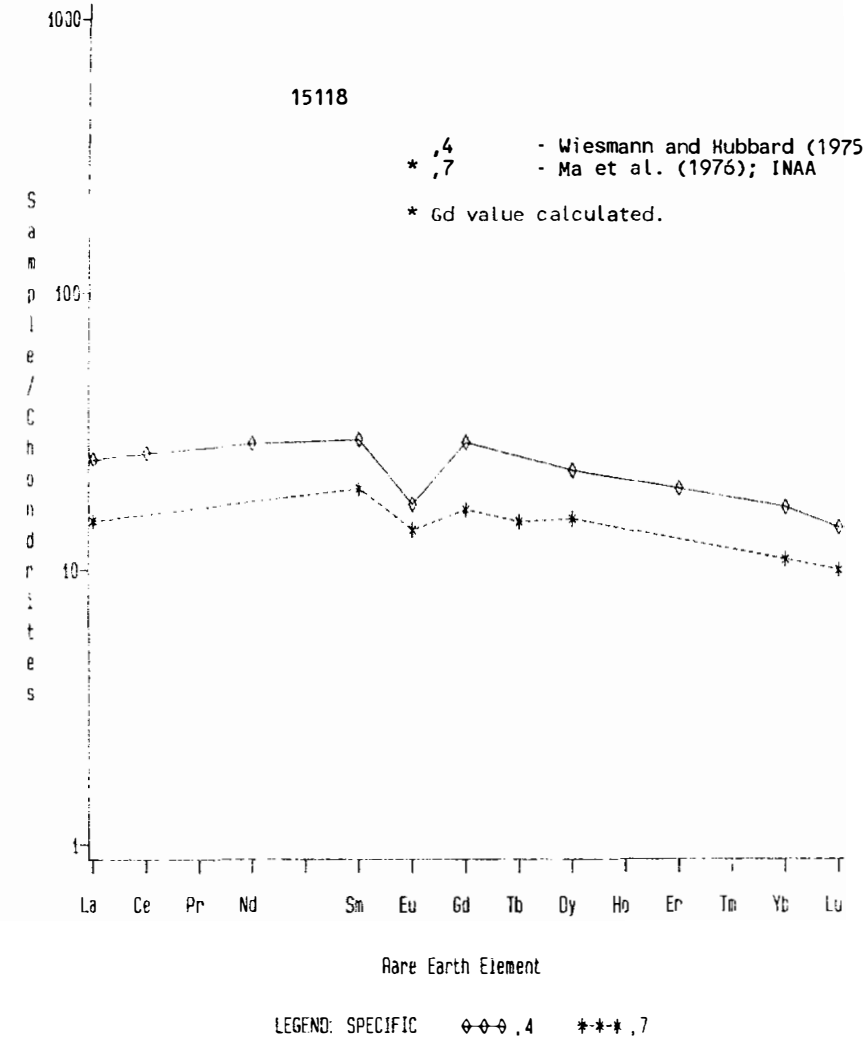

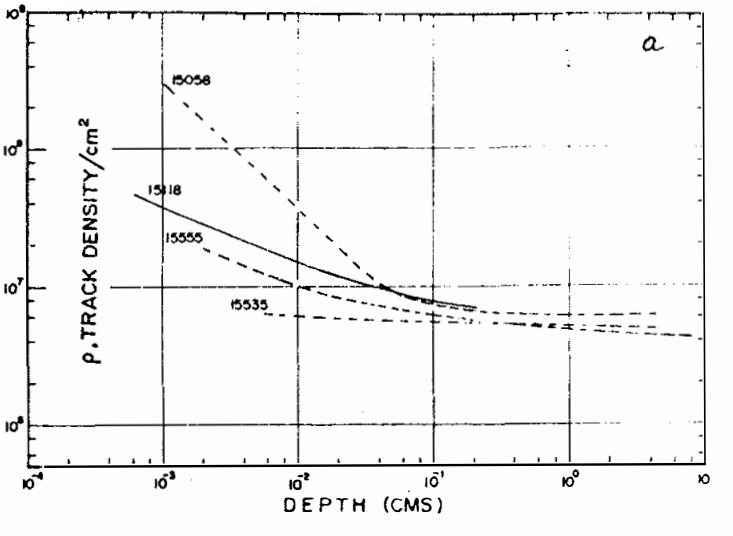

Figure 6. Track density vs. depth for 15118 (solid line) and other Apollo 15 samples (dashed lines) (Bhandari et al., 1972).

TABLE 15118-1. Chemical analyses

		,4	,4	,7
Wt %	SiO2	47.6		
	TiO2	2.05	2.05	2.00
	Al2O3	10.72		10.6
	FeO	20.39		24.0
	MgO	6.49		7.7
	CaO	11.65		10.1
	Na2O	0.32	0.31	0.354
	K2O	0.06	0.076	0.065
	P2O5	0.10		
(ppm)	Sc			42
	V			204
	Cr		2266	3970
	Mn	2170		1970
	Co			44
	Ni			<66
	Rb		1.32	
	Sr		131	
	Y			
	Zr			
	Nb			
	Hf			3.1
	Ba		83.8	80(a)
	Th		0.79	
	U		0.21	
	Pb			
	La		8.39	5.0
	Ce		23.4	
	Pr			
	Nd		17.3	
	Sm		5.40	3.6
	Eu		1.20	0.97
	Gd		7.25	
	Tb			0.71
	Dy		7.33	4.9
	Ho			
	Er		3.99	
	Tm			
	Yb		3.40	2.2
	Lu		0.49	0.34
	Li		8.3	
	Be			
	B			
	C			
	N			
	S	700		
	F			
	Cl			
	Br			
	Cu			
	Zn			
(ppb)	I			
	At			
	Ga			
	Ge			
	As			
	Se			
	Mo			
	Tc			
	Ru			
	Rh			
	Pd			
	Ag			
	Cd			
	In			
	Sn			
	Sb			
	Te			
	Cs			
	Ta			
	W			450
	Re			
	Os			
	Ir			
	Pt			
	Au			
	Hg			
	Tl			
	Bi			
		(1)	(2)	(3)

TABLE 15118-2. Defocussed beam microprobe analysis (Dowty et al., 1973a, b)

Wt %	SiO2	48.7
	TiO2	2.10
	Al2O3	9.7
	FeO	21.1
	MgO	7.0
	CaO	9.9
	Na2O	0.39
	K2O	0.08
	P2O5	0.09
ppm	Cr	1780
	Mn	2090

References and methods:

(1) Rhodes and Hubbard (1973); XRF
(2) Wiesmann and Hubbard (1975); isotope dilution, atomic abs.
(3) Ma et al. (1976); INAA

Notes:

(a) ±35

15119 FINE-GRAINED OLIVINE-NORMATIVE MARE BASALT AND REGOLITH BRECCIA ST. 2 14.1 g

INTRODUCTION: 15119 is an olivine-normative mare basalt with a microporphyritic texture. The phenocrysts are small, sparse, and yellow-green olivines. A regolith breccia adheres to the basalt (Fig. 1), hence the basalt is actually a clast. The basalt is tough; the regolith breccia is friable and brownish-gray. Zap pits occur on the regolith breccia, and the basalt has a few vugs. 15119 was collected as part of the rake sample 5 m east of the boulder at Station 2 (see Fig. 15105-2).

PETROLOGY: The basalt in 15119 consists of a groundmass of granular-looking pyroxene enclosed in plagioclase, and contains sparse olivine phenocrysts (Fig. 2). It is fairly similar to 15105 except that some of its plagioclases are bigger. The regolith breccia has not been sectioned. Macroscopically it contains glass including green glass spheres, basaltic clasts, and chalky white clasts.

CHEMISTRY: Analyses are listed in Table 1 with rare earths plotted in Figure 3. The analyses are of an olivine-normative mare basalt, on the Mg-poor end of the spectrum.

PHYSICAL PROPERTIES: Gose et al. (1972) and Pearce et al. (1973), using a Develco Cryogenic magnetometer, found a natural remanent magnetism intensity of 8.6×10^{-6} emu/g for the sample, typical of Apollo 15 mare basalts.

PROCESSING AND SUBDIVISIONS: The breccia easily broke from the basalt (Fig. 1). The basalt was chipped to provide allocations and is now ,0 (6.90 g). Thin sections ,3 and ,12 were made from ,3 and are only basalt. The breccia has not been allocated and is dominantly chips ,1 (2.5 g) and ,4 (2.53g).

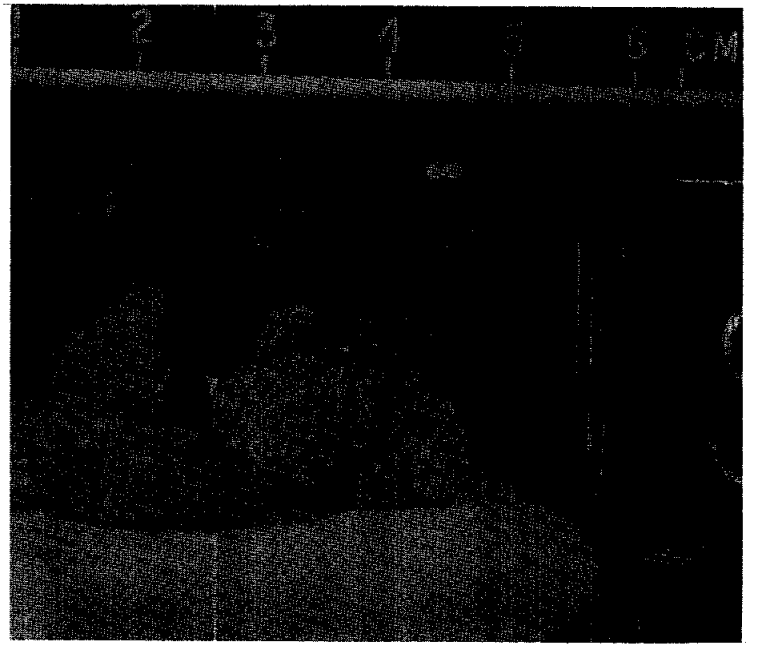

Figure 1. Sample 15119 before chipping the basalt. S-71-48776

Figure 2. Photomicrograph of 15119,12 (a poor section) An olivine microphenocryst is on the center left edge. Crossed polarizers. Width about 1.25 mm.

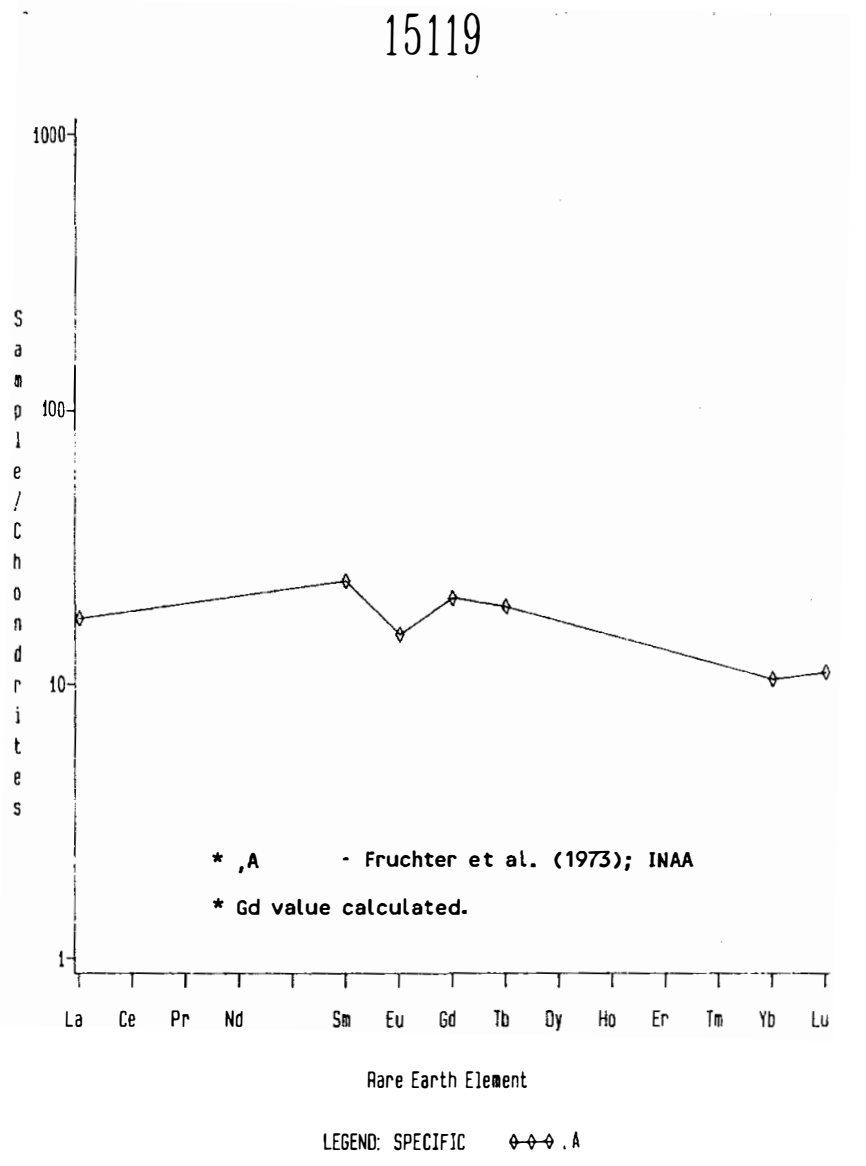

Figure 3. Rare earths in the basalt in 15119 (Fruchter et al., 1973).

TABLE 15119-1. Chemical analyses of the mare basalt in 15119

			,5
Wt %	SiO2		45.23
	TiO2	2.86	2.64
	Al2O3	8.9	9.24
	FeO	21.9	22.25
	MgO		8.93
	CaO		10.55
	Na2O	0.290	0.30
	K2O		0.05
	P2O5		0.09
(ppm)	Sc	45	
	V		
	Cr	3400	3220
	Mn		2405
	Co	47	
	Ni		
	Rb		
	Sr		
	Y		
	Zr		
	Nb		
	Hf	2.8	
	Ba		
	Th		
	U		
	Pb		
	La	5.7	
	Ce		
	Pr		
	Nd		
	Sm	4.3	
	Eu	1.05	
	Gd		
	Tb	0.9	
	Dy		
	Ho		
	Er		
	Tm		
	Yb	2.1	
	Lu	0.38	
	Li		
	Be		
	B		
	C		
	N		
	S		500
	F		
	Cl		
	Br		
	Cu		
	Zn		
(ppb)	I		
	At		
	Ga		
	Ge		
	As		
	Se		
	Mo		
	Tc		
	Ru		
	Rh		
	Pd		
	Ag		
	Cd		
	In		
	Sn		
	Sb		
	Te		
	Cs		
	Ta		
	W		
	Re		
	Os		
	Ir		
	Pt		
	Au		
	Hg		
	Tl		
	Bi		
		(1)	(2)

References and methods:

(1) Fruchter et al. (1973); INAA
(2) Chappell and Green (1973); XRF

15125 PORPHYRITIC SPHERULITIC QUARTZ-NORMATIVE MARE BASALT ST. 2 6.5 g

INTRODUCTION: 15125 is a pyroxene-phyric basalt belonging to the quartz-normative group. The pyroxenes are so pale-colored that in PET they were misidentified as plagioclase. The sample is medium dark gray; its groundmass is fine-grained but not glassy. The basalt is tough, with no obvious vugs but the surface has some zap pits. 15125 was collected as part of the rake sample 5 m east of the boulder at Station 2 (see Fig. 151052).

PETROLOGY: 15125 is pyroxene-phyric with generally small, skeletal, euhedral, and strongly zoned pyroxenes in a fine, dark, but wholly crystalline groundmass (Fig. 2). It was described by Dowty et al. (1973a, b; 1974) with microprobe analyses of silicates and metals in Dowty et al. (1973c). Opaque mineral analyses were reported by Nehru et al. (1973, 1974). Dowty et al. (1973a, b) reported a mode of 44% pyroxene, 4% olivine, 0.4% opaque minerals, and 51.6% groundmass. Grove and Walker (1977) found 45.3% pyroxene, 3.10% olivine, 0.2% opaque minerals, and 51.4% groundmass. The olivines are skeletal and about the same size as the pyroxene phenocrysts; their compositions range from Fo_{70} to fayalitic (Fig. 3). The pyroxene zoning trends were described by Dowty et al. (1974) (Fig. 4). The phenocrysts (0.5 to 2.0 mm x 0.08 to 0.19 mm) are smaller than groundmass pyroxenes in many coarse-grained quartz-normative basalts. The groundmass consists of spherulitic alternating plagioclase and pyroxene needles in a feathery arrangement. Groundmass pyroxenes are 0.02 to 0.07 x 0.005 mm. Dowty et al. (1974) reported cell parameters for pyroxene, and found the for pigeonite-augite intergrowths to be 1.6, consistent with very fast cooling. Nehru et al. (1974) found that chromite had a more restricted range of Fe/Mg than most other samples; ulvospinel was too small to analyze.

Lofgren et al. (1975) compared the textures of 15125 as described by Dowty et al. (1973a, b) with the products of dynamic experiments on a synthetic quartz-normative basalt composition. They inferred cooling rates of around 5°C/hour for the phenocrysts and more than 30°C/hour for the groundmass. Grove and Walker (1977) used a similar but more sophisticated method to investigate cooling rates. The high pyroxene nucleation (10.7 phenocrysts/mm^2) corresponds with cooling at about 30°C/hour for the early stages. An integrated rate of about 10°C/hour was inferred from the total phenocryst sizes, and a late stage rate of 85 to 250°C/hour was inferred from plagioclase sizes. The final cooling rates correspond with a distance of about 6 to 9 cms from a conductive boundary.

CHEMISTRY: The analysis of Helmke et al. (1973) is of an average member of the quartz-normative mare basalt group (Table 1). The rare earths are shown in Figure 5. Helmke et al. (1973) postulatd two groups of quartz-normative basalts on the basis of Sm/Eu ratios; 15125 was similar to vitrophyre 15597. The defocussed beam analysis (Table 2) is in reasonable agreement with the analysis of Helmke et al. (1973).

PROCESSING AND SUBDIVISIONS: 15125 was chipped to produce daughters ,1 to ,4 (Fig. 1). Thin sections ,6 and ,7 were made from ,1. ,0 is now 4.9 g.

Figure 1. Post-split view of 15125. S-71-55548

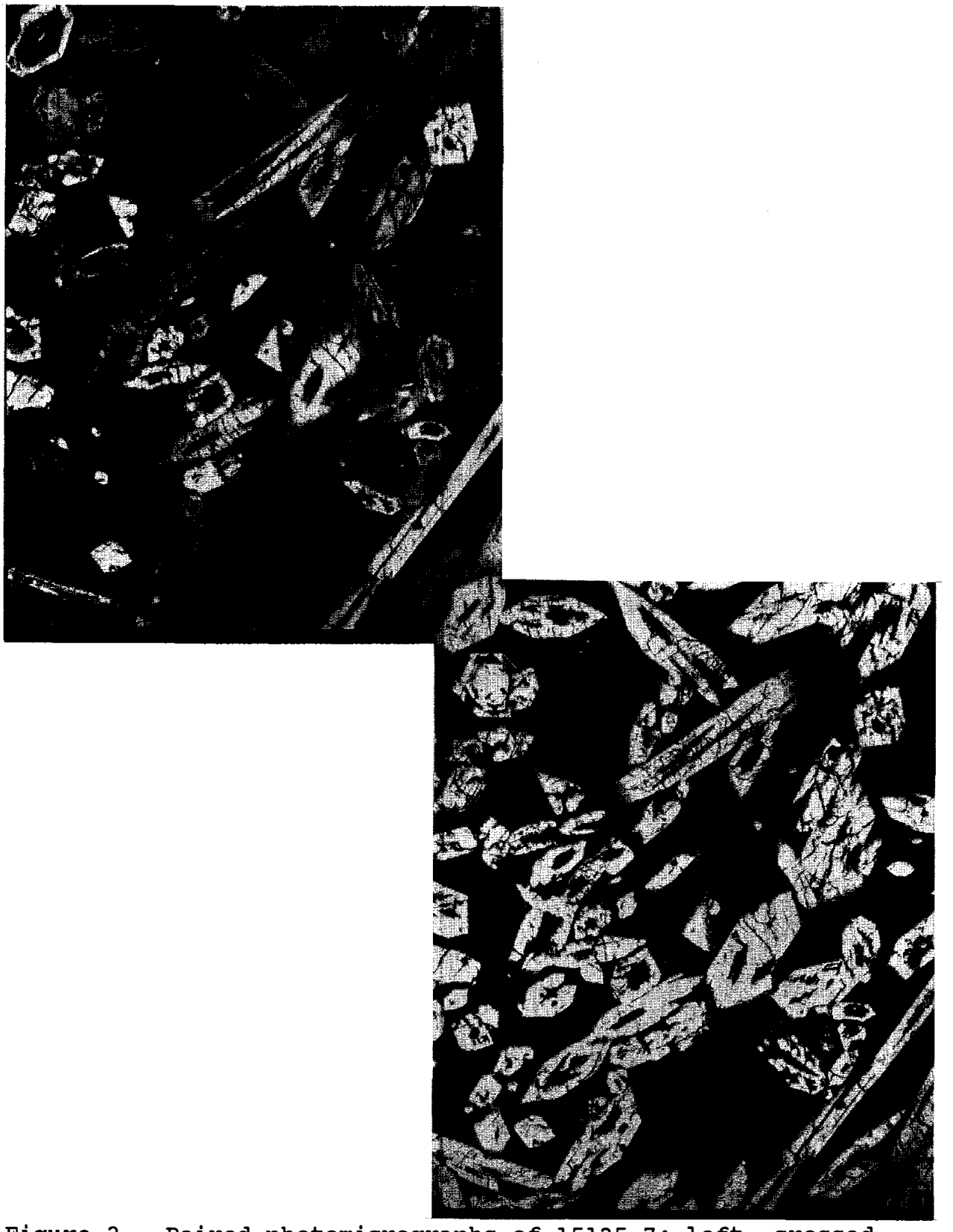

Figure 2. Paired photomicrographs of 15125,7; left, crossed polarizers; right, plane transmitted light. Widths about 1.25 mm.

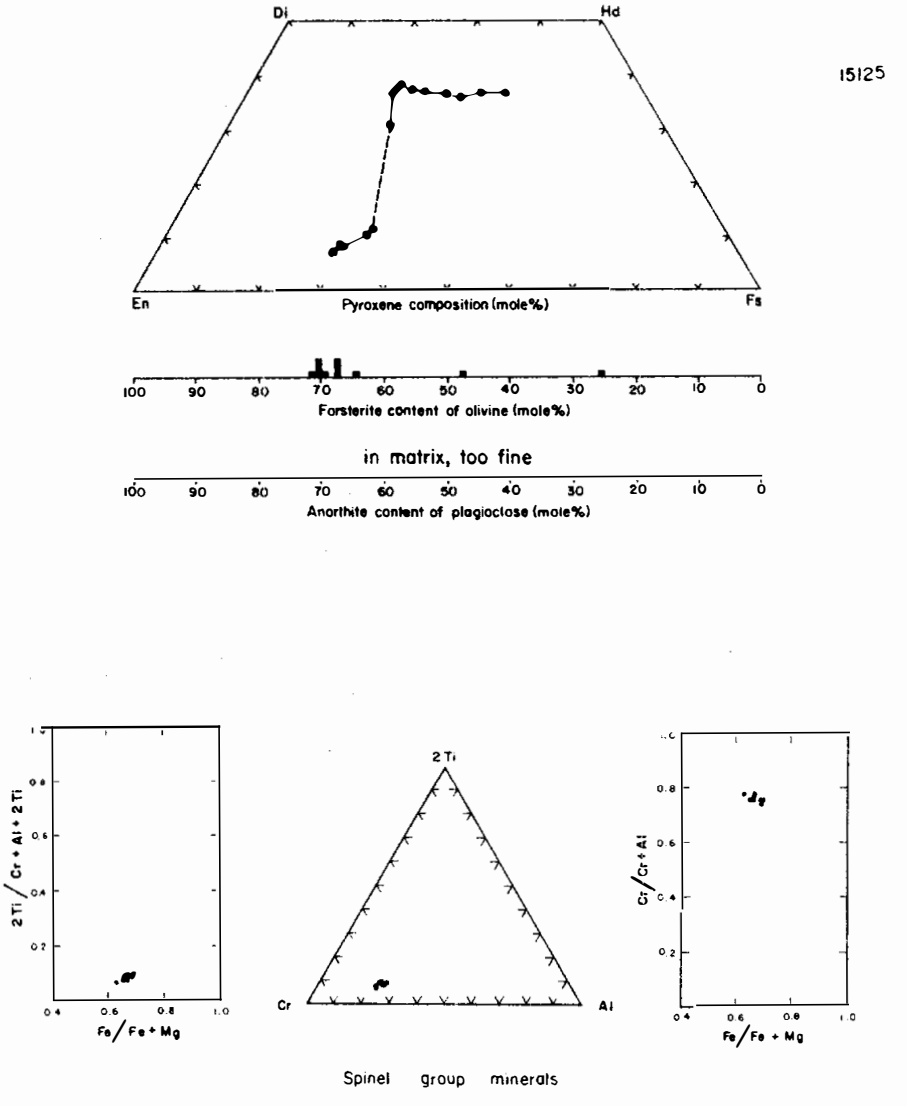

Figure 3. Mineral analyses (Dowty et al., 1973b).

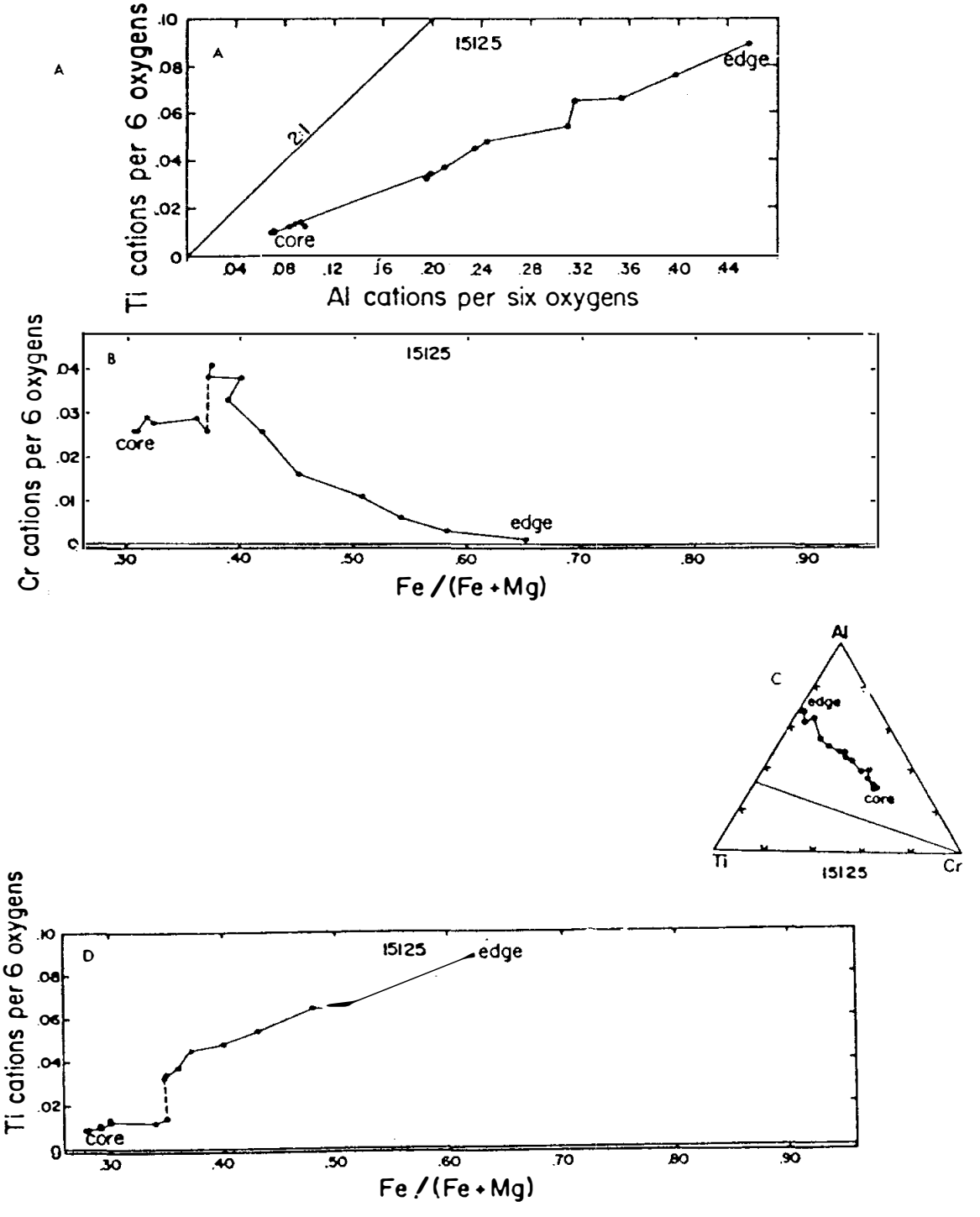

Figure 4. Phenocryst zoning trends. a) Ti-Al; b) Cr-Fe/(Fe+Mg); c) Ti-Al-Cr; d) Ti-Fe/(Fe+Mg) (Dowty et al., 1974).

15125

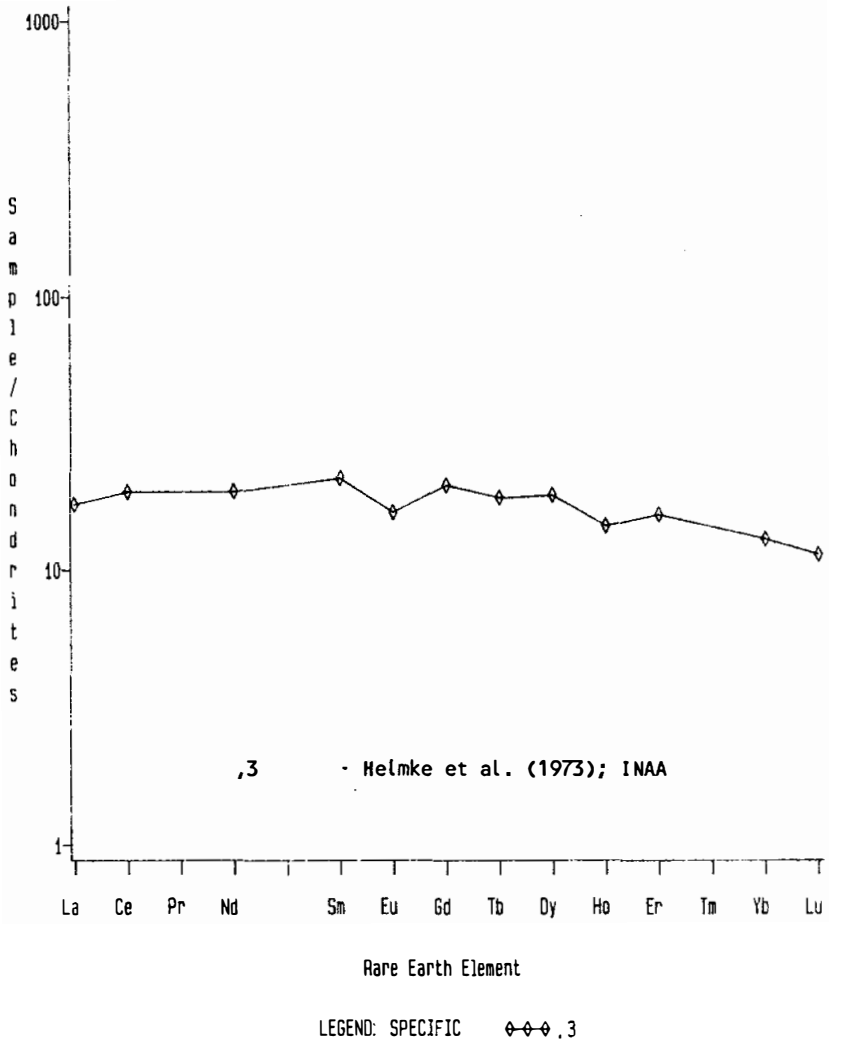

Figure 5. Rare earths in 15125.

TABLE 15125-1. Chemical analyses

		,3
Wt %	SiO2	48.4
	TiO2	1.80
	Al2O3	9.11
	FeO	20.3
	MgO	9.19
	CaO	8.04
	Na2O	0.351
	K2O	0.053
	P2O5	
(ppm)	Sc	41.5
	V	
	Cr	4140
	Mn	2080
	Co	53
	Ni	
	Rb	0.8
	Sr	
	Y	
	Zr	
	Nb	
	Hf	2.1
	Ba	
	Th	
	U	
	Pb	
	La	5.75
	Ce	17.1
	Pr	
	Nd	11.7
	Sm	3.92
	Eu	1.12
	Gd	5.1
	Tb	0.87
	Dy	6.00
	Ho	1.02
	Er	3.2
	Tm	
	Yb	2.59
	Lu	0.39
	Li	
	Be	
	B	
	C	
	N	
	S	
	F	
	Cl	
	Br	
	Cu	
	Zn	<5
(ppb)	I	
	At	
	Ga	3300
	Ge	
	As	
	Se	
	Mo	
	Tc	
	Ru	
	Rh	
	Pd	
	Ag	
	Cd	
	In	
	Sn	
	Sb	
	Te	
	Cs	20
	Ta	
	W	
	Re	
	Os	
	Ir	
	Pt	
	Au	
	Hg	
	Tl	
	Bi	
		(1)

TABLE 15125-2. Microprobe Defocussed beam analysis (Dowty et al., 1973a,b)

Wt %	SiO2	47.5
	TiO2	2.27
	Al2O3	8.3
	FeO	22.3
	MgO	9.4
	CaO	9.3
	Na2O	0.33
	K2O	0.05
	P2O5	0.08
ppm	Cr	3700
	Mn	2090

References and methods:

(1) Helmke et al. (1973); INAA, RNAA, atomic abs.

15135 AGGLUTINATE ST. 2 1.6 g

INTRODUCTION: 15135 is a dark gray, heterogeneous agglutinate containing shocked lithic and mineral fragments. It contains about 35% vugs and vesicles up to 2 mm diameter. It is tough and subangular. It was collected as part of the rake sample 5 m east of the boulder at Station 2 (See Fig. 15105-2).

PETROLOGY: 15135 consists of a vesicular dark glassy matrix containing lithic and mineral clasts (Fig. 2). It was briefly described by Steele et al. (1977), who found it to consist of 45% glass/fine matrix, 5% lithic clasts (mare), 20% mineral fragments, and 30% vesicles. The largest mineral clasts are shocked plagioclase. One pyroxene is exsolved into compositions of $En_{60}Wo_3$ and $En_{40}Wo_{45}$.

PROCESSING AND SUBDIVISIONS: 15135 was sawn to produce ,1 (Fig. 3) from which thin sections ,6 to ,8 were made.

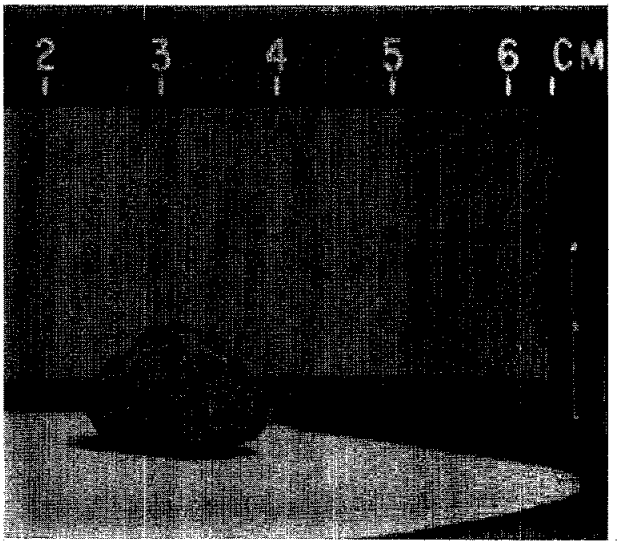

Figure 1. Pre-split view of 15135. S-71-48782

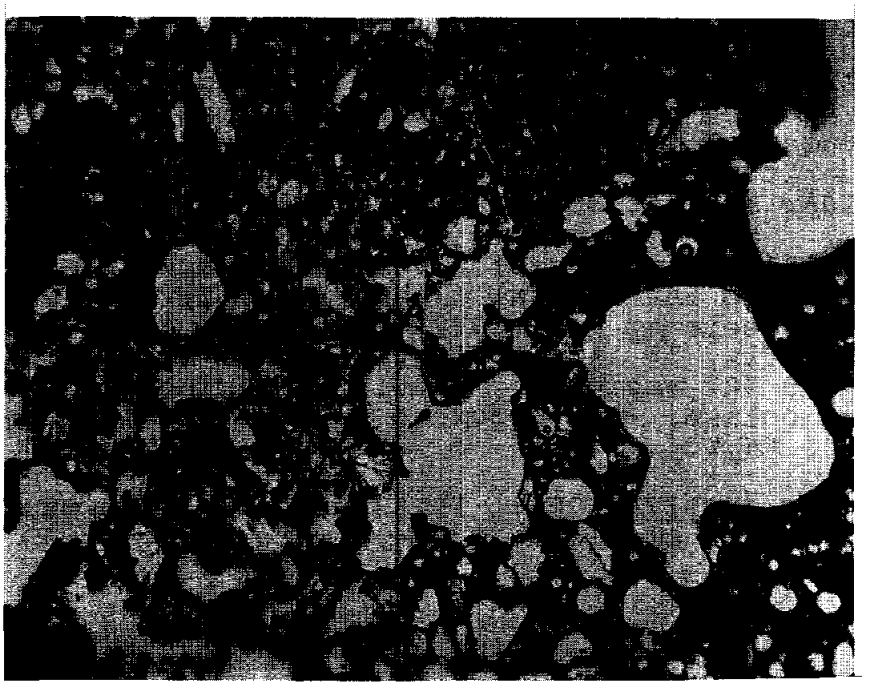

Figure 2. Photomicrograph of 15135,6, showing vesicles, fine matrix, and a melt clast. Width about 1.25 mm. Plane transmitted light.

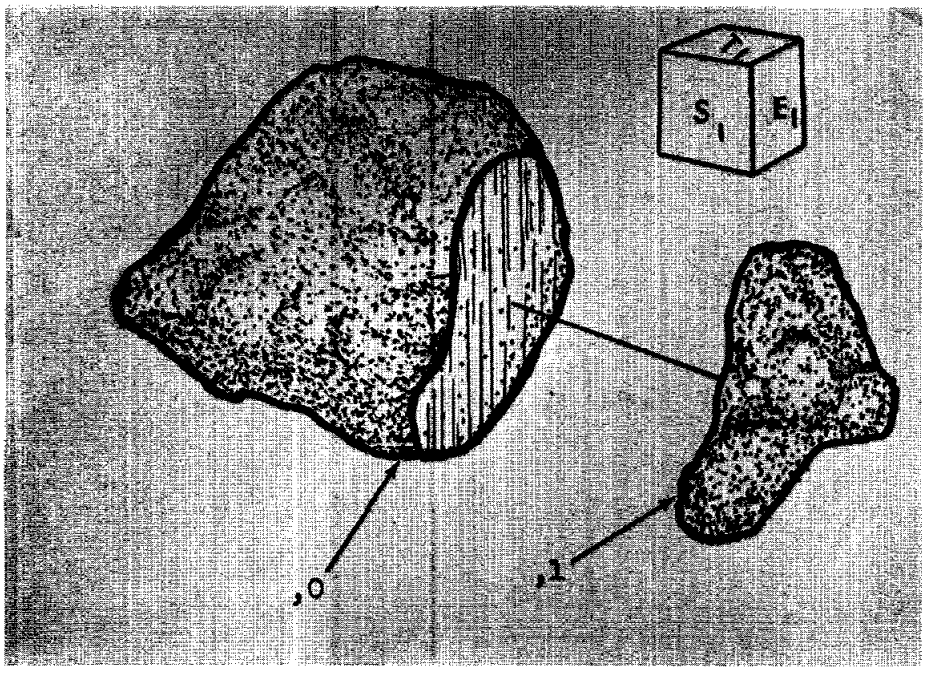

Figure 3. Sawing diagram of 15135.

15145 OLIVINE-NORMATIVE(?) MARE BASALT BRECCIA ST. 2 15.1 g

INTRODUCTION: 15145 is a breccia which appears to be almost monomict and formed of coarse mare basalt clasts. It is light gray, subangular, and tough (Fig. 1). One piece of surface area is slickensided and has a little splash glass. Zap pits occur on this and other surfaces. 15145 was collected as part of the rake sample 5 m east of the boulder at Station 2 (See Fig. 15105-2).

Figure 1. Sawing products of 15145. S-71-57439

Figure 2. Photomicrograph of thin section 15145,8. Width about 2 mm. Transmitted light.

PETROLOGY: 15145 consists predominantly of clasts of coarse mare basalts in a ground up, mainly mare-derived breccia (Fig. 2). It was briefly described by Dowty et al. (1973b). Very large pyroxenes (about 3 mm across) are commonly twinned, without obvious zoning. A few fine-grained and recrystallized mare basalt clasts are also present, along with a few glass spherules and chondrules.

CHEMISTRY: A partial analysis was made by Fruchter et al. (1973) (Table 1, Fig. 3). The Ti abundance suggests a dominantly olivine-normative basalt derivation; the high rare-earths suggest possible KREEP contamination.

PROCESSING AND SUBDIVISIONS: 15145 was sawn to produce daughters from one end (Fig. 1). Thin sections ,8 to ,10 were made from chip ,2. ,0 is now 11.52 g and ,1 is 1.34 g.

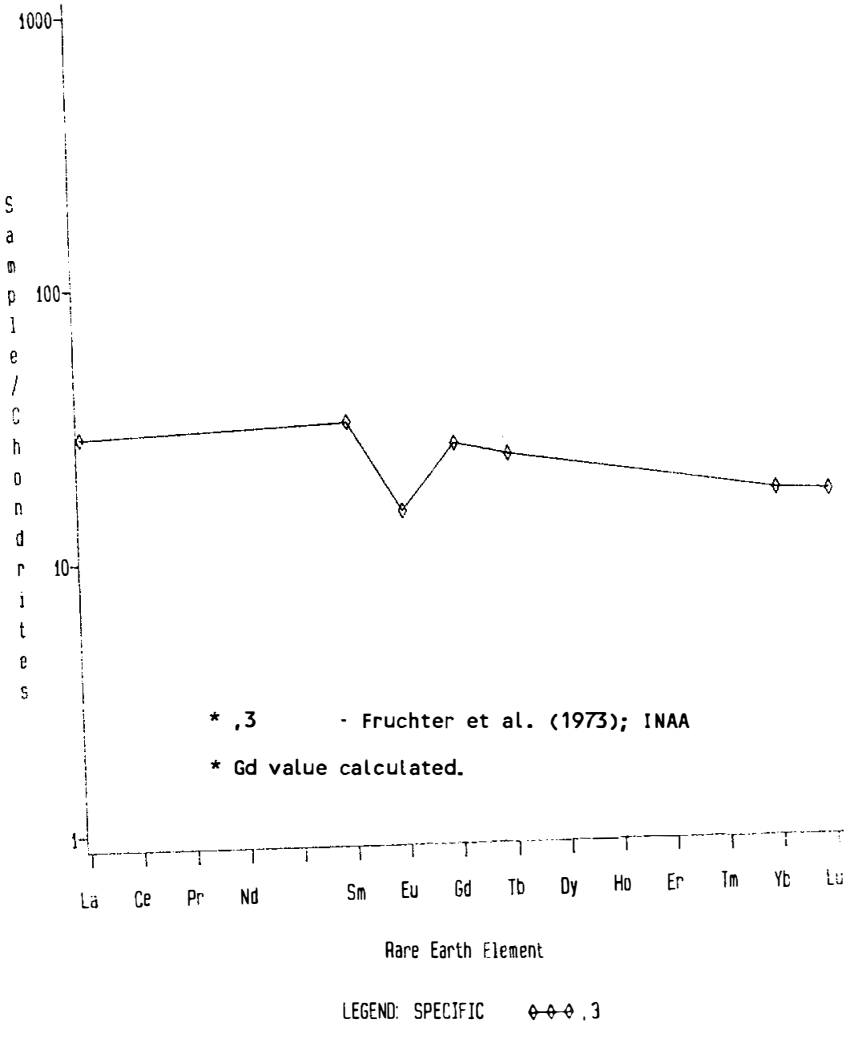

Figure 3. Rare earths in 15145.

TABLE 15145-1. Chemical analyses

		,3
Wt %	SiO_2	
	TiO_2	2.49
	Al_2O_3	8.12
	FeO	21.3
	MgO	
	CaO	
	Na_2O	0.275
	K_2O	
	P_2O_5	
(ppm)	Sc	37
	V	
	Cr	3950
	Mn	
	Co	64
	Ni	
	Rb	
	Sr	
	Y	
	Zr	
	Nb	
	Hf	3.8
	Ba	
	Th	0.36
	U	
	Pb	
	La	9.4
	Ce	
	Pr	
	Nd	
	Sm	5.7
	Eu	1.02
	Gd	
	Tb	1.1
	Dy	
	Ho	
	Er	
	Tm	
	Yb	3.3
	Lu	0.55
	Li	
	Be	
	B	
	C	
	N	
	S	
	F	
	Cl	
	Br	
	Cu	
	Zn	
(ppb)	I	
	At	
	Ga	
	Ge	
	As	
	Se	
	Mo	
	Tc	
	Ru	
	Rh	
	Pd	
	Ag	
	Cd	
	In	
	Sn	
	Sb	
	Te	
	Cs	
	Ta	560
	W	
	Re	
	Os	
	Ir	
	Pt	
	Au	
	Hg	
	Tl	
	Bi	
		(1)

Reference and method:

(1) Fruchter et al. (1973); INAA

15146 MARE BASALT (MONOMICT?) BRECCIA ST. 2 1.0 g

INTRODUCTION: 15146 (Fig. 1) is a breccia consisting almost entirely of mare basalt clasts and debris and may be monomict. It was collected with the rake sample 5 m east of the boulder at Station 2 (see Fig. 15105-2).

PETROLOGY: 15146 consists of coarse poikilitic clasts and coarse mineral fragments in a brown, fine-grained (glassy?) matrix (Fig. 2). It was described by Steele et al. (1977) and Steele et al. (1972). According to Steele et al. (1977), 15146 is a near-monomict breccia consisting of 15% lithic clasts, 75% mineral fragments, 10% fine matrix, and traces of glass. Pyroxene compositions are shown in Figure 3. The appearance of the materials is generally coarse mare, but Steele et al. (1977) referred to the pyroxene type as "other", and plagioclase as low-Fe, not like mare plagioclases. Pyroxenes are about $En_{55}Wo_{11}$; plagioclases are An_{85-90}; and olivines are Fo_{59}. Ilmenite and chromite are also present. The bulk chemistry appears to be similar to green glass, but the TiO_2 is higher. One clast referred to as pyroxenite is shown as a photomicrograph in Steele et al. (1977) (in the caption misprinted as 15164) and consists mainly of pyroxene and olivine; but some plagioclase is also present. The affinity of the clast is unclear but appears to be mare, perhaps a cumulate.

PROCESSING AND SUBDIVISIONS: ,0 was chipped to produce ,1 (Fig. 1) from which thin sections ,1 and ,6 were made.

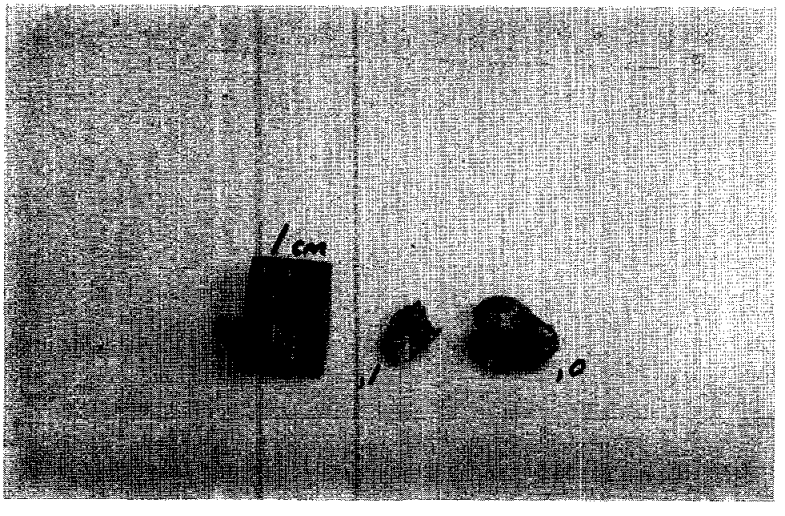

Figure 1. Splits of 15146. S-71-56161

Figure 2. Photomicrograph of 15146,6, showing coarse clasts and mineral fragments. Cross polarizers. Width about 2.5 mm.

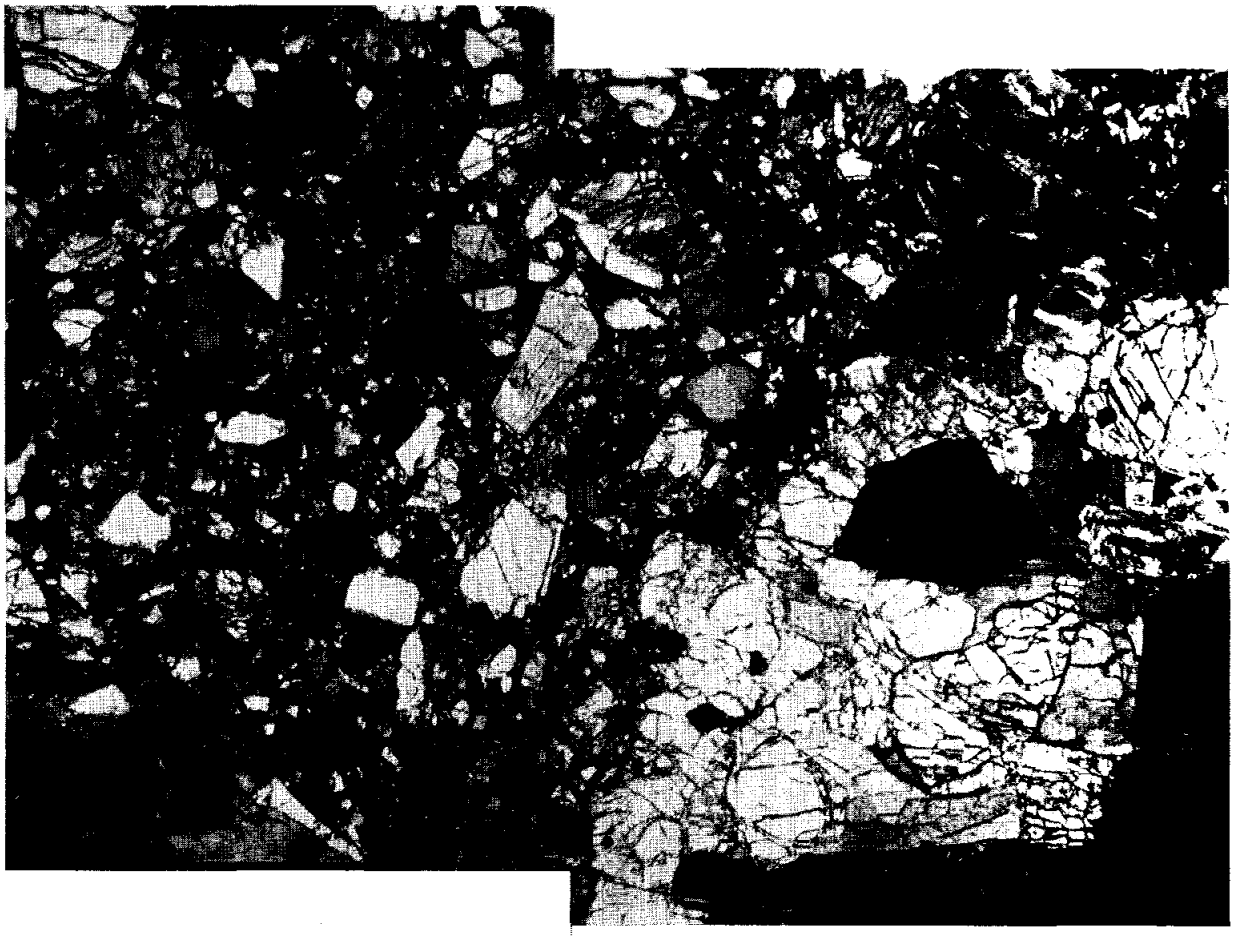

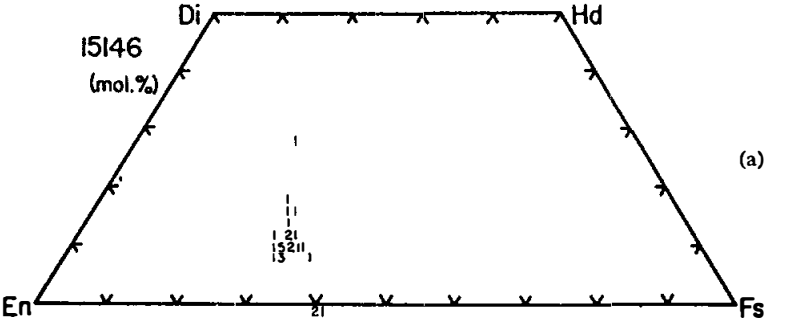

Figure 3. Pyroxenes in 15146,1. (Steele et al., 1977).

15147 REGOLITH BRECCIA ST. 2 3.7 g

INTRODUCTION: 15147 is a light gray to medium gray regolith breccia (Fig. 1). It is angular and tough, lacks zap pits, and has no cavities. Mare basalt clasts are visible and fine matrix makes up 95% of the rock. The sample was collected as part of the rake sample 5 m east of the boulder at Station 2 (see Fig. 15105-2). It has never been subdivided or allocated.

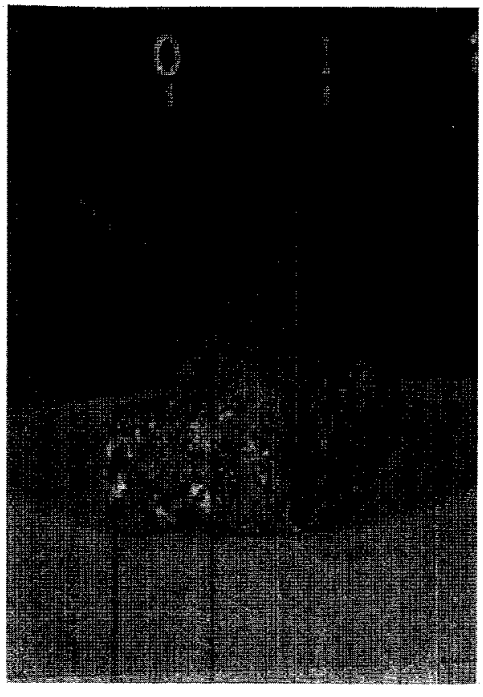

Figure 1. Sample 15147. S-71-49329

15148 REGOLITH BRECCIA ST. 2 3.0 g

INTRODUCTION: 15148 is a medium to light gray breccia (Fig. 1). It contains about 10% basaltic and other lithic fragments, and green spherules are visible. The sample is subangular to blocky, coherent, and has no cavities. It has never been subdivided. It was collected with the rake sample 5 m east of the boulder at Station 2 (see Fig. 15105-2).

PHYSICAL PROPERTIES: Gose et al. (1972) and Pearce et al. (1973), using a Develco Cryogenic magnetometer, found a natural remanent magnetism intensity of 1.9×10^{-5} emu/g. This is higher than for most mare basalts, though not as high as most other breccias.

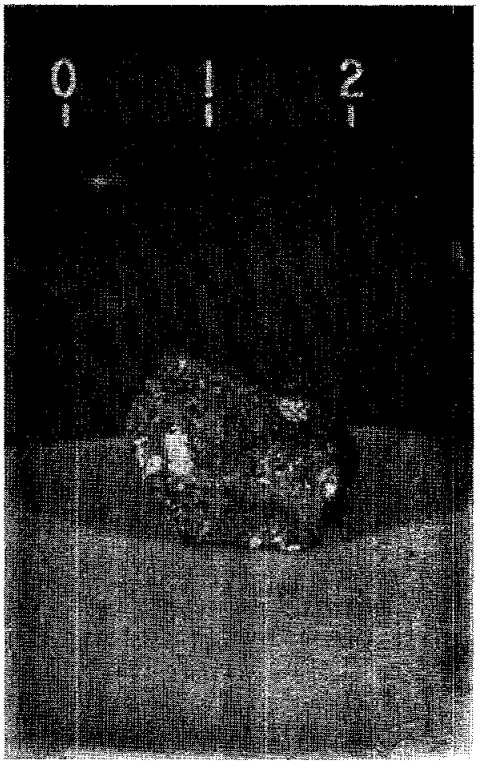

Figure 1. Sample 15148. S-71-49321

15205 REGOLITH BRECCIA, GLASS-COATED ST. 2 337.3 g

INTRODUCTION: 15205 has the characteristics of a breccia formed from an exceptionally immature regolith, but is unique among Apollo 15 regolith samples: it is gray, not brown, is tough, and consists almost entirely of Apollo 15 KREEP basalt fragments with some mare basalt fragments (especially pyroxene-phyric). While it contains green glass as clods and impact glasses, mature regolith components such as agglutinates are rare to absent, and the clast size is much larger than for mature regoliths (Fig. 1). The finest matrix appears to be glass and tiny mineral and lithic fragments. The rock has a distinct fabric.

Glass coats most surfaces (Fig. 1) and is vesicular. These surfaces were not all exposed on the Moon and the glass surfaces penetrated a fracture system in the host boulder. The rock is angular with orthogonal joints and more than one penetrative fracture system. Zap pits are present on several surfaces, with most on one surface.

15205 was chipped from a boulder at St. 2 (Fig. 2 and Fig. 15105-2); 15206 was chipped from the same boulder. The boulder is anomalously large for the area and appears to have been thrown in less than 1 m.y. ago from the north or north-west and rolled to the southern end of its own crater.

PETROLOGY: 15205 is a tough breccia with light-colored basaltic lithic clasts (KREEP basalt) dominant (Fig. 1c). It was described by Dymek et al. (1974) as a regolith breccia, but it is not similar to other Apollo 15 regolith breccias: it has a I_s/FeO of 0 (McKay et al., 1984). According to McKay and Wentworth (1983) it has little intergranular porosity, agglutinates and glass spheres are rare, but shock features are common. Nagle (1982a) found that 15205 had lineation and other characteristics expected for rocks produced by subcrater lithification. Nagle (1982b) tabulated grain size distribution, rounding, and packing data for one thin section.

Dymek et al. (1974) concluded that 15205 was a layered, lithified regolith breccia. They described most of its characteristics as inferred from macroscopic descriptions and inspection of a series of thin sections (see Fig. 13). They found it to consist of about 75% clasts (~40% lithic, ~15% glass, and ~20% mineral fragments) from 10 microns to 1 cm diameter, set in a finer-grained, clastic matrix of glass and mineral particles (Fig. 3). Reaction between clasts and matrix is not present, and much of the glass shows no devitrification. Takeda et al. (1980) found a similar matrix. They noted that most pyroxene fragments are derived from KREEP basalts, and that none contain exsolution lamellae. Lithic clasts exhibit a wide range of granulation and shock effects which preceded accumulation. Dymek et al. (1974) also found a distinct fabric marked by a consistent alignment of clasts in thin section.

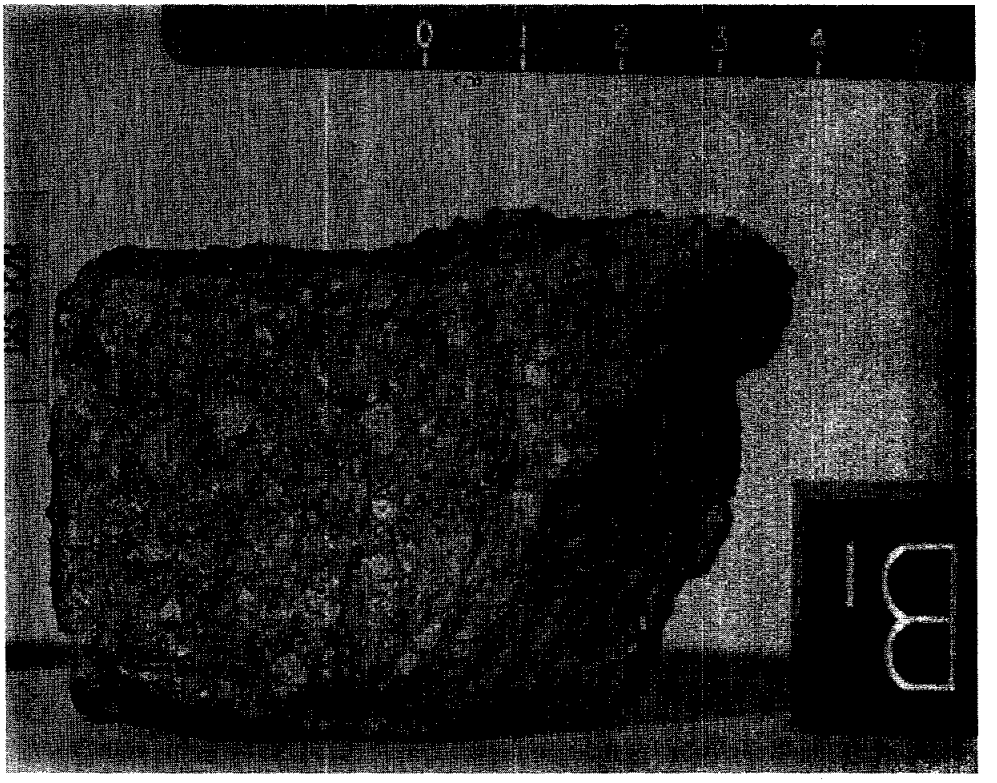

Fig. 1a

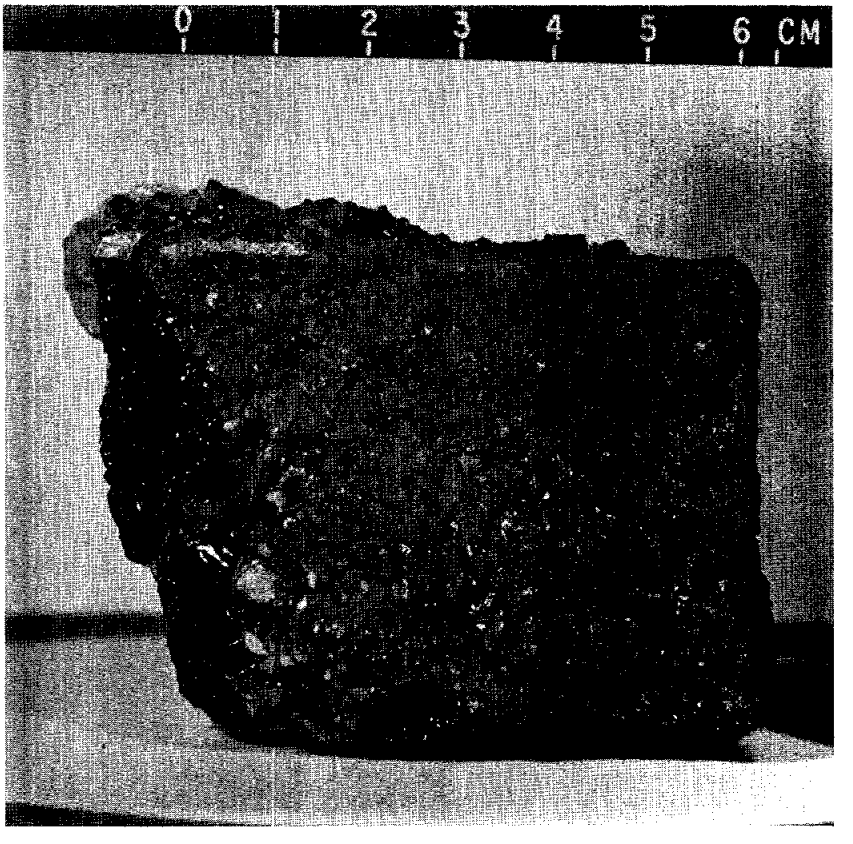

Fig. 1b

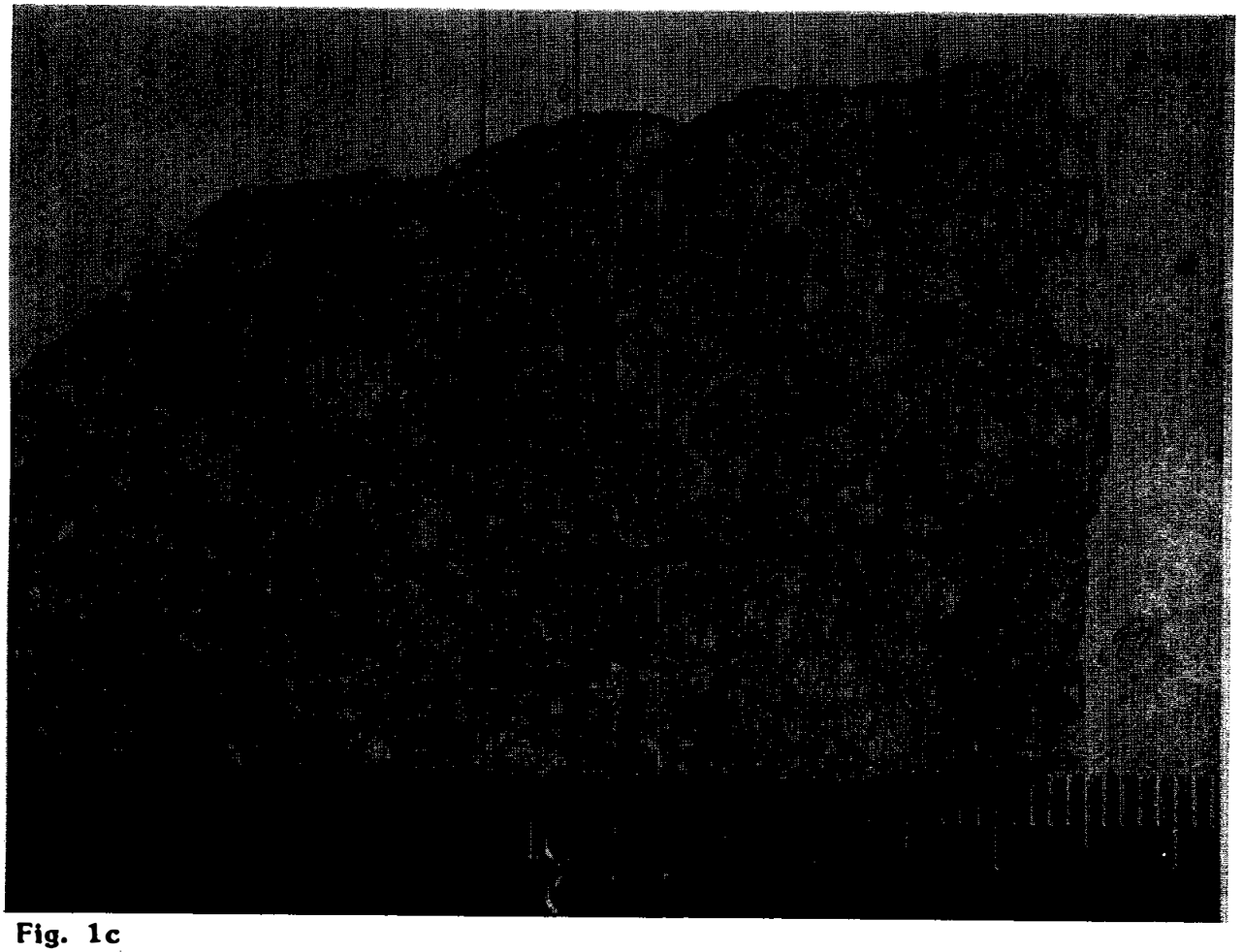

Fig. 1c

Figure 1. Macroscopic views of 15205. a) freshly broken interior piece showing large pale lithic clasts, fractures, and blocky nature. S-71-46350; b) opposite view from a), showing exposed vesicular, planar glass. S-71-46341; c) close up of fractured face of ,0, showing large KREEP basalt clasts, solid matrix, and pieces chipped off. S-77-22162

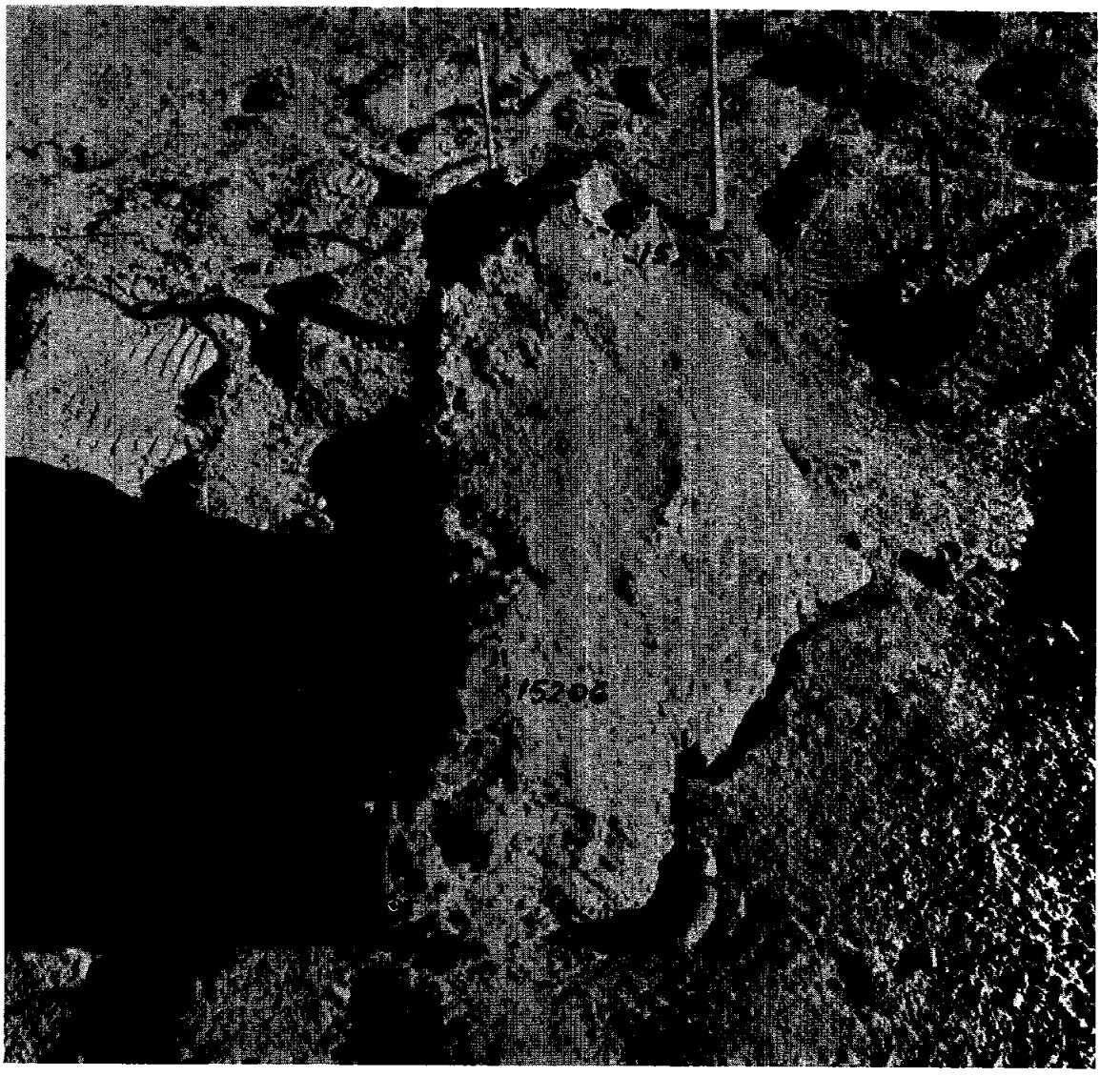

Figure 2. Locations of 15205 and 15206 on the boulder from which they were taken, post-sampling, pre-turning-over of the boulder. AS15-86-11559

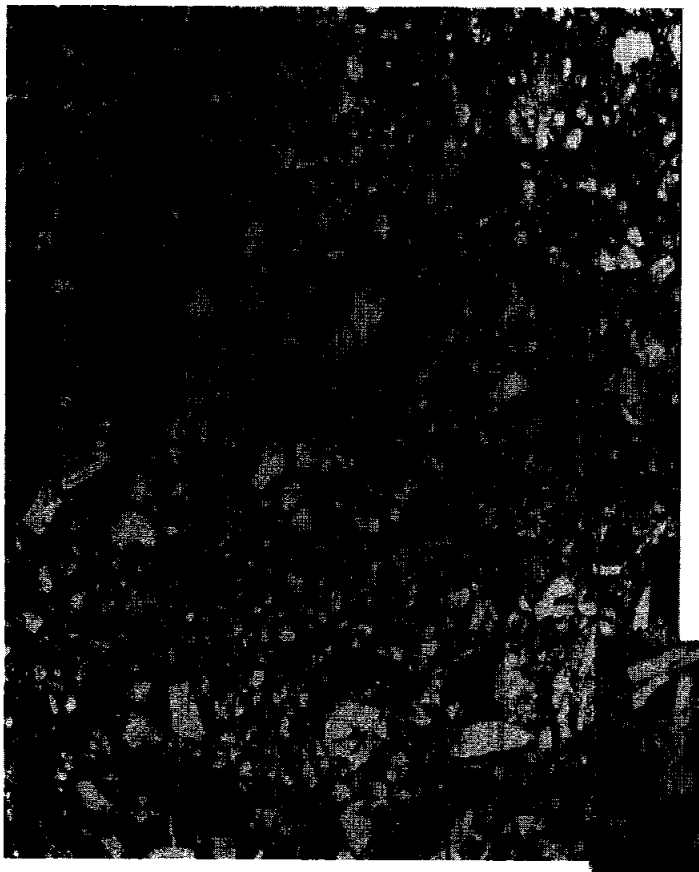

Fig. 3a

Fig 3b

Figure 3. Photomicrographs of 15205. All transmitted light, widths about 1.25 mm. a) 15205,4. general matrix view showing predominance of material larger than 10 microns; b) 15205,4. clast of KREEP basalt (top) and brown, perlitic brown glass with vesicular rind; c) 15205,4. matrix and small clast of mare(?) basalt of uncertain affinity; d) 15205,110. glass coat, vesicular, banded, and with inclusions.

Fig. 3c

Fig.3d

Dymek et al. (1974) found that Apollo 15 KREEP basalt clasts make up about 20% of the sample, and pyroxene-phyric mare basalts a similar amount, while other, olivine-bearing mare basalts make up about 1% of the rock. Inspection of other thin sections and the bulk chemistry of the rock suggests that overall 15205 may contain much less mare basalt (which appears to be locally concentrated) and much more KREEP basalt than suggested by Dymek et al. (1974).

Dymek et al. (1974) divided the feldspathic basalts (Apollo 15 KREEP basalts) into five textural groups: subophitic to intersertal; intersertal; porphyritic intersertal; "ladder structure"; and variolitic. They described each type and provided mineral analyses (Fig. 4) which show them to be similar to other described Apollo 15 KREEP basalts. Takeda et al. (1980) also briefly described KREEP basalt fragments, with mineral compositions given. Dymek et al. (1974) divided the pyroxene-phyric basalts (quartz-normative mare) into three textural groups: aphanitic groundmass; ~10 micron groundmass; ~25 micron groundmass. They described each type and provided mineral analyses (Fig. 5) which show them to be very similar to the typical pyroxene-phyric mare basalts found at the Apollo 15 site. The few other mare basalt fragments include olivine-bearing varieties and may be similar to some of the olivine-normative mare basalts found at the site, as suggested by their mineral compositions (Fig. 6). Conspicuously absent are highlands lithologies; a few fragments of "moderately recrystallized metaclastic rock" are present.

Dymek et al. (1974) described and analyzed glass, which ranges from the glass coat and fracture surface glass, to brown veins, to variously-colored alkalic, high-alumina basalt glasses and layers, to the Apollo 15 green glass which exists as aggregates, and to sparse glasses of mare basalt composition. Conspicuously rare are highlands glasses. Some examples of the compositional range are shown in Figures 7 and 8, which show the several distinct groups. The glass coat forms a distinct cluster, similar to but not the same as the brown glass veins, and also distinct from bulk rock compositions (Tables 1, 2). The coating is dark green-brown and contains abundant spherical vesicles (Fig. 3d) up to 1 cm across. It is flow-banded and the contact between the breccia and the coat is sharp with a 100 micron-wide reaction zone. The coat was not produced by in situ melting. It is distinct from local soil compositions and must predate emplacement of the boulder at its present location. Thin (50-200 micron) brown-glass veins cut the layering and are at least 2 cm long. They are sharp and contain mineral particles and vesicles. They are uniform in composition and different from the glass coat; they were probably injected along microfractures. Yellow to pale-green glass veins are also present. Alkalic, high-alumina (KREEP) basalt glass is most abundant among glass fragments, and is white, yellow, brown, or purple. These glasses are anglular to subrounded, and range from homogeneous nondevitrified to agglutinate-like layers. The compositions show a range

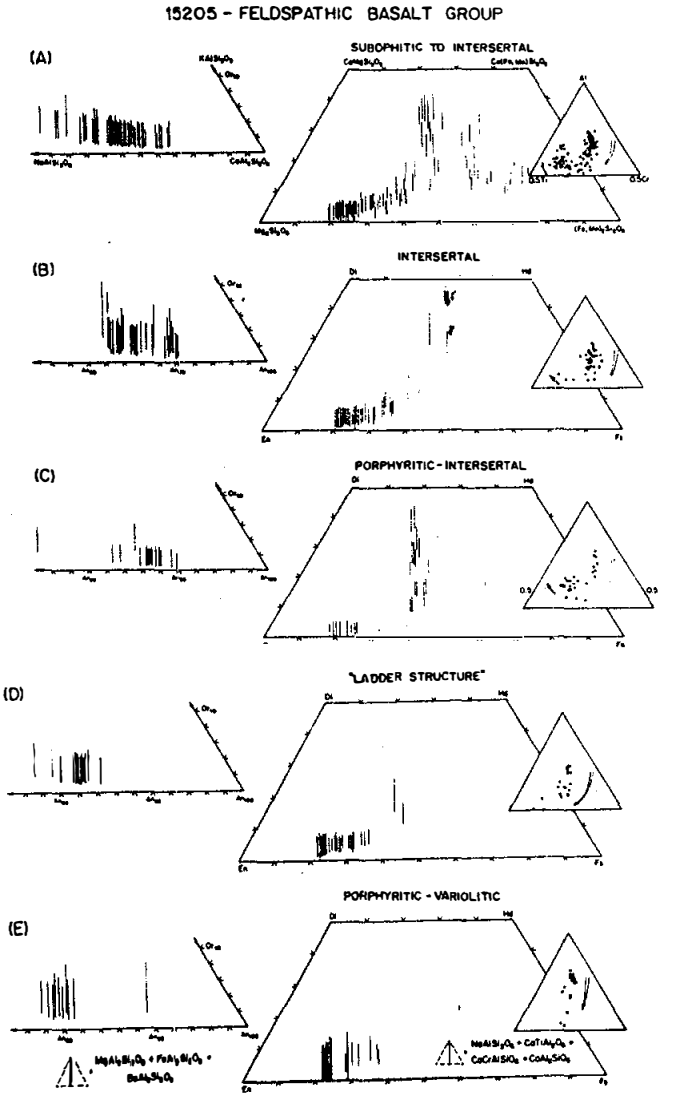

Figure 4. Compositions of plagioclases and pyroxenes in KREEP basalt clasts (Dymek et al., 1974).

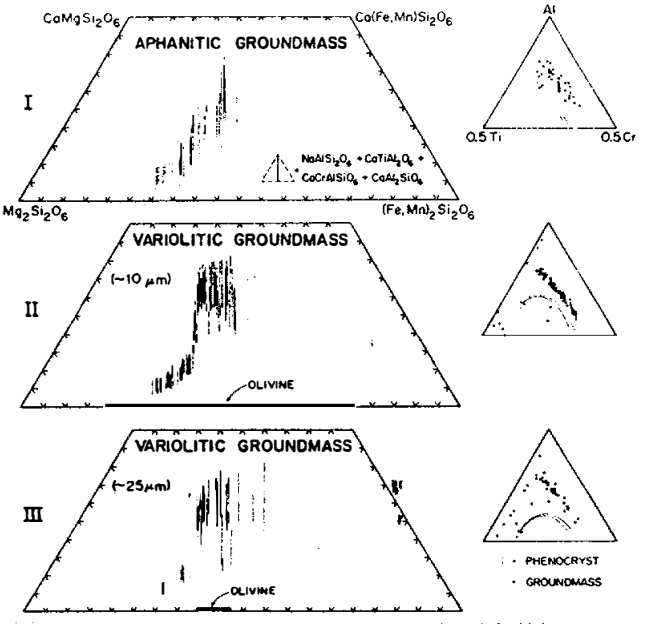

Figure 5. Compositions of pyroxene-phyric (quartz-normative) basalt clasts (Dymek et al., 1974).

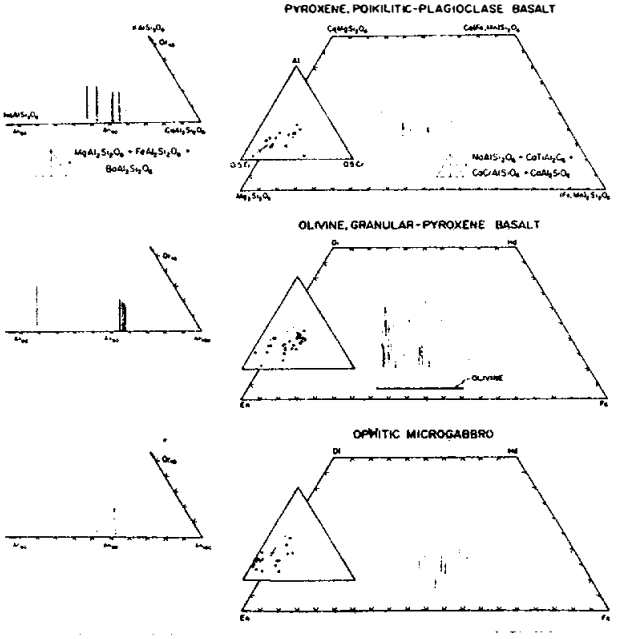

Figure 6. Compositions of plagioclases and pyroxenes in mare basalt clasts in 15205 (Dymek et al., 1974).

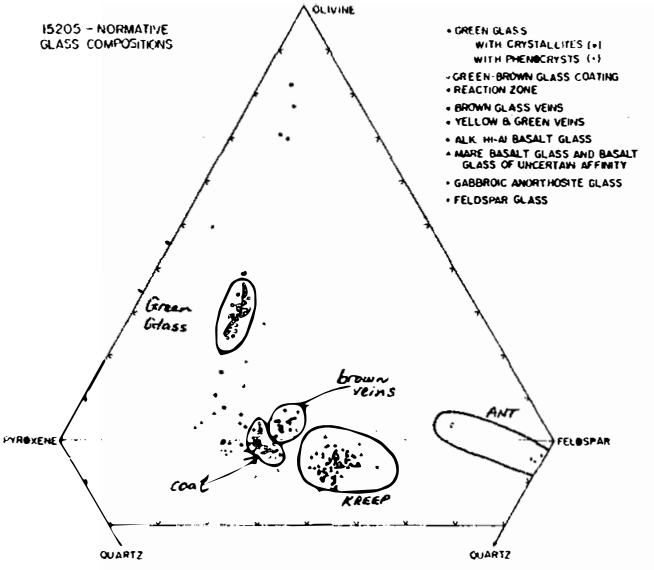

Figure 7. Compositions of glasses in 15205 on catatom ol-px-feldspar-qz diagram (Dymek et al., 1974).

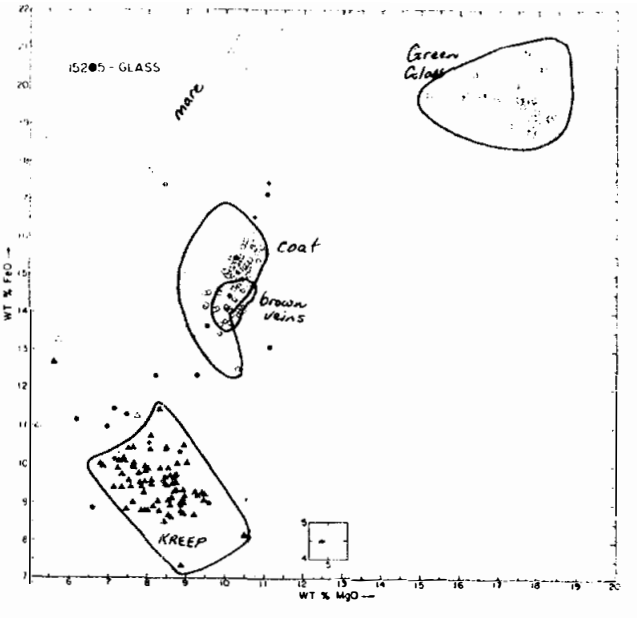

Figure 8. Compositions of glasses in 15205 on FeO vs. MgO diagram; symbols as in Figure 7. (Dymek et al., 1974).

TABLE 15205-1. Part of glass data of Dymek et al. (1974) (see original for minor element data and ranges.

	1	2	3	4	5	6	7	8
SiO2	48.4	47.3	47.5	51.4	45.6	50.5	44.6	47.7
TiO2	1.82	1.60	1.49	1.94	0.43	1.77	0.23	1.67
Al2O3	12.6	14.2	10.9	15.9	7.4	16.3	27.4	9.4
FeO	15.1	14.1	17.0	10.4	19.6	9.6	4.5	20.1
MgO	10.3	10.3	10.9	7.7	17.5	8.3	4.8	9.8
CaO	9.9	10.8	10.1	10.2	8.3	10.5	16.6	10.4
Na2O	0.54	0.50	0.47	0.88	0.15	0.77	0.24	0.36
K2O	0.25	0.22	0.13	0.52	0.02	0.61	0.03	0.07
P2O5	0.25	0.24	0.15	0.56	0.03	0.52	0.05	0.06
Cr ppm	3000	2600	3100	900	3800	1800	750	3800
Mn ppm	1600	1400	1800	700	2100	1100	1600	1200

References for Table 15205-2

References and methods:

(1) Keith et al. (1972); gamma ray spectroscopy
(2) Rancitelli et al. (1972); gamma ray spectroscopy
(3) Willis et al. (1972); XRF
(4) Korotev (1984 unpublished); INAA
(5) Allen et al. (1973); leach and RNAA
(6) Baedecker et al. (1973); RNAA
(7) Reed and Jovanovic (1972); NAA
(8) Moore et al. (1973); combustion, gas chromatography

TABLE 15205-2. Bulk rock chemical analyses

		,0(a)	,0	,37	,114	,35	,38	,35	,32
Wt %	SiO2			51.03					
	TiO2			1.99					
	Al2O3			14.92					
	FeO			11.28	13.3				
	MgO			8.23					
	CaO			9.94	8.9				
	Na2O			0.73	0.66				
	K2O	0.528	0.562	0.528					
	P2O5			0.557					
(ppm)	Sc				28.5				
	V								
	Cr			2330	2770				
	Mn			1232					
	Co				30.2				
	Ni				59		28		
	Rb			14.4					
	Sr			171	150				
	Y			201					
	Zr			979	710				
	Nb			59.4					
	Hf				18.5				
	Ba			673	500				
	Th	12.0	12.6		8.0				
	U	2.9	3.28		2.2			3.2	
	Pb								
	La				49.6				
	Ce				131				
	Pr								
	Nd				76				
	Sm				22.8				
	Eu				2.02				
	Gd								
	Tb				4.54				
	Dy								
	Ho								
	Er								
	Tm								
	Yb				15.5				
	Lu				2.16				
	Li							22	
	Be								
	B								
	C								22
	N								
	S			800					
	F								
	Cl							67.6	
	Br							0.41	
	Cu								
	Zn					6.4	4.5		
(ppb)	I							1.1(b)	
	At								
	Ga						5000		
	Ge						84		
	As								
	Se								
	Mo								
	Tc								
	Ru								
	Rh								
	Pd								
	Ag								
	Cd						16		
	In						2.6		
	Sn								
	Sb								
	Te								
	Cs				480				
	Ta				2150				
	W								
	Re								
	Os								
	Ir				<3		0.14		
	Pt								
	Au				<4		0.41		
	Hg								
	Tl								
	Bi					1.91			
		(1)	(2)	(3)	(4)	(5)	(6)	(7)	(8)

distinct from other glass types and their average is similar to that of Apollo 15 KREEP basalts. Green-glass fragments are spheres or sphere fragments, occurring singly and in aggregates, and are the common Apollo 15 volcanic glass (Table 1) and include devitrified varieties. A few contain vesicles; a few contain euhedral phenocrysts (Fo_{79-82}) similar to the experimentally determined liquidus composition. The chemical variation of clear green glasses is outside of analytical error and consistent with removal of about 5% liquidus olivine. Glass in partly crystallized spheres including that with olivine phenocrysts is more evolved, suggesting that the phenocrysts do not reflect processes occurring during ascent and eruption. The green glass aggregates occur as clasts (clods) up to 1 cm long; the matrix of the clods is also green glass. The green glass clods also contain a few fragments of plagioclase, pyroxene, and pyroxene-phyric basalt. Glass with mare basalt compositions occurs as bright yellow to orange fragments (and as melts at the edge of mare basalt clasts) but are rare. A single angular white fragment with the composition of gabbroic anorthosite was identified, and rare plagioclase glass (An_{81-88}) is present.

Both glass and lithic fragments suggest that a typical highland region was not an important contributor to the 15205 "soil". Dymek et al. (1974) concluded that feldspathic basalt (KREEP) fragments and glass equivalents together compose about 30% of sample 15205; in light of other observations and the bulk rock chemistry it is likely that the percentage is considerably higher.

Wilshire and Moore (1974) briefly discussed the planar glass on 15205. The glass veneers orthogonal fracture surfaces, are quite thin, and have thin spokes projecting out of the rock surface. The spikes suggest that the boulder was separated from a larger rock mass, which was cut by the orthogonal fractures, while the glass was still molten.

CHEMISTRY: Analyses of bulk material of 15205 are listed in Table 2. The rare earths are plotted in Figure 9. Most analyses seem to be of nearly pure Apollo 15 KREEP basalt; that of Korotev (1984 unpublished) contains more mare component. The coarse size of the clasts and heterogeneous nature of the population distribution suggest that considerable sampling problems could arise for bulk rock analyses, especially for small splits. The consistent gamma ray data, which are for the total rock and also similar to those for 15206, suggest the A15 KREEP basalt is the dominant chemical component, consistent with most other analyses. Korotev's (1984 unpublished) data was determined on a small (less than 1/2 g) chip compared with that of Willis et al. (1972) (nearly 2 g). Willis et al. (1972) noted the high incompatible element abundances and the high SiO_2 content. The rare earth pattern is that of KREEP, and Reed and Jovanovic (1972) noted that halogens and other elements were strikingly similar to those in Apollo 14 soils. Schonfeld (1975) used a mixing model to infer 84 ± 2% of Apollo 15 KREEP basalt in 15205. Baedecker et

15205

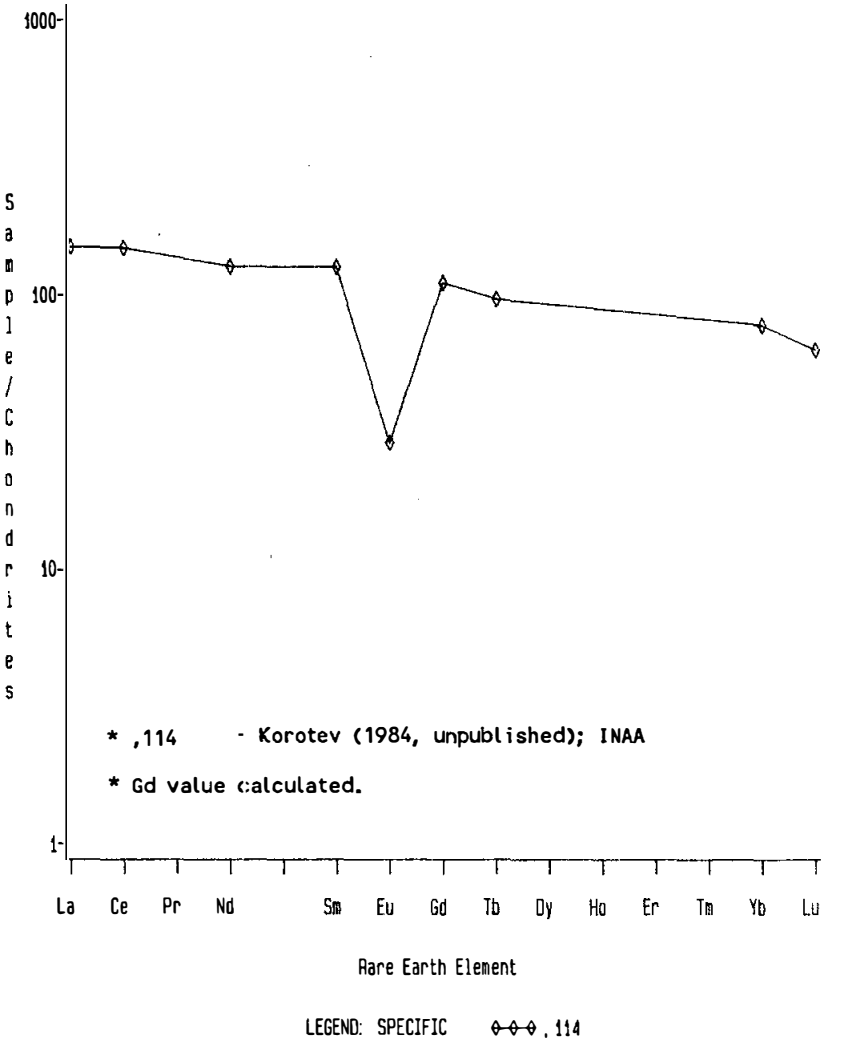

Figure 9. Rare earths in 15205 bulk rock (Korotev, 1984 unpublished).

al. (1973) used their data to infer a very low upper limit for siderophiles in A15 KREEP basalts, similar to mare basalts; they appear to be unaware of the mare basalts in 15205 in considering an origin for the rock as Imbrium ejeta.

Anderson and Hinthorne (1973) used an ion microprobe to determine the concentrations of Ba and rare earths in Y-Zr phosphate, whitlockite, and zircon, presumably derived from KREEP basalt clasts. These minerals have pronounced negative Eu anomalies and flat trivalent rare earth patterns.

STABLE ISOTOPES: Epstein and Taylor (1972) determined δO^{18} values of 5.92 parts per mil and 6.07 parts per mil for gray matrix and black glass samples respectively. These are typical lunar values.

RADIOGENIC ISOTOPES AND GEOCHRONOLOGY: Anderson and Hinthorne (1973) used an ion microprobe to determine Pb isotopic ratios and Th/U ratios in zircon in 15205, determining an age of 4.01 ± 0.11 b.y. for the zircon. They did not specifically discuss the data.

RARE GASES, COSMOGENIC NUCLIDES, TRACKS, CRATERING, AND EXPOSURE: Drozd et al. (1976) made noble gas analyses of whole rock samples, primarily in pursuit of information on the excess xenon present in some lunar samples. They tabulated Kr and Xe isotopic data and tabulated summarized results. The excess xenon factor of 1.5 ± 0.2 is of low magnitude, easily understood in terms of in situ U and Pu decay. They determined an ^{81}Kr exposure age of 169 ± 7 m.y., which is rigorously an upper limit to the present configuration of the boulder. The high $^{131}Xe/^{126}Xe$ and the long exposure suggest a complex, multistage exposure history, as also suggested by the much shorter track and microcratering ages (below).

Schaeffer et al. (1976) used a laser probe to analyse He, Ne, and Ar on exposed surfaces, comparing the spall zones of 100-micron craters with intercrater surfaces. Ne is of solar origin, but the irregular ^{40}Ar and high $^{40}Ar/^{36}Ar$ (cf. solar) suggest a non-surface correlated origin for most ^{40}Ar. The two spall zones had 1/3 and 1/2 the "normal" content of all three gases, but one host had very low gases, possibly a result of a recent splash glass.

Keith et al. (1972) and Rancitelli et al. (1972) reported disintegration count data for cosmogenic radionuclides. They both found that ^{22}Na was at equilibrium but that ^{26}Al was at one-half or one-third of saturation values, indicating a less-than-1-m.y. exposure. The low ^{26}Al is not an artifact of composition (as confirmed by data for soil beneath the boulder and by the Yokoyama et al., 1974, analysis of the data). These cosmogenic nuclide data are similar to those for 15206. Fruchter et al. (1978) made new determinations and found ^{26}Al to be 50% saturated and ^{53}Mn to be 58% saturated, corresponding with

exposure of 0.7 ± 0.1 m.y.and 4.5 ± 0.5 m.y. respectively. These ages are not consistent with each other nor with the Drozd et al. (1976) rare gas age, leading to the conclusion that 15205 was shielded at a depth of approximately 1 m for time period long with respect to the half-life of ^{53}Mn. An exposure history consistent with ^{26}Al age of 0.7 m.y., ^{53}Mn age of 4.5 m.y., and ^{81}Kr age of 169 m.y. requires the boulder to have been buried just below the surface for 200 m.y., then ejected by a small event to its present position where it has remained for less than 100,000 years, consistent with the solar flare track and micro-crater ages (below). Bhandari (1977) also produced ^{26}Al data for different depths (0-0.140 g/cm^2 and 1.5-1.64 g/cm^2) for an exterior surface. He deduced an exposure age of less than or equal to 0.1 m.y., similar to other studies, from the unsaturated ^{26}Al.

Schneider et al. (1973) derived a solar flare track age of about 3 x 10^4 years, which was revised following new calibrations to 7.9 x 10^4 years (Fechtig et al., 1974). These studies outline the depth dependance of solar flare tracks in the glass studied.

Schneider et al. (1973) reported cumulative crater number densities for a statistically significant number of craters (Fig. 10). The specimens were from the top corner of the boulder, and counting was done at several magnifications. The population is in production. The distribution is bimodal. These results have been discussed by Brownlee et al. (1973), Fechtig et al. (1974), and Horz et al. (1975, 1977) because of their implications for the micrometeoroid flux. Brownlee et al. (1973) noted that the bimodal distribution suggested two different source areas for micrometeoroid mass regimes. Hartung and Storzer (1974) continued the work with a study of the microcrater density and solar flare particle track exposure age measurements for the population, using iron-group solar flare tracks to yield exposure ages for host surface and 56 microcraters. (Figs. 11, 12). They found individual microcrater exposure ages indicating an increasing microcrater production rate (flux) over the last 10,000 years (they suggested Comet Encke as the reason). This rate is higher than the present day production rate estimated from satellite and Apollo window data (Fig. 12), and Hartung and Storzer (1974) suspected that a systematic error existed in the analysis of solar flare particle tracks. However, this systematic error would not change the pattern of increasing micrometeoroid flux towards the present. According to Horz et al. (1975), the data for the last 3000 years are in good agreement with the present day flux. Zook et al. (1976) suggested that the Hartung and Storzer result should be inverted: probably solar activity fluctuates more.

PHYSICAL PROPERTIES: Adams and McCord (1972) measured the diffuse reflectance spectra (0.35 - 2.5 microns), and from the pyroxene bands deduced that 15205 had one of the least calcic pyroxenes among Apollo 15 rocks, which is in accordance with petrographic observations. Charette and Adams (1977) obtained

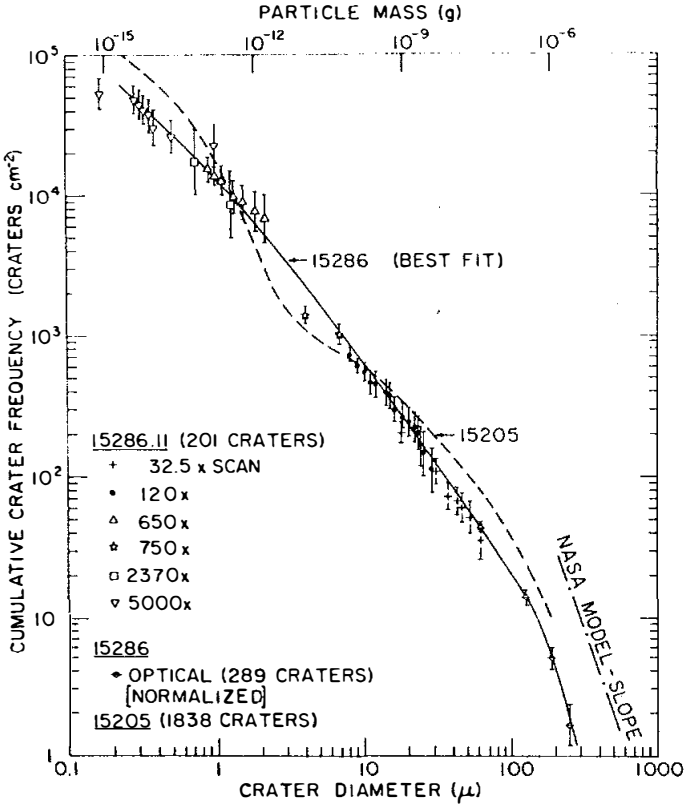

Figure 10. Size frequency data for microcraters on 15205 and for 15286. (15205 data from Schneider et al., 1973; diagram from Brownlee et al., 1973).

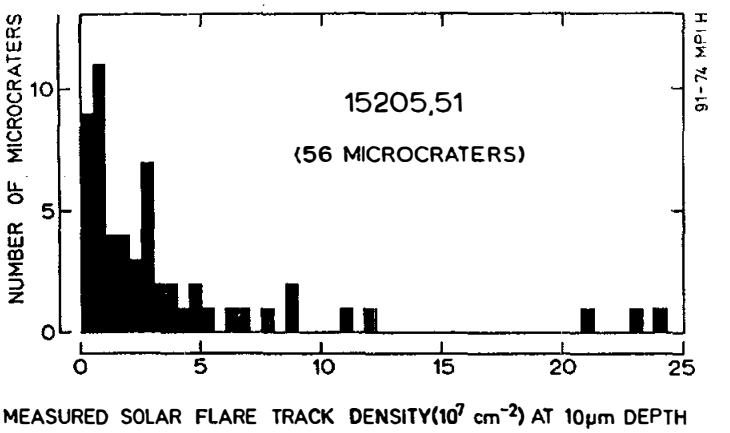

Figure 11. Distribution of microcraters according to measured solar flare track density at a depth of about 10 microns below the surface of a microcrater pit (Hartung and Storzer, 1974).

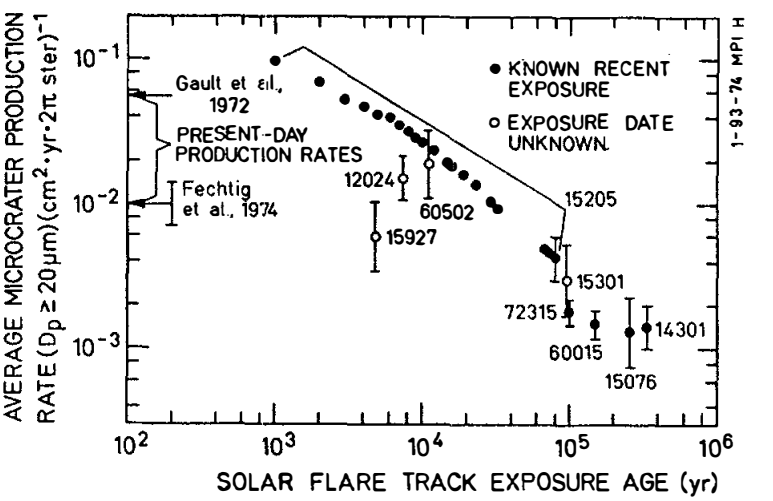

Figure 12. Exposure age data for individual microcraters on 15205 indicating a decreasing average microcrater production rate with time in the past (Hartung and Storzer, 1974).

similar spectra and distinguished the sample (although KREEP) from poikilitic (= low-K Fra Mauro, Apollo 16, 17) rocks on spectral characteristics.

PROCESSING AND SUBDIVISIONS: A small chip (,2) was knocked off (location uncertain) and was used to make thin sections ,3 through ,7. Subsequently the rock was sawn parallel to two faces and the slabs (which have exterior glass) further dissected (Fig. 13). Most allocations have been made from these subdivisions. In 1977 ,0 was further subdivided to produce a few small pieces (,96 - ,102, total less than 15 g) (e.g., Fig. 1c) so that interior pieces could be obtained. One chip was partly used to make thin section ,122. A small chip of glass coat was also removed to make thin section ,110. ,0 is now 139.8 g; no other pieces larger than 25 g exist.

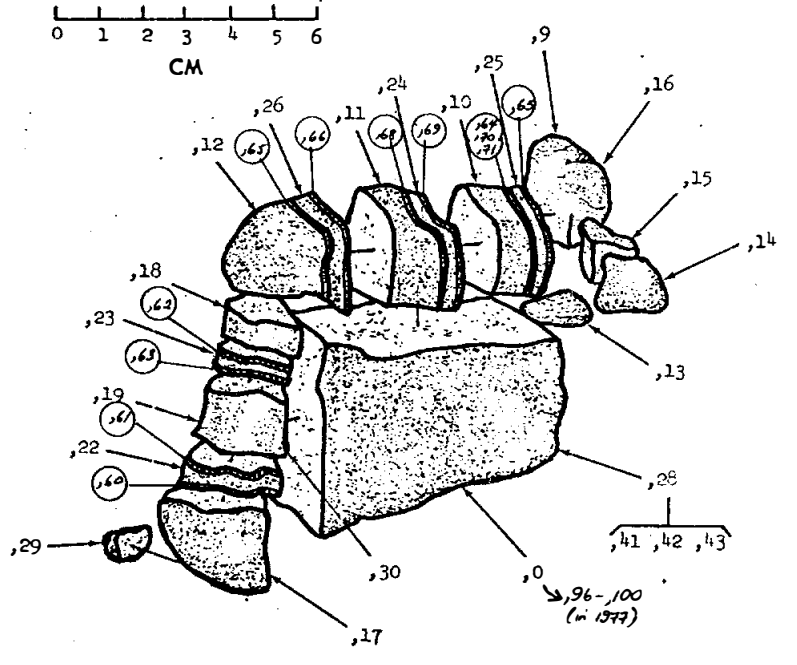

Figure 13. Sawing of 15205 into slablets, 1972. Circled numbers show locations of thin sections cut from these slablets. Other thin sections were also cut.

15206 MELTED REGOLITH BRECCIA ST. 2 92.0 g

INTRODUCTION: 15206 is a vesicular glassy breccia (Fig. 1) containing KREEP basalt clasts and some mare basalt (at least pyroxene-phyric) clasts. The clasts are shocked and penetrated by glass. 15206 is medium gray, blocky, and angular. It has extreme variations in vesicularity and banding, with clasts locally concentrated. It is tough; zap pits occur on only one surface. 15206 was chipped from the same boulder as 15205 (Fig. 15205-2), and appears to be a shock-melted version of that sample. Its collection was documented.

PETROLOGY: 15206 is very dark and vesicular with a glassy matrix, and is rather agglutinitic in appearance (Fig. 2). It contains abundant clasts of Apollo 15 KREEP basalts with rare pyroxene-phyric mare basalts. All the clasts are shocked and some are melted, and are penetrated by dark brown glass fissures. Dymek et al. (1974) noted that it was similar to 15205 except that it had been affected by later impact events with in situ vesiculation and melting. Wilshire and Moore (1974) noted that it differs from 15205 in its extensive fusion; there is no distinguishable contact between glass selvage and partly fused interior of the rock as is so clearly evident on 15205. The selvage is defined by an increase in the size and abundance of cavities towards the original surface of the boulder. The cavity distribution also indicates that the boulder was isolated from any surrounding rock before the glass had congealed.

CHEMISTRY: The limited chemical data (Table 1) show that 15206 is very similar to 15205 for those elements measured, and thus probably consists predominantly of Apollo 15 KREEP basalts.

COSMOGENIC RADIONUCLIDES AND EXPOSURE: Keith et al. (1972) and Rancitelli et al. (1972) provided disintegration count data for cosmogenic radionuclides. The data is similar to that for 15205, indicating that ^{26}Al is unsaturated and ^{22}Na is saturated, and that the boulder moved to its present location less than 1 m.y. ago. The ^{26}Al non-saturation was confirmed by the analysis of the data by Yokoyama et al. (1974).

PROCESSING AND SUBDIVISIONS: ,1 was chipped off the "W" top corner and largely used up in making thin sections ,3 through ,8. Subsequently the sample was sawn (Figs. 1, 3) to produce a series of slablets. Potted butts ,14 and ,15 were made from part of ,11 and partly used to make thin sections ,29 through ,34. All allocations were made from these pieces. ,0 is now 55.89 g.

Fig. 2a

Fig. 2b

Figure 2. Photomicrographs of 15206. Transmitted light. Widths about 1.25 mm. a) 15206,5. Vesicular glassy breccia with KREEP basalt clasts; b) 15206,33. Vesicular but less glassy portion than 15206,5, more like relict 15205, but still substantially molten.

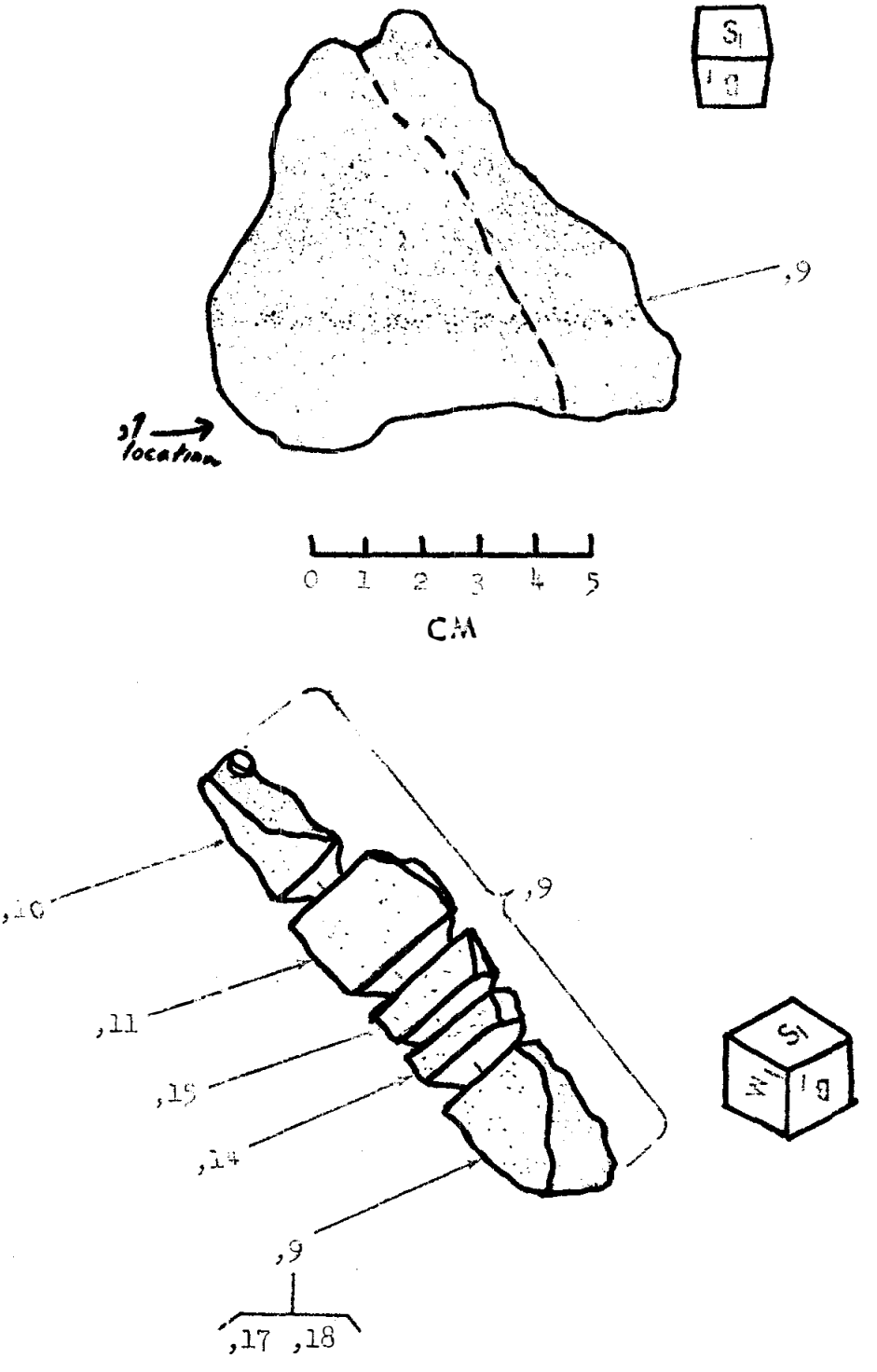

Figure 3. Sawing of 15206.

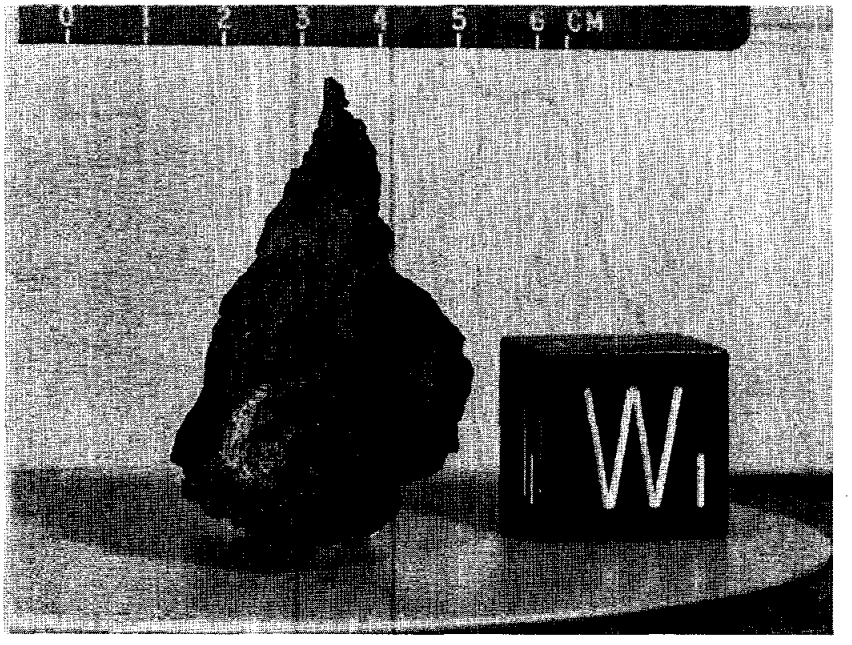

Fig. 1b

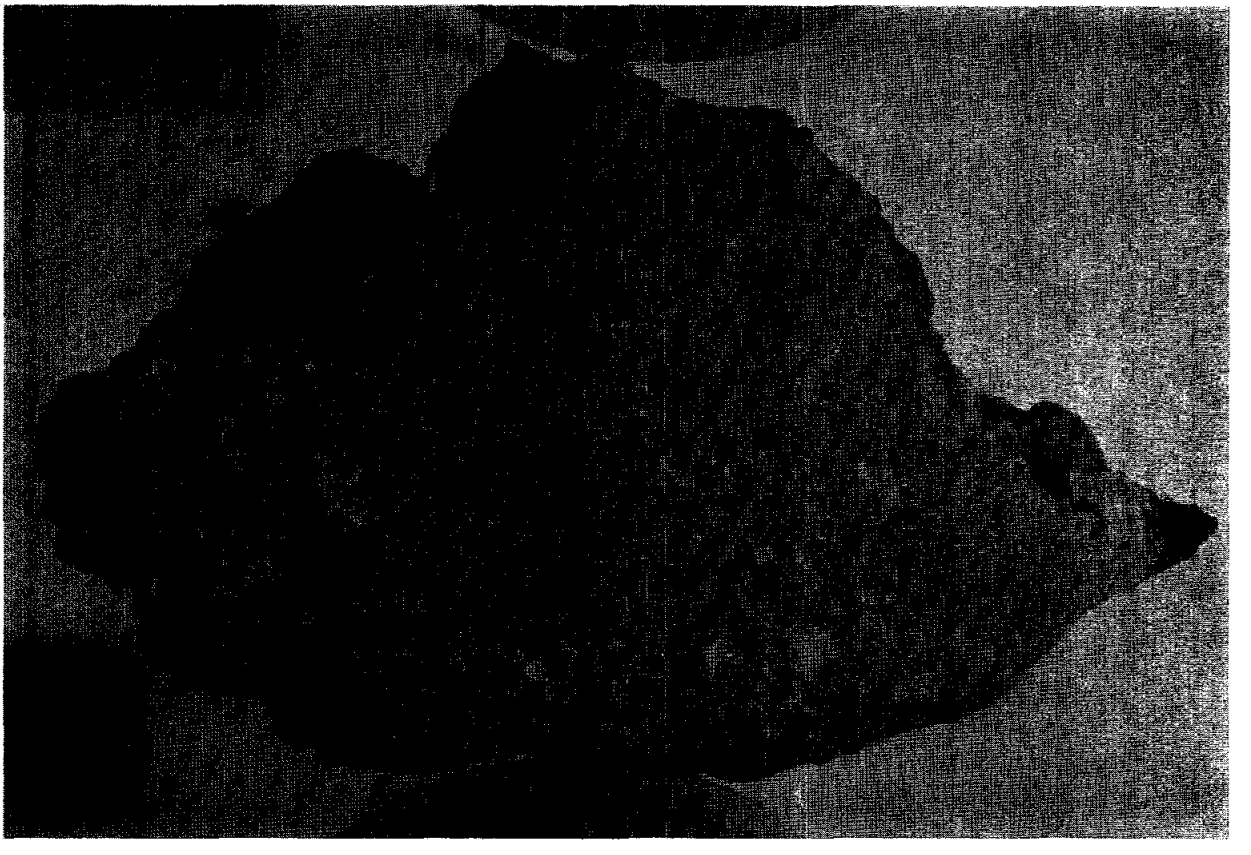

Figure 1. a) Pre-saw view of 15206. Broken face to left, lunar exposed to right. S-71-46057;b) sawn face of 15206,0. Broken face to bottom, lunar exposed to top. S-74-33198

TABLE 15206-1. Chemical analyses

		,0	,0	,17
Wt %	SiO2			
	TiO2			
	Al2O3			
	FeO			
	MgO			
	CaO			
	Na2O			
	K2O	0.584	0.598	
	P2O5			
(ppm)	Sc			
	V			
	Cr			
	Mn			
	Co			
	Ni			
	Rb			
	Sr			
	Y			
	Zr			
	Nb			
	Hf			
	Ba			
	Th	12.0	12.4	
	U	3.2	3.22	4.9
	Pb			
	La			
	Ce			
	Pr			
	Nd			
	Sm			
	Eu			
	Gd			
	Tb			
	Dy			
	Ho			
	Er			
	Tm			
	Yb			
	Lu			
	Li			21
	Be			
	B			
	C			
	N			
	S			
	F			
	Cl			66
	Br			0.51
	Cu			
	Zn			
(ppb)	I			2.3(a)
	At			
	Ga			
	Ge			
	As			
	Se			
	Mo			
	Tc			
	Ru			
	Rh			
	Pd			
	Ag			
	Cd			
	In			
	Sn			
	Sb			
	Te			
	Cs			
	Ta			
	W			
	Re			
	Os			
	Ir			
	Pt			
	Au			
	Hg			
	Tl			
	Bi			
		(1)	(2)	(3)

References and methods:

(1) Keith et al. (1972); gamma ray spectroscopy
(2) Rancitelli et al. (1972); gamma ray spectroscopy
(3) Reed and Jovanovic (1972);

Notes:

(a) detected in leach only

15245 FRAGMENTS OF REGOLITH BRECCIA AND GLASS ST. 6 115.5 g

INTRODUCTION: 15245 consists of 89 pieces ranging from smooth breccia pieces to glass-coated and cemented breccias, to agglutinates. The pieces were arranged in order of increasing degree of porosity, irregularity of surface, and amount of glass, and were individually numbered (,1 to ,89) accordingly (see Fig. 1 and 2 for examples). The breccias are all friable regolith breccias containing glass as spherules, shards, and lapilli, and those analyzed have compositions similar to the local regolith. Some of the vesicular glasses have a few zap pits. The samples constituting 15245 were scooped from the floor of a 1 m crater (with regolith 15240), approximately 20 m south and upslope from the LRV at Station 6, which was described as a "fresh little crater."

PETROLOGY: Few pieces have been inspected other than macroscopically. Thin sections ,107 and ,117, from piece ,24, are of brown glassy regolith breccia (Fig. 3), which is not very porous. The fragment contains glass as blebs, shards, and lapilli, and includes colorless, green, yellow, and orange/red varieties. The red glass is more abundant than is usual for regolith breccias and is almost all as tiny spheres. Lithic fragments are small, and include glassy breccias, feldspathic crystalline breccias, including melt and granulitic anorthosites, and some KREEP-basalt fragments. Mare basalt fragments are not obvious. McKay et al. (1984) listed I_s/FeO of 29 to 44 for ,118 (from ,18) and 29-45 for ,120 (from ,19) respectively; Korotev (1984, unpublished) listed these both with an I_s/FeO of 41. Both of the fragments are regolith breccias. These are submature indices, yet the thin sections contain almost no identifiable agglutinates. Nagle (1982a) listed 15245 as showing the characteristics expected of rocks produced by subcrater lithification and Nagle (1982b) gave grain size distributions and statistics, and also data on rounding, packing, and clast orientation, but no specific split number was listed.

Fabel et al. (1972) gave x-ray emission shift data for SiKβ , AlKβ and OKα for a brown-black spatter glass (,56). Microprobe analyses include heterogeneous zones indicating that mineral inclusions of plagioclase and pyroxene in the glass were analyzed.

CHEMISTRY: Chemical analyses of regolith breccia fragments are listed in Table 1. Rare earth elements are shown in Figure 4. The C and N analysis of Moore et al. (1973) and Moore and Lewis (1976) is on a glass-rich piece, but it is not known whether the analysis was of breccia, glass, or both. The analyses are all very similar to each other and to Station 6 soils, indicating that the breccias were made by shallow-level lithification of local soil (somehow destroying agglutinates). Most analyses in Table 1 were reported without discussion.

RARE GASES: Megrue (1972, 1973a,b) analyzed ,53, a "glassy

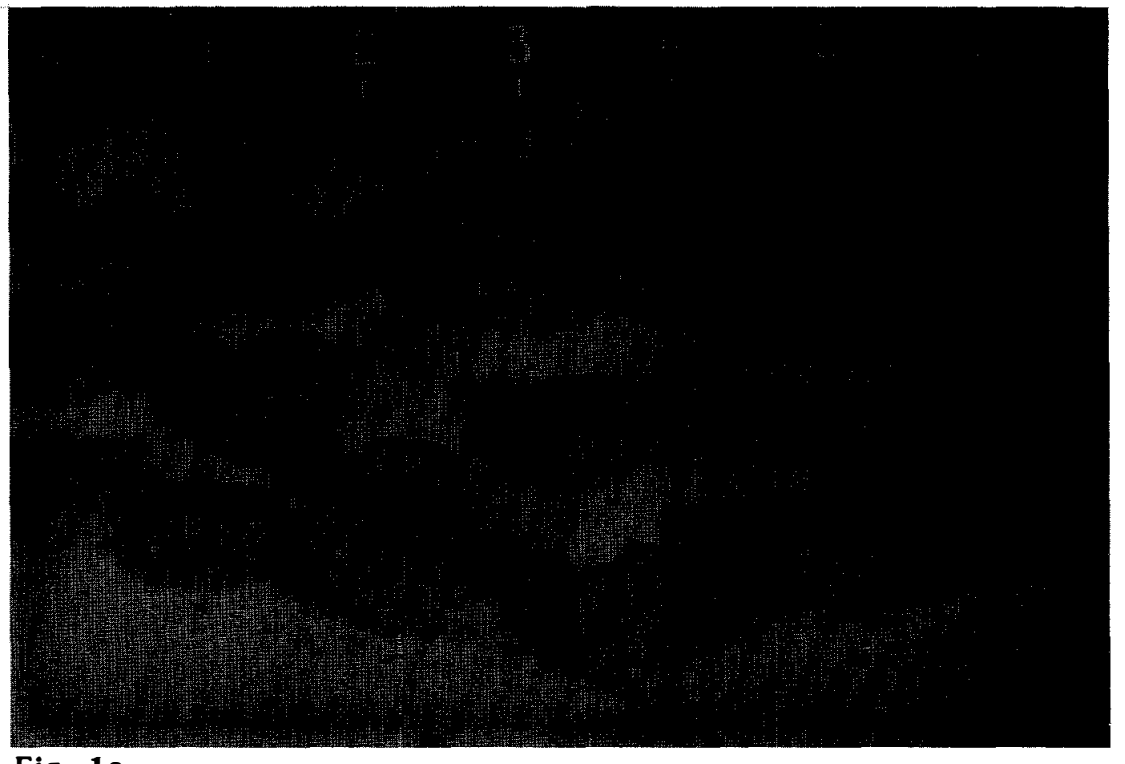

Fig. 1a

Figure 1. Example photographs of 15245 pieces a) regolith breccias ,1 to ,16. S-71-47912; b) glass-coated regolith breccias ,40 to ,47. S-71-47927; c) glassy agglutinates ,85 to ,89.

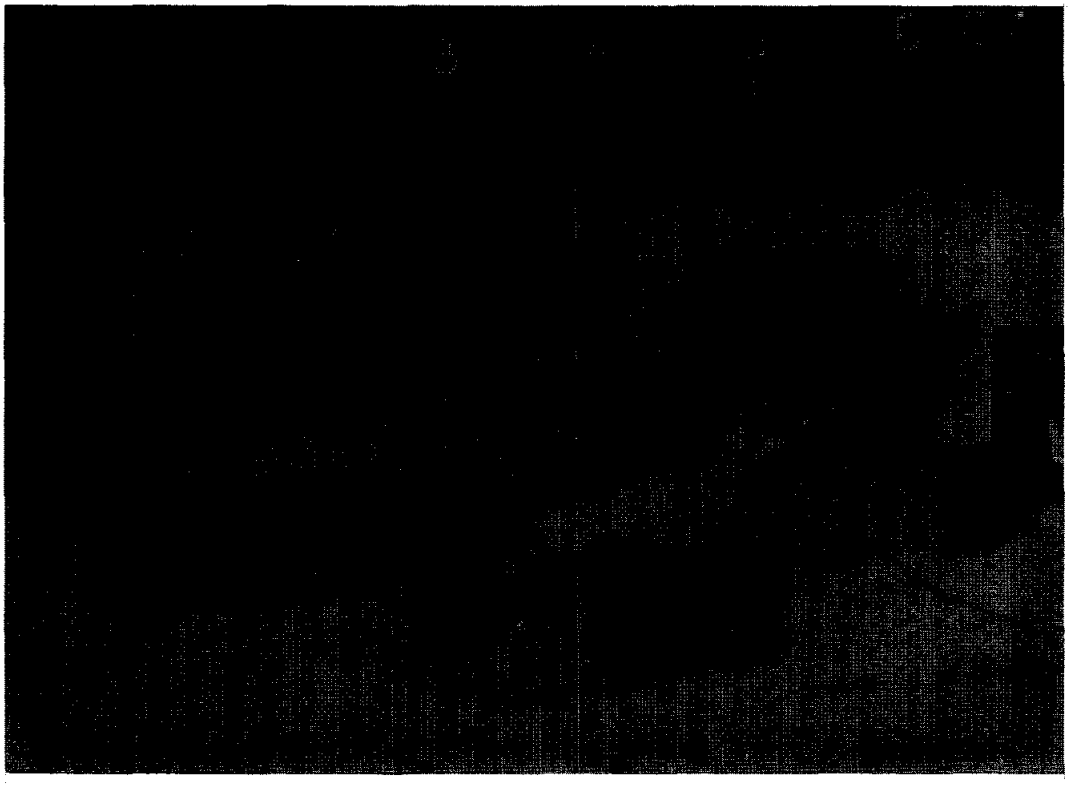

Fig. 1b

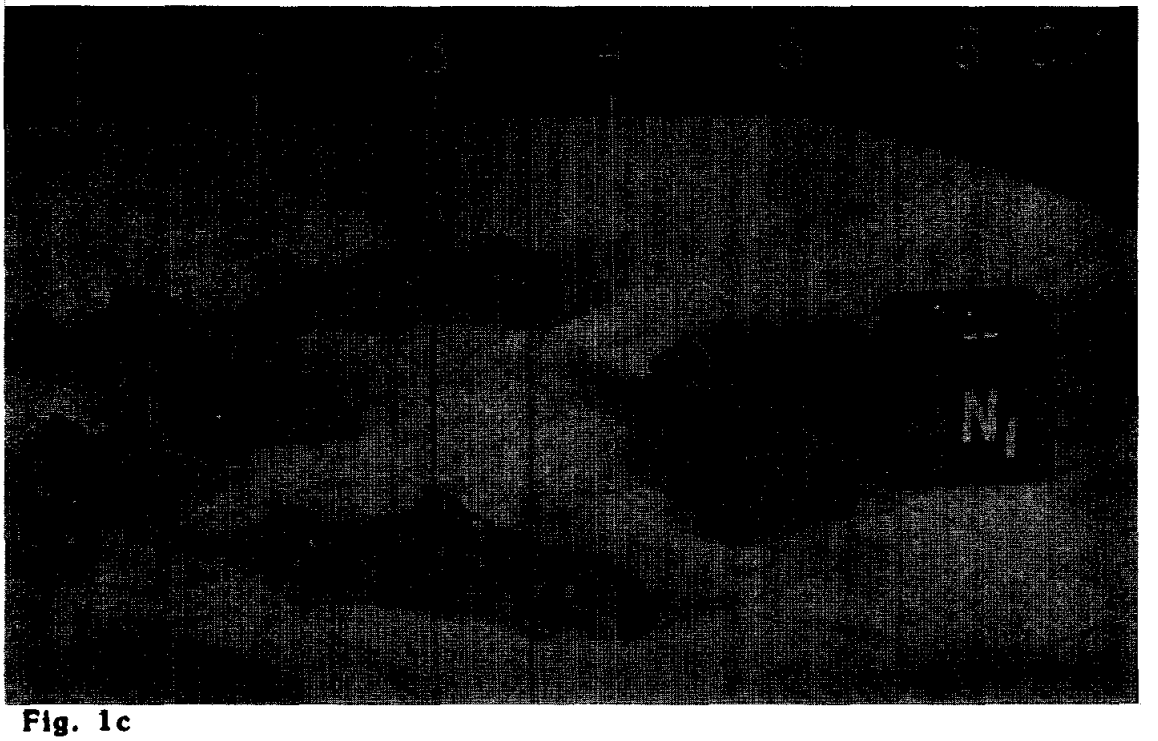

Fig. 1c

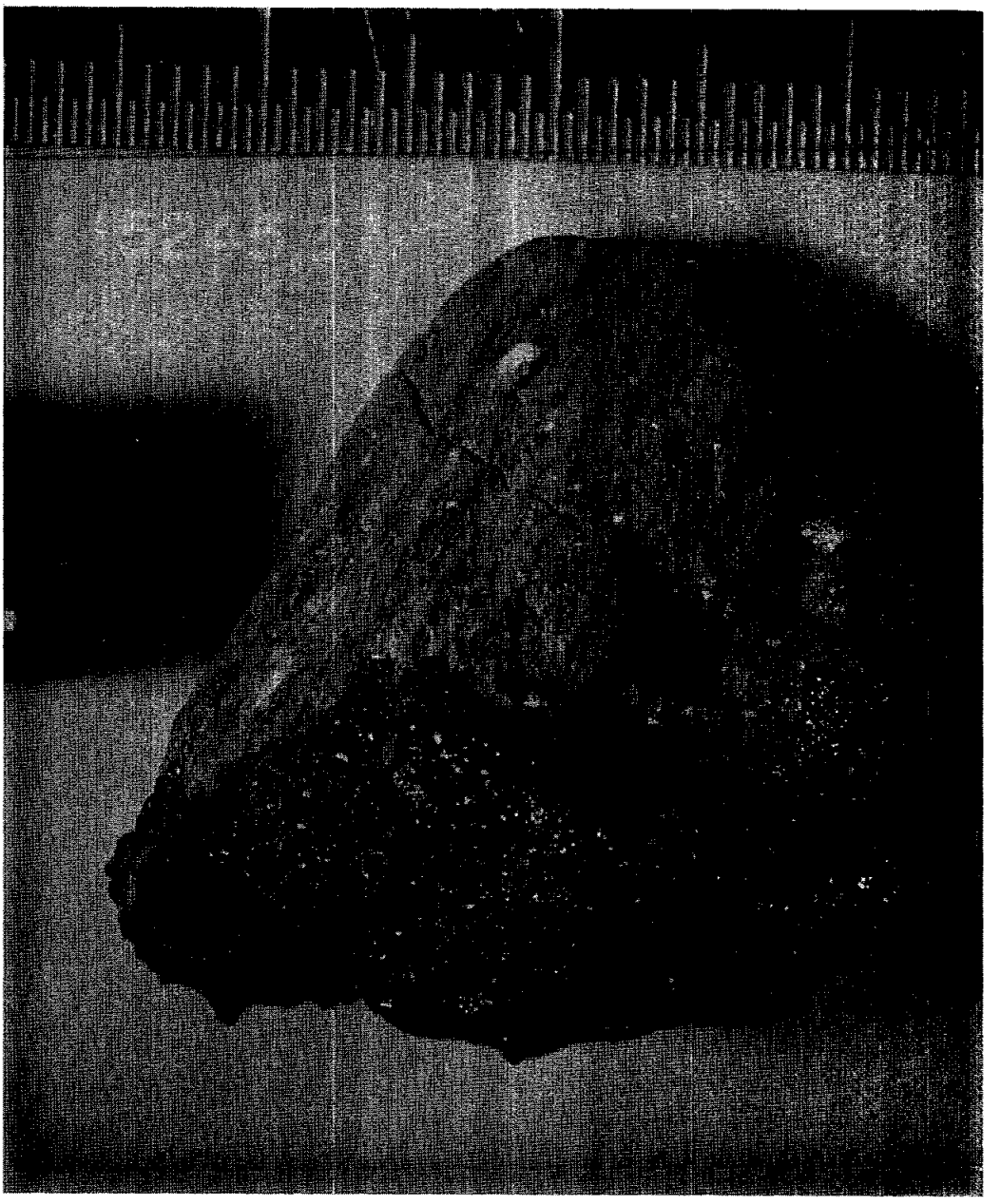

Figure 2. Glass-coated regolith breccia 15245,37. S-75-33758

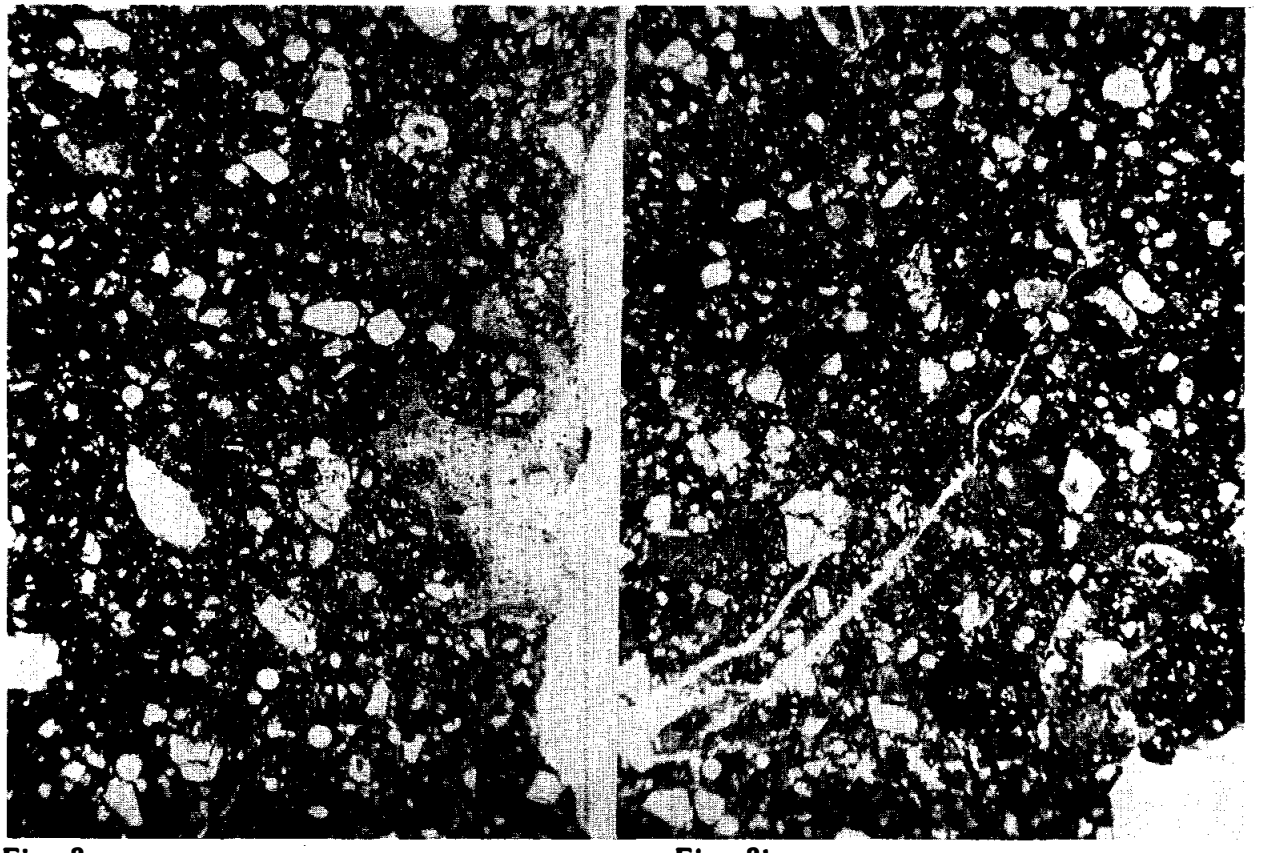

Fig. 3a Fig. 3b

Figure 3. Photomicrographs of 15245,107. Widths about 2 mm. Transmitted light.

TABLE 15245-1. Chemical analyses of 15245 fragments

		,17	,8	,18 (,118)	,19 (,120)	,60	,60
Wt %	SiO2		48.41				
	TiO2	1.24		1.45			
	Al2O3	15.78	17.37	16.3			
	FeO	12.0	11.87	11.8	11.9		
	MgO	10.0	10.84	10.6			
	CaO	9.8	10.78	10.2	11.4		
	Na2O	0.46	0.474	0.47	0.49		
	K2O		0.205				
	P2O5						
(ppm)	Sc	21.9	23.5	22.8	22.6		
	V	76	83.9	69			
	Cr	3295	2210	2160	2180		
	Mn	1690	1230	1240			
	Co	38.8	35.9	38.5	37.1		
	Ni	180	215	229	192		
	Rb	6.3					
	Sr	115	160	145	130		
	Y						
	Zr		368	350	410		
	Nb						
	Hf	10.5	8.92	9.7	10.2		
	Ba	210	290	257	277		
	Th	3.98	4.6	4.3	4.6		
	U	1.02		1.13	1.10		
	Pb						
	La	25	26.3	25.7	27.5		
	Ce		71.2	68	73		
	Pr						
	Nd		45.6	38	40		
	Sm	12.1	11.1	12.0	13.1		
	Eu	1.80	1.42	1.44	1.49		
	Gd						
	Tb	2.71	2.57	2.36	2.58		
	Dy	10.0	15.5				
	Ho		3.7				
	Er						
	Tm						
	Yb	10.7	8.62	8.4	8.9		
	Lu		1.16	1.16	1.25		
	Li						
	Be						
	B						
	C					132	130(a)
	N						78
	S						
	F						
	Cl						
	Br						
	Cu						
	Zn						
(ppb)	I						
	At						
	Ga						
	Ge						
	As						
	Se						
	Mo						
	Tc						
	Ru						
	Rh						
	Pd						
	Ag						
	Cd						
	In						
	Sn						
	Sb						
	Te						
	Cs	490	280	290	290		
	Ta	1250	1080	1170	1250		
	W						
	Re						
	Os						
	Ir		8	8.7	6.7		
	Pt						
	Au			3.1	2.0		
	Hg						
	Tl						
	Bi						
		(1)	(2)	(3)	(3)	(4)	(5)

References to Table 15245-1

References and methods:

(1) Brunfelt et al. (1972); INAA
(2) Wanke et al. (1976, 1977); XRF, INAA, RNAA
(3) Korotev (1984, unpublished); INAA
(4) Moore et al. (1973); pyrolysis, gas chromatography
(5) Moore and Lewis (1976); Pyrolysis, gas chromatography

Notes:

(a) Seems to be a repeated report of the Moore et al. (1973) data.

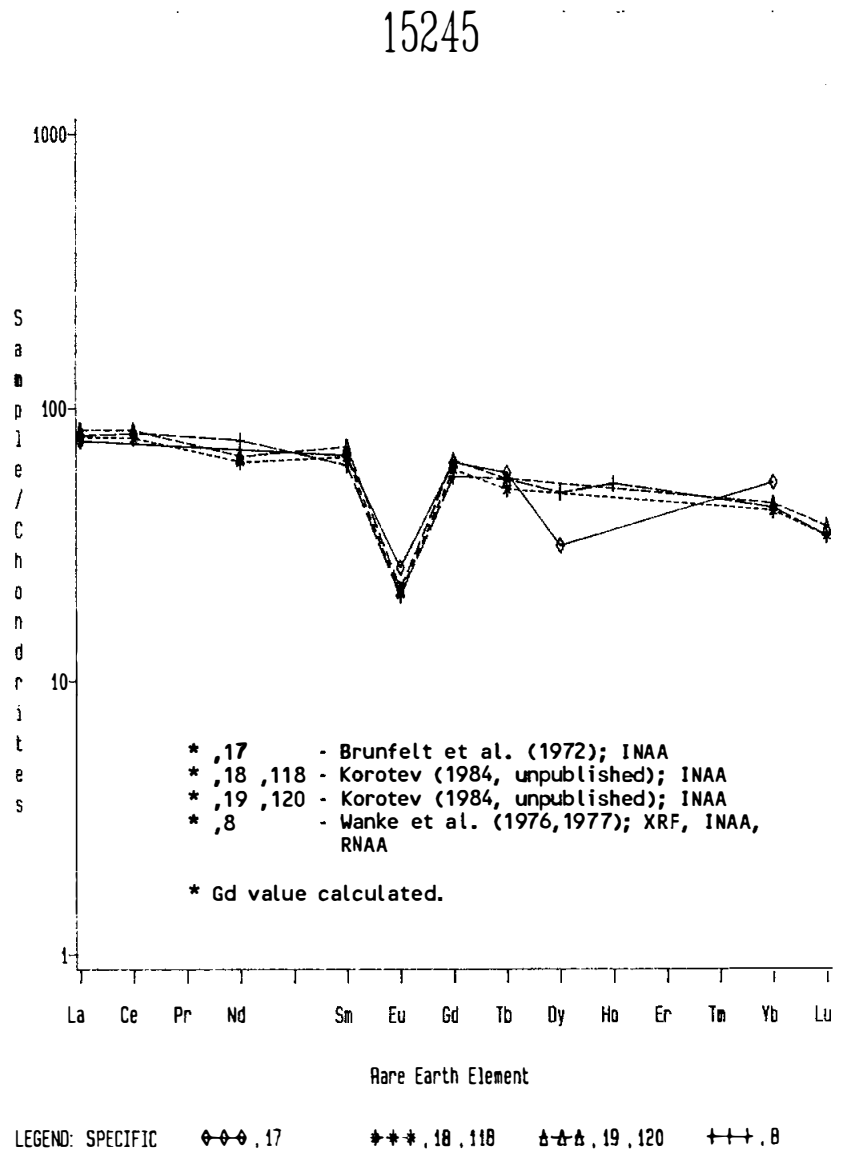

Figure 4. Rare earths in 15245 regolith breccias.

agglutinate", to determine the gradient of He, Ne, and Ar in the sample. The gases were identified as of solar wind origin, and fractionated by the thermal event which produced the glass. The average $^{4}He/^{20}Ne$ is 23; $^{4}He/^{36}Ar$ = 71, and the corresponding fines are 23 and 50% greater. The gases were found below the normal penetration depth of a few microns, suggesting that the glass formed from previously irradiated lunar soil. Other ratios found within the glass and the breccia fines are: $^{4}He/^{3}He$ = 2500 ± 100; $^{20}Ne/^{22}Ne$ = 12.5 ± 0.2; $^{21}Ne/^{22}Ne$ = 0.038 ± 0.002; $^{36}Ar/^{38}Ar$ = 5.2 ± 0.01. A lithic fragment showed no solar gas, but contained cosmogenic and radiogenic argon. Megrue (1973b) suggested that the soil was transported from Dune to St. 6, because of the similarity of fractionated solar gases, in the matrix of 15498,55 and in 15245,53. However, the silicate chemistry of these two samples is substantially different, a fact unknown to Megre (1973b).

PROCESSING AND SUBDIVISIONS: All subdivisions have been made by chipping, following general numbering of individual pieces according to macroscopic characteristics. Only ,8; ,17; ,18; ,37; ,38; ,53; ,56; ,57; ,59; and ,60 have been subdivided. ,37 and ,38 are stored at Brooks.

15255 REGOLITH BRECCIA, GLASS-COATED ST. 6 240.4 g

INTRODUCTION: 15255 is a tough, medium-light brownish gray regolith breccia which has a glass-coat (Fig. 1), mainly on one ("N") side. It contains a typically regolith assemblage of glass, minerals, and lithic fragments. The fragments are not heavily shocked. Some mare basalt is present, but KREEP basalts are not obvious. The breccia appears to be a little less KREEP-rich than local soils; the glass is distinctly different from local soil in having lower alumina and higher rare-earths.

15255 is subangular, rounded, and fairly homogeneous. The glass coating is finely fractured and has vesicles up to 15 mm in size. Although the original catalog (Lunar Sample Information Catalog Apollo 15, 1971) reported many zap pits, a later description by Horz (data packs) found only one, a secondary, even under binocular to 80x, in a 6 to 8 cm^2 area and none with the naked eye on the sample. This observation apparently refers only to the glass. 15255 was collected less than 1 m from 15256, 30 m west of the LRV and approximately 25 m southwest and upslope of the 12 m crater at Station 6. Its orientation is known and the glass coat was on the underside.

PETROLOGY: The breccia is non-porous, with a brown glassy matrix (Fig. 2). Glass shards and spheres include colorless, pale yellow, and some green glass. Red/orange glass appears to be absent. There are also schlieren of brown devitrified glass, and glassy breccias. Mare basalt fragments are definitely present, and include coarse pyroxene-poikilitic rocks, and others with a variety of textures. KREEP basalts are not evident. The lithic and mineral fragments are not strongly shocked. Nava et al. (1977) found that the breccia consisted of 45% undevitrified glass, with fragments of plagioclase, olivine, pyroxene, ilmenite, and minor cristobalite and chromian ulvospinel. The lithic fragments are small and most of the igneous areas ones are "norites". The mafic minerals have a wide compositional range, including pyroxferroite and fayalite (Fig. 3), and at least these Fe-rich minerals are probably mare-derived. Winzer (1978) tabulated area analyses (focussed beam, scans) for ten clasts, which have several sources including mare basalt, green glass, VHA-poik, and others; most have Al_2O_3 in the range 20-25 wt %.

The glass coat is banded, pale-green, and vesicular. The contact with the host breccia is sharp but in some places uneven. Nava et al. (1977) reported the presence of a fine-vesicular layer at the contact, such as might be produced from a hot melt splash on a cooler breccia, with local degassing. The chemistry and texture indicates that the glass is not a melt of the rock. It includes tiny metal spherules. Winzer et al. (1978) found that 15255 had the most fragment-free glass coat of several they studied; the glass exhibited flowage.

Nava et al. (1977) analyzed glasses in 15255, including the rind glass (Fig. 4). There is a variety of glass compositions. The

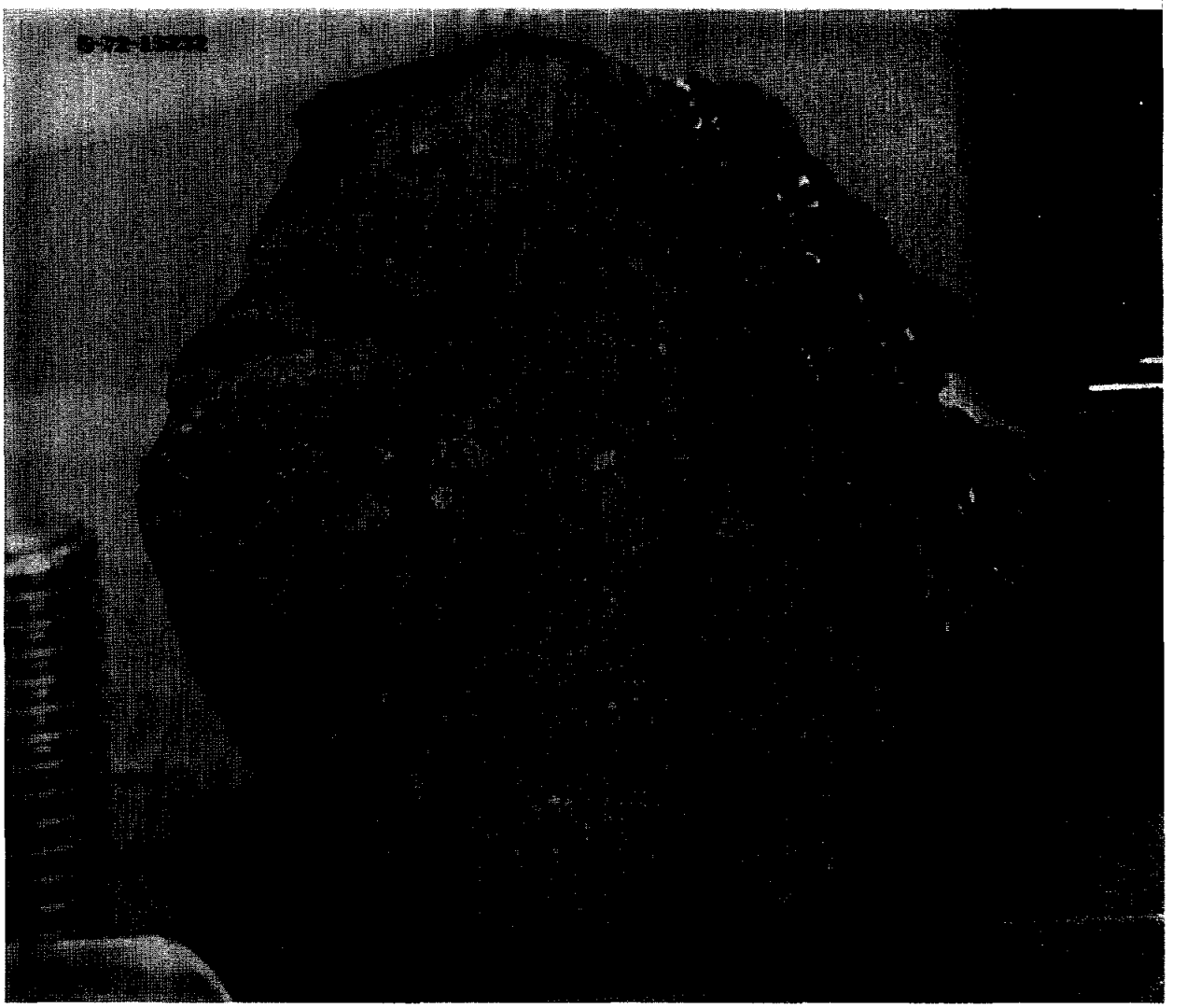

Figure 1. Post-saw view of ,0, showing interior of breccia, and vesicular glass coat on "N" side.

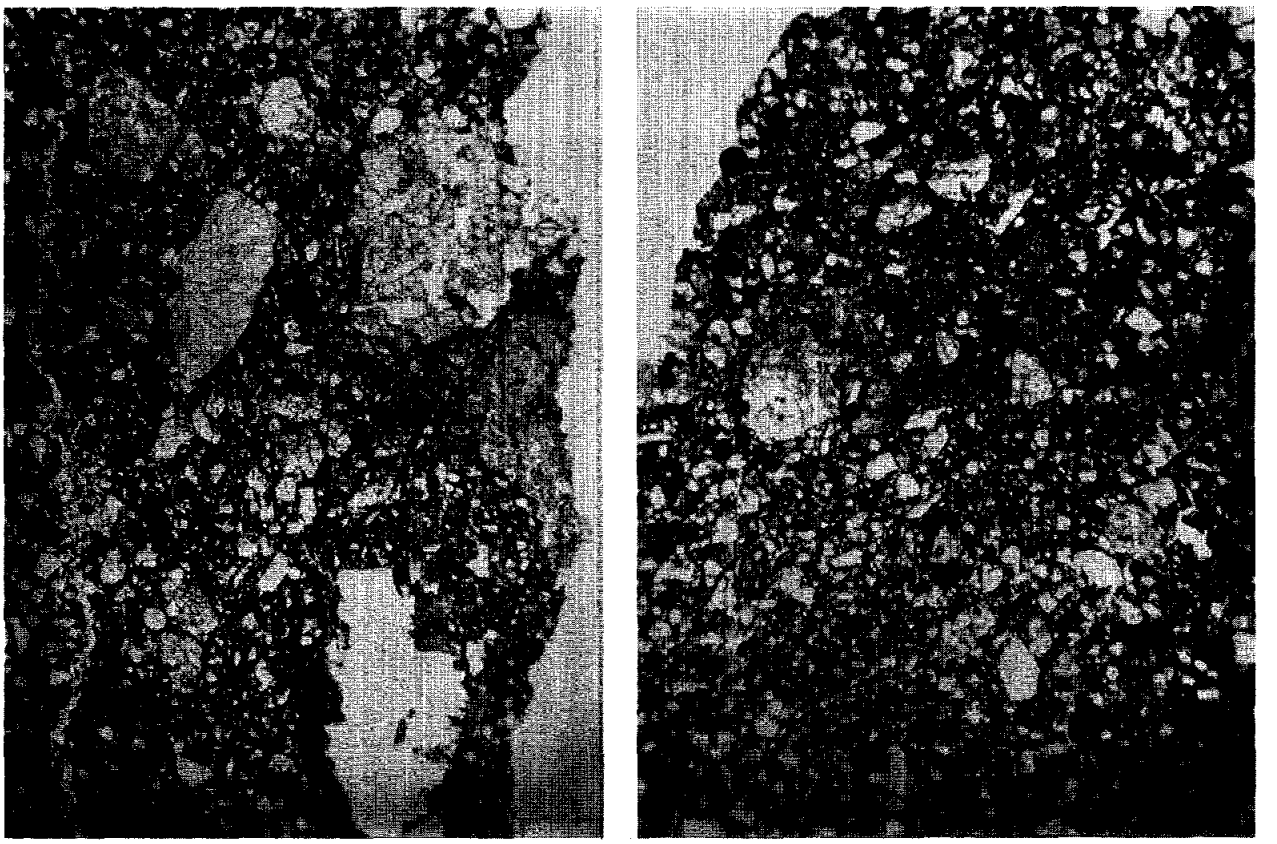

Figure 2. General photomicrographs of 15255,76. Widths about 2 mm. Transmitted light. a) shows a mare basalt clast in the upper right.

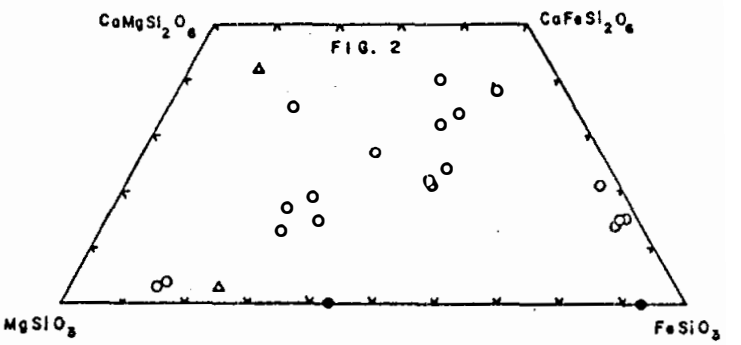

SEM-EDS analyses of pyroxene and olivine in 15255 breccia.
○ = Matrix pyroxene; △ = Clast pyroxene; ● = Matrix olivine.

Figure 3. Plots of mafic mineral compositions for 15255 (Nava et al., 1978).

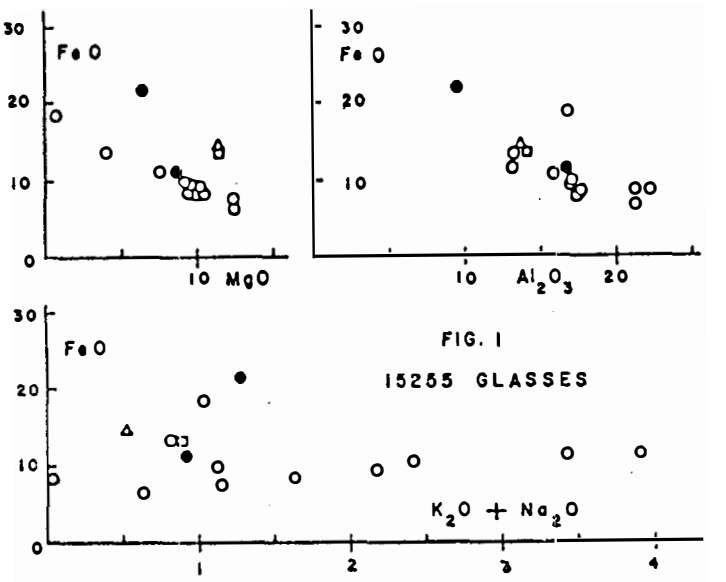

Compositions, in weight %, of glasses in 15255.
□ = Rind glass (SEM-EDS average of 20);
△ = Rind glass (EMP average of 13-19);
● = Glass patches within rind glass (SEM-EDS);
○ = Matrix glasses (SEM-EDS).

Figure 4. Plots of glass compositions for 15255 (Nava et al., 1978).

TABLE 15255-1. Chemical analyses of bulk matrix

		,0	,15	,34
Wt %	SiO_2			
	TiO_2			
	Al_2O_3			
	FeO			
	MgO			
	CaO			
	Na_2O			
	K_2O	0.187		0.181
	P_2O_5			
(ppm)	Sc			
	V			
	Cr			
	Mn			
	Co			
	Ni			
	Rb			4.91
	Sr			122
	Y			
	Zr			290
	Nb			
	Hf			7.9
	Ba			225
	Th	3.5		
	U	0.92		
	Pb			
	La			
	Ce			
	Pr			
	Nd			35.1
	Sm			10.2
	Eu			1.30
	Gd			
	Tb			
	Dy			13.5
	Ho			
	Er			8.05
	Tm			
	Yb			7.26
	Lu			1.11
	Li			13.3
	Be			
	B			
	C		123	
	N			
	S			
	F			
	Cl			
	Br			
	Cu			
	Zn			
(ppb)	I			
	At			
	Ga			
	Ge			
	As			
	Se			
	Mo			
	Tc			
	Ru			
	Rh			
	Pd			
	Ag			
	Cd			
	In			
	Sn			
	Sb			
	Te			
	Cs			
	Ta			
	W			
	Re			
	Os			
	Ir			
	Pt			
	Au			
	Hg			
	Tl			
	Bi			
		(1)	(2)	(3)

References and methods:

(1) Keith et al. (1972); gamma ray spectroscopy
(2) Moore et al. (1973); pyrolysis, gas chromatography
(3) Nava et al. (1977); isotope dilution/mass spectrometry

TABLE 15255-2. Chemical analyses of rind glass

		,77(a)	,77	,34	,38
wt %	SiO_2	48.0	46.4		46.76
	TiO_2	1.61	1.80		1.74
	Al_2O_3	14.37	14.1		13.91
	FeO	13.24	14.7		14.58
	MgO	11.43	11.1		11.29
	CaO	10.26	10.7		11.06
	Na_2O	0.77	0.38		0.18
	K_2O	0.10	0.16	0.282	0.16
	P_2O_5		0.11		
(ppm)	Sc				
	V				
	Cr		3010		3150
	Mn	1550	1700		
	Co				
	Ni				
	Rb			7.49	
	Sr			134	
	Y				
	Zr			501	
	Nb				
	Hf				
	Ba			383	
	Th				
	U				
	Pb				
	La				
	Ce			71.5	
	Pr				
	Nd			53.9	
	Sm			15.0	
	Eu			1.67	
	Gd				
	Tb				
	Dy			20.0	
	Ho				
	Er			12.2	
	Tm				
	Yb			11.0	
	Lu			1.54	
	Li			18.0	
	Be				
	B				
	C				
	N				
	S				
	F				
	Cl				
	Br				
	Cu				
	Zn				
(ppb)	I				
	At				
	Ga				
	Ge				
	As				
	Se				
	Mo				
	Tc				
	Ru				
	Rh				
	Pd				
	Ag				
	Cd				
	In				
	Sn				
	Sb				
	Te				
	Cs				
	Ta				
	W				
	Re				
	Os				
	Ir				
	Pt				
	Au				
	Hg				
	Tl				
	Bi				
		(1)	(2)	(3)	(4)

References and methods:

(1) Nava et al. (1977); SEM-EDS
(2) Nava et al. (1977); microprobe
(3) Nava et al. (1977); isotope dilution, mass spectrometry
(4) Winzer et al. (1978); SEM-EDS

Notes:

(a) some uncertanties very large (especially Mn, Na, K)

15255

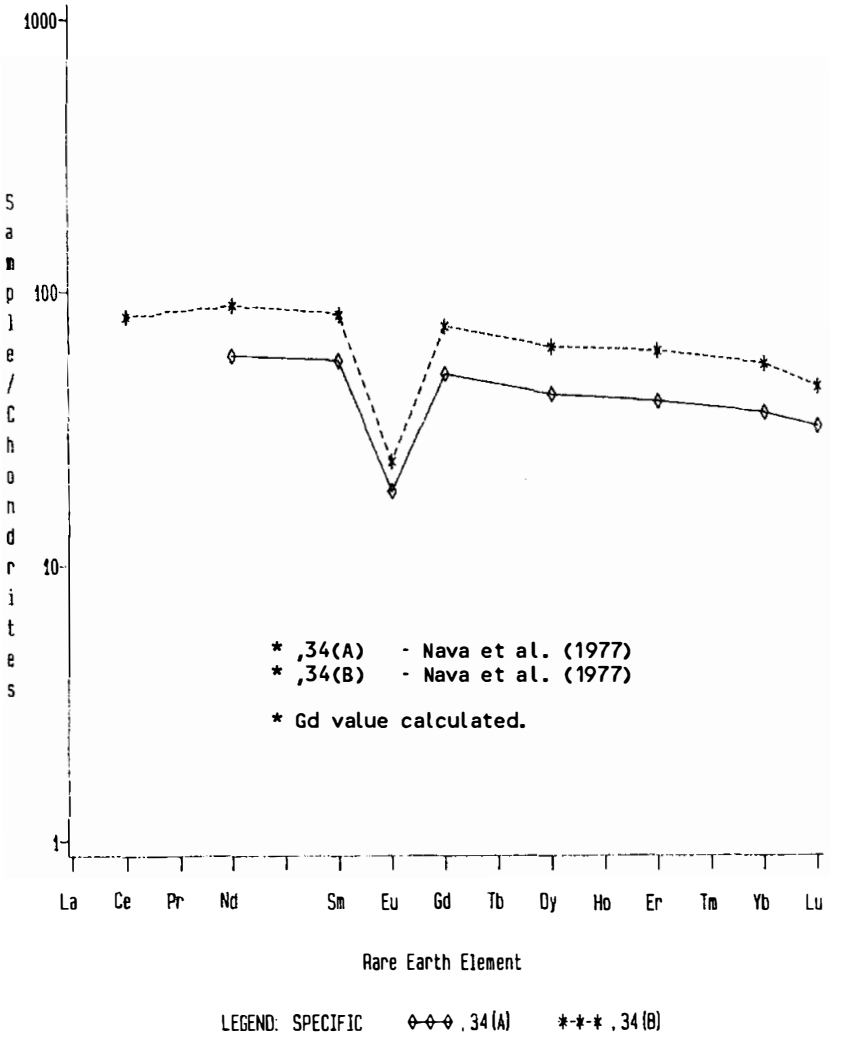

Figure 5. Rare earths in 15255 lithologies.

rind glass has a higher mafic content and a lower alkali and alumina content than most matrix glasses.

Reflection spectra for 15255 shows that the sample has among the most high-Ca pyroxene of Apollo 15 breccias, as indicated in a plot of the wavelengths of the positions of the pyroxene absorption bands against each other (Adams and McCord, 1972).

CHEMISTRY: Limited chemical data for the breccia (Table 1) and for the rind glass (Table 2) are available. Rare earths are shown in Figure 5. The limited data suggest that the breccia composition is similar to, but a little less KREEP-rich than Station 6 soils; the glass is distinctly more mafic and more KREEP-rich (Fig. 5). The difference in composition precludes the formation of the glass by melting of the rock.

EXPOSURE: Cosmogenic radionuclide disintegration count data by Keith et al (1972) (^{26}Al, ^{22}Na, ^{54}Mn, ^{56}Co, ^{46}Sc) implies that ^{26}Al is saturated, indicating a surface residence of about a million years or more. Yokoyama et al. (1974) reanalyzed the data with the ^{26}Al-^{22}Na method and verified that ^{26}Al was saturated. The lack of impact craters led Horz (data pack notes) to believe that the glass had never been exposed.

PROCESSING AND SUBDIVISIONS: 15255 was sawn to produce two ends (,0 and ,1) and multiple thin slab chips ,2 and ,3 (Fig. 6). Subsequently thin sections were made from two daughters of ,3 (,19 and ,20). ,1 was further split and most allocations made from it, and a further potted butt from ,1 (,33) produced another thin section which had glass coat on it. ,0 is now 193.4 g and ,1 is now 13.8 g; no other piece is as large as 7 g.

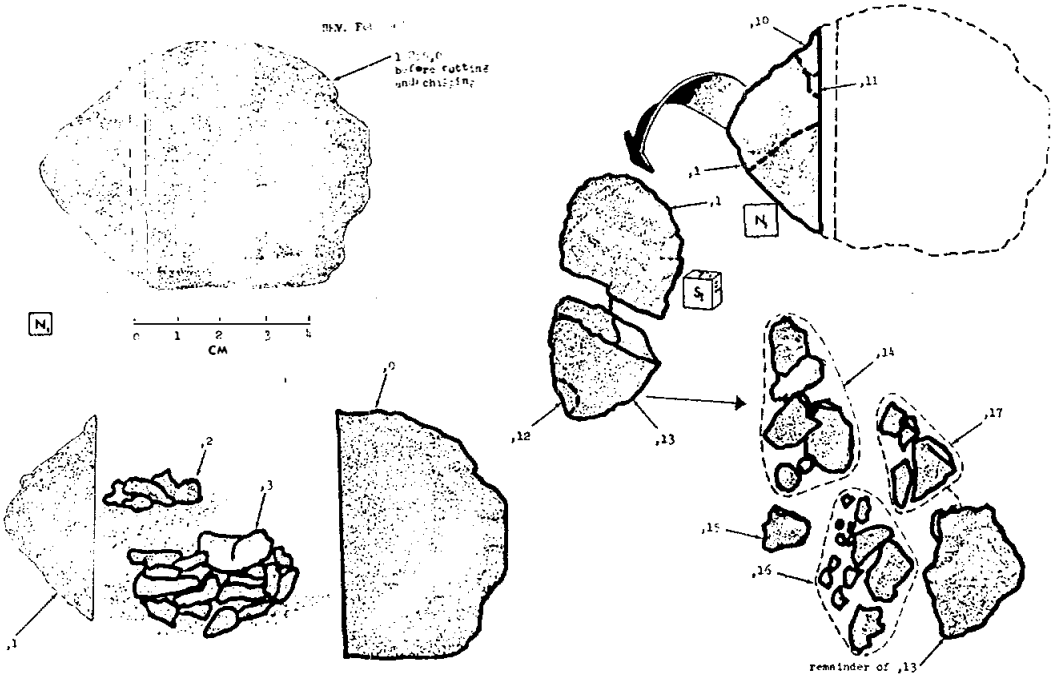

Figure 6. Sawing and splitting of 15255.

15256 SHOCK-MELTED OLIVINE-NORMATIVE MARE BASALT (BRECCIA?) ST. 6 201.0 g

INTRODUCTION: 15256 has the composition of an average olivine-normative basalt, but has a very heterogeneous, generally fine-grained texture. It has always been described as consisting of clasts of basalt in an impact melt matrix, i.e., a melt breccia; however, certain features suggest that virtually the entire sample could have been shock-molten at one time and crystallized rapidly into different textural zones under heterogeneous nucleation. It lacks meteoritic contamination.

15256 is blocky, coherent, aphanitic, and a light greenish gray (Fig. 1). It had glass on a small portion of its surface. Zap pits were scattered on all surfaces, but "B" had the fewest. The orientation is known; "N" was the underside. The sample was collected less than 1 m from 15255, 30 m west of the LRV and approximately 25 m southwest and upslope of the 12 m crater at Station 6.

Figure 1. Major split of 15256 to produce ,27 and ,0. S-71-60578

PETROLOGY: 15256 is an extremely heterogeneous mare basalt appearing to be a breccia (Figs. 2,3). Brief descriptions of the petrography of 15256 were given by Engelhardt et al. (1972, 1973) and Mason et al. (1972). According to Engelhardt et al. (1972, 1973) the rock has a fluidal texture, and is a breccia composed of several mare-type basalts with an original matrix which has been recrystallized such that clast boundaries are indistinct. The matrix contains much clinopyroxene and also plagioclase and ilmenite of varied crystal sizes. The basalts consist of light-colored aphanites, and olivine-bearing, dark, coarse and fine-grained vitrophyres, and a few devitrified glasses. The sample is interpreted as of impact origin. Engelhardt et al. (1973) noted the presence of some narrow fissues filled with yellow vesicular glass. Mason et al. (1972) reported similar characteristics and conclusions, referring to 15256 as a "welded breccia." The grain size is less than 0.5 mm, and contains fragments larger than 1 mm. Large olivine clasts (Fo_{65}) are present on some portions; some basaltic clasts are vitrophyric with abundant olivine phenocrysts and microlites (Fo_{65-50}). Engelhard (1979) tabulated the paragenesis of ilmenite in 15256 samples: it commenced crystallization after plagioclase.

The evidence that 15256 is a melt breccia in which the different zones are clasts is not compelling. Most of the non-glassy zones are extremely heterogeneous within themselves, much more so than single mare basalts, and several contain apparent boundaries which fade out elsewhere in the same zone. Nearly all the basaltic regions are finer-grained than any other known olivine-normative mare basalts (which are not vitrophyric) suggesting that a "clast" population did not sample a typical flow. The sample shows no meteoritic contamination (Chemistry section, below), nor has recrystallization caused the indistinct grain boundaries, as several glassy fragments remain undevitrified. Therefore, it seems at least possible that 15256 has a different,

Figure 2. Whole thin section photograph of 15256,47. Transmitted light. Width about 1.5 cm.

Fig. 3a

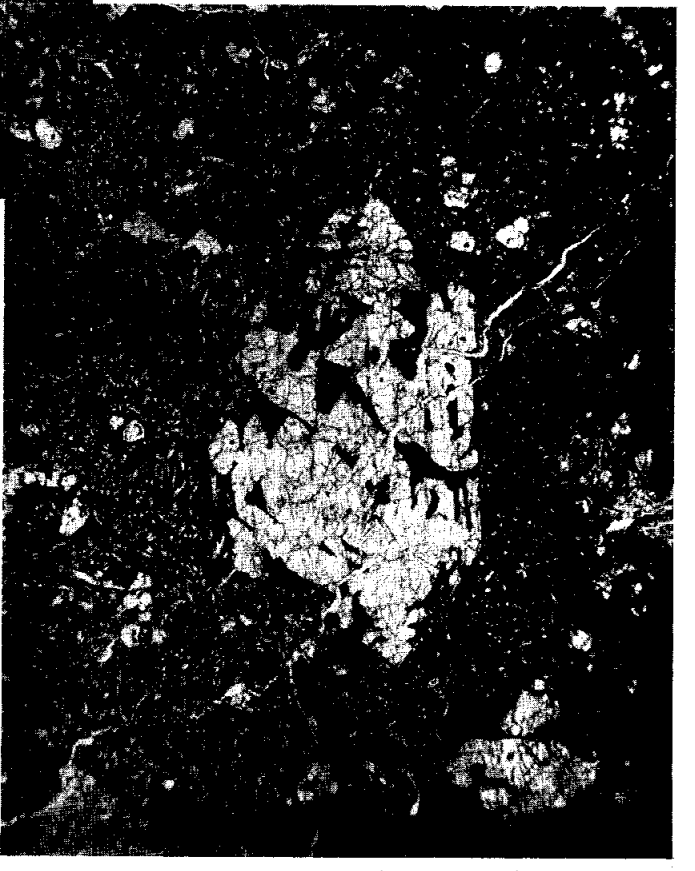

Fig. 3b

Figure 3. Photomicrographs of 15256,47. Transmitted light. widths about 2 mm. a) olivine-vitrophyric patch surrounded and intruded(?) by heterogeneous olivine-phyric, fine-grained basalt; b) zone of fine-grained basalt containing a large euhedral olivine containing patches of fine-grained to glassy melt; small phenocrysts are also olivine.

though still impact origin: by impact melting of an olivine-normative basalt flow, and resolidification from a near-total melt but with heterogeneous nucleation, in a small pool. The angular glassy and fine-grained fragments are then the only clasts and might represent chilled portions of the flow. The impact did not penetrate into underlying flows, nor is there any obvious regolith admixture. It is even possible that the impact was into a still substantially molten flow; such an origin might better explain the large, euhedral, olivine phenocrysts (Fig. 3b) in some zones. However such an event is an unlikely one to have had its products sampled.

CHEMISTRY: Chemical analyses are listed in Table 1, and the rare-earths are plotted in Figure 4. The analyses are consistent with each other, confirming the contention of Mason et al. (1972) that samples as small as 500 mg are adequate to characterize this fine-grained rock, and suggesting that all the textural zones are at least roughly isochemical. The chemical composition is that of an average olivine-normative basalt in almost all respects. However, 15256 was referred to as a non-mare basalt by Ganapathy et al. (1973), Wolf et al. (1979), and Wolf and Anders (1980); they stated that it formed part of a distinct population of high U, Rb, Cs, Cd, and In content and excluded it from mare averages. Examination of the data shows that 15256 is enriched in the very volatile elements Cd, In, Br, and Te compared with other mare basalts, but not in U, Rb, or Cs. Less volatile elements such as Zn are not enriched. The reason for this enrichment in the very volatile elements is presumably related either to the impact history of the rock (although Ir, Re, Au, Ni, and Co are not enriched), or possibly to fumarolic activity at the surface of the lava flow.

RADIOGENIC ISOTOPES: Nyquist et al. (1972, 1973) reported Rb-Sr isotopic data for a whole-rock sample of 15256. The data (Table 2) show that the sample is isotopically identical with other Apollo 15 mare basalts.

EXPOSURE: Radionuclide data by Keith et al. (1972) show that the activity of ^{26}Al is saturated (Keith and Clark, 1974; Yokoyama et al. (1974). Therefore 15256 was exposed for about a million years or more on the lunar surface.

PROCESSING AND SUBDIVISIONS: 15256 was split by chipping, producing several small chips. Thin sections were made from several different fragments. Subsequently the rock split along a major fracture to produce ,27 (Fig. 1) which is 70.3 g and stored at Brooks. ,0 is now 85.4 g; ,4 is 14.72 g. No other pieces are as large as 6 g.

TABLE 15256-1. Chemical analyses

		,22	,10	,15	,22	,22	,0	,6
Wt %	SiO2		45.32	44.93	45.12			
	TiO2	2.46	2.54	2.54	2.51	2.47		
	Al2O3		9.20	8.89	8.95			
	FeO		22.51	22.21	22.52	22.2		
	MgO		9.45	9.08	9.32	9.03		
	CaO		10.17	10.27	10.14	9.93		
	Na2O		0.30	0.28	0.25	0.26		
	K2O	0.038	0.12	0.03	0.04	0.038	0.036	
	P2O5		0.07	0.06	0.07			
(ppm)	Sc							
	V		135					
	Cr		4200(a)					
	Mn			2250				
	Co		46					46
	Ni		60		48			
	Rb		<5		0.6	0.680		0.67
	Sr		88	100	98	99.9		
	Y		48		25			
	Zr		100	90	89			
	Nb				5.3			
	Hf							
	Ba		41			49.9		
	Th						0.42	
	U	0.139				0.139	0.139	
	Pb		<2					
	La					4.82		
	Ce					14.5		
	Pr							
	Nd					10.5		
	Sm					3.43		
	Eu					0.893		
	Gd					4.65		
	Tb							
	Dy					4.98		
	Ho							
	Er					2.75		
	Tm							
	Yb					2.25		
	Lu					0.330		
	Li		8					
	Be							
	B		3					
	C							
	N							
	S			800	700			
	F							
	Cl							
	Br							0.051
	Cu		11					
	Zn		<10					0.92
(ppb)	I							
	At							
	Ga		4000					
	Ge							3.8
	As							
	Se							119
	Mo							
	Tc							
	Ru							
	Rh							
	Pd							
	Ag		<1000					0.78
	Cd		<2000					104
	In							6.8
	Sn							
	Sb							0.43
	Te							2
	Cs							29(b)
	Ta							
	W							
	Re							0.0049
	Os							
	Ir							0.022
	Pt							
	Au							0.019
	Hg							
	Tl							1.45
	Bi		<2000					0.41
		(1)	(2)	(3)	(4)	(5)	(6)	(7)

References to Table 15256-1

References and methods:

(1) Church et al. (1972); isotope dilu ion mass spectrometry (overlap with Hubbard et al. (1973)
(2) Mason et al. (1972); seve al techniques, including emission spectrometry
(3) LSPET (1972), Rhodes and Hubbard (1973); XRF
(4) Rhodes and Hubbard (1973); isotope dilution, mass spectrometry
(5) Hubbard et al. (1973), Nyqui t et al. (1972, 1973); isotope dilut on, mass spectrometry, colorimetry, AA
(6) Keith et al. (1972); gamma ray spectroscopy
(7) Ganapathy et al. (1973), Morgan et al. (1972a,b); RNAA

Notes:

(a) also value of 0.31% Cr_2O_3 listed (2120 ppm Cr), seems erroneously low.
(b) corrected from original publication (H uchi et al., 1975).

15256

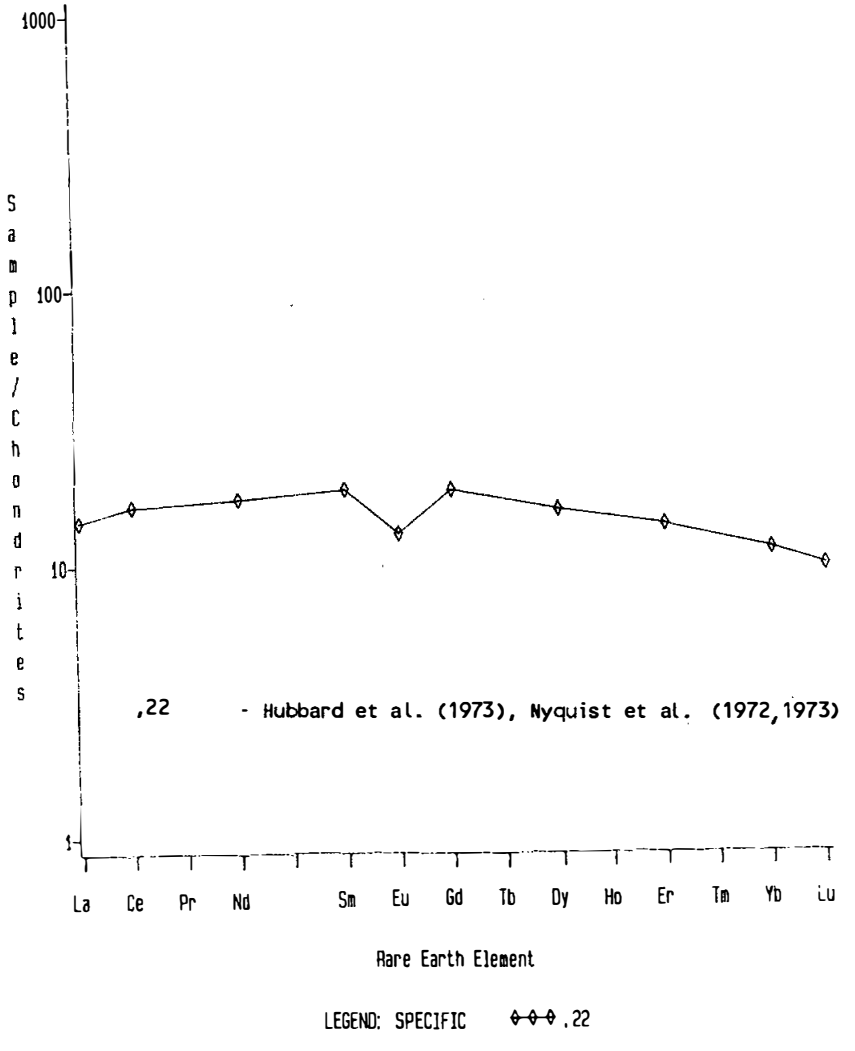

Figure 4. Rare earths in 15256.

TABLE 15256-2. Rb-Sr isotopic data

Split	$^{87}Rb/^{86}Sr$	$^{87}Sr/^{86}Sr$	$^{a}T_{BABI}$ (b.y.)	$^{b}T_{LUNI}$ (b.y.)
,22	0.0197±5	0.70042±7	4.67±.36	5.01±.36

(a) model age assuming I = 0.69910 (BABI plus lab bias)
(b) model age assuming I = 0.69900 (from Apollo 16 anorthosites assuming T = 4.6 b.y.)

15257 REGOLITH BRECCIA, GLASS-COATED ST. 6 22.5 g

INTRODUCTION: 15257 is a coherent regolith breccia with a glass coat on one side (Fig. 1). It contains typical regolith breccia constituents, including glasses and mare basalt fragments. It is blocky, subangular to rounded, with a freshly-broken surface, and is a medium-dark gray. The glass is vesicular and grayish-black. Zap pits occur mainly on one side ("S"). The sample was not documented on collection nor identified in photographs and it is possibly a small piece broken from 15255. It was returned in the same sample bag as 15255 and 15256, which was filled 30 m west of the LRV and approximately 25 m southwest and upslope of the 12 m crater at Station 6.

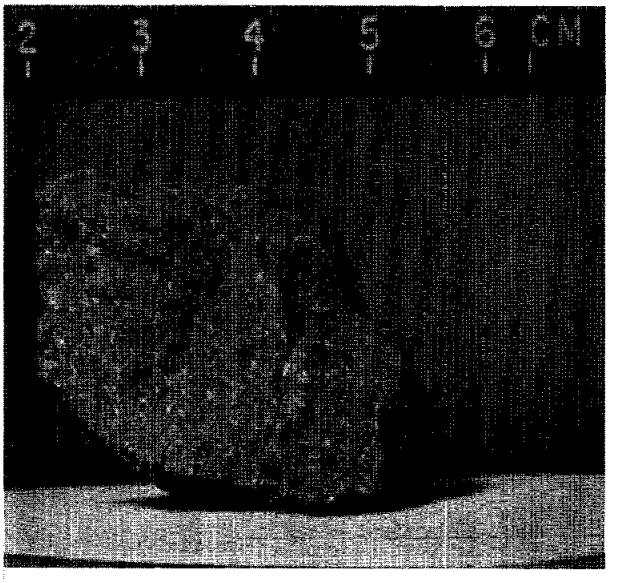

Fig. 1a

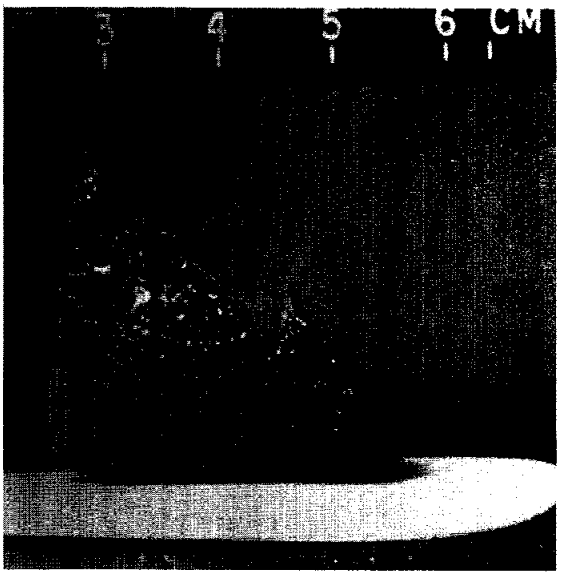

Fig. 1b

Figure 1. Pre-split view of 15257 a) S-71-45818; b) S-71-45814.

PETROLOGY: 15257 is a non-porous regolith breccia with coarse clasts, rather like 15255 (Fig. 2). It contains abundant glass, including colorless, green, and yellow, though red glass is rare to absent. Lithic fragments include fine- and medium-grained basalts, many of which look like mare fragments. According to McKay et al. (1984) the I_s/FeO is 20 to 30, and Korotev (1984, unpublished) refined this to 23. Hence the sample is immature to submature.

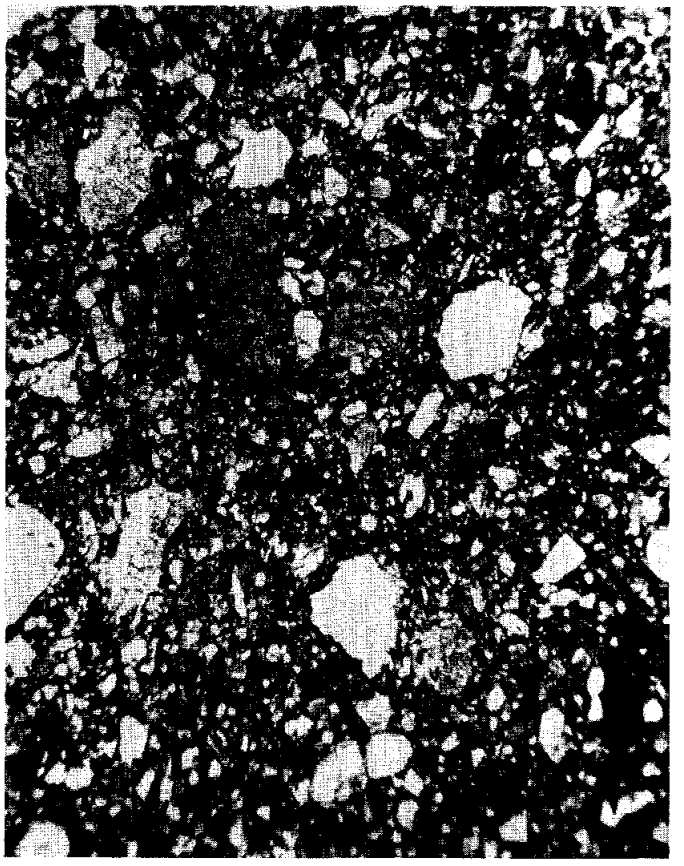

Figure 2. Photomicrograph of 15257,4. Width about 2 mm. Transmitted light.

CHEMISTRY: Only one analysis has been made (Table 1, Fig. 3). The chemistry is more mafic than local soil. For those elements for which comparison can be made, the data are very similar to those for 15255, consistent with suggestions that 15257 was broken from 15255 in transit.

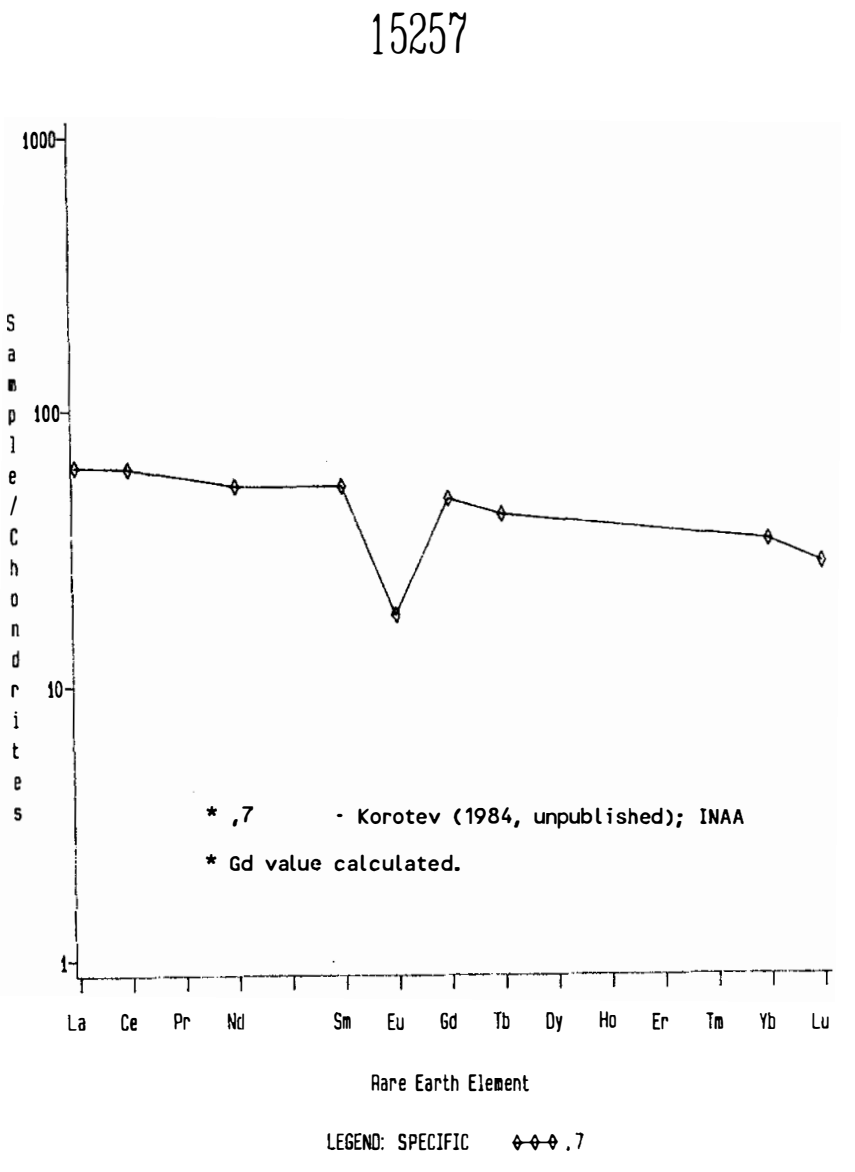

Figure 3. Rare earths in 15257,7.

TABLE 15257-1. Chemical analysis

		,7
Wt %	SiO2	
	TiO2	1.67
	Al2O3	13.2
	FeO	15.5
	MgO	10.8
	CaO	9.5
	Na2O	0.39
	K2O	
	P2O5	
(ppm)	Sc	29.9
	V	107
	Cr	2840
	Mn	1550
	Co	43.6
	Ni	164
	Rb	
	Sr	140
	Y	
	Zr	280
	Nb	
	Hf	7.8
	Ba	208
	Th	3.2
	U	0.8
	Pb	
	La	20.6
	Ce	54
	Pr	
	Nd	32
	Sm	9.6
	Eu	1.25
	Gd	
	Tb	1.96
	Dy	
	Ho	
	Er	
	Tm	
	Yb	6.7
	Lu	0.94
	Li	
	Be	
	B	
	C	
	N	
	S	
	F	
	Cl	
	Br	
	Cu	
	Zn	
(ppb)	I	
	At	
	Ga	
	Ge	
	As	
	Se	
	Mo	
	Tc	
	Ru	
	Rh	
	Pd	
	Ag	
	Cd	
	In	
	Sn	
	Sb	
	Te	
	Cs	240
	Ta	980
	W	
	Re	
	Os	
	Ir	4.7
	Pt	
	Au	1.6
	Hg	
	Tl	
	Bi	
		(1)

References and methods:

(1) Korotev (1984, unpublished); INAA

PROCESSING AND SUBDIVISIONS: Only a few small chips have been removed from ,0 (Fig. 4). Two thin sections (,4 and ,9) were made from a chip ,1 and do not include the glass coat. ,0 consists of one main piece and some small pieces and has a mass of 18.7 g. Some of the chips were numbered (,5 to ,8) in 1983.

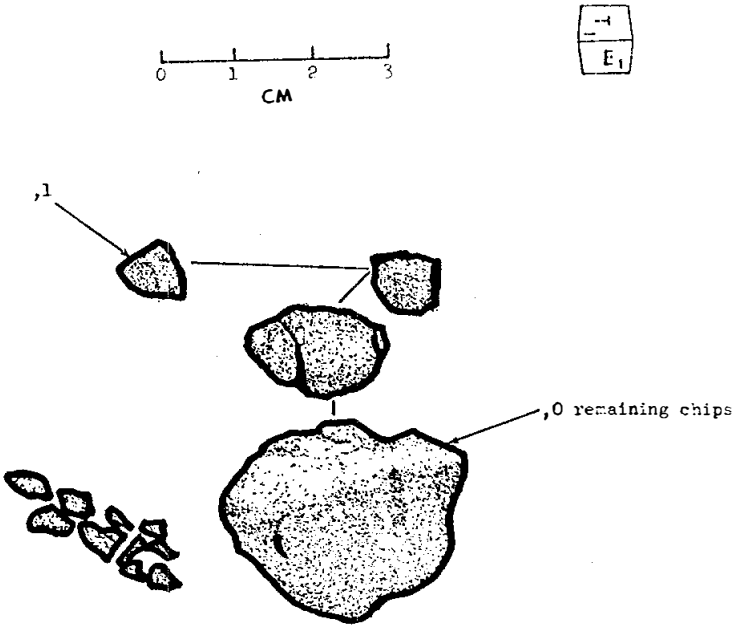

Figure 4. Original chipping of 15257 to produce ,1, which was used for two thin sections.

15259 REGOLITH BRECCIA ST. 6 0.7 g

INTRODUCTION: 15259 is a medium-light gray regolith breccia (Fig. 1). It is friable and slabby, and homogeneous. Its friable surface precludes zap pits. It was collected (with 15265 to 15259 and 15285 to 15289) from the crest of an inner bench on the north-east wall of the 12 m diameter crater at Station 6, downslope 15 m from the LRV. 15259 has never been subdivided or allocated.

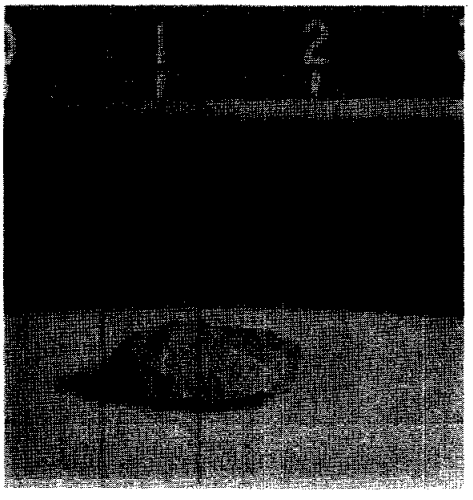

Figure 1. Macroscopic view of 15259. S-71-44958

15265 REGOLITH BRECCIA ST. 6 314.1 g

INTRODUCTION: 15265 is a coherent regolith breccia with a composition a little richer in incompatible elements than Station 6 soils. It contains typical regolith breccia constituents, and contains both KREEP and mare basalt fragments. One mare basalt, apparently an olivine-normative basalt, was dated as 3.16 ± 0.11 b.y. It was studied in a Consortium headed by Burlingame.

15265 is slabby (Fig. 1), with a series of penetrative fractures parallel to the "N" and "S" faces. It has slickensides on one end, and many zap pits on two surfaces, with a few on all other surfaces except one. 15265 was collected (along with 15259, 15266 to 15269, and 15285 to 15289) from the crest of an inner bench on the northeast wall of the 12 m crater at Station 6, downslope 15 m from the LRV. A single large rock was broken by the Commander into three pieces (15265 to 15267). The sample was documented on the lunar surface both before and after it had been broken and moved. It was originally partly buried, possibly a result of an original impact as a secondary projectile.

PETROLOGY: Little petrographic data has been published. It was originally described (Lunar Sample Information Catalog Apollo 15, 1972) as a glassy polymict breccia of non-mare origin, but it does contain mare material in addition to its "metaclastic" clasts and KREEP basalts. In thin section it is a typical regolith breccia (Fig. 2) with some coarse clasts. Glass is common, both as beads and as irregular bodies. Lithic and mineral fragments are generally unshocked and the appearance is fairly immature. Wentworth et al. (1984) found it to be porous (33.4%) with a density of 2.05 g/cc (3.08 g/cc intrinsic), and McKay and Wentworth (1983) described it as porous with a low fracture porosity, minor agglutinates, minor spheres, and minor shock features. McKay et al. (1984) found it had an I_s/FeO of 23, and Korotev (1984, unpublished) working in the same group, reported a value of 21. Kaplan et al. (1976) reported the sample to contain 0.4% Fe^o.

One thin section of grain mounts of small pieces from a prominent clast on the "N" face appears to be of mare basalt.

CHEMISTRY: Chemical analyses of bulk breccia are listed in Table 1, with rare earths plotted in Figure 3. Few authors have discussed their results. Partial analyses of two clasts are listed in Table 2.

The bulk breccia has a composition similar to local regolith, but enriched in incompatible elements; hence it is probably exotic but not from a far distant source. Analyses are fairly consistent except the U content of Reed and Jovanovic (1972) is excessively low; perhaps their split was a clast. Kaplan et al. (1976) also provided CH_4 data. The analyses listed under clasts (Table 2) are uncharacterized, except for column b, which is definitely a mare basalt (for which an internal Rb-Sr isochron

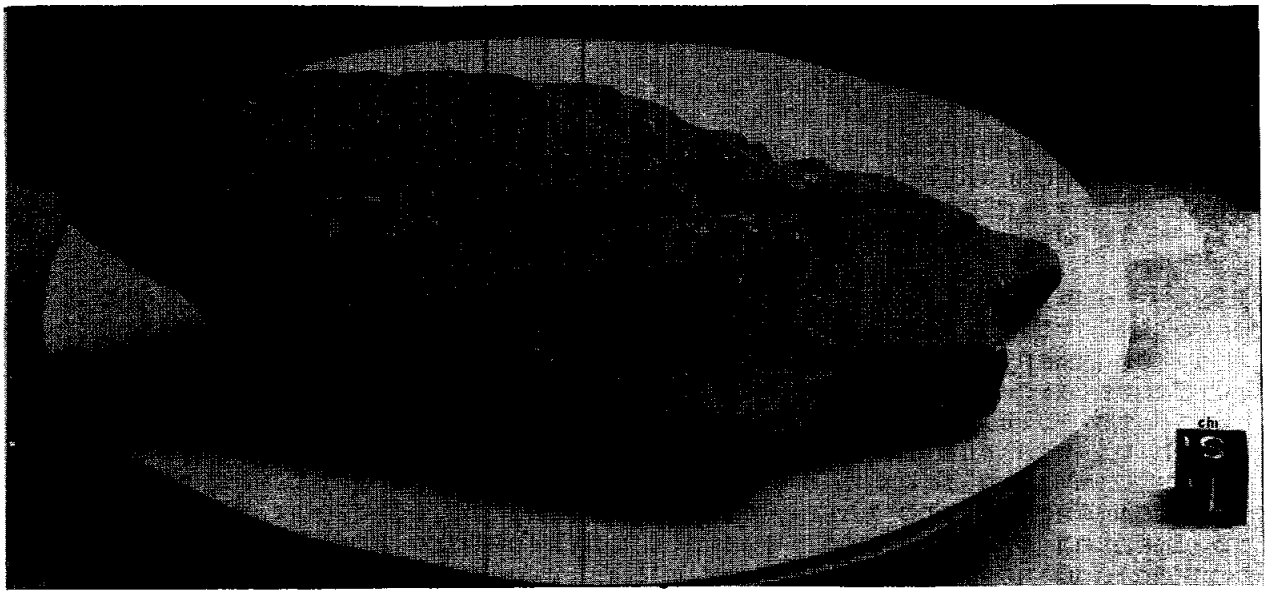

Figure 1. View of 15265 prior to removal of ,2 which lies on top front. The slab has already broken with ,4 lying at front bottom and ,0 at rear.

Figure 2. Photomicrograph of 15265,7. Width about 2 mm. Transmitted light. Basalt is an Apollo 15 KREEP basalt fragment.

15265

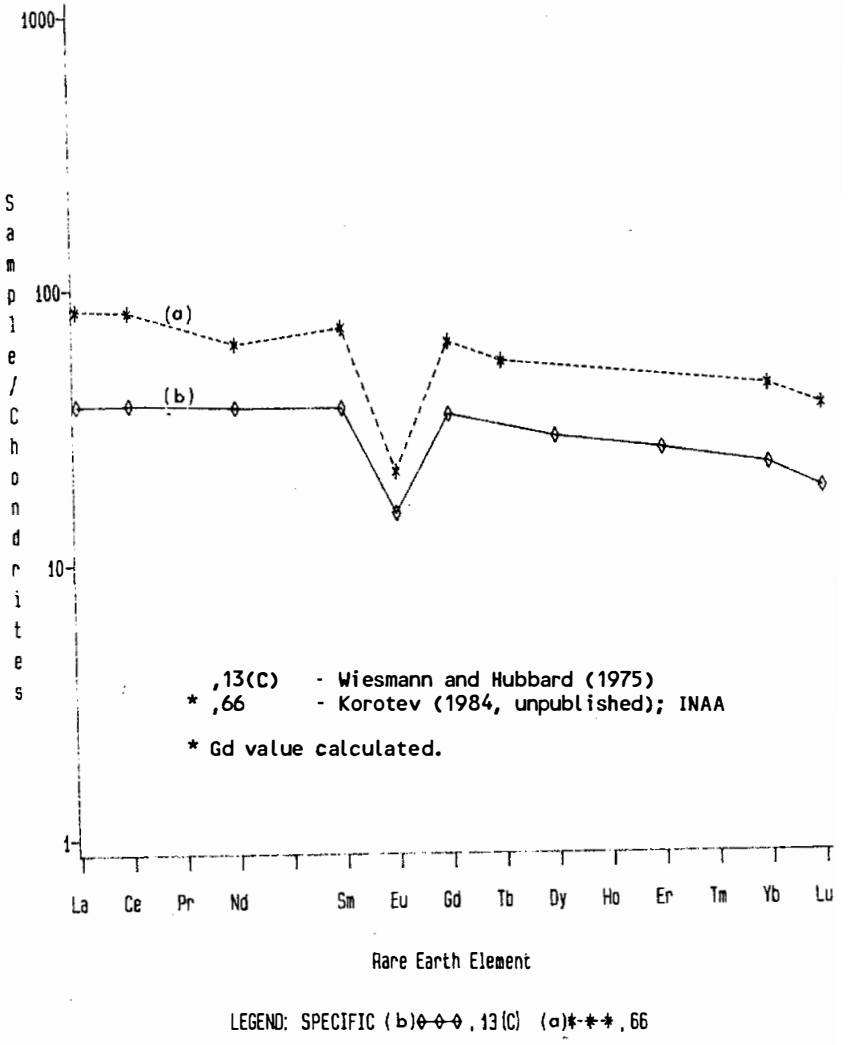

Figure 3. Rare earths in 15265 a) matrix (Korotev, 1984, unpublished); b) clast? (Wiesmann and Hubbard, 1975).

TABLE 15265-1. Chemical analyses

			,66	,0	,13,5	,13	,9004	,9004	,13	,17	,9009
Wt %	SiO2	46.94									
	TiO2	1.40									
	Al2O3	16.71									
	FeO	11.18	11.2								
	MgO	9.95									
	CaO	11.19	11.4								
	Na2O	.51	0.51								
	K2O	.25		0.253							0.263
	P2O5	.25									
(ppm)	Sc		21.4								
	V										
	Cr	2260	2070								
	Mn	1160									
	Co		34.0								
	Ni		214		205						
	Rb	7.8			6.1						6.96
	Sr	150	165								142
	Y	100									
	Zr	469(a)	420								
	Nb	29									
	Hf		10.0								
	Ba		292								
	Th	4.8	4.6	5.05							
	U		1.21	1.27	1.33					0.067	
	Pb										
	La		27.8								
	Ce		73								
	Pr										
	Nd		38								
	Sm		13.1								
	Eu		1.48								
	Gd										
	Tb		2.55								
	Dy										
	Ho										
	Er										
	Tm										
	Yb		8.8								
	Lu		1.26								
	Li									9.1	
	Be										
	B										
	C					57	76				
	N						41				
	S	800					870	830	1010		
	F										
	Cl									26.2	
	Br				0.140					0.62	
	Cu										
	Zn				16.8						
(ppb)	I									0.24	
	At										
	Ga										
	Ge				360						
	As										
	Se				236						
	Mo										
	Tc										
	Ru										
	Rh										
	Pd										
	Ag				10.9						
	Cd				0.62						
	In										
	Sn										
	Sb				2.15						
	Te				16						
	Cs		330		420						
	Ta		1220								
	W										
	Re				0.619						
	Os										
	Ir		7.8		6.22						
	Pt										
	Au		2.1		3.46						
	Hg										
	Tl				2.7						
	Bi				1.9						
		(1)	(2)	(3)	(4)	(5)	(6)	(7)	(8)	(9)	(10)

References to Table 15265-1

References and methods:

(1) LSPET (1972); XRF
(2) Korotev (1984, unpublished); INAA
(3) Keith et al. (1972), LSPET (1972); gamma ray spectroscopy
(4) Ganapathy et al. (1973); RNAA
(5) Moore et al. (1973); combustion, gas chromatography
(6) Kaplan et al. (1976); combustion
(7) Kaplan et al. (1976); hydrolysis
(8) Moore (1974); combustion, gas chromatography
(9) Reed and Jovanovic (1972); neutron activation, leaching
(10) Mark et al. (1974); isotope dilution, mass spectrometry

Notes:

(a) erroneously listed as 169 ppm in NASA SP-289 LSPET report.

TABLE 15265-2. Chemical analyses of clasts

		,13,6(a)	,9005(b)	,13(c)
Wt %	SiO2			
	TiO2			2.13
	Al2O3			
	FeO			
	MgO			
	CaO			
	Na2O			
	K2O		0.040	0.112
	P2O5			
(ppm)	Sc			
	V			
	Cr			3225
	Mn			
	Co			
	Ni	55		
	Rb	0.84	0.743	2.71
	Sr		98.06	109
	Y			
	Zr			181
	Nb			
	Hf			
	Ba			130
	Th			1.95
	U	0.167		0.54
	Pb			
	La			12.5
	Ce			33.5
	Pr			
	Nd			22.2
	Sm			6.66
	Eu			1.05
	Gd			8.66
	Tb			
	Dy			9.11
	Ho			
	Er			5.19
	Tm			
	Yb			4.54
	Lu			0.625
	Li			9.6
	Be			
	B			
	C			
	N			
	S			
	F			
	Cl			
	Br	.03		
	Cu			
	Zn	0.97		
(ppb)	I			
	At			
	Ga			
	Ge	6.2		
	As			
	Se	117		
	Mo			
	Tc			
	Ru			
	Rh			
	Pd			
	Ag	6.4		
	Cd	0.66		
	In			
	Sn			
	Sb	0.14		
	Te	2.8		
	Cs	36		
	Ta			
	W			
	Re	0.006		
	Os			
	Ir	0.023		
	Pt			
	Au	0.09		
	Hg			
	Tl	0.25		
	Bi	0.20		
		(1)	(2)	(3)

References and methods:

(1) Ganapathy et al. (1973, 1974); RNAA
(2) Mark et al. (1974); isotope dilution, mass spectrometry
(3) Wiesmann and Hubbard (1975); isotope dilution, mass spec. and others

Notes:

(a) Norite(?)
(b) Mare basalt
(c) ?

Additional notes for norite(?) clast:
(see errata, 8th Proceedings, p. i)

(i) Te incorrect in Ganapathy et al. (1974)
(ii) U incorrect in Ganapathy et al. (1973)
(iii) Ag and Ge superior values of Ganapathy et al. (1974)
(iv) Incorrectly listed as "matrix" in Ganapathy et al. (1974)

was derived) and whose Rb and Sr contents suggest it is an olivine-normative mare basalt. The Ganapathy et al. (1973, 1974) analysis is ostensibly of a norite(?) clast, but its composition is compatible with a mare basalt. It is not contaminated with meteoritic material. The analysis of Wiesmann and Hubbard (1975) is not claimed as a clast but is obviously dissimilar to bulk breccia analyses; it cannot however be a pure mare basalt clast because its incompatible elements are a factor of 2 too high. It could be a mare-rich fragment of matrix. Full documentation on Burlingame's Consortium samples is not available. A clast was analyzed by Wasson's group in a search for pristine highlands clasts; the data was never reported and the clast is presumably a mare basalt, as indicated by the thin sections (see end of PETROLOGY section).

STABLE ISOTOPES: Kaplan et al. (1976) reported isotopic analyses for C, N, and S. $\delta^{13}C$ °/oo PDB is -20.6, which is not as low as most soils but more like basalts. $\delta^{34}S$ °/oo CDT is +7.7 (combustion) and +6.4 (hydrolysis), values which are lower than most soils but not as low as basalts. $\delta^{15}N$ °/oo AIR is +74 which is slightly higher than soils. The nature of the Kaplan et al. (1976) samples is not known but presumably is bulk breccia.

RADIOGENIC ISOTOPES: Mark et al. (1974) reported a mineral isochron for a mare basalt clast (Fig. 4) from mineral separate Rb-Sr isotopic data (Table 3). The age and initial Sr isotopic ratio are consistent with Apollo 15 mare basalts. Mark et al. (1974) also provided an analysis of the breccia matrix (Table 3). This analysis differs from that of a split of 15265 reported by Wiesmann and Hubbard (1975) ($^{87}Sr/^{86}Sr = 0.70340 \pm 5$) which appears to be a mixture of matrix and mare basalt.

RARE GASES AND EXPOSURE: Rare gas data for apparently bulk breccia samples were reported by LSPET (1972) and Bogard and Nyquist (1972), and by Kaplan et al. (1976). LSPET (1972) provided data for ^{3}He, ^{4}He, ^{22}Ne, ^{36}Ar, ^{84}Kr, and ^{132}Xe. The ratios are similar to those of most other fines and breccias (i.e., $^{20}Ne/^{22}Ne$, $^{21}Ne/^{22}Ne$, $^{36}Ar/^{38}Ar$, $^{40}Ar/^{36}Ar$, $^{4}He/^{36}Ar$). Bogard and Nyquist (1972) found spallation ^{126}Xe to be 0.81 ± 0.7 (10×10^{-10} cc/g) but provided no specific discussion on the Kr and Xe isotopic data they added to their LSPET (1972) report. Kaplan et al. (1976) found 4.74×10^{-2} cc/g of He from combustion, and 4.55×10^{-2} cc/g from hydrolysis.

Radionuclide data by Keith et al. (1972) shows that ^{26}Al is unsaturated, as confirmed by Yokoyama et al. (1974). Keith and Clark (1974) derived an exposure age of 0.97 m.y. (+0.48 m.y., -0.33 m.y., 1 sigma error). Bhandari et al. (1972, 1973) studied tracks in surface chips ,14 and ,15, finding densities of 10×10^{6} cm^{-2} and 6×10^{6} cm^{-2} respectively, both having "suntan" ages of less than 1 m.y.

PROCESSING AND SUBDIVISIONS: 15265 was easily chipped (Fig. 5). ,4 was substantially divided for allocation with its remaining

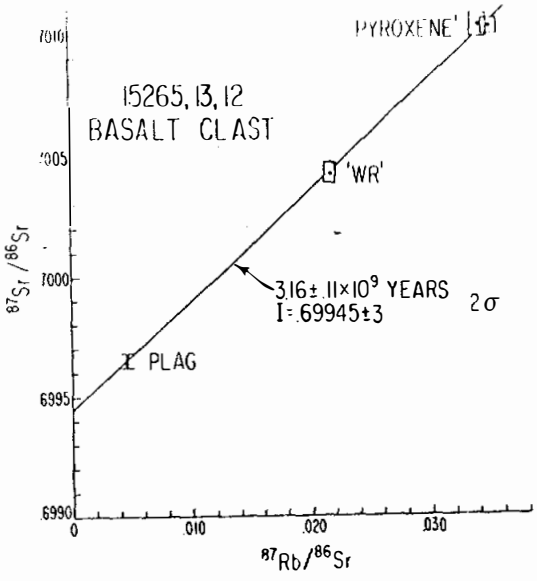

Figure 4. Rb-Sr internal isochron for a mare basalt clast (Mark et al., 1974).

TABLE 15265-3. Rb-Sr isotopic data (Mark et al., 1974)

Sample	K (ppm)	Rb (ppm)	Sr (ppm)	K/Rb (weight)	$^{87}Rb/^{86}Sr$ (atomic)	$^{87}Sr/^{86}Sr \pm 2\sigma$
15265,9005						
plagioclase (H)	487	0.461	289.8	1056	0.00458	0.69965±6
"whole rock" (F)	337	0.743	98.06	507	0.0218	0.70043±8
"clinopyroxene" (I)	338	0.762	63.79	444	0.0343	0.70102±10
"clinopyroxene" (I')	359	0.809	65.88	444	0.0353	0.70101±6
15265,9009						
breccia matrix (B)	2188	6.96	142.0	314	0.140	0.70771±22

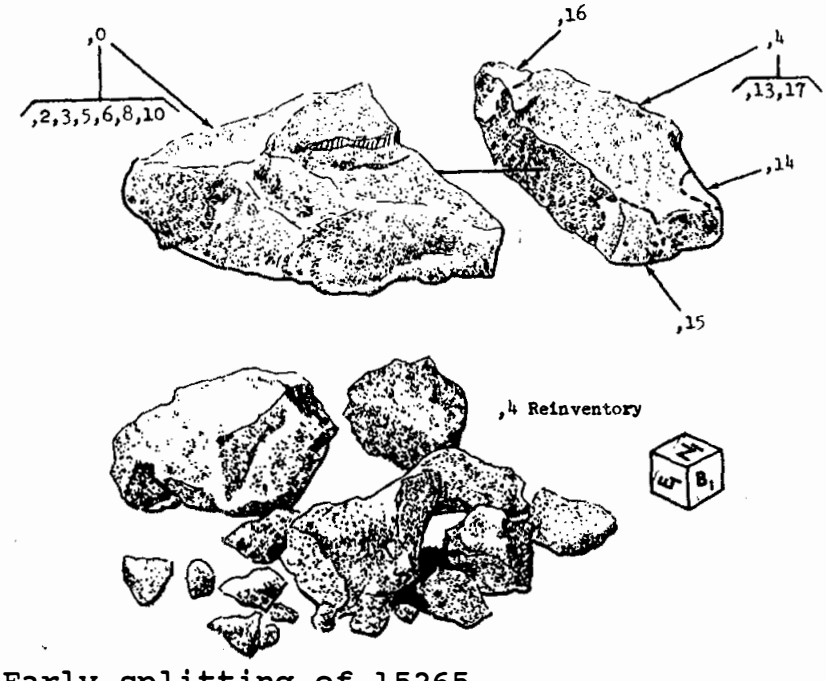

Figure 5. Early splitting of 15265.

mass being 28.8 g. A small chip ,1 was used for thin sections ,7 to ,12, and further matrix thin sections were made from ,13 (,26 and ,62) and from ,69 (,74). A clast grain mount (,65) was made from the material allocated to Wasson. Several generations of chipping have been done: 1972, 1975, 1977, and 1983. ,13 (from ,4) was allocated to the Burlingame Consortium and is now 36 g. ,0 is now 180 g. Several subsplits of ,4, and ,4 itself, are stored at Brooks.

15266 REGOLITH BRECCIA ST. 6 271.4 g

INTRODUCTION: 15266 is a coherent to friable regolith breccia (Fig. 1). It contains typical regolith breccia constituents such as glass spheres, glassy breccias, and numerous mineral fragments, most of which are little shocked. It is blocky and angular, medium gray, and about one half of its "T" surface is grooved and slickensided. Many zap pits are present on several faces. 15266 was collected (along with 15259, 15265, 15267 to 15269, and 15285 to 15289) from the crest of an inner bench on the northeast wall of the 12 m crater at Station 6, downslope 15 m from the LRV. A single large rock was broken by the Commander into three pieces (15265 to 15267). The sample was documented on the lunar surface both before and after it had been broken and moved.

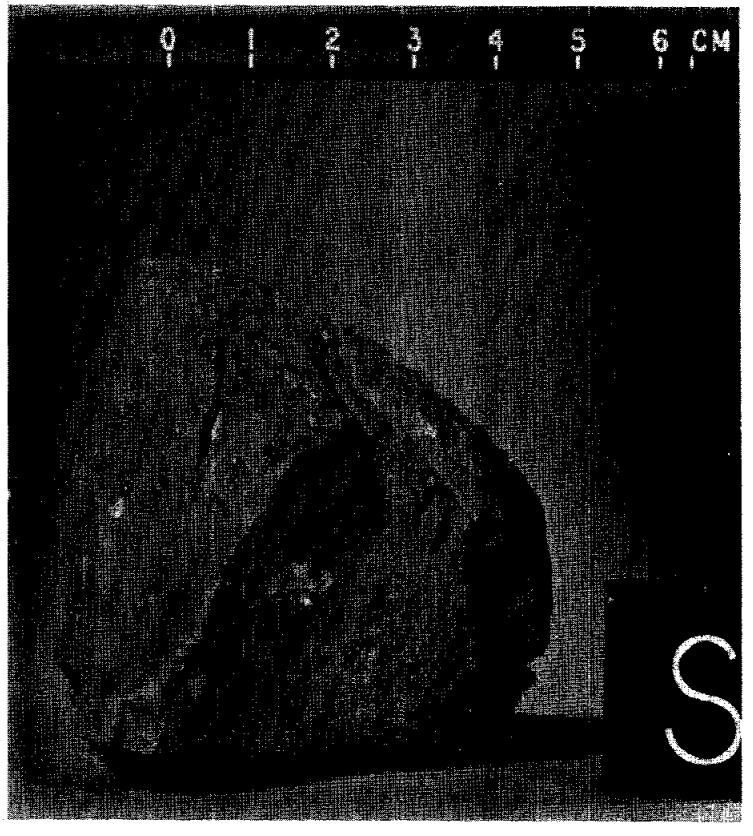

Figure 1. Pre-split view of 15266. S-71-46410

PETROLOGY: 15266 is a porous regolith breccia (Fig. 2) with many glass spheres which are mainly colorless or green. Orange/red and yellow glasses are rare to absent. Small lithic fragments include KREEP and mare basalts, as well as fine-grained impact melts. Glasses, mineral fragments, and lithic fragments are not heavily shocked. Wentworth and McKay (1984) reported the sample to be porous, with a density of only 1.98 g/cc. McKay et al. (1984) found an I_s/FeO of 10-15, which is immature; Korotev (1984, unpublished) listed I_s/FeO of 14. The porosity and maturity are a little lower than for 15265 which is from the same original rock.

CHEMISTRY: An analysis by Korotev (1984, unpublished) (Table 1, Fig. 3) is different from that of local soils and from 15265 in that its incompatible elements are about 50% higher. It is even higher than 15265, which is part of the same rock, and may have been richer in clasts (of KREEP basalts) than typical matrix.

PROCESSING AND SUBDIVISIONS: Several small pieces were chipped from 15266,0 (Fig. 4). Thin sections ,17 to ,20 were made from ,9. The materials allocated to McKay and his coworkers were interior chips from ,4.

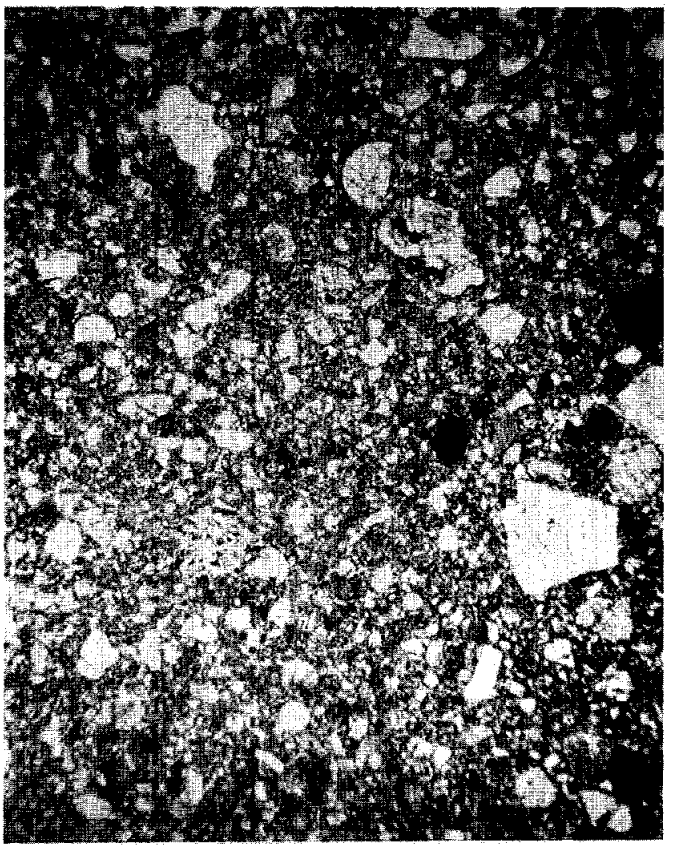

Figure 2. Photomicrograph of 15266,17. Width about 2 mm. Transmitted light.

TABLE 15266-1. Chemical analysis

		,23
wt %	SiO2	
	TiO2	
	Al2O3	
	FeO	12.2
	MgO	
	CaO	10.8
	Na2O	0.58
	K2O	
	P2O5	
(ppm)	Sc	23.7
	V	
	Cr	2290
	Mn	
	Co	34.0
	Ni	151
	Rb	
	Sr	140
	Y	
	Zr	560
	Nb	
	Hf	14.3
	Ba	379
	Th	6.2
	U	1.68
	Pb	
	La	39.0
	Ce	101
	Pr	
	Nd	59
	Sm	17.6
	Eu	1.71
	Gd	
	Tb	3.51
	Dy	
	Ho	
	Er	
	Tm	
	Yb	12.3
	Lu	1.66
	Li	
	Be	
	B	
	C	
	N	
	S	
	F	
	Cl	
	Br	
	Cu	
	Zn	
(ppb)	I	
	At	
	Ga	
	Ge	
	As	
	Se	
	Mo	
	Tc	
	Ru	
	Rh	
	Pd	
	Ag	
	Cd	
	In	
	Sn	
	Sb	
	Te	
	Cs	430
	Ta	1680
	W	
	Re	
	Os	
	Ir	3.7
	Pt	
	Au	1.0
	Hg	
	Tl	
	Bi	
		(1)

References and methods:

(1) Korotev (1984 unpublished); INAA

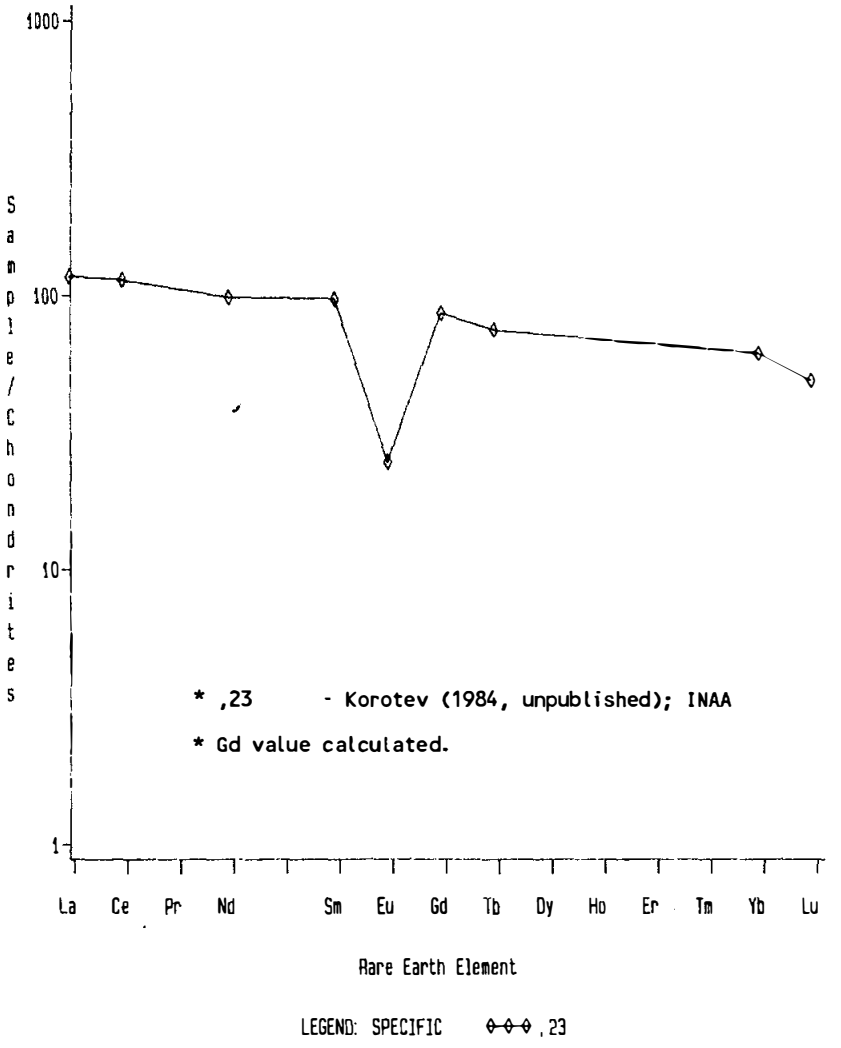

Figure 3. Rare earths in 15266.

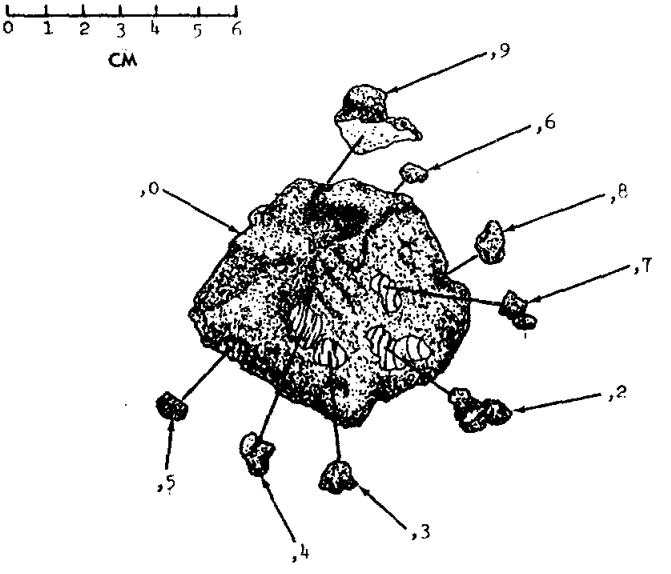

Figure 4. Chipping of 15266.

15267 REGOLITH BRECCIA ST. 6 1.8 g

INTRODUCTION: 15267 is a medium dark gray regolith breccia. It is blocky, subangular, and coherent. It appears to lack zap pits. There is a glass cover on one side, which contains vesicles. 15267 was collected (with 15259, 15265, 15266, 15268, 15269, and 15285 to 15289) from the crest of an inner bench on the northeast wall of the 12 m crater at Station 6, downslope 15 m from the LRV. It was part of the same rock from which 15265 and 15266 came, broken by the Commander, but 15267 has not been identified on surface photographs. It has never been subdivided or allocated.

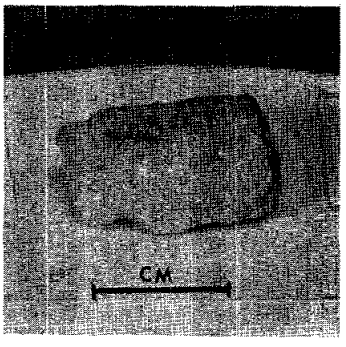

Figure 1. 15267. S-71-44225

15268 REGOLITH BRECCIA ST. 6 11.0 g

INTRODUCTION: 15268 is a coherent regolith breccia with a typical complement of regolith breccia components. It is chemically fairly similar to Station 6 soils. It is medium gray, slabby, subrounded, and fairly homogeneous, except for a white breccia band (Fig. 1). There were a few zap pits dominantly on the "B" side. 15268 was collected (with 15259, 15265 to 15267, 15269, and 15285 to 15289) from the crest of an inner bench on the northeast wall of the 12 m diameter crater, downslope 15 m from the LRV. It was lying very close to 15265-15267 and may have spalled from it.

PETROLOGY: 15268 is a porous regolith breccia, in appearance quite similar to 15266 (Fig. 2). It contains abundant glass as spheres and shards, although red/orange and yellow glasses appear to be very rare. Several small lithic clasts appear to be mare basalts. Few of the constituents are heavily shocked. Gleadow et al. (1974) studied 15268 but did not publish details; in the same study Sewell et al. (1974) reported defocussed beam analyses of several clasts ranging from anorthosites to "metabasalts" to breccias. They also analyzed pyroxenes and plagioclases, and several glasses which include medium-K KREEP, mare basalt, green glass, and aluminous varieties. McKay et al. (1984) reported an I_s/FeO of 22-34, which was reported by Korotev (1984 unpublished) as 32. The pale band visible macroscopically (Fig. 1) does not occur in the thin sections.

CHEMISTRY: A single analysis by Korotev (1984 unpublished) is a little enriched in incompatible elements compared with local soils (Table 1, Fig. 3), and is more like 15265-15267, from which it may have spalled.

PROCESSING AND SUBDIVISIONS: ,1 was originally chipped from ,0 (Figs. 1, 4), and two thin sections (,4 and ,7) produced from it. Interior chips ,8 and ,9 were later removed from ,0 to fulfill the McKay and coworker allocations. ,0 is now 8.9 g.

Figure 1. 15268 following chipping. S-71-59880

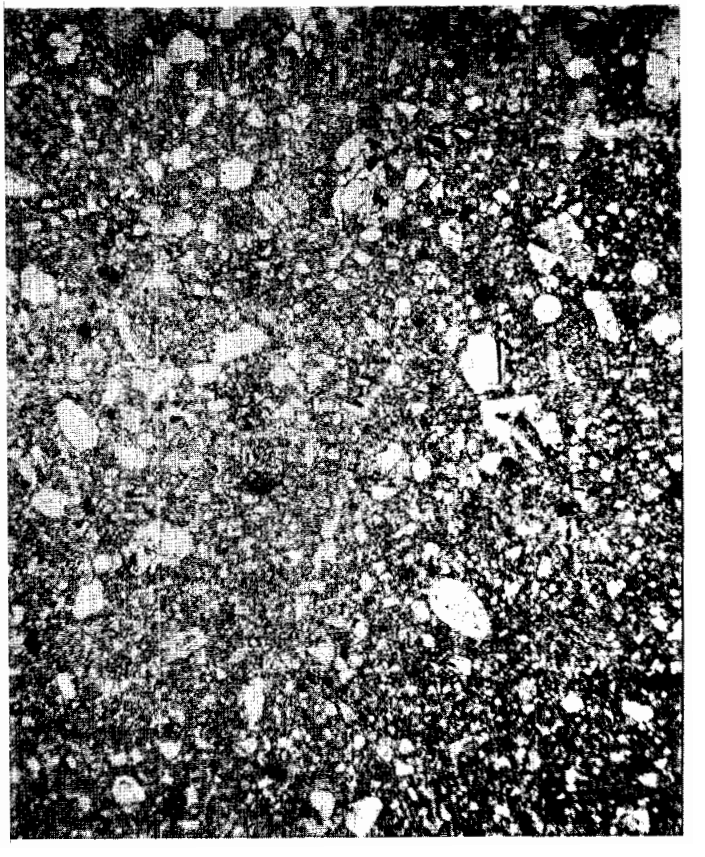

Figure 2. Photomicrograph of 15268,4. Width about 2 mm. Transmitted light.

TABLE 15268-1. Chemical analysis

		,8
Wt %	SiO2	
	TiO2	
	Al2O3	
	FeO	11.8
	MgO	
	CaO	11.3
	Na2O	0.53
	K2O	
	P2O5	
(ppm)	Sc	23.2
	V	
	Cr	2150
	Mn	
	Co	36.8
	Ni	217
	Rb	
	Sr	160
	Y	
	Zr	450
	Nb	
	Hf	11.4
	Ba	334
	Th	5.3
	U	1.6
	Pb	
	La	30.7
	Ce	81
	Pr	
	Nd	45
	Sm	14.4
	Eu	1.54
	Gd	
	Tb	2.80
	Dy	
	Ho	
	Er	
	Tm	
	Yb	10.0
	Lu	1.39
	Li	
	Be	
	B	
	C	
	N	
	S	
	F	
	Cl	
	Br	
	Cu	
	Zn	
(ppb)	I	
	At	
	Ga	
	Ge	
	As	
	Se	
	Mo	
	Tc	
	Ru	
	Rh	
	Pd	
	Ag	
	Cd	
	In	
	Sn	
	Sb	
	Te	
	Cs	330
	Ta	1340
	W	
	Re	
	Os	
	Ir	6.7
	Pt	
	Au	1.9
	Hg	
	Tl	
	Bi	
		(1)

References and methods:

(1) Korotev (1984 unpublished); INAA

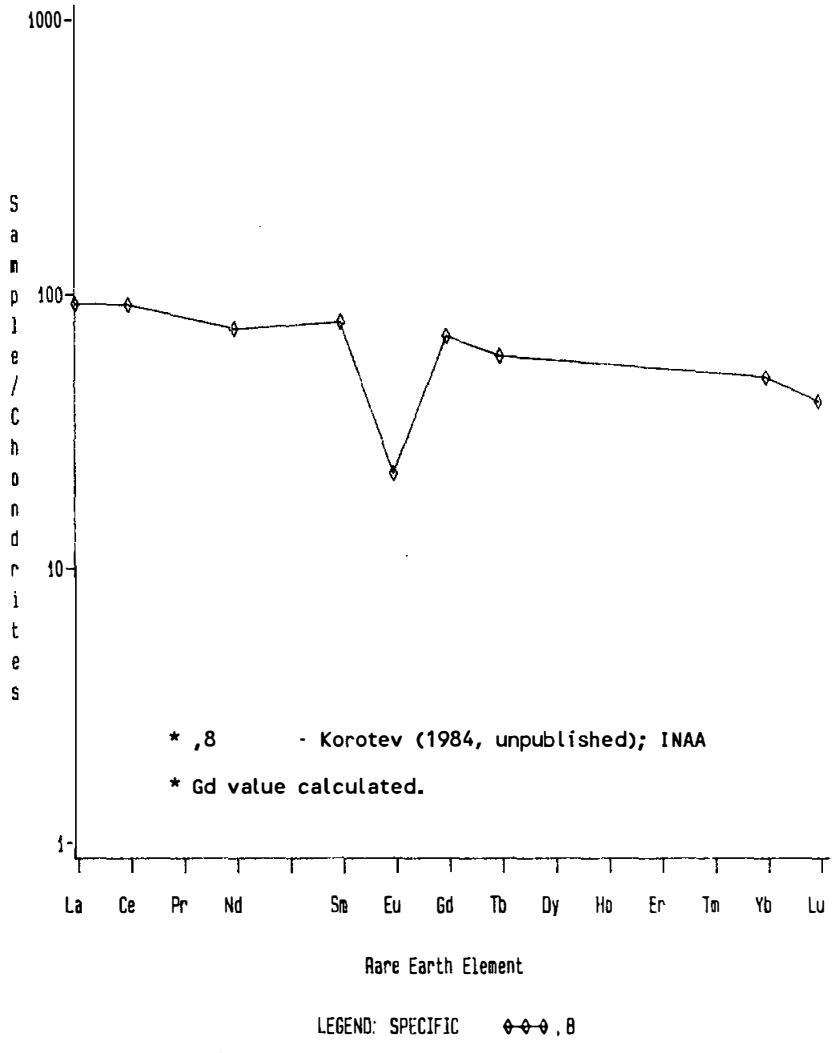

Figure 3. Rare earths in 15268,8.

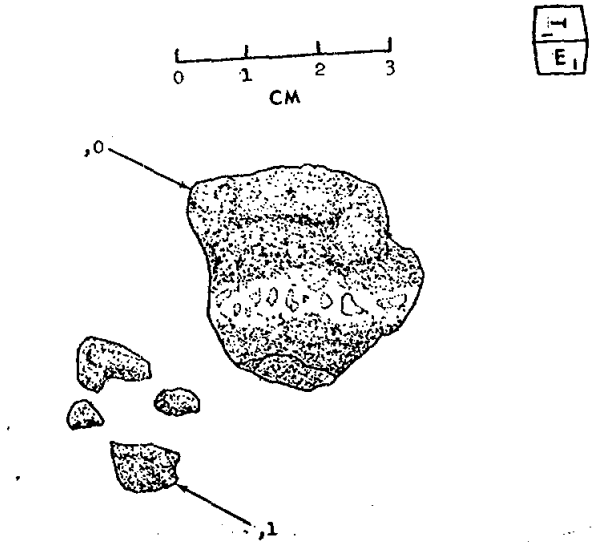

Figure 4. Original chipping of 15268.

15269 REGOLITH BRECCIA, GLASS-COATED ST. 6 6.0 g

INTRODUCTION: 15269 is a glassy regolith breccia with a vesicular glass coat (Fig. 1). It is tough, grayish black, and prismatic or angular. The glass coat is black. The contact of glass coat and glassy breccia is locally sharp, but elsewhere they grade, either rapidly or through a porous, sintered zone. The appearance is of melted breccia, not splash glass. 15269 was collected (with 15259, 15265 to 15268, and 15285 to 15289) from the crest of an inner bench on the north-east wall of the 12 m crater 15 m downslope from the LRV. Like 15268, it was lying very close to 15265-15267 and may have spalled from it.

PETROLOGY: 15269 is a very glassy, coherent, foliated regolith breccia. It contains abundant colorless glass shards. Lithic clasts are generally small, and include fine-grained feldspathic impact melts, as well as anorthositic materials. KREEP and mare basalt fragments are not conspicuous. The glass coat is vesicular and extremely heterogeneous, containg clasts. In thin sections the contact with underlying breccia is quite sharp but irregular.

PROCESSING AND SUBDIVISIONS: Two chips were taken, only one of which was numbered (,1) (Fig. 3). This produced thin sections ,4 and ,6. ,0 is now 5.9 g.

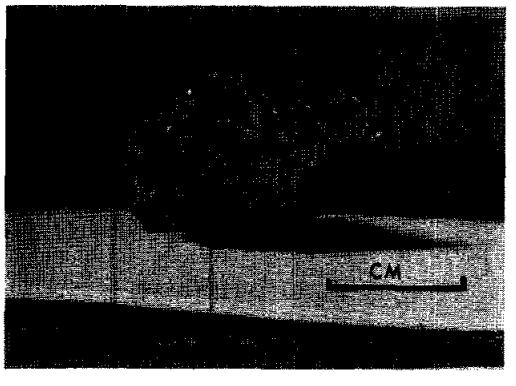

Figure 1. Pre-split view of 15269. S-71-45827

Figure 2. Photomicrograph of 15269,4. Width about 2 mm. Transmitted light. Glass coat is at top.

Figure 3. Chipping of 15269.

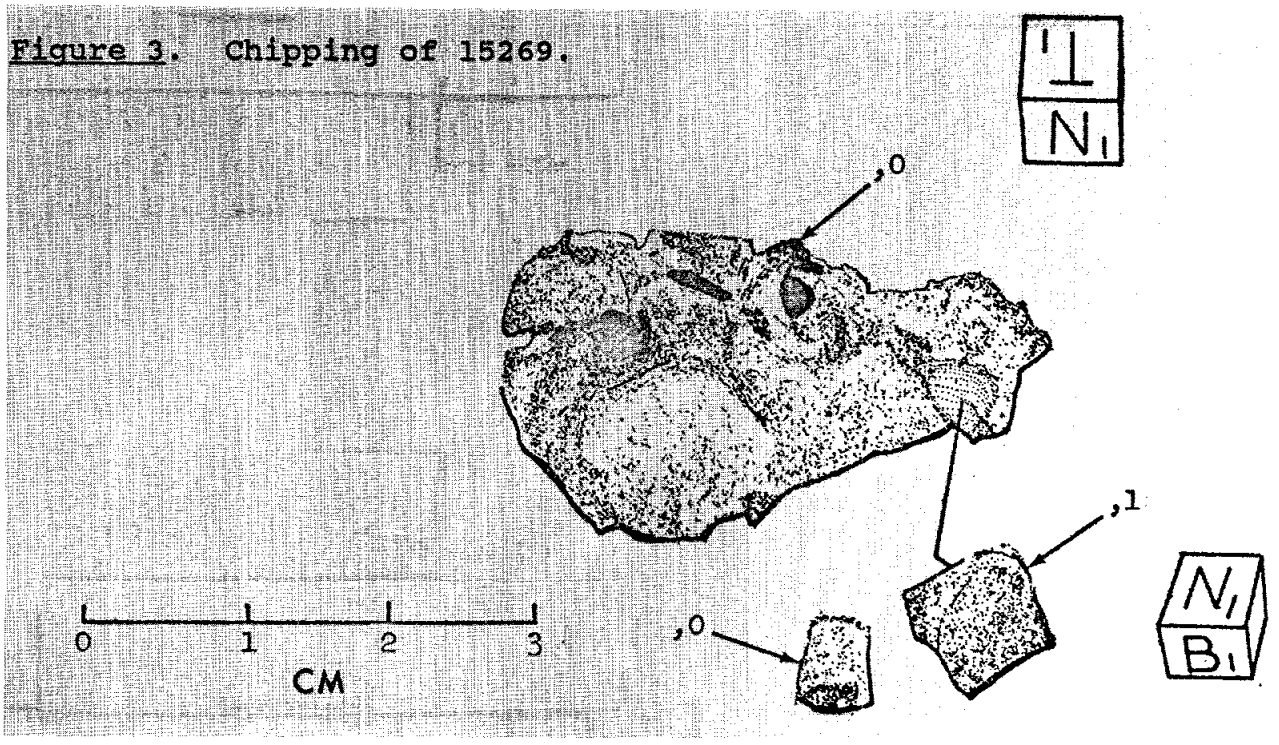

15285 REGOLITH BRECCIA, GLASS-COATED ST. 6 264.2 g

INTRODUCTION: 15285 is a medium dark gray regolith breccia which is partly glass-coated (Fig. 1). Its composition is similar to local soils. It contains a normal complement of regolith breccia constituents and fragments of mare basalt, KREEP basalt, and poikilitic melt clasts in addition to glass and mineral fragments. 15285 was collected (with 15259, 15265 to 15269, and 15286 to 15289) from the crest of an inner bench on the northeast wall of the 12 m crater, downslope 15 m from the LRV. Like several other samples, it was lying very close to 15265-15267 and could have spalled from it, although its composition is not the same. Its orientation is known.

Figure 1. Post-split view of 15285 showing interior matrix and exterior glass coat.

PETROLOGY: 15285 is a regolith breccia (Fig. 2). Wentworth and McKay (1984) found it to be compact, with a density of 2.35 g/cc (intrinsic density of 3.11 g/cc), with a calculated porosity of 23.8%. O'Kelley et al. (1972) listed a density of 2.4 g/cc.

The matrix of 15285 is fairly dark and has a vague foliation. Glass exists as spheres and shards which are mainly colorless or devitrified to brown, with some yellow and very rare red/orange shards. Lithic clasts include mare basalts, KREEP basalts, and various highlands breccias. One fragment is a high-Ti mare basalt, apparently unique in Apollo 15 breccias. Mineral clasts include some which are heavily shocked. The glass coat is gray, and very vesicular, and has tiny vesicles along its sharp contact with the breccia.

Engelhardt et al. (1972, 1973) described 15285 as a regolith breccia with a mafic/plagioclase ratio of 1.2, and noted that its matrix was fragmental and perhaps partly glassy. They mentioned ophitic and intersertal basalts, and "Apennine Mountain" fragments (plagioclase-rich breccias). Lovering and Wark (1973) depicted an Apollo 15 KREEP basalt ("KREEP-rich non-mare basalt") in one thin section. Reid et al. (1977) noted that 15285 contained poikilitic clasts, and was one of only two Apollo 15 breccias they studied which contained such material. They also depicted an Apollo 15 KREEP basalt clast and gave brief mineral data for it. Sewell et al. (1974) presented defocussed beam analyses of several clasts with a range of compositions, and also presented a variety of glass analyses. This data was used in the summary petrology of Gleadow et al. (1974) without specific reference.

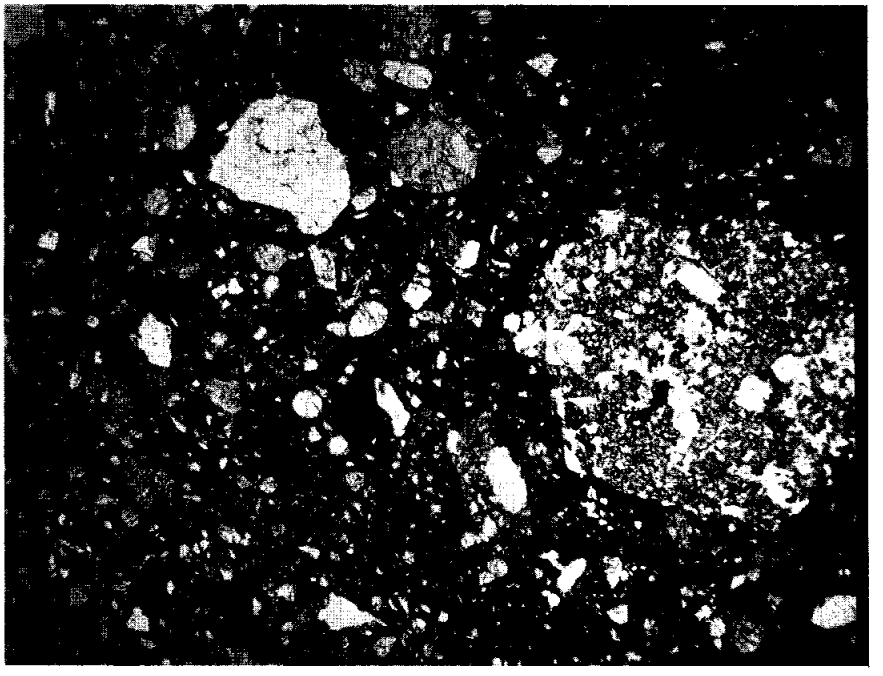

Figure 2. Photomicrograph of 15285,57. Width about 2mm. Transmitted light. Large clast is a poikilitic impact melt.

CHEMISTRY: Chemical analyses for 15285 breccia are listed in Table 1 and rare earths are shown in Figure 3. The authors presented little specific discussion. The compositions are similar to each other and to local soils, although the "total" analysis by S.R. Taylor et al. (1973) has higher iron and slightly lower alumina than either other analyses or the local soil. The two rare earths determined by Christian et al. (1973) appear anomalous. S.R. Taylor (1973) and S.R. Taylor et al. (1972) plotted the analysis as a 30% highland basalt (HB) and 70% low-K Fra Mauro (LKFM) mixture; S.R. Taylor et al. (1973) changed these figures to 11.8% HB and 88.2% LKFM for their "total" analysis and 9.7% HB and 90.3% LKFM for their "black" analysis. Gros et al. (1976) referred to 15285 as a "misclassified soil breccia" for some unknown reason.

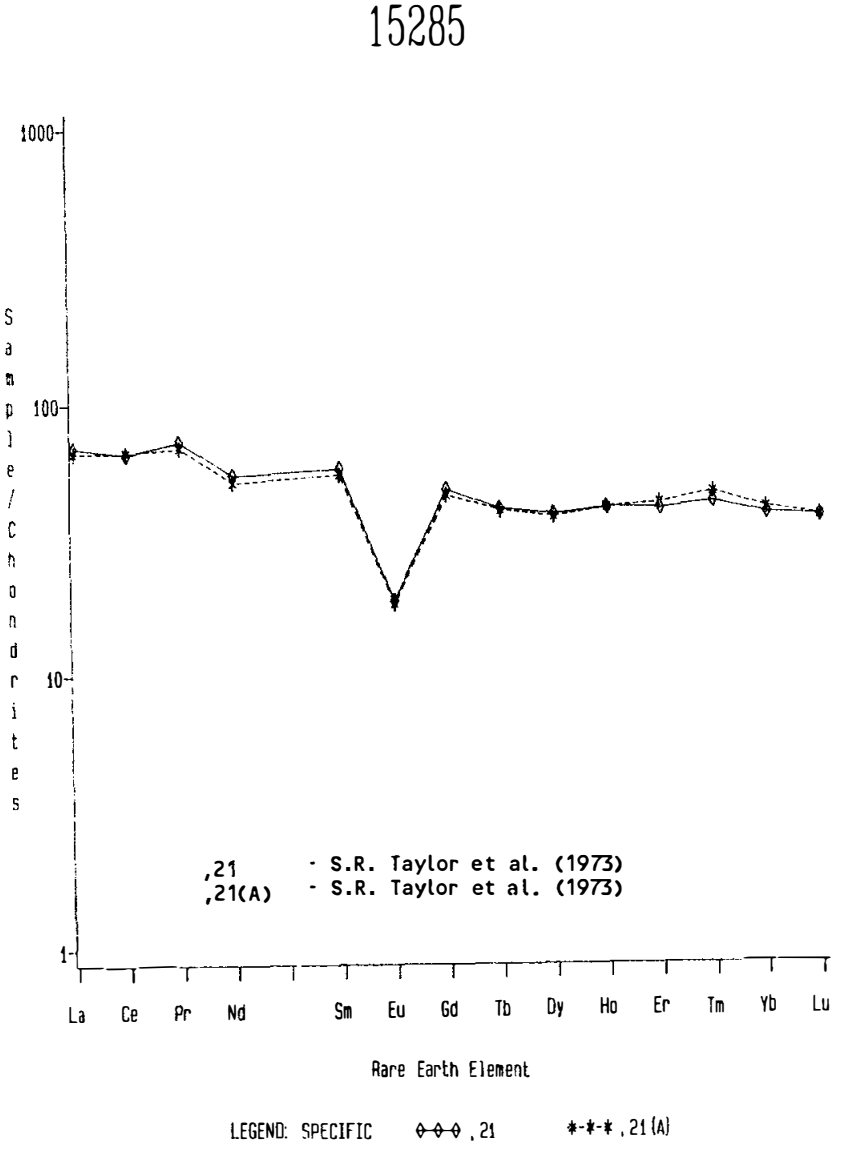

Figure 3. Rare earths in 15285 matrix.

EXPOSURE: O'Kelley et al. (1972a,b,c) and Eldrige et al. (1972) presented disintegration count data for radionuclides, without discussion. Yokoyama et al. (1974) used the ^{22}Na-^{26}Al method to determine that ^{26}Al activity was unsaturated, hence the surface residence time has been less than about 1 m.y. Bhattacharya (1976) included 15285 in a track study, but presented little specific data.

PROCESSING AND SUBDIVISIONS: Pieces were chipped from several parts of 15285 (e.g., Figs. 1, 4). ,1 (not shown) produced thin sections ,6 to ,15 which are of interior breccia. ,16 produced thin section ,43. ,25 produced thin sections ,31 and ,32, also interior breccia. ,54 produced thin sections ,36 and ,55 to ,59, which are of breccia and glass coat. ,0 is now 221 g and no other split is as large at 7 g.

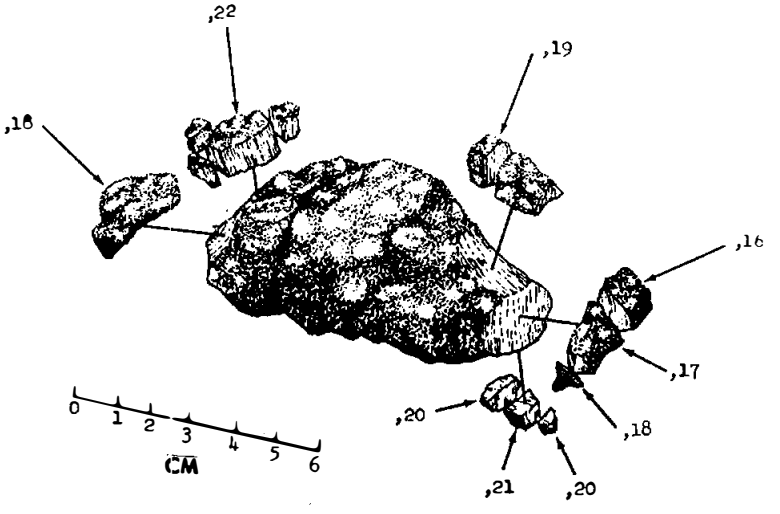

Figure 4. Part of chipping of 15285.

TABLE 15285-1. Chemical analyses of breccia

		,21	,21(a)	,5	,24	,18	,0
Wt %	SiO2	45.6	46.7	45.71			
	TiO2	1.34	1.31	1.56			
	Al2O3	15.2	15.7	16.55			
	FeO	15.0	12.9	12.83			
	MgO	11.6	11.4	11.05			
	CaO	10.3	10.8	10.76			
	Na2O	0.44	0.38	0.46			
	K2O		0.15	0.27			0.192
	P2O5			0.26			
(ppm)	Sc	17.0	19.0	24			
	V	102.0	98.0	68			
	Cr	2600	3100	2054			
	Mn	1300		1400			
	Co	56.0	66.0	36			
	Ni	300	190	180	198		
	Rb	4.1	4.5	4.8	4.77		
	Sr			120			
	Y	80.0	65.0	84			
	Zr	340.0	322.0	390			
	Nb	24.0	23.0	22			
	Hf	6.5	7.7				
	Ba	280	260	270			
	Th	3.5	4.2				3.4
	U	0.81	1.03		0.980		0.93
	Pb	1.7	3.6	2.8			
	La	23.0	22.0	15			
	Ce	58.0	59.0				
	Pr	8.2	7.8				
	Nd	33.0	31.0				
	Sm	10.5	10.0				
	Eu	1.3	1.27				
	Gd	12.0	11.4				
	Tb	1.93	1.9				
	Dy	12.4	12.1				
	Ho	2.9	2.9				
	Er	8.2	8.6				
	Tm	1.3	1.4				
	Yb	7.8	8.2	11			
	Lu	1.3	1.3				
	Li			8.0			
	Be			2.6			
	B						
	C						
	N						
	S					1170	
	F						
	Cl						
	Br				0.121		
	Cu	9.2	11.2	8.8			
	Zn			18	22.4		
(ppb)	I						
	At						
	Ga	3600	4500	4200			
	Ge				391		
	As						
	Se				220	290	
	Mo						
	Tc						
	Ru						
	Rh						
	Pd				6.8		
	Ag				7.62	9.9	
	Cd				57.0		
	In				3.94		
	Sn	270	290				
	Sb				1.39		
	Te				12.1		
	Cs	150	190		234		
	Ta						
	W	80	300				
	Re				0.480	0.49	
	Os				6.69	6.5	
	Ir				5.18	6.7	
	Pt						
	Au				2.25	3.1	
	Hg						
	Tl				3.2	2.3	
	Bi				0.78	0.60	
		(1)	(1)	(2)	(3)	(4)	(5)

References and methods:

(1) S.R. Taylor et al. (1973); electron probe, spark source mass spectrography, emission spec.
(2) Christian et al. (1976); XRF, semi-micro, emission spectrographic
(3) Gros et al. (1976); RNAA
(4) Hughes et al. (1973); RNAA
(5) O'Kelley et al. (1972a,b,c); gamma ray spectroscopy

Notes:

(a) listed as "black"

15286 GLASS AND REGOLITH BRECCIA ST. 6 34.6 g

INTRODUCTION: 15286 is a two-component rock: a piece of regolith breccia is intruded by and/or coated with a vesicular black glass (Fig. 1). Limited data suggest that the glass is fairly similar to but not identical with local soils. The glass composition is a moderately good glass-former, though not equivalent to commercial glass. The breccia is a typical medium gray regolith breccia with glass, mineral, and lithic fragments in a low-porosity matrix. It is coherent to tough. Zap pits occur as few to many on all surfaces, and are especially well developed on the glass. The sample was collected (along with 15159, 15265 to 15269, 15285, and 15287 to 15289) from the crest of an inner bench on the northeast rim of the 12 m crater, downslope 15 m from the LRV. Like several other samples, it was lying very close to 15265-15267 and may have spalled from it. However, it has not been identified in photographs.

PETROLOGY: The breccia and glass were described by Wosinski et al. (1973) and by Winzer et al. (1978) and Winzer (1978). According to Wosinski et al. (1973), the glass is vesicular, with clear and devitrified patches, and vesicles are 100 micron to 10 microns in diameter (however, much larger ones up to 5 mm can be seen macroscopically and in thin sections). The glass contains tiny FeNi and (Fe,Ni)S spheres. The dendritic, devitrified phase is scattered throughout the glass. Winzer et al. (1978) noted that a thin vesicular region separates the breccia and the glass, and that the vesicles are deformed. The Fe and FeS droplets are complex. The glass contains one of the highest proportions of fragments among those of Apollo 15 analyzed by the Winzer group, and is the most heterogeneous (other patches are not so heterogeneous; see Fig. 2a). The dendritic phase consists of tiny crystallites of olivine (Fo_{78-76}), with some elongated, larger (80 microns) crystals being more magnesian (Fo_{83-78}). No pyroxene was observed. Analyses of the rind glass show it to be fairly similar to local soil, but the analysis of Uhlmann and Klein (1976) is less aluminous and more iron-rich.

Mehta et al. (1979) investigated the submicroscopic metal particles in the glass coat. Almost all are rounded and consist of the two-phase assemblage metal and FeS. In the metal, Ni constitutes 9.4 to 15.5%. The sulfide is nearly stoichiometric troilite with up to 1.3% Ni. Coarse (larger than 1 micron) patches are similar to fine particles in both chemistry and structure, indicating that both are meteoritic debris; experiments suggest that the metal formed as fine silicate melt. The structure indicates rapid solidification of metal-sulfide liquids, and does not display the cubic-shaped metal found for reduction to Fe^{o} metal.

The breccia was found by McKay et al. (1974) to be immature (Is/FeO = 9 to 15; listed by Korotev, 1984 unpublished, as 13). It consists of anhedral and angular fragments, including pigeonite, augite, and plagioclase, and many are shocked (Wosinski et al., 1973). Winzer (1978) analyzed five clasts (possibly in the glass coat?) with an area scan technique, finding a fairly restricted range of compositions (23.3 to 25.6% Al_2O_3) which he suspected was a function of the portion sampled, and not a good indicator of a limited provenance. Inspection of several thin sections indicates a wide variety of clasts, including mare basalts and possibly KREEP basalts. Glasses are dominantly colorless or yellow, but rare orange/red glass is present. Best and Minkin (1972) included 15286 in an analytical study of glasses, but did not specify data from 15286. An average composition of matrix glass was given by Handwerker et al. (1972) and was deemed to be similar to the coat glass (Table 1).

TABLE 15286-1. Analyses of glass

	Coat	Coat	Matrix
SiO2 %	47.35	46.1	47.6
TiO2	1.44	1.6	1.2
Al2O3	15.86	14.3	13.3
FeO	12.76	14.2	13.6
MgO	10.42	12.5	13.6
CaO	10.78	10.4	9.8
Na2O	0.45	0.8	0.7
K2O	0.21	0.1	0.3
Cr ppm	3080	---	---
	(1)	(2)	(3)

(1) Winzer et al. (1978); SEM, considerable uncertanities
(2) Uhlmann and Klein (1976), Hardwerker et al. (1977); microprobe
(3) Hardwerker et al. (1977); microprobe

In a series of papers, the Uhlmann group carried out experiments on their glass and matrix glass compositions to investigate their glass-forming properties, cooling rates, and inferred body sizes for the 15286 glasses (Uhlmann and Klein, 1976; Handwerker et al., 1977; Uhlmann and Onorato, 1979; Uhlmann et al., 1979, 1981; Yinnon et al., 1980). They measured the viscosities of molten glass made to their coat and matrix glass compositions (Fig. 3), and measured crystal growth rates as a function of temperature (Fig. 4). For the glass coat, the glass transition temperature was about 650°C, and maximum growth was 1.1×10^{-2} cm^{-1} at an undercooling of about 120°C. The liquidus temperature was determined to be 1210 ± 10°C. From TTT diagrams, CT curves show it would be necessary to cool 15286 glass coat at 120°C min^{-1} or faster to produce a glass (Uhlmann and Klein, 1976). Such a rate is consistent with the thickness presently observed (about 1 cm) suggesting that the molten material intruded (or coated) cold rock. Yinnon et al. (1980) used differential thermal analysis and revised the cooling rate using newly determined nucleation barriers and crystallization statistics analysis to determine a rate of 1.3°C sec^{-1} (80°C min^{-1}) for the glass coat. Uhlmann et al. (1981) used the simplified glass formation model of Uhlmann and Onorato (1979) to determine a critical cooling rate of 6.2°C sec^{-1} for the glass coat composition (compared with 2°C sec^{-1} measured). Handwerker et al. (1977) found that the matrix glass (which they treated as forming in a separate event from the glass coat) had a transition temperature of 644°C. Its liquidus temperature is 1270°C ± 10; viscosity and crystal growth rates as a function of temperature are shown in Figures 3 and 4 respectively. From CT curves (Fig. 6) this matrix glass must have cooled in the region below the liquidus at 80°C min^{-1}; from crystallization statistics the cooling rate was determined to be 42°C min^{-1} to form a glass, i.e., the breccia matrix glass is a better glass-former than the coat. Annealing tests indicate that the matrix formed by cooling of molten material, not a shock-induced crystal-to-glass transition. The calculated thickness for the appropriate cooling is about 3 cm, about that observed for the rock; a more sophisticated analysis would still suggest cooling in a small body, or at the edge of a large body. The matrix glass also precludes much reheating by the glass coat, locally to 825°C perhaps. Yinnon et al. (1980) used differential thermal analysis and used newly determined nucleation barriers and crystallization statistics analyses to determine a cooling rate of 0.11°C sec^{-1} for the matrix glass. Uhlmann et al. (1981) determined a critical cooling rate of 7.4°C sec^{-1} for the matrix glass (compared with 0.3°C sec^{-1} measured).

CHEMISTRY: An analysis, mainly for trace elements, of the matrix was made by Korotev (1984, unpublished) (Table 2, Fig. 7). The rare earths and other incompatibles are enriched a little over local soils, and is more like 15265, from which it may well have spalled.

MICROCRATERS: Brownlee et al. (1973, 1975) studied the depth/diameter relationships for craters on a surface glass chip (Figs. 8, 9). They found no strong dependence of P/Dp on Dp (Fig. 8). Combined with data from other rocks, the indications are that most of the projectiles had mean densities of 2 to 4 gm cm^{-2} (i.e., silicates, not iron), and had velocities of 20 ± 5 km/sec. The size-frequency distribution (Fig. 9) was made by optical examination of the entire surface glass and SEM examination of a 7 mm^2 chip (,11). The data agree well with that for 15205 but do not show a depletion in the 1 to 20 micron size range. Horz et al. (1975) noted that the distribution was unique in not showing bimodality (i.e., 1 to 20 micron depletion), and suggested the possibility that the surface was pointing out of the ecliptic and sampling a different micrometeorite population.

PROCESSING AND SUBDIVISIONS: Two loose chips in the sample bag were determined to be fragments of 15286 and numbered ,1 and ,2. Both chips are very glassy and heavily cratered. Both were entirely subdivided (Fig. 10), ,1 by sawing to produce a chip of the glass coat. Most allocations were made from daughters of ,1. ,6 produced thin sections ,33 to ,36 and ,11 produced thin section ,41. A daughter of ,2 (,3) produced thin section ,15. A new chip directly from ,0 (,27) produced thin sections ,29 and ,30, which are regolith breccia, unlike the other dominently vesicular glass sections. Further chipping from ,0 produced the McKay and co-workers (e.g., Korotev) samples of interior breccia.

TABLE 15286-2. Chemical analyses

		,42
Wt %	SiO2	
	TiO2	
	Al2O3	
	FeO	12.3
	MgO	
	CaO	9.6
	Na2O	0.56
	K2O	
	P2O5	
(ppm)	Sc	24.1
	V	
	Cr	2440
	Mn	
	Co	37.9
	Ni	199
	Rb	
	Sr	135
	Y	
	Zr	490
	Nb	
	Hf	12.7
	Ba	345
	Th	5.4
	U	1.53
	Pb	
	La	34.0
	Ce	90
	Pr	
	Nd	52
	Sm	15.8
	Eu	1.61
	Gd	
	Tb	3.09
	Dy	
	Ho	
	Er	
	Tm	
	Yb	11.0
	Lu	1.51
	Li	
	Be	
	B	
	C	
	N	
	S	
	F	
	Cl	
	Br	
	Cu	
	Zn	
(ppb)	I	
	At	
	Ga	
	Ge	
	As	
	Se	
	Mo	
	Tc	
	Ru	
	Rh	
	Pd	
	Ag	
	Cd	
	In	
	Sn	
	Sb	
	Te	
	Cs	380
	Ta	1490
	W	
	Re	
	Os	
	Ir	5.9
	Pt	
	Au	2.2
	Hg	
	Tl	
	Bi	
		(1)

References and methods:

(1) Korotev (1984, unpublished); INAA

Fig. 1a

Fig. 1b

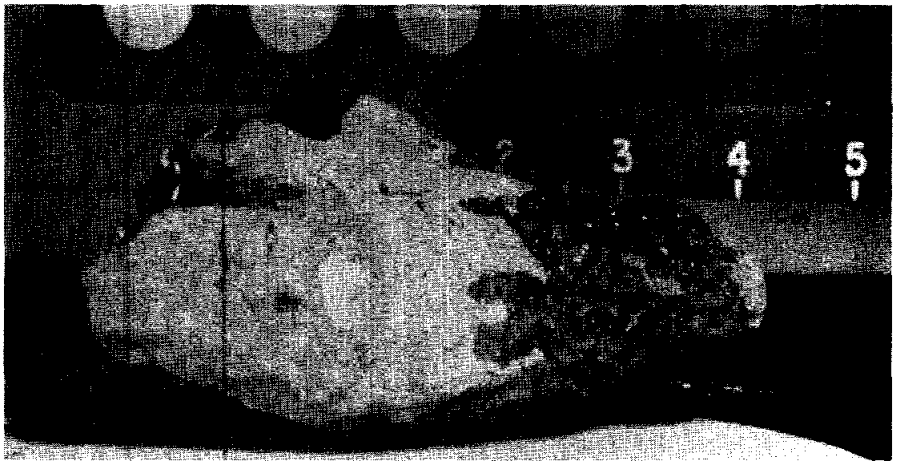

Figure 1. Main mass of 15286. (a) S-71-44952, (b) S-71-44951.

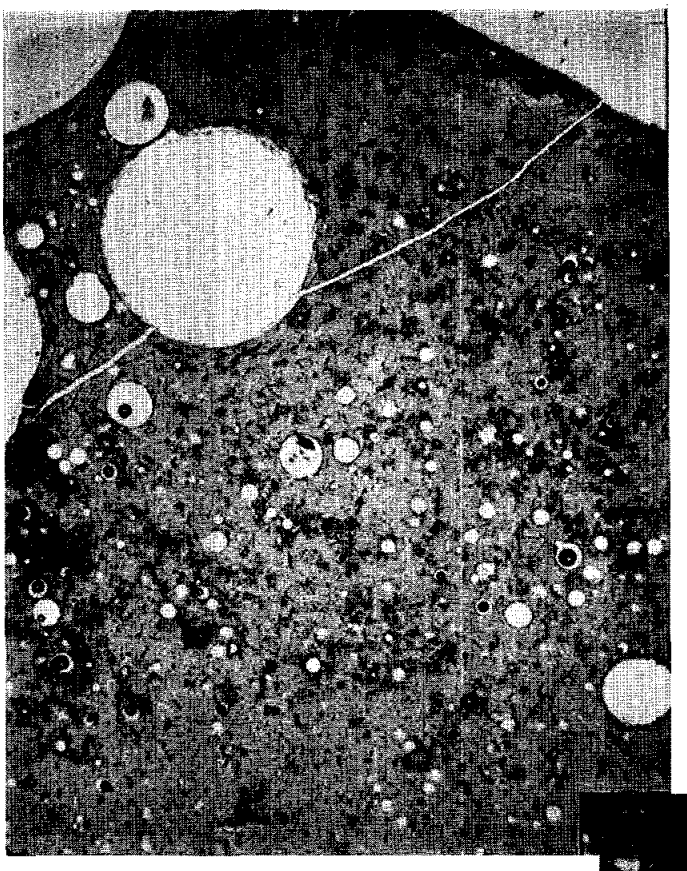

Fig. 2a

Fig. 2b

Figure 2. Photomicrographs of 15286. Widths about 2 mm. Transmitted light. a) 15286,33, vesicular glass coat; b) 15286,30, general matrix.

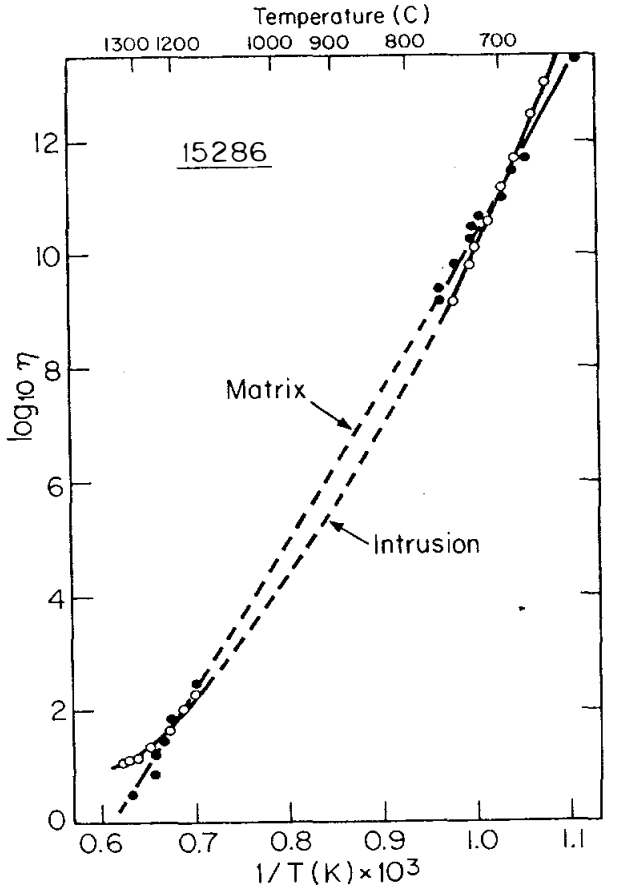

Figure 3. Viscosity vs. temperature for matrix and intrusion (coat) compositions (Handwerker et al., 1977).

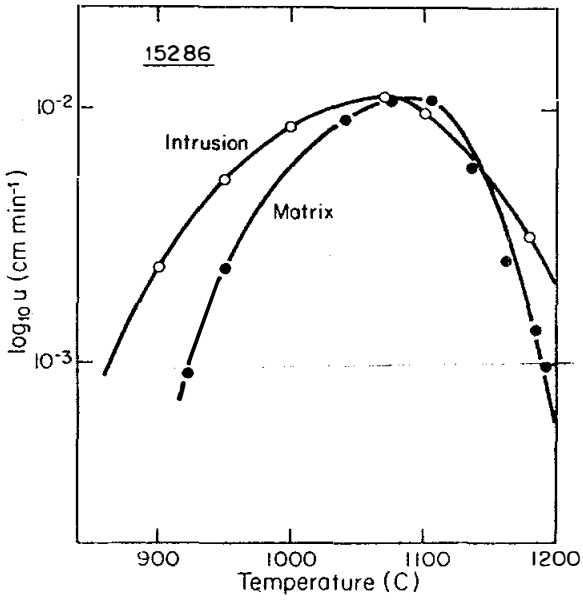

Figure 4. Crystal growth rates vs. temperature for matrix and intruction (coat) compositions (Handwerker et al., 1977).

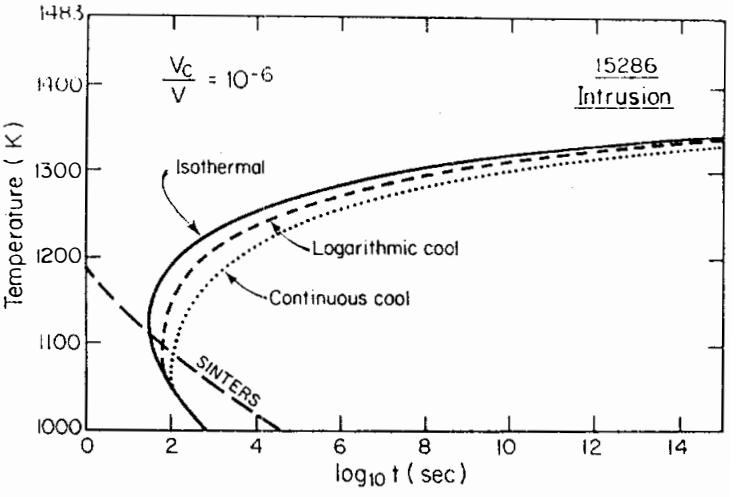

Figure 5. Isothermal time-temperature-transformation, logarithmic cooling (CT), and constant-rate continuous cooling CT curves for glassy intrusion (coat) on 15286 (Handwerker et al., 1977).

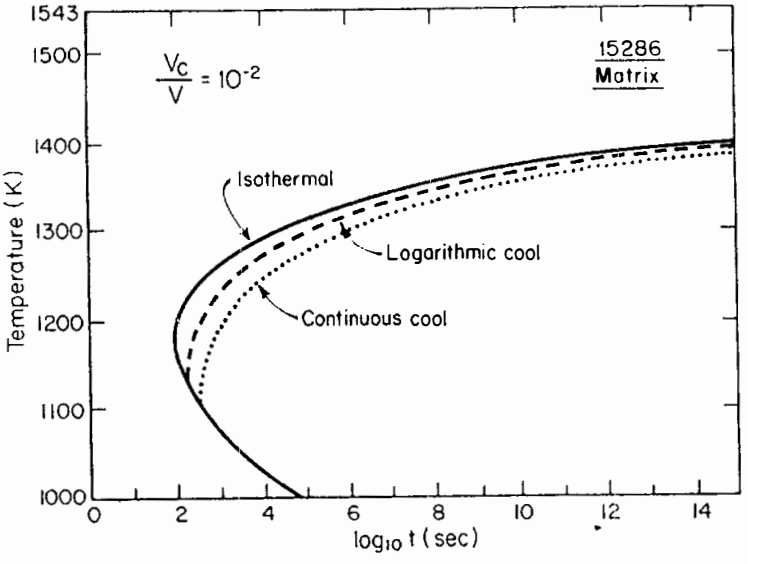

Figure 6. Isothermal time-temperature-transformation, logarithmic cooling (CT), and constant-rate continuous cooling CT curves for the matrix composition of 15286 (Handwerker et al., 1977).

15286

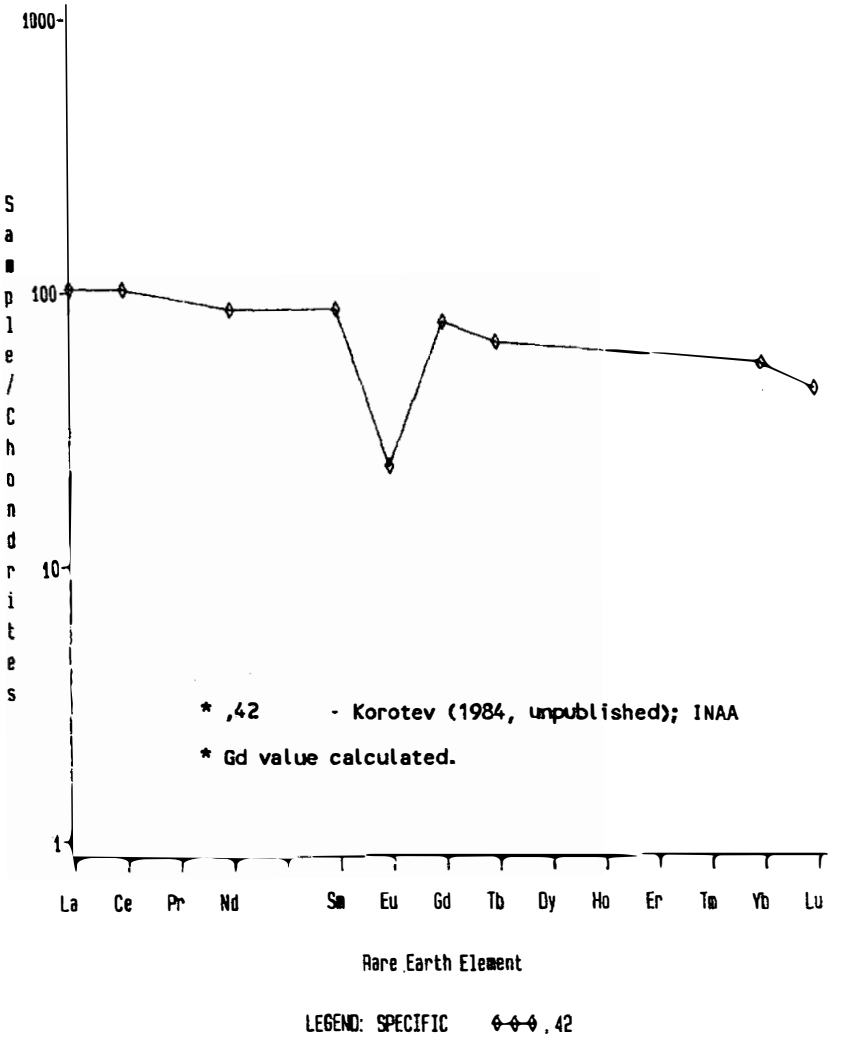

Figure 7. Rare earths in breccia matrix.

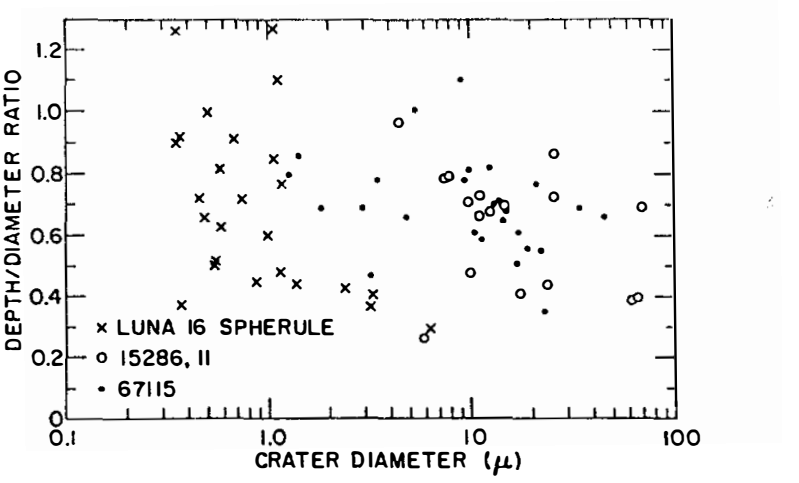

Figure 8. Depth/diameter vs. diameter in glass of 15286 (Brownlee et al., 1973).

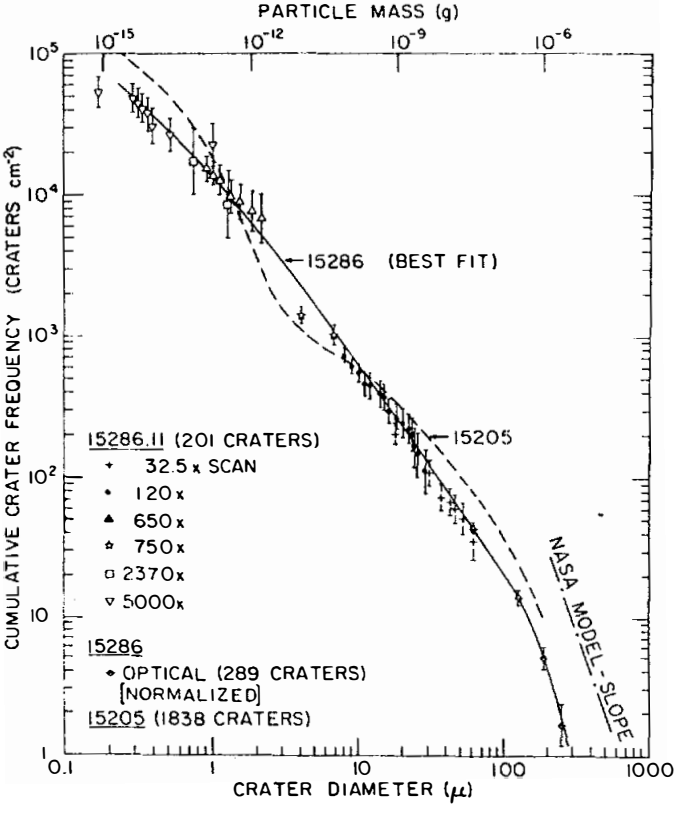

Figure 9. Size frequency for craters on 15286 and 15205. Error bars indicate uncertainty from counting only (Brownlee et al., 1973).

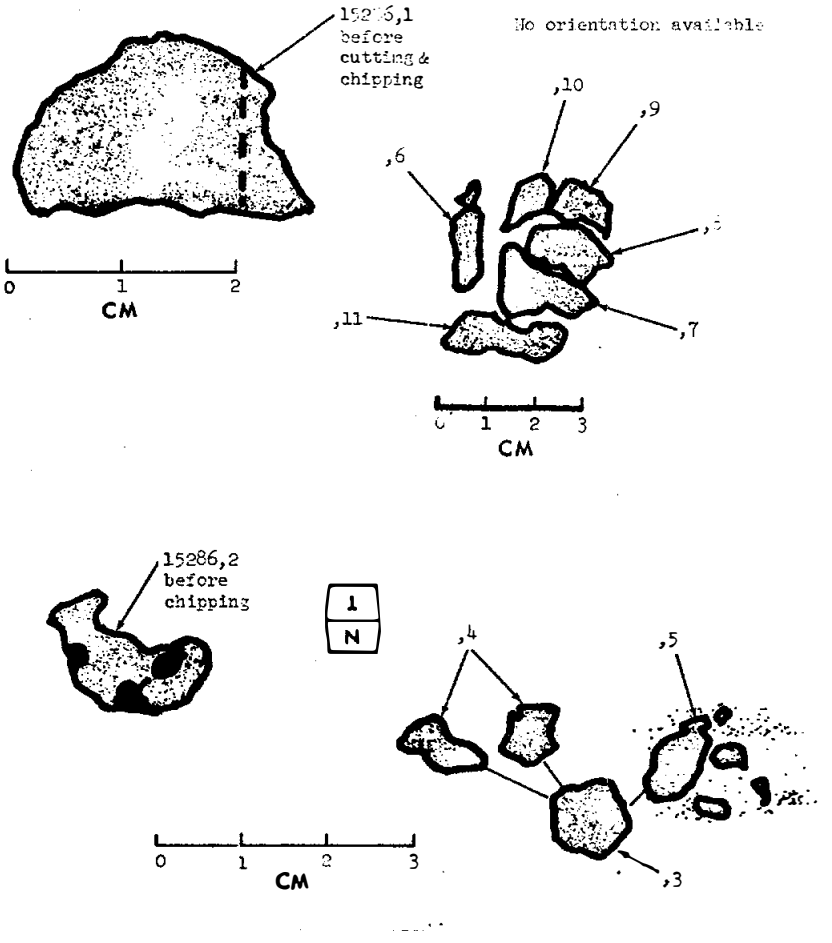

Figure 10. Subdivision of 15286,1 and 15286,2.

15287 REGOLITH BRECCIA ST. 6 44.9 g

INTRODUCTION: 15287 is a coherent regolith breccia which is generally fine-grained. It has a typical complement of regolith breccia constituents. Its composition is more KREEP-rich than local soils. It is olive gray, blocky, subrounded, and smooth (Fig. 1). It had many zap pits on one side but few on others. The sample was collected (along with 15259, 15256 to 15269, 15285, 15286, 15288, and 15289) from the crest of an inner bench on the northeast rim of the 12 m crater, downslope 15 m from the LRV. Like several other samples, it was lying very close to 15265-15267 and may have spalled from it. However, it has not been identified in site photographs.

PETROLOGY: 15287 is a fine-grained regolith breccia (Fig. 2). It is very porous, and generally it constituents are unshocked. Its glass fragments are mainly colorless or devitrified brown. Varied glassy or glassy breccia clasts are present. A few partly crystalline green glass spheres are present. Lithic clasts include mare basalts and possibly small KREEP basalt fragments. McKay et al. (1984) reported an I_s/FeO of 19 to 29, which Korotev (1984 unpublished) reported as 28.

CHEMISTRY: An analysis, mainly for trace elements, was made by Korotev (1984 unpublished) (Table 1, Fig. 3). 15287 appears to be more KREEP-rich than local soils, is like 15265 and its other possible spalls, and is possibly exotic and spalled off 15265-15267.

PROCESSING AND SUBDIVISIONS: ,1 was knocked cleanly off the top (Fig. 4) and was made into a potted butt. Thin sections ,5; ,7; and ,8 have been cut from it. ,0 was later chipped to obtain interior matrix chips ,10 and ,11.

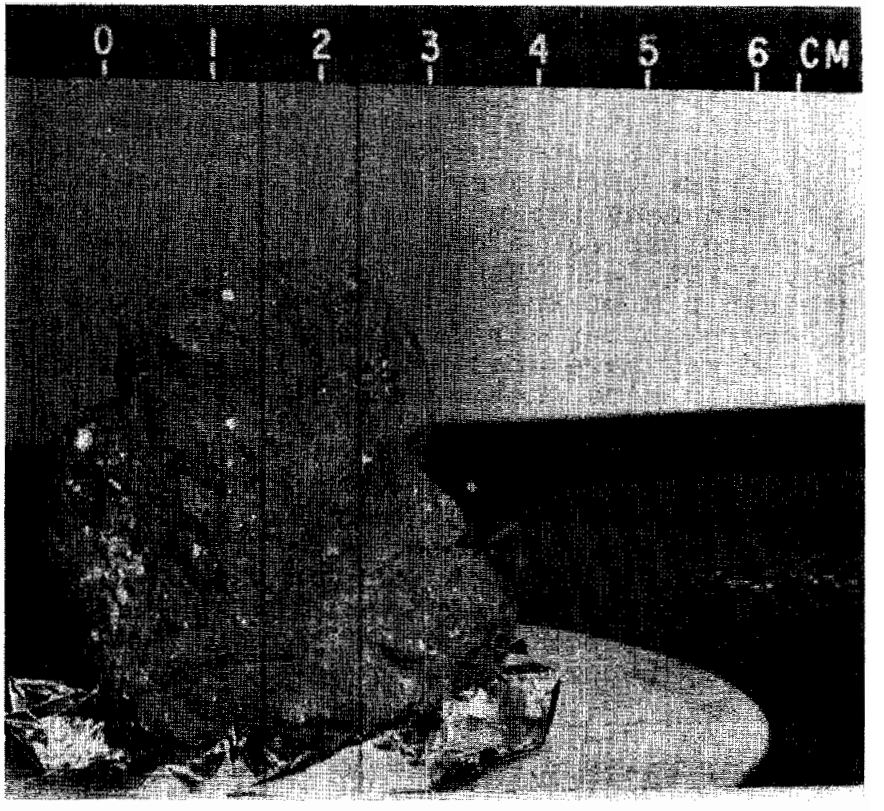

Figure 1. Pre-split view of 15287. S-71-44537

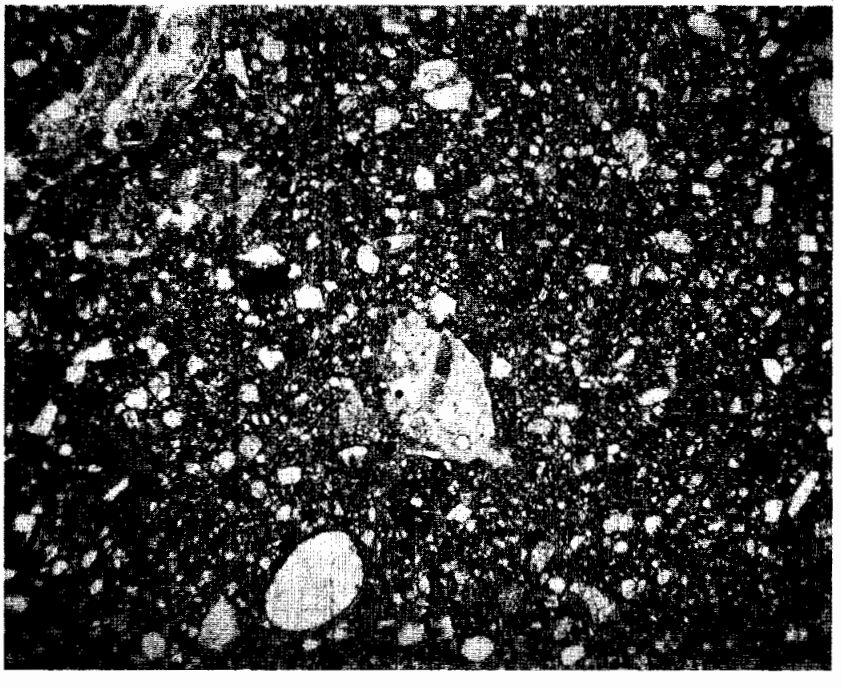

Figure 2. Photomicrograph of 15287,7. Width about 2 mm. Transmitted light.

15287

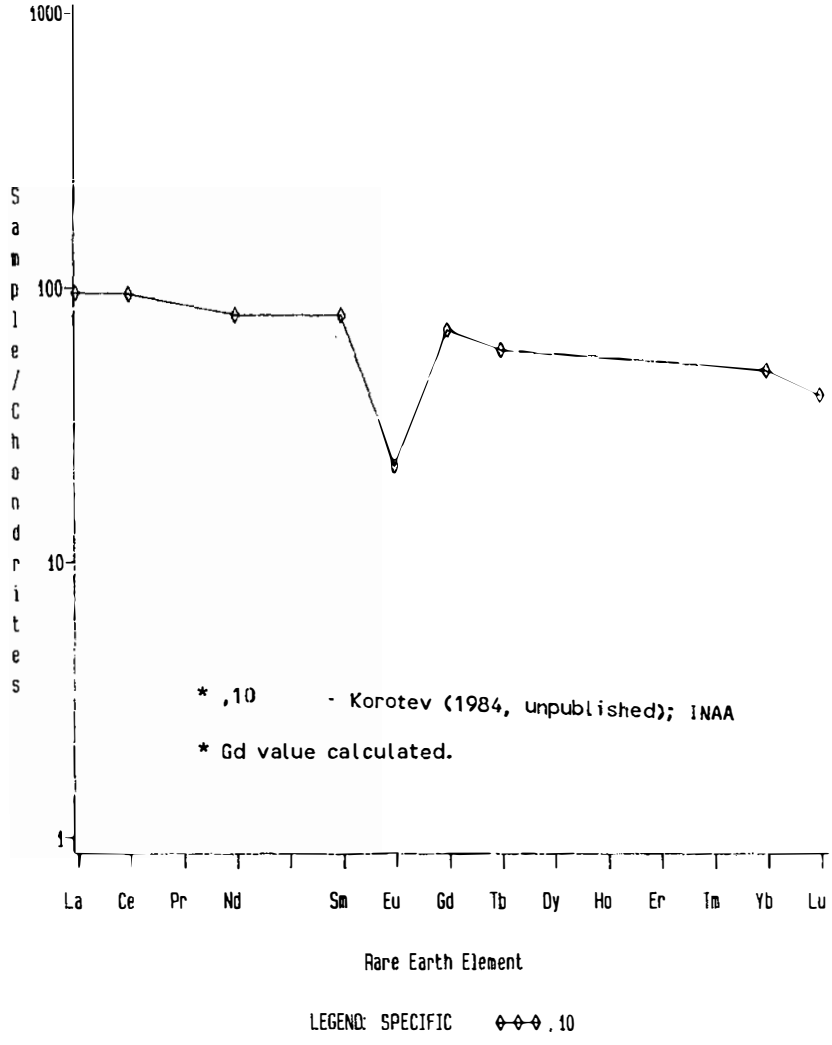

Figure 3. Rare earths in 15287 matrix.

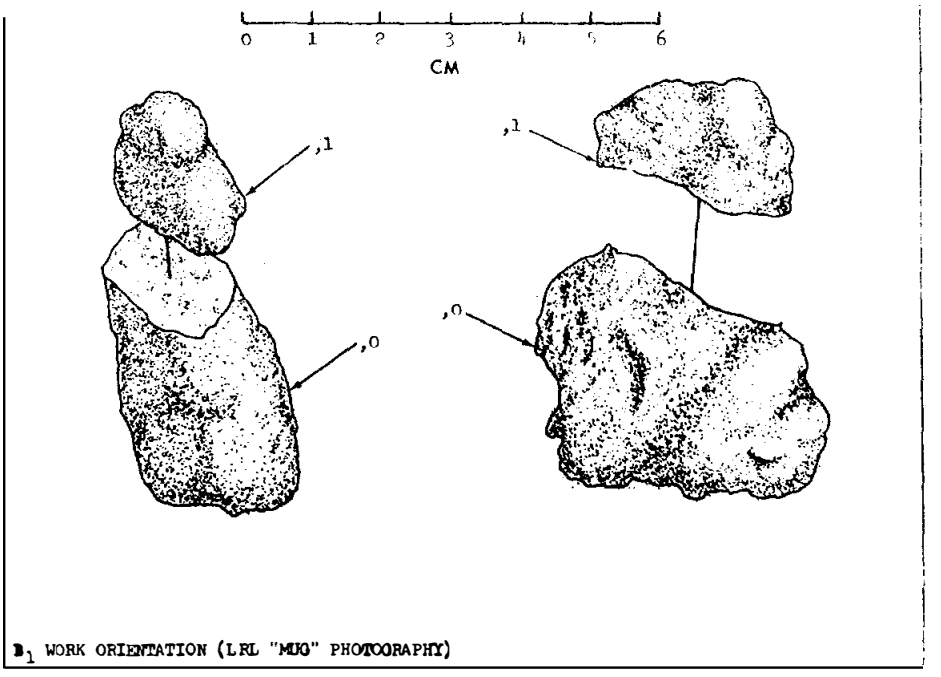

Figure 4. Original chipping of 15287.

TABLE 15287-1. Chemical analyses

		,10
Wt %	SiO2	
	TiO2	
	Al2O3	
	FeO	11.4
	MgO	
	CaO	10.3
	Na2O	0.50
	K2O	
	P2O5	
(ppm)	Sc	22.2
	V	
	Cr	2100
	Mn	
	Co	41.5
	Ni	239
	Rb	
	Sr	130
	Y	
	Zr	440
	Nb	
	Hf	12.0
	Ba	324
	Th	5.6
	U	1.3
	Pb	
	La	31.7
	Ce	84
	Pr	
	Nd	48
	Sm	14.4
	Eu	1.57
	Gd	
	Tb	2.82
	Dy	
	Ho	
	Er	
	Tm	
	Yb	10.2
	Lu	1.41
	Li	
	Be	
	B	
	C	
	N	
	S	
	F	
	Cl	
	Br	
	Cu	
	Zn	
(ppb)	I	
	At	
	Ga	
	Ge	
	As	
	Se	
	Mo	
	Tc	
	Ru	
	Rh	
	Pd	
	Ag	
	Cd	
	In	
	Sn	
	Sb	
	Te	
	Cs	360
	Ta	1400
	W	
	Re	
	Os	
	Ir	6.8
	Pt	
	Au	3.0
	Hg	
	Tl	
	Bi	
		(1)

References and methods:

(1) Korotev (1984, unpublished); INAA

15288 REGOLITH BRECCIA, GLASS-COATED ST. 6 70.5 g

INTRODUCTION: 15288 is a tough, glassy, regolith breccia (Fig. 1) with some vesicular black surface glass, mainly on one surface. It is medium-gray, subangular, and seems to be more mafic than local soils, and less-KREEP-rich than 15265-15267. It has few to no zap pits. The sample was collected (along with 15259, 15266 to 15269, 15285 to 15287, and 15289) from the crest of an inner bench on the northeast wall of the 12 m crater at Station 6, downslope 15 m from the LRV. Like several other samples, it was lying very close to 15265-15267 and may have spalled from it; however its chemical composition is a little different. Its sampling was documented.

PETROLOGY: 15288 is a non-porous, dark regolith breccia (Fig. 2) with spheres of green, red, yellow, and colorless glass. Some parts are clearly foliated. Mare basalt clasts are present.

CHEMISTRY: A comprehensive analysis was reported by Wanke et al. (1977) (Table 1, Fig. 3). The alumina is a little lower and the iron and titanium a little higher than St. 6 soils, and the rare earths are lower than the 15265-15267 rock and its inferred spalls.

PROCESSING AND SUBDIVISIONS: A sample numbered 15258 was renamed 15288,1 when its fresh face was found to fit 15288,0. Chipping of ,0 produced ,7 and ,8 (Figs. 1, 4). ,7 was made into a potted butt from which thin section ,9 was made. Part of ,8 was made into potted butt ,12, from which thin sections ,14 and ,15 were made. Another split of ,8 (,11) was used for the chemical analysis. ,0 is now 54.95 g; ,1 is 7.4 g.

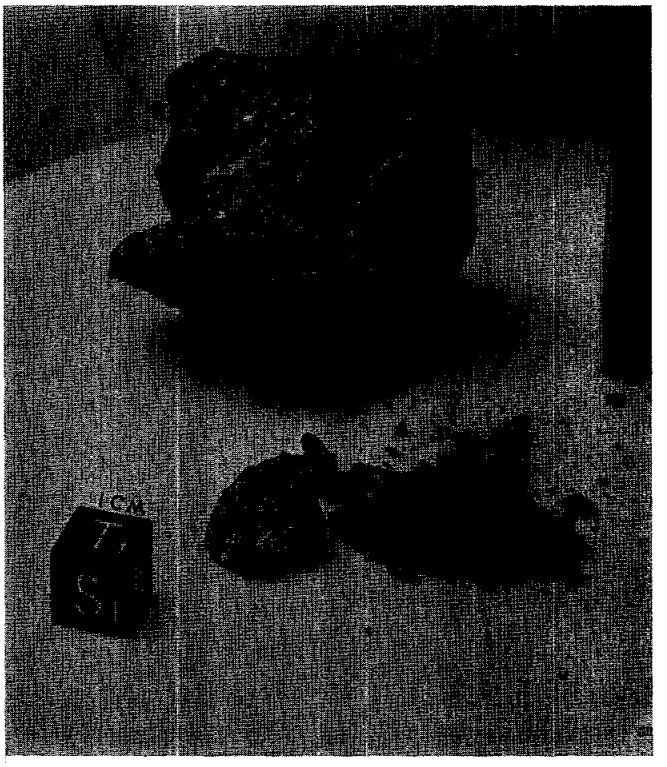

Fig. 1a

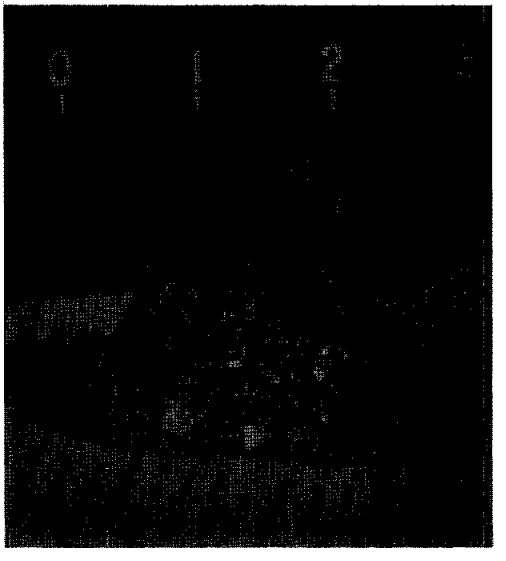

Fig. 1b

Figure 1. a) Splitting of ,0 to produce ,8. S-71-60570; b) 15288,1. S-71-44802.

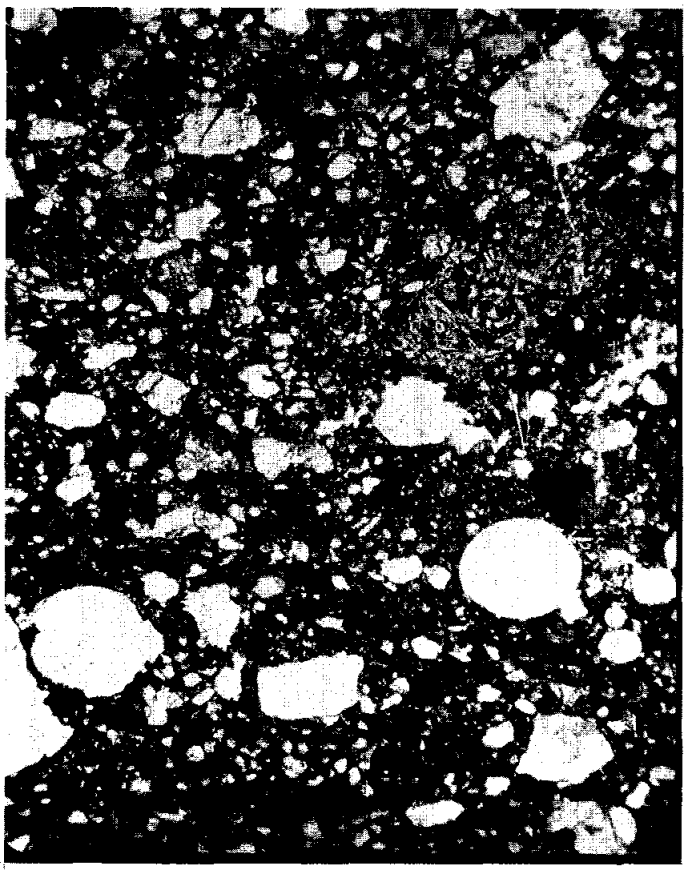

Figure 2. Photomicrograph of 15288,9 showing dense matrix and weak foliation. Width about 2 mm. Transmitted light.

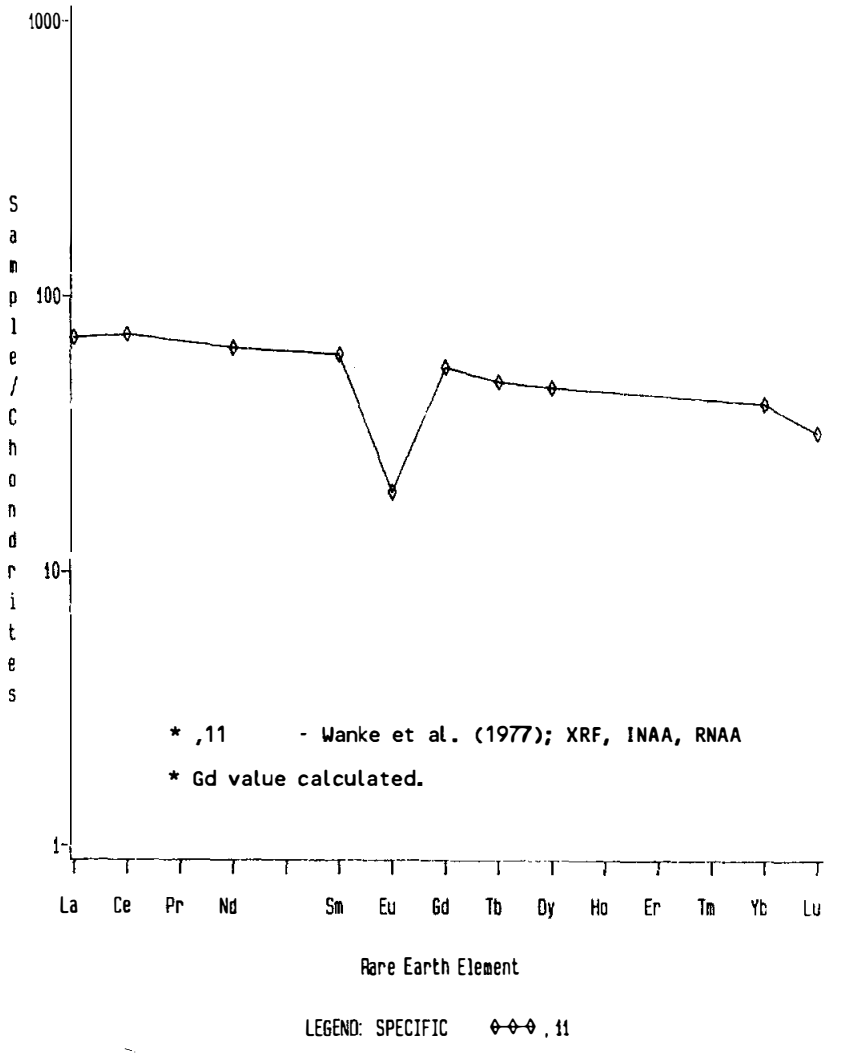

Figure 3. Rare earths in 15288.

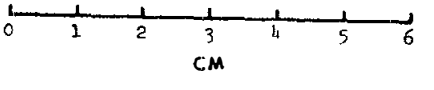

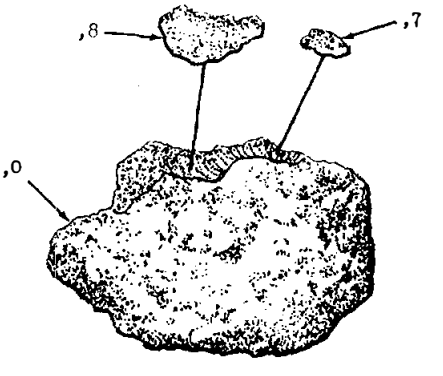

Figure 4. Chipping of 15288,0.

TABLE 15288-1. Chemical analysis

		,11
Wt %	SiO2	46.1
	TiO2	1.57
	Al2O3	15.1
	FeO	13.2
	MgO	10.9
	CaO	11.0
	Na2O	0.45
	K2O	0.188
	P2O5	0.197
(ppm)	Sc	27.1
	V	95.1
	Cr	2780
	Mn	1390
	Co	44.6
	Ni	200
	Rb	
	Sr	129
	Y	83
	Zr	324
	Nb	23
	Hf	8.22
	Ba	246
	Th	3.70
	U	
	Pb	
	La	23.4
	Ce	64.0
	Pr	
	Nd	39
	Sm	11.1
	Eu	1.35
	Gd	
	Tb	2.30
	Dy	14.7
	Ho	
	Er	
	Tm	
	Yb	8.18
	Lu	1.09
	Li	
	Be	
	B	
	C	
	N	
	S	420
	F	
	Cl	
	Br	
	Cu	
	Zn	
(ppb)	I	
	At	
	Ga	
	Ge	
	As	
	Se	
	Mo	
	Tc	
	Ru	
	Rh	
	Pd	
	Ag	
	Cd	
	In	
	Sn	
	Sb	
	Te	
	Cs	
	Ta	1110
	W	
	Re	
	Os	
	Ir	
	Pt	
	Au	
	Hg	
	Tl	
	Bi	
		(1)

References and methods:

(1) Wanke et al. (1977); XRF, INAA, RNAA

15289 REGOLITH BRECCIA ST. 6 24.1 g

INTRODUCTION: 15289 is a regolith breccia which is medium dark gray, blocky, angular, and coherent to friable (Fig. 1). Its friability is a result of penetrative fractures. It has a few zap pits on some surfaces. The sample was collected (along with 15259, 15265 to 15269, and 15285 to 15288) from the crest of an inner bench on the northeast rim of the 12 m crater, downslope 15 m from the LRV. Like several other samples it was lying very close to 15265-15267 and may have spalled from it. However, it has not been identified in site photographs.

PETROLOGY: 15289 is a non-porous, dense, glassy regolith breccia (Fig. 2). It is faintly foliated. Glasses include colorless and yellow shards and spheres, but no red/orange spherules have been observed. Mineral fragments are generally fine-grained. Lithic fragments include small highland crystallines, and mare basalts.

PROCESSING AND SUBDIVISIONS: ,0 was chipped to produce ,1 and ,2 (Figs. 1, 3). ,1 was made into a potted butt and thin sections ,5 to ,7 made from it. ,0 is now 19.3 g.

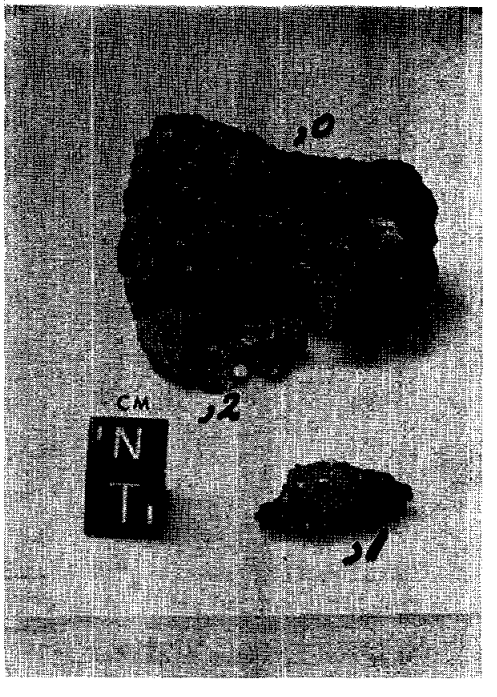

Figure 1. Post-split view of 15289. S-71-60572

Figure 2. Photomicrograph of 15289,6. Width about 2 mm. Transmitted light. Clast in lower center is a mare basalt.

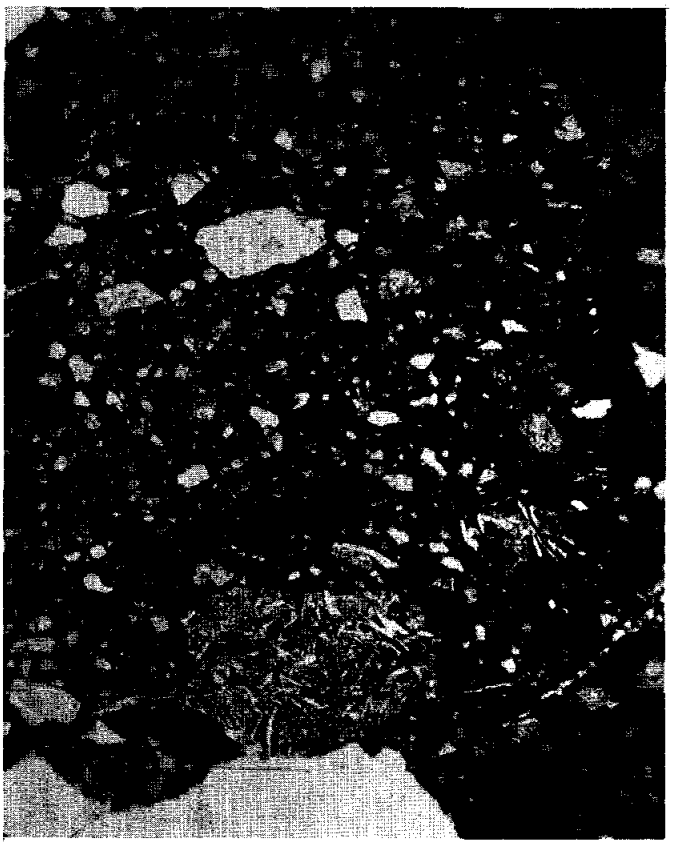

Figure 3. Chipping of 15289.

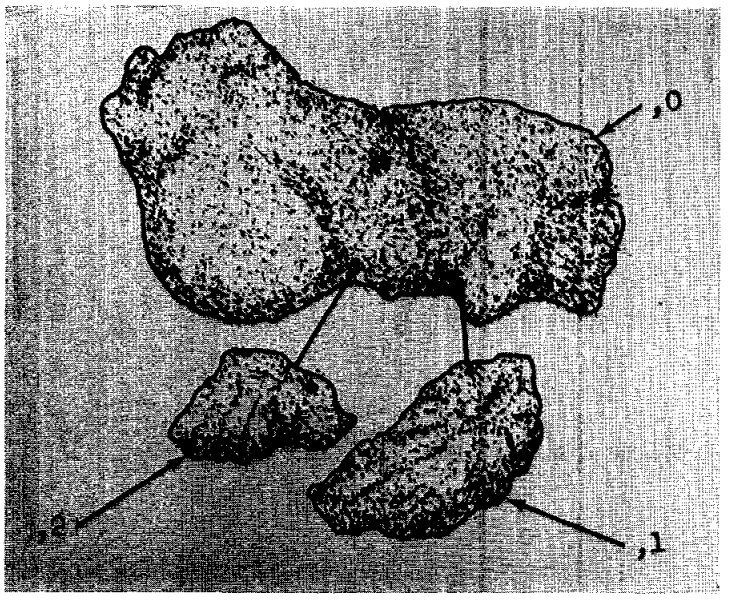

15295 REGOLITH BRECCIA ST. 6 947.3 g

INTRODUCTION: 15295 is a glassy matrix regolith breccia with some conspicuous white clasts, at least one large one of which is a pristine ferroan anorthosite. It contains vesicular glass veins. Its composition is very similar to local regolith.

15295 was collected along with soil samples upslope (south) about 10 or 15 m from the LRV. It was distinctive because of its large size and angularity (Figs. 1, 2), and because it had a fillet on its uphill side. It is medium light gray, tough, and penetrated with glass. It has a few zap pits on some surfaces.

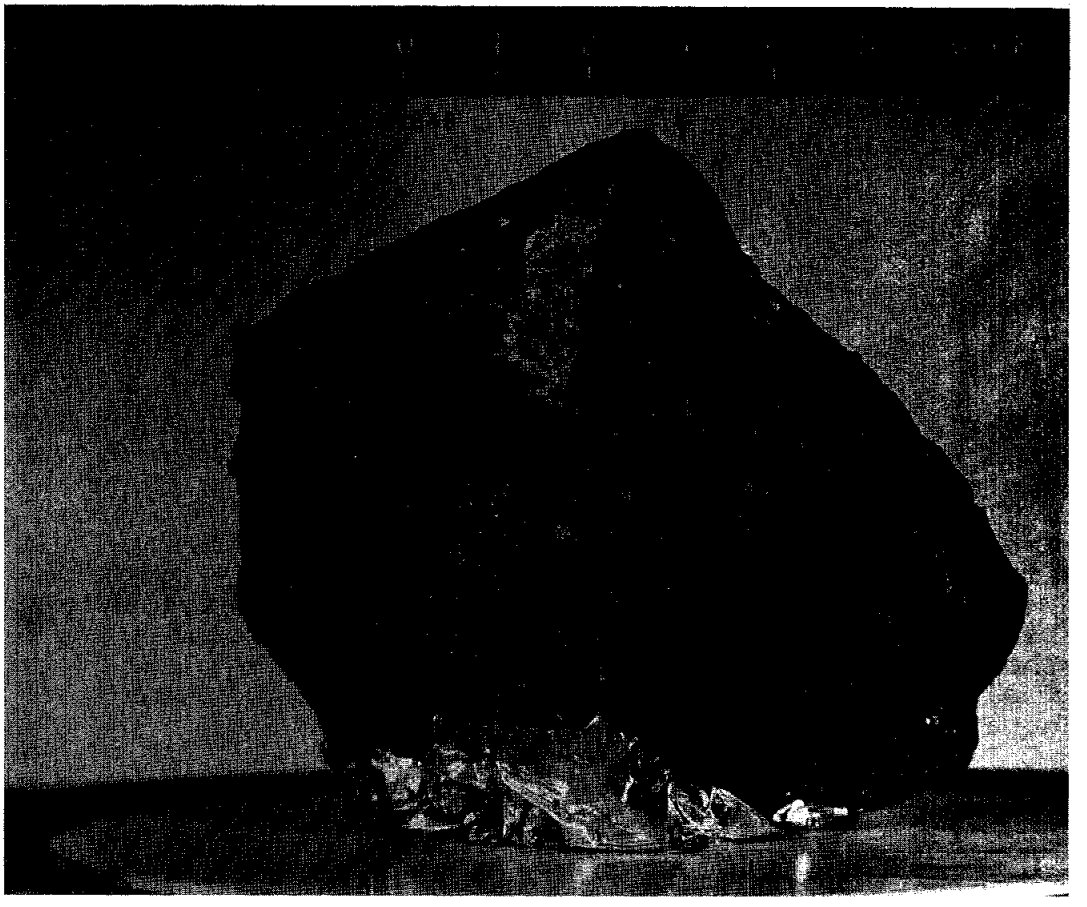

Figure 1. Macroscopic view of 15295 prior to its splitting, showing prominent white clast and bubbly glass.

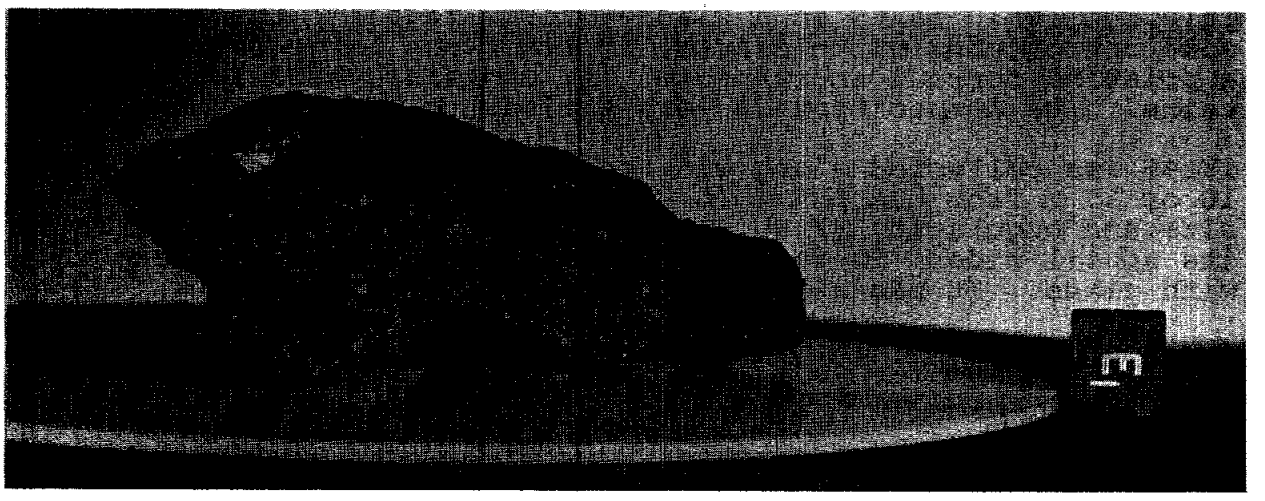

Figure 2. Fresh breccia surface exposed on ,2.

PETROLOGY: 15295 has a glassy brown matrix containing lithic, mineral, and glass fragments (Fig. 3a). The lithic fragments include mare basalt and cataclastic anorthosites. One large white clast was described by Warren and Wasson as a cataclastic, ferroan anorthosite similar to Apollo 16 anorthosites. It contains plagioclases ($An_{95.1-95.8}$) and sparse, tiny pyroxenes ($En_{41}Wo_{42}$). The chemistry of the fragment indicates that it is pristine. This clast appears to be the centimeter-sized anorthosite in thin sections ,12, ,17, and ,19 (Fig. 3b). It might also be the white clast in Figure 1, but there is inadequate documentational evidence.

McKay and Wentworth (1983) found 15295 to have a compact intergranular porosity, a low fracture porosity, very rare agglutinates, minor spheres, and common shock features. An I_s/FeO of 36 (McKay et al., 1984) or 38 (Korotev, 1984 unpublished) was determined, i.e., the sample is submature.

Glass veins penetrate the rock and are flow-banded and greenish brown. Wilshire and Moore (1974) interpret the glass on the surface of the rock to be exposed veins which had developed along conjugate fracture surfaces in the original rock mass.

Fig. 3a

Fig. 3b

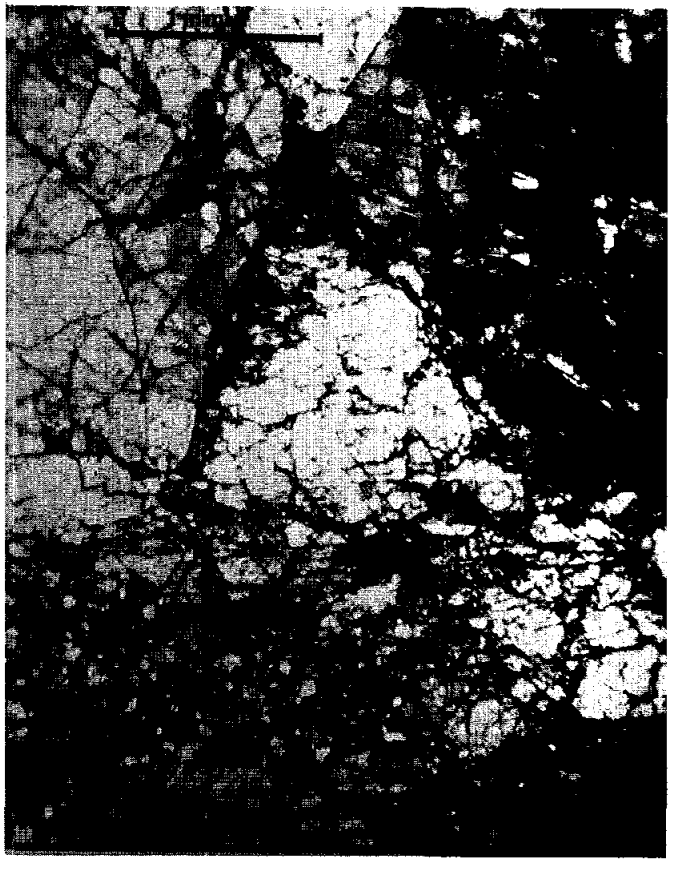

Figure 3. Photomicrographs of 15295,17 (a) breccia matrix, transmitted light; (b) cataclastic anorthosite clast, crossed polarizers.

CHEMISTRY: Analysis for major and trace elements for the matrix agree well for most elements (Table 1, Fig. 4). Its chemical composition is very similar to the Station 6 soils, hence it was probably locally-produced.

Warren and Wasson (1978) presented an analysis of the ferroan anorthosite clast, whose trace abundances indicate it to be free of meteoritic or KREEP contamination (Table 2). It has very low rare earth abundances with the positive europium anomaly typical for anorthosites.

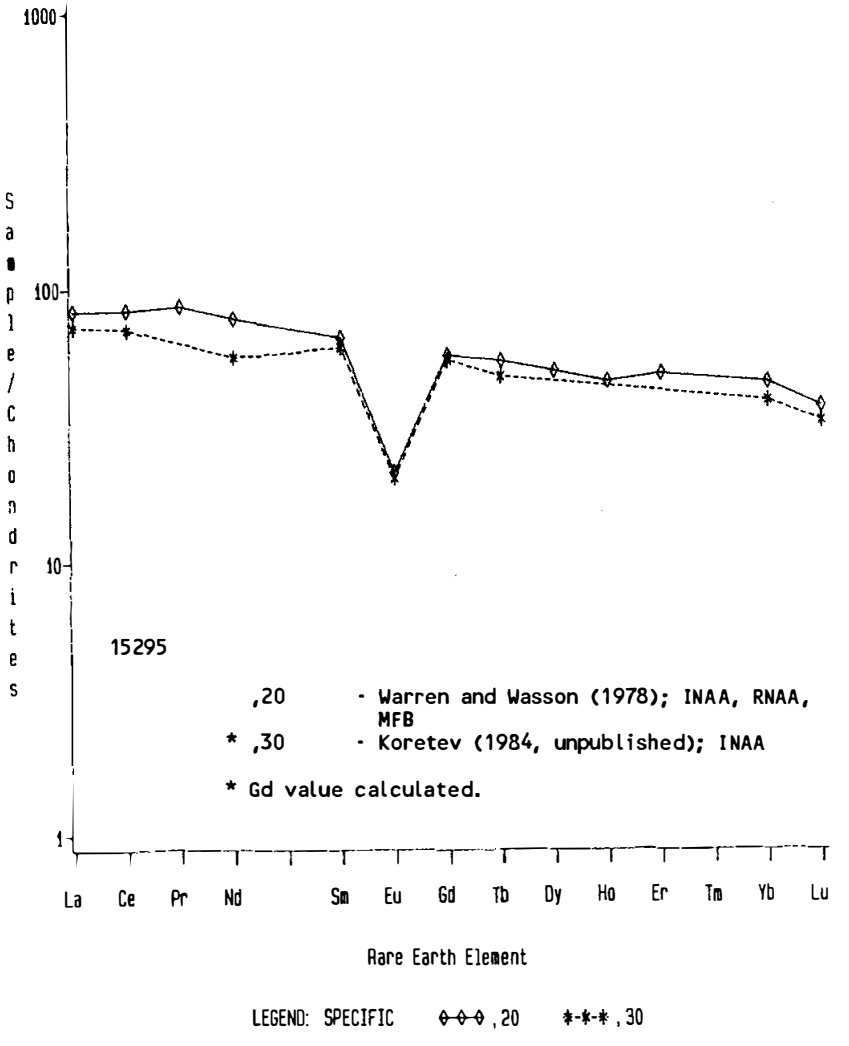

Figure 4. Rare earths in matrix.

TABLE 15295-1.

		,20 MATRIX	,22 ANORTHOSITE CLAST
Wt %	SiO2	46.68	43.9
	TiO2	1.48	
	Al2O3	16.29	35.5
	FeO	11.87	0.23
	MgO	10.24	0.18
	CaO	11.33	19.5
	Na2O	0.4979	0.402
	K2O	0.2247	
	P2O5	0.2222	
(ppm)	Sc	24.7	0.38
	V	76.9	
	Cr	2440	17.8
	Mn	1275	38
	Co	39.4	1.4
	Ni	250	<15
	Rb	5.70	
	Sr	135,147	
	Y	101	
	Zr	394	
	Nb	28	
	Hf	9.65	
	Ba	279	
	Th	3.89	
	U	1.04	
	Pb		
	La	27.7	0.19
	Ce	74.3	
	Pr	9.83	
	Nd	47	
	Sm	12.1	0.049
	Eu	1.47	0.78
	Gd	14.2	
	Tb	2.58	
	Dy	15.9	
	Ho	3.2	
	Er	9.75	
	Tm		
	Yb	9.07	
	Lu	1.26	
	Li	14.3	
	Be	5.47	
	B		
	C		
	N		
	S	610	
	F	59	
	Cl	20.4	
	Br	0.073	
	Cu	4.72	
	Zn	18.0	25.2
(ppb)	I		
	At		
	Ga	4170	3970
	Ge	500	8.2
	As	23	
	Se	150	
	Mo		
	Tc		
	Ru		
	Rh		
	Pd		
	Ag		
	Cd		11[a]
	In		<0.6
	Sn		
	Sb		
	Te		
	Cs	270	
	Ta	1170	
	W	550	
	Re	0.71	
	Os		
	Ir		0.021
	Pt		
	Au	2.9	0.041
	Hg		
	Tl		
	Bi		
		(1)	(2)

References and methods:

(1) Wanke et al. (1977); XRF, RNAA, etc.
(2) Warren and Wasson (1978); INAA, RNAA, MFB

PROCESSING AND SUBDIVISIONS: The sample was broken into several large and small pieces. The bulk of the sample is in ,1 (387.3 g), which is in remote storage, and ,0 (430.7 g). Thin sections ,12, ,17, and ,19 were made from ,4 (10.68 g). The white clast was separated from ,5 as ,22 and appears to be the same white clast as in ,4. Thin sections ,24 and ,28 made from this white clast in ,5 are mainly dark breccia matrix with small pieces of the anorthosite. The large white clast in Figure 1 might be the same clast; it now is part of ,0.

15297 REGOLITH BRECCIA FRAGMENTS ST. 6 34.9 g

INTRODUCTION: 15297 consists of 13 breccia chips which are the residue of SCB 3 (i.e., from Station 6) that are greater than 1 cm (the finer material is 15281 to 15284). The samples have never been split or allocated.

15298 REGOLITH BRECCIA, GLASS-COATED ST. 6 1731.0 g

INTRODUCTION: 15298 is a regolith breccia whose coherency is varied, mainly because of numerous and penetrative fractures. It has a glassy matrix and contains numerous small glass, mineral, and lithic fragments, with few large clasts. It has a small area of glass coat (or vein filling) and slickensides. Its composition is similar to local regolith.

15298 is blocky and angular (Fig. 1), very fractured, and greenish gray. Its lunar orientation is partly known, it was one-fourth to one-third buried at collection, and zap pits are particularly common on one surface. 15298 was collected 10 m south of the LRV parking spot.

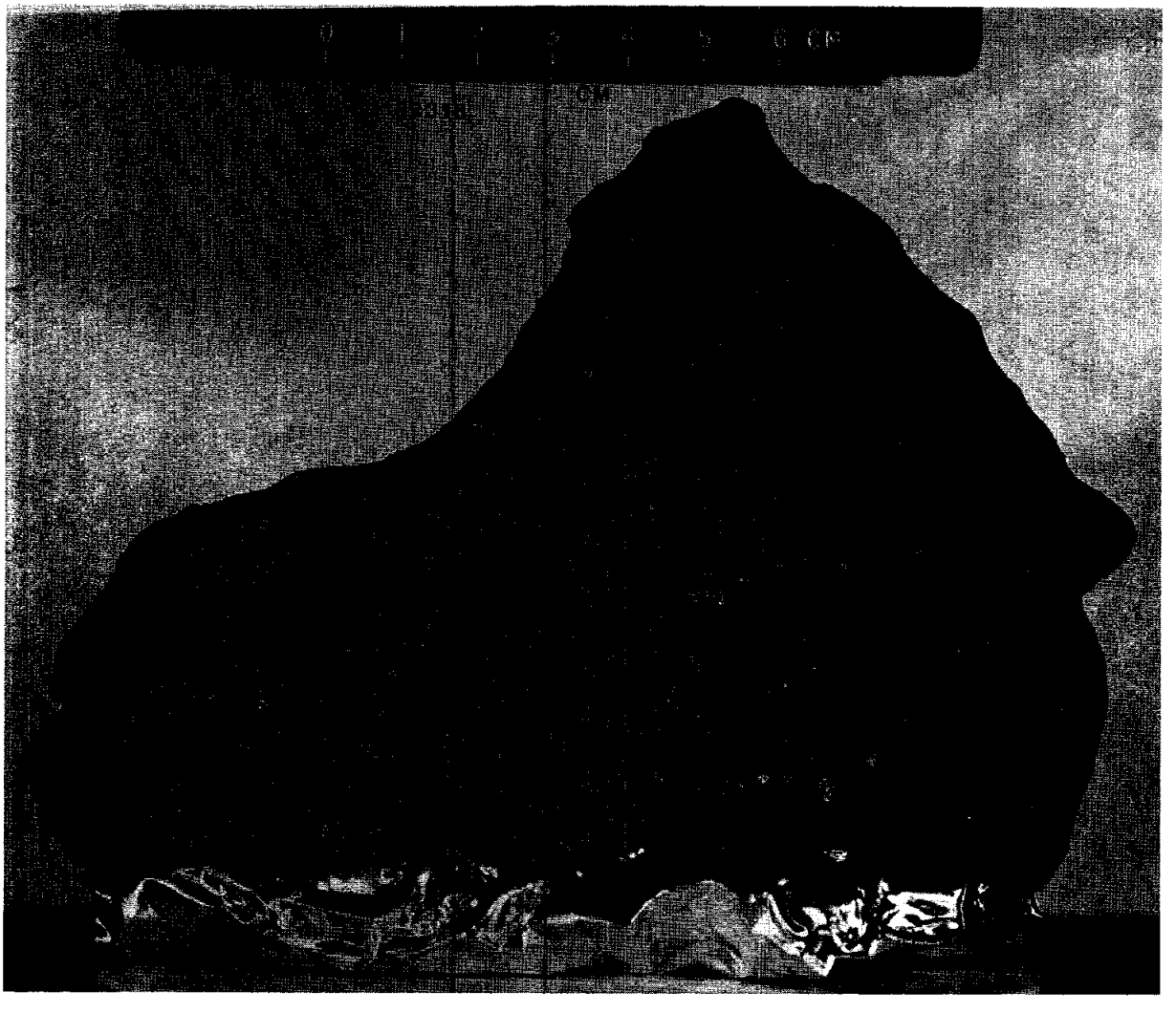

Figure 1. Whole rock sample prior to disintegration.

PETROLOGY: 15298 is a generally fine-grained, brown, glassy breccia (Fig. 2) in which fragments down to a few microns across tend to be angular. Glasses are common as yellow, red, colorless, pale-green, and pale-brown balls and shards; the one (13.6% TiO_2) glass analysis presented by Best and Minkin (1972) is the only olivine-normative of such high-Ti glasses that they found among Apollo 15 glasses. Lithic fragments include mare basalts and various breccias. McKay et al. (1984) determined an I_s/FeO of 46 to 71; Korotev (1984 unpublished) reported this as 59. Thus 15298 is as mature as most Apollo 15 regoliths.

CHEMISTRY: Chemical analyses are presented in Tables 1 to 3. The composition is very similar to Station 6 soils, although the analysis by Korotev (1984 unpublished) is a little more mafic. Rare earths are plotted in Figure 3. The sample has high C and volatiles normal for soil breccias. The data of Florey et al. (1972) may contain contributions to some elements (e.g., N) from terrestrial contamination. Their CO_2 values were very high. Christian et al. (1976) also reported an "excess reducing capacity" determination.

Figure 2. Photomicrograph of breccia matrix in 15298,6, transmitted light.

RARE GASES: Data for ^{3}He, ^{4}He, ^{22}Ne, ^{36}Ar, ^{84}Kr, and ^{132}Xe were presented by LSPET (1972), and Kr and Xe isotopic data were presented by Bogard and Nyquist (1972). The abundances and particularly the ratios are generally similar to Apollo 15 regoliths and other regolith breccias, and are predominantly of solar wind origin.

PROCESSING AND SUBDIVISIONS: The sample was subdivided by chipping, and because of its fragility fell into several parts. The largest pieces are ,8 (607.3 g) in remote storage and ,0 (926.3 g). ,10 to ,19 are pieces up to 20 g which formed during the disintegration. All thin sections (,5 to ,7, and ,20 to ,23) were made from a single chip ,4.

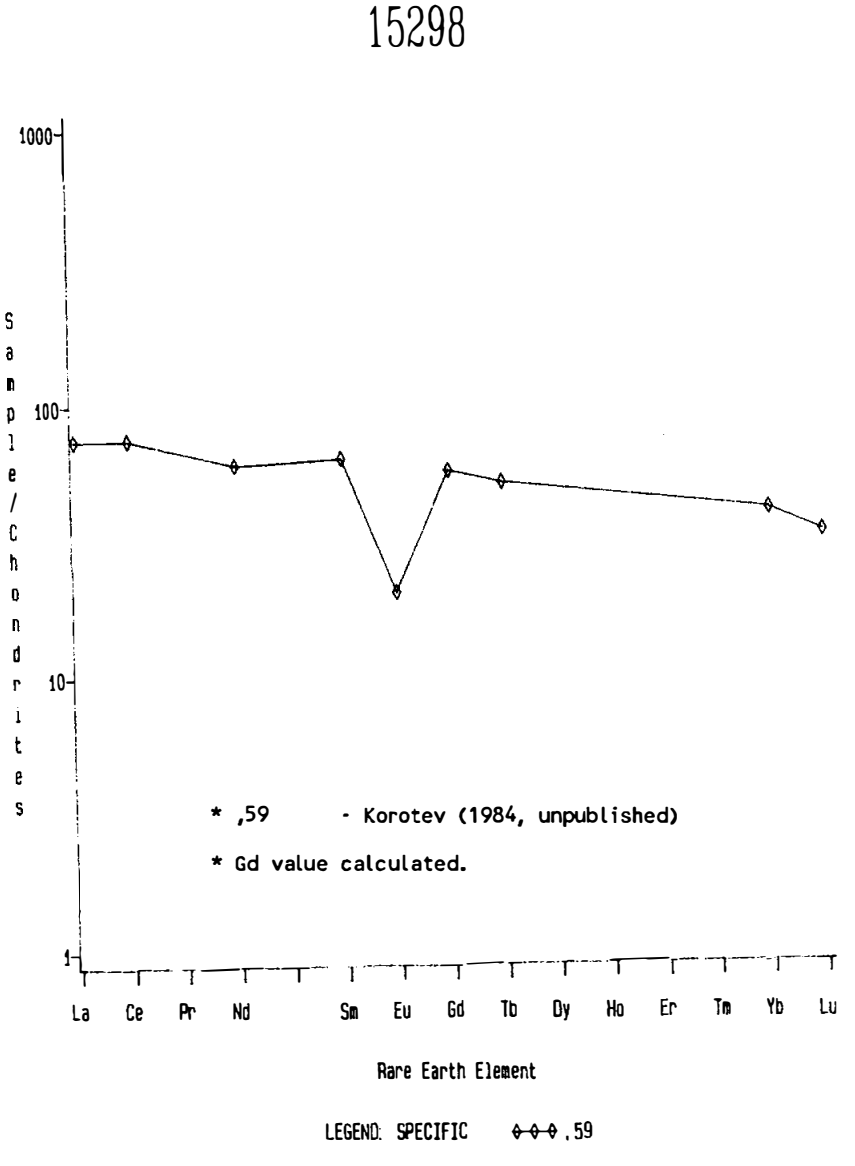

Figure 3. Rare earths in 15298 matrix.

TABLE 15298-1

		,5	,2	,26
Wt %	SiO2	45.71		
	TiO2	1.56		
	Al2O3	16.55		
	FeO	12.83		
	MgO	11.05		
	CaO	10.76		
	Na2O	0.46		
	K2O	0.27		
	P2O5	0.26		
(ppm)	Sc	24		
	V	68		
	Cr	2000		
	Mn	1400		
	Co	36		
	Ni	180		
	Rb	4.8		
	Sr	120		
	Y	84		
	Zr	390		
	Nb	22		
	Hf			
	Ba	270		
	Th			
	U			
	Pb	2.8		
	La	15		
	Ce			
	Pr			
	Nd			
	Sm			
	Eu			
	Gd			
	Tb			
	Dy			
	Ho			
	Er			
	Tm			
	Yb	11		
	Lu			
	Li	8.0		
	Be	2.6		
	B			
	C		160	130
	N			
	S			
	F			
	Cl			
	Cu	8.8		
	Zn	18		
(ppb)	I			
	At			
	Ga	4200		
	Ge			
	As			
	Se			
	Mo			
	Tc			
	Ru			
	Rh			
	Pd			
	Ag			
	Cd			
	In			
	Sn			
	Sb			
	Te			
	Cs			
	Ta			
	W			
	Re			
	Os			
	Ir			
	Pt			
	Au			
	Hg			
	Tl			
	Bi			
		(1)	(2)	(2)

References and methods:

(1) Christian et al. (1976); XRF and others
(2) Moore et al. (1972, 1973)

TABLE 15298-2. Organogenic compounds in 15298,24(2) from acidolysis (ppm) (Florey et al. 1972)

	H_2	N_2	CO_2	CH_4	CO_2	C_2	CD_4/CH_4
15298,24,2	310	8.8	70	45	1200	3.8	2.5

TABLE 15298-3. Organogenic compounds in 15298,24(3) released by volatilization (ppm) (Flory et al. 1972)

°C	N_2	CO	CH_4	CO_2	H_2O
250				59	74
500	33	46	11	53	52
800	130	200	7.6	100	40
1100	130	390		37	55

15299 REGOLITH BRECCIA ST. 6 1692.0 g

INTRODUCTION: 15299 is a regolith breccia consisting of glass, mineral, and lithic fragments in a glassy matrix. The clasts are rarely large as large as a centimeter (Figs. 1, 2) and define a foliation or lineation (Fig. 3). The sample is friable from abundant penetrative fractures. Some of these fractures contain glass.

15299 was collected about 25 m west-southwest of the Rover parking spot. It was not buried, had no fillet, and appeared to the astronauts to have struck the surface about 30 cm east of its collection site. The sample is dark gray, blocky, and angular (Fig. 1). Its lunar orientation is unknown, and its surface too fragile to allow detection of zap pits.

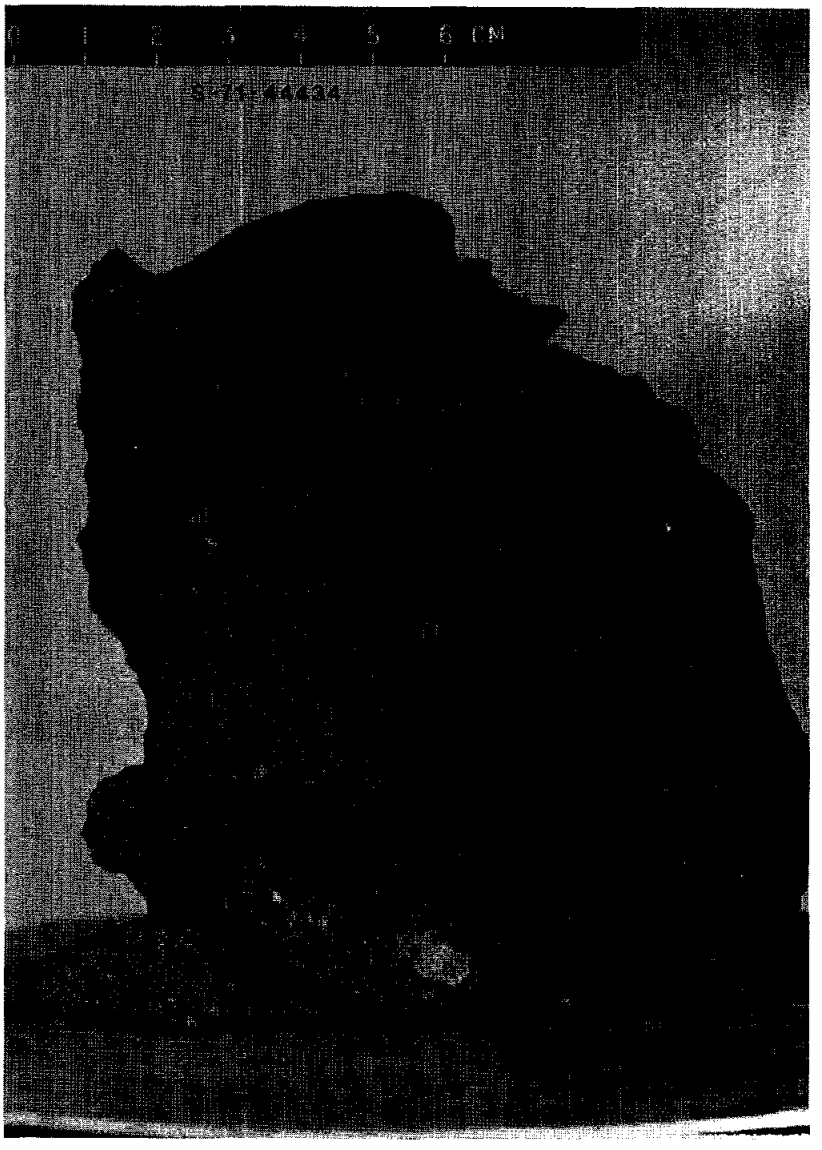

Figure 1. Pre-split photograph.

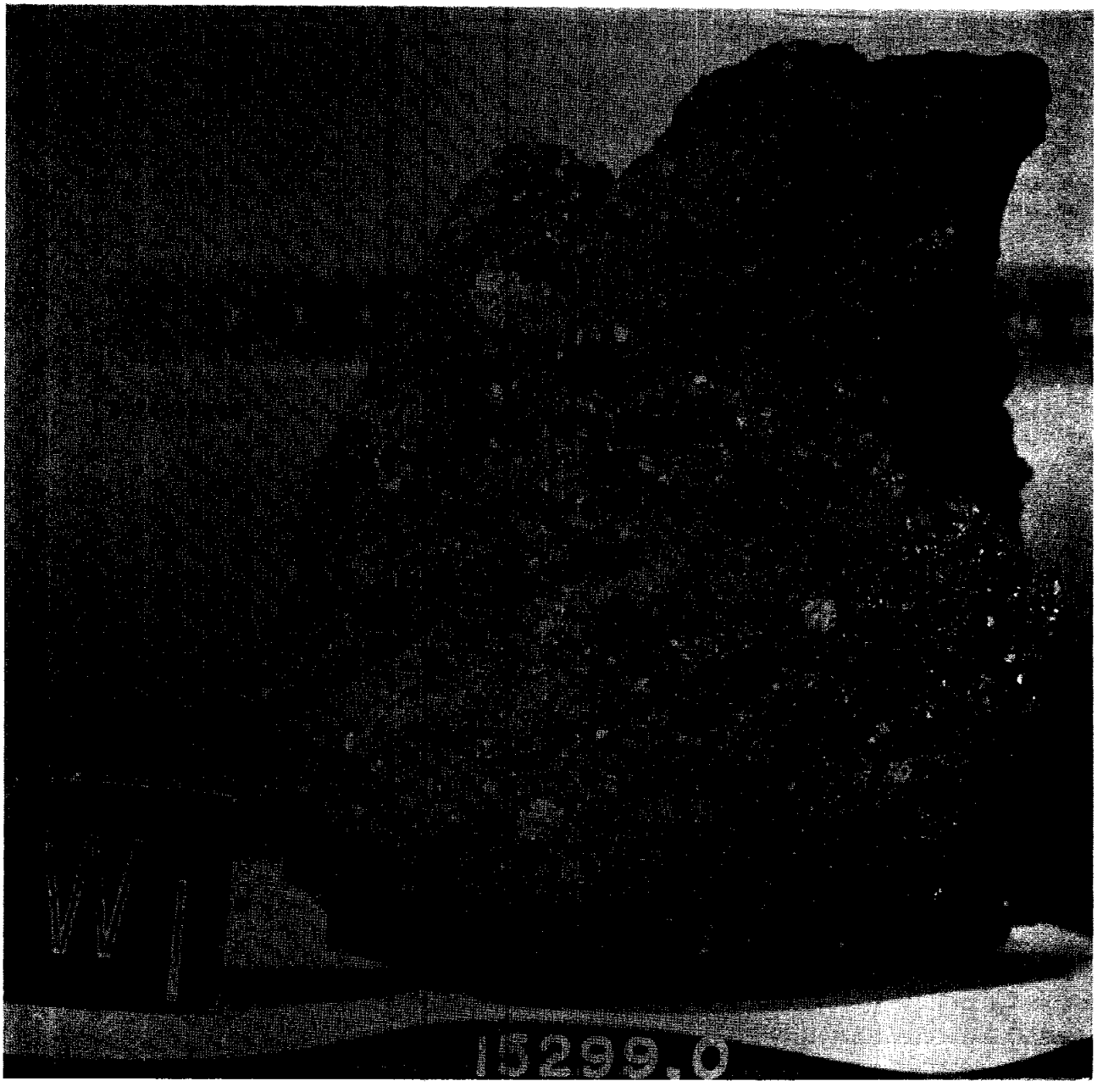

Figure 2. Close up of matrix of 15299,0.

PETROLOGY: 15299 has a gray brown matrix containing conspicuous, generally small white clasts and some pale green, red brown, and orange glasses are visible. McKay and Wentworth (1984) found 15299 to have a compact intergranular porosity, a low fracture porosity, very rare agglutinates, minor spheres, and minor shock features. McKay et al. (1984) determined an I_s/FeO of 22 to 34, which Korotev (1984 unpublished) reported as 32, i.e., submature. Wentworth and McKay (1983) determined a bulk density of 2.49 gm/cm^3. In thin section a foliation is apparent (Fig. 3), formed by alignment of elongated lithic and glass fragments and the long axis of ellipsoidal glass balls. According to Nagle (1982a) the fabric is that expected of subcrater lithification. Nagle (1982b) tabulated data on grain rounding, packing, and clast orientations.

Juan et al. (1972) described thin section ,106 as consisting of 70% glassy matrix, 12% subangular to subrounded lithic clasts (including mare, older breccia, and anorthositic varieties), 11% mineral clasts, 3% glass fragments, and 4% glass spheres. Many of the clasts and mineral fragments show shock effects (undulatory extraction, etc.). Juan et al. (1972) preferred the hypothesis that 15299 is a welded breccia formed in a base surge, i.e., thermal sintering. The largest clast visible in Figure 1 is a mare basalt.

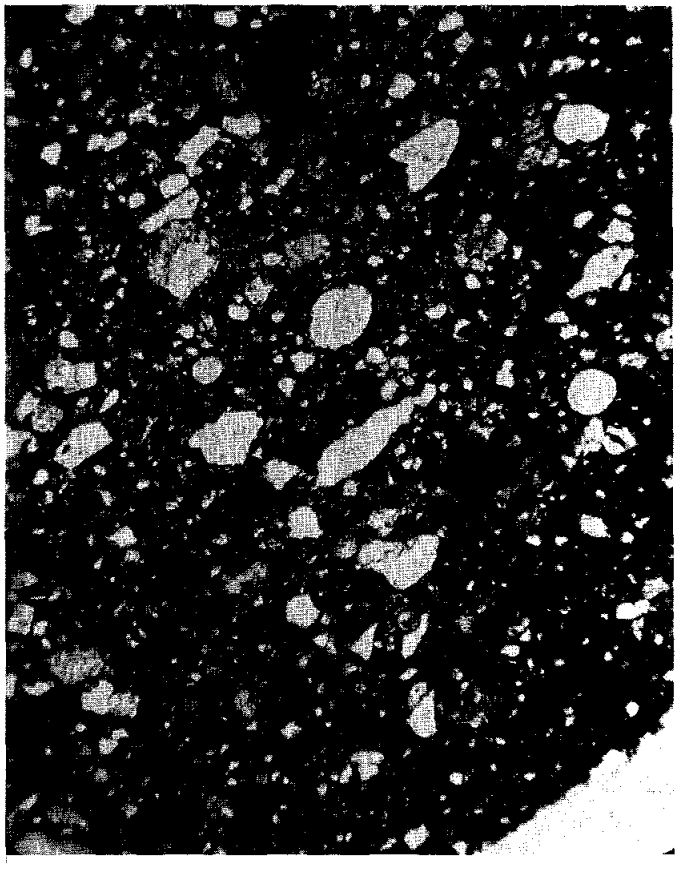

Figure 3. Photomicrograph of matrix in 15299,154 showing foliation.

CHEMISTRY: Several analyses of the breccia have been made (Table 1, Figure 4), and these show a similarity with soils from Station 6. The data of Wanke et al. (1973) is revised from earlier publication (Wanke et al., 1972), and that of Kothari and Goel (1973) includes more replicates than their early publication (Kothari and Goel, 1972). The sample analyzed by Baedecker et al.(1978) had its surface "sand blasted" to reduce contamination. S.R. Taylor et al. (1973) calculated that 15299 consists of a mixture of 15.8% "highland basalt" and 84.2% low-K Fra Mauro.

Merlivat et al. (1974) measured H_2 and H_2O and provide hydrogen isotopic data from extraction at different temperatures. They found that 6% of the total water was extracted above 700°C. Filleux et al. (1978) measured carbon in the near-surface and surface of two exterior pieces of 15299, finding lower "volume" carbon than did Moore et al. (1972, 1973).

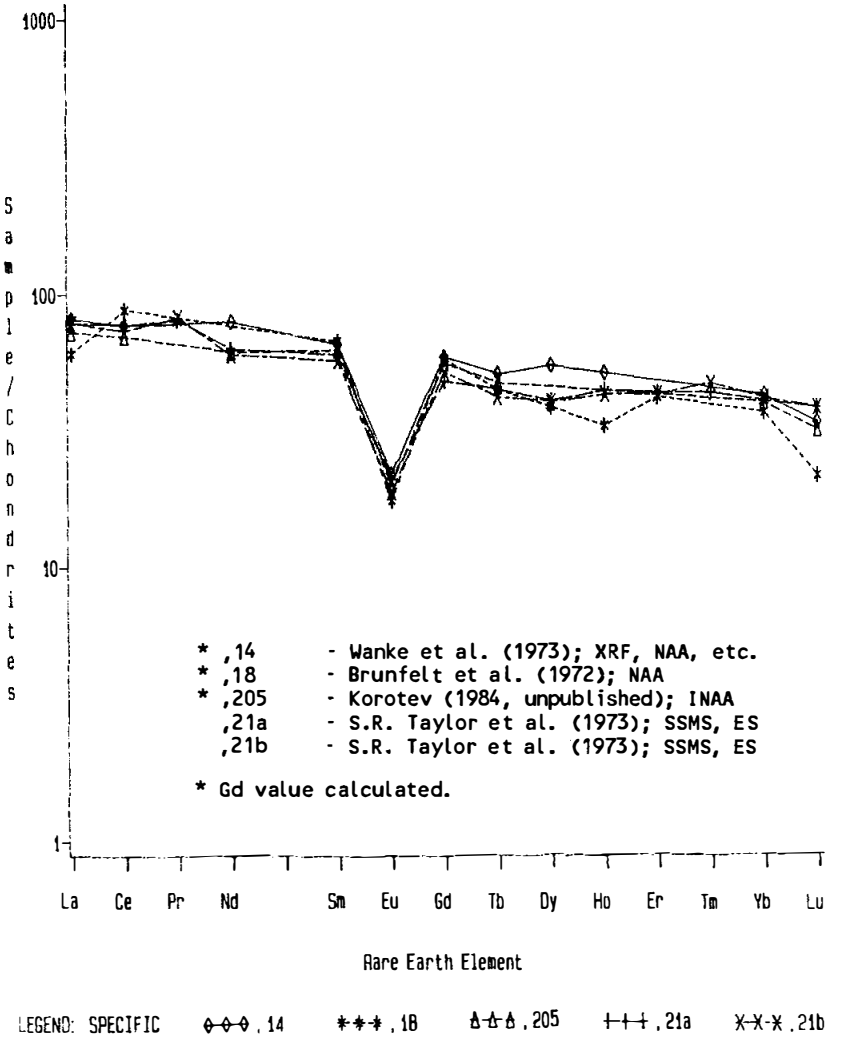

Figure 4. Rare earths in 15299 matrix samples a) Brunfelt et al. (1972); b) S.R. Taylor et al. (1973), "total"; c) S.R. Taylor et al. (1973), "matrix"; d) Wanke et al. (1973); e) Korotev (1984 unpublished).

TABLE 15299-1.

		,13	,18	,21a	,21b	,14	,17	,14	,2
Wt %	SiO2	45.90		46.9		46.4			
	TiO2	1.49	1.21	1.33		1.5			
	Al2O3	18.50	16.48	17.9		16.27			
	FeO	11.65	11.7	10.9		11.96			
	MgO	10.08		10.1		11.08			
	CaO	10.90	10.8	11.6		11.8			
	Na2O	0.430	.047	0.45		0.478			
	K2O	0.224		0.17		0.1960			
	P2O5								
(ppm)	Sc		22.2	16.0	16.0	23.2			
	V		104	45.0	24.0				
	Cr	2340	1570	2000	1750	2290			
	Mn	1180	950			1200			
	Co	71	39.3	44.0	40.0	39.6			
	Ni	244	230	195	215	150		239	
	Rb	5.0	4.5	5.0	4.7				
	Sr	265	100						
	Y			82.0	76.0				
	Zr			385.0	393.0				
	Nb			27.0	27.0				
	Hf		9.8	7.0	7.6	8.7			
	Ba		221	320	300				
	Th		3.5	3.72	4.31				4.271
	U		0.97	0.99	1.2				1.175
	Pb			2.6	3.0				3.031
	La		20	26.0	26.0	27.0			
	Ce		78	68.0	65.0	68			
	Pr			9.1	9.3				
	Nd			38.0	36.0	48			
	Sm		12.2	10.8	10.3	11.9			
	Eu		1.21	1.45	1.3	1.51			
	Gd			11.9	12.9				
	Tb		2.09	2.1	1.97	2.4			
	Dy		12.2	12.9	12.8	17.4			
	Ho		2.3	3.1	3.0	3.6			
	Er		8.4	8.7	8.6				
	Tm			1.3	1.4				
	Yb		7.3	8.1	8.3	8.5			
	Lu		0.73	1.3	1.3	1.15			
	Li	15							
	Be								
	B								
	C								
	N						74c		
	S								
	F								
	Cl								
	Br								
	Cu	3	5.5	4.7	4.2				
	Zn	35	14					17.7	
(ppb)	I								
	At								
	Ga	10000	4300	3800	2200			4500	
	Ge							410	
	As		170						
	Se		330						
	Mo								
	Tc								
	Ru								
	Rh								
	Pd								
	Ag	38	19						
	Cd							49	
	In		4					3.8	
	Sn			220	280				
	Sb								
	Te								
	Cs		220	190	180				
	Ta		1080			1060			
	W		910	190	230				
	Re								
	Os								
	Ir		6.0					7.8	
	Pt								
	Au	6	3.9					2.2	
	Hg								
	Tl								
	Bi								
		(1)	(2)	(3)	(3)	(4)	(5)	(6)	(7)

References and methods:

(1) Juan et al. (1972b); AAS, colorimetric
(2) Brunfelt et al. (1972); NAA
(3) S.R. Taylor et al. (1973); SSMS, ES
(4) Wanke et al. (1973); XRF, NAA, etc.
(5) Kothari and Goel (1973); NAA
(6) Baedecker et al. (1973); RNAA
(7) Silver (1973); ID/MS

Notes:

(a) Referred to as "total".
(b) Referred to as "matrix".
(c) Weighted mean of four replicates.

RADIOGENIC ISOTOPES: Silver (1973) provided Pb isotopic data (as well as U, Th, and Pb abundances), finding 15299 to be similar to local soils.

PHYSICAL PROPERTIES: Dran et al. (1973) tabulated fracture and albedo data for 15299 under a list of "metamorphic characters".

PROCESSING AND SUBDIVISIONS: ,1 was removed from the sample and sawn into several pieces (Fig. 5) from which many of the allocations were made. Subsequently the remaining sample was sawn to produce end piece ,161 (372.7 g), now in remote storage, and ,0 (1131.8 g). The 1-cm white mare basalt clast in Figure 1 (called clast 74) has also been subdivided and allocated.

Many thin sections were made from potted butts ,9, ,10 and ,11 (Fig. 5) and from ,162 which was a split from the major sawing. Most of those from ,11 and ,162 are in educational packages. ,197 is a thin section of basalt clast 74, and thin section ,200 is mainly matrix but also contains part of the clast.

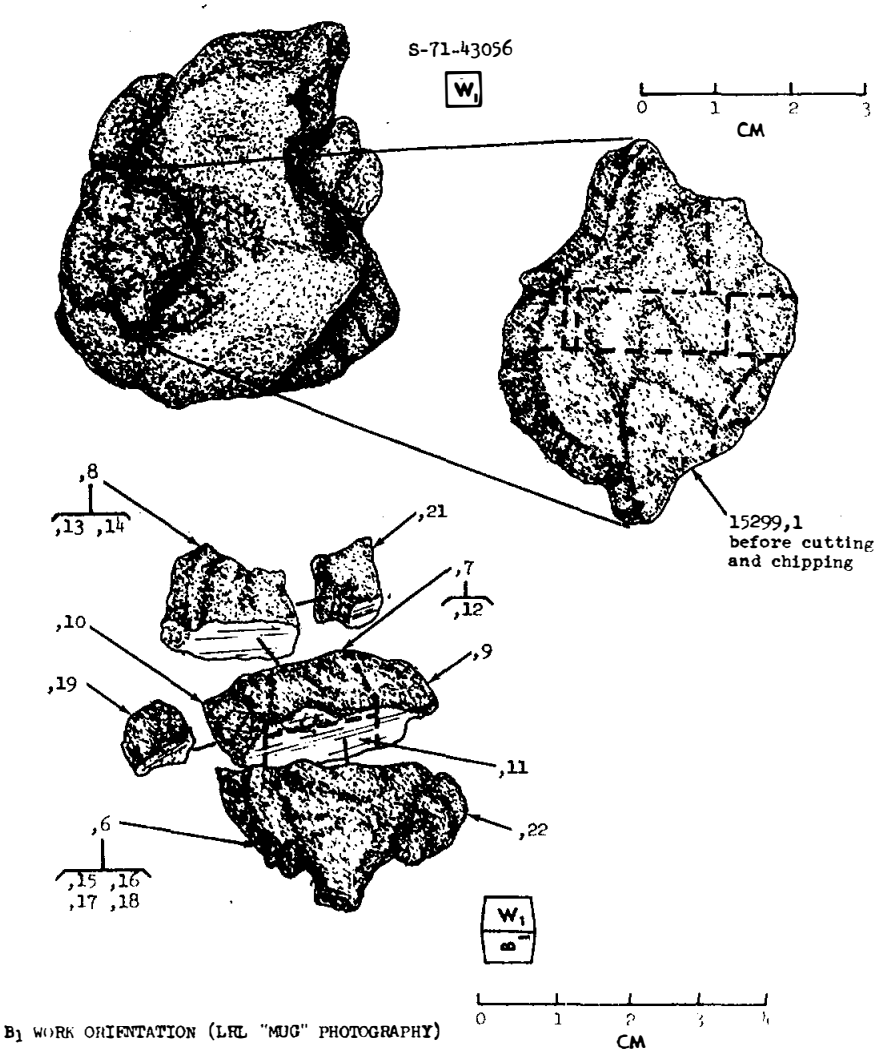

Figure 5. Splitting of ,1.

☆ U.S. GOVERNMENT PRINTING OFFICE: 1991—561-014/40051